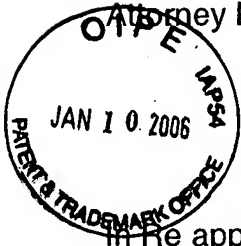Appl. No. 10/290,631

Attorney Docket: DX0670KB1

IN THE UNITED STATES PATENT AND TRADEMARK OFFICE

In re application of:
Gosse Jan ADEMA, et al.

Examiner: B. E. Bunner

Art Unit: 1647

Application No.: 10/290,631

Conf. No.: 3394

Filing Date: November 8, 2002

For: ANTIBODIES THAT
SPECIFICALLY BIND TO FDF03
(as amended)

Commissioner for Patents
P.O. Box 1450
Alexandria, VA 22313-1450

DECLARATION OF JOSEPH H. PHILLIPS PURSUANT TO 37 C.F.R. 1.132

Sir:

I, Joseph H. Phillips, declare as follows:

1. I am a co-inventor of the above-referenced application, and am familiar with the contents thereof.

2. I have been employed by DNAX Research, Inc. for 14 years, and have approximately 30 years of experience in the field of immunology research, as evidenced by my attached *curriculum vitae.*

1   DX0670KB1

3. I understand that the Examiner has rejected the present invention, antibodies or antibody fragments which bind to SEQ ID NO: 2 (FDF03), as not being supported by either a credible, specific and substantial asserted utility or a well established utility.

4. My laboratory has performed several experiments that show that the present invention is, in fact, supported by a credible, specific and substantial asserted utility, i.e., specific staining of myeloid lineage cells (Dendritic Cells) and use of antibodies against FDF03 to modulate immune function of these myeloid lineage cells (see, page 87, lines 26-27, and page 2, respectively, of the specification).

5. Antibodies specifically binding to human or mouse FDF03 were generated by standard immunization and hybridoma technology protocols (see, e.g., Coligan (ed.) (1991 and subsequent supplements) Current Protocols in Immunology, Wiley/Greene, NY.).

6. Antibodies that specifically bound to either mouse or human FDF03 were screened using the supernatants from fused hybrids and subjecting the supernatants to differential ELISA techniques. The FDF03 monoclonal antibodies were further tested for specificity by FACs analysis of FDF03 expressing cell lines.

7. Once mAbs specific for FDF03 were identified, these antibodies were used in FACS staining of CD11c+ dendritic cells (DCs) from peripheral blood and tonsils. As illustrated in the figure labeled "Figure 1" panels A and B, PE conjugated FDF03 specifically binds to myeloid lineage cells, e.g., dendritic cells.

8. A further FACS analysis was performed on CD34+ hematopoietic progenitor cells that were cultured with DC differentiation conditions (see Figure 2, panel A). FDF03 specifically stained these differentiated DC cells.

9. Hematopoietic progenitor cells were also cultured with SCF, GM-CSF, and TNFα for 6 days and subsequently sorted into CD14+ and CD1a+ subsets, which were further cultured with GM-CSF and TNFα at day 12 (see Figure 2, panel B). RNA expression was also analyzed. Only CD14+ derived DCs showed expression of FDF03 on both the

DX0670KB1

cellular and molecular level. Thus, FDF03 expression is restricted to monocyte derived DCs.

10. Monocyte derived DCs were cultured for 7 days with GM-CSF and IL-4 and then activated with LPS or CD40 ligand expressing cells. Cells were stained with PE conjugated FDF03 mAb and analyzed by FACS. Figure 2, panel C, shows specific staining of the activated monocyte derived DCs.

11. PE conjugated FDF03 mAb was also used to stain several immune lineage cells. As shown in Figure 3, panel B, the FDF03 mAb exhibits specificity for myeloid lineage cells, e.g., monocytes and granulocytes, while no staining was detected in non-myeloid lineage cells. Figure 3, panel A shows similar expression patterns on a molecular level.

12. We further performed a mast cell degranulation bioassay using agonist mAbs for both mouse and human FDF03. The degranulation assays were performed essentially as described in, e.g., Cherwinski, et al. (2005) J. Immunol. 174:1348-1356. Results of these experiments showed that agonist antibodies raised against FDF03 could prevent mast cell degranulation, thus impairing the inflammatory cascade associated with mast cell function (see Figure 4). These experiments prove that FDF03 acts as a traditional inhibitory receptor to modulate inflammatory responses caused by myeloid lineage cells.
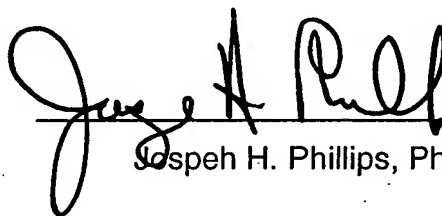
13. The experiments described above establish that the present invention is supported by credible, substantial and specific asserted utilities. Antibodies that bind to FDF03 are specific for myeloid lineage cells and can be used to ascertain the presence of these cells in biological samples. Identification of myeloid lineage cells infiltrating various tissues is important in the analysis of inflammatory diseases. Further, agonist antibodies against FDF03 function to modulate the immune inflammatory response by inhibiting mast cell degranulation. Both utilities are asserted in the present specification.

I hereby declare that all statements made herein of my own knowledge are true and that all statements made on information and belief are believed to be true; and

DX0670KB1

further that these statements were made with the knowledge that willful false statements and the like are so made are punishable by fine or imprisonment, or both, under Section 1001 of Title 18 of the United States Code, and that such willful false statements may jeopardize the validity of the application, any patent issuing thereon, or any patent to which this verified statement is directed.

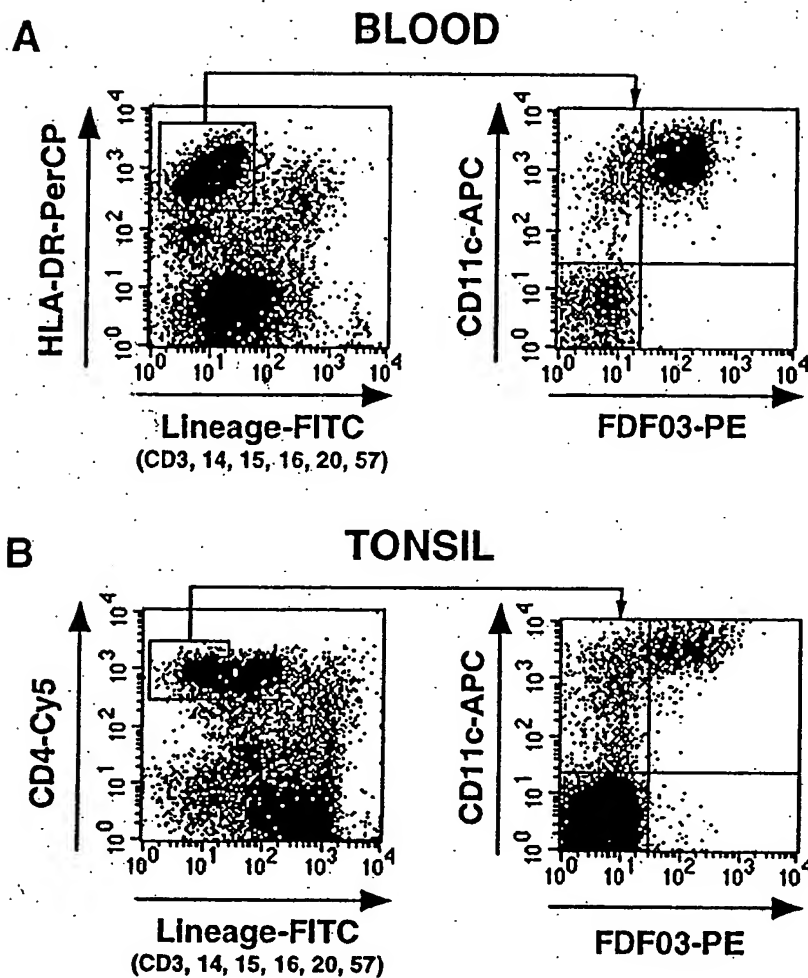Executed at Palo Alto, California on _____4/27/2005_____

Jospeh H. Phillips, Ph.D.
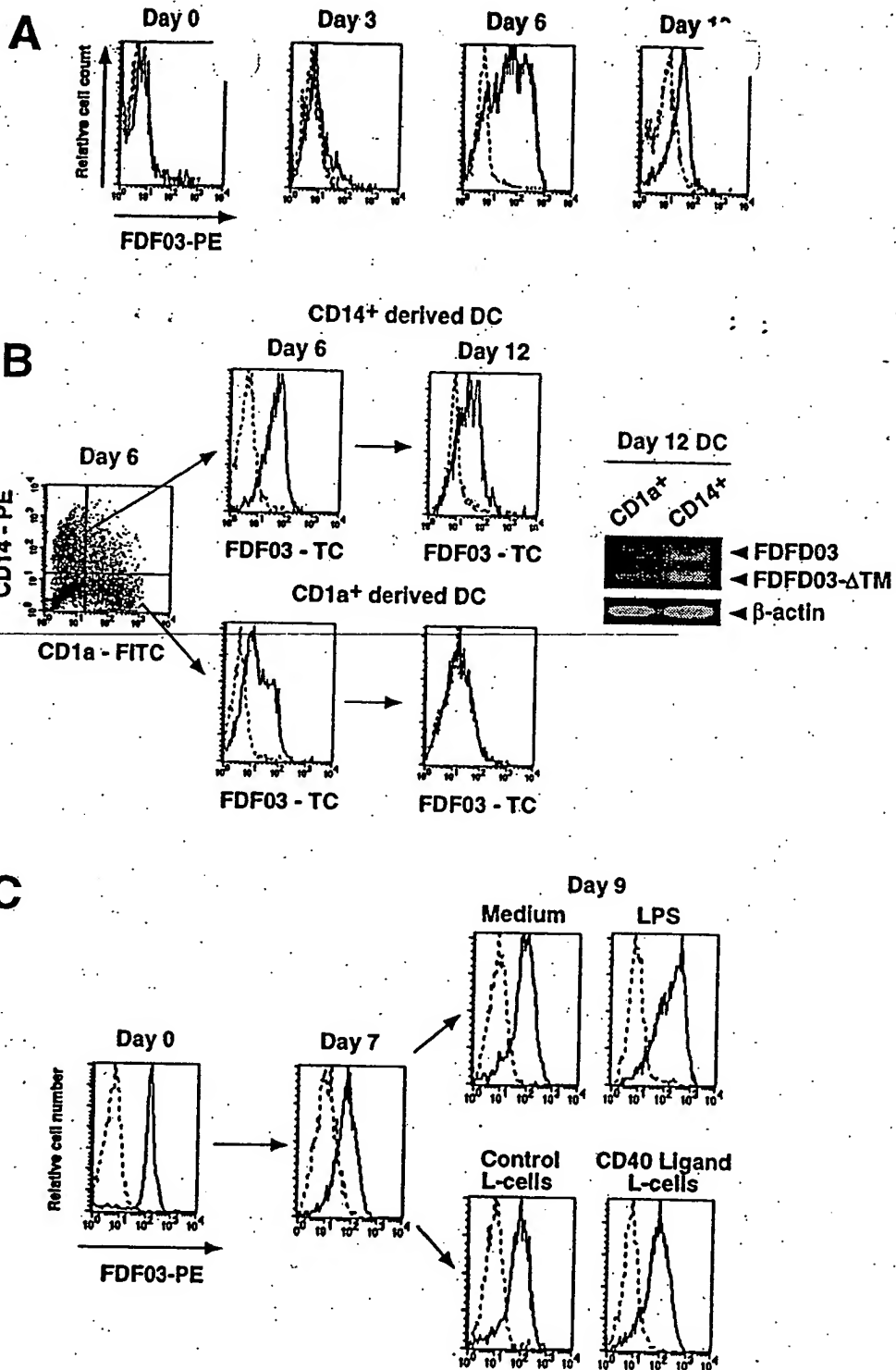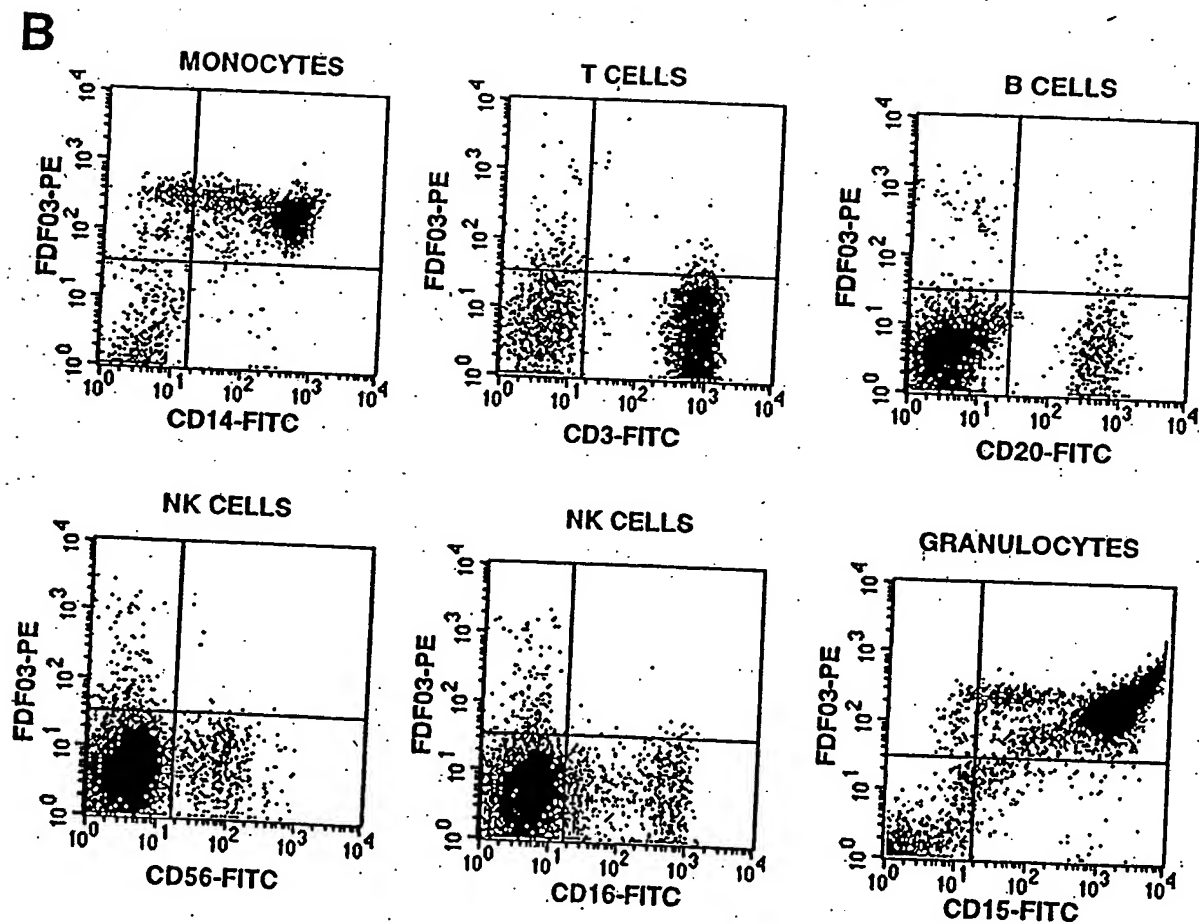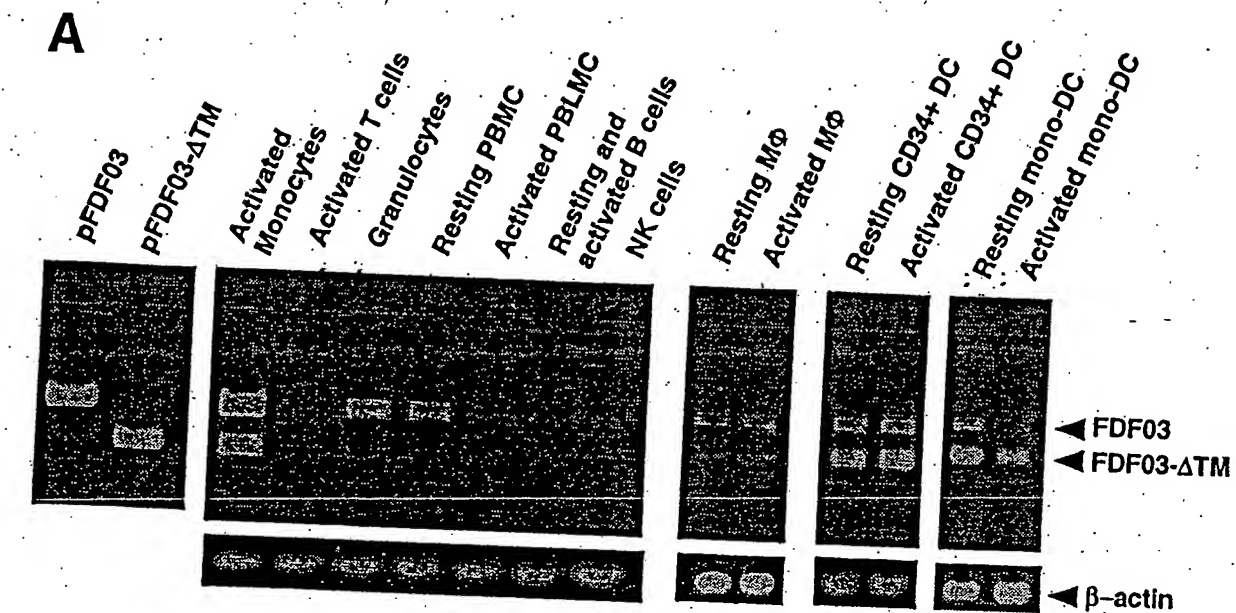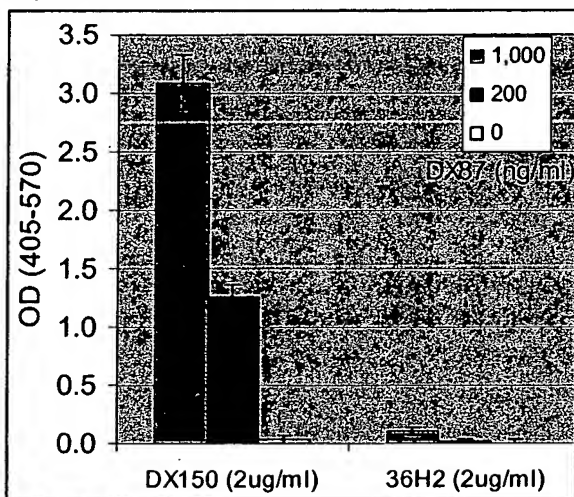
A BLOOD

B TONSIL

Figure 1

Figure 2

Figure 3

In this experiment (MB569), the agonistic anti-human FDF03 mAb, 36H2, inhibited the anti-mouse CD200R mAb (DX87) induced degranulation of the mouse mast cell line DT797, which over-expresses the inhibitory form of human FDF03. This assay measures the activity of Beta-Hexosaminidase that is released upon degranulation from mast cell granules. After the anti-FDF03 (or the isotype control DX150) and the anti-CD200R mAbs are bound to the mouse mast cells a cross-linking mAb is added that will induce degranulation of the mast cells if no inhibition occurs.

In this experiment, (MB509), another agonistic anti-human FDF03 mAb, DX173, inhibits the anti-mouse CD200R mAb (DX87) induced degranulation of the mouse mast cell line DT755, which over-expresses the inhibitory form of mouse FDF03. This is also a Beta-Hexosaminidase assay.
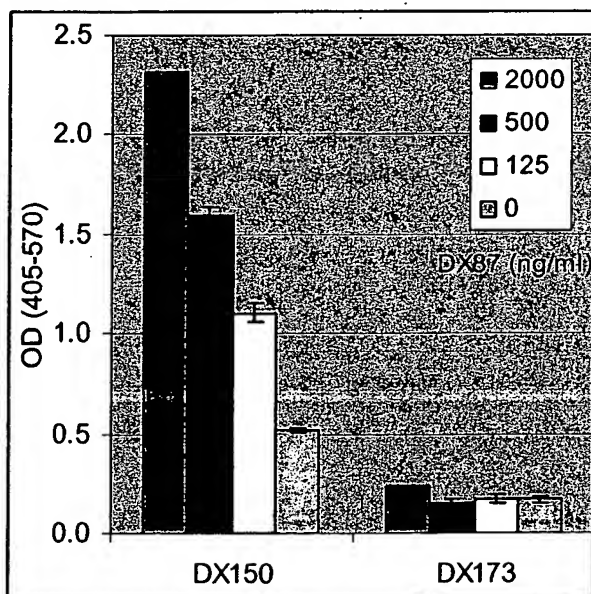

Figure 4

CURRICULUM VITAE

Name: **JOSEPH H. PHILLIPS**

Work Address: DNAX Research Institute for Molecular and Cellular Biology
                    Department of Immunology
                    901 California Avenue
                    Palo Alto, CA 94304-1104

Birthdate: September 27, 1952

Birthplace: Boston, MA

Citizenship: USA

Education:

Ph.D. - University of Texas, M.D. Anderson Hospital and Tumor Institute,
         Houston, Texas 1983

M.A. - William College, Williamstown, Massachusetts 1977

B.A. - Williams College, Williamstown, Massachusetts 1975

Awards and Honors:

Highest Honors in Biology, Williams College, 1975 and 1977

Sigma XI,1975

Whitehall Foundation Research Fellowship, 1975

Professional Activities:

American Association of Immunologists
Associate Editor, *Journal of Immunology*, 1990-1993
American Association for the Advancement of Science
The New York Academy of Sciences,member.

Experience:

Principal Staff Scientist, Department of Immunology/Department of Discovery Research, DNAX Research Institiute, 2000-present.

Research Fellow, Department of Immunology, DNAX Research Institute for Molecular and Cellular Biology, Inc., 1991-2000.

Senior Research Scientist, Becton Dickinson Immunocytometry Systems, 1986-1991.

Research Scientist, Becton Dickinson Monoclonal Center, Inc., 1985-1986.

Postdoctoral Research Fellow, Becton Dickinson Monoclonal Center, Inc., 1983-1985.

Graduate Student in Immunology, University of Texas, M.D. Anderson Hospital and Tumor Institute. 1977-1983.

Research Interests:

Research in the last five years has clearly indicated that the immune system functions successfully by maintaining a critical balance between states of activation and inhibition. Understanding the molecules and mechanism through which leukocytes are stimulated, as well as inhibited, will delineate the balance points at which therapeutic manipulation can be directed. The well characterized CD28/CTLA4 system of counterbalanced receptors has presented strong evidence that these regulatory circuits are critical for normal immune functions. Likewise, defects in these receptors can cause profound effects on the immune system resulting in autoimmune and neoplastic pathologies.

My research interest for the last 20 years have focused primarily on delineating the cell surface molecules expressed on human leukocytes (particularly NK cells, Mast cells and monocytes) that regulate immune interactions. These regulatory molecules encompass both stimulatory and inhibitory pathways and clearly play important roles in balancing immune responses. Understanding the regulation of these receptors may thus allow us to manipulate the immune response and direct the outcome of immunological reactions.

Publications:

1. Koppenheffer, T.L., J. H. Phillips and G.L. Vankin. 1978. C type virus interactions in the normal developing mouse thymus. Am. J. Anat. 153:165.

2. Phillips, J. H. and T.L. Koppenheffer. 1978. Age related appearance of a unique class of cytoplasmic filaments in murine lymphocytes. Develop. Comparat. Immunol. 2: 741.

3. Savary, C.A, J. H. Phillips and E. Lotzova. 1978. Inhibition of murine natural killer cell-mediated cytotoxicity by pretreatment with ammonium chloride. J. Immunol. Methods 25:189.

4. Nishioka, K., G.F. Babcock, J. H. Phillips and D. Noyes. 1981. Antitumor effects of tuftsin. J. Molec.Cell. Biochem. 41:13.

5.   Phillips, J. H., G.F. Babcock and K. Nishioka. 1981. Tuftsin: A naturally occurring immunopotentiating factor. I. In vitro enhancement of murine natural cell-mediated cytotoxicity. J. Immunol. 126:915.

6.   Babcock, G. F., J.H. Phillips and K. Nishioka. 1982. The immunotherapeutic effects of the peptide tuftsin on the B cell lymphoma, CH-1. In, B and T cell Tumors: Biological and Clinical Aspects. UCLA Symposium on Molecular and Cellular biology. Eds. Ellen Vitetta and C.F. Fox, Academic Press, New York.

7.   Babcock, G. F. and J.H. Phillips. 1982. Human NK cells: Light and electron microscopic characteristics. Survey Immunol. Res. 2:88.

8.   Phillips, J. Hl and G.F. Babcock. 1982. NKP-15: A monoclonal antibody reactive against purified human natural killer cells and granulocytes. Immunol Letters 6: 143.

9.   Phillips, J. H., G.F. Babcock and K. Nishioka. 1983. Tuftsin-induced enhancement of human and murine natural cell-mediated cytotoxicity. In, Antineoplastic, Immunogenic and other effects of Tuftsin: A natural macrophage activator. Ann. New York Acad. Science.

10. Nishioka, K., A.A. Amoscato, G.F. Babcock, R. Banks and J.H. Phillips. 1984. Tuftsin: A imunomodulating peptide horone and its clinical potential as a natural biological response modifier. Cancer Invest. 2:39.

11. Lanier, L.L., A.M. Le. J.H. Phillips, N.L. Warner and G.F. Babcock. 1983. Subpopulations of human natural killer cells defined by expression of the Leu 7 (HNK-1) and Leu 11 (NK-15) antigens. J. Immunol. 131:1789.

12. Lanier, L.L., J.H. Phillips, N.L. Warner and G.F. Babcock. 1984. A human natural killer cell associated antigen defined by monoclonal antibody anti-Leu 11 (NKP-15): Functional and two color flow cytometry analysis. J. Leukocyte Biol. 35:11.

13. Phillips, J.H., A.M. Le and L.L. Lanier. 1984. Natural killer cells activated in a human mixed lymphocyte response culture identified by expression of Leu 11 and class II histocompatibility antigens. J. Exp. Med. 159:993.

14. Chen, Y.X., R. Evans, M.S. Pollack. L.L. Lanier, J.H. Phillips, C. Rousso. N.L. Warner and F.M. Brodsky. 1984. Characterization and expression of the HLA- DC antigens defined by anti-Leu 10 antigen. Human Immunology 10:221.

15. Phillips, J.H., N.L. Warner and L.L. Lanier. 1984. Correlation of biophysical properties and cell surface antigenic profile of Percoll gradient separated natural killer cells. Natural Immunity and Cell Growth Regulation 3:73.

16. Lanier, L.L., J.H. Phillips and N.L. Warner. 1986. Antibodies to human lymphocytes. In: Methods in Haematology, Ed. P. Beverley, Chapter 9.

17. Lanier, L.L., C.J. Benike, J.H. Phillips and E.G. Engleman. 1985. Recombinant interleukin-2 enhanced natural killer cell-mediated cytotoxicity in human lymphocyte subpopulations expressing the Leu 7 and Leu 11 antigens. J. Immunol. 134:794.

18. Lanier, L.L. and J.H. Phillips. 1986. A map of the cell surface antigens expressed on resting and activated human natural killer cells. In: Leukocyte Typing II, Eds. E.L. Reinherz, B.F. Haynes, L.M. Nadler and I.D. Bernstein, Springer-Verlag, New York, p. 157.

19. Phillips, J.H. and L.L. Lanier. 1985. K562 tumor cells preferentially activate Leu 11+ human large granular lymphocytes in a mixed lymphocyte response culture. In: Mechanisms for Cytotoxicity by NK Cells. Eds. R.B. Herberman and D.M. Callewaert, Academic Press, NY, p. 563.

20. Phillips, J.H. and L.L. Lanier. 1985. A model for the differentiation of human natural killer cells: Studies on the in vitro activation of Leu 11$^+$ granular lymphocytes with a NK-sensitive tumor cell, K562. J. Exp. Med. 161:1464.

21. Phillips, J.H. and L.L. Lanier. 1986. Lectin-dependent and anti-CD3 induced cytotoxicity are preferentially mediated by peripheral blood cytotoxic T lymphocytes expressing Leu 7 antigen. J. Immunol. 136:1579.

22. Lanier, L.L., T.J. Kipps and J.H. Phillips. 1985. Functional properties of a unique subset of cytotoxic CD3$^+$ T lymphocytes that express Fc receptors for IgG (CD16/Leu 11 antigen). J. Exp. Med. 162:2089.

23. Lanier, L.L., S. Cwirla, N. Federspiel and J.H. Phillips. 1986. Human natural killer cells isolated from peripheral blood do not rearrange the T cell antigen receptor □-chain genes. J. Exp. Med. 163:209.

24. Lanier, L.L. and J.H. Phillips. 1986. Evidence for three types of human cytotoxic lymphocyte. Immunology Today 7:132.

25. Lanier, L.L., and J.H. Phillips. 1986. A schema for the classification of human cytotoxic lymphocytes based on T-cell antigen receptor gene rearrangement and Fc receptor (CD16) or Leu 19/NKH-1 antigen expression. In: Proceedings of the International Symposium on Natural Immunity, Eds. R.B. Herberman, et al., Krager, New York.

26. Lanier, L.L., A.M. Le, C.I. Civin, M.R. Loken and J.H. Phillips. 1986. The relationship of CD16 (Leu 11) and Leu 19 (NKH-1) antigen expression on human peripheral blood NK cells and cytotoxic T lymphocytes. J. Immunol. 136:4480.

27. Lanier, L.L., J.J. Ruitenberg and J.H. Phillips. 1986. Human CD3$^+$ T lymphocytes that express neither CD4 nor CD8 antigens. J. Exp. Med. 164:339.

28.   Freimark. B., L. Lanier, J. Phillips, T. Quertermous and R. Fox. 1987. Comparison of T-cell receptor gene rearrangements in patients with large granular T-cell leukemia and Felty's syndrome. J. Immunol. 138:1724.

29.   Lanier, L.L., J.P. Allison and J.H. Phillips. 1986. Correlation of cell surface antigen expression on human thymocytes by multi-color flow cytometric analysis: Implications for differentiation. J. Immunol. 137:2501.

30.   Phillips, J.H. and L.L. Lanier. 1986. Dissection of the lymphokine activated killer phenomenon: Relative contribution of natural killer cells and T lymphocytes to cytolysis. J. Exp. Med. 164:814.

31.   Lanier, L.L., A.M. Le, S. Cwirla, N. Federspiel and J.H. Phillips. 1986. Antigenic, functional and molecular genetic studies on human natural killer cells and non-MHC restricted cytotoxic T lymphocytes. Fed. Proc. 45:2823.

32.   Lanier, L.L., S. Cwirla and J.H. Phillips. 1986. Genomic organization of T-cell receptor gamma genes in human peripheral blood natural killer cells. J. Immunol. 137:3375.

33.   Lanier, L.L., J.H. Phillips, J. Hackett, Jr., M. Tutt and V. Kumar. 1986. Natural killer cells: Definition of a cell type rather than a function. J. Immunol. 137:2735.

34.   Lanier, L.L. and J.H. Phillips. 1986. Human thymic and peripheral blood non- MHC restricted cytotoxic lymphocytes. Med. Oncol. & Tumor Pharmacother. 3:247.

35.   Lanier, L.L., A.T. Serafini, J.J. Ruitenberg, S. Cwirla, N.A. Federspiel, J.H. Phillips, J.P. Allison and A. Weiss. 1987. The gamma T cell antigen receptor. J. Clin. Immunol. 7:429.

36.   Lanier, L.L., A.M. Le, A.H. Ding, E.L. Evans, A.M. Krensky, C. Clayberger and J.H. Phillips. 1987. Expression of Leu 19 (NKH-1) antigen on IL-2 dependent cytotoxic and non-cytotoxic T cell lines. J. Immunol. 138:2019.

37.   Phillips, J.H., B.T. Gemlo, W.W. Myers, A.A. Rayner and L.L. Lanier. 1988. The contribution of NK and T-cells to the lymphokine activated killer cell phenomenon. In: Cytolytic lymphocyte clones and complement as effectors of the immune system, Vol. II, Ed. E.R. Podack, CRC Press, Boca Raton, FL, pp. 193.

38.   Lanier, L.L., N.A. Federspiel, J.J. Ruitenberg, J.H. Phillips, J.P. Allison, D. Littman and A. Weiss. 1987. The T cell antigen receptor complex expressed on normal peripheral blood CD4-,CD8- T lymphocytes: A CD3-associated disulfide- linked □-chain heterodimer. J. Exp. Med. 165:1076.

39.   Phillips, J.H. and L.L. Lanier. 1987. Acquisition of non-MHC restricted cytotoxic function by IL-2 activated thymocytes with an "immature" antigenic phenotype. J. Immunol. 139:683.

40. Phillips. J.H., B.T. Gemlo, W.W. Myers, A.A. Rayner and L.L. Lanier. 1987. In vivo and in vitro activation of natural killer cells in advanced cancer patients undergoing combined interleukin-2 and LAK cell therapy. J. Clin. Oncol. 5:1933.

41. Herberman, R.B., J. Hiserodt, N. Vujanovic, C. Balch, E. Lotzova. R. Bolhuis, S. Golub, L.L. Lanier, J.H. Phillips, C. Riccardi, J. Ritz, A. Santoni, R.E. Schmidt and A. Uchida. 1987. Lymphokine-activated killer cell activity: Characteristics of effector cells and their progenitors in blood and spleen. Immunology Today 8:178.

42. Phillips, J.H., A. Weiss, B.T. Gemlo, A.A. Rayner and L.L. Lanier. 1987. Evidence that the T cell antigen receptor may not be involved in cytotoxicity mediated by □□ and □□ thymic cell lines. J. Exp. Med. 166:1579.

43. Lanier, L.L. and J.H. Phillips. 1988. What are natural killer cells? ISI Atlas of Science: Immunology. Philadelphia, PA, vol. 1, pp. 15.

44. Nagler, A., P. Greenberg, L.L. Lanier and J.H. Phillips. 1988. The effect of rIL-2 activated NK cells on autologous peripheral blood hematopoietic progenitors. J. Exp. Med. 168:47.

45. Lanier, L.L., D.W. Buck, L. Rhodes, A. Ding, E. Evans, C. Barney and J.H. Phillips. 1988. Interleukin-2 activation of NK cells rapidly induces the expression and phosphorylation of the Leu 23 activation antigen. J. Exp. Med. 167:1572.

46. Nagler, A., L.L. Lanier and J.H. Phillips. 1988. The effects of interleukin-4 on human natural killer cells: A potent regulator of interleukin-2 activation and proliferation. J. Immunol. 141:2349.

47. Skettino, S., J.H. Phillips, L.L. Lanier, A. Nagler and P.L. Greenberg. 1988. Selective generation of erythroid burst promoting activity by recombinant interleukin- 2 stimulated T lymphocytes and natural killer cells. Blood 71:907.

48. Lanier, L.L., J.J. Ruitenberg and J.H. Phillips. 1988. Functional and biochemical analysis of CD16 antigen on NK cells and granulocytes. J. Immunol. 141:3478.

49. Testi, R., J.H. Phillips and L.L. Lanier. 1988. Constitutive expression of a phosphorylated activation antigen (Leu 23) by CD3bright human thymocytes. J. Immunol. 741:2557.

50. Lanier, L.L. and J.H. Phillips. 1988. Effectors, repertoire and receptors involved in lymphocyte-mediated MHC-unrestricted cytotoxicity. Annules d'Immunologie 139:450.

51. Loh, E.Y., S. Cwirla, A.T. Serafini, J.H. Phillips. and L.L. Lanier. 1988. The human T-cell receptor delta chain: Genomic organization, diversity and expression in populations of T-cells. Proc. Natl. Acad. Sci. USA 85:9714.

52.   Lanier, L.L., J.J. Ruitenberg, R.L.H. Bolhuis, J. Borst, J.H. Phillips and R. Testi. 1988. Structural and serological heterogeneity of □□ T cell antigen receptor expression in thymus and peripheral blood. Eur. J. Immunol. 18:1985.

53.   Testi, R., J.H. Phillips and L.L. Lanier. 1989. Leu 23 induction as an early marker of functional CD3/T cell antigen receptor triggering: Requirement for receptor crosslinking, prolonged elevation of intracellular [Ca^{++}] and activation of protein kinase C. J. Immunol. 142:1854.

54.   Lanier, LL., Phillips and R. Testi. 1989. Membrane-anchoring and spontaneous release of CD16 (FcR III) by natural killer cells and granulocytes. Eur. J. Immunol. 19:775.

55.   Lanier, L.L., R. Testi, J. Bindl and J.H. Phillips. 1989. Identity of Leu 19 (CD56) leukocyte differentiation antigen and neural cell adhesion molecule (N-CAM). J. Exp. Med. 169:2233.

56.   Lanier, L.L. and J.H. Phillips. 1990. NK Cells: Membranes structures triggering cell-mediated cytotoxicity. In: Leucocyte Typing IV, Eds. W. Knapp et al., Oxford University Press, UK, p. 1064.

57.   Testi, R., J.H. Phillips and L.L. Lanier. 1989. T cell activation via Leu 23 (CD69). J. Immunol. 143:1123.

58.   Phillips, J.H., T. Takeshita, K. Sugamura and L.L. Lanier. 1989. Activation of NK cells via the p75 interleukin 2 receptor. J. Exp. Med. 170:291.

59.   Nagler, A., L.L. Lanier, S. Cwirla and J.H. Phillips. 1989. Comparative studies of FcRIII positive and negative NK cells. J. Immunol. 143:3183.

60.   Lanier, L.L., S. Cwirla, G. Yu, R. Testi and J.H. Phillips. 1989. A single amino acid determines membrane anchoring of a human Fc receptor for IgG (CD16). Science 246:1611.

61.   Lanier, L.L., G. Yu and J.H. Phillips. 1989. Co-association of CD3□ with an IgG Fc receptor (CD16) on human natural killer cells. Nature 342:803.

62.   Nagler, A., L.L. Lanier and J.H. Phillips. 1990. Constitutive expression of high affinity interleukin-2 receptors on human CD16negative NK cells in vivo. J. Exp. Med. 171:1527.

63.   Lanier, L.L., G. Yu and J.H. Phillips. 1991. Analysis of Fc□RIII (CD16) membrane expression and association with CD3□ and Fc□RI-□ by site-directed mutation. J. Immunol. 146:1571.

64.   Phillips, J.H., C. Chang and L.L. Lanier. 1991. Platelet-induced expression of Fc□RIII (CD16) on human monocytes. Eur. J. Immunol. 21:895.

65.   Lanier, L.L., C. Chang, M. Azuma, J. Ruitenberg, J. Hemperly and J.H. Phillips. 1991. Molecular and functional analysis of human NK cell-associated neural cell adhesion molecule (N-CAM/CD56). J. Immunol. 146:4421.

66.   Phillips, J.H., A. Nagler, H. Spits and L.L. Lanier. 1992. Immunomodulating effects of IL-4 on human natural killer cells. In: Interleukin-4: Structure and Function, Ed. H. Spits, CRC Press, Boca Raton, FL, Chapter 11.

67.   Azuma, M., M. Cayabyab, D. Buck, J.H. Phillips and L.L. Lanier. 1992. CD28 interaction with B7 co-stimulates primary allogeneic proliferative responses and cytotoxicity mediated by small, resting T lymphocytes, J. Exp. Med. 175:353.

68.   Harrison, D.H., J.H. Phillips and L.L. Lanier. 1991. Involvement of a metalloprotease in spontaneous and phorbol ester-induced release of NK cell-associated Fc□RIII (CD16-II), J. Immunol. 147:3459.

69.   Phillips, J.H., L. McKinney, M. Azuma, H. Spits and L.L. Lanier. 1991. A novel □4,□6 integrin-associated epithelial cell antigen involved in NK cell and antigen-specific CTL cytotoxicity. J. Exp. Med. 174:1527.

70.   Lanier, L.L. and J.H. Phillips. 1992. Natural killer cells.   Current Opinions in Immunology. 4:38.

71.   Phillips, J.H., T. Hori, A. Nagler, N. Bhat, H. Spits and L.L. Lanier, 1992. Ontogeny of human natural killer cells: Fetal NK cells mediate cytolytic function and express cytoplasmic CD3□□ proteins. J. Exp. Med. 175:1055.

72.   Lanier, L.L., C. Chang, H. Spits and J.H. Phillips. 1992. Expression of cytoplasmic CD3□ proteins in activated human adult NK cells and CD3□□□ complexes in fetal NK cells: Implications for the relationship of NK and T lymphocytes. J. Immunol. 149:1876.

73.   Lanier, L.L. and J.H. Phillips. 1993. Triggering structures on NK cells. In: Cytotoxic Cells: Recognition, Effector Function, Generation and Methods, ed., M. Sitkovsky and P. Henkart, Birkhauser Press, Boston, MA, pp. 84-95.

74.   Azuma, M., M. Cayabyab, D. Buck, J.H. Phillips and L.L. Lanier. 1992. Involvement of CD28 in major histocompatibility complex-unrestricted cytotoxicity mediated by a human NK leukemia cell line. J. Immunol. 149:1115.

75.   Hori, T., J.H. Phillips, B. Duncan, L.L. Lanier and H. Spits. 1992. Human fetal liver-derived CD7+CD2lowCD3-CD56- clones that express CD3□□ and □ and proliferate in response to IL-2, IL-3, IL-4, or IL-7: Implications for the relationship to T and NK cells. Blood 80:1270.

76.   Lanier, L.L., H. Spits and J.H. Phillips. 1992. The developmental relationship between NK cells and T cells. Immunology Today 13:392.

77. Azuma, M., J.H. Phillips and L.L. Lanier. 1992. CD28 co-stimulation of T cell-mediated cytotoxicity. Int. J. Cancer, Supplement 7, pp. 33.

78. Azuma, M., M. Cayabyab, J.H. Phillips and L.L. Lanier. 1993. Requirements for CD28-dependent T cell-mediated cytotoxicity. J. Immunol. 150:2091.

79. Azuma, M., J.H. Phillips and L.L. Lanier. 1993. CD28⁻ T lymphocytes: Antigenic and functional properties. J. Immunol. 150:1147.

80. Azuma, M., H. Yssel, J.H. Phillips, H. Spits and L.L. Lanier. 1993. Functional expression of B7 on activated T lymphocytes. J. Exp. Med. 177:845.

81. M. Cayabyab, J.H. Phillips and L.L. Lanier. 1994. CD40 preferentially costimulates activation of CD4⁺ T lymphocytes. J. Immunol. 152:1523.

82. Litwin, V., J. Gumperz, P. Parham, J.H. Phillips and L.L. Lanier. 1993. Specificity of HLA class I antigen recognition by human NK clones: Evidence for clonal heterogeneity, protection by self and non-self alleles and influence of the target cell type. J. Exp. Med. 178:1321.

83. Sanchez, M.J., H. Spits, L.L. Lanier and J.H. Phillips. 1993. Human NK cell committed thymocytes and their relationship to the T cell lineage. J. Exp. Med. 178:1857.

84. Sanchez, M.J., M. Muench, M.-G. Roncarolo, L.L. Lanier and J.H. Phillips. 1994. Identification of a common T/NK cell progenitor in human fetal thymus. J. Exp. Med. 180:569.

85. Azuma, M., D. Ito, H. Yagita, K. Okumura, J.H. Phillips, L.L. Lanier and C. Somoza. 1993. B70 antigen is a second ligand for CTLA-4 and CD28. Nature 366:76.

86. Litwin, V., J. Gumperz, P. Parham, J.H. Phillips and L.L. Lanier. 1994. NKB1: An NK cell receptor involved in the recognition of polymorphic HLA-B molecules. J. Exp. Med. 180:537.

87. Lanier, L.L., C. Chang and J.H. Phillips. 1994. Human NKR-P1A: A disulfide-linked homodimer of the C-type lectin superfamily expressed by a subset of NK and T lymphocytes. J. Immunol. 153:2417.

88. Lanier, L.L., S. O'Fallon, C. Somoza, J. H. Phillips, P. S. Linsley, K. Okumura, D. Ito and M. Azuma 1995. CD80 (B7) and CD86 (B70) provide similar costimulatory signals for T cell proliferation, cytokine production and generation of cytotoxic T lymphocytes. J. Immunol. 154:97.

89. Gumperz, J.E., V. Litwin, J.H. Phillips, L.L. Lanier and P. Parham. 1995. The Bw4 public epitope of HLA-B molecules confers reactivity with NK cell clones that express NKB1, a putative HLA receptor. J. Exp. Med. 181:1133.

90. Lanier, L.L. and J.H. Phillips. 1995. NK cell recognition of major histocompatibility complex class I molecules. Seminars in Immunology 7:75.

91. Phillips, J.H., J. Gumperz, P. Parham and L.L. Lanier. 1995. Superantigen-dependent, cell-mediated cytotoxicity inhibited by MHC class I receptors on T lymphocytes. Science 268:403.

92. Lanier, L.L, J. Gumperz, P. Parham, I. Melero, M. López-Botet and J.H. Phillips. 1995. The NKB1 and HP-3E4 NK cell receptors are structurally distinct glycoproteins and independently recognize polymorphic HLA-B and HLA-C molecules. J. Immunol. 154:3320.

93. Warren, H.S., B.F. Kinnear, J.H. Phillips and L.L. Lanier. 1995. Production of IL-5 by human NK cells and regulation of IL-5 secretion by IL-4, IL-10 and IL-12. J. Immunol. 154:5144.

94. Spits, H., L.L. Lanier and J.H. Phillips. 1995. Development of human T and NK cells. Blood 85:2654.

95. Chang, C., A. Rodríguez, M. Carretero, M. López-Botet, J. H. Phillips and L.L.. Lanier. 1995. Molecular characterization of human CD94: A type II membrane glycoprotein related to the C-type lectin superfamily. Eur. J. Immunol. 25:2433.

96. Lanier, L.L. and J.H. Phillips. 1996. Inhibitory MHC class I receptors on NK cells and T cells. Immunology Today 17:86.

97. Barber, L.D., T.P. Patel, L. Percival, J.E. Gumperz, L.L. Lanier, J.H. Phillips, J.C. Bigge, M.R. Wormald, R.B. Parekh and P. Parham. 1996. Unusual uniformity of the N-linked oligosaccharides associated with class I HLA-A, -B and -C glycoproteins expressed by EBV-transformed B cells. J. Immunol. 156:3275.

98. D'Andrea, A., C. Chang, K. Bacon, J.H. Phillips and L.L. Lanier. 1995. Molecular cloning of NKB1: A natural killer cell receptor for HLA-B allotypes. J. Immunol. 155:2306.

99. Baker, E., A. D'Andrea, J.H. Phillips, G.R. Sutherland and L.L. Lanier. 1995. Natural killer cell receptor for HLA-B allotypes, NKB1: Map position 19q13.4. Chromosome Research 3:511.

100. Barber, L.D., L. Percival, N. Valiante, L. Chen, C. Lee, J.E. Gumperz, J.H. Phillips, L.L. Lanier, J.C. Bigge, R.B. Parekh and P. Parham. 1996. The inter-locus recombinant HLA-B*4601 has high selectivity in peptide binding and functions characteristic of HLA-C. J. Exp. Med. 184:735.

101. Onishi, M., S. Kinoshita, Y. Morikawa, A. Shibuya, J. Phillips, L.L. Lanier, D.M. Gorman, G.P. Nolan, A. Miyajima and T. Kitamura. 1996. Applications of retrovirus-mediated expression cloning. Exp. Hematol. 24:324.

102. Shibuya, A., D. Campbell, C. Hannum, H. Yssel, K. Franz-Bacon, T. McClanahan, T. Kitamura, J. Nicholl, G.R. Sutherland, L.L. Lanier and J.H. Phillips. 1996. DNAM-1, a novel adhesion molecule involved in the cytolytic function of T lymphocytes. Immunity 4:573.

103. D'Andrea, A., C. Chang, J.H. Phillips and L.L. Lanier. 1996. Regulation of T cell lymphokine production by killer cell inhibitory receptor recognition of self HLA class I alleles. J. Exp. Med. 184:789.

104. Phillips, J.H., C. Chang, J. Mattson, J. Gumperz, P. Parham and L.L. Lanier. 1996. CD94 and a novel associated protein (94AP) form a NK cell receptor involved in the recognition of HLA-A, -B and -C allotypes. Immunity 5:163.

105. Gumperz, J.E., L.D. Barber, N.M. Valiante, L. Percival, J.H. Phillips, L.L. Lanier and P. Parham. 1997. Conserved and variable residues within the Bw4 motif of HLA-B make separable contributions to recognition by the NKB1 killer cell inhibitory receptor. J. Immunol. 158:5237.

106. Lanier, L.L. B. Corliss and J.H. Phillips. 1997. Arousal and inhibition of human NK cells. Immunological Reviews 155: 145.

107. Houchins, J.P., L.L. Lanier, E. Niemi, J.H. Phillips and J. Ryan. 1997. Natural killer cell cytolytic activity is inhibited by NKG2A and activated by NKG2C. J. Immunol. 158:3603.

108. Valiante, N.M., J.H. Phillips, L.L. Lanier and P. Parham. 1996. Killer cell inhibitory receptor recognition of human leukocyte antigen (HLA) class I blocks formation of a pp36/PLC-□ signaling complex in human natural killer (NK) cells. J. Exp. Med. 184:2243.

109. Lazetic, S., C. Chang, J.P. Houchins, L.L. Lanier and J.H. Phillips. 1996. Human NK cell receptors involved in MHC class I recognition are disulfide-linked heterodimers of CD94 and NKG2 subunits. J. Immunol. 157:4741.

110. Soderstrom, K., B. Corliss, L.L. Lanier and J.H. Phillips. 1997. CD94/NKG2 is the predominant inhibitory receptor involved in recognition of HLA-G by decidual and peripheral blood NK cells. J. Immunol. 159:1072.

111. Jaleco, A.C., B. Blom, P. Res, K. Weijer, L.L. Lanier, J.H. Phillips and H. Spits. 1997. The fetal liver contains committed NK progenitors but is not a site for T cell development. J. Immunol. 159:694.

112. Meyaard, L., G.J. Adema, C. Chang, E. Woollatt, G.R. Sutherland, L.L. Lanier and J.H. Phillips. 1997. LAIR-1, a novel inhibitory receptor expressed on human mononuclear leukocytes. Immunity 7:283.

113. Bakker, L., J.H. Phillips, C.G. Figdor and L.L. Lanier. 1998. Killer cell inhibitory receptors (KIR) for MHC class I molecules regulate lysis of melanoma cells mediated by NK cells, □□ T cells, and antigen-specific CTL. J. Immunol. 160:5239.

114. Valiante, N.M., M. Uhrberg, H.G. Shilling, K. Lienert-Weidenbach, K.L. Arnett, A. D'Andrea, J.H. Phillips, L.L. Lanier and P. Parham. 1997. Functionally and structurally distinct NK cell receptor repertoires in the peripheral blood of two human donors. Immunity 7:739.

115. Lanier, L.L., B.C. Corliss, J. Wu, C. Leong and J.H. Phillips. 1998. Immunoreceptor DAP12 bearing a tyrosine-based activation motif is involved in activating NK cells. Nature 391:703.

116. Braud, V.M., D.S.J. Allan, C.A. O'Callaghan, K. Soderstrom, A. D'Andrea, G.S. Ogg, S. Lazetic, N.T. Young, J.I. Bell, J.H. Phillips, L.L. Lanier and A.J. McMichael. 1998. HLA-E binds to natural killer cell receptors CD94/NKG2A, B and C. Nature 391:795.

117. Leong, C.C., T. Chapman, P. Bjorkman, D. Formankova, E. Mocarski, J.H. Phillips and L.L. Lanier. 1998. Modulation of natural killer cell cytotoxicity in human cytomegalovirus infection: the role of endogenous class I MHC and a viral class I homolog. J. Exp. Med. 187:1681.

118. Tangye, S.G., J.H. Phillips, L.L. Lanier, J.E. deVries and G. Aversa. 1998. CD148, a receptor-type protein tyrosine phosphatase involved in the regulation of human T cell activation. J. Immunol. 161:3249.

119. Smith, K.M., J. Wu, A.B.H. Bakker, J.H. Phillips, and L.L. Lanier. 1998. Ly49D and Ly49H associate with mouse DAP12 and form activating receptors. J. Immunol. 161:7.

120. Lanier, L.L., B.C. Corliss, J. Wu, and J.H. Phillips. 1998. Association of DAP12 with activating CD94/NKG2C NK cell receptors. Immunity 8:693.

121. Tangye, S.G., J. Wu, G. Aversa, J.E. deVries, L.L. Lanier, and J.H. Phillips. 1998. Negative regulation of human T cell activation by the receptor-type protein phosphatase CD148. J. Immunol. 161:3803.

122. Shibuya, A., L.L. Lanier, and J.H. Phillips. 1998. Protein kinase C is involved in the regulation of both signaling and adhesion mediated by DNAX accessory molecule-1 receptor. J. Immunol. 161:1671.

123. Meyaard, L., J. Hurenkamp, H. Clevers, L.L. Lanier, and J.H. Phillips. 1999. Leukocyte-associated Ig-like receptor-1 functions as an inhibitory receptor on cytolytic T cells. J. Immunol. 162:5800.

124. Shibuya, K., L.L. Lanier, J.H. Phillips, H.D. Ochs, K. Shimizu, E. Nakayama, H. Nakauchi, and A. Shibuya. 1999. Physical and functional association of LFA-1 with DNAM-1 adhesion molecule. Immunity 11:615.

125. Tangye, S.G., S. Lazetic, E. Woollatt, G.R. Sutherland, L.L. Lanier, and J.H. Phillips. 1999. Human 2B4, an activating NK cell receptor, recruits the protein tyrosine phosphatase SHP-2 and the adaptor signaling protein SAP. J. Immunol. 162:6981.

126. Bakker, A.B.H., E. Baker, G.R. Sutherland, J.H. Phillips, and L.L. Lanier. 1999. Myeloid DAP12-associating lectin (MDL)-1 is a cell surface receptor involved in activation of myeloid cells. Proc. Natl. Acad. Sci. USA 96:9792.

127. Bauer, S., V. Groh, J. Wu, J.H. Phillips, L.L. Lanier, and T. Spies. 1999. Activation of natural killer cells and T cells by NKG2D, a receptor for stress-inducible MICA. Science 285:727.

128. Wu, J., Y. Song, A.B.H. Bakker, S. Bauer, T. Spies, L.L. Lanier, and J.H. Phillips. 1999. An activating immunoreceptor complex formed by NKG2D and DAP10. Science 285:730.

129. Bakker, A.B.H., J. Wu, L.L. Lanier and J.H. Phillips. 2000. NK cell activation: distinct stimulatory pathways counterbalancing inhibitory signals. Human Immunology 61:18.

130. Tangye, S., J.H. Phillips, and L.L. Lanier. 2000. The CD2-aubset of the Ig superfamily of dell surface molecules: Receptor-ligand pairs expressed by NK Cells and other immune cells. Seminars in Immunology, In press.

131. Arase H, Saito T, Phillips JH, Lanier LL. Cutting edge: the mouse NK cell-associated antigen recognized by DX5 monoclonalantibody is CD49b (alpha 2 integrin, very late antigen-2).J Immunol. 2001 Aug 1;167(3):1141-4.

132. Meyaard L, van der Vuurst de Vries AR, de Ruiter T, Lanier LL, Phillips JH,Clevers H. The epithelial cellular adhesion molecule (Ep-CAM) is a ligand for theleukocyte-associated immunoglobulin-like receptor (LAIR).J Exp Med. 2001 Jul 2;194(1):107-12.

133. Shibuya A, Sakamoto N, Shimizu Y, Shibuya K, Osawa M, Hiroyama T, Eyre HJ,Sutherland GR, Endo Y, Fujita T, Miyabayashi T, Sakano S, Tsuji T, Nakayama E,Phillips JH, Lanier LL, Nakauchi H. Fc alpha/mu receptor mediates endocytosis of IgM-coated microbes.Nat Immunol. 2000 Nov;1(5):441-6.

134. Young NT, Uhrberg M, Phillips JH, Lanier LL, Parham P. Differential expression of leukocyte receptor complex-encoded Ig-like receptors correlates with the transition from effector to memory CTL.J Immunol. 2001 Mar 15;166(6):3933-41.

135. Uhrberg M, Valiante NM, Young NT, Lanier LL, Phillips JH, Parham P. The repertoire of killer cell Ig-like receptor and CD94:NKG2A receptors in Tcells: clones sharing identical alpha beta TCR rearrangement express highly diverse killer cell Ig-like receptor patterns.J Immunol. 2001 Mar 15;166(6):3923-32.

136. Westfaard, IH, Dissen, E. Torgersen, KM, Lazetic, S, Lanier,LL, and Phillips, JH.. 2003. The lectin-like receptor KLRE1 inhibits natural killer cell cytotoxicity. J. Exp. Med. 197:1551-61

137. Wright, GJ, Cherwinski, H. Foster-Cuevas, M., Brooke, G., Puklavec, MJ, Bigler, M., Song, Y., Jenmalm, M., Gorman, D., McClanahan, T., Liu, MR., Brown, MH., Sedgwick, JD., Phillips, JH, Barclay, N. 2003. Characterization of the CD200 receptor family in mice and humans and their interactions with CD200. J. Immunol. 171:3034-46.

138. Pflanz, S, Hibbert, L, Mattson, J, Rosales, R, Vaisberg, E, Baszan, JF, Phillips, JH, McClanahan, TK, de Waal Malefyt, R, and Kastelein, RA. 2004. WSX-1 and glycoprotein 130 constitute a signal-transducing receptor for IL-27. J. Immunol. 172:2225-31.

139. Zhang S, Cherwinski, H, Sedgwick, JD, and Phillips, JHl 2004. Molecular mechanisms of CD200 Inhibition of mast cell activation. J. Immunol. 173:6786-93.

140. Cherwinski, HM, Murphy, CA, Joyce, BL, Bigler, ME, Song YS, Zurawski, SM, Moshrefe MM, Gorman, DM, Miller, KL, Zhang, S, Sedgwick, JD, and Phillips, JH. 2005. The CD200 receptor is a novel and potent regulator of murine and human mast cell function. J. Immunol. 174:1348-56.

FDF03, a Novel Inhibitory Receptor of the Immunoglobulin Superfamily, Is Expressed by Human Dendritic and Myeloid Cells[1]

Nathalie Fournier,* Lionel Chalus,* Isabelle Durand,* Eric Garcia,* Jean-Jacques Pin,* Tatyana Churakova,[†] Segal Patel,[†] Constance Zlot,[†] Dan Gorman,[†] Sandra Zurawski,[†] John Abrams,[†] Elizabeth E. M. Bates,* and Pierre Garrone[2]*

In this study, we describe human FDF03, a novel member of the Ig superfamily expressed as a monomeric 44-kDa transmembrane glycoprotein and containing a single extracellular V-set Ig-like domain. Two potential secreted isoforms were also identified. The gene encoding FDF03 mapped to chromosome 7q22. FDF03 was mostly detected in hemopoietic tissues and was expressed by monocytes, macrophages, and granulocytes, but not by lymphocytes (B, T, and NK cells), indicating an expression restricted to cells of the myelomonocytic lineage. FDF03 was also strongly expressed by monocyte-derived dendritic cells (DC) and preferentially by CD14$^+$/CD1a$^-$ DC derived from CD34$^+$ progenitors. Moreover, flow cytometric analysis showed FDF03 expression by CD11c$^+$ blood and tonsil DC, but not by CD11c$^-$ DC precursors. The FDF03 cytoplasmic tail contained two immunoreceptor tyrosine-based inhibitory motif (ITIM)-like sequences. When overexpressed in pervanadate-treated U937 cells, FDF03 was tyrosine-phosphorylated and recruited Src homology-2 (SH2) domain-containing protein tyrosine phosphatase (SHP)-2 and to a lesser extent SHP-1. Like engagement of the ITIM-bearing receptor LAIR-1/p40, cross-linking of FDF03 inhibited calcium mobilization in response to CD32/FcγRII aggregation in transfected U937 cells, thus demonstrating that FDF03 can function as an inhibitory receptor. However, in contrast to LAIR-1/p40, cross-linking of FDF03 did not inhibit GM-CSF-induced monocyte differentiation into DC. Thus, FDF03 is a novel ITIM-bearing receptor selectively expressed by cells of myeloid origin, including DC, that may regulate functions other than that of the broadly distributed LAIR-1/p40 molecule. *The Journal of Immunology,* 2000, 165: 1197–1209.

I nhibitory receptors containing one or several cytoplasmic immunoreceptor tyrosine-based inhibitory motifs (ITIM)[3] are members of the C-type lectin family or Ig superfamily (Ig-SF). The ITIM is generally defined by the consensus sequence L/V/IxYxxL/V that, following phosphorylation on tyrosine, recruits Src homology-2 (SH2) domain-containing protein tyrosine phosphatases SHP-1 and/or SHP-2, as well as the SH2 domain-bearing inositol phosphatase (SHIP) in the case of FcγRIIB (1–5). ITIM-bearing receptors negatively regulate cellular functions when coaggregated with stimulatory receptors that signal through an immunoreceptor tyrosine-based activation motif (ITAM). The growing number of novel ITIM-bearing receptors identified thus far and their expression by virtually all leukocyte populations suggest that inhibitory receptors may regulate various aspects of immune responses (6, 7), as well as the fate of nonhemopoietic cells, as described for the SHPS-1/SIRPα molecules (8, 9).

Among APCs, dendritic cells (DC) are unique leukocyte populations using their role as sentinels to capture Ag at the periphery of an organism and by their capacity to present processed Ag to both CD4$^+$ and CD8$^+$ naive T cells, thus initiating primary immune responses (for review, see Refs. 10 and 11). In our effort to identify receptors involved in Ag capture and presentation by human DC, we previously described an ITIM-containing C-type lectin, designated DCIR, that displayed features intermediate between NK cell receptors and typical type II lectins involved in ligand internalization (12). While the function of DCIR is not yet determined, its restricted expression on APCs, and particularly on DC, has lead to questions on the potential role(s) of inhibitory receptors in DC function. Different groups have previously reported the presence on APCs of the ITIM-bearing molecules ILT3/LIR-5, ILT2/LIR-1, and ILT4/LIR-2 belonging to the ILT/LIR/MIR family (13–16). It has been shown that these Ig-SF members can function as negative regulators of monocyte and DC activation, most probably through recruitment of SHP-1 (15, 17–20). Both ILT2/LIR-1 and ILT4/LIR-2, but not ILT3/LIR-5, bind to HLA class I molecules (14, 17, 19). While the physiological role of inhibitory receptors for HLA class I on monocytes and DC is not yet understood, the demonstration that ILT2/LIR-1 is also a receptor for the UL18 molecule, an homologue of human MHC class I encoded by CMV (19, 21), suggests that pathogens may use inhibitory receptors of APCs to down-regulate immune responses. In addition to its inhibitory activity, ILT3/LIR-5 is also internalized following cross-linking on monocytes and may be involved in Ag capture and loading for presentation into MHC class II (15). As reported

for the FcγRIIB (22, 23), internalization of ILT3/LIR-5 might be mediated through its cytoplasmic ITIMs, because the ITIM sequence contains the tyrosine-based internalization motif Yxxφ, where φ represents any hydrophobic residue (24). Finally, the recent demonstration that the broadly expressed inhibitory receptor LAIR-1/p40 (25) can inhibit the differentiation of monocytes into DC in response to GM-CSF (26) suggests that ITIM-bearing receptors may also play an important regulatory role during the early commitment of DC precursors by interfering with signaling mediated through growth factor receptors.

In the present study, we report the cloning and characterization of FDF03, a novel member of the Ig-SF that has a restricted expression in myelomonocytic cells including in vitro-derived DC and in vivo CD11c-positive DC. The FDF03 cytoplasmic tail contains two ITIM-like sequences and preferentially associates with SHP-2 in pervanadate-activated monocytic U937 cells. Moreover, we show that coaggregation of FDF03 with CD32/FcγRII inhibits intracellular Ca^{2+} mobilization in U937 cells, as does LAIR-1/p40, thus indicating that FDF03 possesses an inhibitory activity. However, in contrast to LAIR-1/p40, FDF03 failed to inhibit monocyte differentiation into DC in response to GM-CSF, suggesting that FDF03 may be involved in the regulation of different pathways or may use different inhibitory signals to that of LAIR-1/p40.

Materials and Methods

Hemopoietic factors, cytokines, and reagents

All cultures were performed in RPMI 1640 medium supplemented with 10% heat-inactivated FCS, 2 mM L-glutamine (all from Life Technologies, Gaithersburg, MD), and 160 μg/ml gentamicin (Schering-Plough, Levallois-Perret, France). The source and sp. act. of recombinant human cytokines used in this study have been previously described (12). The following factors were used at optimal concentration: GM-CSF (100 ng/ml), TNF-α (2.5 ng/ml), stem cell factor (SCF), and M-CSF (25 ng/ml), G-CSF (25 ng/ml), and IL-4 (50 U/ml). In some experiments, cells were activated with 1 ng/ml PMA (Sigma, St. Louis, MO) and 1 μg/ml ionomycin (Calbiochem, La Jolla, CA) or with 25 ng/ml LPS (Sigma).

Cell preparations

Umbilical cord blood samples, peripheral blood samples, and tonsils were obtained according to institutional guidelines. PBMC were purified from human peripheral blood by Ficoll-Hypaque centrifugation. Monocytes were purified from PBMC by centrifugation over a 50% Percoll gradient followed by immunomagnetic depletion of contaminating T, B, and NK cells as described elsewhere (12). The isolated cells were >95% $CD14^+$ as judged by staining with anti-CD14 mAb and flow cytometric analysis. Granulocytes were purified from whole blood, T lymphocytes (>95% $CD3^+$) were purified from PBMC by immunomagnetic depletion, and B cells (>98% $CD19^+$) were isolated from tonsils essentially as previously described (12, 27). $CD34^+$ hemopoietic progenitors were purified from umbilical cord blood as previously described (28). In all experiments, the isolated cells were 80–95% $CD34^+$ as judged by staining with anti-CD34 mAb.

Granulocytes and macrophages were also generated in vitro from $CD34^+$ hemopoietic progenitors in the presence of G-CSF and SCF for 12 days and M-CSF and SCF for 12 days, respectively. Aliquots of cells were further treated with 1 ng/ml PMA and 1 μg/ml ionomycin for 1 and 6 h and then pooled. Activated and nonactivated cells were lysed for RNA extraction.

Generation of DC from $CD34^+$ progenitors and from monocytes

Cultures of $CD34^+$ cells were established in the presence of SCF, GM-CSF, TNF-α, and 5% AB^+ pooled human serum, as described (28, 29). By day 6, human serum was removed and cells were further cultured in the presence of GM-CSF and TNF-α until day 12. At this time point, aliquots of cells were activated with PMA and ionomycin for 1 and 6 h, then pooled and lysed for RNA extraction. For analysis of FDF03 expression by flow cytometry, cells were collected at the time points indicated within the text. In some experiments, $CD1a^+$ and $CD14^+$ DC precursor subsets were sorted at day 6 by flow cytometry and further cultured until day 12 in the presence of GM-CSF and TNF-α. Monocyte-derived DC were produced by

culturing purified blood monocytes for 6 days in the presence of GM-CSF and IL-4 (30). In some experiments, 5 × 10^5 monocyte-derived DC per well (24-well culture plate) were further activated with LPS (25 ng/ml) for 72 h or by coculture with 4 × 10^4 irradiated (7500 rad) murine fibroblastic L cells untransfected or transfected with the cDNA for CD40 ligand (27).

Northern blot analysis

Human mRNA adult tissue blots (Clontech, Palo Alto, CA) were hybridized with a 377-bp DNA probe from the 3'-end of FDF03 cDNA, produced by PCR amplification of a region defined by the oligonucleotides 5'-CAG CAGCGGACTAAAGCCAC (forward primer) and 5'-GCATCTCGCTC CATTATCAA (reverse primer). This fragment was labeled with ^{32}P-dCTP using the High Prime kit (Boehringer Mannheim, Meylan, France). Membranes were prehybridized and hybridized under standard conditions (31). Low and high stringency washes were 2× SSC/0.2% SDS and 0.2× SSC/ 0.2% SDS, respectively, each done twice for 30 min. The membranes were incubated with Biomax MR film (Kodak, Rochester, NY) for 7 days.

RNA, DNA, and RT-PCR analysis

Cells were lysed, total RNA was extracted (32), and first-strand cDNAs were prepared after DNase I treatment (in the presence of RNase inhibitor) of 5 μg of total RNA using oligo(dT) primers (Pharmacia, Uppsala, Sweden) and the Superscript kit (Life Technologies). Synthesis of cDNAs was controlled by performing RT-PCR using β-actin primers. RT-PCR with the primers 5'-CCCCTTCTCCTTCTATTACC (forward primer) and 5'-TTT AGTCCGCTGCTGACCTT (reverse primer) specific for human FDF03 cDNA (1 ng/ml) was performed using the AmpliTaq enzyme and buffer (Perkin-Elmer, Paris, France), dNTPs at 0.8 mM, and DMSO at 5% final concentration. Cycle conditions were 94°C, 40 s; 55°C, 1 min; 72°C, 2 min, for 35 cycles.

Cloning of FDF03-ΔTM and FDF-M14 isoforms was performed by RT-PCR using a pair of primers designed in the 5'-untranslated region (UTR) and 3'-UTR of FDF03 cDNA (forward 5'-ACAGCCCTCTTCG GAGCCTCA and reverse 5'-AAGCTGGCCCTGAACTCCTGG). PCR products were cloned using the pCRII vector (TA cloning kit; Invitrogen, San Diego, CA). Double-stranded plasmid DNA was sequenced on an ABI 373A sequencer (Applied Biosystems, Foster City, CA) using dye terminator technology. Sequencher (Gene Codes Corporation, Ann Arbor, MI) and Lasergene (DNASTAR, London, U.K.) software were used to analyze sequences. Comparisons against the GenBank databases were performed using the BLAST algorithm.

Identification of a mouse homologue of FDF03

tBlastn searches against the mouse expressed sequence tag (EST) database identified different ESTs (gb, AI606524, AI595493, and AV021745) with homology to human FDF03 cDNA and allowed to build a contig coding for a mouse protein homologous to human FDF03. PCR amplification of cDNAs from mouse spleen using oligonucleotides designed in the 5'- and 3'-ends of this sequence (forward 5'-CCTGAGCACCCCAGTGTCCC and reverse 5'-GTGAATTTCTGTGTCTGCCT) permitted the amplification of the entire open reading frame (ORF) of mouse FDF03 (mFDF03).

Chromosomal localization of the FDF03 gene

Chromosomal localization was performed with the Stanford G3 radiation hybrid medium resolution panel (Research Genetics, Huntsville, AL). PCR was as described above using oligonucleotides that amplify a 505-bp fragment specific to the human gene (forward 5'-ACAGCCCTCTTCGGAGC CTCA, reverse 5'-GGCAGAAATACACAGACTGG). The results were scored manually, and analysis was performed with the radiation hybrid mapper program (http//shgc-www.stanford.edu).

Generation of anti-FDF03 mAb 36H2

Female Lewis rats were primed using DNA immunization via intradermal injection into the tail of 50 μg of a pCDM8 expression plasmid (Invitrogen) encoding the FDF03 molecule. Plasmid immunizations were repeated thereafter on day 7 (40 μg) and day 29 (10 μg). Animals were boosted with FDF03-Ig fusion protein on day 67 (10 μg i.p. in CFA) and on day 82 (2.5 μg i.p. in IFA). On day 127, a combined immunizing dose (2 μg i.v. in saline; 2 μg i.p. in IFA) was administered, and splenocytes were harvested 4 days later and fused with the mouse myeloma P3X63-AG8.653. Hybridomas were initially selected that recognized FDF03-Ig (but not control-Ig) fusion protein in indirect ELISA. Hybridomas were then further selected based on their ability to immunoprecipitate an FDF03-AP fusion protein, as previously described (33), and to recognize PBMC via FACS staining. The rat IgG2a mAb TC17-36H2 (mAb 36H2) was selected for use in this study.

Surface biotinylation, immunoprecipitation, and Western blot analysis

For surface-biotinylation, purified blood monocytes were washed three times with ice-cold PBS, pH 8, then resuspended in freshly prepared solution of 0.5 mg/ml sulfo-N-hydroxy succinimidester of biotin (Pierce, Rockford, IL) in PBS and agitated at room temperature for 30 min. Cells were washed three times with ice-cold PBS, pH 8, and then treated in a lysis buffer containing 50 mM Tris-HCl, pH 8, 1% Nonidet P-40, 150 mM NaCl, and protease inhibitors (Boehringer Mannheim). Lysates were then incubated at 4°C for 20 min, and the insoluble material was pelleted by centrifugation at 12,000 × g for 10 min at 4°C. Soluble extracts were precleared three times with control mAb and protein G-Agarose (Boehringer Mannheim). The extract was then incubated with the mAb of interest for 1 h before adding protein G-Agarose for at least 3 h. Beads were washed three times in lysis buffer, resuspended in SDS-PAGE sample buffer with or without 5% 2-ME, boiled for 3 min, and centrifuged. Immunoprecipitates were separated by SDS-PAGE using 12% polyacrylamide gel and then transferred to a polyvinylidene difluoride membrane (Immobilon P; Millipore, Bedford, MA). Blots were blocked with 1% BSA, 0.1% Tween-20 in PBS, then incubated with HRP-conjugated avidin (ExtrAvidin peroxidase; Sigma) for 30 min. Proteins were detected by enhanced chemiluminescence (Boehringer Mannheim). To analyze FDF03 glycosylations, precipitates were untreated or digested overnight at 37°C with N-glycosidase F (0.2 U/50 μl), or with O-glycosidase (2 mU/50 μl) with or without neuraminidase (5 mU/50 μl) before SDS-PAGE in reducing conditions. All enzymes were from Boehringer Mannheim, and digestions were performed in 0.1 M potassium/phosphate buffer, pH 7, 0.05% SDS, 1% 2-ME, 1% Nonidet P-40, and 50 mM EDTA.

Flow cytometric analysis and cell sorting

Cell-surface expression of FDF03 was determined by immunofluorescence staining and flow cytometric analysis with a FACScalibur (Becton Dickinson, Mountain View, CA). For single staining, cells were incubated for 30 min at 4°C with 5 μg/ml purified rat anti-FDF03 mAb 36H2, then washed twice in PBS, 1% BSA, 0.1% NaN₃, and labeled with PE-conjugated F(ab')₂ goat anti-rat IgG (H+L) or with biotin-conjugated F(ab')₂ goat anti-rat IgG (H+L) (Biosource International, Camarillo, CA) followed by PE-conjugated streptavidin (Becton Dickinson). Nonspecific staining was determined by using control rat IgG mAb. For double staining, cells were first labeled with anti-FDF03 mAb 36H2 or isotype control mAb and further with biotin-conjugated F(ab')₂ goat anti-rat IgG, then washed and incubated for 15 min in 5% normal mouse serum (Dako, Glostrup, Denmark) for saturation. Cells were then labeled with PE-conjugated streptavidin and with FITC-conjugated anti-CD3, anti-CD19, anti-CD16, anti-CD56, anti-CD14, or anti-CD15 mAbs (all from Becton Dickinson). To analyze expression of FDF03 on CD34⁺ progenitor-derived CD1a⁺ and CD14⁺ DC, cells were labeled as described above but FDF03 was revealed with tricolor-conjugated streptavidin (Caltag, Burlingame, CA). Separation of CD1a⁺ and CD14⁺ DC subsets from cultured CD34⁺ cord blood cells was performed by sorting on a FACStar^Plus (Becton Dickinson) as previously described (12, 29).

To analyze FDF03 expression on blood and tonsil DC, blood mononuclear cells (obtained after centrifugation over Ficoll gradient) and tonsil mononuclear cells (obtained by digestion with collagenase) were first depleted of T and B cells by using a cocktail of anti-CD3 and anti-CD19 mAbs and goat anti-mouse IgG-coated magnetic beads essentially as previously described (34). The resulting cell population was labeled with a cocktail of FITC-conjugated anti-CD3, anti-CD14, anti-CD15, anti-CD16, anti-CD20, and anti-CD57 mAbs (lineage-FITC), APC-conjugated anti-CD11c mAb, peridinin chlorophyl protein-conjugated anti-HLA-DR mAb (all mAbs from Becton Dickinson) or PE-Cy5-conjugated anti-CD4 mAb (Immunotech, Marseille, France) and with biotin-conjugated anti-FDF03 mAb 36H2 followed by PE-conjugated streptavidin. Simultaneous acquisition of the four fluorescence parameters was performed on a FACScalibur.

Transfection of FDF03 cDNA in U937 cells

A synthetic Sal-CD8α-myc-Bam fragment was first generated by annealing two single-stranded oligonucleotides corresponding to the sequence of the human CD8α signal peptide followed by the c-myc epitope (EQKLI SEEDL), introducing SalI and BamHI restriction sites on 5' and 3', respectively. FDF03 deleted of the leader sequence (FDF03delSP) was amplified by PCR from a full-length FDF03 cDNA clone using a forward primer 5'-GGATCCACAGGATCTGGTCCAAGCTACCTTTATGGG introducing a BamHI site (underlined) and a reverse primer 5'-ATAGCG GCCGCCTTAGGCCTTTAAGACAGAGTACAGGGTC introducing a

Not site (underlined) 3' to the FDF03 stop codon. Following cloning in pCRII vector and enzymatic digestions, the fragments Sal-CD8α-myc-Bam and Bam-FDF03delSP-Not were ligated together into the SalI-NotI site of pMET7. The resulting CD8-myc-FDF03 construction was transfected into U937 cells (20 μg cDNA for 10 × 10⁶ cells) by electroporation in a GenePulser at 250 V with 975 μF capacitance (Bio-Rad, Richmond, CA). After 48 h of culture, cells expressing FDF03 were positively selected by staining with anti-FDF03 mAb 36H2 and sorting on a FACStar^Plus (Becton Dickinson). After four successive rounds of culture and sorting, a cell line stably expressing FDF03 was obtained.

Tyrosine phosphorylation and phosphatase recruitment

To analyze tyrosine phosphorylation and association with SHP-1 and SHP-2 of FDF03 and LAIR-1, FDF03-transfected U937 cells were stimulated or not with 100 mM sodium pervanadate for 10 min at 37°C and cells were lysed in 1% Nonidet P-40 in the presence of protease and phosphatase inhibitors essentially as previously described (35). Lysates were immunoprecipitated by anti-FDF03 mAb 36H2 or anti-LAIR-1 mAb DX26 (25) and protein G-Agarose. Immunoprecipitates were separated by SDS-PAGE on 12% polyacrylamide gels and transferred to Immobilon-P membranes. The membranes were blocked and then incubated with HRP-anti-phosphotyrosine mAb 4G10 (Upstate Biotechnology, Lake Placid, NY) or with polyclonal rabbit Abs against SHP-1 (C19) or SHP-2 (C18) (Santa Cruz Laboratories, Santa Cruz, CA) followed by HRP-conjugated anti-rabbit Igs (Amersham, Arlington Heights, IL). Proteins were detected by enhanced chemiluminescence.

Analysis of intracellular calcium mobilization

FDF03-transfected U937 cells were loaded with 5 μM Indo-1 AM and 5 μM Pluronic F-27 (Molecular Probes, Eugene, OR) for 45 min at 37°C. Cells were washed and kept at room temperature in the dark in RPMI 1640 supplemented with 10% FCS (complete medium) until analysis. For each experiment, an aliquot of Indo-1-loaded cells (10⁶ cells) was resuspended in 1 ml complete medium at 37°C, and the ratio of violet/blue fluorescent emissions at 405 and 530 nm, respectively, was analyzed on a FACStar^Plus flow cytometer (Becton Dickinson) equipped with an argon laser tuned at 350–364 nm (Spectra-Physics, Mountain View, CA) used for UV excitation. When the 405/530 nm ratio baseline was stable, 10 μg/ml of the Abs to be tested were added and the fluorescent emissions were recorded for 2 min. Cells were then kept at 37°C for 2 min, and cross-linking of Abs was achieved by adding 20 μg/ml of a goat F(ab')₂ anti-mouse Ig (Fcγ fragment-specific) that cross-reacts with rat IgG (Jackson ImmunoResearch, West Grove, PA). Fluorescent emissions were then recorded for the remaining time (≈5 min). The ratio of Indo-1 violet to blue fluorescence (405/530 nm ratio) was displayed as a function of the elapsed time. The anti-CD32 mAb IV.3 used to induce Ca²⁺ mobilization was obtained from Medarex (Lebanon, NH).

Results

Cloning of FDF03 cDNA

By random sequencing of a cDNA library from human activated monocytes (500 sequences), we selected a clone containing a putative leader sequence and representative of a cell-surface receptor, designated FDF03. Fig. 1A shows the nucleotide and deduced amino acid sequences of FDF03. The nucleotide sequence was 1249 bp in length and contained an ORF of 912 nt with the first start codon ATG contained in a consensus Kozak sequence and preceded by a stop codon. The 3'-untranslated sequence of 184 nt contained a classical AATAAA polyadenylation signal. The deduced polypeptide conformed to a type I transmembrane protein composed of 303 aa including a 21-aa signal peptide, a 175-aa extracellular domain, a hydrophobic sequence of 22 aa characteristic of a transmembrane segment, and a 85-aa cytoplasmic tail. The predicted molecular mass of the FDF03 polypeptide was 34 kDa.

FDF03 belongs to the Ig-SF

Searching databases of known polypeptide sequences indicated that the extracellular domain of FDF03 shared significant homology only with the variable (V) domain of human and mouse Igs. Further alignment studies (exemplified in Fig. 1B) confirmed that FDF03 was a novel member of the Ig-SF with a single Ig-related
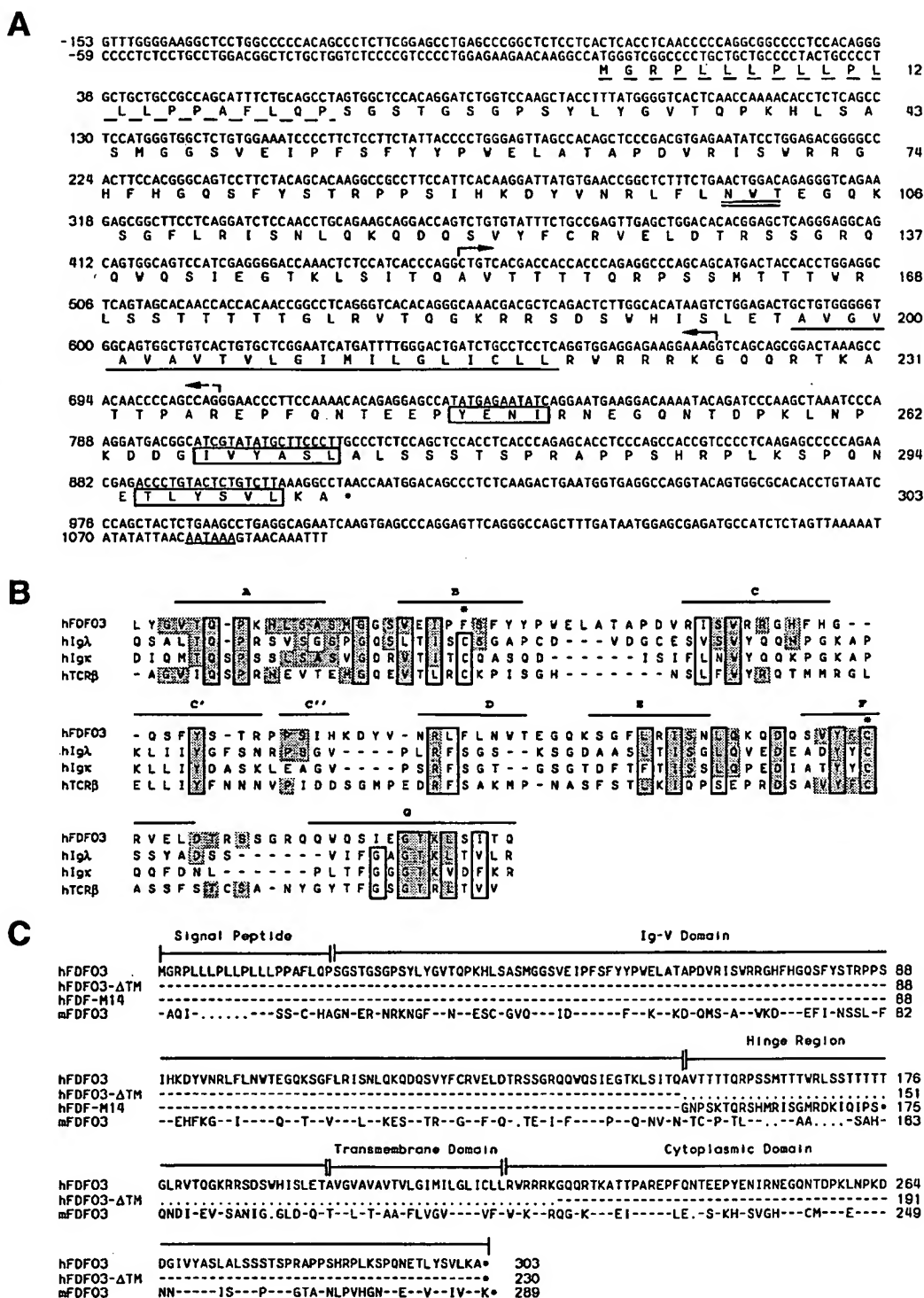
A

```
-153 GTTTGGGGAAGGCTCCTGGCCCCCACAGCCCTCTTCGGAGCCTGAGCCCGGCTCTCCTCACTCACCTCAACCCCCAGGCGGCCCCTCCACAGGG
 -59 CCCCTCTCCTGCCTGGACGGCTCTGCTGGTCTCCCCGTCCCCTGGAGAAGAACAAGGCCATGGGTCGGCCCCTGCTGCTGCCCCTACTGCCCCT
                                                                   M  G  R  P  L  L  L  P  L  L  P  L   12

  38 GCTGCTGCCGCCAGCATTTCTGCAGCCTAGTGGCTCCACAGGATCTGGTCCAAGCTACCTTTATGGGGTCACTCAACCAAAACACCTCTCAGCC
      L  L  P  P  A  F  L  Q  P  S  G  S  T  G  S  G  P  S  Y  L  Y  G  V  T  Q  P  K  H  L  S  A      43

 130 TCCATGGGTGGCTCTGTGGAAATCCCCTTCTCCTTCTATTACCCCTGGGAGTTAGCCACAGCTCCCGACGTGAGAATATCCTGGAGACGGGGCC
      S  M  G  G  S  V  E  I  P  F  S  F  Y  Y  P  V  E  L  A  T  A  P  D  V  R  I  S  V  R  R  G      74

 224 ACTTCCACGGGCAGTCCTTCTACAGCACAAGGCCGCCTTCCATTCACAAGGATTATGTGAACCGGCTCTTTCTGAACTGGACAGAGGGTCAGAA
      H  F  H  G  Q  S  F  Y  S  T  R  P  P  S  I  H  K  D  Y  V  N  R  L  F  L  N  W  T  E  G  Q  K   106

 318 GAGCGGCTTCCTCAGGATCTCCAACCTGCAGAAGCAGGACCAGTCTGTGTATTTCTGCCGAGTTGAGCTGGACACACGGAGCTCAGGGAGGCAG
      S  G  F  L  R  I  S  N  L  Q  K  Q  D  Q  S  V  Y  F  C  R  V  E  L  D  T  R  S  S  G  R  Q      137

 412 CAGTGGCAGTCCATCGAGGGGACCAAACTCTCCATCACCCAGGCTGTCACGACCACCACCCAGAGGCCCAGCAGCATGACTACCACCTGGAGGC
       Q  V  Q  S  I  E  G  T  K  L  S  I  T  Q  A  V  T  T  T  T  Q  R  P  S  S  M  T  T  T  V  R   168

 506 TCAGTAGCACAACCACCACAACCGGCCTCAGGGTCACACAGGGCAAACGACGCTCAGACTCTTGGCACATAAGTCTGGAGACTGCTGTGGGGGT
      L  S  S  T  T  T  T  T  G  L  R  V  T  Q  G  K  R  R  S  D  S  V  H  I  S  L  E  T  A  V  G  V   200

 600 GGCAGTGGCTGTCACTGTGCTCGGAATCATGATTTTGGGACTGATCTGCCTCCTCAGGTGGAGGAGAAGGAAAGGTCAGCAGCGGACTAAAGCC
      A  V  A  V  T  V  L  G  I  M  I  L  G  L  I  C  L  L  R  V  R  R  R  K  G  Q  Q  R  T  K  A    231

 694 ACAACCCCAGCCAGGGAACCCTTCCAAAACACAGAGGAGCCATATGAGAATATCAGGAATGAAGGACAAAATACAGATCCCAAGCTAAATCCCA
      T  T  P  A  R  E  P  F  Q  N  T  E  E  P Y  E  N  I R  N  E  G  Q  N  T  D  P  K  L  N  P      262

 788 AGGATGACGGCATCGTATATGCTTCCCTTGCCCTCTCCAGCTCCACCTCACCCAGAGCACCTCCCAGCCACCGTCCCCTCAAGAGCCCCCAGAA
      K  D  D  G  I  V  Y  A  S  L A  L  S  S  S  T  S  P  R  A  A  P  P  S  H  R  P  L  K  S  P  Q  N   294

 882 CGAGACCCTGTACTCTGTCTTAAAAGGCCTAACCAATGGACAGCCCTCTCAAGACTGAATGGTGAGGCCAGGTACAGTGGCGCACACCTGTAATC
      E T  L  Y  S  V  L K  A  *                                                                      303

 978 CCAGCTACTCTGAAGCCTGAGGCAGAATCAAGTGAGCCCAGGAGTTCAGGGCCAGCTTTGATAATGGAGCGAGATGCCATCTCTAGTTAAAAAT
1070 ATATATTAACAATAAAGTAACAAATTT
```

B

C

FIGURE 1. FDF03 belongs to the Ig-SF. *A*, Nucleotide and predicted amino acid sequences of human FDF03. The nucleotide sequence of the 1249-bp cDNA clone and the derived amino acid sequence are numbered starting from the start codon ATG and methionine, respectively. The predicted signal peptide (dotted) and the transmembrane domain are underlined. The potential *N*-linked glycosylation site in extracellular domain is underlined twice, and the three tyrosine-based motifs within the cytoplamic tail are boxed. A consensus polyadenylation signal (AATAAA) in the 3'-UTR is underlined. Arrows above the nucleotide sequence indicate sequences deleted in FDF03-ΔTM and FDF-M14 isoforms. This sequence has been submitted to the GenBank, EMBL, and DDBJ databases under accession no. AJ400841. *B*, Alignment of the putative Ig-like domain of FDF03 with the variable (V) domain of Ig and Ig-like proteins. Amino acids conserved between FDF03 (aa 32–151) and V-set domains of human Igλ (P01713), Igκ (P01608), and TCRβ (P01733) are shaded. Residues characteristic of the V-set and generally conserved among Ig-like proteins are boxed. Asterisks indicate the position of the conserved cysteines in the Ig fold. The positions of the predicted β-strands are indicated above the sequences. Sequences were analyzed using the MegAlign function of Lasergene (DNASTAR). *C*, Putative soluble forms of human FDF03 (hFDF03) and sequence of a mouse homologue (mFDF03) of hFDF03. Amino acid sequences of hFDF03-ΔTM, hFDF-M14, and mFDF03 (GenBank, EMBL, and DDBJ accession nos. AJ400842, AJ400843, and AJ400844, respectively) are aligned with that of hFDF03. Only amino acids that differ from that of hFDF03 are noted, and residues identical with hFDF03 are indicated by dashes. Gaps introduced to optimize the sequence alignment are indicated by points.

domain of the V-set (36, 37). While most Ig domains are characterized by the presence of a pair of cysteines forming a disulfide bridge that stabilizes the Ig fold, the FDF03 extracellular domain contained only one cysteine at position 125 (asterisks in Fig. 1*B*). However, typical residues conserved among Ig-like proteins and contained in strands forming the two β-sheets of the Ig domain were also present within the FDF03 extracellular region (boxes in Fig. 1*B*). Moreover, a long spacing between the predicted β-strands C and D identified the two additional strands C' and C" that are characteristics of the V-set of Ig domain (36, 37). A single-potential N-linked glycosylation site (NWT) was present in the Ig domain at position 100. Finally, the membrane-proximal region of the FDF03 extracellular domain contained a high proportion of threonine and serine that represent potential sites for O-linked glycosylation. By analogy with other Ig-SF members, this region is predicted to display an extended open conformation typical of hinge-like sequences.

The 85-aa intracellular domain of FDF03 possessed two putative protein kinase C phosphorylation sites (on serine residues 279 and 285 within the motifs SPR and SHR, respectively) and three tyrosine residues at position 246, 269, and 298 in sequences YENI, YASL, and YSVL, respectively. Following tyrosine phosphorylation, these motifs may represent potential binding sites for SH2 domain-containing signaling molecules (38). In particular, tyrosine 269 is centered within the sequence IVYASL that perfectly matches the consensus L/V/IxYxxL/V of the ITIM (2, 5, 39), and is spaced by 28 aa from the more distal tyrosine that is also contained within an ITIM-like sequence TLYSVL (Fig. 1*A*).

Identification of a mouse homologue of human FDF03

Searching mouse cDNA databases, we identified ESTs with homology to human FDF03 cDNA and we used them to build a contig coding for a protein homologous to human FDF03 and to design oligonucleotides in the 5'-end and 3'-end of this sequence (see *Materials and Methods*). PCR amplification of cDNAs from mouse spleen further permitted the amplification of a 1.2-kb nucleotide sequence containing an entire ORF encoding a predicted protein (mFDF03) of 289 aa in length (Fig. 1*C*). The mFDF03 extracellular region also contained a single Ig-like domain of the V-type and shared the amino acid residues characteristics of human FDF03. In particular, the IPFSFY sequence (at position 45–50 of mFDF03) in the predicted strand B is conserved within both proteins. However, mFDF03 contained an YFGRV sequence instead of the YFCRV sequence in strand F of human FDF03 (aa 117 to 121 in mFDF03), thus indicating that the mouse protein possessed none of the two cysteines typical of the Ig domains. Of importance, the intracytoplasmic tail of mFDF03 contained two tyrosines in tandem sequence IVYASI-x23-TVYSIV that is homologous to the tandem IVYASL-x23-TLYSVL of ITIM-like sequences in human FDF03 (Fig. 1*C*).

Soluble forms of FDF03 can be produced by alternative splicing

During the analysis of FDF03 expression by RT-PCR (see below), we identified a second PCR product shorter than the expected size. This product, amplified by RT-PCR from activated PBMC cDNA using primers designed in the 5'-UTR and 3'-UTR of FDF03 cDNA, was purified, cloned, and sequenced. All cDNA clones but one had an identical insert of 943 bp that matched with FDF03 cDNA sequence but contained a deletion of 219 nt coding for the extracellular threonine-rich region and the transmembrane domain of FDF03 (FDF03 nucleotides 455–673, arrows in Fig. 1*A*). The resulting nucleotide sequence coded for a putative protein designated FDF03-ΔTM of 230 aa, composed of the extracellular Ig like-domain directly linked to the entire intracytoplasmic domain
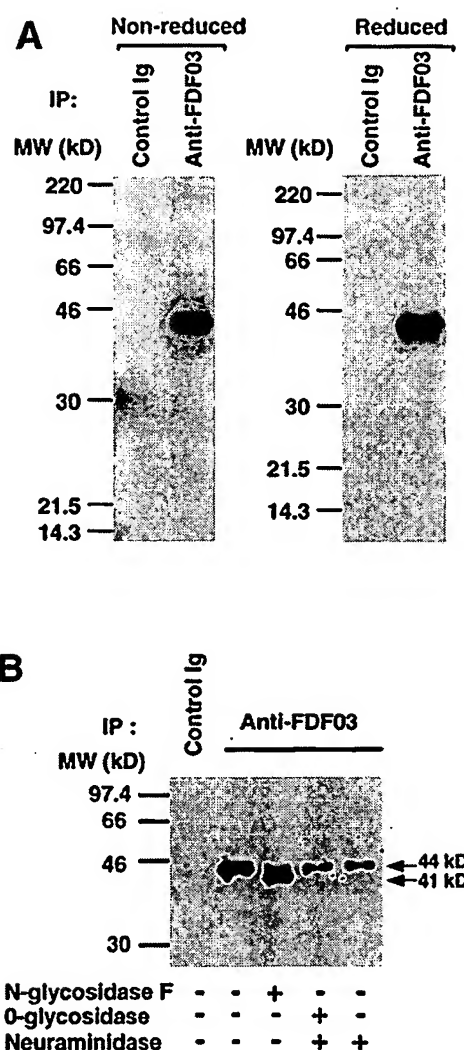

FIGURE 2. FDF03 is a cell-surface monomeric glycoprotein. *A*, Lysates of surface biotinylated monocytes were immunoprecipitated with anti-FDF03 mAb 36H2 or control rat IgG with protein G-Agarose, boiled in nonreducing or reducing conditions, and analyzed by SDS-PAGE on 12% gels. Following transfer on membranes, blots were incubated with HRP-streptavidin and proteins were revealed by enhanced chemiluminescence. *B*, Precipitates of biotin-labeled monocytes with mAb 36H2 were treated with N-glycosidase F or with neuraminidase and/or O-glycosidase before SDS-PAGE in reducing conditions and Western blot analysis as above.

of FDF03 (Fig. 1*C*). The other cDNA clone identified was designated FDF-M14. It contained a 900-bp insert that matched the FDF03 nucleotide sequence but with a 253-bp deletion (FDF03 nucleotides 455–707, arrows in Fig. 1*A*) that also resulted in deletion of the region coding for the hinge region and transmembrane domain of FDF03. In this case, a change in reading frame introduced premature stop codons and the deduced FDF-M14 protein was a short 175-aa polypeptide composed of the extracellular FDF03 Ig-like domain linked to 24 aa at the carboxyl terminus that are not related to the full-length FDF03 amino acid sequence (Fig. 1*C*).

These two molecules lacking the transmembrane domain may thus represent soluble isoforms of FDF03 generated by alternative splicing of FDF03 mRNA (see *Discussion*).

FDF03 is expressed as a monomeric glycoprotein

The anti-FDF03 mAb 36H2, produced by immunizing rats against human FDF03 extracellular domain, was used throughout this

study. Immunoprecipitation from lysates of biotin-labeled blood monocytes using this mAb revealed a 44-kDa protein under both nonreducing and reducing conditions (Fig. 2A). Incubation of the precipitate with N-glycosidase F resulted in a shift of the molecular mass to $\approx$41 kDa, while treatment with neuraminidase and O-glycosidase did not change the electrophoretic migration of the molecule (Fig. 2B). Taken together, these data indicate that FDF03 is expressed as a monomer and that N-linked glycosylations at the single site (N100) within the FDF03 Ig domain account for the observed molecular mass (44 kDa) of the FDF03 polypeptide.

The gene encoding FDF03 is localized on chromosome 7q22 and FDF03 mRNA is mostly expressed in immune tissues

Using human radiation hybrid mapping panels and PCR analysis, the gene coding for FDF03 was mapped to chromosome 7q22, within the interval D7S479–D7S2545 of microsatellite anchor markers AFM036xg5 and AFMa052ya5 (data not shown). The closest marker was SGC33905 localizing the gene encoding human fetal liver cytochrome P450 subfamily IIIA polypeptide 7, CYP3A7.

Northern blot analysis on the Clontech immune system blots, performed with a 377-bp probe that hybridized the 3'-end ORF and 3'-UTR of FDF03 mRNA, showed the highest levels of expression in PBL, strong levels of expression in spleen and bone marrow, and lower expression in lymph node (Fig. 3). FDF03 mRNA was not detected in thymus, appendix, and fetal liver (Fig. 3). On total RNA tissue blots, detectable expression was seen in spinal cord, placenta, and lung, but no expression was seen in heart, brain, liver, skeletal muscle, kidney, pancreas, prostate, testis, ovary, small intestine, and colon (Fig. 3 and data not shown). This analysis generally showed the presence of two bands of $\approx$1.4 and $\approx$1.3 kb that may represent mRNA for FDF03 and for the transmembrane-deleted isoforms FDF03-ΔTM and FDF-M14, respectively, because the probe used in these experiments could hybridize with all three transcripts.

FDF03 expression is restricted to cells of myelo-monocytic origin, including DC

The cellular distribution of FDF03 was first determined by RT-PCR analysis on various isolated cells and cell lines using a pair of primers able to amplify both FDF03 and FDF03-ΔTM cDNAs. As shown in Fig. 4A, FDF03 and FDF03-ΔTM cDNAs were strongly detected in PBMC, blood monocytes, and granulocytes, while no signal was amplified from purified blood T cells, NK cells, and tonsillar B cells. FDF03 and FDF03-ΔTM cDNAs were also present in macrophages (Mϕ in Fig. 4A) derived from CD34$^+$ cells in the presence of M-CSF, as well as in DC generated either from CD34$^+$ cord blood progenitors with GM-CSF and TNF-α (CD34$^+$-DC in Fig. 4A) or from blood monocytes with GM-CSF and IL-4 (mono-DC in Fig. 4A). Moreover, FDF03 was not expressed by the cell lines JY, RAMOS, DAUDI, BL2 (B cell lines), JURKAT, and MOLT4 (T cell lines), TF1 (erythro-leukemia), CHA (kidney carcinoma), MRC5 (fetal lung fibroblasts), and SW620 and HT29 (colon carcinoma cell lines) (data not shown).

In accordance with the RT-PCR analysis, two-color flow cytometry analysis of human PBL performed with mAb 36H2 showed that FDF03 was strongly expressed by all circulating CD14$^+$ monocytes and by freshly isolated CD15$^+$ blood granulocytes (Fig. 4B). In contrast, mAb 36H2 did not react with peripheral blood CD3$^+$ T cells, CD20$^+$ B cells, and CD56$^+$ or CD16$^+$ NK cells (Fig. 4B).
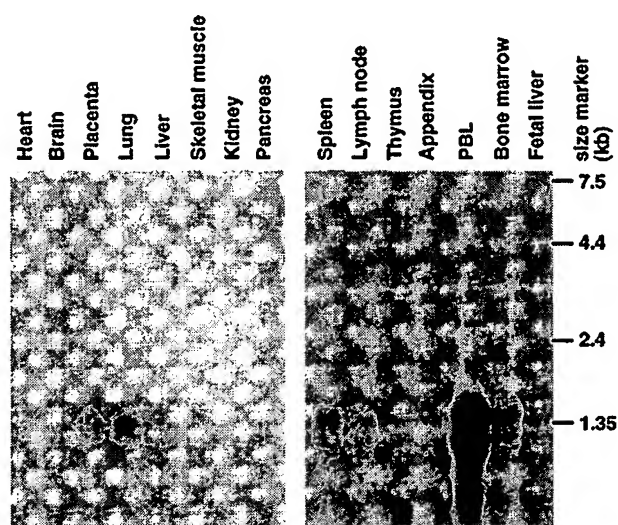

FIGURE 3. FDF03 is mostly expressed in immune tissues. Northern blots of human tissues were analyzed with a probe corresponding to 277 bp overlapping the 3' of the ORF and 3'-UTR of FDF03 cDNA labeled with [^{32}P]dCTP. Two bands were obtained, with the major band at $\approx$1.4 kb corresponding to the expected size for FDF03 mRNA and both the FDF03-ΔTM and/or FDF-M14 isoforms.

Taken together, these data indicate that FDF03 is mostly expressed by cells of myelo-monocytic origin and by in vitro-derived DC. However, it should be noted that FDF03 mRNA was not detected in a number of myeloid cell lines including U937, HL60, and THP-1 (data not shown).

FDF03 is preferentially expressed by monocytic/CD14$^+$-derived DC and by CD11c$^+$ DC

DC represent heterogeneous populations of cells according to their origin and stage of activation/maturation (10, 40, 41). Because FDF03 mRNA was detected in bulk preparations of in vitro-derived DC (Fig. 4A), we further analyzed whether cell-surface expression of the FDF03 receptor could be differently regulated during DC differentiation as well as on DC subpopulations. As shown in Fig. 5A, FDF03 was not expressed on the surface of CD34$^+$ cord blood progenitor cells, but was induced during their culture with a combination of SCF, GM-CSF, and TNF-α, with the strongest expression observed on immature DC on days 5–7 of culture. On day 6, three-color flow cytometric analysis demonstrated that FDF03 was mostly expressed by the CD14$^+$/CD1a$^-$ subset of cells, when compared with the CD14$^-$/CD1a$^+$ subset (Fig. 5B). These two populations were sorted on day 6 according to their CD14 and CD1a expression and recultured for 6 days in the presence of GM-CSF and TNF-α. As shown in Fig. 5B, on day 12, CD14$^+$-derived DC still expressed detectable levels of surface FDF03, and both FDF03 mRNA and FDF03-ΔTM mRNA were amplified by RT-PCR in those DC (day 12 DC in Fig. 5B). In contrast, the DC derived from the CD1a$^+$ subset of cells no longer expressed FDF03 at day 12, both at the cell surface and mRNA levels (Fig. 5B). In contrast, DC generated from peripheral blood monocytes in the presence of GM-CSF and IL-4 expressed high levels of FDF03 both at their immature stage (day 7 in Fig. 5C) and after further activation by signals inducing DC maturation (day 9 in Fig. 5C), such as LPS and CD40 ligand (42). Taken together, these results indicate a preferential expression of FDF03 by monocyte- and CD14$^+$/CD1a$^-$-derived DC and suggest that FDF03 can be expressed by both immature and mature DC.

FIGURE 4. FDF03 is expressed by cells of myelo-monocytic origin. *A,* RT-PCR analysis of FDF03 and FDF03-ΔTM mRNA expression in various cell populations. Pools of cDNA from different samples were prepared as described in *Materials and Methods.* cDNA of macrophages (Mφ) and granulocytes were derived from cord blood CD34⁺ progenitors cultured in the presence of M-CSF or G-CSF, respectively. DC were generated from cord blood CD34⁺ cells with GM-CSF and TNF-α for 12 days (CD34⁺ DC) or from blood monocytes with GM-CSF and IL-4 for 7 days (mono-DC). Freshly isolated cells were PBMC, monocytes, T cells, NK cells, and tonsillar B cells. RT-PCR was performed with primers that amplified both FDF03 and FDF03-ΔTM, but not FDF-M14, as described in *Materials and Methods.* Amplification of plasmids containing FDF03 or FDF03-ΔTM cDNA (pFDF03 and pFDF03-ΔTM) was used as control of specificity, and amplification of β-actin was used as control for cDNA quantity and quality. *B,* Expression of FDF03 on peripheral blood leukocytes. FDF03 expression was analyzed by flow cytometry after staining of circulating mononuclear or polynuclear cells with anti-FDF03 mAb 36H2 followed by PE-conjugated goat anti-rat Ig. After saturation with mouse serum, cells were incubated with FITC-conjugated anti-CD20, anti-CD3, anti-CD16, anti-CD56 (for lymphocytes), anti-CD14 (for monocytes), or with anti-CD15 mAb for granulocytes. Acquisition was performed by gating on the different cell populations according to their forward and right angle scatter parameters.
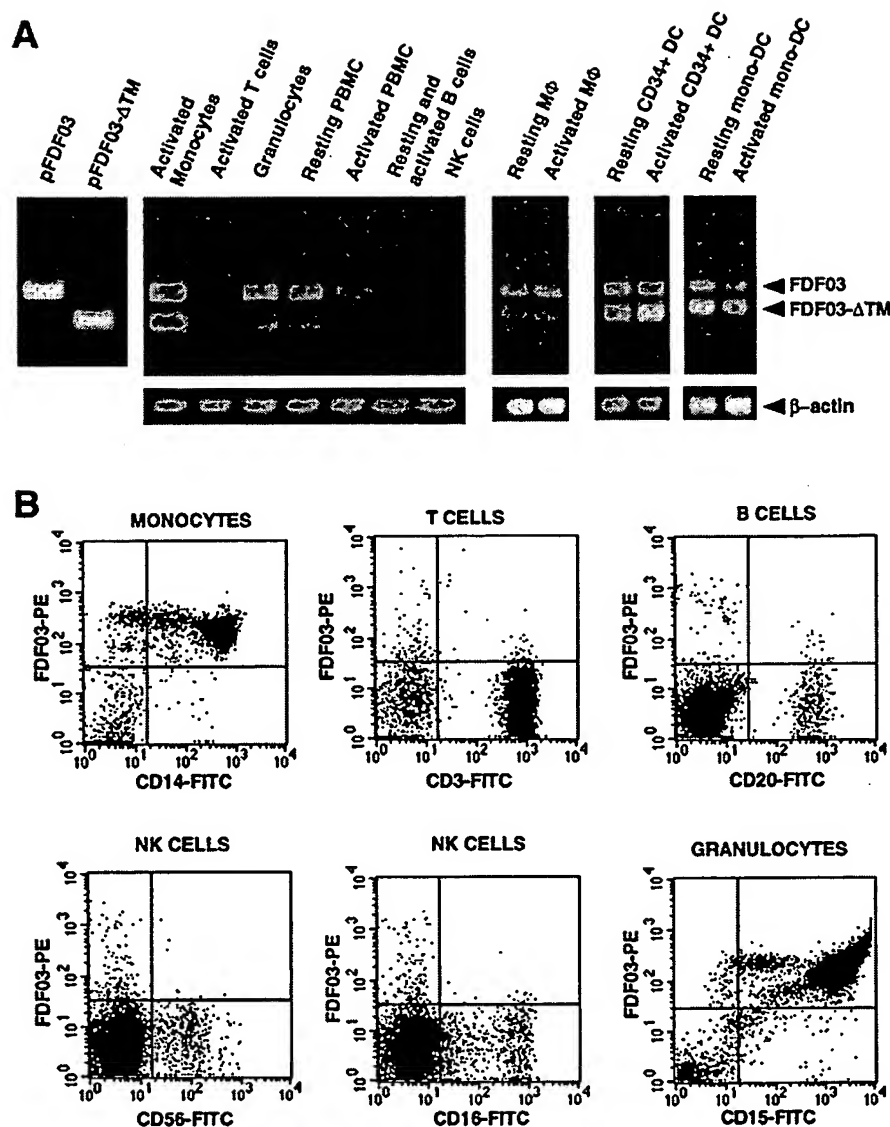

To determine whether in vivo DC also expressed FDF03, we performed four-color FACS analysis on blood and tonsillar mononuclear cell suspensions enriched in DC by immunomagnetic beads depletion. The FDF03 expression was analyzed vs CD11c expression on DC identified on the basis of 1) absence of expression of lineage markers (CD3, CD14, CD15, CD16, CD20, and CD57) but 2) strong expression of MHC class II or CD4 molecules, as previously reported (34, 43–46). As shown in Fig. 6A, analysis of FDF03 expression on blood HLA-DR⁺⁺/lineage⁻ DC demonstrated that the majority of CD11c⁺ DC expressed FDF03, while mAb 36H2 did not stain the CD11c⁻ DC precursor population. On tonsil CD4⁺/lineage⁻ DC, FDF03 was also expressed by the CD11c⁺ population, but not by the CD11c⁻ subset (Fig. 6B).

FDF03 is phosphorylated and recruits SHP-2 and to a lesser extent SHP-1 in U937 cells

Following tyrosine phosphorylation, ITIM-bearing receptors can recruit protein tyrosine phosphatases SHP-1 and/or SHP-2 (5, 47). To determine whether the two ITIM-like sequences contained in the FDF03 intracytoplasmic tail could associate with SHP-1 and/or SHP-2, we transfected FDF03 cDNA in the monocytic U937 cell line and positively selected FDF03-expressing cells by using stain-

ing with mAb 36H2 and FACS sorting. This strategy was chosen because we did not find any cell line, including U937 (Fig. 7A, *left histogram*), that spontaneously expressed FDF03. After four rounds of successive sorting and culture, >90% of the cells expressed relatively high levels of FDF03 (Fig. 7A, *right panel*). This cell line (FDF03-U937 cells) was stimulated or not with sodium pervanadate (an inhibitor of protein tyrosine phosphatases that induces tyrosine phosphorylation) then lysed, and lysates were immunoprecipitated with anti-FDF03 mAb 36H2 or rat control IgG. Because FDF03-U937 cells also expressed the inhibitory receptor LAIR-1/p40 (25) (Fig. 7A), lysates were precipitated in parallel with anti-LAIR-1 mAb DX26 used as a positive control for ITIM-bearing molecule. After SDS-PAGE, Western blot analysis with the anti-phosphotyrosine mAb 4G10 revealed the presence of a major band of ≈44 kDa, corresponding to FDF03 molecular mass, in mAb 36H2 precipitates of pervanadate-activated, but not untreated, cells (Fig. 7B). A ≈40-kDa tyrosine-phosphorylated protein was specifically detected in mAb DX26 precipitates of pervanadate-treated FDF03-U937 cells (Fig. 7B), which corresponds to the previously reported molecular mass of LAIR-1/p40 on NK cells, monocytes, and DC (25, 26). When blots were probed with specific anti-SHP-1 Abs, a faint band of ≈73 kDa was specifically

FIGURE 5. Expression of FDF03 by in vitro-derived DC. *A* and *B,* Expression of FDF03 on CD34⁺-derived DC. *A,* Purified cord blood CD34⁺ progenitor cells were cultured with SCF, GM-CSF, and TNF-α from day 0 to day 6, then washed and recultured with GM-CSF and TNF-α until day 12. At the time indicated, FDF03 expression was analyzed by flow cytometry after staining of cells with anti-FDF03 mAb 36H2 (histograms in solid line) or control rat IgG (histograms in dotted line) followed by PE-conjugated goat anti-rat Ig. *B,* Cord blood CD34⁺ cells cultured for 6 days as described above were labeled with PE-conjugated anti-CD14 and FITC-conjugated anti-CD1a mAbs and then FACS sorted according to CD14 and CD1a expression. CD14⁺/CD1a⁻ cells and CD14⁻/CD1a⁺ cells were further cultured with GM-CSF and TNF-α. FDF03 expression was determined just after cell sorting (day 6) and after 6 days of the second culture (day 12), after staining with anti-FDF03 mAb 36H2 (histograms in solid line) or control rat IgG (histograms in dotted line) followed by biotin-labeled anti-rat Ig and tricolor (TC)-conjugated streptavidin. Data presented in *A* and *B* are representative of at least three independent experiments. FDF03 expression was also analyzed by RT-PCR as described in Fig. 4. *C,* Expression of FDF03 on monocyte-derived DC. Purified blood monocytes were cultured with GM-CSF and IL-4. On day 7, cells were washed and recultured for 2 days with GM-CSF alone (medium), GM-CSF plus LPS (25 ng/ml), or with GM-CSF plus irradiated untransfected (control L cells) or CD40 ligand-transfected L cells. FDF03 expression was determined by flow cytometry after staining with anti-FDF03 mAb 36H2 (histograms in solid line) followed by PE-conjugated goat anti-rat Ig. Histograms in dotted line represent staining obtained with a rat IgG control mAb. Results presented are representative of five independent experiments.
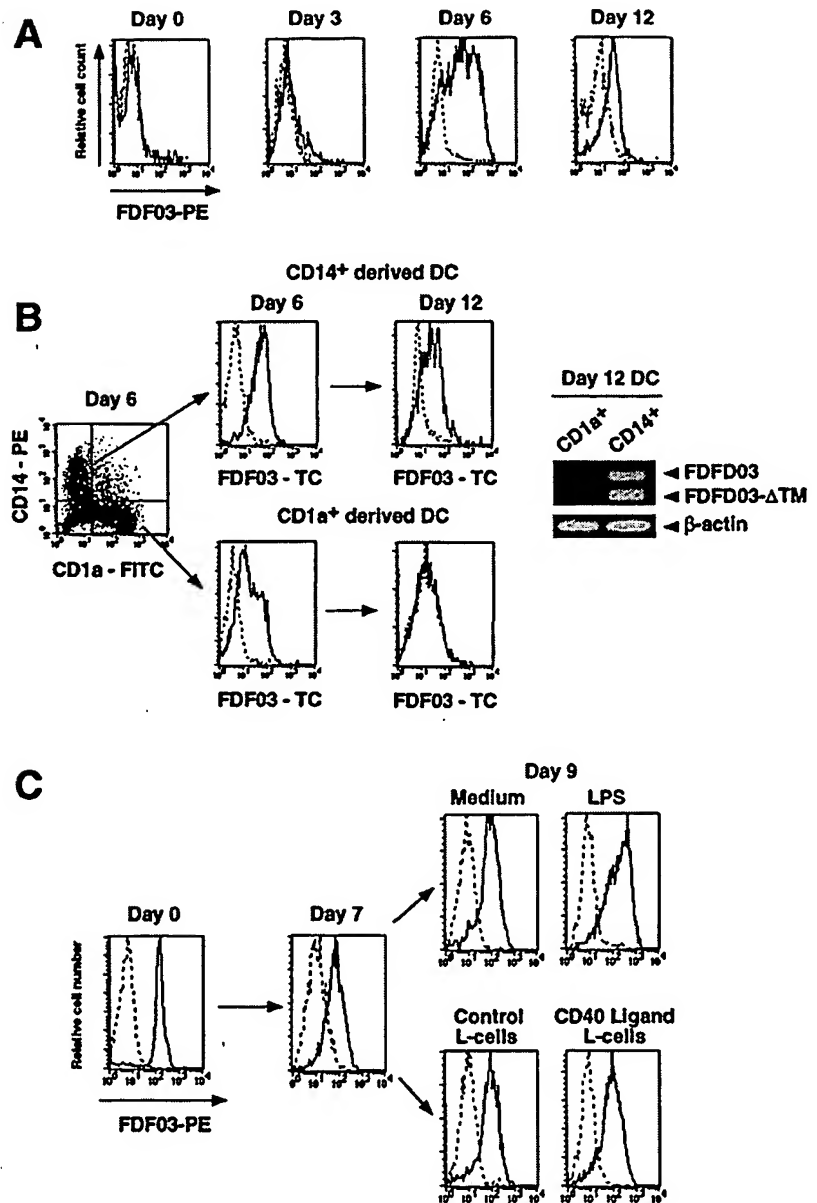
revealed in mAb 36H2 precipitates of pervanadate-treated FDF03-U937 cells (Fig. 7C), while a strong signal was observed in mAb DX26 precipitates, thus suggesting that FDF03 was less efficient than LAIR-1 in association with SHP-1. In contrast, anti-SHP-2 Abs demonstrated that FDF03 recruited SHP-2 as efficiently as LAIR-1 (Fig. 7D). Taken together, these results indicate that FDF03 is tyrosine-phosphorylated and can associate with SHP-2, and to a lesser extent with SHP-1, in pervanadate-activated U937 cells.

FDF03 inhibits CD32/FcγRII-induced calcium mobilization in U937 cells

ITIM-bearing receptors inhibit activation signals, such as intracellular calcium mobilization, when coaggregated with ITAM-bearing receptors (4). Therefore, we analyzed whether FDF03 could also antagonize signaling of stimulatory receptors in FDF03-U937 cells. Efficient cross-linking of the different molecules was performed with a goat F(ab')₂ anti-mouse Ig (Fcγ-specific) that also reacts with rat IgG, so that the same reagents could be used re-

gardless of the origin of the mAbs. As shown in Fig. 8, cross-linking of mAb 36H2 did not increase intracellular Ca²⁺ concentration in Indo-1-loaded FDF03-U937 cells. In contrast, aggregation of CD32/FcγRII by cross-linking of mAb IV.3, which preferentially recognizes the activating isoforms of CD32 (48, 49), induced intracellular Ca²⁺ mobilization. Of interest, the coaggregation of CD32 with FDF03, but not with a control mAb, resulted in strong inhibition of calcium mobilization (Fig. 8). Similar inhibition of Ca²⁺ flux was observed when CD32 was coaggregated with LAIR-1 (Fig. 8). Altogether, these results indicate that FDF03 can function as an inhibitory receptor in monocytic U937 cells, similarly to LAIR-1/p40.

In contrast to LAIR-1/p40, cross-linking of FDF03 does not inhibit the differentiation of monocytes into DC in response to GM-CSF

Because it has been reported that engagement of LAIR-1/p40 inhibited differentiation of monocyte into DC by interfering with GM-CSF activities (26), we wondered whether FDF03 could also
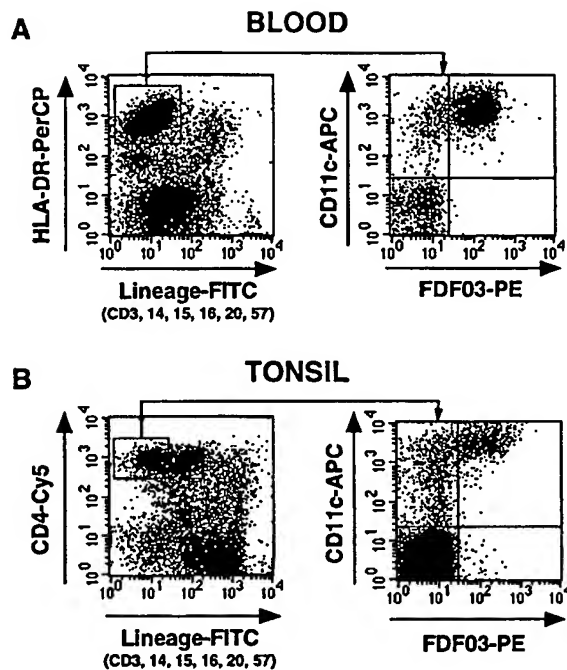
A **BLOOD**

HLA-DR-PerCP / Lineage-FITC (CD3, 14, 15, 16, 20, 57)

CD11c-APC / FDF03-PE

B **TONSIL**

CD4-Cy5 / Lineage-FITC (CD3, 14, 15, 16, 20, 57)

CD11c-APC / FDF03-PE

FIGURE 6. Blood and tonsil CD11c⁺ DC, but not CD11c⁻ DC, express FDF03. *A*, Blood mononuclear cells were first depleted with anti-CD3 and anti-CD19 mAbs and magnetic beads, then stained with FITC-conjugated mAbs against CD3, CD14, CD15, CD16, CD20, and CD57 (lineage-FITC), peridinin chlorophyl protein-conjugated anti-HLA-DR mAb, APC-conjugated CD11c mAb, and biotin-labeled anti-FDF03 mAb 36H2 revealed by PE-conjugated streptavidin. Following total cell acquisition, the expression of FDF03 vs CD11c was analyzed on HLA-DR^{high}/lineage-FITC⁻ DC (gate in left dot plot). *B*, Total tonsil cells were first depleted with anti-CD3 and anti-CD19 mAbs and magnetic beads, then stained with FITC-conjugated mAbs against CD3, CD14, CD15, CD16, CD20, and CD57 (lineage-FITC), PE-Cy5-conjugated anti-CD4 mAb, APC-conjugated CD11c mAb, and biotin-labeled anti-FDF03 mAb 36H2 revealed by PE-conjugated streptavidin. Following acquisition, the expression of FDF03 vs CD11c was analyzed on CD4⁺/lineage-FITC⁻ DC (gate in left dot plot). Quadrant locations in FDF03 vs CD11c dot plots were determined according to the nonspecific fluorescence intensity obtained with APC-conjugated mouse and biotinylated rat control mAbs on HLA-DR^{high}/lineage-FITC⁻ (in *A*) or CD4⁺/lineage-FITC⁻ (in *B*) cells. Data presented are representative of three experiments.

regulate monocyte differentiation. To do this, blood monocytes were cultured with GM-CSF alone or GM-CSF plus IL-4, in the presence of anti-FDF03 mAb 36H2 or anti-LAIR-1 mAb DX26, together with goat F(ab')₂ anti-mouse/rat IgG used as cross-linker. As previously described (30, 50), GM-CSF rapidly down-regulated the expression of CD14 on monocytes, but induced expression of CD1a, as determined by flow cytometry at day 2 of culture (control mAb in Fig. 9*A*). Engagement of FDF03 by mAb 36H2 only weakly decreased CD1a expression and did not inhibit CD14 down-regulation whether the cells were cultured with GM-CSF alone (Fig. 9*A*, *left panel*) or in the presence of IL-4 (Fig. 9*A*, *right panel*). In contrast, and as expected, down-regulation of CD14 and induction of CD1a expression by GM-CSF was almost completely blocked by engagement of LAIR-1 with mAb DX26, even in the presence of IL-4 (Fig. 9*A*). Similar results (lack of inhibition by FDF03 but blockade by LAIR-1 cross-linking) were obtained after 6 days of culture with GM-CSF and were also observed for GM-CSF-induced up-regulation of CD1b and MHC class II molecules (data not shown). Moreover, cross-linking of FDF03 did not modify the percentage of viable cells recovered after 6 days of culture
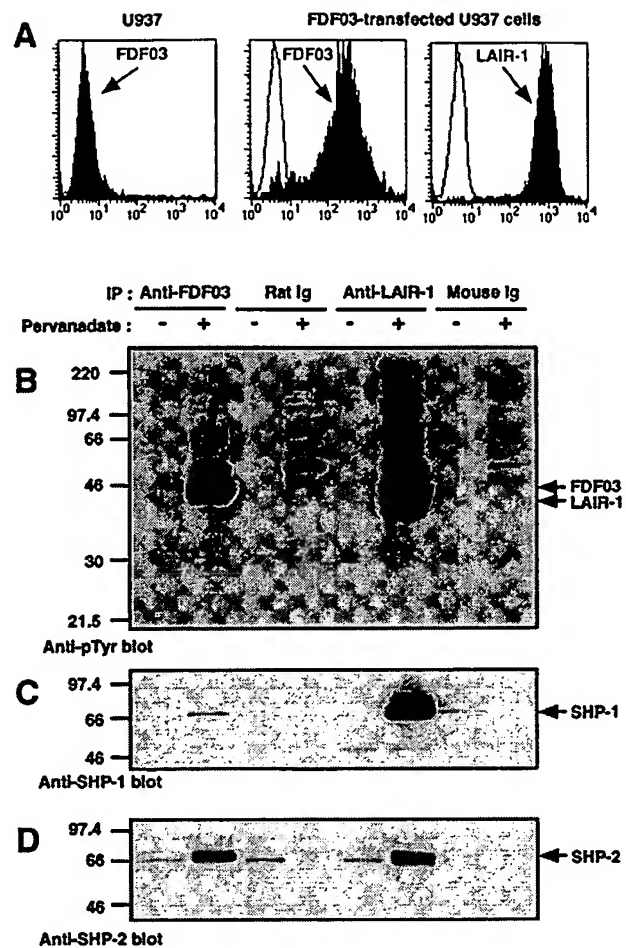

A U937 | FDF03-transfected U937 cells

FDF03 | FDF03 | LAIR-1

IP : Anti-FDF03 Rat Ig Anti-LAIR-1 Mouse Ig
Pervanadate : − + − + − + − +

B 220 97.4 66 46 30 21.5 — FDF03, LAIR-1
Anti-pTyr blot

C 97.4 66 46 — SHP-1
Anti-SHP-1 blot

D 97.4 66 46 — SHP-2
Anti-SHP-2 blot

FIGURE 7. FDF03 and LAIR-1 are tyrosine-phosphorylated and recruit SHP-1 and SHP-2 in pervanadate-activated U937 cells. *A*, Expression of FDF03 and LAIR-1 on U937 cells. U937 cells were transfected with FDF03 cDNA, then positively selected for FDF03 expression by flow cytometry after staining with mAb 36H2. Filled histograms represent surface expression of FDF03 or LAIR-1 (staining with mAb DX26) on transfected cells after four successive rounds of FACS sorting and culture. Unfilled histograms show staining obtained with a rat (for FDF03) or a mouse (for LAIR-1) IgG control mAb. *B–D*, FDF03-transfected U937 cells were unstimulated (−) or stimulated (+) for 5 min with sodium pervanadate and then lysed in 1% Nonidet P-40 lysis buffer. Lysates were immunoprecipitated with anti-FDF03 mAb 36H2 or control rat IgG, or with anti-LAIR-1 mAb or control mouse IgG. After SDS-PAGE and Western blots (precipitate from lysate of 30 × 10⁶ cells/line), precipitated proteins were analyzed using Abs specific for (*B*) proteins phosphorylated on tyrosines (anti-pTyr); (*C*) SHP-1 (anti-SHP-1); and (*D*) SHP-2 (anti-SHP-2).

in the presence of GM-CSF with or without IL-4, while cross-linking of LAIR-1 resulted in a decrease in cell viability (Fig. 9*B*). Thus, engagement of LAIR-1, but not of FDF03, inhibits differentiation of monocytes into DC, most likely by interfering with the GM-CSF receptor signaling pathway (26).

Discussion

In this report, we have described FDF03, a novel inhibitory receptor of the Ig-SF. The FDF03 extracellular domain has no significant homology to other members of the Ig-SF that also contain a single Ig-like domain of the V-set and that represent putative ITIM-bearing or activation receptors such as the PD-1 molecule (51), the CMRF-35 and CMRF-35-H9 pair of molecules (52, 53),

FIGURE 8. Cross-linking of FDF03 inhibits CD32/FcγRII-induced calcium mobilization in U937 cells. FDF03-transfected U937 cells were loaded with Indo-1 AM then stored at room temperature before analysis on FACStar^Plus flow cytometer using an argon laser for UV excitation. For each experiment, aliquots of cells were incubated at 37°C until the baseline of violet vs blue fluorescent emissions (405/530 nm ratio) was stable. Then 10 μg of Abs to be tested were added (arrowhead in each figure) and the 405/530 nm ratio was recorded for 120 s. After a further incubation of 120 s, 20 μg/ml of cross-linker were added (goat F(ab')₂ anti-mouse/rat IgG, arrow in each figure), and the 405/530 nm fluorescence ratio was recorded for the remaining time. Data showed are representative of three experiments.
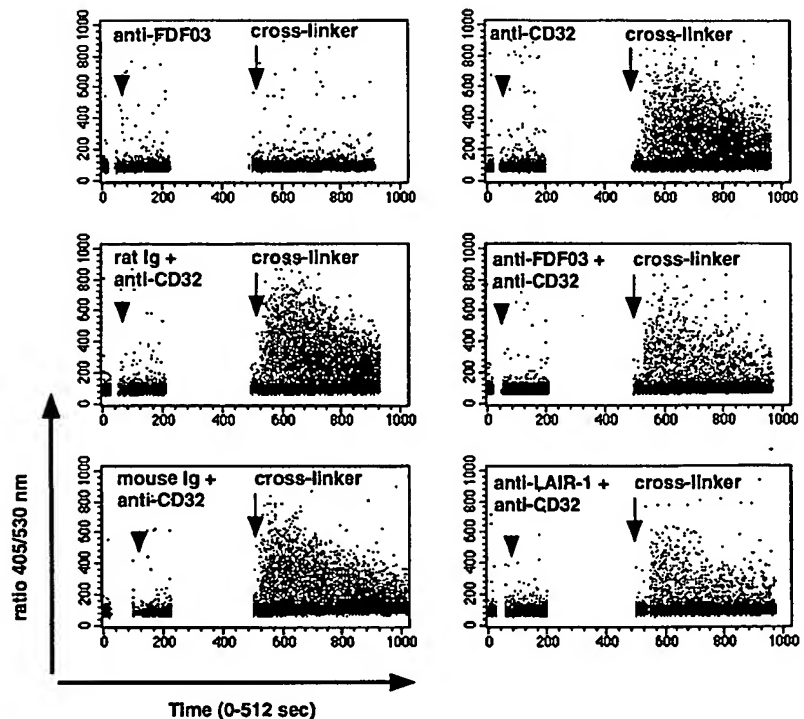
and the NKp44 receptor (54). It is interesting to note that these molecules are encoded by genes localized on different human chromosomes, with the PD-1 gene on chromosome 2q37 (51), the NKp44 gene on chromosome 6 (54), and the FDF03 gene on chromosome 7q22 (the present study). This contrasts with the clustered localization on human chromosome 19q13.4 of genes encoding the inhibitory receptors KIRs (55), ILTs/LIRs/MIRs (13, 16, 19, 56), LAIR-1 (25), and NKp46 (57). All of these molecules carry one or several Ig domain(s) of the C2-set and are related in sequence to bovine Fcγ2R and human FcαR/CD89, the latter also mapping to chromosome 19q13.4 (58). Moreover, genes encoding members of the recently defined sialic acid-binding Ig-like lectins (Siglecs) are localized close to this region on human chromosome 19. In particular, this includes CD33/Siglec-3, CD22/Siglec-2, OB-BP-1/Siglec-6, and OB-BP-2/Siglec-5 (59, 60) that contain intracytoplasmic ITIM or ITIM-like sequences and are composed of one N-terminal V-type Ig domain followed by one or several membrane proximal Ig domain(s) of the C2 type.

We have shown that FDF03 is preferentially expressed in immune tissues and has a restricted expression in cells of the myelomonocytic lineage including monocytes, macrophages, DC, and granulocytes. Flow cytometric analysis demonstrated that FDF03 was expressed by the majority of the CD11c⁺ DC both in blood and tonsils, but not by the CD11c⁻ DC precursors. This preferential expression of FDF03 was confirmed at the mRNA levels because neither FDF03 nor FDF03-ΔTM messengers could be amplified by RT-PCR in purified blood CD11c⁻ DC, while both cDNAs were detected in CD11c⁺ DC (data not shown). This is in agreement with the restricted expression of FDF03 in cells of the myeloid origin, because blood and tonsil CD11c⁻ DC precursors, corresponding to the previously so called plasmacytoid T cells or plasmacytoid monocytes, do not express myelomonocytic markers such as CD14, CD13, and CD33 (43, 44, 46, 61) and have been proposed to be of lymphoid origin. On in vitro-generated DC, FDF03 was preferentially expressed by monocyte-derived DC and by DC derived from the CD14⁺/CD1a⁻ precursors that display

features of the interstitial/dermal-type DC, rather than by the CD1a⁺ subsets of cells that may represent precursors of epidermal/Langerhans cells (29, 40). In keeping with this, anti-FDF03 mAb did not stain Langerhans cells in skin epithelium nor immature CD1a⁺ Langerhans-like DC in tonsil epithelium, and we failed to detect FDF03 mRNA in purified skin Langerhans cells (data not shown). Moreover, FDF03 expression on DC was not down-regulated by signals inducing DC maturation such as LPS or CD40 ligand, suggesting that FDF03 can be expressed by both immature and mature DC. However, immunohistochemical analysis performed on frozen tonsil sections indicated that mAb 36H2 stained neither the CD11c⁺ germinal center DC in B cell follicles (34) nor the mature interdigitating DC in T cell areas (data not shown). This suggests that, in situ, these DC express very low, if any, levels of FDF03, but we cannot exclude that a low sensitivity of our immunostaining procedures may decrease FDF03 detection on tissue sections. However, FDF03 was strongly expressed by cells localized in close contact to the epithelial crypts of the tonsils, some of them expressing the CD11c marker (data not shown). We are currently isolating and characterizing the FDF03-expressing cell populations from tonsils.

The presence of ITIM-like sequences in the FDF03 cytoplasmic tail suggested that FDF03 might principally function as an inhibitory receptor of cell function and activation, as generally described for ITIM-bearing molecules (1, 3, 5, 6). This was confirmed by demonstrating that FDF03 blocked intracellular Ca²⁺ mobilization induced by CD32/FcγRII aggregation in FDF03-transfected U937 cells, as did the ITIM-bearing receptor LAIR-1/p40. However, while cross-linking of LAIR-1 strongly inhibited the effects of GM-CSF and IL-4 on monocyte differentiation and survival, cross-linking of FDF03 only weakly decreased expression of CD1a and did not block down-regulation of CD14, nor affected survival of monocytes. While we cannot exclude that engagement of FDF03 by mAb 36H2 was not optimal in our experimental protocols, these results suggest that FDF03 may have function(s) different to that of the broadly expressed LAIR-1/p40
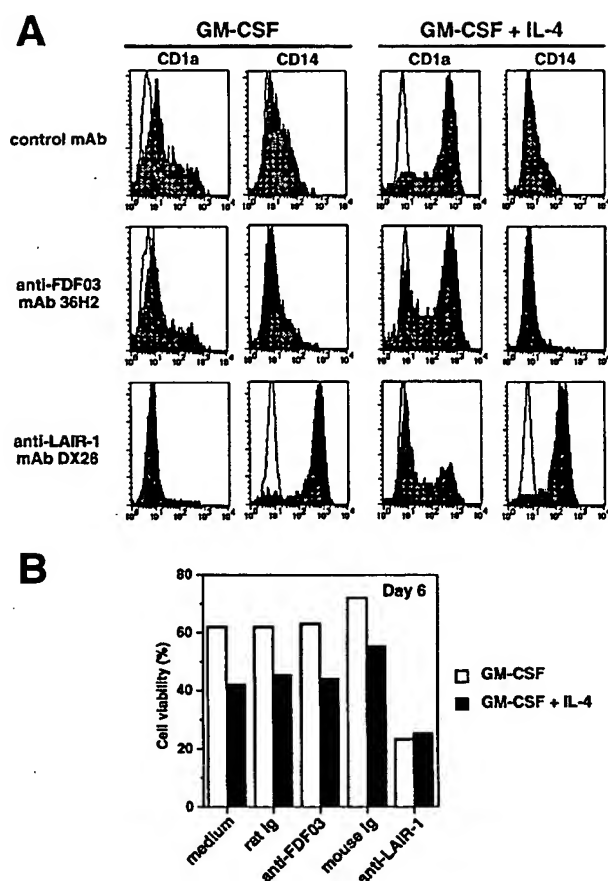
FIGURE 9. Cross-linking of FDF03 does not inhibit the effects of GM-CSF on monocytes. Blood monocytes were cultured with GM-CSF alone or GM-CSF plus IL-4, in the presence of anti-FDF03 mAb 36H2 or anti-LAIR-1 mAb DX26 or with rat or mouse control mAb, respectively. Abs (final concentration of 10 μg/ml) were added at the onset of the culture together with 10 μg/ml of goat F(ab')$_2$ anti-mouse IgG that cross-reacts with rat IgG and that was used as cross-linker. A, On day 2, cells were collected and expression of CD1a and CD14 was determined by flow cytometry following staining with FITC-conjugated anti-CD1a or anti-CD14 mAb. Filled histograms represent CD14 or CD1a expression on cells treated with control IgG, anti-FDF03, or anti-LAIR-1 mAb. Expression of CD1a and CD14 was equivalent on cells cultured with mouse or rat control IgG, and only results with rat IgG are shown (control mAb). Unfilled histograms represent nonspecific staining obtained with a FITC-conjugated negative control mAb. B, On day 6 of culture, cell viability was determined by flow cytometry after staining with propidium iodide. Results are expressed as percentage of viable cells (propidium iodide-negative cells) and are representative of one experiment of three.

molecule (25, 26). Moreover, this discrepancy between FDF03 and LAIR-1 inhibitory activities might be explained by the stronger association of LAIR-1 with SHP-1 (as observed in U937 cells), because SHP-1 has been implicated in the down-regulation of signaling by receptors for erythropoietin, IL-3, and GM-CSF (62–64). Equally, we were unable to demonstrate that engagement of FDF03 negatively regulated functions of FDF03-expressing cells (monocytes and DC) using different assays including proliferation of CD34$^+$ progenitor cells in response to SCF and GM-CSF or IL-3, or DC activation and maturation induced by CD40 ligand or LPS as measured by phenotypic parameters (increase expression of CD80, CD86, CD83, MHC class II, and CD40) and cytokine secretion (IL-12, IL-8, and IL-6) (data not shown). Moreover, anti-FDF03 mAb 36H2 did not affect T cell proliferation induced in

allo-reactions with in vitro-derived DC (data not shown). Finally, unlike some ITIM-bearing receptors such as ILT3 and FcγRIIB (15, 22, 23), FDF03 was not internalized in monocytes and in vitro-derived DC, suggesting that FDF03 does not function as an endocytic receptor for Ag capture and presentation (data not shown).

The cytoplasmic tail of FDF03 contains three tyrosine-based motifs that, following phosphorylation, may represent binding sites for SH2 domain-containing signaling molecules (38). However, the membrane proximal tyrosine in YENI motif is not present within the cytoplasmic region of the mouse homologue of FDF03, while both human and mouse proteins display an ITIM-like tandem IVYASL-x23-TLYSVL and IVYASI-x23-TVYSIV, respectively, which are closest to the motif allowing high-affinity binding to the tandem SH2 domains of SHP-2 (65). We have shown that FDF03 was tyrosine phosphorylated in pervanadate-treated transfected U937 cells and associated with SHP-2. We have also observed association of FDF03 with SHP-1, but apparently with a weaker efficiency when compared with SHP-1 recruitment by the LAIR-1 receptor in the same cells. In contrast to FDF03, but similarly to SHP-1 recruiting inhibitory receptors such as the KIRs (3, 4), the LAIR-1 cytoplasmic tail contains two typical ITIMs in the tandem VTYAQL-x24-ITYAAV (25). Interestingly, it has been shown that the hydrophobic residue (I/V/L) at position −2 upstream of phosphorylated tyrosine in ITIM is critical for binding to and activation of SHP-1 by peptides as well as the cytoplasmic tail of the KIR (47, 66). Moreover, as recently shown for the KIR molecules (67), the N-terminal and C-terminal ITIMs may have different efficiencies to associate with phosphatases in vivo, because the N-terminal ITIM was found to be sufficient to recruit SHP-2 but not SHP-1, while both ITIMs were required to recruit SHP-1. In keeping with this, the recently described T cell transmembrane adaptor protein SIT, which contains only one I/VxYxxV ITIM among its four cytoplasmic YxxL/V tyrosine motifs, associates in vivo with SHP-2, but not with SHP-1 and SHIP (68). Thus, this suggests that the presence of a threonine (T) instead of a hydrophobic residue at position −2 of the C-terminal tyrosine-based motif of FDF03 (TLYSVL), may decrease its potential association with SHP-1 but not with SHP-2, as seen in our study. It should be noted that a similar motif (TVYSIV) is also present at the C-terminal end of mouse FDF03. Interestingly, a threonine is also present at position −2 of the second tandem tyrosine motif YxxV/L of the molecules SHPS-1/SIRPα, CD31/PECAM-1, and CD33 that have been primarily found to associate with SHP-2 as well as, in some studies, with SHP-1 (8, 9, 69–72). Moreover, the TxYxxV/I sequence is present in the cytoplasmic tail of the two CD33-related Siglecs, OB-BP-1/Siglec-6 and OB-BP-2/Siglec-5 (59, 60), and in human and mouse PD-1 molecules (51, 73), but it has not been yet demonstrated whether these molecules can recruit SHP-1 and/or SHP-2. Finally, four TxYxxV/I motifs are present in the intracellular domain of human and mouse 2B4 molecules (74, 75), and three are in the signaling lymphocytic activation molecule SLAM (76), both receptors preferentially recruiting SHP-2. In both SLAM and 2B4 molecules, these motifs also represent docking sites for the SLAM-associated protein SAP (75, 77), an SH2-containing adaptor protein that competes with SHP-2 for recruitment to SLAM and 2B4, and is defective in the inherited X-linked lymphoproliferative syndrome XLP (77–79). Thus, although SAP does not appear to be expressed in myeloid cells, it would be of interest to analyze whether FDF03 may also associate with SAP or with homologous protein such as EAT-2 that recognizes a similar TxYxxV/I motif (80).

In conclusion, FDF03 represents a novel member of the Ig-SF selectively expressed in cells of the myelomonocytic lineage, including monocytes/macrophages, granulocytes, and DC that express the CD11c marker. Tyrosine-phosphorylated FDF03 preferentially recruits SHP-2 and can function as an inhibitory receptor, at least when overexpressed in the monocytic U937 cell line. However, we cannot exclude that FDF03 may have other regulatory functions because recruitment of SHP-2 may also mediate cellular activation (81–83). Of note, by screening molecules associating with SHP-1, Mousseau et al. (84) recently identified a protein designated PIRLα (for paired Ig-like receptor, accession no. AF161080) whose amino acid and cDNA sequences are identical with that of FDF03. The description of the genomic organization of PIRLα/FDF03 (84) clearly confirms that FDF03-ΔTM and FDF-M14 are produced by alternative splicing of FDF03/PIRLα cDNA. It should be noted that all the primers and probes used in our study are specific for FDF03 and cannot hybridize with the nucleotide sequence of PIRLβ (accession no. AF161081), a putative activating counterpart of PIRLα/FDF03 described by Mousseau et al. (84), the gene of which being also localized on chromosome 7q22. Of interest, this localization is close to a region associated with several chromosomal abnormalities relating to tumors and particularly with deletion in myelodysplastic syndrome and acute myeloid leukemia (85–87). We are currently analyzing whether abnormalities in the FDF03 gene locus may be associated with such malignancies.

Acknowledgments

References

1. Burshtyn, D., and E. Long. 1997. Regulation through inhibitory receptors: lessons from natural killer. *Trends Cell. Biol. 7:473.*
2. Cambier, J. C. 1997. Inhibitory receptors abound? *Proc. Natl. Acad. Sci. USA 94:5993.*
3. Lanier, L. L. 1998. NK cell receptors. *Annu. Rev. Immunol. 16:359.*
4. Renard, V., A. Cambiaggi, F. Vely, M. Blery, L. Olcese, S. Olivero, M. Bouchet, and E. Vivier. 1997. Transduction of cytotoxic signals in natural killer cells: a general model of fine tuning between activatory and inhibitory pathways in lymphocytes. *Immunol. Rev. 155:205.*
5. Vivier, E., and M. Daëron. 1997. Immunoreceptor tyrosine-based inhibition motifs. *Immunol. Today 18:286.*
6. Long, E. O. 1999. Regulation of immune responses through inhibitory receptors. *Annu. Rev. Immunol. 17:875.*
7. Yokoyama, W. M. 1997. What goes up must come down: the emerging spectrum of inhibitory receptors. *J. Exp. Med. 186:1803.*
8. Fujioka, Y., T. Matozaki, T. Noguchi, A. Iwamatsu, T. Yamao, N. Takahashi, M. Tsuda, T. Takada, and M. Kasuga. 1996. A novel membrane glycoprotein, SHPS-1, that binds the SH2-domain-containing protein tyrosine phosphatase SHP-2 in response to mitogens and cell adhesion. *Mol. Cell. Biol. 16:6887.*
9. Kharitonenkov, A., Z. Chen, I. Sures, H. Wang, J. Schilling, and A. Ullrich. 1997. A family of proteins that inhibit signalling through tyrosine kinase receptors. *Nature 386:181.*
10. Banchereau, J., and R. M. Steinman. 1998. Dendritic cells and the control of immunity. *Nature 392:245.*
11. Steinman, R. M. 1991. The dendritic cell system and its role in immunogenicity. *Annu. Rev. Immunol. 9:271.*
12. Bates, E. M., N. Fournier, E. Garcia, J. Valladeau, I. Durand, J. J. Pin, S. M. Zurawski, S. Patel, J. S. Abrams, S. Lebecque, P. Garrone, and S. Saeland. 1999. Antigen-presenting cells express DCIR, a novel C-type lectin surface receptor containing an immunoreceptor tyrosine-based inhibitory motif. *J. Immunol. 163:1973.*
13. Arm, J. P., C. Nwankwo, and K. F. Austen. 1997. Molecular identification of a novel family of human Ig superfamily members that possess immunoreceptor tyrosine-based inhibition motifs and homology to the mouse gp49B1 inhibitory receptor. *J. Immunol. 159:2342.*
14. Borges, L., M. L. Hsu, N. Fanger, M. Kubin, and D. Cosman. 1997. A family of human lymphoid and myeloid Ig-like receptors, some of which bind to MHC class I molecules. *J. Immunol. 159:5192.*
15. Cella, M., C. Dohring, J. Samaridis, M. Dessing, M. Brockhaus, A. Lanzavecchia, and M. Colonna. 1997. A novel inhibitory receptor (ILT3) expressed on monocytes, macrophages, and dendritic cells involved in antigen processing. *J. Exp. Med. 185:1743.*
16. Wagtmann, N., S. Rojo, E. Eichler, H. Mohrenweiser, and E. O. Long. 1997. A new human gene complex encoding the killer cell inhibitory receptors and related monocyte/macrophage receptors. *Curr. Biol. 7:615.*
17. Colonna, M., F. Navarro, T. Bellon, M. Llano, P. Garcia, J. Samaridis, L. Angman, M. Cella, and M. Lopez-Botet. 1997. A common inhibitory receptor for major histocompatibility complex class I molecules on human lymphoid and myelomonocytic cells. *J. Exp. Med. 186:1809.*
18. Colonna, M., J. Samaridis, M. Cella, L. Angman, R. L. Allen, C. A. O'Callaghan, R. Dunbar, G. S. Ogg, V. Cerundolo, and A. Rolink. 1998. Human myelomonocytic cells express an inhibitory receptor for classical and nonclassical MHC class I molecules. *J. Immunol. 160:3096.*
19. Cosman, D., N. Fanger, L. Borges, M. Kubin, W. Chin, L. Peterson, and M. L. Hsu. 1997. A novel immunoglobulin superfamily receptor for cellular and viral MHC class I molecules. *Immunity 7:273.*
20. Fanger, N. A., D. Cosman, L. Peterson, S. C. Braddy, C. R. Maliszewski, and L. Borges. 1998. The MHC class I binding proteins LIR-1 and LIR-2 inhibit Fc receptor-mediated signaling in monocytes. *Eur. J. Immunol. 28:3423.*
21. Cosman, D., N. Fanger, and L. Borges. 1999. Human cytomegalovirus, MHC class I and inhibitory signalling receptors: more questions than answers. *Immunol. Rev. 168:177.*
22. Amigorena, S., C. Bonnerot, J. R. Drake, D. Choquet, W. Hunziker, J. G. Guillet, P. Webster, C. Sautes, I. Mellman, and W. H. Fridman. 1992. Cytoplasmic domain heterogeneity and functions of IgG Fc receptors in B lymphocytes. *Science 256:1808.*
23. Daëron, M., O. Malbec, S. Latour, C. Bonnerot, D. M. Segal, and W. H. Fridman. 1993. Distinct intracytoplasmic sequences are required for endocytosis and phagocytosis via murine FcγRII in mast cells. *Int. Immunol. 5:1393.*
24. Marks, M. S., H. Ohno, T. Kirchhausen, and J. S. Bonifacino. 1997. Protein sorting by tyrosine-based signals: adapting to the Ys and werefores. *Trends Cell. Biol. 7:124.*
25. Meyaard, L., G. J. Adema, C. Chang, E. Woollatt, G. R. Sutherland, L. L. Lanier, and J. H. Phillips. 1997. LAIR-1, a novel inhibitory receptor expressed on human mononuclear leukocytes. *Immunity 7:283.*
26. Poggi, A., E. Tomasello, E. Ferrero, M. R. Zocchi, and L. Moretta. 1998. p40/LAIR-1 regulates the differentiation of peripheral blood precursors to dendritic cells induced by granulocyte-monocyte colony-stimulating factor. *Eur. J. Immunol. 28:2086.*
27. Garrone, P., E. M. Neidhardt, E. Garcia, L. Galibert, C. van Kooten, and J. Banchereau. 1995. Fas ligation induces apoptosis of CD40-activated human B lymphocytes. *J. Exp. Med. 182:1265.*
28. Caux, C., C. Dezutter-Dambuyant, D. Schmitt, and J. Banchereau. 1992. GM-CSF and TNF-α cooperate in the generation of dendritic Langerhans cells. *Nature 360:258.*
29. Caux, C., B. Vanbervliet, C. Massacrier, C. Dezutter-Dambuyant, B. de Saint-Vis, C. Jacquet, K. Yoneda, S. Imamura, D. Schmitt, and J. Banchereau. 1996. CD34+ hematopoietic progenitors from human cord blood differentiate along two independent dendritic cell pathways in response to GM-CSF+TNF-α. *J. Exp. Med. 184:695.*
30. Sallusto, F., and A. Lanzavecchia. 1994. Efficient presentation of soluble antigen by cultured human dendritic cells is maintained by granulocyte/macrophage colony-stimulating factor plus interleukin 4 and downregulated by tumor necrosis factor α. *J. Exp. Med. 179:1109.*
31. Sambrook, J., E. F. Fritsch, and T. Maniatis. 1989. *Molecular Cloning: A Laboratory Manual*, 2nd Ed. Cold Spring Harbor Lab. Press, Plainview, NY.
32. Chomczynski, P., and N. Sacchi. 1987. Single-step method of RNA isolation by acid guanidium thiocyanate-phenol-chloroform extraction. *Anal. Biochem. 162: 156.*
33. Castro, A. G., T. M. Hauser, B. G. Cocks, J. Abrams, S. Zurawski, T. Churakova, F. Zonin, D. Robinson, S. G. Tangye, G. Aversa, et al. 1999. Molecular and functional characterization of mouse signaling lymphocytic activation molecule (SLAM): differential expression and responsiveness in Th1 and Th2 Cells. *J. Immunol. 163:5860.*
34. Grouard, G., I. Durand, L. Filgueira, J. Banchereau, and Y. J. Liu. 1996. Dendritic cells capable of stimulating T cells in germinal centers. *Nature 384:364.*
35. Phillips, J. H., C. Chang, J. Mattson, J. E. Gumperz, P. Parham, and L. L. Lanier. 1996. CD94 and a novel associated protein (94AP) form a NK cell receptor involved in the recognition of HLA-A, HLA-B, and HLA-C allotypes. *Immunity 5:163.*
36. Williams, A. F., and A. N. Barclay. 1988. The immunoglobulin superfamily-domains for cell surface recognition. *Annu. Rev. Immunol. 6:381.*
37. Smith, D. K., and H. Xue. 1997. Sequence profiles of immunoglobulin and immunoglobulin-like domains. *J. Mol. Biol. 274:530.*
38. Songyang, Z., S. E. Shoelson, J. McGlade, P. Olivier, T. Pawson, X. R. Bustelo, M. Barbacid, H. Sabe, H. Hanafusa, T. Yi, et al. 1994. Specific motifs recognized by the SH2 domains of Csk, 3BP2, fps/fes, GRB-2, HCP, SHC, Syk, and Vav. *Mol. Cell. Biol. 14:2777.*
39. Burshtyn, D. N., A. M. Scharenberg, N. Wagtmann, S. Rajagopalan, K. Berrada, T. Yi, J. P. Kinet, and E. O. Long. 1996. Recruitment of tyrosine phosphatase HCP by the killer cell inhibitory receptor. *Immunity 4:77.*
40. Caux, C., and J. Banchereau. 1996. In vitro regulation of dendritic cell development and function. In *Blood Cell Biochemistry.* T. Whetton, and J. Gordon, eds. Plenum Press, London, p. 263.
41. Cella, M., F. Sallusto, and A. Lanzavecchia. 1997. Origin, maturation and antigen presenting function of dendritic cells. *Curr. Opin. Immunol. 9:10.*

42. Sallusto, F., M. Cella, C. Danieli, and A. Lanzavecchia. 1995. Dendritic cells use macropinocytosis and the mannose receptor to concentrate macromolecules in the major histocompatibility complex class II compartment: down-regulation by cytokines and bacterial products. *J. Exp. Med. 182:389.*

43. Grouard, G., M. C. Rissoan, L. Filgueira, I. Durand, J. Banchereau, and Y. J. Liu. 1997. The enigmatic plasmacytoid T cells develop into dendritic cells with IL-3 and CD40-ligand. *J. Exp. Med. 185:1101.*

44. O'Doherty, U., R. M. Steinman, M. Peng, P. U. Cameron, S. Gezelter, I. Kopeloff, W. J. Swiggard, M. Pope, and N. Bhardwaj. 1993. Dendritic cells freshly isolated from human blood express CD4 and mature into typical immunostimulatory dendritic cells after culture in monocyte-conditioned medium. *J. Exp. Med. 178:1067.*

45. Olweus, J., A. BitMansour, R. Warnke, P. A. Thompson, J. Carballido, L. J. Picker, and F. Lund-Johansen. 1997. Dendritic cell ontogeny: a human dendritic cell lineage of myeloid origin. *Proc. Natl. Acad. Sci. USA 94:12551.*

46. Thomas, R., L. S. Davis, and P. E. Lipsky. 1993. Isolation and characterization of human peripheral blood dendritic cells. *J. Immunol. 150:821.*

47. Burshtyn, D. N., W. Yang, T. Yi, and E. O. Long. 1997. A novel phosphotyrosine motif with a critical amino acid at position −2 for the SH2 domain-mediated activation of the tyrosine phosphatase SHP- 1. *J. Biol. Chem. 272:13066.*

48. Daëron, M., S. Latour, O. Malbec, E. Espinosa, P. Pina, S. Pasmans, and W. H. W. H. Fridman. 1995. The same tyrosine-based inhibition motif, in the intracytoplasmic domain of FcγRIIB, regulates negatively BCR-, TCR-, and FcR- dependent cell activation. *Immunity 3:635.*

49. Warmerdam, P. A., I. E. van den Herik-Oudijk, P. W. Parren, N. A. Westerdaal, J. G. van de Winkel, and P. J. Capel. 1993. Interaction of a human FcγRIIb1 (CD32) isoform with murine and human IgG subclasses. *Int. Immunol. 5:239.*

50. Kasinrerk, W., T. Baumruker, O. Majdic, W. Knapp, and H. Stockinger. 1993. CD1 molecule expression on human monocytes induced by granulocyte-macrophage colony-stimulating factor. *J. Immunol. 150:579.*

51. Finger, L. R., J. Pu, R. Wasserman, R. Vibhakar, E. Louie, R. R. Hardy, P. D. Burrows, and L. G. Billips. 1997. The human PD-1 gene: complete cDNA, genomic organization, and developmentally regulated expression in B cell progenitors. [Published erratum appears in *1997 Gene 203:253.*] *Gene 197:177.*

52. Green, B. J., G. J. Clark, and D. N. Hart. 1998. The CMRF-35 mAb recognizes a second leukocyte membrane molecule with a domain similar to the poly Ig receptor. *Int. Immunol. 10:891.*

53. Jackson, D. G., D. N. Hart, G. Starling, and J. I. Bell. 1992. Molecular cloning of a novel member of the immunoglobulin gene superfamily homologous to the polymeric immunoglobulin receptor. *Eur. J. Immunol. 22:1157.*

54. Cantoni, C., C. Bottino, M. Vitale, A. Pessino, R. Augugliaro, A. Malaspina, S. Parolini, L. Moretta, A. Moretta, and R. Biassoni. 1999. NKp44, a triggering receptor involved in tumor cell lysis by activated human natural killer cells, is a novel member of the immunoglobulin superfamily. *J. Exp. Med. 189:787.*

55. Dupont, B., A. Selvakumar, and U. Steffens. 1997. The killer cell inhibitory receptor genomic region on human chromosome 19q13. 4. *Tissue Antigens 49: 557.*

56. Samaridis, J., and M. Colonna. 1997. Cloning of novel immunoglobulin superfamily receptors expressed on human myeloid and lymphoid cells: structural evidence for new stimulatory and inhibitory pathways. *Eur. J. Immunol. 27:660.*

57. Pessino, A., S. Sivori, C. Bottino, A. Malaspina, L. Morelli, L. Moretta, R. Biassoni, and A. Moretta. 1998. Molecular cloning of NKp46: a novel member of the immunoglobulin superfamily involved in triggering of natural cytotoxicity. *J. Exp. Med. 188:953.*

58. Kremer, E. J., V. Kalatzis, E. Baker, D. F. Callen, G. R. Sutherland, and C. R. Maliszewski. 1992. The gene for the human IgA Fc receptor maps to 19q13.4. *Hum. Genet. 89:107.*

59. Cornish, A. L., S. Freeman, G. Forbes, J. Ni, M. Zhang, M. Cepeda, R. Gentz, M. Augustus, K. C. Carter, and P. R. Crocker. 1998. Characterization of siglec-5, a novel glycoprotein expressed on myeloid cells related to CD33. *Blood 92:2123.*

60. Patel, N., E. C. Brinkman-Van der Linden, S. W. Altmann, K. Gish, S. Balasubramanian, J. C. Timans, D. Peterson, M. P. Bell, J. F. Bazan, A. Varki, and R. A. Kastelein. 1999. OB-BP1/Siglec-6, a leptin- and sialic acid-binding protein of the immunoglobulin superfamily. *J. Biol. Chem. 274:22729.*

61. O'Doherty, U., M. Peng, S. Gezelter, W. J. Swiggard, M. Betjes, N. Bhardwaj, and R. M. Steinman. 1994. Human blood contains two subsets of dendritic cells, one immunologically mature and the other immature. *Immunology 82:487.*

62. Bone, H., U. Dechert, F. Jirik, J. W. Schrader, and M. J. Welham. 1997. SHP1 and SHP2 protein-tyrosine phosphatases associate with β-chain after interleukin-3-induced receptor tyrosine phosphorylation: identification of potential binding sites and substrates. *J. Biol. Chem. 272:14470.*

63. Jiao, H., W. Yang, K. Berrada, M. Tabrizi, L. Shultz, and T. Yi. 1997. Macrophages from motheaten and viable motheaten mutant mice show increased proliferative responses to GM-CSF: detection of potential HCP substrates in GM-CSF signal transduction. *Exp. Hematol. 25:592.*

64. Yang, W., M. Tabrizi, K. Berrada, and T. Yi. 1998. SHP-1 phosphatase C-terminus interacts with novel substrates p32/p30 during erythropoietin and interleukin-3 mitogenic responses. *Blood 91:3746.*

65. Hof, P., S. Pluskey, S. Dhe-Paganon, M. J. Eck, and S. E. Shoelson. 1998. Crystal structure of the tyrosine phosphatase SHP-2. *Cell 92:441.*

66. Vely, F., S. Olivero, L. Olcese, A. Moretta, J. E. Damen, L. Liu, G. Krystal, J. C. Cambier, M. Daeron, and E. Vivier. 1997. Differential association of phosphatases with hematopoietic co-receptors bearing immunoreceptor tyrosine-based inhibition motifs. *Eur. J. Immunol. 27:1994.*

67. Bruhns, P., P. Marchetti, W. H. Fridman, E. Vivier, and M. Daeron. 1999. Differential roles of N- and C-terminal immunoreceptor tyrosine-based inhibition motifs during inhibition of cell activation by killer cell inhibitory receptors. *J. Immunol. 162:3168.*

68. Marie-Cardine, A., H. Kirchgessner, E. Bruyns, A. Shevchenko, M. Mann, F. Autschbach, S. Ratnofsky, S. Meuer, and B. Schraven. 1999. SHP2-interacting transmembrane adaptor protein (SIT), a novel disulfide- linked dimer regulating human T cell activation. *J. Exp. Med. 189:1181.*

69. Jackson, D. E., K. R. Kupcho, and P. J. Newman. 1997. Characterization of phosphotyrosine binding motifs in the cytoplasmic domain of platelet/endothelial cell adhesion molecule-1 (PECAM-1) that are required for the cellular association and activation of the protein-tyrosine phosphatase, SHP-2. *J. Biol. Chem. 272: 24868.*

70. Newton-Nash, D. K., and P. J. Newman. 1999. A new role for platelet-endothelial cell adhesion molecule-1 (CD31): inhibition of TCR-mediated signal transduction. *J. Immunol. 163:682.*

71. Sagawa, K., T. Kimura, M. Swieter, and R. P. Siraganian. 1997. The protein-tyrosine phosphatase SHP-2 associates with tyrosine-phosphorylated adhesion molecule PECAM-1 (CD31). *J. Biol. Chem. 272:31086.*

72. Taylor, V. C., C. D. Buckley, M. Douglas, A. J. Cody, D. L. Simmons, and S. D. Freeman. 1999. The myeloid-specific sialic acid-binding receptor, CD33, associates with the protein-tyrosine phosphatases, SHP-1 and SHP-2. *J. Biol. Chem. 274:11505.*

73. Ishida, Y., Y. Agata, K. Shibahara, and T. Honjo. 1992. Induced expression of PD-1, a novel member of the immunoglobulin gene superfamily, upon programmed cell death. *EMBO J. 11:3887.*

74. Mathew, P. A., B. A. Garni-Wagner, K. Land, A. Takashima, E. Stoneman, M. Bennett, and V. Kumar. 1993. Cloning and characterization of the 2B4 gene encoding a molecule associated with non-MHC-restricted killing mediated by activated natural killer cells and T cells. *J. Immunol. 151:5328.*

75. Tangye, S. G., S. Lazetic, E. Woollatt, G. R. Sutherland, L. L. Lanier, and J. H. Phillips. 1999. Human 2B4, an activating NK cell receptor, recruits the protein tyrosine phosphatase SHP-2 and the adaptor signaling protein SAP. *J. Immunol. 162:6981.*

76. Cocks, B. G., C. C. Chang, J. M. Carballido, H. Yssel, J. E. de Vries, and G. Aversa. 1995. A novel receptor involved in T-cell activation. *Nature 376:260.*

77. Sayos, J., C. Wu, M. Morra, N. Wang, X. Zhang, D. Allen, S. van Schaik, L. Notarangelo, R. Geha, M. G. Roncarolo, et al. 1998. The X-linked lymphoproliferative-disease gene product SAP regulates signals induced through the co-receptor SLAM. *Nature 395:462.*

78. Coffey, A. J., R. A. Brooksbank, O. Brandau, T. Oohashi, G. R. Howell, J. M. Bye, A. P. Cahn, J. Durham, P. Heath, P. Wray, et al. 1998. Host response to EBV infection in X-linked lymphoproliferative disease results from mutations in an SH2-domain encoding gene. *Nat. Genet. 20:129.*

79. Nichols, K. E., D. P. Harkin, S. Levitz, M. Krainer, K. A. Kolquist, C. Genovese, A. Bernard, M. Ferguson, L. Zuo, E. Snyder, et al. 1998. Inactivating mutations in an SH2 domain-encoding gene in X-linked lymphoproliferative syndrome. *Proc. Natl. Acad. Sci. USA 95:13765.*

80. Poy, F., M. B. Yaffe, J. Sayos, K. Saxena, M. Morra, J. Sumegi, L. C. Cantley, C. Terhorst, and M. J. Eck. 1999. Crystal structures of the XLP protein SAP reveal a class of SH2 domains with extended, phosphotyrosine-independent sequence recognition. *Mol. Cell. 4:555.*

81. Gadina, M., L. M. Stancato, C. M. Bacon, A. C. Larner, and J. J. O'Shea. 1998. Involvement of SHP-2 in multiple aspects of IL-2 signaling: evidence for a positive regulatory role. *J. Immunol. 160:4657.*

82. Neel, B. G. 1997. Role of phosphatases in lymphocyte activation. *Curr. Opin. Immunol. 9:405.*

83. Qu, C. K., Z. Q. Shi, R. Shen, F. Y. Tsai, S. H. Orkin, and G. S. Feng. 1997. A deletion mutation in the SH2-N domain of Shp-2 severely suppresses hematopoietic cell development. *Mol. Cell. Biol. 17:5499.*

84. Mousseau, D. D., D. Banville, D. L'Abbé, P. Bouchard, and S.-H. Shen. 2000. PILRα, a novel immunoreceptor tyrosine-based inhibitory motif-bearing protein, recruits SHP-1 upon tyrosine phosphorylation and is paired with the truncated counterpart PIRLβ. *J. Biol. Chem. 275:4467.*

85. Johnson, E. J., S. W. Scherer, L. Osborne, L. C. Tsui, D. Oscier, S. Mould, and F. E. Cotter. 1996. Molecular definition of a narrow interval at 7q22.1 associated with myelodysplasia. *Blood 87:3579.*

86. Le Beau, M. M., R. Espinosa, 3rd, E. M. Davis, J. D. Eisenbart, R. A. Larson, and E. D. Green. 1996. Cytogenetic and molecular delineation of a region of chromosome 7 commonly deleted in malignant myeloid diseases. *Blood 88:1930.*

87. Willman, C. L. 1998. Molecular genetic features of myelodysplastic syndromes (MDS). [Published erratum appears in *1999 Leukemia 13:315.*] *Leukemia 12(Suppl. 1):S2.*

PILRα, a Novel Immunoreceptor Tyrosine-based Inhibitory Motif-bearing Protein, Recruits SHP-1 upon Tyrosine Phosphorylation and Is Paired with the Truncated Counterpart PILRβ*

Darrell D. Mousseau‡, Denis Banville‡, Denis L'Abbé‡, Patrice Bouchard‡, and Shi-Hsiang Shen‡§¶

From the ‡Mammalian Cell Genetics, National Research Council-Biotechnology Research Institute, Montreal, Quebec H4P 2R2 and §Department of Medicine, McGill University, Montreal, Quebec H3G 1A4, Canada

SHP-1-mediated dephosphorylation of protein tyrosine residues is central to the regulation of several cell signaling pathways, the specificity of which is dictated by the intrinsic affinity of SH2 domains for the flanking sequences of phosphotyrosine residues. By using a modified yeast two-hybrid system and SHP-1 as bait, we have cloned a human cDNA, PILRα, encoding a 303-amino acid immunoglobulin-like transmembrane receptor bearing two cytoplasmic tyrosines positioned within an immunoreceptor tyrosine-based inhibitory motif. Substrate trapping in combination with pervanadate treatment of 293T cells confirms that PILRα associates with SHP-1 in vivo upon tyrosine phosphorylation. Mutation of the tyrosine residues in PILRα indicates the pivotal role of the Tyr-269 residue in recruiting SHP-1. Surface plasmon resonance analysis further suggests that the association between PILRα-Tyr-269 and SHP-1 is mediated primarily via the amino-terminal SH2 domain of the latter. Polymerase chain reaction amplification of cDNA in combination with genomic sequence analysis revealed a second gene, PILRβ, coding for a putative activating receptor as suggested by a truncated cytoplasmic tail and a charged lysine residue in its transmembrane region. The PILRα and PILRβ genes are localized to chromosome 7 which is in contrast with the mapping of known members of the inhibitory receptor superfamily.

The initiation of cell signaling pathways relies on a dynamic interaction between activating and inhibiting processes that can include, among other things, changes in the phosphorylation status of certain tyrosine residues within the target proteins. Dephosphorylation of these residues is mediated by such phosphatases as the cytosolic SHP-1 (also known as SHP, PTP1C, SH-PTP1, or PTPN6 (1)) which is expressed in hematopoietic cells, and to a lesser extent in non-hematopoietic cells, and which contains tandem amino-terminal Src homology 2 (SH2)[1] domains. The importance of SHP-1 in cellular signal

delivery is underscored by the motheaten mouse that carries a natural mutation in the SHP-1 locus and is characterized by widespread autoimmune phenomena resulting from an inability to modulate immune responses (2, 3).

Affinity for the SH2 domains is pivotal for interaction of substrates with SHP-1. The flanking sequence of the phosphotyrosine residue promotes the recruitment of specific SH2-containing phosphatases and, thus, determines the specificity of the signaling pathway. The consensus sequence (S/L/I/V)XYXX(L/V), based on sequences originally deduced from several receptors known to bind to the carboxyl-terminal SH2 domain of the protein tyrosine phosphatase SHP-1 (4–6), defines all immunoreceptor tyrosine-based inhibitory motif (ITIM)-bearing receptors (7) including natural killer cell, B cell, and monocyte and dendritic cell inhibitory receptors (reviewed in Refs. 8 and 9). Members of the inhibitory receptor superfamily (10, 11) can be divided into two groups. The immunoglobulin (Ig) superfamily includes luminal amino-terminal (e.g. type I) transmembrane glycoproteins with two or more Ig-like domains such as p58/KIR2DL3, FcγRIIB, Ig-like transcripts as well as the mouse PIR-B. The other group is comprised of CD94/NKG-2, CD72, and the mouse Ly49 and NKR-P1 which are cytoplasmic amino-terminal (e.g. type II) transmembrane proteins expressing C-type lectin extracellular architecture.

The existence of complementary proteins expressing similar extracellular domains as the inhibitory receptors, while having distinctive transmembrane and frequently truncated cytoplasmic tails, suggests similar ligand-binding specificities but contrasting signaling capabilities for each individual of the protein pair. The truncated protein would have cellular activating properties, in contrast with its ITIM-bearing counterpart which would inhibit cell signaling through recruitment of SHP-1, SHP-2, or SHIP phosphatases (9) seemingly via their respective carboxyl-terminal SH2 domains (12, 13). Human immunoreceptors map to the "complex" or "leukocyte receptor cluster" located on chromosome region 19q13.4 or to the natural killer complex on chromosome 12 (11). Mouse immunoreceptors are located on chromosomes 7 and 6 in regions syntenic to human chromosome 19 and 12, respectively (11), or to band B4 of mouse chromosome 10 (14) which does not appear to have any conserved linkage homology to either human chromosome 19 or 12.

We now present evidence of a novel pair of receptors express-

[1] The abbreviations used are: SH2, Src homology 2; PILRα, paired immunoglobulin-like receptor α; PILRβ, paired immunoglobulin-like receptor β; ITIM, immunoreceptor tyrosine-based inhibitory motif; PCR, polymerase chain reaction; kb, kilobase pair; HA, hemagglutinin; PAGE, polyacrylamide gel electrophoresis; SPR, surface plasmon resonance; FBS, fetal bovine serum; mAb, monoclonal antibody; pAb, polyclonal antibody; GST, glutathione S-transferase; MHC, major histocompatibility complex; PNGase:F, peptide:N-glycosidase F.

ing a single extracellular Ig-like domain that we have designated as "paired immunoglobulin-like receptor" (PILR)α and PILRβ to distinguish their putative inhibitory and activating gene products, respectively. The ITIM-bearing receptor PILRα recruits SHP-1 via its amino-terminal SH2 domain and is likely to have cellular inhibitory potential. The lack of a cytoplasmic tail and the presence of the transmembrane lysine residue in the second receptor PILRβ suggest its potential activating function. Both genes map cytogenetically to human chromosome 7.

EXPERIMENTAL PROCEDURES

Cells and Culture Conditions—All cell lines were obtained from American Type Culture Collection except where indicated. The human embryonic kidney epithelial cell line 293T (Edge Biosystems) was maintained in Dulbecco's modified Eagle's medium, 10% fetal bovine serum (FBS). The T cell-derived KG-1, Jurkat and K562 cell lines were maintained in RPMI, 10% FBS. The B cell-derived cell lines WIL2-NS, Namalwa, Daudi, and Raji were maintained in RPMI, 10% inactivated FBS. The 6F11 B cell line was cultured in Iscove's modified Dulbecco's medium containing 2 mM L-glutamine and 15% FBS. The macrophage 28SC cell line was maintained in Iscove's medium supplemented with 0.03 mM thymidine, 0.1 mM hypoxanthine, 0.05 mM β-mercaptoethanol, and 10% FBS. NK-92ci cells (ImmuneMedicine, Vancouver, British Columbia, Canada) transformed with a pCep-IL-2 construct were maintained by selection in interleukin-2-free Myelocult medium (Stem Cell Technologies, Vancouver, British Columbia, Canada).

Antibodies—SHP-1 was precipitated and detected using a monoclonal antibody (mAb; P17320; Transduction Laboratories) or an inhouse polyclonal antibody (pAb; 237, see Ref. 15). PILRα cDNA was subcloned in-frame with a carboxyl-terminal triple HA tag. The HA epitope was precipitated with a high affinity rat anti-HA mAb (3F10; Roche Molecular Biochemicals) and detected with a mouse mAb (12CA5; Roche Molecular Biochemicals). Separate membranes were also probed with anti-phosphotyrosine 4G10 mAb (Upstate Biotechnology, Inc.) and anti-ubiquitin pAb (U-5379; Sigma). Secondary antibodies were horseradish peroxidase-conjugated to goat anti-mouse or goat anti-rabbit antibody (Bio-Rad) and detection relied on enhanced chemiluminescence (NEN Life Science Products).

Yeast Two-hybrid Screen—Screening of a human mammary gland cDNA library (CLONTECH) with the SHP-1-C455S catalytic mutant (16) was performed as follows. The full-length SHP-1-C455S was cloned into SalI-restricted pBTM116-Src by standard polymerase chain reaction (PCR) procedures and thus was fused in-frame with the carboxyl terminus of the DNA binding domain of the bacterial activator LexA. pBTM116-Src contains a mutant c-Src kinase expression cassette designed for the phosphorylation of protein tyrosine residues in yeast (17). The pBTM116-Src-SHP-1-C455S construct was then used to transform the yeast reporter strain, L40α (*MATa trp1 leu2 his3 LYS2::lexA-HIS3 URA3::lexA-lacz*). Following transformation using Li²⁺ acetate (18), L40α expressing pBTM116-Src-SHP-1-C455S was further transformed with the library. Positive interactors were isolated according to the manufacturer's specifications (CLONTECH Laboratories, Inc.). The positive control consisted of a pBTM-116-cnx1+ and pGADGH-hus5+ combination kindly provided by M. Pelletier and D.Y. Thomas² (NRC Biotechnology Research Institute, Montreal, Quebec, Canada). cDNA sequences were determined and subjected to the BLAST search of the NCBI data bases. The target sequence of interest was used as a probe for screening of cDNA libraries.

Screening of Human cDNA Libraries—³²P-Labeled probes were prepared by random labeling of the PILRα PCR product using Ready-to-Go DNA Labeling Beads (Amersham Pharmacia Biotech) and [α-³²P]dCTP. Placenta, acute myelocytoma leukemia (KG-1), bone marrow, and leukocyte cDNA libraries were screened using the labeled probes. Positive clones were subjected to PCR using λ GT11-specific primers.

Mutant Expression, Immunoprecipitation, and Immunoblotting—Single and double tyrosine to phenylalanine mutants of PILRα-HA, i.e. Y269F, Y298F, Y269F/Y298F, were generated by PCR-based site-directed mutagenesis. 293T cells were transfected either alone or in combination with SHP-1 by calcium phosphate precipitation. Forty-eight hours after transfection the cells were treated with pervanadate (100 μM, 30 min at 37 °C), a phosphatase inhibitor that induces maximal tyrosine phosphorylation (19), and then washed with phosphate-

buffered saline and lysed on ice. Solubilized extracts were immunoprecipitated with the appropriate antibodies followed by protein A- or protein G-Sepharose. The immunoprecipitates were resolved by SDS-PAGE and revealed by standard immunoblotting techniques.

Glycosylation and Ubiquitination Status of PILRα-HA—293T cells were transiently transfected with PILRα-HA. Following immunoprecipitation with an HA-directed antibody, immune complexes were washed and denatured, and N-glycosylation status was determined by overnight incubation at 37 °C with 5 milliunits of N-glycosidase F (PNGase:F, Roche Molecular Biochemicals) while a parallel series of experiments determined O-glycosylation status by incubation with 1 milliunit of neuraminidase (to remove sialic acid residues, Roche Molecular Biochemicals) and/or 1 milliunit of endo-α-N-acetylgalactosaminidase (O-glycosidase, Roche Molecular Biochemicals). The various reactions were resolved on 10% SDS-PAGE gels. To test for the presence of covalently bound ubiquitin in the 55-kDa expressed PILRα-HA species, transiently transfected 293T cells were treated with pervanadate, and HA-bound immunoprecipitates were collected, resolved by SDS-PAGE, and probed with an anti-ubiquitin pAb.

Preparation and Expression of GST Fusion Proteins Containing the SH2 Domains of SHP-1—A 300-base pair segment encoding either the amino-terminal SH2 domain (SH2(N)) or the carboxyl-terminal SH2 domain (SH2(C)) of SHP-1 were generated by PCR amplification of human SHP-1 cDNA (20) and subcloned into pGEX-2T (Amersham Pharmacia Biotech). The SHP-1.SH2(N) and SHP-1.SH2(C) GST fusion proteins were produced in *Escherichia coli* DH5α cultures transformed with the corresponding plasmid and induced with 25 μM isopropyl-β-D-thiogalactoside for 22 h at 28 °C. The GST fusion proteins were isolated using glutathione-Sepharose 4B beads (Amersham Pharmacia Biotech). Protein expression and purity were determined by SDS-PAGE and Coomassie Blue staining.

Surface Plasmon Resonance Measurements—Surface plasmon resonance (SPR) was performed on a BIAcore apparatus using CM5-sensor chips (Biosensor AB, Uppsala, Sweden). The tyrosyl-phosphorylated (pY) synthetic peptides, KDDGIV(pY)ASLALSSSTS and PQNETL(pY)-SVLKA, corresponding, respectively, to the Tyr-269- and Tyr-298-based motifs contained in PILRα were immobilized at 0.5 mg/ml on the Biosensor chip. Immobilization efficiency was verified using the anti-phosphotyrosine 4G10 mAb. GST-SH2 domain fusion proteins (see above) were initially dialyzed in 10 mM Hepes buffer (pH 7.4) containing 150 mM NaCl and 3.4 mM EDTA (HBS). The GST fusion proteins (0.5–2000 nM), diluted in HBS, 0.05% P20, were injected over the test surfaces at a flow rate of 5 μl/min. Regeneration of the Biosensor chip using 46 mM HCl, 1 M NaCl did not result in loss of subsequent signal. Dissociation constants (K_D) were calculated by saturation (nonlinear regression) analysis as well as by kinetic analysis (e.g. the ratio of k_{off} and k_{on} determined using BIAevaluation software; Biosensor AB, Uppsala, Sweden).

Northern Blot Analysis—Human multiple tissue Northern blots (CLONTECH Laboratories, Inc.) containing 2 μg of poly(A)⁺ RNA per lane were hybridized consecutively with ³²P-labeled full-length PILRα cDNA and with ³²P-labeled β-actin cDNA probes. The level of expression in a series of human cells was also examined. Total RNAs from the individual cell lines were extracted by the TriZOL method (Life Technologies, Inc.) and enriched in poly(A)⁺ RNA by passage on oligo(dT) spun columns (Amersham Pharmacia Biotech). Ten μg of poly(A)⁺ RNA were loaded per lane, transferred to membrane, probed as above, and then washed (maximum stringency being 2 × 15 min, 0.1× SSC, 0.1% SDS, 55 °C).

Long Range PCR—The sequence of the 5'-untranslated region was amplified by 5'-rapid amplification of cDNA ends from Marathon-Ready cDNA (CLONTECH), whereas the genomic organization of *PILRα* and *PILRβ* genes was partially determined using the proofreading *Taq* polymerase GenomeWalker™ kit (CLONTECH).

RESULTS

The SHP-1 Catalytic Mutant SHP-1-C455S Interacts with Several ITIM-bearing Protein Fragments—A SHP-1-C455S catalytic mutant was used as bait in a yeast two-hybrid screening of a human mammary gland cDNA library. 4.5 × 10⁶ clones were screened to reveal 24 interactors able to grow on Trp⁻/Leu⁻/His⁻ medium and able to induce β-galactosidase activity (Fig. 1). These positive clones were sequenced and identified as a novel ITIM-bearing protein, subsequently named PILRα, as well as known interactors of SHP-1 namely SHPS-1 (21), EGFRBP-Grb2 (22), and the leukocyte-associated Ig-like recep-

---

² M. Pelletier and D. Y. Thomas, unpublished data.

tor LAIR-1 (23). The sequence of the novel interactor was extended by PCR amplification of the target cDNA library and was ultimately confirmed following its use as a probe in the cDNA library screening which yielded the full-length sequence.
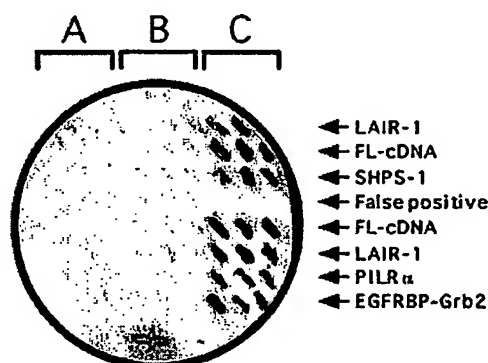

FIG. 1. **SHP-1 interacts with a number of known proteins and a novel inhibitory receptor PILRα.** Interactions were assayed in the yeast strain, L40α, which requires Trp, Leu, and His to grow. pBTM-116-Src-SHP-1-C455S (bait) and pACT2 (target, library) constructs carry Trp and Leu, respectively, as their selective markers. Library plasmids from positive clones were cured and used in combination with irrelevant (*A*, negative control), pBTM-116-Src (*B*, vector control) or pBTM-116-Src-SHP-1-C455S (*C*, the bait) plasmid, to retransform yeast. These yeast transformants were randomly plated in triplicate onto Trp⁻/Leu⁻/His⁻ master plates, grown to a visible biomass, and then submitted to colony-lift β-galactosidase assay. The positive control (+) was a pBTM-116-cnx1+ (bait)/pGADGH-hus5+ (target) combination. FL-cDNA is an unknown interactor described in the NCBI dbEST data base as "fetal lung cDNA."

The nucleotide sequence and deduced amino acid sequence, indicating a theoretical mass of 31.8 kDa, are depicted in Fig. 2. Structurally the gene product does not contain an IgG domain *per se*, although the single extracellular cysteine residue (Cys-125) is flanked by a motif, *e.g.* YXCXVXL, reminiscent of the carboxyl-terminal cysteine-based motif, *e.g.* (F/Y)XCX(V/A)XH, involved in the intradomain disulfide bond of immunoglobulin and major histocompatibility complex (MHC) proteins (PROSITE data base; reference number PS00290). This same segment bears a slight homology to extracellular regions of sialoadhesin (24). In addition, there is a potential *N*-glycosylation site (NX(T/S)), numerous serine and threonine residues capable of being *O*-glycosylated, a transmembrane domain, and three potential tyrosine phosphorylation sites, two of which, *e.g.* Tyr-269 and Tyr-298, reside within an immunoreceptor tyrosine-based inhibitory motif.

PILRα-HA Interacts with SHP-1 in Vivo—To examine protein-protein interactions, 293T cells were co-transfected with PILRα-HA and SHP-1 and treated with pervanadate. Fig. 3 demonstrates that PILRα-HA is phosphorylated in 293T cells (Fig. 3*A*, *top*), that PILRα-HA and SHP-1 co-precipitate (Fig. 3*A*, *middle*), and that tyrosine phosphorylation was essential for binding to SHP-1 (Fig. 3*A*, *bottom*). In addition, confirmation that the association occurred *in vivo* was accomplished by co-immunoprecipitation of PILRα-HA as part of an immune complex containing the SHP-1-D421A substrate-trapping mutant (25) (Fig. 3*B*).

PILRα-HA migrated with an apparent molecular mass of 55 kDa rather than the expected theoretical molecular mass of 36 kDa. The 55-kDa molecular mass includes 4.6 kDa contributed

```
AATAGGGGAAAATAAGCCAGATGGATAAAGGAAGTGCTGGTCACCCTGGAGGTGCACTGGTTTGGGGAAGGCTCCTGGCCCCCACAGCCC
TCTTCGGAGCCTGAGCCCGGCTCTCCTCACTCACCTCAACCCCTCCACAGGCGGCCCCTCCACAGGGCCCGTCTCCTGCCTGGACGGCTCTGCT
GGTCTCCCCGTCCCCTGGAGAAGAACAAGGCCATGGGTCGGCCCCCTGCTGCTGCCCCTACTGCCCTTGCTGCTGCCGCCAGCATTTCTGC    270
                                      M  G  R  P  L  L  L  P  L  L  P  L  L  L  P  P  A  F  L  Q    20

AGCCTAGTGGCTCCACAGGATCTGGTCCAAGCTACCTTTATGGGGTCACTCAACCAAAACACCTCTCAGCCTCCATGGGTGGCTCTGTGG    360
P  S  G  S  T  G  S  G  P  S  Y  L  Y  G  V  T  Q  P  K  H  L  S  A  S  M  G  G  S  V  E    50

AAATCCCCTTCTCCTTCTATTACCCCTGGGAGTTAGCCACAGCTCCCGACGTGAGAATATCCTGGAGACGGGGCCACTTCCACAGGCAGT    450
I  P  F  S  F  Y  Y  P  W  E  L  A  T  A  P  D  V  R  I  S  W  R  R  G  H  F  H  R  Q  S    80

CCTTCTACAGCACAAGGCCGCCTTCCATTCACAAGGATTATGTGAACCGGCTCTTTCTGAACTGGACAGAGGGTCAGAAGAGCGGCTTCC    540
F  Y  S  T  R  P  P  S  I  H  K  D  Y  V  N  R  L  F  L  N  W  T  E  G  Q  K  S  G  F  L    110

TCAGGATCTCCAACCTGCAGAAGCAGGACCAGTCTGTGTATTTCTGCCGAGTTGAGCTGGACACACGGAGCTCAGGGAGGCAGCAGTGGC    630
R  I  S  N  L  Q  K  Q  D  Q  S  V  Y  F  C  R  V  E  L  D  T  R  S  S  G  R  Q  Q  W  Q    140

AGTCCATCGAGGGGACCAAACTCTCCATCACCCAGGCTGTCACGACCACCACCCAGAGGCCCAGCAGCATGACTACCACCTGGAGGCTCA    720
S  I  E  G  T  K  L  S  I  T  Q  A  V  T  T  T  Q  R  P  S  S  M  T  T  T  W  R  L  S    170

GTAGCACAACCACCACAACCGGCCTCAGGGTCACACAGGGCAAACGACGCTCAGACTCTTGGCACATAAGTCTGGAGACTGCTGTGGGGG    810
S  T  T  T  T  T  G  L  R  V  T  Q  G  K  R  R  S  D  S  W  H  I  S  L  E  T  A  V  G  V    200

TGGCAGTGGCTGTCACTGTGCTCGGAATCATGATTTTGGGACTGATCTGCCTCCTCAGGTGGAGGAGAAGGAAAGGTCAGCAGCGGACTA    900
A  V  A  V  T  V  L  G  I  M  I  L  G  L  I  C  L  L  R  W  R  R  R  K  G  Q  Q  R  T  K    230

AAGCCACAACCCCAGCCAGGGAACCCTTCCAAAACACAGAGGAGCCATATGAGAATATCAGGAATGAAGGACAAAATACAGATCCCAAGC    990
A  T  T  P  A  R  E  P  F  Q  N  T  E  E  P  Y  E  N  I  R  N  E  G  Q  N  T  D  P  K  L    260

TAAATCCCAAGGATGACGGCATCGTCTATGCTTCCCTTGCCCTCTCCAGCTCCACCTCACCCAGAGCACCTCCCAGCCACCGTCCCCTCA   1080
N  P  K  D  D  G  I  V  Y  A  S  L  A  L  S  S  S  T  S  P  R  A  P  P  S  H  R  P  L  K    290

AGAGCCCCCAGAACGAGACCCTGTACTCTGTCTTAAAGGCCTAACAATGGACAGCCCTCTCAAGACTGAATGGTGAGGCCAGGTACAGTG   1170
S  P  Q  N  E  T  L  Y  S  V  L  K  A  *                                                        303

GCGCACACCTGTAATCCCAGCTACTCTGAAGCCTGAGGCAGAATCAAGTGAGCCCAGGAGTTCAGGGCCAGCTTTGATAATGGAGCGAGA   1260
TGCCATCTCTAGTTAAAAATATATATTAACAATAAAGTAACAAATTTA                                               1308
```

FIG. 2. **Nucleotide sequence and deduced amino acid sequence of human PILRα.** The signal peptide (*underlined*), the transmembrane region (*bold, underlined*), a potential *N*-glycosylation site (*boxed*), and putative binding sites for SHP-1 SH2 domains (*shaded*) are indicated. The AATAAA polyadenylation signal is also shown (*bold*). The *bold numbers* to the *right* indicate the nucleotide position, and the *italicized numbers* indicate the amino acid position.
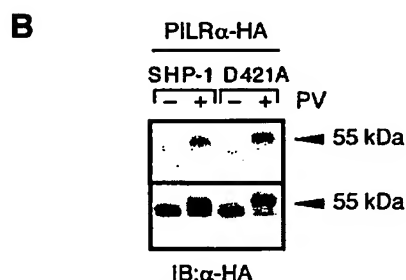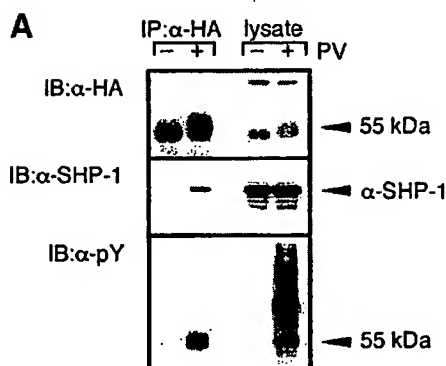
A

IP:α-HA   lysate

IB:α-HA

IB:α-SHP-1

IB:α-pY

55 kDa

α-SHP-1

55 kDa

B

PILRα-HA

SHP-1   D421A

55 kDa

55 kDa

IB:α-HA

FIG. 3. **The phosphorylation of PILRα-HA is required for *in vivo* association with SHP-1.** *A*, pervanadate (*PV*)-treated (+) and non-treated (−) 293T cells co-transfected with PILRα-HA and SHP-1 were lysed. Total cell lysates as well as proteins co-immunoprecipitated with a mAb directed at the HA tag of the PILRα construct were resolved by SDS-PAGE and immunoblotted with anti-HA mAb (*top*), anti-SHP-1 mAb (*middle*), or anti-phosphotyrosine mAb (*bottom*). *B*, pervanadate-treated (+) and non-treated (−) 293T cells transiently co-transfected with PILRα-HA and either SHP-1 or the SHP-1-D421A (D421A) substrate-trapping mutant were lysed, and immune complexes were immunoprecipitated with anti-SHP-1 mAb (*top*). Bound proteins were resolved by SDS-PAGE, and the association of PILRα-HA with SHP-1 was determined by immunoblotting with anti-HA mAb. Expression of PILRα-HA in these same cells was monitored by immunoblotting cell lysate proteins with anti-HA mAb (*bottom*). *Arrowheads* indicate the molecular mass of the expressed PILRα-HA protein (*e.g.* 55 kDa).

by the triple HA tag. The significant difference between the deduced and the apparent molecular mass of PILRα-HA on Western blotting led to the examination of the glycosylation and/or ubiquitination status of this protein. Samples of PILRα-HA immunoblotted for ubiquitin did not reveal any signal (data not shown). Digestion of immunoprecipitates with either PNGase:F or with neuraminidase plus O-glycosidase revealed shifts in the migration of expressed PILRα-HA. The combination of PNGase:F and neuraminidase plus O-glycosidase reduced the molecular mass to approximately 42 kDa thus revealing that post-translation addition of *N*- and *O*-linked carbohydrate residues accounts for a substantial portion of expressed 55-kDa PILRα-HA (Fig. 4).

Mutation of Tyrosine Residues of PILRα-HA Alters Its Interaction with SHP-1—The role of the ITIM-based tyrosine residues of PILRα-HA in recruiting SHP-1 was investigated by mutational analysis. Immunodetection of SHP-1 following co-immunoprecipitation with an HA-directed antibody indicated that the Tyr-269 motif, *e.g.* IVYASL, was the target for binding with SHP-1 (Fig. 5*A*). Indeed, whereas the Y298F substitution seems to have had only a slight effect on the association with SHP-1, the Y269F mutant and the Y269F/Y298F double mutant significantly decreased the SHP-1 signal. PILRα-HA (Fig.
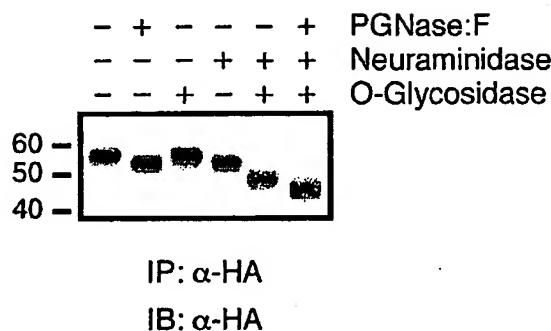

PGNase:F
Neuraminidase
O-Glycosidase

60 —
50 —
40 —

IP: α-HA

IB: α-HA

FIG. 4. **Characterization of the glycosylation status of expressed PILRα-HA.** 293T cells were transiently transfected with PILRα-HA. Tyrosine phosphorylation was maintained by treatment with pervanadate. *N*- and *O*-glycosylation status was examined by immunoprecipitation with anti-HA mAb followed by digestion with peptide:*N*-glycosidase F (*PNGase:F*) and/or neuraminidase (to remove sialic acid residues) and/or endo-α-*N*-acetylgalactosaminidase (*O*-glycosidase). The reactions were resolved by SDS-PAGE and immunoblotted with an anti-HA mAb. *Numbers* to the *left* indicate the molecular mass (kDa) of protein standards.

pcDNA3
PILRα-HA
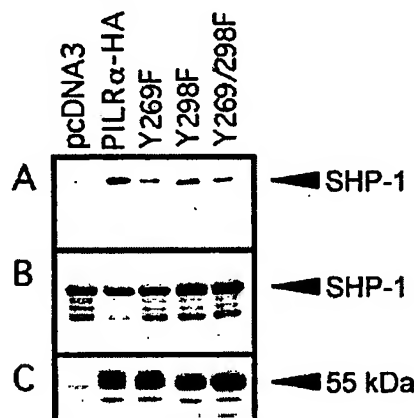Y269F
Y298F
Y269/298F

A   SHP-1

B   SHP-1

C   55 kDa

FIG. 5. **SHP-1 interacts with the first tyrosine within the PILRα-HA ITIM.** Standard PCR-based procedures were used to create Tyr to Phe substitutions of the two ITIM-based tyrosine residues either individually or as the Y269F/Y298F double mutant of PILRα-HA. *A*, pervanadate-treated 293T cells transiently co-transfected with the indicated PILRα-HA mutants and SHP-1 were lysed and immunoprecipitated with anti-HA mAb. Bound proteins were resolved by SDS-PAGE and immunoblotted with anti-SHP-1 mAb. Expression of the co-transfected constructs was monitored by immunoblotting the lysates from these same cells with (*B*) anti-SHP-1 mAb or (*C*) anti-HA mAb.

5*C*) and SHP-1 (Fig. 5*B*) were equally expressed in the corresponding lysates.

Determination of the K_D Values of Interactions between PILRα Phosphotyrosyl Peptides and SH2 Domains of SHP-1 by SPR—The importance of the Tyr-269 motif in recruiting SHP-1 is supported using BIAcore detection. The immobilized phosphorylated peptide corresponding to this motif, *e.g.* KDD-GI(pY)-ASLALSSSTS, demonstrated high affinity for the SHP-1-SH2(N) domain (Fig. 6, *top*) and intermediate affinity for the SHP-1-SH2(C) domain (Fig. 6, *bottom*). Interestingly, the SHP-1-SH2(C) domain selectively recognized the Tyr-298 phosphopeptide, *e.g.* PQNETL(pY)SVLKA, but with much lower affinity (Fig. 6, *bottom*). The dissociation constants (K_D) for the various interactions were determined by saturation analysis (nonlinear regression analysis) and supported by those obtained by kinetic analysis (*e.g.* $K_D = k_{off}/k_{on}$: Table I). Saturation analysis revealed K_D values of 167 ± 4 and 1091 ± 196 nM
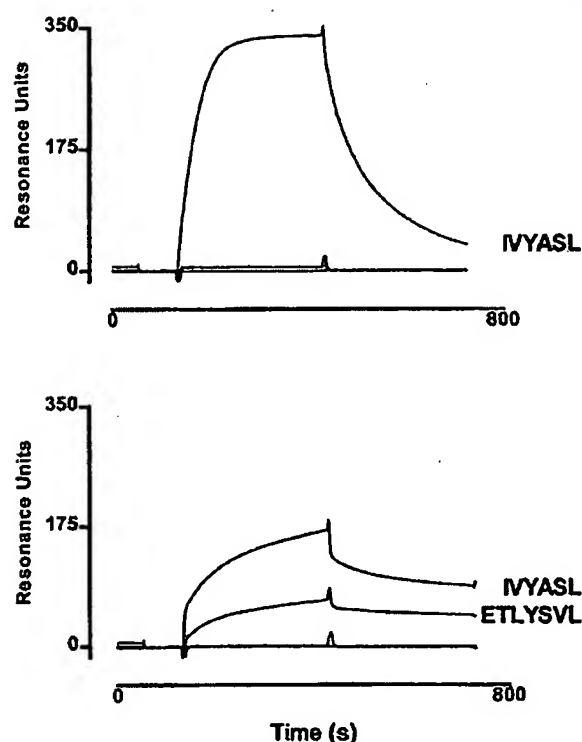
FIG. 6. The binding potential of candidate tyrosine residues in the PILRα cytoplasmic domain was analyzed by surface plasmon resonance. The tyrosyl-phosphorylated synthetic peptides, KDDGIV(pY)ASLALSSSTS (IVYASL) and PQNETL(pY)SVLKA (ETLYSVL), corresponding, to the Tyr-269- and Tyr-298-based YXX(L/V/I) motifs of PILRα were immobilized on separate flow cells of the CM5 sensor chip. GST fusion proteins of the amino-terminal (SHP-1-SH2(N)) and carboxyl-terminal (SHP-1-SH2(C)) SH2 domains of SHP-1 were injected (concentrations ranging from 0.5 to 2000 nM) over the test surfaces. The representative curves shown here correspond to the binding of 400 nM of SHP-1-SH2(N) (*top*) and SHP-1-SH2(C) (*bottom*) to the various test surfaces. Only the tyrosyl-phosphorylated peptide(s) recognized by either SH2 domain are indicated. Curves such as these were used to obtain the kinetic data presented in Table I. The control surface did not bind either of the SH2 domains, and thus the resultant data appear as *straight lines* on both graphs.

TABLE I
Binding potential of the SHP-1 amino- and carboxyl-terminal SH2 domains with human PILRα tyrosyl-phosphorylated peptides

Values represent the mean (±S.E.) of five separate experiments. ND, no detectable binding.

Phosphorylated peptides	KDDGIV(pY)ASLALSSSTS	PQNETL(pY)SVLKA
SHP-1.SH2(N)		
k_{on} (10^4 M^{-1} s^{-1})	5.10 ± 0.53	ND
k_{off} (10^{-3} s^{-1})	2.48 ± 0.65	ND
K_D (nM)	47.8 ± 10.5	ND
SHP-1.SH2(C)		
k_{on} (10^4 M^{-1} s^{-1})	2.42 ± 0.99	0.46 ± 0.05
k_{off} (10^{-3} s^{-1})	3.78 ± 0.96	12.9 ± 0.59
K_D (nM)	214.0 ± 77.7	3000 ± 431

following binding of the SHP-1-SH2(N) and -SH2(C) GST fusion proteins, respectively, to the Tyr-269 phosphopeptide. A K_D value of 3777 ± 447 nM was obtained upon binding of the SHP-1-SH2(C) GST fusion protein to the Tyr-298 phosphopeptide. GST itself did not bind to any of the test surfaces (data not shown) and neither of the GST-SH2 domain fusion proteins bound significantly (*e.g.* less than 5 resonance units) to the control Biosensor chip surface.

The Genomic Organization of PILR Reveals Two Distinct, yet Structurally Related, Receptors—Rapid amplification of cDNA ends designed to clone the 5′ end of the PILRα cDNA revealed the presence of a second cDNA displaying long regions of near sequence identity to PILRα but differing in its 5′ non-coding sequence. The existence of a related gene was also suggested from long range PCR performed on human genomic DNA (results not shown) and was confirmed by the sequence of a 200-kilobase segment of human chromosome 7 deposited subsequently in GenBank™ under the accession number RG161A02. The *PILRα* gene consists of seven exons and six introns spanning approximately 26.7 kb. The second gene, designated *PILRβ*, is located 5.6 kb upstream of the *PILRα* gene and consists of four exons and three introns spanning approximately 9.8 kb (Fig. 7B). The nucleotide sequence of the first three exons of the two genes is extremely similar, displaying more than 90% sequence identity (Fig. 7A), and suggests that the two genes share a common origin. Tables II and III summarize the nucleotide sequence of the splice sites of the *PILRα* and *PILRβ* genes, respectively, and indicate that in both cases the intron-exon boundaries conform to the GT-AG rule. *PILRβ* codes for a protein with similar extracellular features as those of PILRα but with a short cytoplasmic tail and a charged lysine residue within its transmembrane domain (Fig. 7A).

Expression of PILR in Tissues and Selected Cell Lines—Northern blot analysis of selected human tissues revealed a strong signal in peripheral blood leukocytes and lower intensity signals in lung, spleen, and placenta (Fig. 8A). Analysis of various human cell lines revealed a signal in a two B cell lines, *e.g.* WIL2-NS and 6F11 (Fig. 8B), whereas all other cells tested were negative for *PILR*. Due to the high nucleotide sequence identity of the two genes and the similar length of the two transcripts, the Northern blots do not allow us to discriminate which of the two forms, *e.g. PILRα* or *PILRβ*, is expressed in these tissues and cell lines. To resolve this question, PCR with a forward oligonucleotide primer whose sequence was common to both *PILRα* and *PILRβ* (HUKF1, 5′-GGGAAGCTTAT-GGGTCGGCCCCTGCTGCTGCCC) and reverse primers specific for each form, HUKR3 for *PILRα* (5′-CCATCTCGAGTTT-TGAGAGGGCTG) and HUKR5 for *PILRβ* (5′-TCCTCCGGGG-CTAATACACATCC), were performed on reverse transcribed single-stranded cDNA from various tissues including colon, leukocyte, ovary, prostate, small intestine, spleen, testis, thymus, placenta, and mammary gland. The results indicate that both *PILRα* and *PILRβ* were expressed, *e.g.* were paired, at the mRNA level in the individual samples (results not shown).

DISCUSSION

The cytosolic phosphatase SHP-1 contains tandem SH2 domains that bind tyrosine-phosphorylated proteins and, thus, by virtue of its catalytic subunit, gets recruited as an effector enzyme in a signaling pathway initiated by activated tyrosine kinase receptors (26). Specificity in tyrosine kinase signaling pathways is critical and is often dictated by the intrinsic affinity of SH2 domains for the flanking sequences of phosphotyrosine residues. The ITIM consensus sequence (S/L/I/V)-XYXX(L/V), via its recruitment of phosphatases, is central to inhibiting the signaling cascade initiated by activating receptors and, thus, plays a pivotal role in regulating cells of the immune system (10).

PILRα-HA is expressed as a membrane-bound *N*- and *O*-linked glycoprotein that contains within its cytoplasmic domain three potential tyrosine phosphorylation sites. Two of these tyrosines, *e.g.* Tyr-269 and Tyr-298, are positioned in YXXL consensus sequences in a manner very reminiscent of the ITIM (D/E)XXYXXL(X)$_{26}$YXXL originally described for numerous inhibitory receptors (7–9). In the case of PILRα-HA the

A


```
PILRα  MGRPLLLPLLPLLLPPAFLQPSGSTGSGPSYLYGVTQPKHLSASMGGSVEIPFSFYYPWELATAPDVRIS
PILRβ         L  Q      G                                    IV N


PILRα  WRRGHFHRQSFYSTRPPSIHKDYVNRLFLNWTEGQKSGFLRISNLQKQDQSVYFCRVELDTRSSGRQQWQ
PILRβ       G                     E       R  D              R    L


PILRα  SIEGTKLSITQAVTTTTQRPSSMTTTWRLSSTTTTTGLRVTQGKRRSDSWHISLETAVG▓▓▓▓▓▓▓▓▓▓
PILRβ  K    T           --------  P    IA    ES GH E     L  D  IR▓▓▓▓▓▓▓▓▓▓


PILRα  ▓▓▓▓▓▓▓▓▓▓RWRRRKGQQRTKATTPAREPFQNTEEPYENIRNEGQNTDPKLNPKDDGIVYASLALSSST
PILRβ  ▓▓▓▓▓▓▓▓▓W          SRAPSSDF*


PILRα  SPRAPPSHRPLKSPQNETLYSVLKA*
```
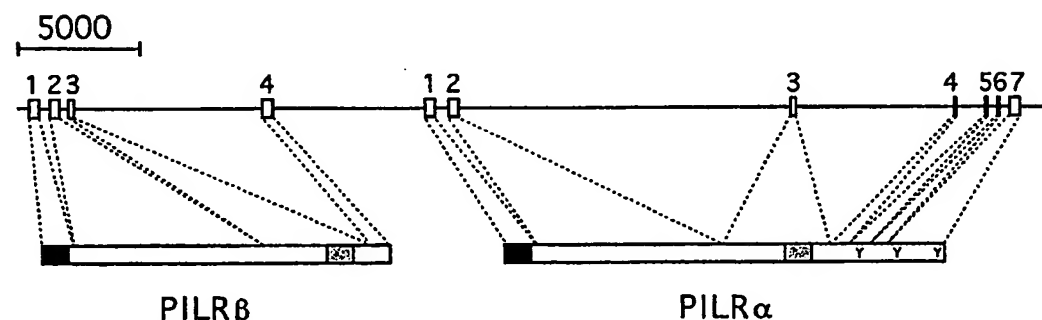
B

FIG. 7. **Genomic organization of the** *PILRα* **and** *PILRβ* **genes and comparison of their respective deduced amino acid sequences.** *A,* the deduced amino acid sequences of PILRα and PILRβ proteins are presented in single letter code. Only those amino acid residues that differ between the two sequences are shown in the PILRβ sequence. The *minus symbol* has been added to facilitate alignment (spacing determined by the respective nucleotide sequences). The amino-terminal signal peptide sequence is *underlined.* The transmembrane domain is displayed as a *shaded box* in both cases, and the charged lysine residue located within this region in PILRβ is highlighted in **bold.** *B,* schematic representation of the *PILRα* and *PILRβ* genes as well as the respective receptors. The *numbers above* the genes indicate the individual exons. The hydrophobic signal peptide *(solid),* the transmembrane region *(hatched),* and the three cytoplasmic tyrosine residues *(e.g. Y)* are indicated. The *bar* represents the scale in base pairs.

TABLE II
Intron-exon splice junction sites of the human PILRα gene

The nucleotide positions within the RG161A02 human genome clone are as follows: exon 1, 170751–171026; exon 2, 171350–171739; exon 3, 187194–187412; exon 4, 195185–195218; exon 5, 196597–196646; exon 6, 196887–196918; exon 7, 197091–197398 (polyadenylation signal at 197381). The "gt-ag" delimiting each intron is underlined.

Exon	Size	Splice donor			Splice acceptor	Intron size
	bp					*bp*
1	276	TTT CTG CAG CCT A	gtgagtacccc...	...cctcctctag	GT GGC TCC ACA GGA	323
2	390	TCC ATC ACC CAG G	gtgagtccagc...	...ctctccccag	CT GTC ACG ACC ACC	15,455
3	219	AGG AGA AGG AAA G	gtaagtgccca...	...cccccctacag	GT CAG CAG CGG ACT	7772
4	34	ACA ACC CCA GCC AG	gtgagtgctgg...	...tcccatacag	G GAA CCC TTC CAA	1378
5	50	ATC AGG AAT GAA G	gtgagtcctt...	...ttattcttag	GA CAA AAT ACA GAT	240
6	32	CTA AAT CCC AAG	gtaagcaatca...	...tctcgcccag	GAT GAC GGC ATC	172
7	308					

spacer between the two portions of the ITIM is 25 amino acids long. By using an SHP-1-D421A substrate-trapping mutant attenuated in its catalytic function but sufficiently stabilized to permit isolation of itself and the "trapped" substrate (25) indicates that tyrosine phosphorylation is required for *in vivo* association with SHP-1. Mutational analysis reveals that Tyr-269 in the motif IVYASL is the essential residue for interaction with SHP-1 although Tyr-298 in the ETLYSVL motif may also contribute marginally to the interaction. Parenthetically, both co-immunoprecipitation and surface plasmon resonance anal-

yses indicate that the membrane-proximal tyrosine residue, *e.g.* Tyr-246, which lies outside of the ITIM consensus sequence and which does not conform to the motif thought to bind to SHP-1 SH2 domains (27) does not, in fact, contribute to the recruitment of SHP-1 by PILRα (data not shown). A parallel series of experiments indicate that PILRα-HA also interacts with the protein tyrosine phosphatase SHP-2 (data not shown) perhaps through its Tyr-298 motif which resembles the tyrosine-based motif, *e.g.* TXYXX(V/I), found in the human NK cell receptor 2B4 as well as in the activation molecule SLAM

TABLE III
Intron-exon splice junction sites of the human PILRβ gene

The nucleotide positions within the RG161A02 human genome clone are as follows: exon 1, ~155,321–155,672; exon 2, 155,996–156,385; exon 3, 156,643–156,843; exon 4, 164,655–165,135 (polyadenylation signal at 165,111). The "gt-ag" delimiting each intron is underlined.

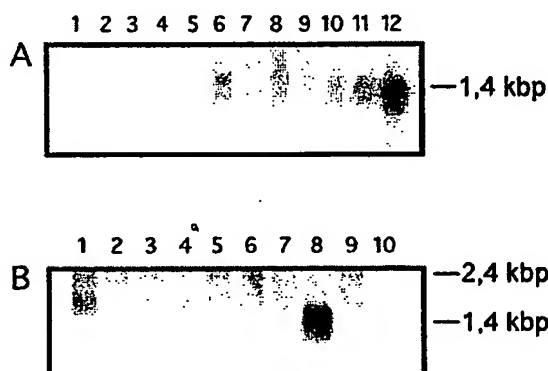| Exo	Size	Splice donor				Splice acceptor	Intron size
	bp						bp
1	≥352	...CTG CAG CCT G	gtgagtaccca...		...cttcctctag	GT GGC TCC AC...	323
2	390	...ATC ACC CAG G	gtgagtccagc...		...ggcccagcag	CT GTC ACA AC...	257
3	201	...AGA AGG AAA G	gtaagtgccca...		...cctcctgcag	GT AGC AGG GC...	7811
4	≥481						

FIG. 8. **Distribution of PILR in selected tissues and cell lines.** Two μg of poly(A)⁺ RNA from selected human tissues (*A*) or 10 μg of poly(A)⁺ RNA from selected human cell lines (*B*) were subjected to Northern blot analysis with ³²P-labeled full-length human *PILRα* cDNA. Probing with ³²P-labeled β-actin cDNA indicated similar signals in the various lanes (data not shown). *A: lane 1*, brain; *lane 2*, heart; *lane 3*, skeletal muscle; *lane 4*, colon; *lane 5*, thymus; *lane 6*, spleen; *lane 7*, kidney; *lane 8*, liver; *lane 9*, small intestine; *lane 10*, placenta; *lane 11*, lung; *lane 12*, peripheral blood leukocyte. *B: lane 1*, macrophage 28SC; *lane 2*, NK92-ci; *lanes 3–5* are T-cells; *lane 3*, Jurkat; *lane 4*, KG-1; *lane 5*, K562; *lanes 6–10* are B cells; *lane 6*, Raji; *lane 7*, Daudi; *lane 8*, WIL2-NS; *lane 9*, Namalwa; and *lane 10*, 6F11.

and thought to be essential for recruitment of SHP-2 and adaptor signaling proteins such as SAP (see Ref. 28 and references therein). Our *in vivo* demonstration of an interaction between SHP-1 and PILRα is supported by our surface plasmon resonance analyses that indicate the high affinity of the amino-terminal SH2 domain of SHP-1 for the Tyr-269 phosphopeptide. A number of receptors, via their (pY)XX(F/P/L/Y) motif, bind the amino-terminal SH2 domain of SHP-1 (27) and, at least in the case of the erythropoietin receptor (29), the interaction with SHP-1 mediates termination of signaling initiated by the receptor itself. In contrast, immunoreceptors such as FcγRIIB (4), CD22 (30), and p58/KIR2DL3 (31, 32), which inhibit signaling initiated by other receptors, apparently do so by recruiting the carboxyl-terminal SH2 domain of SHP-1 (5, 33), an exception being pp130, the product of p91/PIR-B in activated macrophages (34), which does so by interaction with the amino-terminal SH2 domain of SHP-1. PILRα-associated SHP-1 probably exists in an active conformation since activation of SHP-1 resides in amino-terminal SH2 domain occupancy (35, 36). The length of the spacer between Tyr-269 and Tyr-298 of PILRα-HA (25 amino acids), and recognition of the amino-terminal and carboxyl-terminal SH2 domains of SHP-1 by Tyr-269 and Tyr-298, respectively, suggest the potential for tandem occupancy and, thus, maximal phosphatase activity (35, 37). Although no definitive ligand for PILRα has been identified at this time, the lack of homology, extracellular or otherwise, between PILRα and known immunoreceptors, does not necessarily preclude MHC molecules, glycoproteins on self-components, and complex carbohydrates on microbial pathogens as potential ligand candidates.

PILRα-HA is expressed in 293T cells (as well as in Cos-1 and MCF-7 cells; data not shown) as a 55-kDa species that is significantly higher than the molecular mass of 36 kDa expected from the deduced amino acid sequence. We were able to reduce the molecular mass of expressed PILRα-HA to approximately 42 kDa and thus determine that the major portion of this difference was due to the presence of *N*- and *O*-linked carbohydrate residues. An explanation for our inability to reduce completely the mass of PILRα-HA to 36 kDa may well lie in the substrate specificity of the *O*-glycosidase (*e.g.* endo-α-*N*-acetylgalactosaminidase) which only digests unsubstituted Galβ1–3GalNAc moieties while leaving all other types of *O*-glycans untouched (38). It is therefore very possible that a certain portion of *O*-linked carbohydrate residues remained bound to PILRα-HA following treatment.

One of the striking features of the ITIM-bearing family of receptors is the pairing of inhibitory receptors with complementary activating receptors. The importance of a matched receptor pair and their individual cellular regulatory roles is exemplified by the stimulation of natural killer and T cell signaling pathways upon binding of the MHC class I ligand to the killer cell activating receptor which contrasts the disrupting signal initiated by binding of the ligand to the inhibitory counterpart killer cell inhibitory receptor (39). To date, all human immunoreceptors have mapped cytogenetically to the 19q13.4 complex or leukocyte receptor cluster, or to the natural killer complex on chromosome 12. Genomic organization of *PILRα* revealed the presence of two genes, *e.g. PILRα* and *PILRβ*, with high sequence homology on chromosome 7. The ITIM-bearing gene product encoded by *PILRα* has a non-polar transmembrane domain. In contrast, the truncated protein PILRβ with the charged residue (*e.g.* lysine) in its transmembrane domain confirms that it is likely the activating counterpart of PILRα (9). Activating receptors such as the mouse PIR-A associate with FcεRI-γ (40) to deliver activation signals to macrophages. We are presently investigating the possibility that our own activating isoform PILRβ can associate with proteins bearing immunoreceptor tyrosine-based activation motifs (ITAMs) such as the Fc receptors. Control of cellular signaling pathways probably occurs through a balance between PILRα-mediated inhibition and PILRβ-mediated activation.

Based on these data and the current literature which pairs inhibitory and activating receptors such as killer cell inhibitory receptor and killer cell activating receptor, FcγRIIB and FcγRIII, and PIR-B and PIR-A, to name but a few (9, 11), we are confident in stating that PILRα and PILRβ represent a novel ITIM-bearing and non-ITIM-bearing receptor pair. Furthermore, their chromosomal localization and their lack of homology with any of the known inhibitory/activating receptors suggests that they represent a novel family of receptors. Their chromosomal localization may yet reveal itself to include other genes bearing information relevant to our understanding of the regulation of cellular signaling pathways.

REFERENCES

1. Adachi, M., Fischer, E. H., Ihle, J., Imai, K., Jirik, F., Neel, B., Pawson, T., Shen, S., Thomas, M., Ullrich, A., and Zhao, Z. (1996) *Cell* 85, 15
2. Shultz, L. D., Schweitzer, P. A., Rajan, T. V., Yi, T., Ihle, J. N., Matthews, R. J., Thomas, M. L., and Beier, D. R. (1993) *Cell* 73, 1445–1454
3. Tsui, H. W., Siminovitch, K. A., de Souza, L., and Tsui, F. W. (1993) *Nat. Genet.* 4, 124–129
4. D'Ambrosio, D., Hippen, K. L., Minskoff, S. A., Mellman, I., Pani, G., Siminovitch, K. A., and Cambier, J. C. (1995) *Science* 268, 293–297
5. Burshtyn, D. N., Scharenberg, A. M., Wagtmann, N., Rajagopalan, S., Berrada, K., Yi, T., Kinet, J. P., and Long, E. O. (1996) *Immunity* 4, 77–85
6. Olcese, L., Lang, P., Vély, F., Cambiaggi, A., Marguet, D., Blery, M., Hippen, K. L., Biassoni, R., Moretta, A., Moretta, L., Cambier, J. C., and Vivier, E. (1996) *J. Immunol.* 156, 4531–4534
7. Cambier, J. C. (1995) *Immunol. Today* 16, 110
8. Burshtyn, D. N., and Long, E. O. (1997) *Trends Cell Biol.* 7, 473–479
9. Vély, F., and Vivier, E. (1997) *J. Immunol.* 159, 2075–2077
10. Lanier, L. L. (1998) *Annu. Rev. Immunol.* 16, 359–393
11. Long, E. O. (1999) *Annu. Rev. Immunol.* 17, 875–904
12. Vély, F., Nunes, J. A., Malissen, B., and Hedgecock, C. J. (1997) *Eur. J. Immunol.* 27, 3010–3014
13. Bruhns, P., Marchetti, P., Fridman, W. H., Vivier, E., and Daeron, M. (1999) *J. Immunol.* 162, 3168–3175
14. Kuroiwa, A., Yamashita, Y., Inui, M., Yuasa, T., Ono, M., Nagabukuro, A., Matsuda, Y., and Takai, T. (1998) *J. Biol. Chem.* 273, 1070–1074
15. Bouchard, P., Zhao, Z., Banville, D., Dumas, F., Fischer, E. H., and Shen, S. H. (1994) *J. Biol. Chem.* 269, 19585–19589
16. Su, L., Zhao, Z., Bouchard, P., Banville, D., Fischer, E. H., Krebs, E. G., and Shen, S. H. (1996) *J. Biol. Chem.* 271, 10385–10390
17. Keegan, K., and Cooper, J. A. (1996) *Oncogene* 12, 1537–1544
18. Gietz, D., St-Jean, A., Woods, R. A., and Schiestl, R. H. (1992) *Nucleic Acids Res.* 20, 1425
19. O'Shea, J. J., McVicar, D. W., Bailey, T. L., Burns, C., and Smyth, M. J. (1992) *Proc. Natl. Acad. Sci. U. S. A.* 89, 10306–10310
20. Yu, Z., Hoglinger, O., Jaramillo, M. L., Banville, D., and Shen, S. H. (1998) *J. Biol. Chem.* 273, 3687–3694
21. Veillette, A., Thibaudeau, E., and Latour, S. (1998) *J. Biol. Chem.* 273, 22719–22728
22. Kon-Kozlowski, M., Pani, G., Pawson, T., and Siminovitch, K. A. (1996) *J. Biol. Chem.* 271, 3856–3862
23. Meyaard, L., Adema, G. J., Chang, C., Woollatt, E., Sutherland, G. R., Lanier, L. L., and Phillips, J. H. (1997) *Immunity* 7, 283–290
24. Crocker, P. R., Mucklow, S., Bouckson, V., McWilliam, A., Willis, A. C., Gordon, S., Milon, G., Kelm, S., and Bradfield, P. (1994) *EMBO J.* 13, 4490–4503
25. Flint, A. J., Tiganis, T., Barford, D., and Tonks, N. K. (1997) *Proc. Natl. Acad. Sci. U. S. A.* 94, 1680–1685
26. Pawson, T. (1995) *Nature* 373, 477–478
27. Songyang, Z., Shoelson, S. E., McGlade, J., Olivier, P., Pawson, T., Bustelo, X. R., Barbacid, M., Sabe, H., Hanafusa, H., Yi, T., Ren, R., Baltimore, D., Ratnofsky, S., Feldman, R. A., and Cantley, L. C. (1994) *Mol. Cell. Biol.* 14, 2777–27785
28. Tangye, S. G., Lazetic, S., Woollatt, E., Sutherland, G. R., Lanier, L. L., and Phillips, J. H. (1999) *J. Immunol.* 162, 6981–6985
29. Klingmuller, U., Lorenz, U., Cantley, L. C., Neel, B. G., and Lodish, H. F. (1995) *Cell* 80, 729–738
30. Doody, G. M., Justement, L. B., Delibrias, C. C., Matthews, R. J., Lin, J., Thomas, M. L., and Fearon, D. T. (1995) *Science* 269, 242–244
31. Wagtmann, N., Rajagopalan, S., Winter, C. C., Peruzzi, M., and Long, E. O. (1995) *Immunity* 3, 801–809
32. Burshtyn, D. N., Lam, A. S., Weston, M., Gupta, N., Warmerdam, P. A., and Long, E. O. (1999) *J. Immunol.* 162, 897–902
33. Wang, L. L., Blasioli, J., Plas, D. R., Thomas, M. L., and Yokoyama, W. M. (1999) *J. Immunol.* 162, 1318–1323
34. Berg, K. L., Carlberg, K., Rohrschneider, L. R., Siminovitch, K. A., and Stanley, E. R. (1998) *Oncogene* 17, 2535–2541
35. Pei, D., Wang, J., and Walsh, C. T. (1996) *Proc. Natl. Acad. Sci. U. S. A.* 93, 1141–1145
36. Hof, P., Pluskey, S., Dhe-Paganon, S., Eck, M. J., and Shoelson, S. E. (1998) *Cell* 92, 441–450
37. Townley, R., Shen, S. H., Banville, D., and Ramachandran, C. (1993) *Biochemistry* 32, 13414–13418
38. Van den Steen P., Rudd, P. M., Dwek, R. A., and Opdenakker, G. (1998) *Crit. Rev. Biochem. Mol. Biol.* 33, 151–208
39. Biassoni, R., Cantoni, C., Falco, M., Verdiani, S., Bottino, C., Vitale, M., Conte, R., Poggi, A., Moretta, A., and Moretta, L. (1996) *J. Exp. Med.* 183, 645–650
40. Taylor, L. S., and McVicar, D. W. (1999) *Blood* 94, 1790–1796 M9-05253, 806025

REVIEW

The SHP-2 tyrosine phosphatase: Signaling mechanisms and biological functions

QU CHENG KUI
Department of Hematopoiesis, Jerome H. Holland Laboratory for the Biomedical Sciences, American Red Cross, Rockville, Department of Anatomy and Cell Biology, George Washington University School of Medicine and Health Sciences, Washington DC

ABSTRACT

Cellular biological activities are tightly controlled by intracellular signaling processes initiated by extracellular signals. Protein tyrosine phosphatases, which remove phosphate groups from tyrosine phosphorylated signaling molecules, play equally important tyrosine roles as protein tyrosine kinases in signal transduction. SHP-2, a cytoplasmic SH2 domain containing protein tyrosine phosphatase, is involved in the signaling pathways of a variety of growth factors and cytokines. Recent studies have clearly demonstrated that this phosphatase plays an important role in transducing signal relay from the cell surface to the nucleus, and is a critical intracellular regulator in mediating cell proliferation and differentiation.

Key words: *SHP-2, SHP-1, Signal transduction.*

INTRODUCTION

Cells can not survive without environmental factors. Cellular responses to a variety of extracellular cues are mediated by intracellular signaling pathways. A great deal of evidence has demonstrated that dysregulation of such signaling pathways initiated from extracellular factors causes malfunctioning of the targeted cells,

[0]Corresponding address: Dr. Cheng Kui Qu, Department of Hematopoiesis, Holland Laboratory, American Red Cross, 15601 Crabbs Branch Way, Rockville, MD 20855 USA
Tel: (301) 738-0445; Fax: (301) 738-0444; E-mail: quc@usa.redcross.org

and eventually leads to diseases. Many important cellular activities, such as cell proliferation, differentiation, and death, are highly controlled by the cellular signal transduction processes in which protein phosphorylation and dephosphorylation are central events[1-3]. It is increasingly clear that these biochemical processes are carried out by protein tyrosine kinases (PTKs) and protein tyrosine phosphatases (PTPs). Protein phosphorylation and dephosphorylation are closely related to the activities of the signaling proteins and directly mediate protein-protein interaction. Thus, PTPs, which dephosphorylate tyrosine phosphorylated signaling molecules, play an equally important role as PTKs in transducing signal flow and controlling cellular behavior. However, studies regarding PTPs are lagging behind. SHP-2, a Src homology 2 (SH2) domain containing non-transmembrane PTP, has been demonstrated to be involved in a variety of cytokine and growth factor initiated signal transduction processes[4-8]. Increasing evidence has indicated that this phosphatase plays an important role in diverse signaling pathways to regulate cellular biological processes. Even though significant progress has been made in the last several years, many aspects of the activities of this phosphatase still remain unaddressed. This review will focus on the signaling mechanisms and the biological functions of this enzyme. Particular attention will be paid to its role in hematopoietic cell regulation.

Signaling mechanisms

SHP-2, previously called SH-PTP2, PTP1D, SH-PTP3, and Syp, was identified independently by several groups as a cytosolic SH2 domain containing protein tyrosine phosphatase[4-8]. It is ubiquitously expressed in various tissues and cell types. It has a similar overall structure and high homology with the hematopoietic cell specific-SHP-1 phosphatase[9, 10]. Both of these phosphatases contain two tandem SH2 domains at the N-terminus and one phosphatase domain at the C-terminus. The SH2 domain is a 100 amino acid motif which mediates the binding of SHP-2 and SHP-1 to the phosphorylated tyrosine residues on other molecules, thus directing the specific protein-protein interaction for these two phosphatases[11]. Normally, the auto-inhibitory influence of their SH2 domains renders these two enzymes catalytically inefficient. Occupancy of the SH2 domains by phosphotyrosine residues leads to an increase in the catalytic activity of the SHP-2 and SHP-1 phosphatases, possibly by inducing conformational changes in the enzymes[12, 13]. Accumulated biochemical data have shown that both SHP-2 and SHP-1 act downstream of receptor and cytoplasmic tyrosine kinases to propagate the signal relay from the cell surface to the nucleus. Despit high homology between SHP-2 and SHP-1, their functions might be distinct. Genetic analyses on *Xenopus* revealed that both the SH2 domains and the phosphatase domains contribute to signaling, and thus functional specificity of these two PTPs[14, 15].

SHP-2 is expressed in various tissues and cell types, and has been implicated in diverse signaling pathways including those initiated by growth factors such as

PDGF, EGF, and IGF-1, cytokines such as IL-3, GM-CSF, and EPO, as well as insulin and interferon[16, 17]. SHP-2 has compound signaling functions. It appears to be involved in a variety of signal transduction processes, such as the Ras-Raf-MAP kinase, Jak-Stat, and PI3 kinase pathways. Within a single signaling pathway, SHP-2 may act at multiple sites to participate in the signal relay. For instance, SHP-2 directly interacts with cytokine and growth factor receptors, such as PDGF, EGF, SCF, and EPO receptors. It has also been demonstrated to bind with a variety of signaling intermediates such as Grb2, FRS-2, Jak2, p85 subunit of PI3 kinase, IRS-1, and Gab1 and 2. As a protein tyrosine phosphatase, SHP-2 is believed to function by dephosphorylating its associated signaling molecules, thus diminishing the local signaling flow. However, the ultimate effect of SHP-2 action in most signaling pathways is to enhance the signal transduction. The precise mechanism remains to be defined.

. In most circumstances, SHP-2 plays a positive role in transducing the signal relay from receptor PTKs[14, 18-21]. Previous biochemical evidence has demonstrated that the SHP-2 enzymatic activity is required for its function in signal transduction[21, 22]. Cysteine (Cys) at amino acid residue 459 has been identified as critical for its phosphatase activity. While the replacement of cysteine with serine (Ser) at this site completely abolishes its enzymatic activity, the capacity for this mutant molecule to bind to other signaling intermediates via its SH2 domains remains unaltered. This mutant functions thus as a dominant negative molecule over the endogenous wild type SHP-2. Using the dominant negative approach, SHP-2 has been reported, in a number of studies, to positively regulate the signaling pathways of insulin, EGF, PDGF, and FGF. Overexpression of this mutant protein has been shown to block the signaling functions of endogenous SHP-2 in both *in vitro* and *in vivo* models. For example, the introduction of a catalytically inert SHP-2 molecule markedly inhibited the activation of MAP kinase in response to EGF, insulin, and fibronectin stimulation[19, 21, 23-26]. The precise biochemical basis for such positive regulation for this phosphatase still remains unclear. Biochemical studies on the *Drosophila* homologue of SHP-2, csw, revealed that SHP-2 may function at a parallel level or upstream of Ras in the MAP kinase pathway[27].

In some cases, SHP-2 does play a negative role in intracellular signaling processes, thus it may have dual functions in cytokine and growth factor signal transduction. For instance, SHP-2 negatively regulates the Jak-Stat signaling pathway initiated by interferon -α and -γ. As a consequence, SHP-2 mutant cells are more sensitive to the cytotoxicity of interferons, and the activation of downstream Stat2 and Stat1 is elevated[28]. Another prominent example is that SHP-2 was found to function to diminish the signal relay from gp130[29-31]. For instance, the recent knockin mouse model, in which the endogenous gp130 has been replaced with a human gp130 Y759F (equivalent to residue 757 in mouse) mutant, displayed lymphoadenopathy, splenomegaly, and an enhanced acute-phase response. However, the data supporting the negative regulatory role for SHP-2 is based on observed

281

increases in gp130-dependent signaling when Y757 on gp130, a pivotal binding site for SHP-2, is mutated to phenylalanine. The question remaining to be resolved is whether these phenotypes are really mediated by SHP-2, because a more recent finding demonstrated that the Y757 is also the recognition site for SOCS-3, a putative SH2 domain containing cytokine signaling suppressor[32]. SOCS-3 and SHP-2 may compete to bind to this site, and SHP-2 functions to block the effects of SOCS-3 in gp 130 pathway.

SHP-2 is also highly expressed in hematopoietic cells, and has been indicated to be involved in hematopoietic growth factor signal transduction[33-35]. It has been shown to participate in the signal transduction from IL-3, EPO, SCF, GM-CSF, and IL-5. However, compared to SHP-1 phosphatase, understanding of the physiological and biochemical functions of SHP-2 in hematopoietic cells lags far behind. A potential role of SHP-2 phosphatase in hematopoietic cell signaling is indicated by indirect evidence based on receptor-mediated changes in SHP-2 tyrosine phosphorylation and/or its association with receptors or other signaling intermediates. Unfortunately, the cellular significance of SHP-2 involvement in these pathways remains to be elucidated. This could be achieved through the signal transduction studies on the hematopoietic cell lines lacking this phosphotase. Thus, direct evidence showing the biological function and the cellular significance of the enzymatic activity of this signaling protein may be obtained.

Identification of the down-stream targets or substrates of SHP-2 will help to elucidate the biochemical basis of SHP-2 activity in signal transduction. To date, several such molecules have been identified, for instance, SHPS-1[36], PZR[37], and the newly characterized pleckstrin homology domain-containing scaffolding or docking proteins, Gab1[38] and Gab2[39-41]. In fact, Gab2 was originally identified in IL-3 stimulated hematopoietic cells[42], and was shown to be a major SHP-2-binding protein. Subsequently, this strong interaction was further demonstrated to be induced by TPO and EPO stimulation as well as TCR engagement[41]. In addition, the SHP-2/Gab2 complex is also assembled in hematopoietic cells after β1 integrin cross-linking (Qu et al., unpublished data). Our recent studies showed that SHP-1 also associates with Gab2. However, unlike the SHP-2/Gab2 association, SHP-1 and Gab2 are associated in a constitutive manner. Thus both the SHP-2 and SHP-1 phosphatases anchor to the same docking protein Gab2, which may serve as a linker for the functional interaction between these two phosphatases.

Biological functions

An extensive distribution of SHP-2 phosphatase indicates that it might have a wide range of physiological functions. Recent data from SHP-2 gene knockout mice have clearly suggested this notion. Mice homozygous for a SHP-2 mutation are embryonic lethal. Homozygous mutants die at midgestation with multiple developmental defects in the mesodermal pattering and body organization[43, 44]. A

similar requirement for SHP-2 in *Xenopus* development was found to be attributed to its positive role in basic fibroblast growth factor signaling[15]. Chimeric mice generated from homozygous mutant ES cells die at different stages, depending on the contribution from the mutant cells[45]. This strategy has proven to be an alternative approach for further defining the physiological functions that are masked due to the early embryonic lethality of mutant mice. Some interesting phenotypes were observed in chimeric mice containing SHP-2 mutant cells, such as abnormal development of the skeleton and limbs[45, 46]. Another striking observation was that 50% of the chimeric mice had an open eyelid phenotype, which is a typical phenotype of EGF receptor knockout mice, suggesting that SHP-2 is required for *in vivo* action of EGF. Further genetic analyses showed that a SHP-2 heterozygous mutation dominantly enhanced the phenotypes of EGF receptor weak allele (*wa-2/wa-2*). .Reducing SHP-2 protein levels by half further significantly diminished the EGF signaling on the background of EGF receptor mutation[47]. Additionally, subsequent studies showed that the penetrance and severity of the defective cardiac semilunar valvulogenesis was enhanced in wa-2/wa-2 mice with a heterozygous mutation of SHP-2, indicating a functional requirement for SHP-2 in heart development[48].

In vitro studies have revealed that SHP-2 plays critical roles in regulating a number of cellular activities. ES cells are totipotent embryonic stem cells, that can be induced to differentiate into a variety of cell lineages, including hematopoietic cells, cardiomyocytes, and even neuronocytes. SHP-2 mutation in these stem cells severely decreased erythroid lineage differentiation. Myeloid lineage development was completely blocked[49]. Consistently, *in vivo* hematopoietic progenitor development of mutant ES cell origin in the bone marrow and fetal liver from the chimeric mice generated from homozygous mutant ES cells was undetectable[45]. Hematopoietic progenitor analyses demonstrated that hematopoietic activity in the yolk sac from homozygous mutant embryos was dramatically decreased, suggesting that the SHP-2 mutation blocks hematopoietic development at the primitive hematopoiesis stage. Moreover, SHP-2 is also required for lymphoid lineage development, as SHP-2 mutation completely blocked the T and B lymphocyte development in SHP-2-/-/RAG-2-/- chimeric mice. No Thy+ T cells and B220+ B cells derived from mutant ES cells were detected, suggesting T and B lymphocyte development was blocked at the Pro-T and Pro-B stages (Qu et al., unpublished data). It seems that these developmental defects occur at very early stages in the differentiation process of ES cells. Indeed, SHP-2 mutation significantly reduced ES cell differentiation potential[30, 50], the differentiation of other lineages, including cardiomyocytes and fibroblasts from mutant ES cells was also decreased.

In contrast with SHP-2 phosphatase, the hematopoietic cell specific-SHP-1 phosphatase negatively regulates hematopoietic cell regulation[51-54]. Functional studies on SHP-1 phosphatase have been considerably aided by analyses of *motheaten* (*me/me*) and *viable motheaten* (*mev/mev*) mice which have spontaneous mutations in the coding region for the N-terminal SH2 domain and the catalytic do-

main of SHP-1 respectively[55]. Homozygous mutants have obvious hematological abnormalities. Both me/me and mev^v/mev^v mice develop systemic autoimmune disease and die after approximately 3 and 9 w, respectively[56]. High levels of immunoglobulins-particularly autoantibodies-in peripheral blood and excessive erythropoiesis in spleen suggest a primarily negative regulatory role for this phosphatase in hematopoietic development and function. Consistent with this, it has been found that SHP-1 attenuates signals emanating from receptors for EPO, IL-3, GM-CSF, and M- CSF, and mediates inhibitory signals triggered by immunoglobulin γ Fc domains (FcγRIIB1), NK cell inhibitory receptor, TCR, BCR, CD22, and CD72[52-54, 57-60].

Taken together, these findings suggest that SHP-2 and the homologous SHP-1 phosphatase have opposite functions in regulating hematopoietic cell development, despite sharing high homology. Indeed, recent data from SHP-2/SHP-1 double mutant mice strongly support this notion. Defective primitive hematopoiesis caused by the SHP-2 mutation was partially rescued by an additional SHP-1 mutation (Qu et al., unpublished data). A profound biochemical basis for the distinct functions of these phosphatases remains to be elucidated.

In addition, SHP-2 appears to positively regulate fibroblast cell adhesion and migration[23, 24, 61, 62]. SHP-2 homozygous mutant fibroblast cells have reduced cell spreading and migration. Further biochemical studies have indicated that SHP-2 participates in focal adhesion kinase-mediated integrin signaling. Moreover, SHP-2 is required for in vivo insulin action. Transgenic mice expressing dominant negative SHP-2 displayed insulin resistance[25]. Plasma insulin levels in transgenic mice after 4 h fasting were 3 times greater than none-transgenic controls with comparable blood glucose levels. In the presence of physiological concentration of insulin, the insulin-stimulated glucose uptake in muscle and adipocytes from transgenic mice was impaired.

Perspectives

It is clear that SHP-2 tyrosine phosphatase plays critical roles in regulating signal transduction, and mediating a variety of cellular biological processes. However, many questions regarding the biochemical basis for its signaling functions still remain unaddressed. Prominent questions are: why does a protein tyrosine phosphatase play a positive role in transducing signal relay from cell surface receptors, and what is the biochemical significance of the phosphatase activity of this enzyme? Importantly, several recent reports have indicated a clinical relevance of SHP-2 phosphatase to some diseases such as neutropenia (Kostmann's syndrome)[63] and diabetes[64, 65], which further emphasizes the importance of studies on the signaling regulation of this PTP. Understanding the profound mechanisms of SHP-2 action will provide novel insights into the regulation of intracellular signaling processes, and may lead to novel molecular therapeutic approaches for certain diseases.

284

ACKNOWLEDGEMENTS

REFERENCES

[1] Hunter T. Signaling–2000 and beyond. Cell 2000; 100:113-27.

[2] Tonks NK and BG Neel. From form to function: signaling by protein tyrosine phosphatases. Cell 1996; 87:365-8.

[3] Denu JM, JA Stuckey, MA Saper, JE Dixon. Form and function in protein dephosphorylation. Cell 1996; 87:361-4.

[4] Feng GS, CC Hui, T Pawson. SH2-containing phosphotyrosine phosphatase as a target of protein-tyrosine kinases. Science 1993; 259:1607-11.

[5] Freeman RM, JrJ Plutzky, BG Neel. Identification of a human src homology 2-containing protein-tyrosine-phosphatase: a putative homolog of Drosophila corkscrew. Proc Natl Acad Sci USA 1992; 89:11239-43.

[6] Ahmad S, D Banville, Z Zhao, EH Fischer, SH Shen. A widely expressed human protein-tyrosine phosphatase containing src homology 2 domains. Proc Natl Acad Sci USA 1993; 90:2197-201.

[7] Vogel W, R Lammers, J Huang, A Ullrich. Activation of a phosphotyrosine phosphatase by tyrosine phosphorylation. Science 1993; 259:1611-4.

[8] Adachi M, M Sekiya, T Miyachi, K Matsuno, Y Hinoda, K Imai, A Yachi. Molecular cloning of a novel protein-tyrosine phosphatase SH-PTP3 with sequence similarity to the src-homology region 2. FEBS Lett 1992; 314:335-9.

[9] Adachi M, EH Fischer, J Ihle, et al. Mammalian SH2-containing protein tyrosine phosphatases. Cell 1996; 85:15.

[10] Yi T, JL Cleveland, JN Ihle. Identification of novel protein tyrosine phosphatases of hematopoietic cells by polymerase chain reaction amplification. Blood 1991; 78:2222-8.

[11] Koch CA, D Anderson, MF Moran, C Ellis, T Pawson. SH2 and SH3 domains: elements that control interactions of cytoplasmic signaling proteins. Science 1991; 252:668-74.

[12] Hof P, S Pluskey, S Dhe-Paganon, MJ Eck, SE Shoelson. Crystal structure of the tyrosine phosphatase SHP-2. Cell 1998; 92:441-50.

[13] Eck MJ, S Pluskey, T Trub, SC Harrison, SE Shoelson. Spatial constraints on the recognition of phosphoproteins by the tandem SH2 domains of the phosphatase SH-PTP2. Nature 1996; 379:277-80.

[14] Tang TL, RM Freeman, JrAM O'Reilly, BG Neel, SY Sokol. The SH2-containing protein-tyrosine phosphatase SH-PTP2 is required upstream of MAP kinase for early Xenopus development. Cell 1995; 80:473-83.

[15] O'Reilly AM and BG Neel. Structural determinants of SHP-2 function and specificity in Xenopus mesoderm induction. Mol Cell Biol 1998; 18:161-77.

[16] Neel BG and NK Tonks. Protein tyrosine phosphatases in signal transduction. Curr Opin Cell Biol 1997; 9:193-204.

[17] Huyer G and DR Alexander. Immune signalling: SHP-2 docks at multiple ports. Curr Biol 1999; 9:R129-32.

[18] Shi ZQ, W Lu, GS Feng. The Shp-2 tyrosine phosphatase has opposite effects in mediating the activation of extracellular signal-regulated and c-Jun NH2-terminal mitogen-activated protein kinases. J Biol Chem 1998; 273:4904-8.

[19] Bennett AM, SF Hausdorff, AM O'Reilly, RM Freeman, BG Neel. Multiple requirements for SH-PTP2 in epidermal growth factor-mediated cell cycle progression. Mol Cell Biol 1996; 16:1189-202.

[20] Hadari YR, H Kouhara, I Lax, J Schlessinger. Binding of Shp2 tyrosine phosphatase to FRS2 is essential for fibroblast growth factor-induced PC12 cell differentiation. Mol Cell Biol 1998; 18:3966-73.

[21] Milarski KL and AR Saltiel. Expression of catalytically inactive Syp phosphatase in 3T3 cells blocks stimulation of mitogen-activated protein kinase by insulin. J Biol Chem 1994; 269:21239-43.

[22] Yamauchi K, KL Milarski, AR Saltiel, JE Pessin. Protein-tyrosine-phosphatase SHPTP2 is a required positive effector for insulin downstream signaling. Proc Natl Acad Sci USA 1995; 92:664-8.

[23] Inagaki K, T Noguchi, T Matozaki, et al. Roles for the protein tyrosine phosphatase SHP-2 in cytoskeletal organization, cell adhesion and cell migration revealed by overexpression of a dominant negative mutant. Oncogene 2000; 19:75-84.

[24] Manes S, E Mira, C Gomez-Mouton, Z J Zhao, RA Lacalle, AC Martinez. Concerted activity of tyrosine phosphatase SHP-2 and focal adhesion kinase in regulation of cell motility. Mol Cell Biol 1999; 19:3125-35.

[25] Maegawa H, M Hasegawa, S Sugai, et al. Expression of a dominant negative SHP-2 in transgenic mice induces insulin resistance. J Biol Chem 1999; 274:30236-43.

[26] Noguchi T, T Matozaki, K Horita, Y Fujioka, M Kasuga. Role of SH-PTP2, a protein-tyrosine phosphatase with Src homology 2 domains, in insulin-stimulated Ras activation. Mol Cell Biol 1994; 14:6674-82.

[27] Allard JD, HC Chang, R Herbst, H McNeill, MA Simon. The SH2-containing tyrosine phosphatase corkscrew is required during signaling by sevenless, Ras1 and Raf. Development 1996; 122:1137-46.

[28] You M, DH Yu, GS Feng. Shp-2 tyrosine phosphatase functions as a negative regulator of the interferon-stimulated Jak/STAT pathway. Mol Cell Biol 1999; 19:2416-24.

[29] Symes A, N Stahl, SA Reeves, et al. The protein tyrosine phosphatase SHP-2 negatively regulates ciliary neurotrophic factor induction of gene expression. Curr Biol 1997; 7:697-700.

[30] Burdon T, C Stracey, I Chambers, J Nichols, A Smith. Suppression of SHP-2 and ERK signalling promotes self-renewal of mouse embryonic stem cells. Dev Biol 1999; 210:30-43.

[31] Ohtani T, K Ishihara, T Atsumi, et al. Dissection of signaling cascades through gp130 *in vivo*: reciprocal roles for STAT3- and SHP2-mediated signals in immune responses. Immunity 2000; 12:95-105.

[32] Nicholson SE, DDe Souza, LJ Fabri, J Corbin, TA Willson, JG Zhang, A Silva, M Asimakis, A Farley, AD Nash, D Metcalf, DJ Hilton, NA Nicola, M Baca. Suppressor of cytokine signaling-3 preferentially binds to the SHP-2-binding site on the shared cytokine receptor subunit gp130. Proc Natl Acad Sci USA 2000; 97:6493-8.

[33] Fuhrer DK, GS Feng, YC Yang. Syp associates with gp130 and Janus kinase 2 in response to interleukin-11 in 3T3-L1 mouse preadipocytes. J Biol Chem 1995; 270:24826-30.

[34] Tauchi T, GS Feng, MS Marshall, et al. The ubiquitously expressed Syp phosphatase interacts with c-kit and Grb2 in hematopoietic cells. J Biol Chem 1994; 269:25206-11.

[35] Tauchi T, GS Feng, R Shen, et al. Involvement of SH2-containing phosphotyrosine phosphatase Syp in erythropoietin receptor signal transduction pathways. J Biol Chem 1995; 270:5631-5.

[36] Fujioka Y, T Matozaki, T Noguchi, et al. A novel membrane glycoprotein, SHPS-1, that binds the SH2-domain- containing protein tyrosine phosphatase SHP-2 in response to mitogens and cell adhesion. Mol Cell Biol 1996; 16:6887-99.

[37] Zhao ZJ and R Zhao. Purification and cloning of PZR, a binding protein and putative physiological substrate of tyrosine phosphatase SHP-2. J Biol Chem 1998; 273:29367-72.

[38] Holgado-Madruga M, DR Emlet, DK Moscatello, AK Godwin, AJ Wong. A Grb2-associated docking protein in EGF- and insulin-receptor signalling. Nature 1996; **379**:560-4.

[39] Gu H, JC Pratt, SJ Burakoff, BG Neel. Cloning of p97/Gab2, the major SHP2-binding protein in hematopoietic cells, reveals a novel pathway for cytokine-induced gene activation. Mol Cell 1998; **2**:729-40.

[40] Zhao C, DH Yu, R Shen, GS Feng. Gab2, a new pleckstrin homology domain-containing adapter protein, acts to uncouple signaling from ERK kinase to Elk-1. J Biol Chem 1999; **274**:19649-54.

[41] Nishida K, Y Yoshida, M Itoh, et al. Gab-family adapter proteins act downstream of cytokine and growth factor receptors and T- and B-cell antigen receptors. Blood 1999; **93**:1809-16.

[42] Gu H, JD Griffin, BG Neel. Characterization of two SHP- 2- associated binding proteins and potential substrates in hematopoietic cells. J Biol Chem 1997; **272**:16421-30.

[43] Saxton TM, M Henkemeyer, S Gasca, et al. Abnormal mesoderm patterning in mouse embryos mutant for the SH2 tyrosine phosphatase Shp-2. Embo J 1997; **16**:2352-64.

[44] Arrandale JM, A Gore-Willse, S Rocks, et al. Insulin signaling in mice expressing reduced levels of Syp. J Biol Chem 1996; **271**:21353-8.

[45] Qu CK, WM Yu, B Azzarelli, et al. Biased suppression of hematopoiesis and multiple developmental defects in chimeric mice containing Shp-2 mutant cells. Mol Cell Biol 1998; **18**:6075-82.

[46] Saxton TM, BG Ciruna, D Holmyard, et al. The SH2 tyrosine phosphatase shp2 is required for mammalian limb development. Nat Genet 2000; **24**:420-3.

[47] Qu CK, WM Yu, B Azzarelli, GS Feng. Genetic evidence that Shp-2 tyrosine phosphatase is a signal enhancer of the epidermal growth factor receptor in mammals. Proc Natl Acad Sci USA 1999; **96**:8528-33.

[48] Chen B, RT Bronson, LD Klaman, et al. Mice mutant for Egfr and Shp2 have defective cardiac semilunar valvulogenesis. Nat Genet 2000; **24**:296-9.

[49] Qu CK, ZQ Shi, R Shen, FY Tsai, SH Orkin, GS Feng. A deletion mutation in the SH2-N domain of Shp-2 severely suppresses hematopoietic cell development. Mol Cell Biol 1997; **17**:5499-507.

[50] Qu CK and GS Feng. Shp-2 has a positive regulatory role in ES cell differentiation and proliferation. Oncogene 1998; **17**:433-9.

[51] Kozlowski M, L Larose, F Lee, DM Le, R Rottapel, KA Siminovitch. SHP-1 binds and negatively modulates the c-Kit receptor by interaction with tyrosine 569 in the c-Kit juxtamembrane domain. Mol Cell Biol 1998; **18**:2089-99.

[52] Yi T, AL Mui, G Krystal, JN Ihle. Hematopoietic cell phosphatase associates with the interleukin-3 (IL-3) receptor beta chain and down-regulates IL-3-induced tyrosine phosphorylation and mitogenesis. Mol Cell Biol 1993; **13**:7577-86.

[53] Chen HE, S Chang, T Trub, BG Neel. Regulation of colony-stimulating factor 1 receptor signaling by the SH2 domain-containing tyrosine phosphatase SHPTP1. Mol Cell Biol 1996; **16**:3685-97.

[54] Klingmuller U, U Lorenz, LC Cantley, BG Neel, HF Lodish. Specific recruitment of SH-PTP1 to the erythropoietin receptor causes inactivation of JAK2 and termination of proliferative signals. Cell 1995; **80**:729-38.

[55] Shultz LD, PA Schweitzer, TV Rajan, et al. Mutations at the murine motheaten locus are within the hematopoietic cell protein -tyrosine phosphatase (Hcph) gene. Cell 1993; **73**:1445-54.

[56] Shultz LD. Pleiotropic effects of deleterious alleles at the "motheaten" locus. Curr Top Microbiol Immunol 1988; **137**:216-22.

[57] D'Ambrosio D, KL Hippen, SA Minskoff, et al. Recruitment and activation of PTP1C in negative regulation of antigen receptor signaling by Fc gamma RIIB1. Science 1995; **268**:293-7.

[58] Doody GM, LB Justement, CC Delibrias, et al. A role in B cell activation for CD22 and the protein tyrosine phosphatase SHP. Science 1995; **269**:242-4.

[59] Wu Y, MJ Nadler, LA Brennan, et al. The B-cell transmembrane protein CD72 binds to and is an *in vivo* substrate of the protein tyrosine phosphatase SHP-1. Curr Biol 1998; **8**:1009-17.

SHP-2 in signal transduction

[60] Burshtyn DN, AM Scharenberg, N Wagtmann, et al. Recruitment of tyrosine phosphatase HCP by the killer cell inhibitor receptor. Immunity 1996; 4:77-85.

[61] Yu DH, CK Qu, O Henegariu, X Lu, GS Feng. Protein-tyrosine phosphatase Shp-2 regulates cell spreading, igration, and focal adhesion. J Biol Chem 1998; 273:21125-31.

[62] Hakak Y, YS Hsu, GS Martin. Shp-2 mediates v-Src-induced morphological changes and activation of the anti-apoptotic protein kinase Akt. Oncogene 2000; 19:3164-71.

[63] Tidow N, B Kasper, K Welte. SH2-containing protein tyrosine phosphatases SHP-1 and SHP-2 are dramatically increased at the protein level in neutrophils from patients with severe congenital neutropenia (Kostmann's syndrome). Exp Hematol 1999; 27:1038-45.

[64] Bonini JA, J Colca, C Hofmann. Altered expression of insulin signaling components in streptozotocin-treated rats. Biochem Biophys Res Commun 1995; 212:933-8.

[65] Ahmad F and BJ Goldstein. Alterations in specific protein-tyrosine phosphatases accompany insulin resistance of streptozotocin diabetes. Am J Physiol 1995; 268:E932-40.

ELSEVIER

GENE
AN INTERNATIONAL JOURNAL ON
GENES AND GENOMES

Review

The function of the protein tyrosine phosphatase SHP-1 in cancer

Chengyu Wu[1], Mingzhong Sun[1], Lijun Liu, G. Wayne Zhou*

Program in Molecular Medicine, University of Massachusetts Medical School, 373 Plantation Street, Worchester, MA 01605, USA

Abstract

SHP-1, an SH2 domain-containing protein tyrosine phosphatase, is primarily expressed in hematopoietic cells and behaves as a key regulator controlling intracellular phosphotyrosine levels in lymphocytes. SHP-1 has been proposed as a candidate tumor suppressor gene in lymphoma, leukemia and other cancers, as it functions as an antagonist to the growth-promoting and oncogenic potentials of tyrosine kinase. The decreased levels of SHP-1 protein and SHP-1 mRNA observed in various leukemia and lymphoma cell lines have been attributed to either the methylation of the promoter region of the SHP-1 gene or the post-transcriptional block of SHP-1 protein synthesis. In contrast, SHP-1 protein is normally or over-expressed in some non-lymphocytic cell lines, such as prostate cancer, ovarian cancer and breast cancer cell lines. SHP-1 expression also is decreased in some breast cancer cell lines with negative expression of estrogen receptor as well as some prostate and colorectal cancer cell lines. These data suggest that SHP-1 can play either negative or positive roles in regulating signal transduction pathways. Dysfunction in SHP-1 regulation can cause abnormal cell growth and induce different kinds of cancers. In this paper, we summarize recent studies on the expression and regulation of SHP-1 protein and its pathological function in the development of lymphoma, leukemia and other cancers.
© 2003 Elsevier Science B.V. All rights reserved.

Keywords: SHP-1; Tumor suppressor gene; Regulation; Cancer

1. Introduction

Known as a key mechanism for regulating eukaryotic

cellular signaling pathways, the phosphorylation of tyrosine residues in proteins is precisely regulated by two types of enzymes, protein tyrosine kinases (PTKs) and protein tyrosine phosphatases (PTPs). PTKs catalyze the phosphorylation of tyrosine residues, and conversely, PTPs dephosphorylate the phosphotyrosine residues which keep the tyrosine phosphorylation level at a dynamic equilibrium in biological systems (for review see Tonks and Neel, 1996). Any deviation in this balance (generally associated with increased PTK signaling) can promote the intracellular accumulation of tyrosine-phosphorylated proteins, which will cause abnormal cell proliferation and differentiation thereby resulting in different kinds of diseases (Qian and Weiss, 1997; Healy and Goodnow, 1998; Siminovitch et al., 1999). Similar deviation from this equilibrium also can be induced by decreased activity of PTPs resulting from gene mutation or gene deletion, leading to an increase in tyrosine-phosphorylated proteins in cells (Tsui et al., 1993; Lorenz et al., 1996; Pani et al., 1996; Paulson et al., 1996).

SHP-1, an SH2 domain-containing cytosolic PTP, is a key regulator that controls the intracellular phosphotyrosine level in lymphocytes. Cross-linking of immune receptors, such as the B cell receptor (BCR) and T cell receptor (TCR)

on their cognate cells leads to their activation through the sequential activation of PTKs, which then trigger a cascade of intracellular phosphorylation which, in turn, activates the cells. Inhibitory receptors and their associated signaling molecules are responsible for setting the threshold levels for activation signals and the subsequent activation-terminating response (Sen et al., 1999; Bruecher-Encke et al., 2001). In lymphocytes, SHP-1 binds the immunoreceptor tyrosine-based inhibition motif (ITIM) of the inhibitory receptors, such as CD22, CD72, FcγRIIB, p70-NKB1 and KIR, through its SH2 domains, dephosphorylates the downstream proteins, and subsequently either terminates the activated signal or activates other pathways such as apoptosis (Unkeless and Jin, 1997; Famiglietti et al., 1999; Christensen and Geisler, 2000). Therefore, dysfunction of SHP-1 in lymphocytes likely induces lymphoma, leukemia and other related diseases (Tabrizi et al., 1998).

Extensive studies on SHP-1 protein and SHP-1 mRNA revealed that the expression of SHP-1 protein was diminished or abolished in most cancer cell lines and tissues examined (Plutzky et al., 1992; Walton and Dixon, 1993; Banville et al., 1995; Matsushita et al., 1999; Oka et al., 2001; Tsui et al., 2002). On the other hand, the growth of cancer cells was suppressed after introducing the SHP-1 gene into the corresponding cell lines (Bruecher-Encke et al., 2001; Zapata et al., 2002). These findings support the hypothesis that the SHP-1 gene functions as a tumor suppressor. Herein, we review the recent progress in the studies on the relationship between SHP-1 and various cancers. We also discuss the pathological function and the potential therapeutic role of SHP-1 in lymphoma, leukemia and other cancer-related diseases.

2. The SHP-1 gene structure and protein structure

The human SHP-1 gene is located on chromosome 12p13 (Plutzky et al., 1992; Matsushita et al., 1999). It consists of 17 exons and spans approximately 17 kb of DNA with a transcription size of 2.4–2.6 kb (Fig. 1). SHP-1 gene encodes two forms of SHP-1 protein due to different translation initiation codons located within exons 1 and 2, respectively (Fig. 1). Both forms of SHP-1 proteins are synthesized using identically restricted exons. The major differences between the two forms appear at the N-terminal amino acid sequences, MLSRG for form I and MVR for form II. The difference in the activity of the two forms of SHP-1 protein is marginal and negligible (Plutzky et al., 1992; Walton and Dixon, 1993).

Two different and mutually exclusive tissue-specific promoters regulate expression of the two forms of SHP-1 protein (Fig. 1). Promoter 1, located approximately 7 kb upstream from promoter 2, is active in all cells of non-hematopoietic origin, whereas promoter 2 is active exclusively in cells of hematopoietic lineage. Both promoters contain the recognition sequences for transcription

factors such as SP1 and/or AP2. Promoter 2 contains an inverted GATA box approximately 250-bp from the identified transcription starting site (CAP site), a second GATA sequence, a CCAAT box, and a properly-spaced TATA box region between 390- and 470-bp from the CAP site (Banville et al., 1995). In contrast, promoter 1 has an important motif for its expression, located about 190-bp upstream of the CAP site which contains two 12-bp repeats, each with an E-box. This region is regulated by the heterodimer or homodimer of the upstream stimulatory factors USF1 and/or USF2. Promoter 1 also contains another motif containing 12-bp repeats, the NF-κB binding site, located 105-bp upstream of the E-box. This motif is regulated by a different complex of NF-κB dimers (Tsui et al., 2002). Exons 3 and 4, exons 5 and 6, and exons 8–10 encode the N-terminal SH2 domain, C-terminal SH2 domain, and catalytic domain, respectively. The translation stop codon is located within exon 16, and no known protein is encoded by exon 17 (Fig. 1).

The crystal structures of SHP-1 in different conformations have been determined (Yang et al., 1998, 2000, 2001, 2003). As shown in Fig. 2, the C-terminal truncated SHP-1 is in a self-inhibited conformation, with the Nβ4-Nβ5 loop of the N-SH2 domain protruding into the catalytic domain to directly block the entrance into the active site (Yang et al., 2003). The highly mobile C-SH2 domain was expected to function as an antenna to search for the phosphopeptide activator. Binding of a phosphopeptide to the C-SH2 domain results in a large conformational change that restores the distorted conformation of the neighboring N-SH2 domain and subsequently opens up its phosphopeptide-binding pocket to harbor a second phosphopeptide molecule. These events can weaken the self-inhibiting interaction on the interface between the N-SH2 and catalytic domains and permit the subsequent synergistic opening up of the catalytic domain's active site (Yang et al., 2003).

The active site of the catalytic domain of SHP-1 contains three important amino acid residues: Cys455, behaving as the nucleophile to attack the substrate; Arg459, stabilizing the negative charge of the phosphotyrosine substrate; and Asp421, serving as the proton donor and proton acceptor involving the product release. In addition, the activity of the catalytic domain is determined by the flexibility of the WPD loop, which contains the active-site residue Asp421 (Yang et al., 1998). Both biochemical and crystallographic data have shown that the catalytic domain of SHP-1 prefers the substrate with the consensus sequence $(D/E)X(L/I/V)X_{1-2}pYXX(L/I/V)$, and that the substrate-recognition specificity is conferred by the β5-loop-β6 and α5-loop-α6 regions (Yang et al., 1998, 2000).

3. The expression of SHP-1 protein in lymphoma and leukemia cell lines

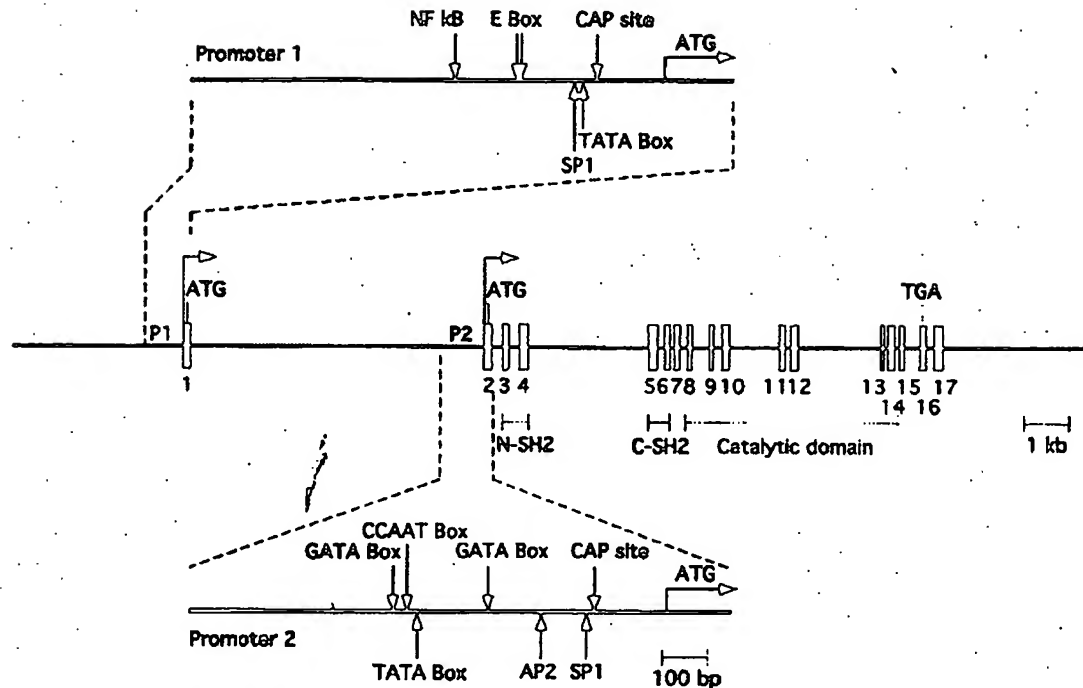Lymphoma comprises a group of neoplasms arising from

Fig. 1. Schematic representation of the human SHP-1 gene. The black boxes represent the exons. P1 and P2 indicate the positions of promoters 1 and 2 which are active in non-hematopoietic and hematopoietic cells, respectively. The positions of the translation initiation sites (ATG) and the termination codon are indicated. The various domains of SHP-1 encoded by different exons are shown below the exons. The schematic representations of promoter regions 1 and 2 are enlarged in the figure. The CAP sites (position +1) and the initiation codons are shown for both promoter regions. The positions of a putative TATA box, an SP-1 recognition sequence, an AP2 binding site, two GATA boxes and a CCAAT box are shown in the promoter 1 region. The positions of a TATA box, an SP-1 recognition site, two repeat E boxes which bind USF1 and/or USF2, and an NF-κB binding site are shown in the promoter 2 region.

lymphoid cells. Lymphomas are classified clinically into Hodgkin's disease and non-Hodgkin's lymphomas. The non-Hodgkin's lymphomas include three major forms: B-cell lymphoma, T-cell lymphoma and putative NK-cell lymphoma (Isaacson, 2000; Ottensmeier, 2001). Lymphoma could be caused by a variety of risk factors such as infection by Epstein–Barr virus (EBV), along with congenital or acquired immune deficiencies, organ transplantation, autoimmune disorders like Hashimoto's thyroiditis and Sjogren's syndrome, malaria, infection with human T-cell leukemia/lymphoma virus, or Kaposi's sarcoma-associated herpes virus (Baris and Zahin, 2000). However, how these risk factors play a role in the development of malignancy remain unknown.

SHP-1 is predominantly expressed in hematopoietic cells. Specifically, it down-regulates intracellular signaling transmembrane receptors: growth factor receptors with an intrinsic tyrosine kinase activity (e.g. c-kit, CSF-1, TrkA and EGF) (Chen et al., 1996; Tomic et al., 1995; Vambutas et al., 1995; Vogel et al., 1993; Yeung et al., 1992; Yi et al., 1993), cytokine receptors (e.g. Epo-R, IFNα/β-R, IL-3R and IL-2R) (Kim et al., 1999; Klingmuller et al., 1995; Kozlowski et al., 1993; Law et al., 1996) and receptors involved in the immune response such as the TCR complex

and CD5 (David et al., 1995; Klingmuller et al., 1995; Yi et al., 1993, 1995). The importance of SHP-1 expression for the maturation and function of hematopoietic cells has been addressed by the studies of moth-eaten (me/me) and moth-eaten viable (me^v/me^v) mice carrying mutations in SHP-1 gene. The homozygous me and me^v mice exhibited multiple abnormalities including neutrophilia, lymphopenia, splenomegaly and/or elevated serum immunoglobulin, severe combined immunodeficiency and systemic autoimmunity, due to the dysregulation of leukocyte development (Kozlowski et al., 1993; Shultz et al., 1993; Tsui et al., 1993; Lorenz et al., 1996). Therefore, decreased or abolished SHP-1 protein expression can be regarded as a characteristic of lymphoma/leukemia cell lines and tissues.

3.1. B-cell lymphoma

The expression of SHP-1 in most of human Burkitt's lymphoma (also known as B-cell lymphoma, high-grade B-cell lymphoma or small non-cleaved cell lymphoma) cell lines was dramatically decreased (Table 1). Burkitt's lymphoma, classified as a non-Hodgkin's lymphoma, is a lymph gland tumor associated with EBV infection. In all 13 EBV-negative Burkitt's lymphoma cell lines (Ramos,
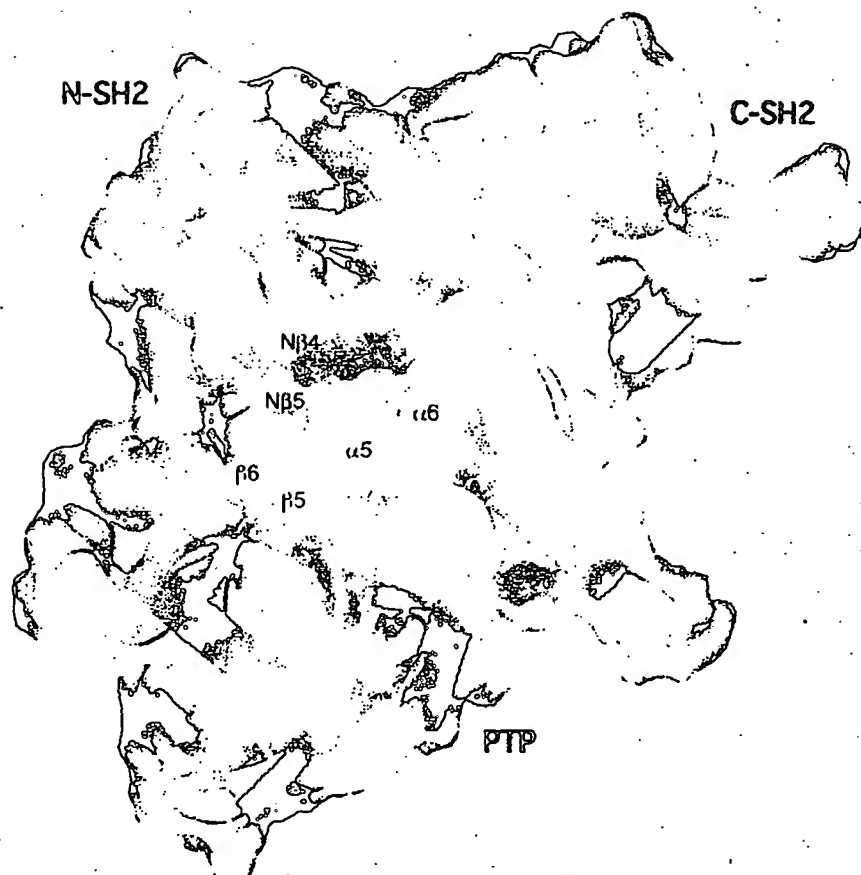
Fig. 2. Schematic drawing of the three-dimensional structure of SHP-1. The N-SH2, C-SH2 and catalytic domains are colored in red, green and blue, respectively. The solvent-accessible surface of the protein is shown in transparent gray and overlapped on the structure of SHP-1.

BL70, BL2, BL28, BL47, CA46, EW6, DG75, MC116, Louckes, WMN, BL41 and DHBL), SHP-1 protein expression was reduced by one to three orders of magnitude compared with in normal lymphocytes. In contrast, in all 11 group I/II EBV-positive Burkitt's lymphomas cell lines (Eli, Kem I, Mutu I, Rael, Raji, Daudi, WW2BL, BL72, OKUBL, ODHI BL and BL74), which have retained the original tumor phenotype and morphologically resemble EBV-negative lines, the expression of SHP-1 protein was decreased by 95% compared to the corresponding normal B cells. Also, the decreased expression of SHP-1 in the above cells was comparable to that of me^V/me^V mice (Kozlowski et al., 1993; Shultz et al., 1993; Tsui et al., 1993). Nevertheless, SHP-1 protein was normally expressed in four group III EBV-positive Burkitt's lymphoma cell lines (AG876BL, KK124, Kem III and WW1BL), and in BJAB, a B lymphoma cell line morphologically resembling EBV-negative Burkitt's lymphoma but lacking the characteristic chromosomal translocation that involves c-myc (Delibrias et al., 1997).

3.2. T-cell lymphoma

Numerous epidemiological and clinical studies have established the connection between human T cell lymphotropic virus type I (HTLV-I) infection and T-cell lymphomas including adult T-cell leukemia/lymphoma (ATLL), cutaneous T cell lymphoma (CTCL), peripheral blood lymphocyte (PBL) and T lymphoma (T-LY) (Johnson et al., 2001; Zucker-Franklin, 2001). Among 14 HTLV-I positive T-lymphoma cell lines, ten (MT-1, MT-2, MT-4, MB3-12A, MB3-12B, ATL-2, C91PL, C10MJ2, EDS and ATLIK) showed diminished or abolished SHP-1 protein expression, whereas three (HUT102B, HUB102B2 and MJ) expressed SHP-1 at normal levels (Table 2) (Migone et al., 1998; Zhang et al., 2000; Oka et al., 2001). The three cell lines with normal SHP-1 protein expression expressed IL-5, a cytokine which mediates the constitutive activation of the JAK-STAT pathway and hence overcomes the requirement for the down-regulation of SHP-1

Table 1
Expression of SHP-1 in cell lines originated from Burkitt's lymphoma

Cell line	Origin	SHP-1[a]	Cell type	Reference
BJAB	Burkitt's LY	+	B cell EB(−)	Delibrias et al. (1997)
Ramos	Burkitt's LY	−	B cell EB(−)	
BL70	Burkitt's LY	−	B cell EB(−)	
BL2	Burkitt's LY	↓	B cell EB(−)	
BL28	Burkitt's LY	↓	B cell EB(−)	
BL47	Burkitt's LY	↓	B cell EB(−)	
CA46	Burkitt's LY	↓	B cell EB(−)	
EW6	Burkitt's LY	↓	B cell EB(−)	
DG75	Burkitt's LY	↓	B cell EB(−)	
MC116	Burkitt's LY	↓	B cell EB(−)	
Louckes	Burkitt's LY	↓	B cell EB(−)	
WMN	Burkitt's LY	↓	B cell EB(−)	
BL41	Burkitt's LY	↓	B cell EB(−)	
DHBL	Burkitt's LY	↓	B cell EB(−)	
Eli	Burkitt's LY	↓	B cell EBgroupI/II(+)	
Kem I	Burkitt's LY	↓	B cell EBgroupI/II(+)	
Mutu I	Burkitt's LY	↓	B cell EBgroupI/II(+)	
Rael	Burkitt's LY	↓	B cell EBgroupI/II(+)	
Raji	Burkitt's LY	↓	B cell EBgroupI/II(+)	
Daudi	Burkitt's LY	−	B cell EBgroupI/II(+)	
WW2BL	Burkitt's LY	−	B cell EBgroupI/II(+)	
BL72	Burkitt's LY	↓	B cell EBgroupI/II(+)	
OKUBL	Burkitt's LY	↓	B cell EBgroupI/II(+)	
ODHIBL	Burkitt's LY	↓	B cell EBgroupI/II(+)	
BL74	Burkitt's LY	↓	B cell EBgroupI/II(+)	
AG876BL	Burkitt's LY	+	B cell EBgroupIII(+)	
KK124	Burkitt's LY	+	B cell EBgroupIII(+)	
KemIII	Burkitt's LY	+	B cell EBgroupIII(+)	
WW1BL	Burkitt's LY	+	B cell EBgroupIII(+)	
WW2LCL	BLCL	+	Lymphoblastoid cell EBV(+)	
JY	BLCL	+	Lymphoblastoid cell EBV(+)	

[a] +, detectable; −, undetectable; ↑, increased; ↓, decreased; N/A, not available (symbols are also used for the following tables).

expression. In contrast to the above 13 cell lines, the IWA1 cell line strongly expressed SHP-1 protein. This difference may be related to the fact that IWA1 is a virus producing cell line with a normal human karyotype which was freshly immortalized in vitro by co-cultivation with an HTLV-1 producer cell line.

The pattern of SHP-1 expression is similar in T lymphoma cell lines regardless of HTLV-I status. The expression of SHP-1 protein in different HTLV-I-negative T-cell lymphomas is summarized in Table 2. In comparison with normal B and T cells, twelve cell lines, including four out of five Hodgkin's cell lines (L540, HDLM, HDLM2 and L428), six out of seven aggressive non-Hodgkin's T-cell lines (2A, 2B, SEZ-4, SUDHL-1, HUT78 and KIT225) and two NK/T lymphoma cells lines (NK-YS and NK-TYZ), exhibited diminished or undetectable protein expression (Zhang et al., 2000; Oka et al., 2001). In contrast, the PB-1 and HD70 cell lines expressed SHP-1 protein at normal levels. These differences might be attributed to the developing stage of T-cell lymphoma, as the loss of SHP-1 expression could be progressive and lymphoma stage-dependent (Oka et al., 2001; Zhang et al., 1999, 2000).

3.3. Leukemia

Leukemia comprises a group of malignancies that originate from hematopoietic cells. There are four kinds of leukemia: acute/chronic lymphocytic leukemia and acute/chronic myelogenous leukemia. Leukemia is related to lymphoma since they exhibit the uncontrolled growth of cells with similar function and origin. The expression of SHP-1 protein in different leukemia cell lines is summarized in Table 3. SKW3, a cell line of T cell chronic lymphocyte leukemia (TCLL), and K562, a cell line of chronic myelogenous leukemia (CML), were negative for SHP-1 expression. In addition, two out of four B cell acute lymphoblastic leukemia (B-ALL) cell lines (SCOTT and KW) and two out of three multiple myeloma (MM) cell lines (U266 and RPM18266) showed decreased or abolished protein expression. However, SHP-1 was normally expressed in some B-ALL cell lines (KCA and BALL1), MM cell line (MOLP2), AML cell line (KG1), ATL cell line (JURKAT) and two low-grade malignant lymphoma/ leukemia cell lines (SP53 and SP50B). It is not clear why SHP-1 is expressed so differently in different leukemia cell

Table 2
Expression of SHP-1 in cell lines originated from other lymphomas[a]

Cell line	Origin	SHP-1	Cell type	Reference
MT-1	ATLL	−	T-cell HTLV1(+)	Migone et al. (1998)
MT-2	ATLL	−	T-cell HTLV1(+)	Migone et al. (1998)
MT-4	ATLL	−	T-cell HTLV1(+)	Migone et al. (1998)
HUT102B2	CTCL	+	T-cell HTLV1(+)	Migone et al. (1998)
MJ	CTCL	+	T-cell HTLV1(+)	Migone et al. (1998)
MB3-12A	PBL	−	T-cell HTLV1(+)	Migone et al. (1998)
MB3-12B	PBL	−	T-cell HTLV1(+)	Migone et al. (1998)
ATL-2	ATLL	−	T-cell HTLV1(+)	Zhang et al. (1999)
C91PL	ATLL	−	T-cell HTLV1(+)	Zhang et al. (1999)
HUT102B	ATLL	+	T-cell HTLV1(+)	Zhang et al. (1999)
C10MJ2	ATLL	−	T-cell HTLV1(+)	Zhang et al. (1999)
EDS	ATLL	↓	T-cell HTLV1(+)	Oka et al. (2001)
ATL1K	T-LY	−	T-cell HTLV1(+)	Oka et al. (2001)
IWAI		↓	T-cell HTLV1(+)	Oka et al. (2001)
PB-1	CTCL	+	T-cell	Zhang et al. (2000)
2A	CTCL	−	T-cell	Zhang et al. (2000)
2B	CTCL	−	T-cell	Zhang et al. (2000)
SEZ-4	CTCL	−	T-cell	Zhang et al. (2000)
SUDHL-1	ALCL	↓	T-cell	Zhang et al. (2000)
HUT78		−	T-cell	Leon et al. (2002)
KIT225		−	T-cell	Leon et al. (2002)
SU-DHL4	B-LY	↓	B-cell	Oka et al. (2001)
L540	HD	↓	T-cell	Zhang et al. (2000)
HDLM	HD	↓	T-cell	Zhang et al. (2000)
HDLM2	HD	−	T-cell	Oka et al. (2001)
L428	HD	↓	T-cell	Oka et al. (2001)
HD70	HD	+	T-cell	Oka et al. (2001)
SP53	MCL	+	Mantle cell	Oka et al. (2001)
SP50B	MCL	+	Mantle cell	Oka et al. (2001)
NK-YS	NK/T-LY	−	T-cell	Oka et al. (2001)
NK-TYZ	NK/T-LY	−	T-cell	Oka et al. (2001)

[a] Abbreviations: ALCL, anaplastic large-cell lymphoma; ATLL, adult T-cell leukemia/lymphoma; B-LY, B lymphoma; CTCL, cutaneous T-cell lymphoma; HD, Hodgkin's disease; MCL, mantle cell lymphoma; PBL, peripheral blood lymphocyte; NK/T-LY, natural killer/T lymphoma; and T-LY, lymphoma.

lines, but the SHP-1 expression in various cancer-related cell lines may be related to the progressive and aggressive

stages of leukemia (Bruecher-Encke et al., 2001; Oka et al., 2001).

In summary, SHP-1 protein is greatly diminished or abolished in highly aggressive lymphomas such as NK/T, ATLL and Burkitt's lymphomas. These results reflect the important function of SHP-1 in normal cell growth by balancing the PTK activity, and supporting the crucial role of SHP-1 in the pathogenesis in a wide range of lymphomas/leukemia.

4. The SHP-1 mRNA level in lymphoma and leukemia cell lines

The diminished or abolished SHP-1 protein expression in lymphoma/leukemia cell lines could be induced either by the decrease or absence of SHP-1 mRNA or the post-transcriptional regulation of protein synthesis. The SHP-1 mRNA levels in different lymphoma/leukemia cell lines have been examined using Northern blot and PCR analyses (Table 4). SHP-1 mRNA was detected in one CTCL cell line (PB-1), one ATLL cell line (HUT102B), one MCL cell line (SP53) and several leukemia cell lines (KCA, BALL1, EDS, ATL1K and JURKAT) (Oka et al., 2001; Zhang et al., 2000). The presence of SHP-1 mRNA confirmed that the SHP-1 gene and transcription of SHP-1 were normal in these cell lines. Also, this implied that decreased SHP-1 protein expression in some of these cell lines, such as EDS and ATL1K (Table 2), could be caused by post-transcriptional modification. In contrast, SHP-1 mRNA expression was undetectable in three CTCL cell lines (2A, 2B and SEZ-4), three ATLL (HTLV-1 positive) cell lines (ATL-2, C10MJ2 and C91PL), one ALCL cell line (L540), and two NK/T lymphoma cell lines (NK-YS and NK-TYZ) (Zhang et al., 2000) due to direct modification of the SHP-1 gene by mutation/deletion, or DNA modification in promoter region.

To investigate whether a genetic disorder or modification is involved in decreased SHP-1 expression, the coding

Table 3
Expression of SHP-1 in cell lines originated from leukemia[a]

Cell line	Origin	SHP-1	Reference
SCOTT	B-ALL	−	Oka et al. (2001)
KCA	B-ALL	+	Oka et al. (2001)
KW	B-ALL	−	Oka et al. (2001)
BALL1	B-ALL	+	Oka et al. (2001)
KG1	AML	+	Oka et al. (2001)
JURKT	ATL	+	Oka et al. (2001)
SKW3	T-CLL	−	Oka et al. (2001)
U266	MM	−	Oka et al. (2001)
MOLP2	MM	↑	Oka et al. (2001)
RPMI8266	MM	↓	Oka et al. (2001)
HairM	HCL	+	Oka et al. (2001)
K562	CML	−	Oka et al. (2001); Bruecher-Encke et al. (2001)

[a] Abbreviations: AML, acute myeloblastic leukemia; ATL, acute T lymphoblastic leukemia; B-ALL, T-lineage acute lymphoblastic leukemia; CML, chronic myelogenous leukemia; MM, multiple myeloma; HCL, hairy cell leukemia; and T-CLL, T-cell lymphocytic leukemia.

Table 4
Expression of SHP-1 mRNA in lymphoma/leukemia cell lines[a]

Cell line	Origin	SHP-1 mRNA	Inducibility	Reference
PB-1	CTCL	+	+ 5-deoxyazacytidine	Zhang et al. (2000)
2A	CTCL	−	+ 5-deoxyazacytidine	Zhang et al. (2000)
2B	CTCL	−	+ 5-deoxyazacytidine	Zhang et al. (2000)
SEZ-4	CTCL	−	N/A	Zhang et al. (2000)
ATL-2	ATLL(HTLV +)	−	+ 5-deoxyazacytidine	Zhang et al. (2000)
C10MJ2	ATLL(HTLV +)	−	+ 5-deoxyazacytidine	Zhang et al. (2000)
C91PL	ATLL(HTLV +)	−	N/A	Zhang et al. (2000)
HUT102B	ATLL(HTLV +)	+	N/A	Zhang et al. (2000)
L540	ALCL	−	+ 5-deoxyazacytidine	Zhang et al. (2000)
NK-YS	NK/T-LY	−	− TPA	Oka et al. (2001)
NK-TYZ	NK/T-LY	−	− TPA	Oka et al. (2001)
SP53	MCL	+	N/A	Oka et al. (2001)
KG1	AML	+	↑ TPA	Oka et al. (2001)
JURKAT	ATL	+	N/A	Leon et al. (2002); Oka et al. (2001)
KCA	B-ALL	+	N/A	Oka et al. (2001)
BALL1	B-ALL	+	N/A	Oka et al. (2001)
EDS	ATL	+	N/A	Oka et al. (2001)
ATL1K	ATL	+	N/A	Oka et al. (2001)
K562	CML	+	− TPA	Bruecher-Encke et al. (2001)
HT93	APL	+	↑ ATRA	Uesugi et al. (1999)
HL60	APL	+	↑ ATRA, ↑ DMSO	

[a] Abbreviations: ALCL, anaplastic large-cell lymphoma; AML, acute myeloblastic leukemia; APL, acute promyelocytic leukemia; ATL, acute T lymphoblastic leukemia; ATLL, adult T-cell leukemia/lymphoma; B-ALL, T-lineage acute lymphoblastic leukemia; CML, chronic myelogenous leukemia; CTCL, cutaneous T-cell lymphoma; MCL, mantle cell lymphoma; and NK/T-LY, natural killer/T lymphoma.

regions and splicing junctions of the SHP-1 gene were examined in nine T-cell lymphoma lines (PB-1, 2A, 2B, Sez-4, C91PL, ATL-2, C10MJ2, L540 and SUDHL01) (Zhang et al., 1999). DNA deletions or single-base mutations were not detected in any of those cell lines. Moreover, in these cells, the intact status of the SHP-1 gene was confirmed further by the induction of SHP-1 expression in response to stimulation with TPA, DMSO and/or ATRA (Table 4). In KG1 cells, although SHP-1 expression is low, it could be strongly induced with TPA treatment. Likewise, SHP-1 expression was detectable in some leukemia cell lines such as HL60 and HT93, and this up-regulation of SHP-1 expression could be observed with ATRA treatment. In addition, DMSO treatment was demonstrated to up-regulate SHP-1 expression in HL60 cells (Uesugi et al., 1999). In contrast, NK-YS and NK-TYZ cells were completely negative for SHP-1 expression with or without TPA stimulation, whereas normal human PBMC cells, as a control, had a transient increase in SHP-1 protein expression induced with TPA stimulation.

Another reason for the absence of SHP-1 mRNA could be the gene silencing resulting from the methylation of the cysteine residue in the CpG islands located in the 5' end of SHP-1 gene. The region encompassing promoter 2 and exon 2 of the SHP-1 gene is particularly rich in the CpG islands (Fig. 1). The promoter region of the SHP-1 gene in malignant T cell lines was resistant to digestion with three different methylation-sensitive restriction enzymes. How-

ever, treatment of cells with 5-deoxyazacytidine, a demethylation agent, could reverse this resistance. For example, in two Burkitt's lymphoma cell lines (Daudi and Ramos), two CTLL cell lines (2A and 2B), two ATLL cell lines (ATL-2, C10MJ2) and one Hodgkin's lymphoma cell line (LD540), SHP-1 mRNA expression could be induced by 5-deoxyazacytidine treatment under standard culture conditions. However, among the five cell lines with inducible SHP-1 mRNA expression, only one cell line (2A) had increased SHP-1 protein levels. Demethylation could increase the expression of SHP-1 mRNA and still might not induce SHP-1 protein expression due to additional post-transcriptional blocks in SHP-1 protein synthesis (Zhang et al., 2000). Therefore, diminished or abolished SHP-1 protein expression could be caused by the silencing of SHP-1 transcription due to the methylation of its promoter (Uesugi et al., 1999; Zhang et al., 2000; Bruecher-Encke et al., 2001; Oka et al., 2001).

5. The SHP-1 protein expression in clinic lymphoma/leukemia specimens

Decreased or abolished SHP-1 expression has been related to both malignant transformation and tumor cell invasiveness in most lymphoma/leukemia cell lines summarized above. Apparently, it is of interest to: (1) determine whether the SHP-1 expression pattern in specimens from

related cancer patients is similar to those observed in cancer cell lines; and (2) evaluate if and how SHP-1 expression changes during tumor progression and invasion.

Analyses, based on 207 paraffin-embedded specimens of various malignant lymphomas/leukemia using cDNA expression array and tissue microarray techniques, showed that 100% of NK/T cell lymphoma specimens and more than 95% of various types of malignant lymphoma specimens (DLL, FL, HD, MCL, PT and ATLL) were negative for SHP-1 protein expression (Fig. 3) (Oka et al., 2001). In comparison, only 60% of low-grade malignant lymphomas such as MZL and MALT were negative for SHP-1 expression, was caused either by methylation of the SHP-1 promoter region or by a post-transcriptional block. In a different study, nearly all follicle center cell lymphoma (29/30) were negative for SHP-1 protein expression due to malignant transformation and tumor aggressiveness (Kossev et al., 2001). These results revealed that the SHP-1 expression patterns in lymphoma/leukemia specimens were essentially consistent to those observed in the corresponding cell lines.

SHP-1 protein was highly expressed in resting B cells and in normal lymphocyte reactive hyperplasia. However, strong expression of SHP-1 protein also was observed in 40% of mantle zone and some inter-follicular zone lymphocytes in reactive lymphoid hyperplasia specimens (Oka et al., 2001). A few lymphoma samples, including four kinds of malignant small B-cell lymphoma tissues, all

mantle cell lymphomas (12/12), marginal zone lymphocytic lymphomas (10/10) and chronic lymphocytic leukemia/ small lymphocytic lymphomas (13/13) were found to express SHP-1 protein at normal levels (Kossev et al., 2001).

6. Expression of SHP-1 protein in other cancers

6.1. Breast cancer

Breast cancer is one of the most commonly diagnosed cancers in women. It has been found that the cellular phosphotyrosine imbalance due to deviation from the dynamic phosphotyrosine equilibrium is a common feature in human breast cancer. Increased PTP activity, followed by increased PTK activity, has been regarded as an important diagnostic parameter in breast cancer (Ouenholf-Kalff et al., 1995).

Yip et al. examined the expression of SHP-1 mRNA in 18 breast cancer cell lines and one HBL-100 cell line that was originally isolated from human breast milk and found to contain SV40-derived sequences (Yip et al., 2000). It was found that SHP-1 mRNA was normally expressed in all eight ER-positive cell lines (MDA-MB-134, MDA-MB-175, MDA-MB-361, MCF-7, BT-474, BT-483, T-47D and ZR-75-1) and in four out of ten ER-negative cell lines (MDA-MB-468, BT-20, SK-BR-3 and MDA-MB-453). In
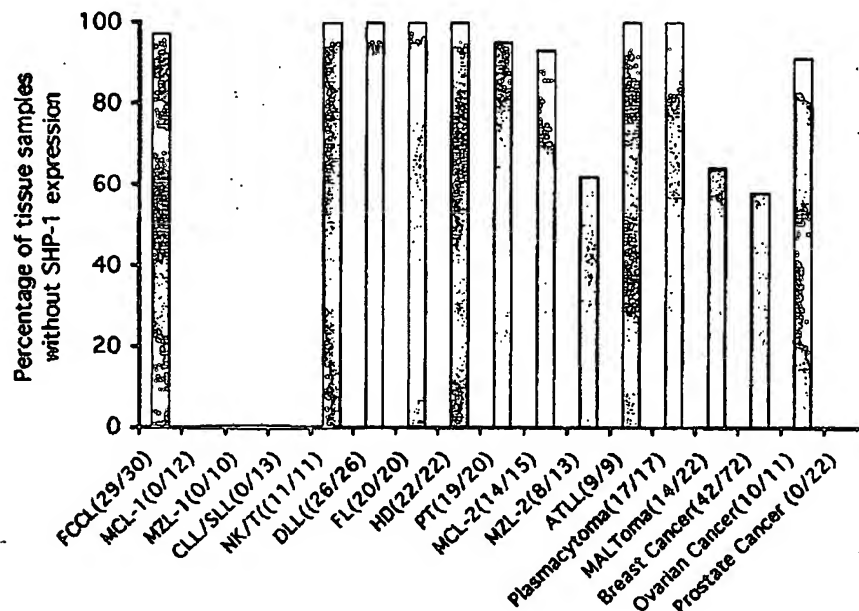
Fig. 3. SHP-1 expression in lymphoma, leukemia and other cancers. The graph shows the percentage of tissue samples from different cancer patients without SHP-1 protein expression. The number of tissue samples examined for each type of cancer is shown in the denominator of the label. Tissue samples without SHP-1 expression are shown in the numerator of the label. Abbreviations: FCCL, follicle center cell lymphoma; MCL, mantle cell lymphoma; MZL, maginal zone lymphoma; CLL/SLL, chronic lymphocytic leukemia/small lymphocytic lymphoma; DLL, diffuse large B cell lymphoma; FL, follicular lymphoma; HD, Hodgkin's disease; PT, peripheral T cell lymphoma; ATLL, adult T cell lymphoma/leukemia. MZL-1 & MCL-1 and MZL-2 & MCL-2 are independent results from two different groups.

contrast, SHP-1 mRNA expression was very low or even undetectable in six other ER-negative cell lines (BT-549, Hs-578T, MDA-MB-157, MDA-MB-231, MDA-MB-330 and MDA-MB-436) and HBL-100 cells (Table 5). Among these cell lines, five exhibited increased levels of SHP-1 mRNA by 2-fold (ZR-75-1 and MCF-7) to 3-fold (BT-20, MDA-MB-361 and MDA-MB-134). SHP-1 protein was undetectable in MDA-MB-231, normal in BT-474 and T-47D, and up-regulated in ZR-75-1. In comparison, 58% (42/72) of primary breast cancer tissues had 2-–12-fold increase in SHP-1 mRNA (Fig. 3) (Yip et al., 2000).

6.2. Ovarian cancer

Ovarian cancer has three main types: epithelial, germ and stromal cell tumors. More than 90% of ovarian cancers are of epithelial cell origin. As SHP-1 is primarily expressed in

Table 5
The SHP-1 expression in other cancer cell lines

Cancer cell line	SHP-1	SHP-1 mRNA	Reference
Breast cancer			
ER(−) cell line			Yip et al. (2000)
BT-549	N/A	−	
Hs-578T	N/A	↓	
MDA-MB-157	N/A	−	
MDA-MB-231	−	−	
MDA-MB-330	N/A	↓	
MDA-MB-436	N/A	−	
BT-20	N/A	↑	
MDA-MB-453	N/A	+	
MDA-MB-468	N/A	+	
SK-BR-3	N/A	+	
ER(+) cell line			Yip et al. (2000)
MDA-MB-134	N/A	↑	
MDA-MB-175	N/A	+	
MDA-MB-361	N/A	↑	
MCF-7	N/A	↑	
BT-474	+	+	
BT-483	N/A	+	
T-470D	+	+	
ZR-75-1	↑	↑	
Ovarian cancer			Mok et al. (1995)
OVCA3	↑	↓	
OVCA20	↑	↑	
OVCA29	↑	↑	
OVCA32	↑	↑	
OVCA32	↑	↑	
CAOV3	↑	↑	
DOV13	↑	↑	
SKOV3	+	+	
Prostate cancer			Zapata et al. (2002)
PC-3	↓		
LNCap	+		
Pancreatic cancer			Douziech et al. (1999)
PANC-1	+		
MIAPaCa-2	−		

hematopoietic and epithelial cells, it has been proposed that SHP-1 is expressed at different levels in malignant and non-malignant ovarian epithelial cell lines (Mok et al., 1995). Indeed, Northern blot analysis indicated that seven out of eight ovarian carcinoma cell lines (OVCA3, OVCA420, OVCA429, OVCA432, OVCA433, CAOV3 and DOV13) showed a 1.8–-4.4-fold increased SHP-1 transcription level in comparison with non-malignant ovarian epithelial cells (Mok et al., 1995; Tsui et al., 2002). An exception is the SKOV3 cell line which expressed SHP-1 mRNA at a normal level. Correspondingly, those seven cell lines showed a 2-–4-fold increase in SHP-1 protein expression, whereas the SKOV3 cell line expressed SHP-1 protein normally (Table 5). Moreover, ten out of 11 ovarian tumor samples showed a 2-–3.3-fold increase in the level of SHP-1 transcription and an up-regulation of SHP-1 protein expression (Fig. 3). Taken together, the SHP-1 protein expression level corresponds to the mRNA level in both normal ovarian cells and cancerous ovarian cells and tissues (Mok et al., 1995). SHP-1 generally is over-expressed in ovarian cancer cell lines and tissues. Thus, the increased level of SHP-1 protein is a reasonable indicator for ovarian cancer.

6.3. Prostate cancer

Prostate cancer is one of the most common malignancies in men and constitutes a major heath problem in industrialized countries. SHP-1 expression has been determined in two prostate carcinoma cell lines, PC-3 and LNCap (Table 5). In these cell lines, an inverse relationship exists between cell proliferation and the amount of secreted Somatostain (SRIF or SS-14). SRIF inhibits PC-3 and LNCap cell proliferation through an autocrine/paracrine loop. Coincident with the increased secretion of SRIF, the activity and expression of SHP-1 present in PC-3 cells were augmented. Transient transfection with a vector containing the SRIF gene into the PC-3 cells resulted in the increase of SRIF protein expression and activity by 244 and 182%, respectively. In contrast, when SRIF secretion was blocked, the expression and activity levels of SHP-1 protein were reduced, and PC-3 cell proliferation was increased (Zapata et al., 2002). The anti-proliferative effect of SRIF was observed only when SHP-1 was expressed. Therefore, SHP-1 could play a key role in controlling prostatic cell proliferation, which also indicated that SHP-1 expression might be a therapeutic target for treatment of prostate cancer (Halmos et al., 2000; Zapata et al., 2002). In addition, the difference in SHP-1 expression between the two cell lines was considered related to the stage of development and degree of aggressiveness of prostate cancer (Webber et al., 1997).

6.4. Pancreatic cancer

Pancreatic cancer is another highly prevalent cancer threatening human health. Studies relating the primary role of SHP-1 and the inhibitory/stimulatory effects of somato-

statin (SRIF or SS-14) and its structural analog SMS 201 – 995 (SMS) on two human pancreatic cancer cell lines, PANC-1 and MIA PaCa-2, revealed that SMS had a dose-dependent effect on human pancreatic cancer cell growth, depending upon the presence or absence of SHP-1 protein. SHP-1 protein expression was observed in the PANC-1 cell line and could be enhanced by treatment with epidermal growth factor follow by SS-14 and SMS treatment. In contrast, in the MIA PaCa-2 cell line where SHP-1 expression is not detectable, SS-14 and SMS treatment were associated with a positive growth response (Table 5). This difference in response between these cell lines was related to SHP-1 protein expression. In response to SS-14 and SMS stimulation, the activity of membrane tyrosine kinase and P42 MAP kinase was inhibited in PANC-1, whereas they were increased in MIAPaCa-2 (Douziech et al., 1999).

SMS also can activate anti-proliferation signaling and induce intracellular acidification-dependent apoptosis in breast cancer cells. Recruitment of SHP-1 to the cell membrane by SMS was an early and necessary event in this anti-proliferation signal pathway. Membrane-associated SHP-1 is required for receptor-mediated cytotoxic signaling, and required for both intracellular acidification and subsequent apoptosis (Thangaraju et al., 1999). These results suggested a role of SHP-1 in controlling cell proliferation, which in turn gives insight into the regulation of cancer cell growth by SMS.

7. The potential tumor suppressor function of SHP-1

It is well established that SHP-1 regulates the intracellular signaling of different transmembrane receptors, including growth factor receptors and cytokine receptors. Though the detailed regulatory mechanism is unclear, SHP-1 can bind the inhibitory receptors via its SH2 domains and dephosphorylate the downstream signal molecules. It also can bind to members of the Janus activated kinases (JAK) family and regulate the activities of both JAK kinase and 'signal transduction and activators of transcription' (STATs). Diminished or abolished SHP-1 expression or activity results in increased JAK kinase activity and can directly cause abnormal cell growth. Also, the role of SHP-1 in terminating proliferation signals was confirmed by evidence of prolonged JAK activity and signaling due to the loss of the receptor tyrosine phosphorylation motifs that recruit SHP-1 to the erythropoietin receptor (Klingmuller et al., 1995). Likewise, a naturally occurring mutation at this site leads to a form of familial erythrocytosis (de la Chapelle et al., 1993). Taken together, these results strongly indicate that SHP-1 is a negative regulator of the JAK/STAT signaling pathway.

The tumor suppressor function of SHP-1 also has been demonstrated from the cell growth studies of cancer cell lines that were transfected with different SHP-1 genes. Bruecher-Encke et al. identified the correlation between the induction of SHP-1 expression and K562 cell differen-

tiation, which suggested that a lack of SHP-1 expression might contribute to the abnormal growth of this leukemic cell line (Bruecher-Encke et al., 2001). In addition, in stable transfection of K562 cells with a vector directing SHP-1 expression versus the vector alone revealed that the SHP-1-transfected cells and the vector-transfected cells exhibited remarkable differences in growth pattern and morphology. Moreover, soft agar growth experiments showed that most SHP-1-transfected clones appeared 10–14 days later than those transfected with vector alone. Interestingly, the 'late' clones exhibited substantially higher levels of SHP-1 expression than the 'early' ones. These data were consistent with the growth inhibitory effect of SHP-1. Likewise, the role of SHP-1 in regulation of cell proliferation was confirmed further by experiments on PC-3 cells in which SHP-1, or empty vector, was stably expressed (Zapata et al., 2002). Two clones expressing high levels of SHP-1 also were found to proliferate more slowly than control cells or cells transfected with empty vector. Further, the proliferation of these two clones with over-expressed SHP-1 was reduced by 35 and 45% after 6 days of culture, respectively.

8. Conclusion

In this paper, we reviewed the recent progress in the studies of the pathological correlation between SHP-1 and a variety of cancers. In summary, SHP-1 protein expression was dramatically decreased in most lymphocytic-related cancers, and was decreased in some non-lymphocytic cancers. The diminished or abolished SHP-1 expression could be due to mutation of the SHP-1 gene, the methylation of the promoter region of the SHP-1 gene or post-transcriptional regulation of SHP-1 protein synthesis. Introduction of the SHP-1 gene back into a leukemia cell line and a prostate cancer cell line demonstrated the tumor suppressor function of SHP-1. Taken together, SHP-1 plays an important role in the pathogenesis of a wide range of cancers including lymphoma/leukemia, breast cancer, ovarian cancer, prostate cancer and pancreatic cancer. These results suggest the potential value for SHP-1 gene as a target for therapy in cancer patients.

References

Banville, D., Stocco, R., Shen, S.H., 1995. Human protein tyrosine phosphatase 1C (PTPN6) gene structure: alternate promoter usage and exon skipping generate multiple transcripts. Genomics 27, 165–173.

Baris, D., Zahm, S., 2000. Epidemiology of lymphomas. Curr. Opin. Oncol. 12, 383–394.

Bruecher-Encke, B., Griffin, J.D., Neel, B.G., Lorenz, U., 2001. Role of the tyrosine phosphatase SHP-1 in K562 cell differentiation. Leukemia 15, 1424–1432.

Chen, H.E., Chang, S., Trub, T., Neel, B.G., 1996. Regulation of colony-stimulating factor 1 receptor signaling by the SH2 domain-containing tyrosine phosphatase SHPTP1. Mol. Cell. Biol. 16, 3685–3697.

Christensen, M.D., Geisler, C., 2000. Recruitment of SHP-1 protein tyrosine phosphatase and signalling by a chimeric T-cell receptor-killer inhibitory receptor. Scand. J. Immunol. 51, 557–564.

David, M., Chen, H.E., Goelz, S., Larner, A.C., Neel, B.G., 1995. Differential regulation of the alpha/beta interferon-stimulated Jak/Stat pathway by the SH2 domain-containing tyrosine phosphatase SHPTP1. Mol. Cell. Biol. 15, 7050–7058.

de la Chapelle, A., Traskelin, A.L., Juvonen, E., 1993. Truncated erythropoietin receptor causes dominantly inherited benign human erythrocytosis. Proc. Natl. Acad. Sci. USA 90, 4495–4499.

Delibrias, C.C., Floettmann, J.E., Rowe, M., Fearon, D.T., 1997. Down-regulated expression of SHP-1 in Burkitt lymphomas and germinal center B lymphocytes. J. Exp. Med. 186, 1575–1583.

Douziech, N., Calvo, E., Coulombe, Z., Muradia, G., Bastien, J., Aubin, R.A., Lajas, A., Morisset, J., 1999. Inhibitory and stimulatory effects of somatostatin on two human pancreatic cancer cell lines: a primary role for tyrosine phosphatase SHP-1. Endocrinology 140, 765–777.

Famiglietti, S.J., Nakamura, K., Cambier, J.C., 1999. Unique features of SHIP, SHP-1 and SHP-2 binding to FcgammaRIIb revealed by surface plasmon resonance analysis. Immunol. Lett. 68, 35–40.

Halmos, G., Schally, A.V., Sun, B., Davis, R., Bostwick, D.G., Plonowski, A., 2000. High expression of somatostatin receptors and messenger ribonucleic acid for its receptor subtypes in organ-confined and locally advanced human prostate cancers. J. Clin. Endocrinol. Metab. 85, 2564–2571.

Healy, J.I., Goodnow, C.C., 1998. Positive versus negative signaling by lymphocyte antigen receptors. Annu. Rev. Immunol. 16, 645–670.

Isaacson, P.G., 2000. The current status of lymphoma classification. Br. J. Haematol. 109, 258–266.

Johnson, J.M., Harrod, R., Franchini, G., 2001. Molecular biology and pathogenesis of the human T-cell leukaemia/lymphotropic virus Type-1 (HTLV-1). Int. J. Exp. Pathol. 82, 135–147.

Kim, C.H., Qu, C., Hangoc, G., Cooper, S., Anzai, N., Feng, G., Broxmeyer, H.E., 1999. Abnormal chemokine-induced responses of immature and mature hematopoietic cells from moth eaten mice implicate protein tyrosine phosphatase SHP-1 in chemoine responses. J. Exp. Med. 190, 681–690.

Klingmuller, U., Lorenz, U., Cantley, L.C., Neel, B.G., Lodish, H.F., 1995. Specific recruitment of SH-PTP1 to the erythropoietin receptor causes inactivation of JAK2 and termination of proliferative signals. Cell 80, 729–738.

Kossev, P.M., Raghunath, P.N., Bagg, A., Schuster, S., Tomaszewski, J.E., Wasik, M.A., 2001. SHP-1 expression by malignant small B-cell lymphomas reflects the maturation stage of their normal B-cell counterparts. Am. J. Surg. Pathol. 25, 949–955.

Kozlowski, M., Mlinaric-Rascan, I., Feng, G.S., Shen, R., Pawson, T., Siminovitch, K.A., 1993. Expression and catalytic activity of the tyrosine phosphatase PTP1C is severely impaired in motheaten and viable motheaten mice. J. Exp. Med. 178, 2157–2163.

Law, C.L., Sidorenko, S.P., Chandran, K.A., Zhao, Z., Shen, S.H., Fischer, E.H., Clark, E.A., 1996. CD22 associates with protein tyrosine phosphatase 1C, syk, and phospholipase C-1 upon B cell activation. J. Exp. Med. 183, 547–560.

Leon, F., Cespon, C., Franco, A., Lombardia, M., Roldan, E., Escribano, L., Harto, A., Gonzalez-Porque, P., Roy, G., 2002. SHP-1 expression in peripheral T cells from patients with Sezary syndrome and in the T cell line HUT-78: implications in JAK3-mediated signaling. Leukemia 16, 1470–1477.

Lorenz, U., Bergemann, A.D., Steinberg, H.N., Flanagan, J.G., Li, X., Galli,

S.J., Neel, B.G., 1996. Genetic analysis reveals cell type-specific regulation of receptor tyrosine kinase c-Kit by the protein tyrosine phosphatase SHP1. J. Exp. Med. 184, 1111–1126.

Matsushita, M., Tsuchiya, N., Oka, T., Yamane, A., Tokunaga, K., 1999. New variations of human SHP-1. Immunogenetics 49, 577–579.

Migone, T.S., Cacalano, N.A., Taylor, N., Yi, T., Waldmann, T.A., Johnston, J.A., 1998. Recruitment of SH2-containing protein tyrosine phosphatase SHP-1 to the interleukin 2 receptor: loss of SHP-1 expression in human T- lymphotropic virus type 1-transformed T cells. Proc. Natl. Acad. Sci. USA 95, 3845–3850.

Mok, S.C., Kwok, T.T., Berkowitz, R.S., Barrett, A.J., Tsui, F.W., 1995. Overexpression of the protein tyrosine phosphatase, non-receptor type 6 (PTPN6), in human epithelial ovarian cancer. Gynecol. Oncol. 57, 299–303.

Oka, T., Yoshino, T., Hayashi, K., Ohara, N., Nakanishi, T., Yamaai, Y., Hiraki, A., Sogawa, C.A., Kondo, E., Teramoto, N., Takahashi, K., Tsuchiyama, J., Akagi, T., 2001. Reduction of hematopoietic cell-specific tyrosine phosphatase SHP-1 gene expression in natural killer cell lymphoma and various types of lymphomas/leukemias: combination analysis with cDNA expression array and tissue microarray. Am. J. Pathol. 159, 1495–1505.

Ottenhoff-Kalff, A.E., van Oirschot, B.A., Hennipman, A., de Weger, R.A., Staal, G.E., Rijksen, G., 1995. Protein tyrosine phosphatase activity as a diagnostic parameter in breast cancer. Breast Cancer Res. Treat. 33, 245–256.

Ottensmeier, C., 2001. The classification of lymphomas and leukemias. Chem. Biol. Interact. 135–136, 653–664.

Pani, G., Fischer, K.D., Mlinaric-Rascan, I., Siminovitch, K.A., 1996. Signaling capacity of the T cell antigen receptor is negatively regulated by the PTP1C tyrosine phosphatase. J. Exp. Med. 184, 839–852.

Paulson, R.F., Vesely, S., Siminovitch, K.A., Bernstein, A., 1996. Signalling by the W/Kit receptor tyrosine kinase is negatively regulated in vivo by the protein tyrosine phosphatase Shp1. Nat. Genet. 13, 309–315.

Plutzky, J., Neel, B.G., Rosenberg, R.D., Eddy, R.L., Byers, M.G., Jani-Sait, S., Shows, T.B., 1992. Chromosomal localization of an SH2-containing tyrosine phosphatase (PTPN6). Genomics 13, 869–872.

Qian, D., Weiss, A., 1997. T cell antigen receptor signal transduction. Curr. Opin. Cell Biol. 9, 205–212.

Sen, G., Bikah, G., Venkataraman, C., Bondada, S., 1999. Negative regulation of antigen receptor-mediated signaling by constitutive association of CD5 with the SHP-1 protein tyrosine phosphatase in B-1 B cells. Eur. J. Immunol. 29, 3319–3328.

Shultz, L.D., Schweitzer, P.A., Rajan, T.V., Yi, T., Ihle, J.N., Matthews, R.J., Thomas, M.L., Beier, D.R., 1993. Mutations at the murine motheaten locus are within the hematopoietic cell protein-tyrosine phosphatase (Hcph) gene. Cell 73, 1445–1454.

Siminovitch, K.A., Lamhonwah, A.M., Somani, A.K., Cardiff, R., Mills, G.B., 1999. Involvement of the SHP-1 tyrosine phosphatase in regulating B lymphocyte antigen receptor signaling, proliferation and transformation. Curr. Top. Microbiol. Immunol. 246, 291–297.

Tabrizi, M., Yang, W., Jiao, H., DeVries, E.M., Platanias, L.C., Arico, M., Yi, T., 1998. Reduced Tyk2/SHP-1 interaction and lack of SHP-1 mutation in a kindred of familial hemophagocytic lymphohistiocytosis. Leukemia 12, 200–206.

Thangaraju, M., Sharma, K., Liu, D., Shen, S.H., Srikant, C.B., 1999. Interdependent regulation of intracellular acidification and SHP-1 in apoptosis. Cancer Res. 59, 1649–1654.

Tomic, S., Greiser, U., Lammers, R., Kharitonenkov, A., Imyanitov, E., Ullrich, A., Bohmer, F.D., 1995. Association of SH2 domain protein tyrosine phosphatases with the epidermal growth factor receptor in human tumor cells. J. Biol. Chem. 270, 21277–21284.

Tonks, N.K., Neel, B.G., 1996. From form to function: signaling by protein tyrosine phosphatases. Cell 87, 365–368.

Tsui, H.W., Siminovitch, K.A., de Souza, L., Tsui, F.W., 1993. Motheaten and viable motheaten mice have mutations in the haematopoietic cell phosphatase gene. Nat. Genet. 4, 124–129.

Tsui, H.W., Hasselblatt, K., Martin, A., Mok, S.C., Tsui, F.W., 2002. Molecular mechanisms underlying SHP-1 gene expression. Eur. J. Biochem. 269, 3057–3064.

Uesugi, Y., Fuse, I., Toba, K., Kishi, K., Purukawa, T., Koike, T., Aizawa, Y., 1999. Involvement of SHP-1, a phosphotyrosine phosphatase, during myeloid cell differentiation in acute promyelocytic leukemia cell lines. Eur. J. Haematol. 62, 239–245.

Unkeless, J.C., Jin, J., 1997. Inhibitory receptors, ITIM sequences and phosphatases. Curr. Opin. Immunol. 9, 338–343.

Vambutas, V., Kaplan, D.R., Sells, M.A., Chenoff, J., 1995. Nerve growth factor stimulates tyrosine phosphorylation and activation of src homology-containing protein tyrosine phosphatase 1 in PC12 cells. J. Biol. Chem. 270, 25629–25633.

Vogel, W., Lammers, R., Huang, J., Ullrich, A., 1993. Activation of a phosphotyrosine phosphatase by tyrosine phosphorylation. Science 259, 1611–1614.

Walton, K.M., Dixon, J.E., 1993. Protein tyrosine phosphatases. Annu. Rev. Biochem. 62, 101–120.

Webber, M.M., Bello, D., Quader, S., 1997. Immortalized and tumorgenic adult human prostatic epithelial cell lines: characteristics and applications. II. Tumorigenic cell lines. Prostate 30, 58–64.

Yang, J., Liang, X., Niu, T., Meng, W., Zhao, Z., Zhou, G.W., 1998. Crystal structure of the catalytic domain of protein-tyrosine phosphatase SHP-1. J. Biol. Chem. 273, 28199–28207.

Yang, J., Cheng, Z., Niu, T., Liang, X., Zhao, Z.J., Zhou, G.W., 2000. Structural basis for substrate specificity of protein-tyrosine phosphatase SHP-1. J. Biol. Chem. 275, 4066–4071.

Yang, J., Cheng, Z., Niu, T., Liang, X., Zhao, Z.J., Zhou, G.W., 2001. Protein tyrosine phosphatase SHP-1 specifically recognizes C-terminal residues of its substrates via helix alpha0. J. Cell. Biochem. 83, 14–20.

Yang, J., Liu, L., He, D., Song, X., Liang, X., Zhao, Z.J., Zhou, G.W., 2003. Crystal structure of human protein tyrosine phosphatase SHP-1. J. Biol. Chem. M210430200, in press.

Yeung, Y.G., Berg, K.L., Pixley, F.J., Angeletti, R.H., Stanley, E.R., 1992.

Protein tyrosine phosphatase-1C is rapidly phosphorylated on tyrosine in macrophages in response to colony stimulationg factor-1. J. Biol. Chem. 267, 23447–23450.

Yi, T., Zhang, J., Miura, O., Ihle, J.N., 1995. Hematopoietic cell phosphatase associates with erythropoietin (Epo) receptor after Epo-induced receptor tyrosine phosphorylation: identification of potential binding sites. Blood 85, 87–95.

Yi, T., Mui, A.L.-F., Krystal, G., Ihle, J.N., 1993. Hematopoietic cell phosphatase associates with the interleukin-3 (IL-3) receptor chain and down-regulates IL-3-induced tyrosine phosphorylation and mitogenesis. Mol. Cell. Biol. 13, 7577–7586.

Yip, S.S., Crew, A.J., Gee, J.M., Hui, R., Blamey, R.W., Robertson, J.F., Nicholson, R.I., Sutherland, R.L., Daly, R.J., 2000. Up-regulation of the protein tyrosine phosphatase SHP-1 in human breast cancer and correlation with GRB2 expression. Int. J. Cancer 88, 363–368.

Zapata, P.D., Ropero, R.M., Valencia, A.M., Buscail, L., Lopez, J.I., Martin-Orozco, R.M., Prieto, J.C., Angulo, J., Susini, C., Lopez-Ruiz, P., Colas, B., 2002. Autocrine regulation of human prostate carcinoma cell proliferation by somatostatin through the modulation of the SH2 domain containing protein tyrosine phosphatase (SHP)-1. J. Clin. Endocrinol. Metab. 87, 915–926.

Zhang, Q., Lee, B., Korecka, M., Li, G., Weyland, C., Eck, S., Gessain, A., Arima, N., Lessin, S.R., Shaw, L.M., Luger, S., Kamoun, M., Wasik, M.A., 1999. Differences in phosphorylation of the IL-2R associated JAK/STAT proteins between HTLV-I(+), IL-2-independent and IL-2-dependent cell lines and uncultured leukemic cells from patients with adult T-cell lymphoma/leukemia. Leuk. Res. 23, 373–384.

Zhang, Q., Raghunath, P.N., Vonderheid, E., Odum, N., Wasik, M.A., 2000. Lack of phosphotyrosine phosphatase SHP-1 expression in malignant T-cell lymphoma cells results from methylation of the SHP-1 promoter. Am. J. Pathol. 157, 1137–1146.

Zucker-Franklin, D., 2001. The role of human T cell lymphotropic virus type I tax in the development of cutaneous T cell lymphoma. Ann. N. Y. Acad. Sci. 941, 86–96.

DIgR1, a Novel Membrane Receptor of the Immunoglobulin Gene Superfamily, Is Preferentially Expressed by Antigen-Presenting Cells

Kun Luo,* Weiping Zhang,† Lili Sui,† Nan Li,† Minghui Zhang,†
Xianwei Ma,* Lihuang Zhang,* and Xuetao Cao*,†,1

*Institute of Immunology, Zhejiang University, 353 Yanan Road, Hangzhou, 310031, People's Republic of China; and †Institute of Immunology, Second Military Medical University, 800 Xiangyin Road, Shanghai 200433, People's Republic of China

A novel membrane receptor of immunoglobulin gene superfamily (IgSF) has been identified from mouse dendritic cells (DC) and designated as DC-derived Ig-like receptor 1 (DIgR1). It encodes a 228-amino-acid (aa) residue polypeptide with a 21-aa signal peptide, a 20-aa transmembrane region, a 189-aa extracellular region, and a 19 aa intracellular region. Its extracellular region contains a single V domain of Ig. So it is a novel type I transmembrane glycoprotein of IgSF. DIgR1 shows significant homologies to human CMRF-35 antigens and polymeric immunoglobulin receptors (pIgR). The mRNA expression of DIgR1 was highly abundant in mouse spleen. The preferential expression of DIgR1 mRNA is observed in the known antigen-presenting cells (APC) including DC, monocytes/macrophages, and B lymphocytes. A 40 kDa of protein in NIH/3T3 cells transfected with the DIgR1 cDNA was detected by Western blot analysis using anti-DIgR1 polyclonal antibodies. The expression of DIgR1 protein on DC is not regulated by LPS stimulation. Further study should be conducted to investigate what were biological functions of DIgR1 in the immunobiology of APC. © 2001 Academic Press

Key Words: membrane receptor; immunoglobulin gene superfamily; antigen-presenting cell; dendritic cell; gene cloning.

The immunoglobulin gene superfamily (IgSF) is a group of cell surface glycoproteins with similar structure. The typical IgSF member shares three conserved regions which mediated protein–protein interaction. In the N-terminus, the extracellular region generally contains one or more Ig-like domains consisting of 90–110 amino acids each and is putatively involved in molecular recognition. The transmembrane region composes of approximately 20 hydrophobic amino acids anchoring the IgSF molecule in cell membrane surface. The cytoplasmic region at the C-terminus with great variant contributes to the function of signal transduction. These molecules locate on the surface of leukocytes, epithelial cells, and nervous cells and make their functions on molecular recognition, cell activation, and cell–cell interaction (1, 2). The known members of IgSF including the major histocompatibility complex (MHC) class I and class II molecules, the T cell receptors, and T cell accessory molecules CD4 and CD8 (3), certain adhesion molecules (4, 5), cytokine receptors (6), and the polymeric immunoglobulin receptors (pIgR) (7, 8).

In recent years, a number of IgSF members including the CMRF-35 antigens have been identified (9–11). The CMRF-35 monoclonal antibody (mAb) produced by immunization with large granular lymphocytes (LGL) recognizes an epitope that presents on the surface of monocytes, neutrophils, a proportion of peripheral blood T and B lymphocytes and lymphocytic cell lines. The recognized epitope was found on at least two cell surface molecules, the CMRF-35A (12, 13) and CMRF-35H (14). These two CMRF-35 molecules share a highly homologus V-Ig domain (>90%) in the extracellular region, but their intracellular regions are quite different. CMRF-35H contains three putative immunoreceptor tyrosine-based inhibitory motifs (ITIM) in the cytoplasmic domain, suggesting that this molecule might play a negative regulatory role in leukocyte function. Meanwhile, CMRF-35A molecule has a short cytoplasmic domain without ITIM or other putative signaling motifs and a glutamic acid residue in its transmembrane domain, suggesting its potential association with an as yet undefined signaling molecule. They are expressed independently of each other on leukocyte populations and on hematopoietic cell lines and are the products of different genes (14, 15). These

1 To whom correspondence should be addressed. Fax: (+86-21) 6538 2502. E-mail: caoxt@public3.sta.net.cn.

suggest that these two molecules may play distinct but related roles in the regulation of leukocyte function.

The function of these molecules remains unknown, however they have been implicated to be associated with cell activation/differentiation, molecular recognition, and regulation. Here, we report a novel member of IgSF isolated from mouse dendritic cells (DC) which shares high homology to CMRF-35A. We designated it as dendritic cell-derived Ig-like receptor 1 (DIgR1). DIgR1 is a type I transmembrane glycoprotein which is highly expressed in spleen and is preferentially expressed in the professional antigen-presenting cells (APC) including DC, monocytes/macrophages, and B lymphocytes.

MATERIALS AND METHODS

Cell preparation. Mouse DC culture procedure used in this study was described previously (16). Briefly, bone marrow cells from BALB/c mice were depleted of red blood cells with ammonium chloride and depleted of T, B cells and Ia⁺ cells using a cocktail containing anti-CD4, anti-CD8, anti-B220/CD45R, and anti-Ia monoclonal antibodies (ATCC). Then, the cells were plated in 24-well culture plates (10^6 cells/well) in RPMI 1640 medium supplemented with 10% heat-inactivated FCS, 50 μM 2-ME, 10 mM Hepes (pH 7.4), 2 mM glutamine, 100 U/ml penicillin, 100 μg/ml streptomycin, 3.3 ng/ml recombinant murine GM-CSF (Sigma), and 1 ng/ml recombinant murine IL-4 (Sigma). At day 3 of culture, floating cells were gently removed and adherent cells were cultured in fresh medium. At day 9, nonadherent and loosely adherent cells were harvested and used as DC population with the purity of >90%. For activation, DC were treated with LPS (2 μg/ml) for 24 h. Freshly isolated T and B lymphocytes from BALB/c mice were prepared using positive selection with anti-CD8, anti-CD4, or anti-B220/CD45R monoclonal antibody (ATCC) and Minimagnetic bead-conjugated secondary antibody (Militenyi Biotec Ginbit). The labeled cells were enriched by passing through a MiniMACS column placed in a magnetic field (MiniMacs, Militeny Biotec, Bergisch, Germany).

Isolation of DIgR1 full-length cDNA. By BLAST analysis of mouse EST databases from the National Center for Biotechnology Information, three mouse ESTs (GenBank Accession Nos. AI645367, AI060397, and AA175302) were found to be highly homologous to human CMRF-35 antigens, from which mouse DIgR1 full-length cDNA was obtained by contig. According to this available sequence, RT-PCR was performed to clone DIgR1 cDNA from mouse DC. The upstream primer of DIgR1 is 5'-GGAATTCACCAGGAAGCAGA-GGA-3', and the downstream primer is 5'-CGGGATCCTCAGCCA-CCAGAGGAGCTGT-3'. The amplification parameters were denaturing of 30 s at 94°C, annealing of 30 s at 57°C, and extension of 45 s at 72°C on a thermocycle PCR9600 (Applied Biosystem Inc.). After 30 cycles of amplification the PCR product was digested by *EcoRI/BamHI* and inserted into pGEM-3Z(f) vector (Promega, Madison, WI) and the sequence was conformed by DNA sequencing.

Northern blotting. Northern blotting was performed as described previously (17). Briefly, DIgR1 cDNA insert excised by enzymatic digestion and ³²P labeled was used as a probe. Ready-to-use blots containing mouse RNA from various tissues (2 μg/lane) were purchased from Clontech Laboratories. The filters were hybridized with ³²P-labeled cDNA probes in ExpressHyb hybridization solution (Clontech Laboratories) according to the manufacturer's instructions. After stringently washing at 50°C for 20 min in 0.1 × SSC and 0.1% SDS, the filters were subjected to autoradiography. The filters were stripped and reprobed with mouse β-actin cDNA probe (Clontech Laboratories).

RT-PCR analysis of DIgR1 expression. Murine cell lines used for analysis of mRNA expression and Western blotting were listed here: NIH/3T3 (embryo fibroblast cell), P815 (mastocytoma), Raw (macrophage; monocyte), B16 (melanoma), YAC-1 (lymphoma), A20 (B lymphocyte), EL4 (T lymphocyte), CTLL-2 (T lymphocyte), E.G7 (lymphoma; T lymphocyte), FBL3 (erythroleukemia), WEHI164 (fibrosarcoma), CT26 (colonocarcinoma). All of these cell lines were obtained from ATCC. Standard procedures were used for cell culture. Total cellular RNA was isolated using Trizol reagent (Life Technologies) and then was reverse-transcribed into cDNA, The PCR was performed with the following primer sets: 5'-GGAATTCACCAGG-AAGCAGAGGA-3' and 5'-CGGGATCCTCAGCCACCAGAGGAGC-TGT-3' for DIgR1; and 5'-TGGAATCCTGTGGCATCCATGAAAC-3' and 5'-TAAAACGCAGTAACAGTCCG-3' for β-actin.

Recombinant expression of GST fusion protein of DIgR1 and generation of anti-DIgR1 polyclonal antibodies. The cDNA encoding DIgR1 extracellular region without signal peptide was amplified by PCR with the sense primer 5'-GGATCCTCTCAGGTCCCAG-GCTGT-3' and antisense primer 5'-GAATTCAGGGAGCAGGAA-TTGTGTCATC-3'. The DIgR1 cDNA sequence and the ORF were confirmed by DNA sequencing, then inserted into the expression vector pGEX-2T (Pharmacia Biotech, Piscataway, NJ). The *Escherichia coli* strain BL21 was used as host to express GST fusion protein. The soluble fusion protein was obtained under the condition of IPTG (0.5 mM) induction at 22°C for 3 h and purified by affinity chromatography (Pharmacia Biotech). Female New Zealand rabbits were immunized with purified fusion protein to produce polyclonal antibodies according to conventional procedure. DIgR1 fusion protein was injected into multiple subcutaneous sites and immunizations were boosted twice at 3-week intervals. Ten days after the last injection, the anti-DIgR1 serum was isolated and purified using protein A affinity chromatography (Pierce, Rockford, IL). The titration of this antiserum was detected by Western blot.

Eukaryotic expression of recombinant DIgR1 protein. To express His-tagged DIgR1 protein in eukaryotic cells, DIgR1 cDNA was amplified by PCR and inserted into vector pcDNA3.1/mic-His (−) (Invitrogen). The DNA sequence was confirmed by DNA sequencing. The transcription was initiated by CMV promoter. NIH/3T3 cells were transfected with DIgR1 expression vector using the Lipofactamine transfection reagent (Gibco) according to the manufacturer's instructions. After 3 weeks of screening in the presence of 800 μg/ml G418 (Calbiochem, La Jolla, CA), the stable positive clones were obtained and confirmed by Western blot analysis using anti-DIgR1 polyclonal antibodies. These stable expression clones were used for immunoblotting.

Immunoblotting analysis. Totally harvested cells were lyzed in cell lysis buffer (1% NP-40, 50 mM Tris–CL, pH 7.8, 150 mM NaCl) containing PMSF (100 μg/ml), aprotinin(1 μg/ml), and leupeptins(1 μg/ml). The lysates were fractionated by 12% SDS–PAGE gel and transferred onto nitrocellulose membrane. After blocked with 10% nonfat dry milk for 2 h, the membrane was washed three times for 5 min each with TBST (100 mM Tris–Cl, pH 7.6, 0.9% NaCl, 0.1% Tween 20). Then the membrane was incubated in anti-DIgR1 polyclonal antibodies (1:2000 dilution) over night at 4°C. After washed three times for 5 min each with TBST, the membrane was incubated in HRP-coupled anti-rabbit secondary antibody (New England Biolabs Inc., 1:20000 dilution) for 1 h. After washed with TBST as above, the membrane was incubated in LumiGLo for 1 min and then wrapped in Saran Wrap to expose to X-ray film.

FACS analysis. Cells growing vigorously were harvested, then were washed twice with PBS, and incubated in anti-DIgR1 polyclonal antibodies for 1 h at 4°C. Preimmune rabbit serum were used as negative control. After being washed three times for 5 min each, the cells were incubated in FITC-conjugated anti-rabbit IgG (DAKO) for 30 min. All cells were analyzed by cytofluograph on a FACScan (Becton–Dickinson, San Jose, CA) equipped with lysis software).

accaggaagcagaggacagaaaggagaactaggcaagagaacattctactgtctagactgaggacagatccttctccactc   80

ttggccctgatgtgggcacaggtgacagcggagctgaagaa ATG ATT CCC AGA GTA ATA AGA TTG TGG CTG   151

                  M   I   P   R   V   I   R   L   W   L   10

CCT TCA GCT CTG TTC CTC TCT CAG GTC CCA GGC TGT GTC CCA CTG CAT GGC CCC AGC ACT   211

   P   S   A   L   F   L   S   Q   V   P   G   C   V   P   L   H   G   P   S   T   30

ATC ACA GGC GCT GTT GGG GAA TCG CTC AGT GTG TCA TGT CAA TAC GAG GAG AAA TTC AAG   271

   I   T   G   A   V   G   E   S   L   S   V   S   C   Q   Y   E   E   K   F   K   50

ACT AAG GAC AAA TTC TGG TGC AGA GGG TCA CTG AAG GTA CTC TGT AAA GAT ATT GTC AAG   331

   T   K   D   K   F   W   C   R   G   S   L   K   V   L   C   K   D   I   V   K   70

ACC AGC AGC TCA GAA GAA GTT AGG AAT GGC CGA GTG ACC ATC AGG GAC CAT CCA GAC AAC   391

   T   S   S   S   E   E   V   R   (N)   G   R   V   T   I   R   D   H   P   D   (N)   90

CTC ACC TTC ACA GTG ACC TAT GAG AGC CTC ACC CTG GAG GAT GCA GAC ACC TAC ATG TGT   451

   L   T   F   T   V   T   Y   E   S   L   T   L   E   D   A   D   T   Y   M   C   110

GCG GTG GAT ATA TCA CTT TTT GAT GGC TCC TTG GGG TTC GAT AAG TAC TTC AAG ATT GAG   511

   A   V   D   I   S   L   F   D   G   S   L   G   F   D   K   Y   F   K   I   E   130

TTG TCT GTG GTT CCA AGT GAG GAC CCA GTC ACA GGT TCG AGC CTT GAG AGT GGT AGA GAT   571

   L   S   V   V   P   S   E   D   P   V   T   G   S   S   L   E   S   G   R   D   150

ATC CTG GAA TCC CCC ACA TCC TCA GTT GGG CAC ACT CAT CCC AGT GTG ACC ACA GAT GAC   631

   I   L   E   S   P   T   S   S   V   G   H   T   H   P   S   V   T   T   D   D   170

ACA ATT CCT GCT CCC TGC CCT CAG CCT CGG TCT CTT CGG AGC AGC CTC TAC TTC TGG GTC   691

   T   I   P   A   P   C   P   Q   P   R   S   L   R   S   S   L   Y   F   W   <u>V</u>   190

CTG GTG TCT CTG AAG TTG TTC CTG TTC CTG AGC ATG CTT GGT GCT GTC CTC TGG GTG   AAC   751

   <u>L   V   S   L   K   L   F   L   F   L   S   M   L   G   A   V   L   W   V</u>   N   210

AGG CCT CAG AGG TGC TCT GGG GGA AGC AGC TCT CGG CCC TGT TAT GAG AAC CAG TGA   811

   R   P   Q   R   C   S   G   G   S   S   R   P   C   Y   E   N   Q   °   228

agtctgttgacatcaaggccctgtccctaaacacagctcctctggtggctga   860

FIG. 1. Sequences of nucleotides and deduced amino acids of DIgR1. The in-frame stop codons in 5′ UTR are boxed. Single underline is the signal peptide. Double underline is the transmembrane domain. The potential N-glycosylation sites are cycled. The sequence of DIgR1 has been deposited in the GenBank/EMBL under the Accession No. AY048685.

RESULTS

Identification and Sequence Analysis of DIgR1

By searching mouse EST database against human CMRF-35 antigens, we obtained three ESTs (GenBank Accession Nos. AI645367, AI060397, and AA175302) which were contiged to form a full-length cDNA with a complete open-reading frame (ORF) potentially encoding a peptide homologous to human CMRF-35A. By amplifying the cDNA with specific primers using RT-PCR from mouse bone marrow derived DC, we identified the full-length cDNA. The 860-bp full-length cDNA contains ORF of 684 bp and a 5′ untranslating region

(UTR) of 121 bp containing a stop codon TGA. It indicated that it was a full-length cDNA clone. The mature DIgR1 protein has a length of 228 aa with four conserved cysteine residues and two potential N-linked glycosylation sites, with the predicted molecular mass of 25.2 kDa before glycosylation. A putative hydrophobic signal anchor sequence of 20 aa extending from nt 689 to 748 was identified as an integral transmembrane region. The 189-aa extracellular region met the structural features of Ig-V domain and is predicted to carry 21-aa signal polypeptide in its NH2-terminus (Fig. 1). So it belongs to type-I transmembrane receptor of IgSF. The novel molecule is designated as DIgR1.
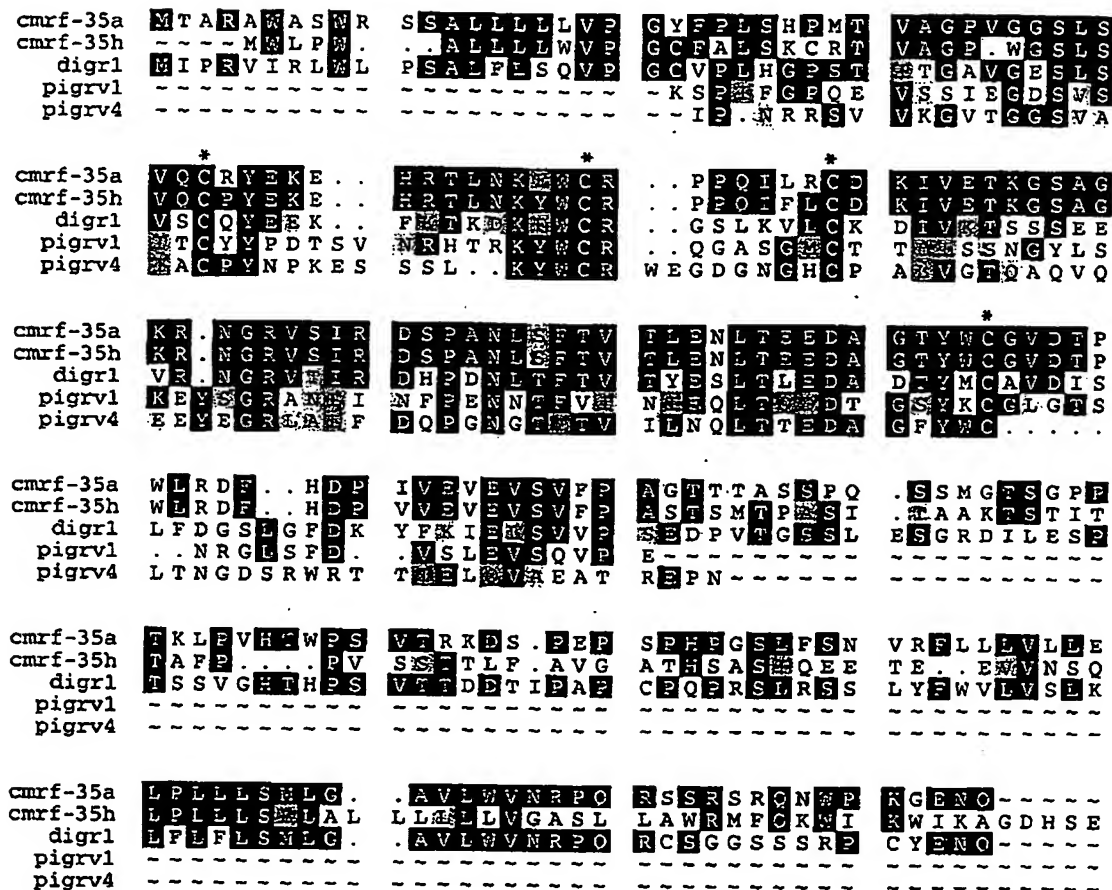
```
cmrf-35a   M T A R A W A S W R    S S A L L L L L V P    G Y F P L S H P M T    V A G P V G G S L S
cmrf-35h   ~ ~ ~ ~ M W L P W .    . . A L L L L W V P    G C F A L S K C R T    V A G P . W G S L S
  digr1    M I P R V I R L W L    P S A L F L S Q V P    G C V P L H G P S T    W T G A V G E S L S
 pigrv1    ~ ~ ~ ~ ~ ~ ~ ~ ~ ~    ~ ~ ~ ~ ~ ~ ~ ~ ~ ~    ~ K S P W F G P Q E    V S S I E G D S W S
 pigrv4    ~ ~ ~ ~ ~ ~ ~ ~ ~ ~    ~ ~ ~ ~ ~ ~ ~ ~ ~ ~    ~ ~ I P . W R R S V    V K G V T G G S W A

                *                          *                    *                    *
cmrf-35a   V Q C R Y E K E . .    H R T L N K W W C R    . . P P Q I L R C D    K I V E T K G S A G
cmrf-35h   V Q C P Y E K E . .    H R T L N K Y W C R    . . P P Q I F L C D    K I V S T K G S A G
  digr1    V S C Q Y E E K . .    F W T K D K W W C R    . . G S L K V L C K    D I V W T S S S E E
 pigrv1    W T C Y Y P D T S V    W R H T R K Y W C R    . . Q G A S G W C T    T W S S N G Y L S
 pigrv4    W A C P Y N P K E S    S S L . . K Y W C R    W E G D G N G H C P    A W V G T Q A Q V Q

cmrf-35a   K R . N G R V S I R    D S P A N L W F T V    I L E N L T E E D A    G T Y W C G V D P P
cmrf-35h   K R . N G R V S I R    D S P A N L W F T V    T L E N L T E E D A    G T Y W C G V D P P
  digr1    V R . N G R V W I R    D H P D N L T F T V    T Y E S L T L E D A    D T Y M C A V D I S
 pigrv1    K E W S G R A W W I    N F P E N G W V W    N W Q L T W W D T    G S W K C G L G T S
 pigrv4    E E W E G R W A W F    D Q P G N G W W T V    I L N Q L T T E D A    G F Y W C . . . . .

cmrf-35a   W L R D W . . H D P    I V E V E V S V F P    A G T T A S S P Q    . S S M G W S G P P
cmrf-35h   W L R D W . . H D P    V V E V E V S V F P    A S T S M T P W S I    . W A A K T S T I T
  digr1    L F D G S L G F D K    Y F W I E W S V V P    W E D P V W G W S L    E S G R D I L E S P
 pigrv1    . . N R G L S F D .    . W S L E V S Q V P    E ~ ~ ~ ~ ~ ~ ~ ~ ~    ~ ~ ~ ~ ~ ~ ~ ~ ~ ~
 pigrv4    L T N G D S R W R T    T W E L W V W E A T    R W P N ~ ~ ~ ~ ~ ~    ~ ~ ~ ~ ~ ~ ~ ~ ~ ~

cmrf-35a   W K L W V H W W P S    W W R K W S . P E P    S P W W G S W F S N    V R W L L W V L W E
cmrf-35h   W A F W . . . . P V    S W W T L P . A V G    A T W S A S W Q E E    T E . . E W W N S Q
  digr1    W S S V G W W H P S    V W W D W T I W A W    C P Q W R S W R W S    L Y W W V W V S W K
 pigrv1    ~ ~ ~ ~ ~ ~ ~ ~ ~ ~    ~ ~ ~ ~ ~ ~ ~ ~ ~ ~    ~ ~ ~ ~ ~ ~ ~ ~ ~ ~    ~ ~ ~ ~ ~ ~ ~ ~ ~ ~
 pigrv4    ~ ~ ~ ~ ~ ~ ~ ~ ~ ~    ~ ~ ~ ~ ~ ~ ~ ~ ~ ~    ~ ~ ~ ~ ~ ~ ~ ~ ~ ~    ~ ~ ~ ~ ~ ~ ~ ~ ~ ~

cmrf-35a   L P L L L S W L G .    . A V L W V N R P Q    R S S R S R Q N W P    K G E W Q ~ ~ ~ ~ ~
cmrf-35h   L P L L L S W L A L    L L W L L V G A S L    L A W R M F C K W I    K W I K A G D H S E
  digr1    L F L F L S W L G .    . A V L W V N R P Q    R C S G G S S S R P    C Y E W Q ~ ~ ~ ~ ~
 pigrv1    ~ ~ ~ ~ ~ ~ ~ ~ ~ ~    ~ ~ ~ ~ ~ ~ ~ ~ ~ ~    ~ ~ ~ ~ ~ ~ ~ ~ ~ ~    ~ ~ ~ ~ ~ ~ ~ ~ ~ ~
 pigrv4    ~ ~ ~ ~ ~ ~ ~ ~ ~ ~    ~ ~ ~ ~ ~ ~ ~ ~ ~ ~    ~ ~ ~ ~ ~ ~ ~ ~ ~ ~    ~ ~ ~ ~ ~ ~ ~ ~ ~ ~
```

FIG. 2. Multiple alignment of the deduced DIgR1 protein with human CMRF-35A, CMRF-35H, V1, and V4 domains of mouse pIgR. Identical amino acids are shown on black background. Similar residues are in gray. The conserved Cys residues in extracellular region are marked with asterisks.

Identity of amino acid sequence (45%) between DIgR1 and human CMRF-35A was revealed (Fig. 2). The extracellular region of DIgR1 was also significantly homologous to human CMRF-35H (53% identity), V1 domain of mouse pIgR (30% identity), and V4 domain of mouse pIgR (36% identity). Similar homology was founded between DIgR1 and rabbit or rat pIgR (not shown).

DIgR1 mRNA Expression Patterns in Mouse Dendritic Cells, Monocytes/Macrophages, and B Cells

Northern blotting revealed approximately 0.9 and 2.0 kb transcripts in several normal mouse tissues (Fig. 3). The greatest expression of DIgR1 mRNA was observed in the spleen and the 0.9 kb transcript was dominant. These two different transcripts might be generated by alternative splicing. Faint expression was detected in heart, spleen, lung, liver, and testis. No expression was observed in kidney, brain, and skeletal
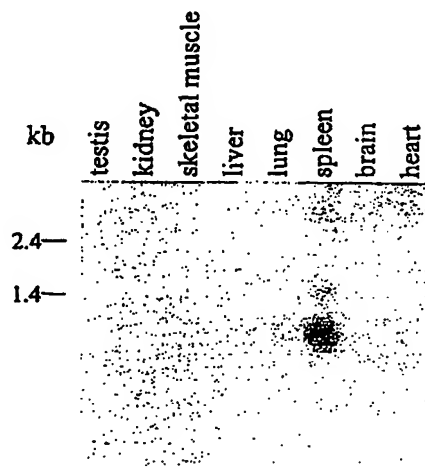
FIG. 3. Northern blot analysis of DIgR1 expression in normal tissues. Poly(A)+ RNA from the indicated tissues were hybridized with radioactive probes which contain the full-length sequence of DIgR1. The mRNA markers are shown in size on the left.
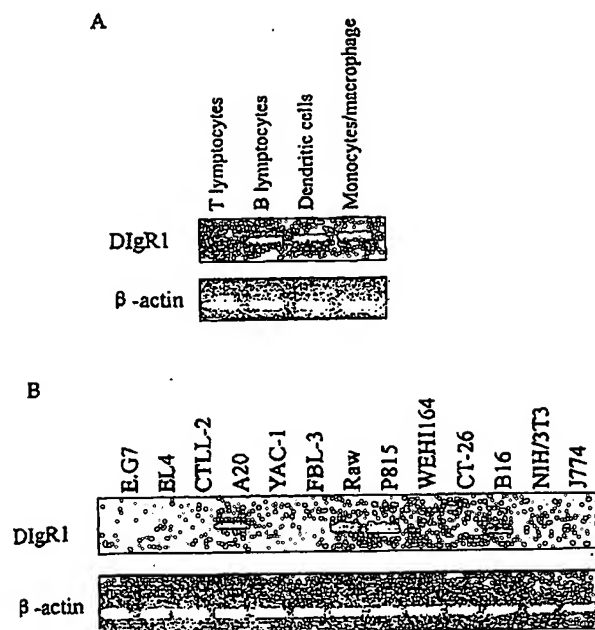
A

DIgR1

β -actin

B

DIgR1

β -actin

FIG. 4. RT-PCR analysis of DIgR1 mRNA expression. Mouse β-actin was amplified as positive control. (A) RT-PCR products of freshly isolated mouse T lymphocytes, B lymphocytes, monocytes, and bone marrow-derived DC. (B) RT-PCR products of partly hematopoietic and tumor cell lines.

muscle. Highly abundant expression of DIgR1 mRNA in spleen indicated that it might possess important function in the immune system. We further investigated its cellar distribution by RT-PCR analysis in various cells or cell lines (Fig. 4). In hematopoietic cells and cell lines, expression of DIgR1 mRNA was observed in freshly isolated murine bone marrow-derived DC, monocytes, B lymphocytes, and B lymphoma cell line (A20), monocytes/macrophage cell line (Raw), but no expression was detected in either freshly isolated T lymphocytes or T cell lines (EL4, CTLL-2, or E.G7). DIgR1 mRNA was expressed in mouse mature DC with high abundance. Different levels of DIgR1 expression were also seen in some tumor cell lines. Therefore, DIgR1 was expression preferentially by DC, monocytes, and B lymphocytes. As we know, DC, monocytes, and B lymphocytes are professional APC which play important roles in the initiation and regulation of immune response. So DIgR1 may be related to the immunobiology of APC.

Expression of DIgR1 Protein in DIgR1-Transfected Cells

To further investigate the biological characterization of DIgR1, we generated GST-DIgR1 fusion protein and produced anti-DIgR1 serum. The purified polyclonal antibodies could react with 0.05 μg of DIgR1 protein at

the titer of 1:4000 and no cross-reactivity with bacterial protein. Then the DIgR1 cDNA with full-length encoding region was inserted into pcDNA3.1 vector that was transfected into NIH/3T3 cells for stable expression of DIgR1 protein. A ~40 kDa protein was detected in transfected NIH/3T3 cells under reduced and non-reduced condition by Western-blotting with rabbit polyclonal antibodies against DIgR1 (Fig. 5). This indicates the mature protein of DIgR1 is a monomer and is highly glycosylated.

Expression of DIgR1 Protein on the Surface of Mouse Dendritic Cells

DC are the most potent professional APC in the immune system, and the one capable of sensitizing naive, unprimed T cells. Importantly, DC express high level of MHC and costimulatory/adherent molecules which are necessary to activate T cells. Because DIgR1 mRNA was expressed in mouse DC with high abundance, we want to know what level of DIgR1 protein expression on DC at different stages in order to further study the role of DIgR1 in immunobiology of DC. DIgR1 on mouse DC was detected by FACS. DCs from mouse bone marrow were cultured in media containing GM-CSF and IL-4 for 7 days DC, 9 days DC, or activated with LPS for 24-h activated DC. FACS analysis revealed high expression of DIgR1 protein on DCs (Fig. 6A). But no significant difference in DIgR1 expression was observed among 7 day DC, 9 day DC, and activated DC. This phenomenon was also confirmed by RT-PCR and Western blotting analysis (Figs. 6B and Fig. 6C).

DISCUSSION

In this study, we isolated a novel cell surface glycoprotein named DIgR1 from mouse DC. Characterized by consisting of a single V-Ig domain in its N-terminus, this 228-residue protein belongs to IgSF. DIgR1 shares the closest homology to CMRF-35A, which putatively has an important function common to diverse leukocyte types. Just like human CMRF-35A, DIgR1 con-
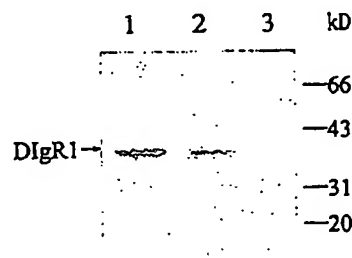

FIG. 5. Western blot analysis of DIgR1 protein expression in DIgR1 cDNA transfected NIH/3T3 cells under reduced (lane 1) and nonreduced (lane 2) conditions. NIH/3T3 cells transfected pcDNA3.1 was subjected to negative control (lane 3). Protein markers are shown on the right.
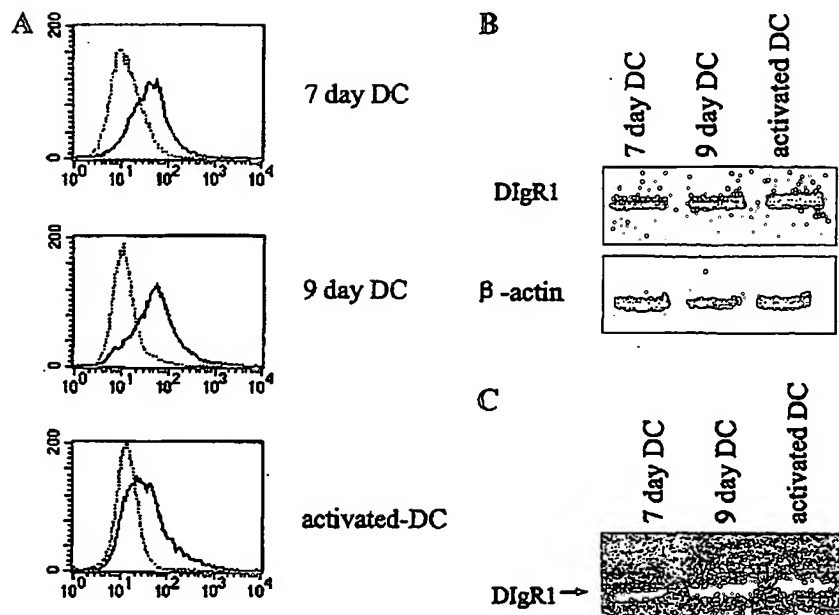
FIG. 6. Analysis of DIgR1 expression on 7 day DC, 9 day DC, and LPS-activated DC. (A) Expression analysis of DIgR1 protein by FACS. Solid lines show that the cells were stained with anti-DIgR1 polyclonal antibodies. Dotted lines show the cells were stained with preimmune sera as negative control. No difference in DIgR1 protein expression was observed on DC at different stages that were consistent with the results of RT-PCR (B) and Western blot analysis (C).

tains a short cytoplasmic domain indicating that this molecule might be associated with an as yet undefined signaling molecule to make functions. Within the extracellular region, DIgR1 shares sequence homology with CMRF-35H (14, 15), but DIgR1 lacks immunoreceptor tyrosine-based inhibitory motif (ITIM) that negatively regulates the activation of cells when cocrosslinked with immunoreceptor tyrosine-based activatory motif (ITAM) in its cytoplasmic domain (18, 19). So DIgR1 might be a noninhibitory (or activated) molecule on the surface of leukocytes. In contrast to expression pattern of CMRF-35A, DIgR1 mRNA is not expressed in T lymphocytes on which CMRF-35A transcripts are positive when confirmed by RT-PCR. Therefore, DIgR1 might have distinct functions when compared to CMRF-35A.

On the other hand, DIgR1 Ig-like domain is most closely related to the V1 and V4 domain of mouse pIgR. The pIgR, which is constitutively expressed on the basolateral surface of secretory epithelial cells, mediates external translocation of polymeric IgA, and pentameric IgM (collectively called pIg) to exocrine secretions (20, 21). Studies on the structure and function of pIgR reveal that there are six Ig-like domains in the extracellular pIg-binding region of the receptor (22). But each domain is not required for IgA binding. Domain I has high affinity for binding to IgA (23). The deletion of domains II and III or individual deletion of domains IV and V of pIgR does not prevent binding to IgA (24, 25). But no study demonstrates that the ex-

tracellular region of pIgR harboring a single domain I can bind to IgA. It is interesting that the expression of DIgR1 mRNA is highly abundant in small intestine and duodenum, which is revealed by RT-PCR analysis (data not shown). These tissues highly expressing pIgR at a high level are vigorous in mucosal immune response. Our further investigation will focus on the binding activity of DIgR1 with IgA.

Northern blotting analysis indicating high expression of DIgR1 in the spleen showed that DIgR1 might possess important function in the immune system. Then, its cellar distribution was analyzed by RT-PCR in various cell lines and freshly isolated cells. High level expression of DIgR1 mRNA was detected in the unactivated DC and activated DC. In hematopoietic cell lines, expression of DIgR1 mRNA was observed in B lymphocytes and B lymphoma cell line (A20), macrophages and cell line (Raw), but no expression was detected in T lymphocytes and T cell lines (EL4, CTLL-2, E.G7). DC, monocytes/macrophages, and B lymphocytes are all of professional APCs. So DIgR1 is speculated to be involved in the immunobiology of APC such as antigen capture, process and presentation.

In conclusion, we identify a novel cell membrane receptor DIgR1 that belongs to IgSF. DIgR1 is highly expressed in spleen and is preferentially expressed in professional APC including DC, monocytes/macrophages, and B lymphocytes, suggesting that DIgR1 might play roles in the immune system. But the expression of DIgR1 on DC can not be regulated by

dangerous signals such as LPS stimulation. What are the factors that can regulate the expression of DIgR1 in the immune system? What are the functions of DIgR1 in the immunobiology of APC? These need to be characterized by further investigation.

ACKNOWLEDGMENTS

REFERENCES

1. Williams, A. F., and Barclay, A. N. (1988) *Annu. Rev. Immunol.* 6, 381–405.

2. Hunkapiller, T., and Hood, L. (1989) *Adv. Immunol.* 44, 1–63.

3. Littman, D. R. (1987) *Annu. Rev. Immunol.* 5, 561–584.

4. Starling, G. C., Egner, W., Mclellan, A. D., Fawcett, J., Simmons, D. L., Hart, D. N. J. (1995) *Eur. J. Immunol.* 25, 2528–2532.

5. Hart, D. N., and Prickett, T. C. (1993) *Cell Immunol.* 148, 447–454

6. Halaby, D. M., and Mornon, J. P. (1998) *J. Mol. Evol.* 46, 389–400.

7. Kushiro, A., and Sato, T. (1997) *Gene* 204, 277–282.

8. Piskurich, J. O., Blanchard, M. H., Youngman, K. R., France, J. A., and Kaetzel, C. S. (1995) *J. Immunol.* 154, 1735–1747.

9. Selvakumar, A., Steffens, U., and Dupont, B. (1996) *Tissue Antigens* 48, 285–295.

10. Cella, M., Dohing, C., Samaridis, J., Dessing, M., Brockhaus, M., Lanzavecchia, A., and Colonna, M. (1997) *J. Exp. Med.* 185, 1743–1751.

11. Fournier, N., Chalus, L., Durand, I., Garcia, E., Pin, J., Abrams, J., E. M. Bates. E., and Garrone, P. (2000) *J. Immunol.* 165, 1197–1209.

12. Jackson, D. G., Hart, D. N., Starling, G., and Bell, J. I. (1992) *Eur. J. Immunol.* 22, 1157–1163.

13. Daish, A., Starling, G. C., Mckenzie, J. L., Nimmo, J. C., Jackson, D. G., and Hart, D. N. (1993) *Immunology* 79, 55–63.

14. Green, B. J., Clark, G. J., and Hart, D. N. (1998) *Int. Immunol.* 10(7), 891–899.

15. Clark, G. J, Green, B. J., and Hart, D. N. (2000) *Tissue Antigens* 55(2), 101–109.

16. Cao, X., Zhang, W., He, L., Xie, Z., Ma, S., Tao, Q., Yu, Y., Hamada, H, and Wang, J. (1998) *J. Immunol.* 161, 6238–6244.

17. Cao, X., Zhang, W., Wan, T., He, L., Chen, T., Yuan, Z., Ma, S., Yu, Y., and Chen, G. (2000) *J. Immunol.* 2588–2595.

18. Bolland, S., and Ravetch, J. (1999) *Adv. Immunol.* 72, 149–177.

19. Gergely, J., Pecht, I., and Sarmay, G. (1999) *Immunol. Lett.* 68, 3–15.

20. Kaetzel, C. S., Robinson, J. K., Chintalacharuvu, K. R., Vaerman, J. P., and Lamm, E. M. (1991) *Proc. Natl. Acad. Sci. USA* 88, 8796–8800.

21. Kaetzel, C. S., Robinson, J. K., and Lamm, E. M. (1994) *J. Immunol.* 152, 72–76.

22. Piskurich, J. F., Blanchard, M. H., Youngman, K. R., France, J. A., and Kaetel, C. S. (1995) *J. Immunol.* 154, 1735–1747.

23. Bakos, M. A., Kurosky, A., Woodard, C. S., and Denney, R. M. (1991) *J. Immunol.* 146, 162–168.

24. Coyne, R. S., Siebrecht, M., Peitsch, M. C., and Casnnovr, J. E. (1994) *J. Biol. Chem.* 269, 31620–31625.

25. Crottet, P. C., Peitsch, M. C., Servis, C., and Corthesy, B. (1999) *J. Biol. Chem.* 274, 31445–3145.

John Trowsdale
Roland Barten
Anja Haude
C. Andrew Stewart
Stephan Beck
Michael J. Wilson

The genomic context of natural killer receptor extended gene families

Authors' addresses
John Trowsdale[1], Roland Barten[1], Anja Haude[1],
C. Andrew Stewart[1], Stephan Beck[2], Michael J. Wilson[1],
[1]Immunology Division, Department of
Pathology, University of Cambridge,
Cambridge, UK.
[2]The Sanger Centre, Wellcome Trust Genome
Campus, Hinxton, Cambridge, UK.

Correspondence to:
John Trowsdale
Immunology Division
Department of Pathology
Tennis Court Road
University of Cambridge
Cambridge CB10 1SA
UK
Fax: 44 1223 333875
e-mail: jt233@mole.bio.cam.ac.uk

Summary: The two sets of inhibitory and activating natural killer (NK) receptor genes belong either to the Ig or to the C-type lectin superfamilies. Both are extensive and diverse, comprising genes of varying degrees of relatedness, indicative of a process of iterative duplication. We have constructed gene maps to help understand how and when NK receptor genes developed and the nature of their polymorphism. A cluster of over 15 C-type lectin genes, the natural killer complex is located on human chromosome 12p13.1, syntenic with a region in mouse that borders multiple Ly49 loci. The equivalent locus in man is occupied by a single pseudogene, LY49L. The immunoglobulin superfamily of loci, the leukocyte receptor complex (LRC), on chromosome 19q13.4, contains many polymorphic killer cell immunoglobulin-like receptor (KIR) genes as well as multiple related sequences. These include immunoglobulin-like transcript (ILT) (or leukocyte immunoglobulin-like receptor genes), leukocyte-associated inhibitory receptor genes (LAIR), NKp46, FcaR and the platelet glycoprotein receptor VI locus, which encodes a collagen-binding molecule. KIRs are expressed mostly on NK cells and some T cells. The other LRC loci are more widely expressed. Further centromeric of the LRC are sets of additional loci with weak sequence similarity to the KIRs, including the extensive CD66(CEA) and Siglec families. The LRC-syntenic region in mice contains no orthologues of KIRs. Some of the KIR genes are highly polymorphic in terms of sequence as well as for presence/absence of genes on different haplotypes. Some anchor loci, such as KIR2DL4, are present on most haplotypes. A few ILT loci, such as ILT5 and ILT8, are polymorphic, but only ILT6 exhibits presence/absence variation. This knowledge of the genomic organisation of the extensive NK superfamilies underpins efforts to understand the functions of the encoded NK receptor molecules. It leads to the conclusion that the functional homology of human KIR and mouse Ly49 genes arose by convergent evolution. NK receptor immunogenetics has interesting parallels with the major histocompatibility complex (MHC) in which some of the polymorphic genes are ligands for NK molecules. There are hints of an ancient genetic relationship between NK receptor genes and MHC-paralogous regions on chromosomes 1, 9 and 19. The picture that emerges from both complexes is of eternal evolutionary restlessness, presumably in response to resistance to disease.

Introduction

Detection of suitable targets by natural killer (NK) cells is mediated by two major families of receptor molecules: the immunoglobulin superfamily (IgSF) and the C-type lectin su-

Table 1. Compilation of some members of the extended family of activating and inhibitory receptors related to receptors on NK cells. This list is not complete and several other members of the family may be identified by searching databases. For further information, see Figs 1 & 2 and text.

| Human				Mouse			
Activating receptors							
Chromosome	Ligand	Chromosome	Receptor	Receptor	Chromosome	Ligand	Chromosome
		6p21.3	NKp30	NKp30	17		
		6p12.3	NKp44	NKp44	17		
		6	TREM	TREM	17		
6p21.3	HLA-E,	12p13.1	NKG2C/E	NKG2C/E	6	Qa1	17
6p21.3	MICA, B	12p13.1	NKG2D	NKG2D	6	H60	10
6q25	ULBP1–3					RAE	10
				NKR-P1B			
	IgA	19q13.4	FCAR				
		19q13.4	NKp46	MAR-1	7		
		19q13.4	KIR2DS1, 3DS	Ly49D, H	6	MHC class I H2	17
		19q13.4	ILT 1, 8 LIR8	PIRA1–7	7		7
	Collagen	19q13.4	gpVI	gpVI		Collagen	
		19q13.4	LAIR				
Inhibitory receptors							
		7q22	FDF03				
6p21.3	HLA-E	12p13.1	NKG2A	NKG2A	6	Qa1	17
		12p13.1	NKR-P1A	NKRP1A/C			
		12p13.1	NKG2A	NKG2A			
		12p13.1	MAFA-L				
		17	IRp60 CMRF35				
	Sialic acid	19q13.2	CD22				
		19q13.2	CD66a, d	CD66/CEA	7		
		19q13.3	CD33				
	Sialic acid	19q13.3	SIGLECe.g.5	SIGLEC	7	Sialic acid	
6p21.3	MHC class I	19q13.4	ILT2, 3, 4, 5 LIR8	PIR	7		7
		19q13.4	LAIR1				
3	CD47	20	SIRP	SIRP		CD47	
Other potential receptors or ligands							
		12p13.1	CLEC1/2				
		12p13.1	CD69	CD69			
		12p13.1	AICL				
		12p13.1	KLFR1				
		12p13.1	Ltt1				
		12p13.1	Ly49-L				
Fc receptors							
Activating receptors							
		1q23	FcεRI	FcεRI	1		
		1q21.1	FcγRI	FcγRI	3		
		1q23–24	FcγRIIA				
		1q23–24	FcγRIIIA	FcγRIIIA	1		
		19q13.4	FcαR	–			
Inhibitory receptors							
		1q	FCγRIIB				
Other receptors							
		1	Fcα/μR				
		1	polyIgR				
		1q23–24	FcγRIIIB				
		19q13.3	FcRN	FcRN	7		
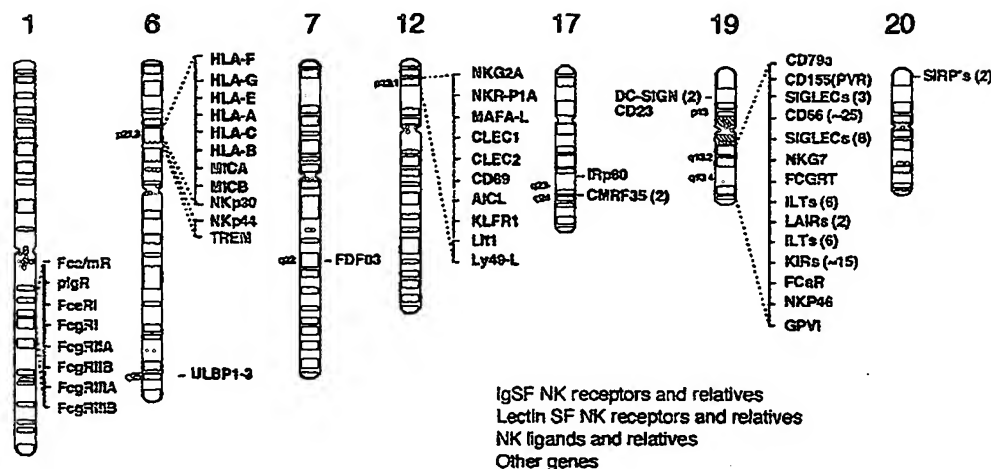
Fig. 1. Chromosomal locations of some NK receptor and ligand gene superfamilies. The approximate locations of the genes listed in Table 1 are shown alongside idiograms of human chromosomes. IgSF and lectinSF genes are coloured green and red, respectively. MHC class I-related ligands are blue. As mentioned in the text, these families of sequences are extensive and not all members are represented here.

These large clusters of receptor and ligand loci must have arisen from prolific duplication. Reference sources: FcR loci (121); MHC (122); MIC (123); NKp44 (124); TREM (125); ULBP (126); FDF03 (127); lectin receptors (NKC) (24); IRp60 (128); CMRF35 (129); LRC (24); SIRPs (130); CD155 (poliovirus receptor) (131); CD79a (132).

perfamily (1–5). Where known, the ligands for many of these receptors are MHC class I molecules (6–8). The receptors can be either activating or inhibitory, depending on the sequence in the transmembrane (TM) and cytoplasmic tails (5, 9). The inhibitory forms function via immunoreceptor tyrosine-based inhibitory motifs (ITIMs) (1, 10). The activating versions have truncated cytoplasmic domains lacking ITIMs. These molecules associate with immunoreceptor tyrosine-based activation motif (ITAM)-bearing adapter molecules (11). In the case of the killer cell Ig-like receptors (KIRs), as well as the murine functional homologues Ly49, the adapter is the DAP12 molecule (12, 13). Association between the regions of receptor and adapter is facilitated by neutralisation of oppositely charged residues, an aspartate in DAP12 and a positively charged residue on the TM region of the receptor (12).

Most of the inhibitory genes encoding these receptors are clustered in two locations. The C-type lectin genes, including CD94 and NKG2, are grouped in a ~2 Mb region of human chromosome 12, which has been called the natural killer complex (NKC) (14). The IgSF genes are clustered in a region of human chromosome 19q13.4 called the leukocyte receptor complex (LRC) (15–17). These complexes in mice also contain some 'paired' Ig-activating receptors (PIRs) that are, as the name suggests, members of the same molecular superfamilies (18).

Additional loci encoding either activating or inhibitory receptors have been identified on NK cells (19). Most of these also fit into the two extended superfamilies. With the benefit of rapid database screening it is apparent that sequences with varying degrees of relatedness are present on a variety of different tissues, especially those of the haemopoietic lineages. The products of some of the related genes, such as the Ig-like transcripts (ILTs) (or leukocyte Ig-like receptors (LIR) or CD85), for example, are expressed on a broad range of cell types (20, 21).

Receptor genes and ligand genes

Ascribing the many receptor cDNA and expressed sequence tag (EST) sequences to individual loci was not reliable in the absence of genomic data. To facilitate this we obtained extensive data on the organisation of NK receptor loci. Here we present an analysis of the gene structures, sequences and polymorphism of NK receptor genes as well as some related sequences.

On Table 1 we have listed some of the main NK receptor-related genes in man and mouse as well as genes encoding their ligands, where known. These families of molecules encompass several subfamilies of both lectins and Igs with related functions in the immune system and beyond. The two major clusters of inhibitory receptors are C-type lectins, in
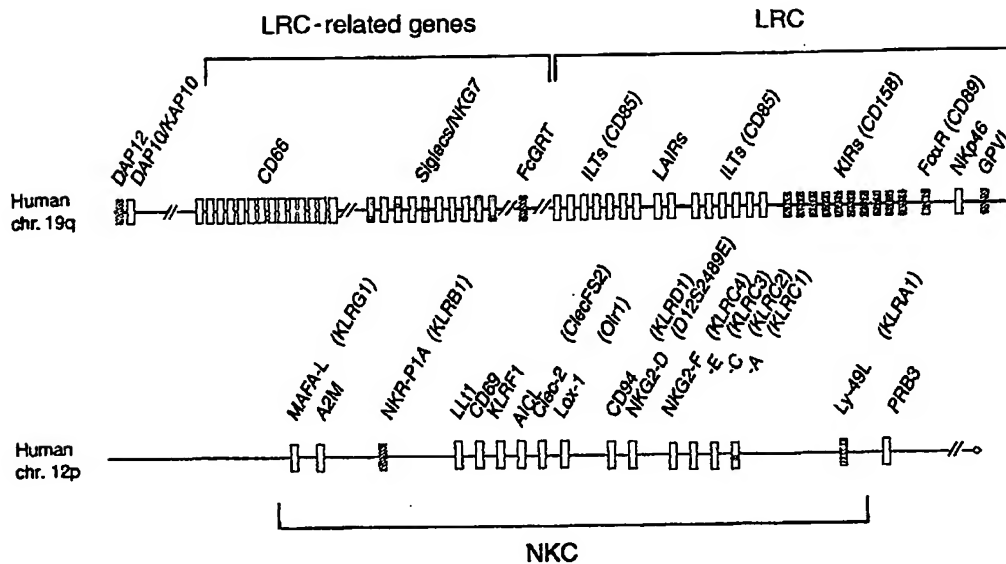
22

Fig. 2. Cartoon map of the organization of the extended LRC and NKC regions. The extended LRC region on chromosome 19q13 encompasses at least 40 members of the IgSF. At the far centromeric end, on chromosome band 19q13.1, are two adapter genes, DAP12 and DAP10 (KAP10), shown in more detail on Fig. 6 (13). Receptor gene families, weakly related to the KIR/ILT superfamily, the Siglecs and CD66 loci, have not been catalogued accurately here. These gene families are extensive and, although not shown here, interspersed with many genes of other types. The LRC extends from ILT8 to the far telomeric end, marked by GPVI, the collagen-binding receptor (28). Next is NKp46, an activating receptor on NK cells (25). Both of these genes are present in mice, presumably in the syntenic region of chromosome 7 (Fig. 11). Direct rodent orthologues of FcaR (CD89) and KIR genes have not been identified. The PIR loci in mice may be homologues of the ILT (CD85) genes (27). The lectin genes in the NKC (below) on chromosome 12p13 extend over several Mbp. Symbols approved by the human gene-mapping workshop are in brackets. Gaps are indicated by pairs of oblique lines. The maps are not to scale.

the NKC on chromosome 12p13.1 and IgSF, in the LRC on chromosome 19q13.4 (Figs 1 & 2). Further centromeric of the LRC are clusters of related sequences we have called the extended LRC. Activating versions, the functions of which are not immediately obvious, are interspersed with the inhibitory genes at these two locations. Some ligand genes are also located on this chromosome in the MHC, at 6p21.3 (22). Other activating receptors on NK cells are dispersed, particularly on human chromosome 6, and include NKp30 and NKp44 (18).

The leukocyte receptor complex

This complex of loci on chromosome 19q13.4 contains over 25 Ig superfamily genes, indicative of prolific duplication (23, 24) (Fig. 2). Since some loci, such as NKp46, are orthologous in humans and mice (25), primordial genes must have been in place for at least 80 million years, before speciation between man and rodents. Some of the other genes are provisionally identified as orthologues, e.g. the PIRs and the ILTs

(26). The existence of chicken Ig-receptors related to PIRs and Fc receptors is also consistent with a common origin (27). The platelet collagen receptor gene, platelet glycoprotein receptor VI (GPVI), is located at the telomeric end of the complex. This gene is clearly related to the other genes in the LRC (28) and, like the ILTs, the protein product associates with Fc common γ chain (FcRγ) for signal transduction.

The extended LRC

Other related molecules are encoded centromeric of the LRC, including the sialic acid-binding Ig-like lectins (Siglecs) (29) and the CD66-related molecules. The CD66 gene family includes a group of molecules commonly known as carcinoembryonic antigen (CEA). In total there are about 29 CD66 genes, 18 of which are expressed (30). There are at least 7 CEA genes encoding membrane-spanning cell surface molecules, with 1–4 Ig domains. Another group of 11 genes belongs to the pregnancy-specific glycoprotein subgroup of secreted molecules. A role in innate immunity has been proposed for these molecules. Some of the CEA molecules
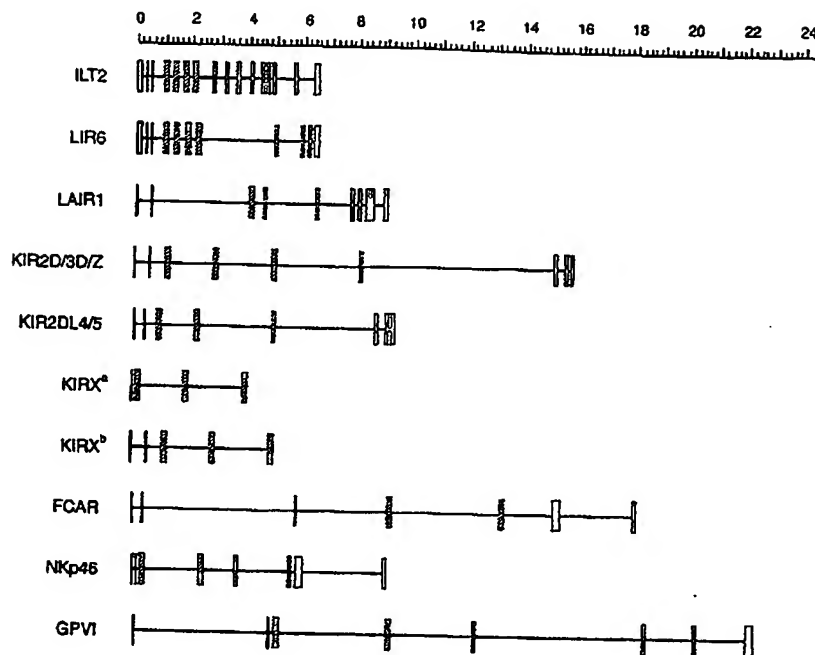
Fig. 3. Exon structure of some members of the Ig receptor superfamily. Exons are depicted as vertical bars. A distinctive feature of these genes is the hydrophobic leader (signal) sequence that is encoded over two exons (solid black), in contrast to many other members of the IgSF. Each Ig domain is on a separate exon (orange) in the same phase of the triplet codon. The genes of the LRC vary 5′ of the Ig domains with differing numbers of stalk or stem exons (light blue), the TM domain is encoded by a single exon (purple), and the cytoplasmic tail can be encoded by up to six exons (red). ILT2 and LIR6 are prototypic inhibitory and activating ILT gene structures, respectively. Many of the ILTs have a predicted 5′ untranslated exon (white) based on some longer cDNA sequences (see (40)), with ILT3 being the single exception (also only having two Ig domains corresponding, by

homology, to the first and last Ig domains of other ILTs). ILT6 is an outriding member of this family having untranslated pseudoexons for the second stalk, TM and cytoplasmic tail (exons 8, 9 and 10 (40)). ILT9 and ILT10 also have pseudoexons for the second and third Ig domains respectively. No transcripts have been identified which omit these exons, suggesting that they are transcribed pseudogenes (133). Exon 3 of the KIRs is also a pseudoexon in 2DL1–3 and 2DS1–5 where it is spliced out (35, 134, 135). KIRZ also has a pseudoexon 3 and a pseudoexon 4 (due to a one base deletion (M. Wilson, unpublished)), with no transcripts having been identified to date. KIRX is polymorphic with respect to the presence (*) or absence (*) of exon 2, as demonstrated on the two haplotypes sequenced to date, and is also missing exons 6–9 from the prototypic KIR gene structure (23).

possess homo- and heterotypic cell adhesion properties. Other IgSF genes mapping to the extended LRC are FCGRT, encoding the neonatal FcRN, as well as CD79a and CD155.

Further centromeric on the same chromosome at 19q13.1 are two of the genes for TM adapter molecules. DAP12 complexes with activating receptors within the LRC and NKC. DAP10/KAP10, on the other hand, has only been shown to associate with NKG2D that is encoded in the NKC (13, 31, 32).

Organization of KIR genes

A consistent feature of the Ig receptor family of genes is the exon–intron organisation. As shown on Fig. 3, intron distances vary widely but the exon boundaries are absolutely conserved. The splitting of the signal sequence between two

exons is highly characteristic of this particular set of loci. Each Ig domain is contained on a separate exon. The remaining C-terminal portion of each encoded protein is encoded on a small number of exons.

KIR loci with two Ig domains appear to have been derived from genes with three domains by skipping of an exon. In some cases the skipped exons have incurred mutations. Interestingly, these mutations may provide part of the means of eliminating the exon in the transcript. This speculation is based on work showing mechanisms for exon skipping as a direct consequence of nonsense or missense mutations in genes, using BRCA1 as an example (33).

There is some variation in organisation within different KIR genes. The Ig domains (and exons) are labelled D0, D1 and D2, from the N-terminus of the prototypic 3-Ig-domain mol-

ecule. The *KIRZ* locus has high homology to *KIR2DL3/2DL2* and *2DL1* at the nucleotide level (>97%). This gene is a component of the most common, short (A), haplotype (34). The exon encoding the D0 domain is a pseudoexon with three base pairs missing and a base change leading to the introduction of an in-frame stop codon, as in other two Ig domain KIRs (35). The D1 domain has a single base pair deletion causing a frame shift that introduces a stop codon, while the D2 domain, common to all KIRs, is intact. If this gene is transcribed, it would have to skip both exon 3 and exon 4, resulting in a unique KIR protein with only a single Ig (D2) domain as well as a classical ITIM motif (36) in the cytoplasmic tail, in addition to an RVYXXL motif.

KIRX is present on both haplotypes sequenced to date (23). On the common A haplotype the second exon is absent due to a deletion, leaving only 74 bp between exons 1 and 3. This compares with 1,550 bp encoding intron 1, exon 2 and intron 2 on the single B haplotype analysed (Fig. 4). (23) Both haplotypes are also missing exons encoding for the stalk, TM and cytoplasmic portions of the KIR protein.

The 14 kb region 3′ of *KIRX* bears no homology with other KIR genes, as demonstrated by a dot plot analysis of one haplotype versus itself. Most of this region encodes various DNA repeat elements resulting in a gap in the reiteration of the KIR gene sequences (23). The D0, D1 and D2 domains of *KIRX* are intact and potentially encode a 3-Ig-domain protein. One would predict that the encoded protein of the *KIRX* gene on the common haplotype would not be secreted, owing to the lack of a classical leader sequence. Conversely, *KIRX* on the B haplotype (with the leader sequence exons intact) would be secreted. To date no transcripts have been identified for either *KIRX* or *KIRZ*.

Inhibitory and activating versions of KIR loci are highly similar in sequence. Minimal alterations in the sequence of an inhibitory receptor are sufficient to create a charged residue upstream of a stop codon, converting an inhibitory sequence into an activating version through recruitment of DAP12 and elimination of ITIMs.

Fig. 4. Feature map of the telomeric end of the KIR complex on chromosome 19q13.4. The sequence was taken from PAC 1060P11 and PAC 550B14 (23) (and unpublished). The positions of genes were identified by comparison of the sequence with EST or cDNA databases, or by gene prediction programs such as NIX. Arrows point in a 5′ to 3′ direction. The positions of Alu, long interspersed nuclear element (LINE) and long terminal repeat (LTR) sequences are indicated on the lines below the genes. All of the genes belong to the extended KIR IgSF except for the pair of loci between *NKp46* and *GPVI*. For further details, see text and (23).
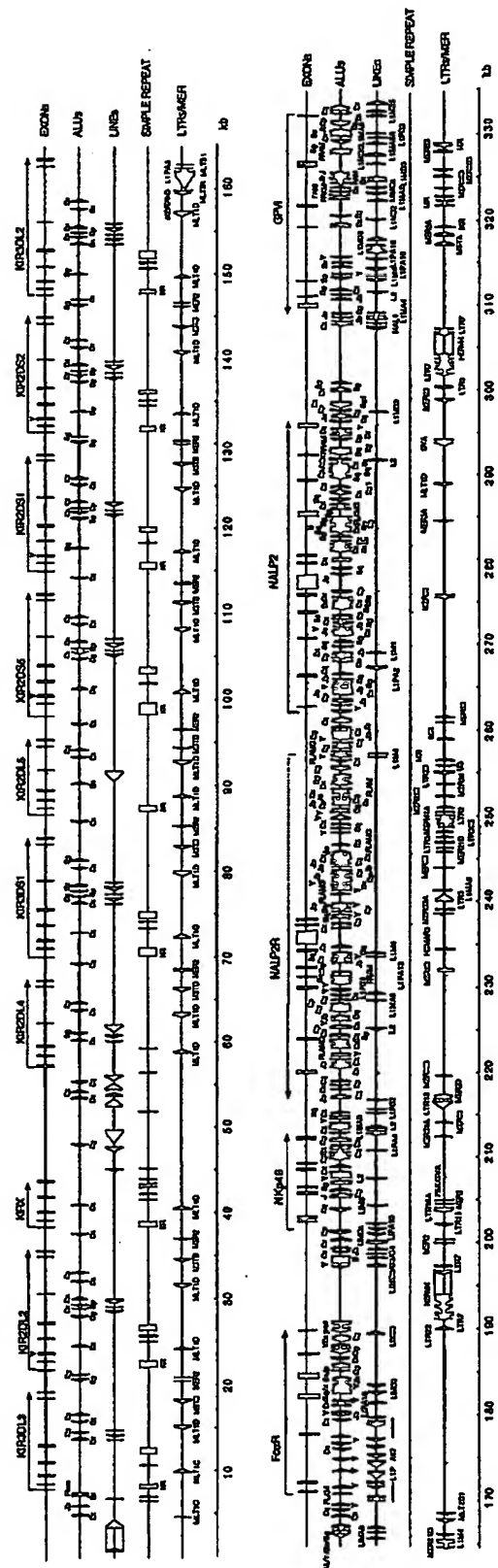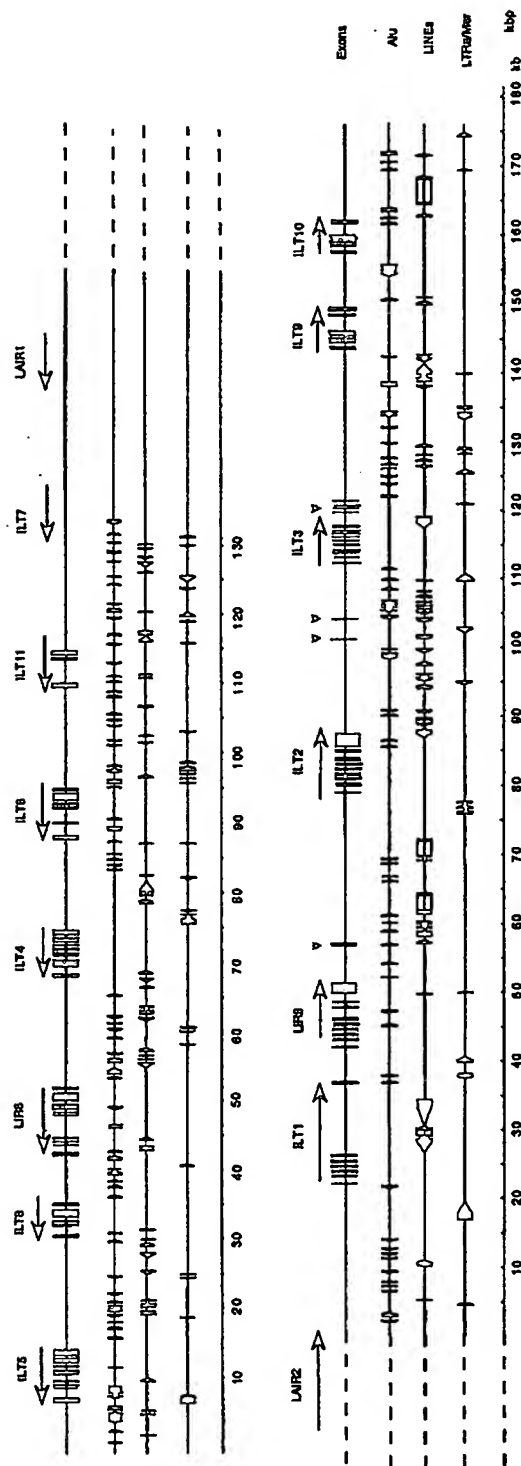
Genomic sequences of *KIR* loci

We have completed an extensive analysis of KIR sequences from two haplotypes (Fig. 4) (23). KIR genes are organised head-to-tail in a tight-knit arrangement. Each gene is approximately 2 kb apart. Dot matrix analysis revealed a series of reiterated sequences with just one substantial 14 kb stretch of unique sequence upstream of KIR2DL4, apart from the ends of the complex. This arrangement is consistent with recent duplication.

Telomeric of the KIR loci, the related FcaR and NKp46 loci are arranged in the same orientation. Between these loci and the related collagen receptor GPVI, which is in the opposite orientation, is a section of DNA containing two NACHT family genes, NALP2 and NALP2R (R for related) arranged head-to-head. The NACHT proteins comprise a group of sequences with several shared motifs including nucleoside triphosphate (NTPase) domains as well as Walker A and B motifs (37). The MHC class II transcription activator CIITA is a member of this family of molecule (38). This stretch of DNA, which is highly repeat-rich, separates the most telomeric member of the Ig superfamily in the LRC, GPVI, encoding the platelet collagen-binding gene from the other sequences. The presence of two human endogenous retroviral (HERV) sequences flanking the NALP2 loci may be related to the insertion of an inverted DNA duplication (39).

ILT loci

The ILT genes fall into two clusters of 6–7 loci, each genetically linked to a single leukocyte-associated inhibitory receptor (LAIR) locus, orientated in opposite directions (16, 40, 41) (Fig. 5). The ILT genes differ markedly from the KIR loci in that their introns and intergenic regions are not highly homologous. This suggests an older origin of the ILT loci than the KIR genes, consistent with the potential orthology of the murine PIRs (42). The ILT region is similar on different haplotypes. Of the ILTs, so far only the ILT6 gene is polymorphic for presence/absence on different chromosomes, due to a simple deletion that removes exons 1–7, spanning 6.7 kbp of the locus (40). Like the NALP2 genes, ILT6 is associated with HERV sequences, which may be related to the deletion (39). The intact ILT6 allele has a gene frequency of 0.72 (23, 40).

Adapter loci on chromosome 19q13.1

Two genes encoding adapters for positive signalling from some KIR as well as lectin products in the NKC, such as NKG2D, are positioned centromeric of the CD66 loci at 19q13.1. The DAP12 and DAP10/KAP10 genes are arranged tail-to-tail, separated by 131 bp (Fig. 6). An uncharacterised

Fig. 5. Feature map of the ILT complex on chromosome 19q13.4. The ILT and LAIR genes are shown from PACs 52N12 and 598H20 (23, 40). Alu, LINE and LTRs are indicated as for Fig. 4. The genes are arranged in two sets, which were most likely the result of an inverted duplication (16, 40).

TYROBP   DAP10/   LEG2.6   APLP1
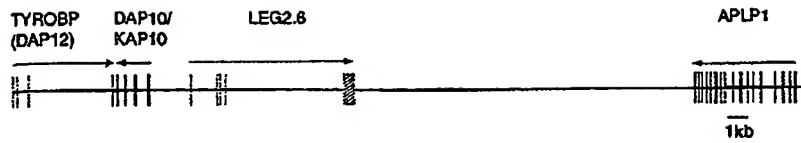(DAP12)   KAP10

1kb

Fig. 6. The adapter genes on chromosome 19q13.1. The two DAP genes are arranged tail to tail. The DAP10 locus shares a promoter region with another gene, LEG2.6, which is expressed in similar tissues (data not shown). The amyloid precursor-like protein 1 (APLP1) gene was described in (136).

gene, with a 2.6 kb transcript, was identified in the course of investigating the DAP complex. Preliminary studies indicate that the expression of this gene, leukocyte-expressed gene (LEG2.6), is co-ordinate with that of DAP10 (M. J. Wilson, A. Haude, C. Chang, unpublished).

Polymorphism and gene organisation

One of the most interesting findings to emerge from the study of NK receptors is their polymorphism (34, 43). The MHC is the paradigm for extreme variation, where some loci now comprise over 300 alleles (22). Another related feature of the MHC is the variation for the presence or absence of loci, such as in the DRB cluster (44, 45). And, like DRB or C4 genes in the MHC, KIR loci exhibit variation in sequence as well as variation for presence/absence on different haplotypes. Some KIR genes are present on most if not all haplotypes. Between these anchor or framework sequences the number of KIR genes varies, as shown on Fig. 7. The continuous reiteration of KIR loci in head-to-tail arrangement may help to facilitate gain–loss variation throughout evolution by non-reciprocal recombination. The precise number of haplotypes remains to be determined but it is over 15 and could exceed 100. So far there are not enough data to obtain an accurate measure of the number of alleles at individual KIR loci, but most have multiple alleles and certain ILT loci are obviously highly variable (Table 2). KIR sequences may vary in a minimal number of base pairs, to convert from an ITIM-bearing inhibitory receptor to an activating molecule, which can associate with the DAP12 adapter. The inhibitory KIR3DS1 and activating KIR3DL1 sequences are examples of such alleles at a single locus (23, 34). The other way in which KIR loci may vary, in the number of Ig domains, was discussed earlier (Fig. 3). So far, there is no indication that regions flanking highly polymorphic loci are also variable, as is the case surrounding MHC class I and class II genes (46).

As mentioned above, apart from the single exception of ILT6, ILT loci are present on all haplotypes. Some of the ILT sequences are, however, highly variable, including, so far, ILT5

and ILT8 (40, 47). Eighteen alleles of ILT5 have been described from 52 individuals screened (47).

Polymorphism of HLA genes is focused on the amino acid residues flanking the peptide-binding grooves (45). From preliminary analysis, variation in KIR sequences appears to concentrate on key residues that impact class I structures (48). As well as influencing protein structure and (presumably) interaction with ligands, KIR variation may affect expression either through alteration in the TM region or possibly in the promoter sequences.

Minisatellites in KIR loci

As mentioned above, the KIR2DL4 gene is flanked by unique sequence. As opposed to the other KIR loci, the gene is expressed in most NK cells. Another unique feature of KIR2DL4 is that it does not have a G+C rich minisatellite in the first intron. G+C rich minisatellites are often associated with recombination and/or variation in other genes. Such sequences are present in all of the other KIR loci (49, 50). Each minisatellite contains a reiterated sequence of 19–20 bp (Fig. 8).
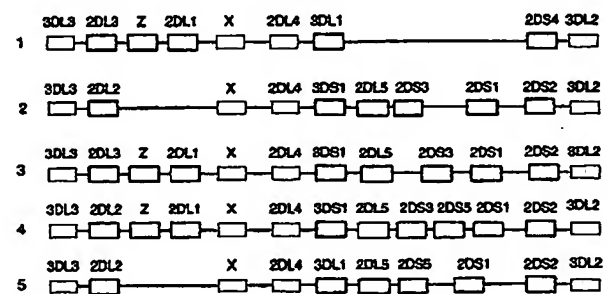

Fig. 7. Organization of KIR haplotypes. Some hypothetical haplotypes based on known genotypes are shown (34) (M. Carrington, unpublished data). Framework loci, present on most or all haplotypes, are shown as filled boxes. Other loci vary in number between different haplotypes. The haplotypes shown have in most cases been inferred from analysis of paired genomic and cDNA samples. Many additional variant haplotypes may exist (M. Wilson, unpublished data) (M. Carrington, personal communication). Example 1 corresponds to the frequent 'A' haplotype (34).

Table 2. Preliminary listing of numbers of alleles at KIR-related loci. The numbers of known alleles are given. The degree of variation in some loci has not been explored so the numbers represent a minimal figure.

ILT/LAIR		KIR	
Name	No. of alleles	Name	No. of alleles
ILT5	18	2DL1	8
ILT8	3	2DL2	4
LIR8	2	2DL3	5
ILT4	6	2DL4	6
ILT6	3*	2DL5	6
ILT11	1	2DS1	4
ILT7	1	2DS2	8
LAIR1	4	2DS3	3
LAIR2	2	2DS4	8
ILT1	5	2DS5	2
LIR6	2	3DL1	11
ILT2	7	3DL2	10
ILT3	4	3DL3	3
ILT9	2	KIRX	2
ILT10	2	KIRZ	1

Other LRC loci			
NKp46	2	GPVI	2
FcaR	5		

* ILT6 has one allelic form that is missing exons 1–7 which is included in this total.

Each KIR locus contains a discrete number of repeat units, ranging from 23 in 2DL5 to 63 in 2DS4 (Table 3). So far, no allelic variation has been identified. The function of the mini-satellites could also relate to the stochastic regulation of KIR expression in different NK clones (34).

Repeat analysis in KIR and ILT loci

We have analysed two LRC genomic sequences for the presence of Alu in addition to other repeat sequences. The ratio of AluS to AluJ sequences can provide a measure of the age of a region since AluS sequences are relatively recent compared to J (51–54). There are ~9 AluS sequences and no AluJ in each KIR gene. The AluS/J ratio is therefore extremely high over the KIR region, consistent with the recent derivation of these genes, the presence of which is restricted to primates (55). The S/J ratio over ILT sequences is closer to the genome average of 3. Further telomeric, over the region between the FcaR and GPVI loci, the S/J ratio is also slightly elevated (~5).

Promoter sequences

Fig. 9 shows an alignment of ~460 bp of 15 different KIR promoter sequence. Those KIR genes expressed on a fraction of the NK-cell population have homology over these regions

with greater than 91% identity (43). On the other hand, the anchor loci KIR3DL3 and KIR2DL4 have more divergent promoter sequence from this group, 89% and 69% identity, respectively. No physiological transcripts of KIR3DL3 have been reported, whilst KIR2DL4 is expressed in 100% of NK-cell clones (43). The sequence homology suggests that although the promoter regulation of KIR2DL4 may be divergent, the majority of KIR promoters are likely to be controlled by similar mechanisms.

Potential transcription factor binding sites are illustrated in Fig. 9. The high level of homology of the KIR promoters provides few clues as to which transcription factors are likely to be specific to KIR gene expression. However, identification of non-expressed KIR2DL5 variants led Vilches et al. to suggest that a mutation in a putative AML1 transcription factor site may prevent these variants from being expressed (56). The promoter of these variants is identical to that of the pseudogene KIRX. The binding site for AML1 is conserved between all other KIR promoters, including KIR2DL4. The AML1 transcription factor regulates a variety of haematopoietic genes and can act as both a positive and negative regulator of transcription. Known partners for AML1 in transcription activation include members of the Ets, AP1, c/EBP, Myb and CBP (CREB binding protein) families (57), some of which have possible binding sites within the KIR promoter regions.

The natural killer complex (NKC)

The NKC is located on human chromosome 12p13.1 (Figs 1 & 2) (58–61). This region encodes type II TM C-type lectin proteins, many of which are expressed on NK cells. Some of the other related genes in the NKC, including NKR-P1, LOX-1, KLRF1 and CLEC are expressed on a broader range of cell types, mostly of the haemopoietic lineage (62–65). As with the LRC, multiple duplications must have been responsible for this extensive group of weakly related loci (66). There is also evidence for recent duplication since some of the genes are extremely similar in sequence. The NKG2 loci, for example, are over 90% identical (67, 68).

Orthologous regions

While there are obvious orthologues maintained between species, such as CD69 and CD94, there are remarkable differences in organization of the NKC (24). Three NKR-P1 genes have been identified in mouse, 2 or 3 in rat, but humans probably possess only one functional gene (69, 70) (R. Barten, unpublished data). The human NKR-P1A protein interacts with FcRγ and p56lck and is an activating receptor. Mice have

KIR3DL1 INTRON 1

Exon 1<-

```
GAGTCCTGGAAGGGAATCGAGGGAG
GGAGTGCGGGGATGGGATCT
CGACCTGGAGGTAAAGATAT
GGGCCTAGAGGTGGAGTTAT
GGGCCTGGAGGTGGAGTTAT
GGGCCTGAAGTGGAGATCT
GGGCCTGGAGTGGAGATCT
GGGCCTGGAGTGGAGATA
GGGGCCTGGGGTGGAGATAT
GTGCCTGGAGTGGAGATCT
GGGCCTGGAGTGGAGATAT
GGGCCTGGGGTGGAGATAT
GTGCCTGGGGTGGAGATAT
GGGCCTGGAGGGGAGATAT
GGGCCTGGAGGGGAGATGT
GGGCCTAGAGGTGGAGTGAT
GGGCCTAGAAGTGGAGCGAT
GGGCCTGGAGTGGAGATAT
GGGCCTGGAGGTGGAGTTAT
GGGCCTGCAGTAGAGATAT
GGGCCTGAAGTGGAGATAT
GGGCCTGGAGTGGAGATAT
GGGCCTAGAGGTGGAGTTAT
GGGCCCGGAGGTGGAGTTAA
GGGCATGAAGTGGAGATCT
GGGCCTGGAGTGGAGATAT
GATCCTGGAGTGGAGATAT
GGGCCTGGGGTGGAGATAC
GGGCCTGGAGCAGACATAC
AAGCCTGGAAAGGAGATAT
GGGCCTGGAGAGGAGATAG
AAGCCTGGAGTGGAAATAT
GGGCCTGGAGTGGAGATAT
GAGCCTGGAGTGGATATAT
GAGCCTGGAGTTGAGATAG
GAGCCTGGAGTGGAGATAT
GGGCCTGGAGTGGACTTAT
CAGCCTGGAGAGGAGATAT
GGGTCTGGAGTGGAGATAC
GGACCTGGAGTGGAGATCT
GGGCCTGTTGTGTAGATCT
AGGCCTGGAGGTAGAGATCT
GGGCCTGGAGGCTGAGTCTCT
GCACAGCCGAGATCCTTGTTCCTGGGGGCAGGTAGGCAGCGAGGGTGAGTTTACCTTCA
GCCCAGCAAGGGCCTGGCTGCCAAGACGCACAACCCAGTGGGGGCAGCAGGGTGCCCTG
GTTTGCCTGCAGATGGATGGTCCATCATGATCTTTCTTTCTAG -> Exon 2
```

Fig. 8. Example of a minisatellite sequence in the first intron of a KIR gene (KIR3DL1). The intron in this gene contains 42 19–20 bp repeating units. The numbers of units in other KIR loci are shown on Table 2. Almost all of this intron is made of repeats of the type described (49).

the NKR-P1A orthologue, the related NKR-P1C gene and an ITIM-containing molecule, NKR-P1B, that exhibits an inhibitory function (71). The most outstanding difference concerns the Ly49 family. The precise number of murine Ly49 genes has not been conclusively determined but estimates are of 12–15 genes (14, 72).

No sequence information about the mouse NKC is known, but it may reveal that the size difference of the human NKC

of 2 Mb and the mouse of 4 Mb is mainly due to the expansion of the Ly49 gene family between NK2GA and Ly49b (24). Southern blot analysis revealed that different inbred mouse strains show not only a high degree of polymorphism but also different numbers of Ly49 genes (72, 73). Without genomic sequence from different strains it is difficult to distinguish between alleles and different loci. Southern blot and limited sequence analysis is suggestive that, like the KIRs,

Table 3. Numbers of microsatellite repeat units (each 19–20 bp) in the first introns of KIR genes. Preliminary data on a small sample suggest that the numbers of repeats are relatively constant in different alleles of the same locus. Similarly there may not be much sequence variation in the repeat region between alleles.

Locus	Intron 1	KIR repeats
2DL1	983	42
2DL2	909	37
2DL3	909	37
2DL4	189	None
2DL5	649	23
2DS1	965	39
2DS2	793	30
2DS4	1398	63
2DS5	1212	52
KIRY	1057	45
3DL2	728	28
3DL3	677	33
3DS1	998	43
3DL1	999	42

there is considerable variation in arrangement of Ly49 genes (14, 74).

Recent evolutionary processes are evident from a comparison of chimpanzee and human NKG2 genes. With the exception of NKG2D, the different NKG2 loci are more similar within a single species than between different species, such as humans and mice (75). This is consistent with a rederivation of different loci in individual species from a single locus in each case, by a birth and death process (76). Although CD94 and NKG2A are highly conserved, NKG2C is more diverse and a chimp NKG2C pseudogene has been found.

Classical MHC class I sequences are similarly non-orthologous between humans and rodents (77). Local gene duplication after speciation could similarly account for these data. An alternative mechanism is intraspecies homogenisation by gene conversion (78).

Phenotypes

Several phenotypic traits have been mapped to the NKC in mouse and rat. Nka in rats controls NK-mediated alloreactivity and is linked to the Ly49 genes (79). The Chok locus is important for differential killing of Chinese hamster ovary cell (CHO), versus YAC-1 targets, by different mouse strains (80). Transfection of the Ly49D gene from B6 mice into BALB/c NK cells made them capable of killing CHO cells (81). A locus mediating resistance to mouse cytomegalovirus has been mapped to the Ly49 region, at the Cmv-1 locus (82–84). B6

mice, but not BALB/c, are resistant to these virus infections. Resistance to ectromelia virus maps to a similar region but it is not known if it is identical to Cmv-1 (85). Resistance to ectromelia virus-induced necrosis (Rmp1) and acute splenic replication of mouse CMV (Cmv-1) is apparently mediated by NK cells, as shown by NK-transfer studies (83, 86). Mapping data from back-cross mice shows that Cmv1 is located between Ly49b and Prp at the telomeric end of the NKC, excluding most of the Ly49 genes (87). Antibody-blocking experiments, using reagents against Ly49, confirm this result (88), but anti-Ly49d did not block the Chok phenotype (80). Therefore, even in the absence of functional Ly49 genes, similar resistance genes against virus infection could be present in humans.

NKC gene structures and encoded proteins

The gene structures of the C-type lectins in the NKC are very similar. One or two exons encode the 3' UTR and cytoplasmic tail. A single exon delineates the Tm region and three separate exons encode the carbohydrate recognition domain (CRD) (Fig. 10). The only notable difference is the presence or absence of a separate exon for a stalk region between the TM and the CRD. CD69, activation-induced C-type lectin (AICL), mast cell function-associated antigen (MAFA), LLt1 are missing this stalk region (24, 66). Interestingly, this region is involved in the ligand specificity of Ly49A and C, as shown in binding assays using chimaeric molecules (73). No ligands have been found for the proteins missing the neck region.

Many C-type lectins recognise carbohydrate structures in a calcium-dependent manner (89). However, for some of the lectins encoded in the NKC, sugar binding does not seem to be absolutely necessary for ligand binding (90). Ligands for the Ly49 homodimers and the NKG2A/C/E CD94 heterodimers are both classical and non-classical MHC class I molecules (91–95). CD94/NKG2 interaction with HLA-E is Ca^{2+} and carbohydrate independent (96). Ly49-A may preferentially bind to a protein structure but other reports stress binding carbohydrate moieties (97).

Divergent, convergent and co-evolution of NK receptors and ligands

The two main gene clusters of receptors, the LRC and NKC, are identifiable in both man and mouse (Fig. 11). Many of the genes in these clusters have remained in order in the two species. However, the highly polymorphic NK receptors appear to have developed from different gene sets in the two species. Early primate lineages may have had functional Ly49
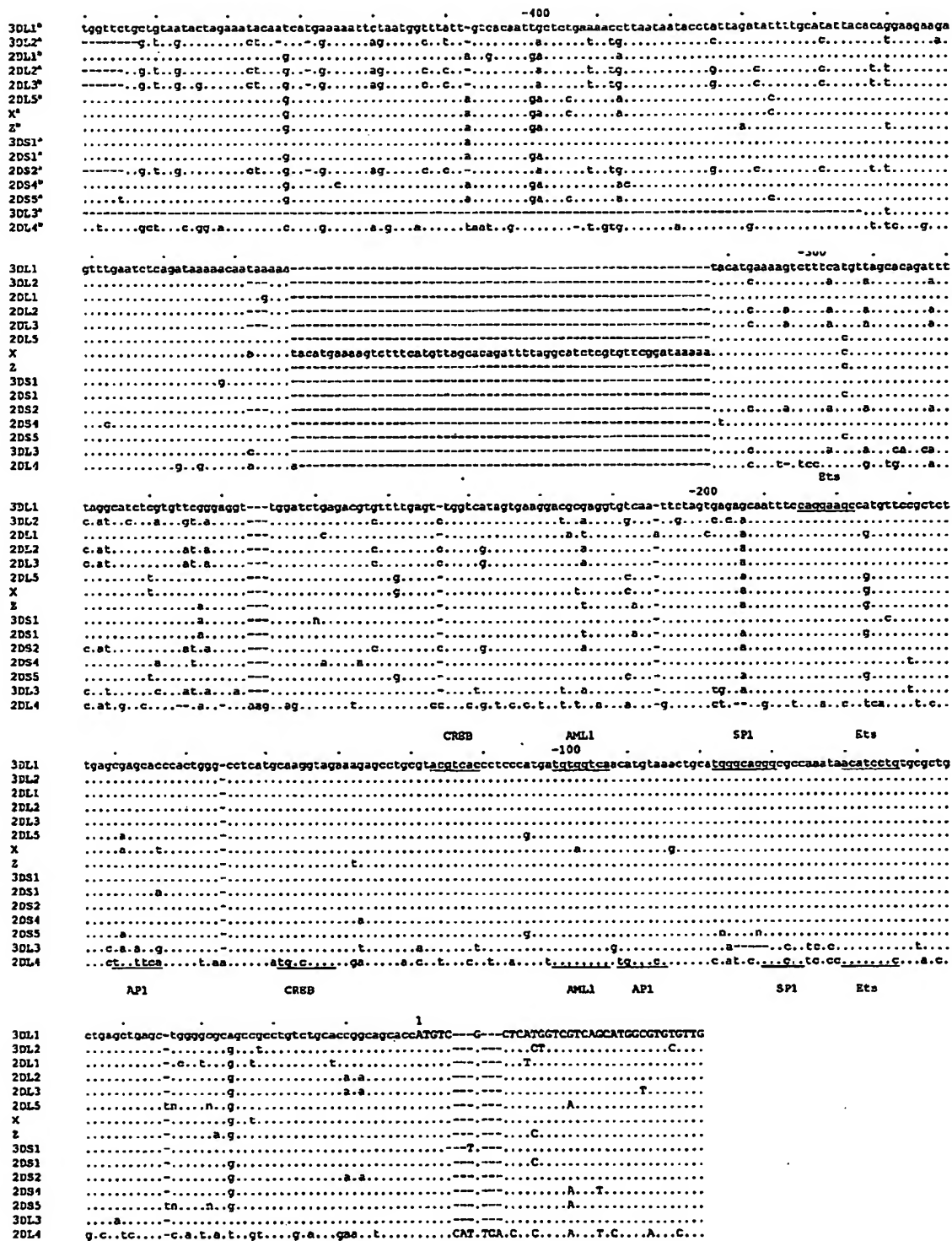
```
                                                                -400
3DL1°  tggttctgctgtaatactagaaatacaatcatgaaaaattctaatggtttatt-gtcacaattgctctgaaaaccttaataataccctattagatattttgcatattacacaggaagaaga
3DL2°  --------g.t..g.........ct..-...-.g.....ag.....c..t..-.....a.....t..tg...........c...............c.......t......a.
2DL1°  ......................g.................a..g...ga.........a...............................c...................
2DL2°  -------.g.t..g.........ct..g..-.g.....ag.....c..c..-.....a.....t..tg...........g.....c........c.......t.t.....
2DL3°  -------..g.t..g..g.....ct..g..-.g.....ag.....c..c..-.....a.....t..tg...........g.....c........c.......t.t.....
2DL5°  ......................g.................a.....ga...c......a...............................c...................
X°     ......................g.................a.....ga..c.....a...............................c...................
Z°     ......................g.................a.....ga..................................a..................t......
3DS1°  ......................g.................a.....ga.........................................................
2DS1°  ......................g.................a.....ga.........................................................
2DS2°  -------.g.t..g.........ct..g..-.g.....ag.....c..c.......a.....t..tg...........g.....c........c.......t.t.....
2DS4°  ......................g.....c.........a.....ga.....bc......................................c...................
2DS5°  ...t..................g.................a.....ga..c......a...............................c...................
3DL3°  ----------------------------------------------------------------------------------------------,..t......
2DL4°  ..t.....gct...c.gg.a.......c....g.....a.g...a.....taat..g........-.t.gtg.....a..........g..................t.tc...g...

                                                                          -300
3DL1   gtttgaatctcagataaaaacaataaaaa----------------------------------------------------------tacatgaaaagtctttcatgttagcacagattt
3DL2   .............................----.....................................................---....c.......a....a..........a..
2DL1   ..................g..........-.....................................................---....c.......a....a.......a..
2DL2   ..................--...........-----................................................---....c.......a....a...a....a..
2DL3   ...............................-----...............................................---....c.......a....a...a....a..
2DL5   ...........................--........................................................---....c......................
X      .............................a.....tacatgaaaagtctttcatgttagcacagatttttaggcatctcgtgttcggataaaa.......c.............
Z      ...........................--..............................................................---....c.............
3DS1   ...............g.............-----.................................................---....c.......a....a.......a..
2DS1   .............................-----................................................---....c.............
2DS2   ..................--.........-----...............................................---....c.......a....a....a..
2DS4   ...c..........................-----..............................................---....t..c.............
2DS5   .............................-----.............................................---....c.............
3DL3   ...........c.................-----............................................---....c.......a....a...ca..ca..
2DL4   ..........g.g.......a.........a-----...........................................---....c...t-.tcc.......g..tg....a..

                                                                   Ets
                                                           -200
3DL1   taggcatctcgtgttcgggaggt---tggatctgagacgtgtttttgagt-tggtcatagtgaaggacgcgaggtgtcaa-ttctagtgagagcaatttccaggaagccatgttccgctct
3DL2   c.at.c..a...gt.a......---.......c.........-.......t..a....g..-..g...c.c.a...............g.........
2DL1   ..........a......---......c.....-...........a.t.....a.....c...a...............g...........
2DL2   c.at.......at.a......---......c.....d....g..........a..........-.....a...............g...........
2DL3   c.at.......at.a......---......c.....c....g..........a..........-.....a...............a...........
2DL5   .......t...............---.........g....-.........c....-.....a...............g...........
X      .........t...........---.........g....-.........t....c....-.....a...............g...........
Z      ..........a..........---.......-...........t....a....-.....a...............g...........
3DS1   ..........a......---....n.....-...........t....a....-.....A...............c...........
2DS1   ..........a..........---......-...........t....a....-.....A...............g...........
2DS2   c.at.......at.a......---......c.....c....g..........a..........-.....a...............g...........
2DS4   .......a....t.......---....a...a...........t....a....-.....c...............t...........
2DS5   .......t...........---.........g....-.........c....-.....a...............g...........
3DL3   c..t.......c...at.a..a.---......-...........t..a....-.....c...............t...........
2DL4   c.at.g..c....,--.a..-....aag..ag.......t...........cc...c.g.t.c.c.t..t.t..a...a...-g......ct.--..g...t...a..c..tca....t.c..

                                CREB            AML1           SP1            Ets
                                                -100
3DL1   tgagcgagcacccactggg-cctcatgcaaggtagaaagagcctgcgtacgtcacccttcccatgatgtggtcaacatgtaaactgcatgggcagggcgccaaataacatcctgtgcgctg
3DL2   ...........................................................................................................
2DL1   ...........................................................................................................
2DL2   ...........................................................................................................
2DL3   ...........................................................................................................
2DL5   .........a..................-..........................g....................................................
X      .....a....t.................-..........................a...........g........................................
Z      ...........................-..........t....................................................................
3DS1   ...........................................................................................................
2DS1   ..........a................................................................................................
2DS2   ...........................................................................................................
2DS4   ...................a.......................................................................................
2DS5   .....a.....................................................g.........................a---n..................
3DL3   ..c.a.a...g.........-.......t.....a.......t.........g.........a----..c..tc.c...........t....
2DL4   ...ct..ttca.......t.aa......atg.c......ga.....a.c..t...c..t..a....t.........tg...c.......c.at.c....g..tc.cc.......c....a.c.

       AP1             CREB                      AML1     AP1         SP1        Ets

                                          1
3DL1   ctgagctgagc-tggggcgcagccgcctgtctgcaccggcagcaccATGTC---G---CTCATGGTCGTCAGCATGGCGTGTGTTG
3DL2   ............-.........g....t...........................---.---....CT...................C....
2DL1   ............-.c..t..g..t...........t...................---.---...T..........................
2DL2   ............-.........g...............a.a..............---.---..............................
2DL3   ............-.........g...............a.a..............---.---..................T.........
2DL5   ...........tn....n..g..................................---.---................A............
X      ............-.........g..t.............................---.---....C........................
Z      ............-.........a.g..............................---.---....C........................
3DS1   ............-.......................................---?.---..............................
2DS1   ............-.........g................................---.---....C........................
2DS2   ............-.........g...............a.a..............---.---..............................
2DS4   ............-.........g................................---.---........A...T...............
2DS5   ...........tn....n..g..................................---.---................A............
3DL3   ....a.......-.........................................---.---..............................
2DL4   g.c..tc....-c.a.t.a.t..gt....g.a...gaa..t...........CAT.TCA.C..C.....A...T.C....A...C....
```

Fig. 9. Comparison of upstream regulatory regions in KIR genes. Multiple alignment using ClustalW of upstream sequence from KIR genes located on PAC1060p11 (*) and Lawrence Livermore BAC52946 (°). The KIR translated region is marked in upper case, and all numbering is for KIR3DL1 from the AUG initiation codon. Potential transcription factors binding sites (underlined) were found using TESS (137) and the TRANSFAC databases (138).
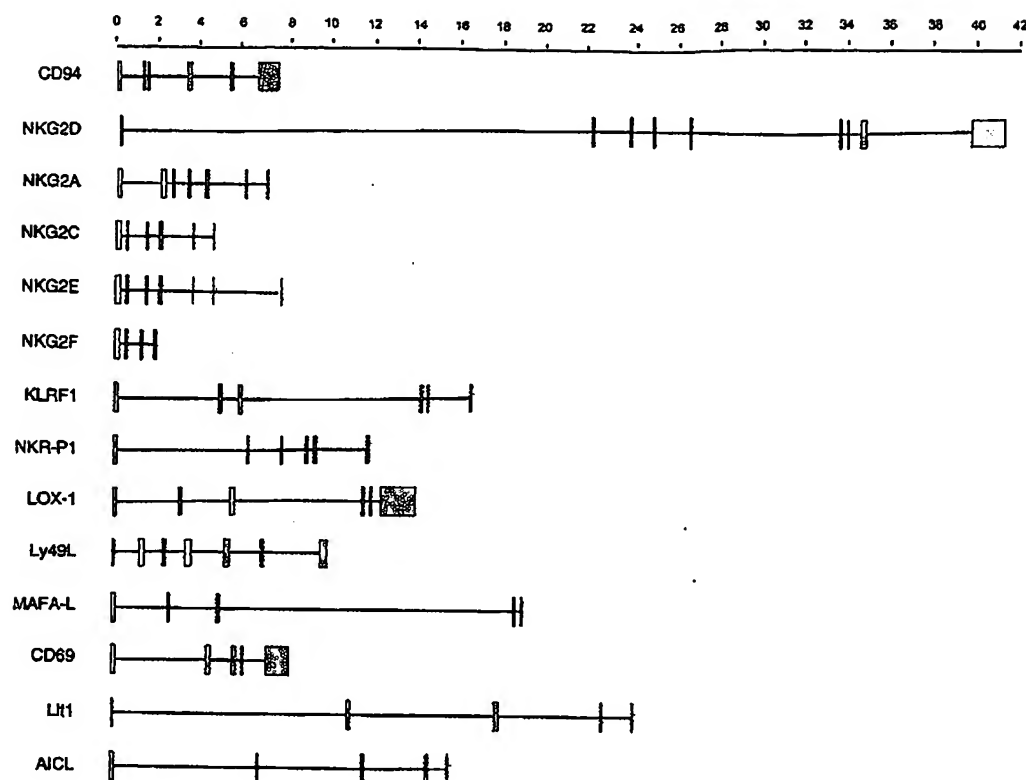
Fig. 10. Exon structure of the NKC genes. Exons are depicted as vertical bars. These lectin-related genes are all type II TM proteins. They are organised in a similar manner, belonging to the Group V of C-type lectins, with one or two exons coding for the 5' UTR and the cytoplasmic tail (black), the TM domain (and a part of the cyoplasmic tail) encoded by a single exon (green) and a CRD shared by three exons (blue). The exon–intron junctions of the CRDs are conserved. Two groups can be distinguished by the presence or absence of a stalk or neck exon (red). Lox-1 (63, 139) CD94 (140), KLRF1 (64), Ly49L (99), NKRP1 (R. Barten, unpublished data) and NKG2A, C and E (68, 141) all have neck exons. CD69 (66), AICL, Llt1 and MAFA (R. Barten, unpublished data) are missing the separate neck exon. Exon 5 of Ly-49L continues over a predicted splice site into a stop codon thereby rendering exons 6 and 7 as untranscribed pseudoexons (99). NKG2D has a unique organisation (68).

genes, but a single pseudogene, Ly49L, is now left in man (98, 99). Similarly, there is no trace of KIR genes in rodents. The two sets of genes, from unrelated superfamilies, share four remarkable features: 1) They both recognise MHC class I; 2) They are expressed in a clonal fashion on NK cells; 3) They are polymorphic in both species; and 4) They utilise similar mechanisms for signal transduction. The finding of sets of genes from different superfamilies performing similar functions in different species is a remarkable example of convergent evolution (24).

The evolution of NK receptors may have taken place in parallel with evolution of their ligands, which comprise only class I MHC molecules so far. Some data call for a more rapid evolution of KIR than the MHC, in terms of type and number

of genes, an idea that suggests that other KIR ligands could exist (55). Examination of the sequence relationships and map positions of the extended NK receptor gene families may help to trace the evolution of the two sets of functionally interacting genes. As was shown on Table 1, the NK receptor genes on chromosome 19 and the other large sets of genes along that chromosome, such as ILT, Siglec, CD66 and CEA include the FcaR locus. This sequence is highly related to those of the other C2-set IgSF molecules (27), and the gene structure is consistent with this. Other IgSF Fc receptors are also part of this group and Fc receptors are highly structurally related to the KIRs. The other Fc receptor loci are all located on human chromosome 1, except for FcRN, the gene for which, FCGRT, is also on chomosome 19q13.3 (100, 101).

This molecule, which is responsible for transfer of IgG molecules across the placenta, shares some sequence similarities with MHC class I molecules (102). Could FcRN represent a primordial class I-related molecule that preceded the evolution of modern class I, Fc receptor and KIR sequences? Although located within the main CD66–GPVI conglomerate of genes, most of which comprise of molecules with C2-set Ig domains, FcRN is more akin to the V-C1-set of structures (102).

Chromosomes 1, 6, 9 and 19 all reveal evidence of an ancient paralogous relationship in that they have similar sets of genes, related MHC class I loci, as well as some more highly conserved NOTCH and RING3 loci. Fc receptor and KIR loci are on two of these chomosomes, 1 and 19 respectively (103). The region of chromosome 19 thought to be paralogous with the MHC is likely to be on the short arm, at 19p13.1–13.3. Two lectin-related DC-SIGN genes and the CD23 gene are located here (104). The chicken MHC contains a highly restricted set of key MHC, genes which include lectin genes, to which DC-SIGN is related (105). These locations hint at the possibility that some subsets of C-type lectin and IgSF genes and their receptors may share an ancient genetic as well as functional relationship (106). Genes of the C1 IgSF are informative. The butyrophilins (6p21.3) (107) and poliovirus receptor (CD155; 19q13.2) are phylogenetically some of the oldest members of this family, which includes tapasin and class II (6p21.3). It has been noted that the location of CD155 and FCGRT genes on 19q13.2–q13.3 is consistent with their being derived following a pericentric inversion of the MHC-paralogous region at 19p13 (106). Such inversions are not uncommon and may have accounted for the separation of the paralogous set of MHC-related genes on chromosome 1.

Obviously much of the genomic clustering of the receptor genes apparent from Fig. 1 and Table 1 is due to serial cis-duplication of genes. Duplications resulting in proliferation of KIR genes, for example, must have occurred recently in evolution, and it is not surprising that the genes lie next to each other. Duplication of IgSF genes has played a key role in the generation of the immune system. It could be argued that the current diaspora of clusters of IgSF-related sequences originated from a single source of duplicating genes that over time seeded all of the relevant chromosomal regions highlighted in Fig. 1 by chromosome rearrangement or duplication (108).

Once duplicated, the product of one gene can perform its original function and the other is free to adopt a modified role (109). An example of this is provided by MHC class II
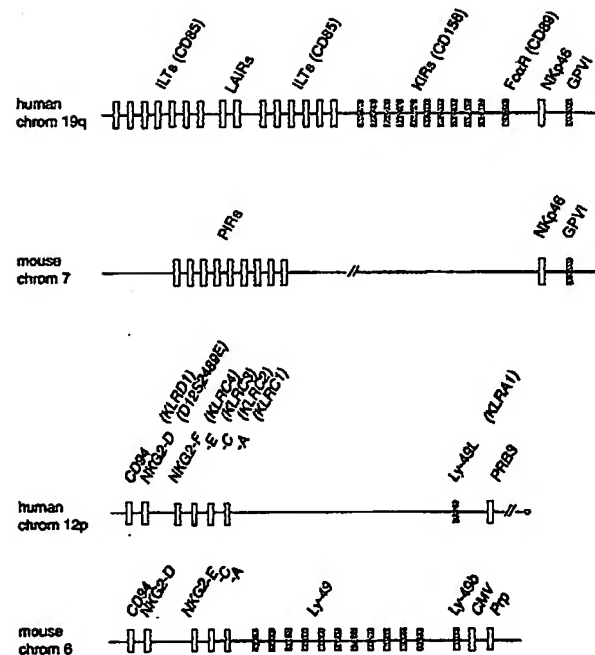
Fig. 11. Proposed convergent evolution of NK receptor genes. The LRC and NKC along with the syntenic mouse complexes are shown. To date, no orthologous KIR loci have been identified on mouse chromosome 7. The syntenic location for such genes would most likely be between the PIR and NKp46 genes. Similarly, no expressed human LY49 genes have been found. However, the Ly49 region is identifiable by a pseudogene, LY49L.

structures. Non-classical HLA-DM and -DO molecules both associate with classical HLA-DR to facilitate peptide loading by subtly, and transiently, altering its properties (110). The genes for all of these molecules are linked, in the MHC, and are obvious duplicates of each other. The propensity of class II molecules to associate with each other, in homotypic interaction, could be a significant evolutionary intermediate in the development of modulatory functions (111). Interactions of classical and non-classical class II could have arisen initially by homotypic associations of a primordial class II molecule, which, as gene duplication took place, then developed into a heterotypic liaison, as one component diversified in sequence. This scenario of duplication, then homotypic, followed by heterotypic association, could be easily imagined for sets of genes like the KIRs. There is structural evidence for multimerisation of KIR, consistent with 'zippering' of multiple KIR with MHC class I ligands when an NK cell interacts with its target (112, 113). As KIR genes duplicate and diversify, homotypic KIR:class I interactions could develop

into heterotypic interactions, provided by a mixture of inhibitory and activating receptors interacting with class I structures. Complexity of this kind could enable the development of exquisite sensitivity in target recognition and diversity of subsequent effector functions, such as cytokine production and killing, in response to modulation of class I molecules by infection. Recognition could be effected by integration of sets of signals from multiple KIRs, both activating an inhibitory, in an array at the cell surface. In this way, the product of a newly duplicated gene could be rapidly exploited during evolution. Incidentally, early development of IgSF receptor-ligand pairs, such as KIR with class I and Ig with poly-Ig receptor, may also have arisen via an intermediate stage of homotypic interaction.

The range of expression patterns, ligands and functions of IgSF molecules along chromosome 19 is very broad. Where known, all the ligands for KIRs are class I molecules, but the various ligands for related molecules such as GPVI and CD66 speak to the extreme versatility of the family of molecules. The superfamily extends, at least in terms of structure, if not identifiable sequence homology, to haematopoietic receptors such as human growth hormone receptor, prolactin receptor and erythropoietin receptor (114). Of the ILTs, only two have been shown to interact with class I molecules (115). The others remain in a functional twilight zone and do not necessarily interact with class I-related structures.

Conclusion

NK receptors such as the KIRs appear to be flexible at several levels. First, their sequences are polymorphic. Second, the number of genes varies in different individuals, in what we term presence/absence variation. Third, there is functional variation since different species use different sets of receptors for recognition of targets. Fourth, receptor expression in different NK clones is stochastic. This flexibility is reflected by the plasticity of gene arrangement. We have argued that multiple head–tail KIR loci are the optimal arrangement for these features (23).

Why are KIR genes polymorphic? The variation of both NK receptor and MHC genes may relate to disease resistance (116). Military analogies are often employed to describe the purpose of the immune system (117, 118). Both groups of polymorphic receptors invoke additional descriptive possibilities. Flexible response and moving target come to mind instantly. It has taken decades to begin to understand the relationship between MHC polymorphism and disease (119, 120). The existence of two sets of polymorphic surface molecules that interact with each other provides all kinds of interesting possibilities for co-operation. Since they are on separate chromosomes, some combinations of MHC and NK haplotypes may have negative as well as positive epistatic interactions — scope for the proverbial military cock-up.

References

1. Long EO. Regulation of immune responses through inhibitory receptors. Annu Rev Immunol 1999;17:875–904.
2. Kärre K, Colonna M, eds. Specificity, function and development of NK cells. Curr Top Microbiol Immunol 1998;230:1–248.
3. Lanier LL. NK cell receptors. Annu Rev Immunol 1998;16:359–394.
4. Lanier LL. On guard-activating NK receptors. Nat Immunol 2001;2:23–27.
5. Houchins JP, Yabe T, McSherry C, Bach FH. DNA sequence analysis of NKG2, a family of related cDNA clones encoding type II integral membrane proteins on human natural killer cells. J Exp Med 1991;173:1017–1020.
6. Moretta A, et al. Major histocompatibility complex class I-specific receptors on human natural killer and T lymphocytes. Immunol Rev 1997;155:105–117.

7. Lazetic S, Chang C, Houchins JP, Lanier LL, Phillips JH. Human NK cell receptors involved in MHC class I recognition are disulphide-linked heterodimers of CD94 and NKG2 subunits. J Immunol 1996;157:4741–4745.
8. Yokoyama WM. Natural killer cell receptors specific for major histocompatibility complex class I molecules. Proc Natl Acad Sci USA 1995;92:3081–3085.
9. Vely F, Vivier E. Conservation of structural features reveals the existence of a large family of inhibitory cell surface receptors and noninhibitory/activatory counterparts. J Immunol 1997;159:2075–2077.
10. Houchins JP, Lanier LL, Niemi EC, Phillips JH, Ryan JC. Natural killer cell cytolytic activity is inhibited by NKG2-A and activated by NKG2-C. J Immunol 1997;158:3603–3609.

11. Isakov N. Role of immunoreceptor tyrosine-base activation motif in signal transduction from antigen and Fc receptor. Adv Immunol 1998;69:183–187.
12. Campbell KS, Colonna M. DAP12: a key accessory protein for relaying signals by natural killer cell receptors. Int J Biochem Cell Biol 1999;31:631–636.
13. Wilson MJ, Lindquist JA, Trowsdale J. DAP12 and KAP10 (DAP10)-novel transmembrane adapter proteins of the CD3zeta family. Immunol Res 2000;22:21–42.
14. Brown MG, Scalzo AA, Yokoyama WM. The NKC and regulation of natural killer cell mediated immunity. In: Kasahara M, ed. MHC–evolution structure and function. Tokyo: Springer; 2000. p. 287–304.

15. Wagtmann N, Rojo S, Eichler E, Mohrenweiser H, Long EO. A new human gene complex encoding the killer cell inhibitory receptors and related monocyte/macrophage receptors.
Curr Biol 1997;7:615–618.

16. Wende H, Volz A, Ziegler A. Extensive gene duplications and a large inversion characterise the human leukocyte receptor cluster.
Immunogenetics 2000;51:703–713.

17. Wende H, Colonna M, Ziegler A, Volz A. Organisation of the leukocyte receptor cluster (LRC) on human chromosome 19q13.4.
Mamm Genome 1998;10:154–160.

18. Moretta A, Biassoni R, Bottino C, Mingari MC, Moretta L. Natural cytotoxicity receptors that trigger human NK-cell-mediated cytolysis.
Immunol Today 2000;21:228–234.

19. Parham P, ed. NK cells, MHC class I antigens and missing self.
Immunol Rev 1997;155:1–221.

20. Borges L, Hsu ML, Fanger N, Kubin M, Cosman D. A family of human lymphoid and myeloid Ig-like receptors, some of which bind to MHC class I molecules.
J Immunol 1997;159:5192–5196.

21. Colonna M, Nakajima H, Navarro F, Lopez-Botet M. A novel family of Ig-like receptors for HLA class I molecules that modulate function of lymphoid and myeloid cells.
J Leukoc Biol 1999;66:375–381.

22. MHC sequencing consortium. Complete sequence and gene map of a human major histocompatibility complex (MHC).
Nature 1999;401:921–923.

23. Wilson MJ, et al. Plasticity in the organization and sequences of human KIR/ILT gene families.
Proc Natl Acad Sci USA 2000;97:4778–4783.

24. Barten R, Torkar M, Haude A, Trowsdale J, Wilson M. Divergent and convergent evolution of NK-cell receptors.
Trends Immunol 2001;22:52–57.

25. Biassoni R, Pessino A, Bottino C, Pende D, Moretta L, Moretta A. The murine homologue of human NKp46, a triggering receptor involved in the induction of natural cytotoxity.
Eur J Immunol 1999;3:1014–1020.

26. Kubagawa H, et al. Paired immunoglobulin-like receptors of activating and inhibitory types.
Curr Top Microbiol Immunol 1999;244:137–149.

27. Dennis G, Kubagawa H, Cooper MD. Paired Ig-like receptor homologs in birds and mammals share a common ancestor with mammalian Fc receptors.
Proc Natl Acad Sci USA 2000;21:13245–13250.

28. Clementson JM, Polgar J, Magnenat E, Wells TN, Clemetson KJ. The platelet collagen receptor glycoprotein VI is a member of the immunoglobulin superfamily closely related to FcαR and the natural killer receptors.
J Biol Chem 1999;274:29019–29024.

29. Munday J, Floyd H, Crocker PR. Sialic acid binding receptors (siglecs) expressed by macrophages.
J Leukoc Biol 1999;66:705–711.

30. Hammarström S. The carcinoembryonic antigen (CEA) family: structures, suggested functions and expresion in normal and malignant tissues.
Semin Cancer Biol 1999;9:67–81.

31. Lanier LL, Corliss B, Wu J, Phillips JH. Association of DAP12 with activating CD94/NKG2C NK cell receptors.
Immunity 1998;8:693–702.

32. Chang C, et al. KAP10, a novel adapter protein genetically linked to DAP12 but with unique signalling properties.
J Immunol 1999;163:4651–4654.

33. Liu HX, Cartegni L, Zhang MQ, Krainer AR. A mechanism for exon skipping caused by nonsense or missense mutations in BRCA1 and other genes.
Nat Genet 2001;27:55–58.

34. Uhrberg M, et al. Human diversity in killer cell inhibitory receptor genes.
Immunity 1997;7:753–763.

35. Wilson MJ, Torkar M, Trowsdale J. Genomic organization of a human killer cell inhibitory receptor gene.
Tissue Antigens 1997;49:574–579.

36. Burshtyn DN, et al. Recruitment of tyrosine phosphatase HCP by the killer cell inhibitory receptor.
Immunity 1996;4:77–85.

37. Koonin EV, Aravind L. The NACHT family – a new group of predicted NTPases implicated in apoptosis and MHC transcription activation.
Trends Biochem Sci 2000;25:223–224.

38. Steimle V, Otten LA, Zufferey M, Mach B. Complementation cloning of an MHC class II transactivator mutated in hereditary MHC class II deficiency (or bare lymphocyte syndrome).
Cell 1993;75:135–146.

39. Dawkins R, et al. Genomics of the major histocompatibility complex: haplotypes, duplication, retroviruses and disease.
Immunol Rev 1999;167:275–304.

40. Torkar M, Haude A, Milne S, Beck S, Trowsdale J, Wilson MJ. Arrangement of the ILT gene cluster: a common null allele of the ILT6 gene results from a 6.7 kbp deletion.
Eur J Immunol 2000;30:3655–3662.

41. Meyaard L, Adema GJ, Chang C, Lanier LL, Phillips JH. LAIR-1, a novel inhibitory receptor expressed on human mononuclear leukocytes.
Immunity 1997;7:283–290.

42. Blery M, Kubagawa H, Chen CC, Vely F, Cooper MD, Vivier E. The paired Ig-like receptor PIR-B is an inhibitory receptor that recruits the protein-tyrosine phosphatase SHP-1.
Proc Natl Acad Sci USA 1998;95:2446–2451.

43. Valiante NM, et al. Functionally and structurally distinct NK cell receptor repertoires in the peripheral blood of two human donors.
Immunity 1997;7:739–751.

44. Trowsdale J, Ragoussis J, Campbell RD. Map of the human MHC.
Immunol Today 1991;12:443–446.

45. Marsh SGE, Parham P, Barber LD. The HLA factsbook. London: Academic Press; 1999.

46. Beck S, Trowsdale J. The human MHC – lessons from the DNA sequence.
Annu Rev Genomics Hum Genet 2000;1:117–137.

47. Colonna M, et al. A common inhibitory receptor for MHC class I molecules in human lymphoid and myelomonocytic cells.
J Exp Med 1997;186:1809–1818.

48. Gardiner CM, et al. Different NK cell surface phenotypes defined by the DX9 antibody are due to KIR3DL1 gene polymorphism.
J Immunol (In press).

49. Jeffreys AJ, Neil DL, Neumann R. Repeat instability at human minisatellites arising from meiotic recombination.
EMBO 1998;17:4147–4157.

50. Jeffreys AJ, Murray J, Neumann R. High-resolution mapping of crossovers in human sperm defines a minisatellite-associated recombination hotspot.
Mol Cell 1998;2:267–273.

51. Jurka J, Smith T. A fundamental division in the Alu family of repeated sequences.
Proc Natl Acad Sci USA 1988;85:4775–4778.

52. Jurka J, Milosavljevic A. Reconstruction and analysis of human Alu genes.
J Mol Evol 1991;32:105–121.

53. Jurka J, Walichiewicz J, Milosavljevic A. Prototypic sequences for human repetitive DNA.
J Mol Evol 1992;35:286–291.

54. Jurka J. A new subfamily of recently retroposed Alu repeats. Nucleic Acids Res 1993;21:2252.

55. Rajalingam R, Hong M, Adams EJ, Shum BP, Guethlein LA, Parham P. Short KIR haplotypes in pygmy chimpanzee (Bonobo) resemble the conserved framework of diverse human KIR haplotypes. J Exp Med 2001;193:135–146.

56. Vilches C, Gardiner CM, Parham P. Gene structure and promoter variation of expressed and nonexpressed variants of the KIR2DL5 gene. J Immunol 2000;165:6416–6421.

57. Lutterbach B, Hiebert SW. Role of the transcription factor AML-1 in acute leukemia and hematopoietic differentiation. Gene 2000;245:223–235.

58. Suto Y, Yabe T, Maenaka K, Tokunaga K, Tadokoro K, Juji T. The human natural killer gene complex (NKC) is located on chromosome 12p13.1–p13.2. Immunogenetics 1997;46:159–162.

59. Ziegler SF, Ramsdell F, Alderson MR. The activation antigen CD69. Stem Cells 1994;12:456–465.

60. Lopez-Cabrera M, et al. Molecular cloning, expression, and chromosomal localization of the human earliest lymphocyte activation antigen AIM/CD69, a new member of the C-type animal lectin superfamily of signal-transmitting receptors. J Exp Med 1993;178:537–547.

61. Schnittger S, Hamann J, Dannenberg C, Fiebig H, Strauss M, Fonatsch C. Regional sublocalization of the human CD69 gene to chromosome bands 12p12.3–p13.2, the predicted region of the human natural killer cell gene complex. Eur J Immunol 1993;23:2711–2713.

62. Poggi A, Rubartelli A, Moretta L, Zocchi MR. Expression and function of NKRP1A molecule on human monocytes and dendritic cells. Eur J Immunol 1997;27:2965–2970.

63. Yamanaka S, Zhang XY, Miura K, Kim S, Iwao H. The human gene encoding the lectin-type oxidized LDL receptor (OLR1) is a novel member of the natural killer gene complex with a unique expression profile. Genomics 1998;54:191–199.

64. Roda-Navarro P, Arce I, Renedo M, Montgomery K, Kucherlapati R, Fernandez-Ruiz E. Human KLRF1, a novel member of the killer cell lectin-like receptor gene family: molecular characterization, genomic structure, physical mapping to the NK gene complex and expression analysis. Eur J Immunol 2000;30:568–576.

65. Colonna M, Samaridis J, Angman L. Molecular characterization of two novel C-type lectin-like receptors, one of which is selectively expressed in human dendritic cells. Eur J Immunol 2000;30:697–704.

66. Santis AG, Lopez-Cabrera M, Hamann J, Strauss M, Sanchez-Madrid F. Structure of the gene coding for the human early lymphocyte activation antigen CD69: a C-type lectin receptor evolutionarily related with the gene families of natural killer cell-specific receptors. Eur J Immunol 1994;24:1692–1697.

67. Plougastel B, Trowsdale J. Sequence analysis of a 62 kbp region overlapping the human KLRC cluster of genes. Genomics 1998;49:193–199.

68. Glienke J, et al. The genomic organization of NKG2C, E, F, and D receptor genes in the human natural killer gene complex. Immunogenetics 1998;48:163–173.

69. Carlyle JR, Martin A, Mehra A, Attisano L, Tsui FW, Zúñiga-Pflücker JC. Mouse NKR-P1B, a novel NK1.1 antigen with inhibitory function. J Immunol 1999;162:5917–5923.

70. Ryan JC, Seaman WE. Divergent functions of lectin-like receptors on NK cells. Immunol Rev 1997;155:79–89.

71. Kung SK, Su RC, Shannon J, Miller RG. The NKR-P1B gene product is an inhibitory receptor on SJL/J NK cells. J Immunol 1999;162:5876–5887.

72. McQueen KL, Freeman JD, Takei F, Mager DL. Localization of five new Ly49 genes, including three closely related to Ly49c. Immunogenetics 1998;48:174–183.

73. Takei F, Brennan J, Mager DL. The Ly-49 family: genes, proteins and recognition of class I MHC. Immunol Rev 1997;155:67–77.

74. Brown MG, et al. A 2-Mb YAC contig and physical map of the natural killer gene complex on mouse chromosome 6. Genomics 1997;42:16–25.

75. Vance RE, Jamieson AM, Raulet DH. Recognition of the class Ib molecule Qa-1(b) by putative activating receptors CD94/NKG2C and CD94/NKG2E on mouse natural killer cells. J Exp Med 1999;190:1801–1812.

76. Nei M, Gu X, Sitnikova T. Evolution by the birth-and-death process in multigene families of the vertebrate immune system. Proc Natl Acad Sci USA 1997;94:7799–7806.

77. Parham P. The rise and fall of great class I genes. Semin Immunol 1994;6:373–382.

78. Ohta T. Effect of gene conversion on polymorphic patterns at major histocompatibility complex loci. Immunol Rev 1999;167:319–325.

79. Dissen E, Ryan JC, Seaman WE, Fossum S. An autosomal dominant locus, Nka, mapping to the Ly-49 region of a rat natural killer (NK) gene complex, controls NK cell lysis of allogeneic lymphocytes. J Exp Med 1996;183:2197–2207.

80. Idris AH, Iizuka K, Smith HRC, Scalzo AA, Yokoyama WM. Genetic control of natural killing and in vivo tumor elimination by the Chok locus. J Exp Med 1998;188:2243–2256.

81. Idris AH, Smith HR, Mason LH, Ortaldo JR, Scalzo AA, Yokoyama WM. The natural killer gene complex genetic locus Chok encodes Ly-49D, a target recognition receptor that activates natural killing. Proc Natl Acad Sci USA 1999;96:6330–6335.

82. Scalzo AA, Lyons PA, Fitzgerald NA, Forbes CA, Yokoyama WM, Shellam GR. Genetic mapping of Cmv1 in the region of mouse chromosome 6 encoding the NK gene complex associated loci Ly49 and musNKR-P1. Genomics 1995;27:435–441.

83. Delano ML, Brownstein DG. Innate resistance to lethal mousepox is genetically linked to the NK gene complex on chromosome 6 and correlates with early restriction of virus replication by cells with an NK phenotype. J Virol 1995;69:5875–5877.

84. Forbes CA, Brown MG, Cho R, Shellam GR, Yokoyama WM, Scalzo AA. The Cmv1 host resistance locus is closely linked to the Ly49 multigene family within the natural killer cell gene complex on mouse chromosome 6. Genomics 1997;41:406–413.

85. Depatie C, Muise E, Lepage P, Gros P, Vidal SM. High-resolution linkage map in the proximity of the host resistance locus Cmv1. Genomics 1997;39:154–163.

86. Brownstein DG, Gras L. Differential pathogenesis of lethal mousepox in congenic DBA/2 mice implicates natural killer cell receptor NKR-P1 in necrotizing hepatitis and the fifth component of complement in recruitment of circulating leukocytes to spleen. Am J Pathol 1997;150:1407–1420.

87. Brown MG, Zhang J, Du Y, Stoll J, Yokoyama WM, Scalzo AA. Localization on a physical map of the NKC-linked Cmv1 locus between Ly49b and the Prp gene cluster on mouse chromosome 6. J Immunol 1999;163:1991–1999.

88. Depatie C, Chalifour A, Pare C, Lee SH, Vidal SM, Lemieux S. Assessment of Cmv1 candidates by genetic mapping and in vivo antibody depletion of NK cell subsets. Int Immunol 1999;11:1541–1551.

89. Drickamer K, Taylor ME. Biology of animal lectins. Annu Rev Cell Biol 1993;9:237–264.

90. Matsumoto N, Ribaudo RK, Abastado JP, Margulies DH, Yokoyama WM. The lectin-like NK cell receptor Ly-49A recognizes a carbohydrate-independent epitope on its MHC class I ligand. Immunity 1998;8:245–254.

91. Chang CS, Shen L, Gong DE, Kane KP. Major histocompatibility complex class I-dependent cell binding to isolated Ly-49A: evidence for high-avidity interaction. Eur J Immunol 1996;26:3219–3223.

92. Brennan J, Mahon G, Mager DL, Jefferies WA, Takei F. Recognition of class I major histocompatibility complex molecules by Ly-49: specificities and domain interactions. J Exp Med 1996;183:1553–1559.

93. Vance RE, Kraft JR, Altman JD, Jensen PE, Raulet DH. Mouse CD94/NKG2A is a natural killer cell receptor for the nonclassical major histocompatibility complex (MHC) class I molecule Qa-1b. J Exp Med 1998;188:1841–1848.

94. Borrego F, Ulbrecht M, Weiss EH, Coligan JE, Brooks AG. Recognition of human histocompatibility leukocyte antigen (HLA)-E complexed with HLA class I signal sequence-derived peptides by CD94/NKG2 confers protection from natural killer cell-mediated lysis. J Exp Med 1998;187:813–818.

95. Lee N, et al. HLA-E is a major ligand for the natural killer inhibitory receptor CD94/NKG2A. Proc Natl Acad Sci USA 1998;95:4789–5420.

96. Braud VM, et al. HLA-E binds to natural killer cell receptors. Nature 1998;391:795–797.

97. Daniels BF, Nakamura MC, Rosen SD, Yokoyama WM, Seaman WE. Ly-49A, a receptor for H-2Dd, has a functional carbohydrate recognition domain. Immunity 1994;1:785–792.

98. Westgaard IH, Berg SF, Orstavik S, Fossum S, Dissen E. Identification of a human member of the Ly-49 multigene family. Eur J Immunol 1998;28:1839–1846.

99. Barten R, Trowsdale J. The human Ly-49L gene. Immunogenetics 1999;49:731–734.

100. Simister NE, Mostov KE. An Fc receptor structurally related to MHC class I antigens. Nature 1989;337:184–187.

101. Kandil E, et al. The human gene encoding the heavy chain of the MHC class I-like Fc receptor. Cytogenet Cell Genet 1996;73:97–98.

102. Simister NE, Ahouse JC. The structure and evolution of FcRN. Res Immunol 1996;147:333–337.

103. Kasahara M. The chromosomal duplication model of the major histocompatibility complex. Immunol Rev 1999;167:17–29.

104. Soilleux EJ, Barten R, Trowsdale J. DC-SIGN, a related gene, DC-SIGNR and CD23 form a cluster on 19p13. J Immunol 2000;165:2937–2934.

105. Kaufman J, et al. The chicken B locus is a minimal essential MHC. Nature 1999;401:923–925.

106. Du Pasquier L. Relationships among the genes encoding MHC molecules and the specific antigen receptors. In: Du Pasquier L, Kasahara M, eds. MHC evolution, structure and function. Tokyo: Springer; 2000. p. 53–65.

107. Rhodes DA, Stammers M, Malcherek G, Beck S, Trowsdale J. BTN genes form a cluster of polymorphic orphan cell surface receptors in the extended MHC. Genomics (in press).

108. Du Pasquier L. The phylogenetic origin of antigen-specific receptors. Top Microbiol Immunol 2000;248:160–185.

109. Ohno S. Evolution by gene duplication. Berlin: Springer; 1970.

110. Sanderson F, Trowsdale J. Kissing cousins exchange CLIP. Curr Biol 1995;5:1372–1376.

111. Schafer PH, Pierce SK, Jardetzky TS. The structure of MHC class II: a role for dimer of dimers. Semin Immunol 1995;7:389–398.

112. Boyington JC, Motyka SA, Schuck P, Brooks AG, Sun PD. Crystal structure of an NK cell immunoglobulin-like receptor in complex with its class I MHC ligand. Nature 2000;405:537–543.

113. Davis DM, Chiu I, Fassett M, Cohen GB, Mandelboim O, Strominger JL. The human natural killer cell immune synapse. Proc Natl Acad Sci USA 1999;96:15062–15067.

114. Fan QR, Mosyak L, Winter CC, Wagtmann N, Long EO, Wiley DC. Structure of the inhibitory receptor for human natural killer cells resembles haematopoietic receptors. Nature 1997;389:96–100.

115. Borges L, Cosman D. LIRs/ILTs/MIRs, inhibitory and stimulatory Ig-superfamily receptors expressed in myeloid and lymphoid cells. Cytokine Growth Factor Rev 2000;11:209–217.

116. Hill AVS. Defence by diversity. Nature 1999;398:668–669.

117. Kronenberg M, Brines R, Kaufman J. MHC evolution: a long term investment in defense. Immunol Today 1994;15:4–6.

118. Parham P. Immunology. Some savage cuts in defence. Nature 1990;344:709–711.

119. Carrington M, et al. HLA and HIV-1: heterozygote advantage and B*35-Cw*04 disadvantage. Science 1999;283:1748–1752.

120. Gilbert SC, et al. Association of malaria parasite population structure, HLA, and immunological antagonism. Science 1998;279:1173–1177.

121. Kinet JP, Launay P. Fcα/μR: single member or first born in the family? Nat Immunol 2000;1:371–372.

122. Aguado B, et al. Complete sequence and gene map of a human major histocompatibility complex (MHC). Nature 1999;401:921–923.

123. Bauer S, et al. Activation of NK cells and T cells by NKG2D, a receptor for stress-inducible MICA. Science 1999;285:727–729.

124. Cantoni C, et al. NKp44, a triggering receptor involved in tumour cell lysis by activated human natural killer cells, is a novel member of the immunoglobulin superfamily. J Exp Med 1999;189:787–796.

125. Bouchon A, Dietrich J, Colonna M. Inflammatory responses can be triggered by TREM-1, a novel receptor expressed on neutrophils and monocytes. J Immunol 2000;164:4991–4995.

126. Chalupny J, et al. Soluble forms of the novel MHC class I-related molecules, ULBP1 and ULBP2, bind to and functionally activate NK cells. FASEB J 2000;14:1018.

127. Fournier N, et al. FDFO3, a novel inhibitory receptor of the immunoglobulin superfamily, is expressed by human dendritic and myeloid cells. J Immunol 2000;165:1197–1209.

128. Cantoni C, et al. Molecular and functional characterization of IRp60, a member of the immunoglobulin superfamily that functions as an inhibitory receptor in human NK cells. Eur J Immunol 1999;29:3148–3159.

129. Jackson DG, Hart DN, Starling G, Bell JL.
Molecular cloning of a novel member of
the immunoglobulin gene superfamily
homologous to the polymeric
immunoglobulin receptor.
Eur J Immunol 1992;22:1157–1163.

130. Kharitonenkov A, Chen Z, Sures I, Wang
H, Schilling J, Ullrich A. A family of
proteins that inhibit signalling through
tyrosine kinase receptors.
Nature 1997;386:181–186.

131. Campadelli-Fiume G, Cocchi F, Menotti
L, Lopez M. The novel receptors that
mediate the entry of herpes simplex
viruses and animal alphaherpesviruses into
cells.
Rev Med Virol 2000;10:305–319.

132. Mason DY, et al. CD79a: a novel marker
for B-cell neoplasms in routinely
processed tissue samples.
Blood 1995;86:1453–1459.

133. Torkar M, Norgate Z, Colonna M,
Trowsdale J, Wilson MJ. Isotypic variation
of novel immunoglobulin-like transcript/
killer cell inhibitory receptor loci in the
leukocyte receptor complex.
Eur J Immunol 1998;28:3959–3967.

134. Vilches C, Pando MJ, Parham P. Genes
encoding human killer-cell Ig-like
receptors with D1 and D2 extracellular
domains all contain untranslated
pseudoexons encoding a third Ig-like
domain.
Immunogenetics 2000;51:639–646.

135. Vilches C, Rajalingam R, Uhrberg M,
Gardiner CM, Young NT, Parham P.
KIR2DL5, a novel killer-cell receptor with
a D0-D2 configuration of Ig-like domains.
J Immunol 2000;164:5797–5804.

136. Lenkkeri U, et al. Structure of the human
amyloid-precursor-like protein gene APLP1
at 19q13.1.
Hum Genet 1998;102:192–196.

137. Schug J, Overton GC. Welcome to TESS:
Transcription Element Search Software on
the WWW. Technical Report CBIL-TR-
1997-1001-v0.0. Philadelphia (PA):
University of Pennsylvania; 1997.
Available from: URL: http://
www.cbil.upenn.edu/tess/index.html.

138. Wingender E, et al. TRANSFAC: an
integrated system for gene expression
regulation.
Nucleic Acids Res 2000;28:316–319.

139. Aoyama T, et al. Structure and
chromosomal assignment of the human
lectin-like oxidized low-density-
lipoprotein receptor-1 (LOX-1) gene.
Biochem J 1999;339:177–184.

140. Rodriguez A, et al. Structure of the
human CD94 C-type lectin gene.
Immunogenetics 1998;47:305–309.

141. Plougastel B, Jones T, Trowsdale J.
Genomic structure, chromosome location
and alternative splicing of the human
NKG2-A gene.
Immunogenetics 1996;44:286–291.

G.J. Clark
B. Cooper
S. Fitzpatrick
B.J. Green
D.N.J. Hart

The gene encoding the immunoregulatory signaling molecule CMRF-35A localized to human chromosome 17 in close proximity to other members of the CMRF-35 family

Abstract: The immunoregulatory signaling (IRS) family includes several
molecules, which play major roles in the regulation of the immune response.
The CMRF-35A and CMRF-35H molecules are two new members of the IRS
family of molecules, that are found on a wide variety of haemopoietic lin-
eages. The extracellular functional interactions of these molecules is pres-
ently unknown, although CMRF-35H can initiate an inhibitory signal and is
internalized when cross-linked. In this paper, we described the gene struc-
ture for the CMRF-35A gene and its localization to human chromosome 17.
The gene consists of four exons spanning approximately 4.5 kb. Exon 1
encodes the 5′ untranslated region and leader sequence, exon 2 encodes the
immunoglobulin (Ig)-like domain, exon 3 encodes the membrane proximal
region and exon 4 encodes the transmembrane region, the cytoplasmic tail
and the 3′ untranslated region. A region in the 5′ flanking sequence of the
CMRF-35A gene, that promoted expression of a reporter gene was identified.
The genes for the CMRF-35A and CMRF-35H molecules are closely linked
on chromosome 17. Similarity between the Ig-like exons and the preceding
intron of the two genes suggests exon duplication was involved in their
evolution. We also identified a further member of the CMRF-35 family, the
CMRF-35J pseudogene. This gene appears to have arisen by gene duplica-
tion of the CMRF-35A gene. These three loci – the CMRF-35A, CMRF-35J
and CMRF-35H genes–form a new complex of IRS genes on chromosome
17.

Authors' affiliations:

G.J. Clark[1],
B. Cooper[1],
S. Fitzpatrick[1],
B.J. Green[2],
D.N.J. Hart[1]

[1]Mater Medical Research
Institute, Aubigny Place,
South Brisbane,
Queensland, Australia,

[2]Centenary Institute, Gene
Therapy Group, Royal Prince
Alfred Hospital, Missenden
Road, Camperdown, New
South Wales, Australia

Correspondence to:
Dr. Georgina Clark
Mater Medical Research
Institute
Aubigny Place
South Brisbane, 4101
Queensland
Australia
Tel: +61 7 3840 2561
Fax: +61 7 3840 2550
e-mail: gclark@
mmri.mater.org.au

The immunoregulatory signaling (IRS) family of molecules are a
group of leucocyte surface molecules, that contribute important ac-
tivating and inhibitory signals to a wide variety of haemopoietic
cell types. It includes molecules which have a C-type lectin structure
and molecules that fall into the immunoglobulin (Ig) superfamily
(1). The Ig superfamily members include the FcγRII molecules (2),
KIR receptors (3–5), the CD85 (ILT) molecules (6), the NKp44 (7) and
NKp46 (8) molecules, the recently described TREM1 and TREM2
molecules (9) and the CMRF-35A and CMRF-35H (IRC1) molecules
(10–12). The hallmarks of the family are pairs of related receptors
that have complementary signaling functions. The inhibitory mem-

415

ber has one or more immunoreceptor tyrosine-based inhibitory motifs (ITIM) in the cytoplasmic domain, which associates with cellular SH2 containing protein tyrosine phosphatases. The activatory counterparts associate with a second signaling molecule such as the FcRγ (13) or DAP12 chain (14), containing an immunoreceptor tyrosine-based activatory motif (ITAM). Functionally, these molecules are involved in the regulation of the effector functions of haemopoietic cells.

The CMRF-35A molecule appears to be the activatory form of the two CMRF-35 molecules, identified (10–12). It contains a single Ig-V-like domain, a proline rich membrane proximal region, a transmembrane region and a short cytoplasmic tail. The transmembrane region encodes a charged residue typical of other activatory receptors. However, most other activatory receptors identified to date have a basic amino acid in the transmembrane region and CMRF-35A is unique to date in having an acidic residue, glutamic acid, in its transmembrane region. The ITAM containing molecule that associates with CMRF-35A is presently unknown.

The genes for the Ig superfamily subset of the IRS molecules are located in clusters throughout the genome. The genes for FcγRII molecules are localized to chromsosome 1q23–24 (15). A region on human chromosome 19q13.4 has been fine mapped (16). Two clusters containing genes for the CD85 or ILT/LIR molecules and LAIR molecules exist in this region. These clusters are centromeric to the genes for KIR, FcαR and NKp46 loci (17). One cluster of ILT genes contains seven genes including ILT5, ILT8, LIR8, ILT4, ILT6, ILT11, ILT7 and LAIR1, whilst the other contains six genes, including ILT1, LIR6, ILT2, ILT3, ILT9, ILT10, of which two are pseudogenes. The syntenic region on mouse chromosome 7 contains the genes for the PIR molecules (18, 19). The genes for the TREM molecules and NKp44 have been localized to human chromosome 6 (7, 9) and the gene for the CMRF-35H molecule localized to human chromosome 17 (20).

The genomic organization for FcαR (21), KIRs (22, 23), PIRs (18, 19), some ILTs (24, 25) and CMRF-35H (20) have now been described. Here, we describe the genomic organization of the CMRF-35A gene, the presence of CMRF-35J, a related pseudogene and localize both of these to human chromosome 17.

Material and methods

Isolation of genomic clones

A human T-lymphocyte genomic library, constructed in the bacteriophage vector λ2001, was screened by plaque hybridization (26). The library was probed with an 873-bp XbaI fragment containing

the coding region of the CMRF-35A cDNA (10) labeled with [32P]-dCTP using a RADprime random priming kit according to the manufacturer's protocol (Life Technologies, Auckland, New Zealand). Following hybridization, the plaque lifts were washed at a final stringency of 0.1×SSC/0.1% SDS at 65°C. Two clones that hybridized to the CMRF-35A probe were identified. Phage inserts were subcloned for further analysis. One clone contained part of the gene for the CMRF-35A molecule.

We have previously described the isolation of two PAC clones containing sequences that hybridized to the CMRF-35A cDNA (20). A human fetal liver genomic DNA library, constructed in the P1 pAD10sacB11 vector (Genome System, St. Loius, MO, USA), was screened firstly with a 342-bp BamHI-SacI fragment containing the Ig domain of the CMRF-35A cDNA (10). A second screen was performed using a 279-bp XbaI cDNA fragment that contained the cytoplasmic and 3' untranslated region of the CMRF-35A molecule. Each cDNA fragment was labeled with [32P]-dCTP by random priming and following hybridization, the filters were washed to a final stringency of 0.1×SSC/0.1% SDS at 65°C. PAC plasmid DNA prepared using standard protocols (27) was digested with BamHI or SacI and subcloned into the SK+ vector (Stratagene, La Jolla, CA, USA) for further analysis. The restriction map of each subclone was determined to produce the overall CMRF-35A gene map.

Southern blot analysis

PAC DNA subclones or PCR products were fractionated through 1% agarose gels and transferred to Hybond N+ (Amersham Pharmacia Biotech, Auckland, New Zealand). Membranes were hybridized to oligonucleotides labeled with digoxigenin (DIG) using a 3'-end labeling kit according to the manufacturer's recommendations (Roche Molecular Biologicals, New Zealand). The oligonucleotide sequences were made from the CMRF-35A cDNA sequence and are shown in Table 1. Following hybridization, membranes probed with oligonucleotides were washed in 6×SSC/0.1% SDS at 2°C below the Tm of the oligonucleotide.

DNA sequencing

Sequence analysis was performed on purified plasmid DNA using dideoxy chain termination technology. Custom made primers directly labeled with IRD40 (MWG-Biotech, Ebersberg, Germany) were used and the reactions were separated on a LiCor automated sequencer. Alternatively sequencing was performed using dye terminator fluorescent cycle sequencing on an ABI Prism 377 automated sequencer (PE Applied Biosytems, Scoresby, Vic, Australia) using the Australian Genome Research Facilities (St. Lucia,

Table 1

Sequences of oligonucleotides used

Oligo	Sequence	Position in CMRF-35A cDNA
35-A	5'ATG ACT GCC AGG GCC TGG3'	240–258
35-B	5'TTC TGC CTG CTT CTA GAG C3'	871–889
35-C	5'AGA GCT CCA TGG GCA CCT C3'	667–685
35-D	5'CCA GCA TGC TCA GGA GCA G3'	819–837
35-F	5'AAT GTC ACC TGC CAC TGT G3'	209–227
35-G	5'TGT CTC AGG TCT GAG GCT3'	96–113
35-H	5'CCT GGA GAA TCT CAC AG3'	527–543
35-I	5'TCC CTG TTC AGC AAT GT3'	768–784
35-J	5'GCT TTC TGG TCA CGC TGG3'	721–738
35-K	5'TGT TGC AGG CCT TGA TG3'	778–784
35-L	5'GAA TGA CCT CCT GAC CA3'	722–738
35-M	5'TTC TGG TCA GGA TGG AC3'	5' flanking region
35-N	5'TTG CTG ATT CTG TGG AG3'	5' flanking region
35-Bext	5'CTC AGA GAA GCT CTA GAA GCA GGC AGA A3'	862–889
L8-BAC	5'ATC CCT GGT CGT GAC CTC ACG3'	Intron 3
35-3UT	5'CGC ATA TTC TAC TCT CCT GGA C3'	
H9b	5'GAT TCT CCA GGG TCA CTG3'	537–520
H9D	5'GATTGTGGAGACCAAAGG3'	439–457

Queensland, Australia). Sequence alignments and motif searches were done using the GCG Wisconsin Package (Madison, WI, USA). Additional analysis was performed using the human GDB (http://www.ncbi.nlm.nih.gov/genome) through NCBI and the Australian National Genome Information Services (ANGIS).

Identification of introns

Intron-exon boundaries were identified by DNA sequence analysis. Intron sizes were determined by polymerase chain reaction (PCR) using oligonucleotides primers (Table 1) to amplify across each intron. PAC DNA was used as template and each PCR product was restriction mapped. Intron sizes were confirmed by restriction mapping of the subclone and sequencing data.

RACE

Rapid amplification of cDNA ends (RACE) for CMRF-35A was performed using a 5' RACE system from Life Technologies according to the manufacturer's instructions or using the methods of Frohman (28). Single stranded cDNA was reverse transcribed using the 35-F primer from total RNA prepared from the histiocytic cell line, U937 and the eyrthro-myeloid cell line, HEL for 5' RACE. The 5' RACE

products were generated using the nested gene-specific primer 35-G or 35SP-1 and the 5' RACE primer from the kit.

For 3' RACE, total RNA was reverse transcribed into cDNA using the following primer 5'GAC TAG TCT GCA GAA TTC TTT TTT TTT TTT TTT TTT TT3'. PCR products were generated using an adapter primer 5'GAC TAG TCT GCA GAA TTC3' and 35Bext.

Reporter gene assay

A 2.9-kb *BamHI* fragment that contained the 5' flanking region, exon 1 and the part of the first intron was cloned into the pGL3-basic vector (Promega, Madison, WI, USA). Deletions of this region were constructed using PCR. Constructs were transiently transfected into the Epstein-Barr virus (EBV)-transformed B-cell line, Mann, using DMRIE-C according to the manufacturer's instructions (Life Technologies). Cells were co-transfected with the pRL-TK plasmid (Promega) to allow normalization of transfections. Cell lysates were prepared from the transfected cells 48 h after transfection and analyzed for luciferase activity on a TD-20/20 luminometer (Turner Designs, Promega, Annadale, NSW, Australia) using a Dual Luciferase Assay system according to the manufacturer's instructions (Promega, Annadale, NSW, Australia). Results are represented as a ratio of

Firefly luciferase to *Renilla* luciferase and given as relative luciferase fluorescence.

Chromosomal localization

Genomic DNA from monochromosomal somatic cell hybrids (BIOS Laboratories, New Haven, CT, USA) was used as a template for PCR. Products were amplified using the primers 35A and H9B that amplified a 297-bp product. The PCR products were Southern blotted and probed with DIG-labeled H9D.

Results

Isolation and characterization of the CMRF-35A gene

A bacteriophage clone encoding the CMRF-35A genomic sequence was isolated from a high stringency screening of a human genomic DNA library with the entire coding region of the CMRF-35A cDNA (10). This bacteriophage clone contained the first three exons of the CMRF-35A gene. The full gene was then isolated from a human genomic DNA PAC library, screened first with a 342-bp *Bam*HI-*Sac*I fragment containing the Ig domain of the CMRF-35A cDNA (10) and secondly with a 279-bp *Xba*I fragment, which contained the cytoplasmic and 3' untranslated region of the CMRF-35A molecule. A single PAC clone was isolated and the CMRF-35A gene characterized. A partial restriction map of the gene is shown in Fig. 1. Restriction fragments were subcloned into the SK$^+$ vector and those encoding the CMRF-35A exons were identified by hybridization to DIG-
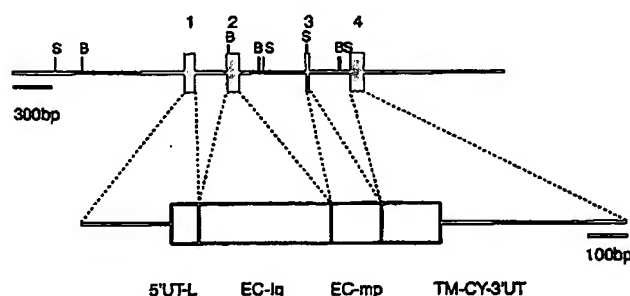
Fig. 1. Genomic organization of the human *CMRF-35A* gene. The exon-intron structure is displayed aligned to the cDNA. Exon 1 encodes the 5' untranslated region and the leader sequence (5'UT-L), exon 2 encodes the single Ig like extracellular domain (EC-Ig), exon 3 encodes the transmembrane proximal region (EC-mp), and exon 4 encodes the transmembrane, cytoplasmic and 3' untranslated regions (TM-CY-3'UT). The Inr sequence is underlined. These sequences have been submitted to genbank (Accession numbers for these sequences are AF373863, AF373864, AF373865, AF373866).

labeled oligonucleotides. The exons and intron-exon boundaries were confirmed by DNA sequencing and comparison to the CMRF-35A cDNA. Intron sizes were determined by PCR using primers specific for the different protein domains of the molecule and restriction fragment analysis of subclones. Confirmation of the sequence and structure was obtained from recent input into the human GDB.

Structure of the CMRF-35A gene

The *CMRF-35A* gene spans approximately 4.5 kb and consists of four exons (Fig. 1). Exon 1 encodes the 5' untranslated region and the entire leader sequence. This exon ends immediately following the predicted site of cleavage of the leader sequence between the proline and glycine residues. Exon 2 encodes the single Ig like extracellular domain, whereas exon 3 encodes the transmembrane proximal region. The transmembrane, cytoplasmic and 3' untranslated regions are encoded by exon 4. The introns range from 0.771 kb to 1.62 kb in length (Table 1).

The sequences of the intron-exon junctions conform with the GT-AG rule (Fig. 2, Table 1) (29). The 3' boundaries for exons 1 and 2 were all situated after the first nucleotide of the codon i.e. in phase I. A feature of many immunoglobulin like region domains is that they are encoded by exons that have a phase I intron-exon junction (30). The CMRF-35A Ig-like domain is encoded by exon 2, which conforms to this feature. The 3' boundary of exon 3 was in phase II.

Characterization of the 5' region of the *CMRF-35A* gene

The CMRF-35A cDNA contained 232 nucleotides of 5' untranslated sequence. The 5' end of the CMRF-35A transcript was examined using 5' RACE. The template for these experiments was cDNA prepared from the histiocytic cell line, U937 and the erythro-myeloid cell line, HEL. Both cell lines express CMRF-35A, however only HEL expresses the CMRF-35H molecule. Two cell lines were chosen to determine the presence of any alternative transcription start sites. No extra 5'UT sequence was identified by the 5'RACE protocol, suggesting that the cDNA contains the near full length sequence.

The sequence of the genomic DNA 4 kb upstream of the transcription start site was sequenced and searched for consensus binding motifs for transcription factors known to influence the expression of leucocyte surface molecules. Sequences representing a TATA box or CCATT box were not identified in the region immediately upstream of the transcriptional start site. A consensus Inr or initiator sequence (Py Py A+1 N T/A Py Py) was found 80 bases 5' to the ATG initiation codon (Fig. 2) (31). This sequence however is in the 5'UT region and not at the transcriptional start site. The 5'

ries
RF.
iers
ric-
nce
DB.

s of
and
ring
the
tra-
oxi-
ited
b to

the
and
iase
that
tion
iich
iase

ated
ined
pre-
loid
only
osen
ites.
ocol,
ie.
ran-
ind-
ires·
ATA
itely
: in-
s 5'
er is
e 5'

```
ccactagcacccatcccagagctgtcagcaccggcctcagcccaggcggctctctccctg
agcttcctgtagccctgaccctctccagcctcagacctgagacagggctggacaaggaag
cagagagcagaagaaaagcagaagcgaagctcagatctgctgggaggaagattacatttt
gtcccctcctggggtcttgcacagtggcaggtgacattcgtgttacaggaATGACTGCCA
                                                   M  T  A  R
```

```
GGGCCTGGGCCTCGTGGCGGTCTTCAGCTCTGCTCCTCCTGCTTGTCCCAGgtgagtggg
A  W  A  S  W  R  S  S  A  L  L  L  L  V  P  G
```

0.771kb   ttgtattttttcagGCTATTTTC
                                              Y F P

```
CTCTGAGCCACCCCATGACCGTGGCGGGCCCCGTGGGGGGATCCCTGAGTGTGCAGTGTC
L  S  H  P  M  T  V  A  G  P  V  G  G  S  L  S  V  Q  C  R
```

```
GCTATGAGAAGGAACACAGGACCCTCAACAAATTCTGGTGCAGACCACCACAGATTCTCC
Y  E  K  E  H  R  T  L  N  K  F  W  C  R  P  P  Q  I  L  R
```

```
GATGTGACAAGATTGTGGAGACCAAAGGGTCAGCAGGGAAAAGGAATGGCCGAGTGTCCA
C  D  K  I  V  E  T  K  G  S  A  G  K  R  N  G  R  V  S  I
```

```
TCAGGGACAGTCCTGCAAACCTCAGCTTCACAGTGACCCTGGAGAATCTCACAGAGGAGG
R  D  S  P  A  N  L  S  F  T  V  T  L  E  N  L  T  E  E  D
```

```
ACGCAGGCACCTACTGGTGTGGGGTGGATACACCGTGGCTCCGAGACTTTCATGATCCCA
A  G  T  Y  W  C  G  V  D  T  P  W  L  R  D  F  H  D  P  I
```

```
TTGTCGAGGTTGAGGTGTCCGTGTTCCCGGgtgagccc        1.62kb
V  E  V  E  V  S  V  P  P  A
```

```
acccacagCCGGGACGACCACACGCCTCCAGCCCCCAGAGCTCCATGGGCACCTCAGGTCC
         G  T  T  A  S  S  P  Q  S  S  M  G  T  S  G  P
```

```
TCCCACGAAGCTGCCCGTGCACACCTGGCCCAGCGTGACCAGAAAGGACAGCCCCGAACC
P  T  K  L  P  V  H  T  W  P  S  V  T  R  K  D  S  P  E  P
```

```
CAGCCCACACCCTGGgtaagg                         0.942kb
S  P  H  P  G
```

```
tgtccccacagCTCCCTGTTCAGCAATGTCCGCTTCCTGCTCCTGGTCCTCTTGGAGCTG
           S  L  F  S  N  V  R  F  L  L  L  V  L  L  E  L
```

```
CCCCTGCTCCTGAGCATGCTGGGTGCCGTCCTCTGGGTGAACAGACCTCAGAGAAGCTCT
P  L  L  L  S  M  L  G  A  V  L  W  V  N  R  P  Q  R  S  S
```

```
AGAAGCAGGCAGAATTGGCCCAAGGGTGAGAACCAGTAGcatctgctgtccatcaaggcc
R  S  R  Q  N  W  P  K  G  E  N  Q  *
ctgtgctgcaacagagcccctctgggggactggaatgacctcctgaccactccctcccgg
gctgctctctccaacatctcctggaatcctttgtgagcctccttcagcctttttccctgtg
cccgatcctcatgtgtcacatgtgaacctgacggacatggacgccctgagctgtgagtcc
acgtctcatgtgcacgccccggccagctaagcctcgggccgtcagcaatacctctgagtg
cccggatgccctccctgcacccttccatttctccaggagcctggcactgcttcctccacc
gttttcacagggagaagcaggtctaggactcccctgcacctttgccaccataatggccca
cactccctgggtccaggagtgtagaatatgcggctgcttccatttgctgagtgtgtcgat
tcaatgatgctttcaaactttaataaa
```

Fig. 2. Nucleotide and deduced amino acid sequence of the human CMRF-35A gene. The translated protein sequence is shown below the nucleotide sequence. The length of each intron and the nucleotide sequence at the junctions are shown. The leader sequence and transmembrane sequence are underlined and the putative polyadenylation site is indicated in bold type.

flanking sequence contains a number of putative transcription factor binding motifs, including elements known to be active in haemopoietic lineages. These included binding sites for transcription factors that are important for myeloid haematopoiesis, such as myeloid zinc finger transcription factor, MZF-1 (32) and the consensus binding site for AML-1 (33), as well as binding sites for more ubiquitous factors such as Ets, Oct-1 and Sp1 (34).

To study the regulation of the CMRF-35A gene, a number of constructs containing the region immediately upstream from the translational start site were made in the pGL3 basic reporter vector.
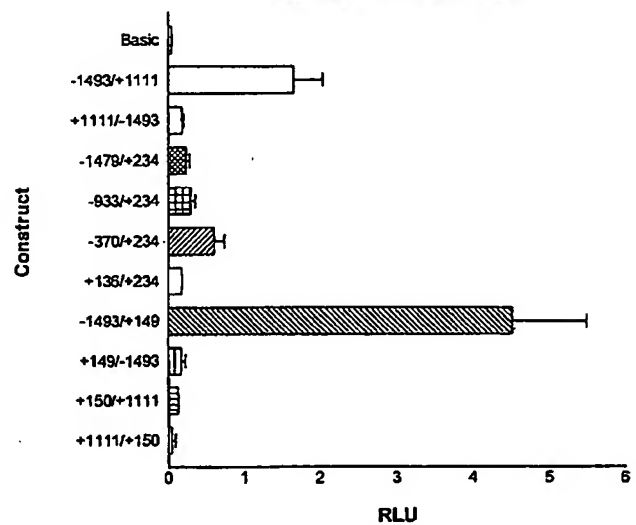
Fig. 3. Promoter activity of the CMRF-35A-pGL3 constructs in the Mann cell line. Cells were transiently transfected with the firefly luciferase reporter plasmids containing fragments of the CMRF-35A 5' flanking region. Luciferase activity was normalized by co-transfection with the Renilla luciferase reporter vector pRL-TK. Data are represented as relative luciferase light units (RLU) and the standard deviation from three independent experiments following normalization to Renilla luciferase activity.

These were transiently transfected into the Mann cell line and assayed for luciferase activity. The region containing the sequence from nucleotides −1493 to +149 initiated transcription of the reporter gene (Fig. 3). Reporter gene activity was diminished if the region from nucleotide −1493 to −933 was removed. In addition, the presence of the first exon and part of the first intron in the constructs resulted in lower reporter gene expression.

Characterization of the 3' region of the CMRF-35A gene

The 3' untranslated region of the original CMRF-35A cDNA (accession number X66171) contains two copies of a 43-bp sequence (10). The origin of this sequence has been questioned. This region should be encoded in exon 4. Comparison of the genomic sequence for exon 4 with CMRF-35A cDNA sequences from different isolates has confirmed that this repeat sequence does not exist in either the gene or other cDNA sequences. The sequence is contained entirely within the exon and is not the product of an exon duplication. Its most likely origin is as an artifact in the library from which the cDNA was cloned.

The CMRF-35A cDNA sequence did not contain a consensus polyadenylation site. Sequencing of the genomic DNA has identified a classic consensus polyadenylation site at 468 bases 3' to the end of the coding region.

Exon-Intron Junctions of the *CMRF-35A* gene

Exon	nts cDNA	Phase	Exon	Intron	Intron length (kb)	Intron	Exon
5-UT-Leader	9–300	I	V P G TGTCCCAG	gtgagtggg	0.771	atttttcag	Y F GCTATTT
Ig Domain	301–638	I	F P G GTTCCCGG	gtgagcc	1.62	acccaca	G T CCGGGAC
Hinge Region	639–766	II	H P G CACCCTGG	gtaagg	0.942	tgtcccacag	S L F CTCCCTGTT
Transmembrane-Cytoplasmic-3'UT	767–1137						

Table 2

Presence of a pseudogene

Analysis of the PAC clone 140L9 identified sequences similar to the CMRF-35A molecule, located 3.2 kb 5′ to the start of the *CMRF-35A* gene. The structure of this apparent gene is similar to the *CMRF-35A* gene and contains regions that correspond to the CMRF-35A 5′-UT region, the Ig-like domain, the membrane proximal domain and the transmembrane-cytoplasmic region. These appear to follow similar exon structures, except that a leader sequence with similarity to the CMRF-35A sequence was not identified. Translation of the Ig domain sequence similar to the CMRF-35A molecule identified a stop codon in the reading frame which was confirmed to be present in genomic DNA from 4 individuals. PCR primers were made to the putative coding regions of this pseudogene and RT-PCR analysis of a large panel of cDNA from different haemopoietic cells failed to identify any specific mRNA product (data not shown).

The genomic sequence of the *CMRF-35J* pseudogene was compared to the *CMRF-35A* gene. The former demonstrated substantial regions of apparent similarity in both the putative exons and introns. The sizes of the introns differ marginally. The intron between the Ig domain coding exon and the membrane proximal region coding exon was 1.62 kb in the *CMRF-35A* gene, compared to 0.974 kb in the putative *CMRF-35J* pseudogene. The intron between the membrane proximal region coding exon and the next exon is 1.107 kb in *CMRF-35J* and 0.942 kb in *CMRF-35A*. The sequence similarity between the CMRF-35A exons and the putative CMRF-35J exons is 88%.

Comparison to the CMRF-35H gene

Blast alignment was used to investigate the similarity between the gene structures of these two molecules. The nucleotide sequence of the introns 5′ to the exons encoding the Ig domain from each gene were aligned. The 3′ end of these introns when aligned with each other exhibited 77% identity over 200 residues. The sequence of the Ig domain encoding exons are 80% similar (11). However, this simi-

larity did not extend more than 22 bases into the intron following the Ig domain containing exon. This suggests that the similarity between these genes evolved from an exon duplication. The size of the corresponding introns in the *CMRF-35A* and *CMRF-35H* genes were compared. The intron following exon 2 was much longer in the *CMRF-35A* gene (1.62 kb) than in the *CMRF-35H* gene (0.656 kb).

Chromosomal localization

The *CMRF-35A* gene was localized by screening a panel of genomic DNA prepared from human/mouse and human/hamster hybrids by PCR. PCR primers from the CMRF-35A leader and Ig like domains were used to amplify a region specific to the *CMRF-35A* gene. Specific PCR products were detected in DNA samples containing DNA from human chromosome 17 only. The result was confirmed by fluorescent *in situ* hybridization, which mapped the *CMRF-35A* gene to Chr 17q22–24 (data not shown).

We have previously localized the *CMRF-35H* gene to human chromosome 17q22–24 (20) and thus the two genes are closely linked. We have described two individual, non-overlapping PAC clones; one for the *CMRF-35A* gene and the other for the *CMRF-35H* gene (20) confirming their close proximity and establishing that the two molecules are encoded for by individual genes. Analysis of the human genomic databases confirmed subsequently that the two genes are linked on chromosome 17. The *CMRF-35J* pseudogene is located 3.2 kb 5′ to the *CMRF-35A* gene. Thus there are three related loci in close proximity to each other establishing the presence of a new gene complex.

Discussion

The IRS family of molecules includes a growing number of members. The genes for these molecules have been localized to a gene complex

on chromosome 19 known as the LRC or leucocyte receptor complex including, amongst others, the genes for the ILT molecules, LAIR, FcαR, and KIR (35). The CMRF-35A and CMRF-35H molecules are two novel members of the IRS family of molecules (10, 20). The CMRF-35H molecule has 3 putative ITIM in its cytoplasmic region (11) and has been shown to be able to initiate an inhibitory signal (12). On the other hand, CMRF-35A is a leucocyte surface molecule that has a relatively short cytoplasmic tail that lacks any ITIM sequences. Instead, the presence of a charged residue in its transmembrane domain suggests that CMRF-35A associates with another molecule, that we predict would contain ITAM sequences and give CMRF-35A a putative activatory function. In this paper, we used PAC clones of human genomic DNA to characterize the gene structure of the CMRF-35A molecule to add to our description of the CMRF-35H gene structure. Whilst this work was in progress, the sequence of the region of chromosome 17 containing the CMRF-35A and CMRF-35H genes, became available through the human genome project. We were therefore able to confirm the genomic organization of CMRF-35A gene as well as analyze the region surrounding this gene.

The CMRF-35A gene consists of four exons spanning 4.5 kb. We have identified a polyadenylation consensus motif 468 nucleotides 3' to the end of the cDNA. A repeat sequence in the 3'UT region of the cDNA has been identified as an artifact of the library from which the cDNA was cloned (10). No evidence for this repeat could be found in the genomic sequence. The gene structures of the CMRF-35A and CMRF-35H molecules are similar in that single exons code for the 5'UT and leader sequences, the single Ig domain and the membrane proximal region. The positions of the intron-exon boundaries, surrounding the Ig domain containing exon are conserved between the two genes. However, the remainder of the genes differ, as do the molecules. The CMRF-35A gene has a single exon encoding the transmembrane, cytoplasmic and 3'UT regions, whereas this region in the CMRF-35H gene is encoded by four exons (20). The similarity of their Ig domain containing exons suggests that these arose by exon duplication. The introns between the similar domains of the two genes are similar in size except for the intron following the Ig domain. This intron is significantly longer in the CMRF-35A gene than the CMRF-35H gene consistent with the observation that the intron between the Ig domain and membrane proximal regions is longer in most genes encoding the activatory counterpart compared to the corresponding intron in the gene for the inhibitory partner (30).

The CMRF-35A molecule has the similarities of the activating family member in that it has a short cytoplasmic tail and a charged residue in the transmembrane domain. The gene structure of the CMRF-35A gene, described here, is similar to the gene structures of that of other activating molecules such as LIR-6 and PIR-A/p91B

in that the transmembrane, cytoplasmic and 3'UT regions are all encoded by a single exon. However, the CMRF-35A gene differs from these genes in the 5' region of the gene. The 5' UT and leader sequence of the CMRF-35A molecule are encoded by one exon, whereas in the other genes, the 5'UT and leader sequences are split between two exons with the second exon often being a mini exon (25, 36). The membrane proximal region of the CMRF-35A molecule is also encoded in a single exon, whereas this is also split into two exons in the LIR-6, LIR-5 and PIRA genes (25).

A third CMRF-35 gene, which we called the putative CMRF-35J pseudogene was identified approximately 3.2 kb upstream of the CMRF-35A gene. This gene was identified to be a pseudogene because of the presence of an insertion in the Ig like domain encoding exon that inserts a premature stop codon into the translated sequence. In addition, no sequence similar to the CMRF-35A leader sequence was identified. The CMRF-35J pseudogene shows approximately 88% similarity to the CMRF-35A gene. The regions of similarity include intronic regions suggesting that the two genes arose from gene duplication. The presence of pseudogenes is a feature of the ILT molecules, with both ILT9 and ILT10 identified as being pseudogenes (17).

The CMRF-35A molecule is expressed in a range of haemopoietic cell lineages including natural killer (NK) cells, granulocytes, most myeloid cells, dendritic cells and a subpopulation of T and B lymphocytes. The expression of the CMRF-35A molecule on the cell surface is both up and downregulated by various stimuli (37). Analysis of the 5' flanking sequences failed to identify a TATA box, thus the CMRF-35A gene is yet another non-housekeeping gene that has a TATA-less promoter. Other genes expressed by haemopoietic cells that lack a TATA box include the CD33 gene (38), the mouse 2B4 gene (39) and the LIR5 (25). Whilst no TATA box was identified, an Inr or initiator consensus sequence was present (40, 41). This sequence is normally located around the transcription start site. However the consensus sequence was found within the 5'UT region of the cDNA. To study the regulation of the gene, a region 1.493 kb upstream of the transcription initiation site was analyzed for evidence of regulatory sequences, involved in expression of the CMRF-35A molecule. The region containing nucleotides −1479 to +149 was able to initiate transcription of a reporter gene and it is this region that contains the Inr consensus sequence. Deletion of nucleotides −1479 to −933 resulted in loss of reporter gene activity, indicating the presence of important regulatory sequences within this region. In addition, the presence of intron 1 appears to diminish the activity of the promoter. Within the putative promoter region, there are a number of binding sites for transcription factors that are predominantly active in the myeloid lineage such as MZF-1 and AML-1, as well as some that have a more ubiquitous activity.

The *CMRF-35A* and *CMRF-35H* genes are regulated independently of each other, although they may be expressed together or alone. A comparison of the 5' flanking sequences of the two genes containing likely promoting elements, showed no similarities between them. A major difference was the number of CG dinucleotides present in this region of the two genes. The sequence of the CMRF-35H 5' flanking region has three times the number of CG dinucleotides to the corresponding region of the *CMRF-35A* gene. Thus, these two molecules are the products of independent genes, that are regulated independently of each other at the RNA level (11) because of their different promoters. Nonetheless, the data does suggest that they arose through a common ancestor and are linked closely on chromosome 17. The genes for members of the IRS family are located throughout the genome. The largest collection of members of this family is in the LRC complex at human chromosome 19q13.4 (17, 25, 35, 42, 43). Other regions that contain members of the family include chromosome 7q22; FDF03 (44), chromosome 6; NKp44 (7), TREM-1 (9), chromosome 16; DORA (45). Generally, the inhibitory and the activatory counterparts are localized within the same regions. This is shown here to be the same for the CMRF-35 genes, with the gene encoding the activatory molecule CMRF-35A and the *CMRF-35H* gene both localizing to chromosome 17q22-24. The presence of the *CMRF-35J* pseudogene identified a third region of chromosome 17, that has evolved from this CMRF-35 family. More detailed analysis of this region of the chromosome is currently underway, to further characterize the extent and nature of this new complex.

This paper describes the organization of the *CMRF-35A* gene as the second transcribed gene of this family, located on chromosome 17. The exon-intron structure of this gene is similar to the structures of other IRS activatory molecules, further indicating that the CMRF-35 molecules are members of the leucocyte receptor molecules that have counteractive activatory and inhibitory roles. The CMRF-35A and CMRF-35H molecules are differentially expressed in haemopoietic cells and this understanding of their gene structures allow better appreciation of their independent regulation. Studies are currently underway to determine the role these molecules play in regulating the immune response.

References

1. Daeron M, Vivier E. Biology of immunoreceptor tyrosine-based inhibition motif-bearing molecules. *Curr Top Microbiol Immunol* 1999; 244: 1–12.
2. Hulett MD, Hogarth PM. Molecular basis of Fc receptor function. *Adv Immunol* 1994: 57: 1–127.
3. Wagtmann N, Biassoni R, Cantoni C et al. Molecular clones of the p58 NK cell receptorreveal immunoglobulin related moleculeswith diversity in both the extra- and intracellular domains. *Immunity* 1995: 2: 439–49.
4. Colonna M, Samaridis J. Cloning of immunoglobulin-superfamily members associated with HLA-C and HLA-B recognition by human natural killer cells. *Science* 1995: 269: 407–8.
5. D'Andrea A, Chang C, Franz-Bacon K, McClanahan T, Phillips JH, Lanier LL. Molecular cloning of NKB1. A natural killer cell receptor for HLA-B allotypes. *J Immunol* 1995: 155: 2306–10.
6. Samaridis J, Colonna M. Cloning of novel immunoglobulin superfamily receptors expressed on human myeloid and lymphoid cells: structural evidence for new stimulatory and inhibitory pathways. *Eur J Immunol* 1997: 27: 660–5.
7. Cantoni C, Bottino C, Vitale M et al. NKp44, a triggering receptor involved in tumor cell lysis by activated human natural killer cells, is a novel member of the immunoglobulin superfamily. *J Exp Med* 1999: 189: 787–95.
8. Pessino A, Sivori S, Bottino C et al. Molecular cloning of NKp46: a novel member of the immunoglobulin superfamily involved in triggering of natural cytotoxicity. *J Exp Med* 1998: 188: 953–60.
9. Bouchon A, Dietrich J, Colonna M. Cutting edge: inflammatory responses can be triggered by TREM-1, a novel receptor expressed on neutrophils and monocytes. *J Immunol* 2000: 164: 4991–5.
10. Jackson DG, Hart DNJ, Starling GC, Bell JL. Molecular cloning of a novel member of the immunoglobulin gene superfamily homologous to the polymeric immunoglobulin receptor. *Eur J Immunol* 1992: 22: 1157–63.
11. Green BJ, Clark GJ, Hart DNJ. The CMRF-35 mAb recognizes a second leukocyte membrane molecule with a domain similar to the poly Ig receptor. *Int Immunol* 1998: 10: 891–9.
12. Cantoni C, Bottino C, Augugliaro R et al. Molecular and functional characterization of IRp60, a member of the immunoglobulin superfamily that functions as an inhibitory receptor in human NK cells. *Eur J Immunol* 1999: 29: 3148–59.
13. Gupta N, Scharenberg AM, Burshtyn DN et al. Negative signaling pathways of the killer cell inhibitory receptor and FcgRIIb1 require distinct phosphatases. *J Exp Med* 1997: 186: 473–8.
14. Lanier LL, Corliss BC, Wu J, Leong C, Phillips JH. Immunoreceptor DAP12 bearing a tyrosine-based activation motif is involved in activating NK cells. *Nature* 1998: 391: 703–7.
15. Daeron M. Fc receptor biology. *Annu Rev Immunol* 1997: 15: 203–34.
16. Wilson MJ, Torkar M, Haude A et al. Plasticity in the organization and sequences of human KIR/ILT gene families. *Proc Natl Acad Sci U S A* 2000: 97: 4778–83.
17. Wende H, Volz A, Ziegler A. Extensive gene duplications and a large inversion characterize the human leukocyte receptor cluster. *Immunogenetics* 2000: 51: 703–13.

18.

19.

20.

21.

22.

23.

24.

25.

26.

18. Alley TL, Cooper MD, Chen M, Kubagawa H. Genomic structure of PIR-B, the inhibitory member of the paired immunoglobulin-like receptor genes in mice. *Tissue Antigens* 1998: 51: 224–31.

19. Kuroiwa A, Yamashita Y, Inui M et al. Association of tyrosine phosphatases SHP-1 and SHP-2, inositol 5-phosphatase SHIP with gp49B1, and chromosomal assignment of the gene. *J Biol Chem* 1998: 273: 1070–4.

20. Clark GJ, Green BJ, Hart DN. The CMRF-35H gene structure predicts for an independently expressed member of an ITIM/ITAM pair of molecules localized to human chromosome 17. *Tissue Antigens* 2000: 55: 101–9.

21. de Wit TPM, Morton HC, Capel PJA, van de Winkel JGJ. Structure of the gene for the human myeloid IgA Rc receptor (CD89). *J Immunol* 1995: 155: 1203–9.

22. Selvakumar A, Steffens U, Palanisamy N, Chaganti RSK, Dupont B. Genomic organisation and allelic polymorphism of the human killer cell inhibitory receptor gene KIR103. *Tissue Antigens* 1997: 49: 564–73.

23. Wilson MJ, Torkar M, Trowsdale J. Genomic organization of a human killer cell inhibitory receptor gene. *Tissue Antigens* 1997: 49: 574–9.

24. Torkar M, Norgate Z, Colonna M, Trowsdale J, Wilson MJ. Isotypic variation of novel immunoglobulin-like transcript/killer cell inhibitory receptor loci in the leukocyte receptor complex. *Eur J Immunol* 1998: 28: 3959–67.

25. Liu WR, Kim J, Nwankwo C, Ashworth LK, Arm JP. Genomic organization of the human leukocyte immunoglobulin-like receptors within the leukocyte receptor complex on chromosome 19q13.4. *Immunogenetics* 2000: 51: 659–69.

26. Le Franc M, Forster A, Baer R, Stinson MA, Rabbitts TH. Diversity and rearrangement of the human T-cell rearranging K genes: nine germ-line variable genes belonging to the two subgroups. *Cell* 1986: 45: 237–46.

27. Ioannou PA, Amemiya CT, Garnes J et al. A new bacteriophage P1-derived vector for the propagation of large human DNA fragments. *Nat Genet* 1994: 6: 84–9.

28. Frohman MA, Dush MK, Martin GR. Rapid amplification of full-length cDNAs from rare transcripts:amplification using a single gene-specific oligonucleotide primer. *Proc Natl Acad Sci U S A* 1988: 85: 8998–9002.

29. Breathnach R, Chambon P. Organization and expression of eucaryotic split genes coding for proteins. *Annu Rev Biochem* 1981: 50: 349–83.

30. Radley E, Alderton RP, Kelly A, Trowsdale J, Beck S. Genomic organisation of HLA-DMA and HLA-DMB: comparison of the gene organisation of all six class II families in the human major histocompatibility complex. *J Biol Chem* 1994: 269: 18834–8.

31. Ernst P, Smale ST. Combinatorial regulation of transcription. I: General aspects of transcription control. *Immunity* 1995: 2: 311–9.

32. Morris JF, Rauscher FJ 3rd, Davis B et al. The myeloid zinc finger gene, MZF-1, regulates the CD34 promoter *in vitro. Blood* 1995: 86: 3640–7.

33. Lutterbach B, Hiebert SW. Role of the transcription factors AML-1 in acute leukemia and hematopoirtic differentiation. *Gene* 2000: 245: 223–35.

34. Faisst S, Meyer S. Compilation of vertebrate-encoded transcription factors. *Nucleic Acids Res* 1992: 20: 3–26.

35. Wende H, Colonna M, Ziegler A, Volz A. Organization of the leukocyte receptor cluster (LRC) on human chromosome 19q13.4. *Mamm Genome* 1999: 10: 154–60.

36. Hogarth PM, Witort E, Hulett MD et al. Structure of the mouse bFcg receptor II gene. *J Immunol* 1991: 146: 369–76.

37. Daish A, Starling GC, McKenzie JL, Nimmo JC, Jackson DG, Hart DNJ. Expression of the CMRF-35 antigen, a new member of the immunoglobulin gene superfamily, is differentially regulated on leucocytes. *Immunology* 1993: 79: 55–63.

38. Bodger MP, Hart DN. Molecular cloning and functional analysis of the CD33 promoter. *Br J Haematol* 1998: 102: 986–95.

39. Chuang SS, Lee Y, Stepp SE, Kumaresan PR, Mathew PA. Molecular cloning and characterization of the promoter region of murine natural killer cell receptor 2B4. *Biochem Biophys Acta* 1999: 1447: 244–50.

40. Lo K, Smale ST. Generality of a functional initiator consensus sequence. *Gene* 1996: 182: 13–22.

41. Smale ST. Transcription inititation from TATA-less promoters within eukaryotic protein-coding genes. *Biochim Biophys Acta* 1997: 1351: 73–88.

42. Wagtmann N, Rojo S, Eichler E, Mohrenweiser H, Long EO. A new human gene complex encoding the killer cell inhibitory receptors and related monocyte/macrophage receptors. *Current Biol* 1997: 7: 615–8.

43. Wilson MJ, Torkar M, Trowsdale J. Genetic analysis of a highly homologous gene family. The killer cell immunoglobulin-like receptors. *Methods Mol Biol* 2000: 121: 251–63.

44. Fournier N, Chalus L, Durand I et al. FDF03, a novel inhibitory receptor of the immunoglobulin superfamily, is expressed by human dendritic and myeloid cells. *J Immunol* 2000: 165: 1197–209.

45. Bates EE, Dieu MC, Ravel O et al. CD40L activation of dendritic cells down-regulates DORA, a novel member of the immunoglobulin superfamily. *Mol Immunol* 1998: 35: 513–24.

G6b, a Novel Immunoglobulin Superfamily Member Encoded in the Human Major Histocompatibility Complex, Interacts with SHP-1 and SHP-2*

Edwin C. J. M. de Vet, Begoña Aguado, and R. Duncan Campbell‡

From the Medical Research Council United Kingdom Human Genome Mapping Project Resource Center, Hinxton, Cambridge CB10 1SB, United Kingdom

The G6b gene, located in the class III region of the human major histocompatibility complex, has been suggested to encode a putative receptor of the immunoglobulin superfamily. Genomic sequence information was used as a starting point to clone the corresponding cDNA. Reverse transcriptase polymerase chain reaction showed that expression of the gene is restricted to certain hematopoietic cell lines including K562, Molt 4, and Jurkat. Several splice variants were detected, varying only in their C-terminal parts. One of the potential membrane-bound isoforms contained two immunoreceptor tyrosine-based inhibitory motifs in its cytoplasmic tail. Four of the isoforms were expressed as epitope-tagged proteins in the cell lines K562 and COS-7. The two splice isoforms lacking the hydrophobic transmembrane segment were secreted from the cell. Glycosidase treatment of the four recombinant proteins provided evidence for N- and O-glycosylation. Immunofluorescence studies indicated that the spliced isoforms having a transmembrane segment were directed to the cell membrane. The G6b isoform containing two immunoreceptor tyrosine-based inhibitory motifs in its cytoplasmic tail was found to be phosphorylated on tyrosine residues after pervanadate treatment of cells and, subsequently, interacts with the SH2-containing protein-tyrosine phosphatases SHP-1 and SHP-2. Mutagenesis studies showed that phosphorylation of tyrosine 211 is critical for the interaction of G6b with SHP-1 and SHP-2.

The Ig superfamily receptors constitute a large group of cell surface proteins involved in the immune system and cellular recognition (1, 2). Members of this family are characterized by an extracellular part containing at least one immunoglobulin domain, a transmembrane segment, and a cytoplasmic tail. A subset of the Ig superfamily is the inhibitory receptor characterized by the presence of one or more immunoreceptor tyrosine-based inhibitory motifs (ITIM)[1] in their cytoplasmic tail.

The consensus sequence of the ITIM is generally described as (L/V/I/S/T)XYXX(L/V) (3). Following phosphorylation of the tyrosine residue within this motif, the SH2 domain containing protein-tyrosine phosphatases SHP-1 and/or SHP-2 can be recruited to the receptor, where they can dephosphorylate membrane-bound phosphoproteins, thus modulating the signaling cascade. SHP-1 is a non-transmembrane protein primarily expressed in hematopoietic cells and is considered to play a negative role in cell signaling (4). Identified substrates for SHP-1 are the linker of activated T-cells (5, 6) and the adapter protein Slp-76 (7). In contrast, SHP-2 has been considered to act primarily as a positive signal transducer (8). Possible substrates for this phosphatase are the platelet-derived growth factor beta receptor (9) and PZR (10). SHP-2 modulates the signal strength of receptor-protein-tyrosine kinases and is also involved in cytokine and antigen signaling not involving receptors with intrinsic kinase activity (11). Although the two phosphatases appear to have opposing roles, there are examples of ITIM-containing receptors that recruit both SHP-1 and SHP-2 (12, 13). Other receptors are reported to recruit primarily only one form (14, 15). Both phosphatases SHP-1 and SHP-2 contain two SH2 domains and a catalytic domain (16, 17).

The human major histocompatibility complex (MHC) is located on chromosome band 6p21.3 and spans ~3.6 megabases of DNA. The complete sequence of this region has been determined (18). The central MHC region is termed the class III region and comprises 0.8 megabases. Of the 59 genes in this region, 40% are known or predicted to have a role in the immune system or inflammation, such as tumor necrosis factor, lymphotoxin-α, and lymphotoxin-β. Susceptibility to a wide range of diseases has been linked to the MHC, including insulin-dependent diabetes mellitus (19), rheumatoid arthritis (20), and ankylosing spondylitis (21). Although disease susceptibility is often due to allelic differences in the class I and class II antigens, there is evidence that loci located in the class III region may also contribute (21, 22). For this reason the detailed characterization of genes located in the class III region with a potential role in the immune system is of great interest.

G6b is an uncharacterized gene located in the class III region of the MHC that encodes a putative cell surface receptor of the Ig superfamily. Its predicted gene product was found to contain a potential signal peptide, a variable type Ig domain, and a transmembrane segment (23). Interestingly, we have observed that the intracellular stretch also contains two tyrosine residues in ITIM consensus sequences.

In this study, the available genomic sequence information was used as a starting point to obtain the cDNA encoding the

amide gel electrophoresis; nt, nucleotide(s); mAb, monoclonal antibodies.

G6b protein. By RT-PCR, several alternative splice variants of the G6b mRNA were identified in the bone marrow-derived cell lines K562, Molt4, and Jurkat but not in other hematopoietic and fibroblast cell lines studied. These mRNAs encode proteins with different C termini, some of which lacked a transmembrane segment. Expression of four of the proteins as epitope-tagged fusion proteins in mammalian cells allowed their further characterization. An association of the splice isoform containing the ITIM motifs with SHP-1 and SHP-2 was shown following pervanadate-induced tyrosine phosphorylation.

EXPERIMENTAL PROCEDURES

Reverse Transcriptase-PCR—RNA isolation from human cell lines was performed as described previously (24). cDNA synthesis was carried out using a Promega Reverse Transcription System and ~1 μg of poly(A)$^+$ RNA according to the manufacturer's instructions. Control PCR reactions with β-actin primers were performed on each cDNA reaction (forward 5'-CTTCGCGGGCGACGATGC-3' and reverse 5'-TGGTGGTGAAGCTGTAGCC-3'). PCR primers for G6b were designed based on the genomic sequence (GenBank™ accession number AF129756). To obtain the complete open reading frame, nested PCR was performed on the cDNA samples. In the first round, forward primer 5'-AGCTTCTCCTCACCACATCC-3' (nt position 26694–26713) and reverse primer 5'-AAAGGGTCAGTCTCCTGACG-3' (nt position 23402–23421) were used. In the second round, forward primer 5'-CCTAACCATGGCTGTGTTTC-3' (nt position 26676–26695) was used in combination with reverse primer 5'-GGGAGGTTTGGAGTAAGGGC-3' (nt position 24972–24991). In each round, 25 cycles were performed using an annealing temperature of 60 °C. PCR fragments were cloned into the pGEM-T vector (Promega). Clones were checked by sequencing on an Applied Biosystems (Applera) 377 automated DNA sequencer using Big Dye terminators.

Expression of Proteins in COS-7 Cells and K562 Cells—For expression of epitope-tagged proteins in mammalian cells, the open reading frames of the different splice isoforms were cloned into the pcDNA3 vector (Invitrogen) fused to a T7-epitope tag (MASMTGGQQMGRDP). To express the G6b isoforms fused at the C terminus to the T7-epitope tag, PCR copies were made of the open reading frames removing the stop codons. The forward primer 5'-TTATAAGCTTACCATGGCTGTGTTTCTGC-3' was used, creating a HindIII site (underlined). The reverse primer (either 5'-TCATGCGGCCGCGCTAGCAACTACAACTGCATAGA-3' (for G6b splice isoforms B and E) or 5'-TCATGCGGCCGCGCTAGCGCAGGGTCCGCTGTGG-3' (for G6b splice isoforms A and D)) was used. These two reverse primers obliterated the stop codons and introduced NheI sites (underlined), allowing direct fusion to the T7 tag sequence in the T7.TagpBlsc vector (25). PCR fragments were cloned into this vector using HindIII-NheI. Constructs were checked by DNA sequencing as described above. The inserts encoding the fusion proteins were cloned into the pcDNA3 vector using HindIII-NotI.

To express the G6b isoforms with the T7-epitope tag fused to the N terminus, an expression vector was created containing the human CD33 signal peptide (26) instead of the G6b signal peptide followed by the T7-epitope tag in pcDNA3. First, a fusion between the CD33 signal peptide and the T7-epitope tag was constructed in pBluescript. The CD33 leader-T7 tag fusion was amplified by PCR using primers 5'-GCTTGGTACCATGCCGCTGCTGCTACTG-3' introducing a NdeI site (underlined) and 5'-GATCTATGGATCCGACCC-3' containing a BamHI site (underlined). The resulting fragment was cloned into the pcDNA3 vector using NdeI and BamHI, yielding the plasmid CD33-T7-pcDNA3. The G6b splice isoforms were PCR-amplified with primer 5'-GTCGGGATCCCAAGGGAACCCTGGGGC-3', introducing a BamHI site (underlined) and removing the first 15 amino acids of the potential signal sequence, and 5'-AATTGCGGCCGCCCTTCAAACTACAACTGC-3', introducing a NotI site (underlined) and maintaining the stop codon. The resulting PCR fragments were digested with BamHI and NotI and cloned into CD33-T7-pcDNA3 digested with BamHI and NotI. The clones were checked by DNA sequencing. Mutations of tyrosine to phenylalanine in the cytoplasmic tail of the N-terminal-tagged G6b-B construct were made using the QuikChange® mutagenesis method (Stratagene) according to the manufacturer's instructions.

Proteins were transiently expressed in COS-7 cells using the DEAE-dextran method as described elsewhere (25). Three days after transfection, cells and supernatants were harvested. K562 cells were transfected with Lipofectin (Life Technologies, Inc.) according to the manufacturer's instructions. Three days after transfection, cells were maintained in the presence of 0.5 mg/ml G418. For direct analysis on

SDS-polyacrylamide gels, cells were washed once with phosphate-buffered saline and lysed in SDS-PAGE sample buffer (27). Supernatants were routinely cleared by centrifugation. SDS-PAGE was done according to Laemmli (27) on 12% polyacrylamide gels. Western blot immunostaining was performed with the anti-T7 tag monoclonal antibody (mAb) (Novagen). Immunoreactive proteins were detected with horseradish peroxidase-coupled secondary antibody followed by detection with ECL (PerkinElmer Life Sciences). Immunofluorescence localization studies were performed as described elsewhere (28), and staining was examined with a Nikon Eclipse E800 microscope linked to a MicroRadiance confocal imaging system (Bio-Rad).

Glycosidase Treatment—G6b splice isoforms were expressed in COS-7 cells as described above, and cell lysates were prepared in 10 mM sodium phosphate buffer, pH 6.5, 0.1% SDS, and 50 mM β-mercaptoethanol. For treatment of secreted G6b forms, the medium was harvested, and SDS (final concentration, 0.1%) and β-mercaptoethanol (final concentration, 50 mM) were added. To denature the proteins, both cell lysates and media were heated for 2 min at 95 °C. Thereafter, Nonidet P-40 (final concentration, 1%), sodium phosphate buffer, pH 6.5 (final concentration, 50 mM), and protease inhibitor mixture (Sigma P8340, 200× diluted) were added. Aliquots of these preparations were treated with N-glycosidase F (25 units/ml), neuraminidase (0.15 units/ml), or O-glycosidase (4 milliunits/ml) for 5 h at 37 °C. (All three enzymes were obtained from Roche Molecular Biochemicals.) Reactions were then stopped by the addition of SDS-PAGE sample buffer and analyzed on 12% polyacrylamide gels followed by Western blot immunostaining as described above.

Pervanadate Treatment—Pervanadate was prepared by mixing sodium orthovanadate (Sigma) and hydrogen peroxide (Sigma) in phosphate-buffered saline to final concentrations of 1 and 10 mM, respectively, and leaving the mixture for 15 min at room temperature. To remove excess hydrogen peroxide, catalase (Sigma) was added to a final concentration of 0.2 mg/ml. Cells were stimulated by a 10× dilution of pervanadate in phosphate-buffered saline for 10 min at 37 °C. Cells were lysed in lysis buffer (10 mM Tris/HCl, pH 7.5, 1% Nonidet P-40, 150 mM NaCl, 0.02% sodium azide, and 1 mg/ml bovine serum albumin) supplemented with protease inhibitor mixture (200× diluted). Lysates were cleared by a 15-min centrifugation at 4 °C, and immunoprecipitations were performed with the anti-T7 mAb and protein A-Sepharose (Sigma) at 4 °C. Proteins were eluted with SDS-PAGE sample buffer at 95 °C for 2 min and analyzed by SDS-PAGE followed by Western blotting. The Western blots were probed with either the anti-T7 tag mAb horseradish peroxidase conjugate (Novagen), anti-phosphotyrosine mAb (4G10) coupled to horseradish peroxidase (Upstate Biotech), anti-SHP-1, or anti-SHP-2 polyclonal antisera (Santa Cruz Biotechnology). In the case of the anti-SHP-1 and SHP-2 antisera, a secondary antibody coupled to horseradish peroxidase was used. Proteins were detected with ECL as before.

RESULTS

RT-PCR—No human expressed sequence tag (EST) clones were found that contained any part of the coding region of G6b, although EST BE750421 was found to encode a putative bovine homologue. However, there were a few human ESTs that corresponded to the genomic sequence ~1000–1600 nt downstream of the putative stop codon. Characterization of some of these clones (*e.g.* AA699838) indicated that they did not contain the complete open reading frame. Because one-step RT-PCR turned out not to be sensitive enough, nested RT-PCR was performed on cDNA preparations from poly(A)$^+$ RNA derived from various human cell lines. The preparations from the bone marrow-derived cell lines K562 (erythroleukemia), Molt4, and Jurkat (T cell leukemias) yielded a number of differently sized PCR fragments (Fig. 1A, *bands A–F*) with the two closely migrating *bands A* and *B* (Fig. 1A) being of the expected size. PCR on the bone marrow-derived cell lines U937 (monocyte-like), Raji (B cell-like), HL60 (promyelocytic), and the fibroblast cell lines Tk and HeLa did not yield any of these products (Fig. 1). Similarly, in a separate experiment, we were not able to amplify by PCR G6b mRNA from human natural killer cell lines NKL, NK92, and YT (data not shown).

Sequence analysis of the generated RT-PCR products showed that the band with the lower molecular weight (*band B*) represents the form predicted by Genscan (23) and also anno-
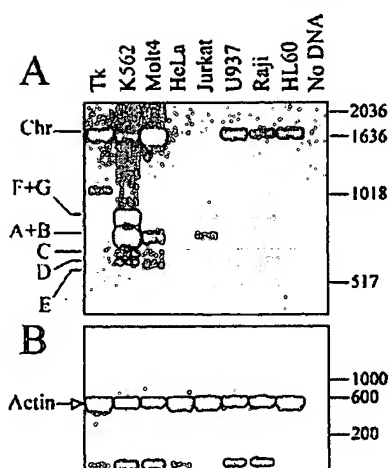
FIG. 1. **RT-PCR of G6b using cDNAs from various human cell lines as template.** *A,* second round of the nested PCR reactions on human cDNA preparations using G6b-specific primers. The cell lines from which the cDNA samples were derived are denoted *above* the gel. Bands are designated *A–G. Chr* corresponds to the band derived from chromosomal contamination. *B,* β-actin control of the cDNA preparations. Molecular weight markers (in base pairs) are indicated on the *right*.

tated in EMBL/GenBank™ entry AF129756). This form contains two ITIM motifs at amino acid positions 209–214 and 235–240 in the encoded polypeptide (Fig. 2*B*). Comparison of the cDNA sequence of the higher molecular weight band (*band A*) with the genomic sequence revealed that this form includes an extra stretch of 19 base pairs relative to G6b-B due to different splicing at the 5' end of coding exon 5 (Fig. 2). This extra stretch shifts the reading frame of the C-terminal end of G6b-A compared with G6b-B, resulting in the absence of the two ITIM motifs in G6b-A. The lower molecular weight bands (*bands C–E*) correspond to variants missing either exon 3 or exons 3 and 4 together (Fig. 2). Because the putative transmembrane segment is encoded by exon 3, these variants would encode proteins that are predicted to be secreted and not to be membrane-associated. Bands that showed higher molecular weights than the ones described above (*bands F* and *G*) turned out to contain intronic sequences. These cDNAs would encode proteins that contain the same signal sequence, Ig domain, and transmembrane domain as the previous forms but with a different cytoplasmic tail. The only PCR band observed in Tk cells (Fig. 1*A*) contained the intron between coding exons 1 and 2, which leads to a premature stop codon. No potentially functional transcript could be amplified from this cell line.

Expression of G6b Isoforms in COS-7 Cells—Four splice isoforms were selected for further characterization, two transmembrane segment-containing isoforms (G6b-A and G6b-B) and two soluble isoforms (G6b-D and G6b-E). The C terminus of G6b-A is identical to the C terminus of G6b-D, and the C terminus of G6b-B corresponds to the C terminus of G6b-E. The four splice isoforms were cloned into a pcDNA3 expression vector as fusions with a T7 epitope. The fusion proteins were transiently expressed in COS-7 cells. Multiple bands per lane were observed on SDS-polyacrylamide gel, which could be indicative of glycosylation, each band representing the protein in a different state of glycosylation (Fig. 3). As expected, only the isoforms lacking transmembrane segments (G6b-D and G6b-E) were present in the medium. The expected molecular sizes for the G6b splice variants without leader peptide are 24.3 (G6b-A), 23.2 (G6b-B), 19.5 (G6b-D), and 18.3 kDa (G6b-E). The observed molecular sizes of the proteins on SDS-polyacryl-

amide gel are in general in good agreement with the expected molecular sizes when considering the lowest band found in each case. An exception to this is the G6b-E form found in the medium, which migrates at ~30–38 kDa. This might be due to the presence of relatively large glycan chains. In this respect, it is noteworthy that G6b-E found within the cell has a molecular size much closer to the theoretical one, probably because these proteins have not been through the complete glycosylation pathway.

Glycosidase Treatment of G6b—To investigate whether the different G6b variants were glycosylated, COS-7 cell lysates and cell supernatants containing the various C-terminal-tagged forms of G6b were incubated with combinations of the glycosidases *N*-glycosidase F, *O*-glycosidase, and/or neuraminidase (Fig. 4). Treatment of *N*-glycosidase F alone causes in all forms (except G6b-E) the disappearance of some of the multiple bands, indicating that the various forms have, at least in part, *N*-glycan chains. Treatment with both neuraminidase and *O*-glycosidase resulted in bands with molecular weights no different from the bands obtained after only neuraminidase treatment, except in the case of the secreted form of G6b-E, indicating that only this form contains a substantial *O*-glycosylation. However, when the molecular weights of the membrane proteins G6b-A and G6b-B treated with only *N*-glycosidase F (devoid of *N*-glycan chains) are compared with these proteins treated with all three glycosidases (devoid of both *N*- as well as *O*-glycan chains), a small difference in the molecular weight is observed (Fig. 4). This difference can be explained by the presence of low molecular weight *O*-glycan chains. Comparing the same treatments in the case of secreted G6b-D shows that the higher molecular weight band observed when the protein is treated with *N*-glycosidase F alone is not detected when the protein is treated with all three glycosidases, indicating that this particular band contains *O*-glycosylation.

In the case of the non-membrane-bound isoforms (G6b-D and G6b-E), the proteins secreted into the medium contain more glycosylation than what is found in the corresponding cell lysates. The proteins found in the cell lysates may also represent misfolded proteins. For that reason they may not be transported through the secretory pathway and thus may not be fully glycosylated. When the same treatments were performed on the N-terminal-tagged isoforms, similar results were obtained (data not shown).

Immunofluorescence—Localization studies with immunofluorescence were performed using the constructs with either the C-terminal or N-terminal T7-epitope tag (Fig. 5). Using the C-terminal-tagged proteins, an overall staining of the cells was observed in the case of the isoforms G6b-A and G6b-B, which contain potential transmembrane segments. This finding is in line with a localization at the plasma membrane. In contrast, G6b-D and G6b-E showed a pattern consistent with endoplasmic reticulum and Golgi labeling.

In the case of the N-terminal-tagged proteins, staining was performed under both permeabilizing as well as non-permeabilizing conditions. With permeabilizing conditions, the patterns observed were similar to the ones observed with the C-terminal-tagged proteins (Fig. 5*B*). Staining under non-permeabilizing conditions clearly indicated that the G6b forms containing a transmembrane segment (G6b-A and G6b-B) were present at the plasma membrane with the T7-epitope tag outside the cell (Fig. 5*C*). In contrast, G6b-D- and G6b-E-expressing cells showed a completely different pattern when stained under non-permeabilizing conditions compared with permeabilizing conditions. G6b-D-expressing cells showed staining around the edges of the cell, in contrast to G6b-E, where this type of

A
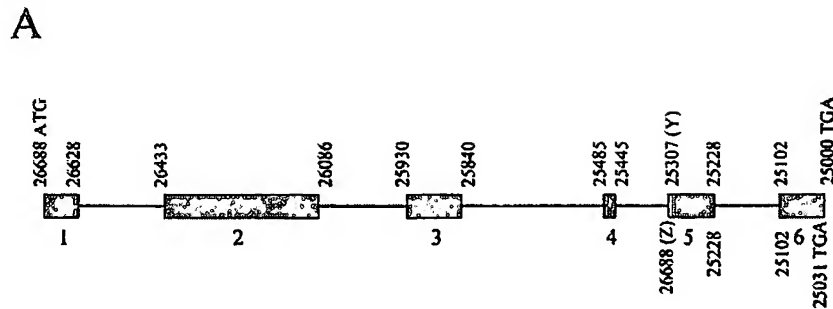
FIG. 2. **Genomic structure and amino acid sequences of the G6b-splice isoforms.** *A,* genomic structure of G6b. The six exons are numbered *1-6.* The *nucleotide numbers* above the exons correspond to GenBank™/EMBL entry AF129756. The two different 5' splice sites of exon 5 are denoted *Y* and *Z.* When exon 5 is spliced at the Y site, the stop codon is located at nt 25000 (G6b-B, G6b-C, and G6b-E). When exon 5 is spliced at the Z site, the stop codon is located at nt 25031 (G6b-A and G6b-D). Exceptions are G6b-F and G6b-G in which the stop codon is located in the intron between exons 5 and 6. *B,* amino acid sequences of the G6b splice variants. For each splice variant, the exon composition is shown. For exon 5, the 5' splice site is denoted as either *Y* or *Z* (in *brackets*). Exon boundaries are shown by a *slash* (*/*), and the intron is indicated with two *slashes* (*//*). The putative signal sequence is *underlined.* The putative transmembrane segment is in **bold.** ITIM sequences are in *italics* and *underlined.*

B

```
G6b-A    exon 1-2-3-4-5(Z)-6
MAVFLQLLPLLLSRAQGNPG/ASLDGRPGDRVNLSCGGVSHPIRWVWAPSFPACKGLSKG
RRPILWASSSGTPTVPPLQPFVGRLRSLDSGIRRLELLLSAGDSGTFFCKGRHEDESRTV
LHVLGDRTYCKAPGPTH/GSVYPQLLIPLLGAGLVLGLGALGLVWWLHR/RLPPQPIRPL
PRF/ALSPPHSSTCENRAPEASKGGRAQDSRGPGPGT/EPALCGSGPSSPQQAPPAVHSG
PC

G6b-B    exon 1-2-3-4-5(Y)-6
MAVFLQLLPLLLSRAQGNPG/ASLDGRPGDRVNLSCGGVSHPIRWVWAPSFPACKGLSKG
RRPILWASSSGTPTVPPLQPFVGRLRSLDSGIRRLELLLSAGDSGTFFCKGRHEDESRTV
LHVLGDRTYCKAPGPTH/GSVYPQLLIPLLGAGLVLGLGALGLVWWLHR/RLPPQPIRPL
PRF/APLVKTEPQRPVKEEEPKIPGDLDQEP/SLLYADLDHLALSRPRRLSTADPADAST
IYAVVV

G6b-C    exon 1-2-4-5(Y)-6
MAVFLQLLPLLLSRAQGNPG/ASLDGRPGDRVNLSCGGVSHPIRWVWAPSFPACKGLSKG
RRPILWASSSGTPTVPPLQPFVGRLRSLDSGIRRLELLLSAGDSGTFFCKGRHEDESRTV
LHVLGDRTYCKAPGPTH/GACPRNRFDHSLDLLCPPHI/APLVKTEPQRPVKEEEPKIPG
DLDQEP/SLLYADLDHLALSRPRRLSTADPADASTIYAVVV

G6b-D    exon 1-2-5(Z)-6
MAVFLQLLPLLLSRAQGNPG/ASLDGRPGDRVNLSCGGVSHPIRWVWAPSFPACKGLSKG
RRPILWASSSGTPTVPPLQPFVGRLRSLDSGIRRLELLLSAGDSGTFFCKGRHEDESRTV
LHVLGDRTYCKAPGPTH/ALSPPHSSTCENRAPEASKGGRAQDSRGPGPGT/EPALCGSG
PSSPQQAPPAVHSGPC

G6b-E    exon 1-2-5(Y)-6
MAVFLQLLPLLLSRAQGNPG/ASLDGRPGDRVNLSCGGVSHPIRWVWAPSFPACKGLSKG
RRPILWASSSGTPTVPPLQPFVGRLRSLDSGIRRLELLLSAGDSGTFFCKGRHEDESRTV
LHVLGDRTYCKAPGPTH/APLVKTEPQRPVKEEEPKIPGDLDQEP/SLLYADLDHLALSR
PRRLSTADPADASTIYAVVV


G6b-F    exon 1-2-3-4-intron-5-6
MAVFLQLLPLLLSRAQGNPG/ASLDGRPGDRVNLSCGGVSHPIRWVWAPSFPACKGLSKG
RRPILWASSSGTPTVPPLQPFVGRLRSLDSGIRRLELLLSAGDSGTFFCKGRHEDESRTV
LHVLGDRTYCKAPGPTH/GSVYPQLLIPLLGAGLVLGLGALGLVWWLHR/RLPPQPIRPL
PRF//GETNSTPFSFSYMPTPHPSIPESEPLLGADTLVTFSPSFSSVPPT

G6b-G    exon 1-2-3-4-5(Z)-intron-6
MAVFLQLLPLLLSRAQGNPG/ASLDGRPGDRVNLSCGGVSHPIRWVWAPSFPACKGLSKG
RRPILWASSSGTPTVPPLQPFVGRLRSLDSGIRRLELLLSAGDSGTFFCKGRHEDESRTV
LHVLGDRTYCKAPGPTH/GSVYPQLLIPLLGAGLVLGLGALGLVWWLHR/RLPPQPIRPL
PRF/ALSPPHSSTCENRAPEASKGGRAQDSRGPGPGT//GKGMGMGRG
```

staining is virtually absent (Fig. 5C). This staining might be explained if the protein sticks to the cell after being secreted.

Pervanadate Treatment and Interaction with SHP-1 and SHP-2—Most inhibitory receptors, either of the Ig superfamily or lectin-like superfamily, contain at least two ITIMs with a typical spacing of 20–32 amino acids in the primary sequence (3) and are known to bind SHP-1 and/or SHP-2 after phosphorylation. G6b-B contains two tyrosine residues in consensus ITIM sequences in its cytoplasmic tail, and the spacing between these two ITIMs is 26 amino acids. To investigate whether this isoform was able to bind SHP-1 and/or SHP-2 after phosphorylation, COS-7 cells expressing the four N-terminal T7-tagged G6b isoforms were treated with pervanadate. In the case of the membrane-bound forms G6b-A and G6b-B, the N-terminal epitope tag (present outside the cell) is expected not to interfere with these interactions, which take place at the cytoplasmic tail. Analysis of total COS-7 lysates by Western blotting with anti-phosphotyrosine antibodies showed that tyrosine phosphorylation in the cells was highly increased due to pervanadate treatment (data not shown). The different G6b isoforms were immunoprecipitated with the anti-T7 mAb from

cells treated or untreated with pervanadate (Fig. 6). Induction of tyrosine phosphorylation on G6b was checked with a phosphotyrosine-specific antibody. Only the G6b-B isoform was found to be tyrosine-phosphorylated after pervanadate stimulation (Fig. 6). In the immunoprecipitate containing tyrosine-phosphorylated G6b-B, both SHP-1 and SHP-2 can be detected by Western blot immunostaining (Fig. 6). The presence of SHP-1 and SHP-2 is strictly dependent on both the presence of the ITIM-containing G6b-B isoform and on the induction of tyrosine phosphorylation by pervanadate on this molecule.

To investigate whether both cytoplasmic tyrosines of G6b-B or just one of them are phosphorylated, three mutant constructs were expressed in COS-7 cells, namely G6b-B(Y211F), G6b-B(Y237F), and G6b-B(Y211F/Y237F). Mutation of Tyr-211 to Phe resulted in a total loss of detectable tyrosine phosphorylation as well as a loss of interaction of G6b-B with SHP-1 and SHP-2 (Fig. 7). Mutation of Tyr-237 to Phe leads to a clearly detectable, although strongly reduced, level of tyrosine phosphorylation and SHP-1 and SHP-2 interaction. These results suggest that Tyr-211 is the only tyrosine residue to be
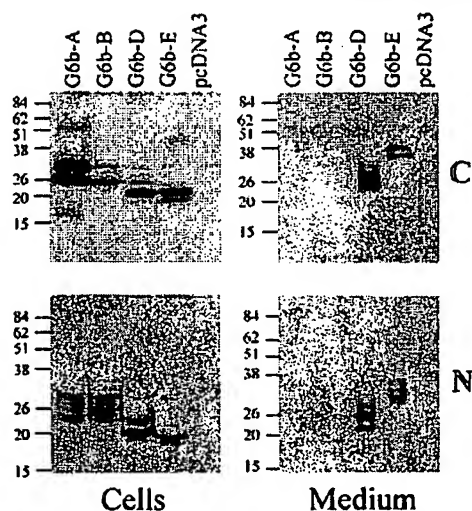
FIG. 3. **Expression of G6b isoforms in COS-7 cells.** The C-terminal (C) and N-terminal (N) T7-epitope-tagged G6b constructs were transiently expressed, and expression was analyzed by Western blot immunostaining using the anti-T7 tag mAb. The negative control cells were transfected with empty pcDNA3 vector. Both medium and cells were analyzed, and samples were run under reducing conditions. Molecular size markers (kDa) are indicated on the *left* of each blot.
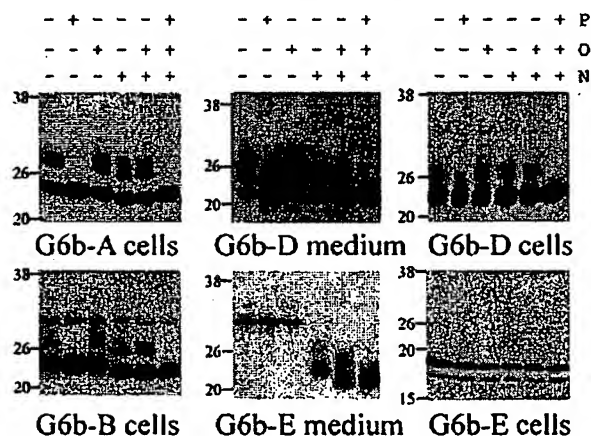
FIG. 4. **Glycosidase treatment of G6b isoforms.** Cell lysates or medium were treated with various glycosidases alone or in combination as indicated and analyzed by Western blot immunostaining with the anti-T7 tag mAb. Molecular size markers (kDa) are indicated on the *left* of each blot. P, N-glycosidase F; O, O-glycosidase; N, neuraminidase.

phosphorylated and to be involved in SHP-1 and SHP-2 binding, even though Tyr-237 is in an ITIM consensus sequence.

To confirm the interaction of G6b-B with SHP-1 and SHP-2 in a human bone marrow-derived cell line, a similar experiment was performed using the human leukemic cell line K562, which expresses G6b at the RNA level (Fig. 1). The two membrane-bound forms of G6b (G6b-A and G6b-B) were expressed in this cell line. Only the G6b-B isoform was phosphorylated upon pervanadate treatment (Fig. 8). Both SHP-1 and SHP-2 can be detected in immunoprecipitates of tyrosine-phosphorylated G6b-B in transfected K562 cells, confirming the results obtained in COS-7 cells.

DISCUSSION

We have characterized the G6b gene located in the class III region of the human MHC, a region known to contain many genes with relevance in the immune system. RT-PCR on cDNA
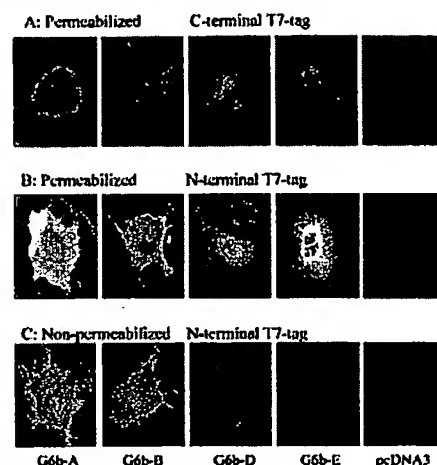
FIG. 5. **Immunofluorescence of G6b isoforms.** The various G6b isoforms were expressed in COS-7 cells as either C-terminal (A) or N-terminal (B and C) T7-epitope-tagged fusions. In the case of the N-terminal-tagged versions, the staining was performed under permeabilizing (B) as well as under non-permeabilizing (C) conditions.
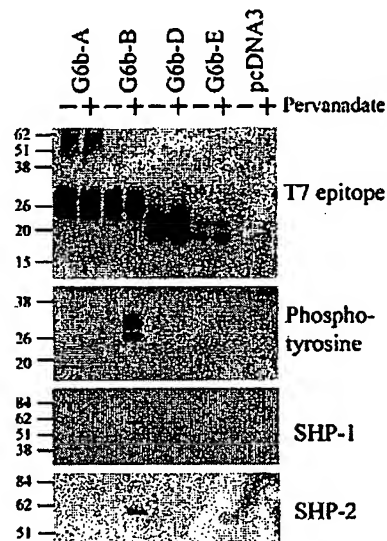
FIG. 6. **Pervanadate treatment of COS-7 cells transfected with the different G6b cDNAs and co-immunoprecipitation of G6b-B with SHP-1 and SHP-2.** Cells expressing T7-epitope-tagged G6b isoforms were untreated (−) or treated (+) with pervanadate, and immunoprecipitations were performed with the anti-T7 mAb. Immunoprecipitates were analyzed by Western blot immunostaining with the anti-T7 mAb, anti-phosphotyrosine mAb, and polyclonal antibodies against SHP-1 and SHP-2. Molecular size markers (kDa) are indicated on the *left* of each blot.

preparations from various human cell lines showed that the G6b gene is only expressed in a restricted set of hematopoietic cell lines, suggesting an immune-related function. Furthermore, it was observed that the RNA derived from this gene is alternatively spliced. One spliced form, which encodes a protein containing two ITIM sequences (G6b-B), appears to be less abundant at the RNA level than the form lacking these motifs (G6b-A). Besides these forms, other variants were detected encoding proteins lacking a transmembrane segment (G6b-D and G6b-E). When expressed in COS-7 cells, these latter forms were secreted, showing that the N-terminal hydrophobic segment indeed serves as a signal sequence.

Glycosidase treatment of the various G6b isoforms provided
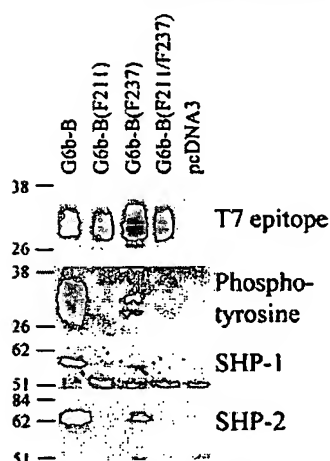
Fig. 7. **Pervanadate treatment of COS-7 cells transfected with the different G6b-B Tyr to Phe mutant cDNAs and co-immunoprecipitation with SHP-1 and SHP-2.** Immunoprecipitations were performed with the anti-T7 mAb. Immunoprecipitates were analyzed by Western blot immunostaining with the anti-T7 mAb, anti-phosphotyrosine mAb, and polyclonal antibodies against SHP-1 and SHP-2. Molecular size markers (kDa) are indicated on the *left* of each blot.
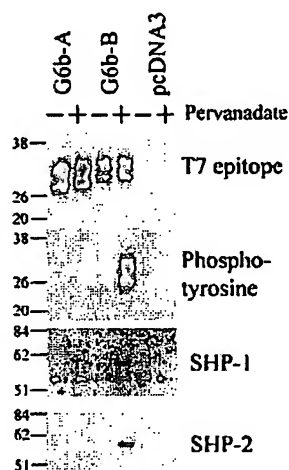
Fig. 8. **Pervanadate treatment of K562 cells transfected with G6b-A and G6b-B cDNAs and interaction with SHP-1 and SHP-2.** K562 cells expressing T7-epitope-tagged G6b-A and G6-B were treated (+) or untreated (−) with pervanadate, and immunoprecipitations were performed using the anti-T7 mAb. Immunoprecipitates were analyzed by Western blot immunostaining with the anti-T7 mAb, anti-phosphotyrosine mAb, and polyclonal antibodies against SHP-1 and SHP-2. Molecular size markers (kDa) are indicated on the *left* of each blot.

evidence that the proteins are both *N*- as well as *O*-glycosylated. The extracellular part of the membrane-bound forms of G6b contains only one consensus *N*-glycosylation site. This site is located in the predicted B-strand of the V-type Ig domain, and the side chain of the asparagine residue (Asn-32) to be glycosylated is likely to be on the surface (see Ref. 29 for a detailed description of V-type Ig domains), making it a suitable residue for glycosylation. Secreted G6b-E contains a relatively high amount of *O*-glycosylation compared with the other isoforms. Because the difference between G6b-D and G6b-E lies in the C-terminal tail, it is likely that there is at least one extra *O*-glycosylation site in this part of G6b-E, which could explain the difference in glycosylation between these two forms. Although G6b-B contains a C terminus identical to the C termi-

nus of G6b-E, in the case of G6b-B, this tail is cytoplasmic and, therefore, not available for glycosylation.

Immunofluorescence with non-permeabilized cells using the N-terminal-tagged constructs showed that the T7 tag is outside the cells in the case of G6b-A and G6b-B. Although these constructs do not carry their own signal sequence, it confirms that the proteins are transported to the plasma membrane and not retained in the endoplasmic reticulum. These observations indicate that these proteins are able to fold correctly in these cells because proteins that are not able to fold correctly are retained in the endoplasmic reticulum and finally broken down (30). For the same reason, it can be assumed that G6b-D and G6b-E are able to correctly fold in COS-7 cells because these variants are secreted into the medium.

Of all the G6b isoforms analyzed, only G6b-B appears to be efficiently phosphorylated when COS-7 and K562 cells expressing this recombinant protein are treated with pervanadate. This is completely in line with expectations as G6b-A does not contain cytoplasmic tyrosine residues and the soluble isoforms do not have a part exposed to the cytoplasmic kinases even though G6b-E contains ITIM sequences identical to G6b-B. The interaction of tyrosine-phosphorylated G6b-B with SHP-1 and SHP-2 could be observed in two different cell lines, one of them (K562) expressing G6b mRNA endogenously. SHP-1 is known to be primarily expressed in hematopoietic cells (4), but we could clearly detect this protein in the monkey fibroblast cell line COS-7.

Although G6b-B contains two tyrosine residues in ITIM consensus sequences in its cytoplasmic tail (Tyr-211 and Tyr-237), site-directed mutagenesis suggested that only one of them (Tyr-211) gets phosphorylated upon pervanadate stimulation of COS-7 cells and that this tyrosine is responsible for SHP-1 and SHP-2 binding. This result was not anticipated because mutagenesis studies with similar receptors containing two tyrosine residues in ITIMs showed the involvement of both residues in SHP-1 or SHP-2 binding (15, 31). It is assumed that in these cases, the tandem SH2 domains of SHP-1 and SHP-2 bind the diphosphorylated receptor with high affinity. However, the absence of detectable tyrosine phosphorylation of the Y211F mutant does not necessarily mean that Tyr-237 does not get phosphorylated in the wild type construct. It cannot be excluded that the phosphorylation of tyrosine 237 is dependent on the prior phosphorylation of tyrosine 211.

It has become clear that inhibitory receptors often have closely related activating homologues that are expressed on the same cell type and are believed to bind similar or identical extracellular ligands (32). Known examples are the killer inhibitory receptor family as well as the Ly49 family (32). In these cases, inhibitory and activating receptors are encoded by different genes. In contrast to the inhibitory proteins, the activating receptors generally have a short cytoplasmic tail lacking ITIM sequences. Furthermore, they possess a positively charged residue in the transmembrane segment involved in binding to signaling effector molecules such as CD3ξ, DAP10, and DAP12 (33, 34). The results obtained in this study with G6b resemble the studies with the mouse natural killer cell receptor 2B4 in which two splice variants exist that differ only in the cytoplasmic tail (35). The longer variant of 2B4 contains four consensus ITIM sequences, interacts with SHP-2 upon tyrosine phosphorylation, and inhibits NK cell-mediated lysis of tumor targets (36). In contrast, the shorter 2B4 isoform contains only one potential ITIM but does not get phosphorylated upon pervanadate stimulation and thus does not recruit SHP-2. This shorter variant has been shown to stimulate NK cell-mediated lysis of tumor targets (36). Analogous to these results, one can speculate that the G6b-A variant is the acti-

vating counterpart of the inhibitory receptor G6b-B. However, both the short form of 2B4 as well as G6b-A lack a positively charged residue in the transmembrane segment, which is in contrast to the killer inhibitory receptor and Ly49 family of activating receptors.

In summary, we have shown that the *G6b* gene located in the class III region of the human MHC is expressed and processed in immune-related cells at the RNA level. Characterization of the different G6b isoforms expressed in mammalian cells is in line with G6b encoding a novel glycosylated cell surface receptor, although soluble variants are found as well. The interaction of G6b-B with SHP-1 and SHP-2 classifies this variant at least as a new member of the family of inhibitory receptors of the Ig superfamily and the first one found so far in the MHC. However, the G6b Ig domain does not contain any significant homology toward other Ig domain-containing proteins with known ligand. Identification of the extracellular ligand might be crucial in understanding the role of the G6b gene product in cellular signaling.

REFERENCES

1. Hunkapiller, T., and Hood, L. (1989) *Adv. Immunol.* **44**, 1–63
2. Williams, A. F., and Barclay, A. N. (1988) *Annu. Rev. Immunol.* **6**, 381–405
3. Vivier, E., and Daeron, M. (1997) *Immunol. Today* **18**, 286–291
4. Zhang, J., Somani, A. K., and Siminovitch, K. A. (2000) *Semin. Immunol.* **12**, 361–378
5. Valiante, N. M., Phillips, J. H., Lanier, L. L., and Parham, P. (1996) *J. Exp. Med.* **184**, 2243–2250
6. Weber, J. R., Orstavik, S., Torgersen, K. M., Danbolt, N. C., Berg, S. F., Ryan, J. C., Tasken, K., Imboden, J. B., and Vaage, J. T. (1998) *J. Exp. Med.* **187**, 1157–1161
7. Binstadt, B. A., Billadeau, D. D., Jevremovic, D., Williams, B. L., Fang, N., Yi, T., Koretzky, G. A., Abraham, R. T., and Leibson, P. J. (1998) *J. Biol. Chem.* **273**, 27518–27523
8. Feng, G. S. (1999) *Exp. Cell Res.* **253**, 47–54
9. Klinghoffer, R. A., and Kazlauskas, A. (1995) *J. Biol. Chem.* **270**, 22208–22217
10. Zhao, Z. J., and Zhao, R. (1998) *J. Biol. Chem.* **273**, 29367–29372
11. Streuli, M. (1996) *Curr. Opin. Cell Biol.* **8**, 182–188
12. Fournier, N., Chalus, L., Durand, I., Garcia, E., Pin, J. J., Churakova, T., Patel, S., Zlot, C., Gorman, D., Zurawski, S., Abrams, J., Bates, E. E., and Garrone, P. (2000) *J. Immunol.* **165**, 1197–1209
13. Cantoni, C., Bottino, C., Augugliaro, R., Morelli, L., Marcenaro, E., Castriconi, R., Vitale, M., Pende, D., Sivori, S., Millo, R., Biassoni, R., Moretta, L., and Moretta, A. (1999) *Eur. J. Immunol.* **29**, 3148–3159
14. Falco, M., Biassoni, R., Bottino, C., Vitale, M., Sivori, S., Augugliaro, R., Moretta, L., and Moretta, A. (1999) *J. Exp. Med.* **190**, 793–802
15. Xu, M., Zhao, R., and Zhao, Z. J. (2000) *J. Biol. Chem.* **275**, 17440–17446
16. Ahmad, S., Banville, D., Zhao, Z., Fischer, E. H., and Shen, S. H. (1993) *Proc. Natl. Acad. Sci. U. S. A.* **90**, 2197–2201
17. Shen, S. H., Bastien, L., Posner, B. I., and Chretien, P. (1991) *Nature* **352**, 736–739
18. The MHC Sequencing Consortium (1999) *Nature* **401**, 921–923
19. Todd, J. A. (1997) *Pathol. Biol.* **45**, 219–227
20. Svejgaard, A., Platz, P., and Ryder, L. P. (1983) *Immunol. Rev.* **70**, 193–218
21. Brown, M. A., Pile, K. D., Kennedy, L. G., Campbell, D., Andrew, L., March, R., Shatford, J. L., Weeks, D. E., Calin, A., and Wordsworth, B. P. (1998) *Arthritis Rheum.* **41**, 588–595
22. Schaffer, F. M., Palermos, J., Zhu, Z. B., Barger, B. O., Cooper, M. D., and Volanakis, J. E. (1989) *Proc. Natl. Acad. Sci. U. S. A.* **86**, 8015–8019
23. Ribas, G., Neville, M., Wixon, J. L., Cheng, J., and Campbell, R. D. (1999) *J. Immunol.* **163**, 278–287
24. Aguado, B., and Campbell, R. D. (1999) *Biochem. J.* **341**, 679–689
25. Milner, C. M., Smith, S. V., Carrillo, M. B., Taylor, G. L., Hollinshead, M., and Campbell, R. D. (1997) *J. Biol. Chem.* **272**, 4549–4558
26. Simmons, D., and Seed, B. (1988) *J. Immunol.* **141**, 2797–2800
27. Laemmli, U. K. (1970) *Nature* **227**, 680–685
28. Aguado, B., and Campbell, R. D. (1998) *J. Biol. Chem.* **273**, 4096–4105
29. Chothia, C., Gelfand, I., and Kister, A. (1998) *J. Mol. Biol.* **278**, 457–479
30. Parodi, A. J. (2000) *Biochem. J.* **348**, 1–13
31. Zhao, R., and Zhao, Z. J. (2000) *J. Biol. Chem.* **275**, 5453–5459
32. Taylor, L. S, Paul, S. P., and McVicar, D. W. (2000) *Rev. Immunogenet.* **2**, 204–219
33. Wu, J., Cherwinski, H., Spies, T., Phillips, J. H., and Lanier, L. L. (2000) *J. Exp. Med.* **192**, 1059–1068
34. Lanier, L. L., Corliss, B., Wu, J., and Phillips, J. H. (1998) *Immunity* **8**, 693–701
35. Stepp, S. E., Schatzle, J. D., Bennett, M., Kumar, V., and Mathew, P. A. (1999) *Eur. J. Immunol.* **29**, 2392–2399
36. Schatzle, J. D., Sheu, S., Stepp, S. E., Mathew, P. A., Bennett, M., and Kumar, V. (1999) *Proc. Natl. Acad. Sci. U. S. A.* **96**, 3870–3875

Decoding Protein−Protein Interactions through Combinatorial Chemistry: Sequence Specificity of SHP-1, SHP-2, and SHIP SH2 Domains[†]

Michael C. Sweeney,[‡,§] Anne-Sophie Wavreille,[‡] Junguk Park,[‡] Jonathan P. Butchar,[∥] Susheela Tridandapani,[§,∥] and Dehua Pei*,[‡,§]

Departments of Chemistry and Internal Medicine and Ohio State Biochemistry Program, The Ohio State University, 100 West 18th Avenue, Columbus, Ohio 43210

ABSTRACT: A general, combinatorial library method for the rapid identification of high-affinity peptide ligands of protein modular domains is reported. The validity of this method has been demonstrated by determining the sequence specificity of four Src homology 2 (SH2) domains derived from protein tyrosine phosphatase SHP-1 and SHP-2 and inositol phosphatase SHIP. A phosphotyrosyl (pY) peptide library was screened against the SH2 domains, and the beads that carry high-affinity ligands of the SH2 domains were identified and peptides were sequenced by partial Edman degradation and mass spectrometry. The results reveal that the N-terminal SH2 domain of SHP-2 is capable of recognizing four different classes of pY peptides. Binding competition studies suggest that the four classes of pY peptides all bind to the same site on the SH2 domain surface. The C-terminal SH2 domains of SHP-1 and SHP-2 and the SHIP SH2 domain each bind to pY peptides of a single consensus sequence. Database searches using the consensus sequences identified most of the known as well as many potential interacting proteins of SHP-1 and/or SHP-2. Several proteins are found to bind to the SH2 domains of SHP-1 and SHP-2 through a new, nonclassical ITIM motif, (V/I/L)XpY(M/L/F)XP, which corresponds to the class IV peptides selected from the pY library. The combinatorial library method should be generally applicable to other protein domains.

Protein−protein interactions are an integral component of many cellular processes such as intracellular signaling. Frequently, the interactions are mediated by modular domains, which recognize small, specific peptide motifs in their partner proteins. The Src homology 2 (SH2) domain was one of the first examples of such domains, which binds to specific phosphotyrosyl (pY)[1] peptides (*1*). A large number of SH2 domains are now known, and it has been estimated that the human genome encodes at least 115 SH2 domains (*2*). Each SH2 domain interacts with a unique subset of pY peptides, and the sequence specificity is primarily determined by the three amino acids immediately C-terminal to pY. Since the initial discovery of the SH2 domain, some 30 other types of modular domains have now been discovered (e.g., SH3, PDZ, FHA, and PTB domains), many of which also recognize various peptide motifs in their target proteins (*3*).

However, for the vast majority of these domains, their sequence specificity or in vivo interaction partners are currently unknown.

One approach to sorting out the complex protein−protein interaction network is to determine the sequence specificity of these modular domains through the screening of combinatorial peptide libraries and then use the consensus sequence-(s) to search the protein databases. Several combinatorial methods have been reported. In their pioneering work with SH2 domains, Cantley and co-workers employed affinity columns containing an immobilized SH2 domain to enrich SH2-binding sequences from a pY peptide library (*4*), a technique later expanded upon by others (*5*). Sequencing of the enriched peptide pool by conventional Edman degradation reveals the preferentially selected amino acid(s) at each position. A variation of this method involved screening support-bound libraries against a fluorescently labeled SH2 domain (*6*). The positive beads with the bound SH2 were removed from the library using a fluorescence-activated bead sorter, and all of the selected beads were pooled and sequenced by Edman degradation. This method of sequencing provides information on the most preferred amino acid-(s) at each position but, importantly, does not give individual sequences. Since the method selects for *both* affinity and abundance of certain types of sequences, a high-affinity peptide of low abundance may not emerge from the consensus sequence(s). A second method involves the iterative synthesis and screening of sublibraries or "positional scanning" (*7*). However, this method suffers from the same

* To whom correspondence should be addressed at the Department of Chemistry, The Ohio State University. Telephone: (614) 688-4068. Fax: (614) 292-1532. E-mail: pei.3@osu.edu.

[‡] Department of Chemistry.

[§] Ohio State Biochemistry Program.

[∥] Department of Internal Medicine.

[1] Abbreviations: BCIP, 5-bromo-4-chloro-3-indolyl phosphate; Nic-OSU, N-hydroxysuccinimidyl nicotinate; MBP, maltose-binding protein; IPTG, isopropyl β-D-thiogalactoside; ITIM, immunoreceptor tyrosine-based inhibition motif; pY, phosphotyrosine; PITC, phenyl isothiocyanate; SH2 domain, Src homology 2 domain; SPR, surface plasmon resonance; TFA, trifluoroacetic acid.

drawbacks as the first method, in addition to being highly labor intensive. In a third method, bacteriophage bearing short random peptide sequences on their surfaces were selected against an immobilized modular domain (8−10). The sequences of the binding peptides were determined by amplifying the bound phage and sequencing their DNA. This method is highly effective for modular domains that recognize unmodified peptides but generally does not work with protein domains that recognize posttranslationally modified peptides (10, 11). Here we describe another method, in which resin-bound peptide libraries are selected against a protein receptor and the positive beads are removed from the library and sequenced by partial Edman degradation, a high-throughput technique recently developed by one of these laboratories. Our method produces a large number of individual sequences, from which a consensus sequence(s) can be derived. This method is applied to determine the sequence specificity of four SH2 domains from phosphatases SHP-1, SHP-2, and SHIP.

EXPERIMENTAL PROCEDURES

Materials. The pMAL-c2 vector, all DNA modifying enzymes, and amylose resin were purchased from New England Biolabs. The pET-28a vector and *Escherichia coli* BL21(DE3) Rosetta CodonPlus strain were purchased from Novagen. All oligonucleotides were purchased from Integrate DNA Technologies. 5-Bromo-4-chloro-3-indolyl phosphate (BCIP), antibiotics, *N*-hydroxysuccinimido-biotin, Sephadex G-25 resin, 4-hydroxy-α-cyanocinnamic acid, and organic solvents were obtained from Sigma-Aldrich. Talon resin for IMAC purification was purchased from Clontech. Reagents for peptide synthesis were from Advanced ChemTech, Peptides International, and NovaBiochem. *N*-Hydroxy-succinimidyl nicotinate (Nic-OSU) was from Advanced ChemTech and was recrystallized from ethyl acetate prior to use. Phenyl isothiocyanate was purchased in 1 mL sealed ampules from Sigma-Aldrich and used without purification. Protein concentration was determined by the Bradford method using bovine serum albumin (Sigma-Aldrich) as standard. The Raw 264.7 murine macrophage cell line was obtained from ATCC and maintained in RPMI supplemented with 10% heat-inactivated fetal bovine serum (FBS) and 1% penicillin/streptomycin, as described previously (12).

SH2 Domain Constructs. A pET-MAL vector was created by subcloning the *malE* gene from pMAL-c2 into pET-28a with the retention of all pMAL-c2 multiple cloning sites. The DNA sequences coding for the SHP-2 N-SH2 domain (aa 1−106), C-SH2 domain (aa 108−220), and SHIP SH2 domain (aa 1−109) were isolated by polymerase chain reaction (PCR) from plasmids pET22-SHP2 (13) and pGEX2T-SHIP (14), respectively. The DNA primers used were as follows: N-SH2, T7 promoter primer, and 5′-AGAT-TAGAAGCTTTCAATCTGCACAGTTCAGAGGATATT-TAAGCA-3′; C-SH2, 5′-ATATAGAATTCATGACCTCT-GAAAGGTGGTTTCATGGACA-3′ and 5′-AGATTAGAAG-CTTTCAACGAGTCGTGTTAAGGGGCTGCT-3′; SHIP SH2, 5′-GCGAATTCATGCCTGCCATGGTCCCTGG-3′ and 5′-CGTCCAAGCTTCACTCCTCCTCCAGGGGCAC-5′. The PCR products were digested with restriction endonucleases *Eco*RI (*Nde*I in the case of N-SH2 domain) and *Hind*III and ligated into their corresponding sites in pET-MAL. This

C-terminus of maltose-binding protein (MBP), facilitating both purification and biotinylation. In addition, each SH2 domain was constructed in its isolated form containing an N-terminal six-histidine tag. This was carried out in a similar manner as described above, except that the PCR products were ligated into plasmid pET-28a instead. The identity of all DNA constructs was confirmed by dideoxy sequencing. SHP-1 SH2 domain constructs have previously been described (15). Recombinant full-length SHP-1 and SHP-2 were prepared as previously described (13, 15).

Purification and Biotinylation of MBP-SH2 Proteins. E. *coli* BL21(DE3) cells harboring the proper pET-MAL-SH2 plasmid were grown in LB medium to the mid-log phase and induced by the addition of 300 μM isopropyl β-D-thiogalactoside (IPTG) for 2.5 h at 30 °C. The cells were harvested by centrifugation and lysed in the presence of protease inhibitors by passing through a French press. The MBP-SH2 protein was purified from the crude lysate on an amylose column according to manufacturer's recommended procedures. The protein was concentrated in an Amicon concentrator to approximately 4 mg/mL (in 20 mM HEPES, pH 8.2, 150 mM NaCl, 2 mM 2-mercaptoethanol, and 10 mM maltose) and treated with 2 equiv of *N*-hydroxysuccin-imido-biotin at room temperature for 45 min. Excess biotin was removed by passing the solution through a Sephadex G-25 column. After concentration and addition of glycerol (final 40%), the protein was quickly frozen in a dry ice/2-propanol bath. MBP alone was prepared and labeled in the same manner as a control.

Purification of Histidine-Tagged SH2 Domains. N-Ter-minally histidine-tagged SH2 domains were expressed in a Rosetta CodonPlus strain of *E. coli* BL21(DE3) cells. Protein expression was induced by the addition of 300 μM IPTG at 30 °C for 3 h. The cells were lysed in a French pressure cell, and the crude lysate was loaded onto a Talon cobalt affinity column (10 mL). After extensive washing, the SH2 protein was eluted with 125 mM imidazole and passed through a size exclusion column (XK-16 Superdex-75) connected to an FPLC system (Pharmacia). The elution buffer contained 10 mM HEPES, pH 7.4, 150 mM NaCl, 3 mM EDTA, and 10 μM tris(carboxyethyl)phosphine. All proteins were flash frozen without the addition of glycerol.

Synthesis of the pY Library. The library was synthesized on 5 g of 90 μm TentaGel S NH$_2$ resin using standard Fmoc chemistry employing HBTU/HOBt/DIPEA as the coupling reagents. The invariant positions (LNBBRM and pY) were synthesized with 4 equiv of Fmoc-amino acids, and the coupling reaction was terminated after ninhydrin tests were negative. The random positions were synthesized using the split-synthesis method (7, 16, 17). The coupling reactions employed 5 equiv of Fmoc-amino acids and were allowed to proceed for 45 min, after which the coupling reaction was repeated once to ensure complete reaction. To facilitate sequence determination by mass spectrometry, 5% Ac-Gly was added to the coupling reactions of Leu and Lys, whereas 5% Ac-Ala was added to the coupling reactions of Nle (18). After removal of the terminal Fmoc group, the resin-bound library was washed with dichloromethane and deprotected using reagent K [7.5% phenol, 5% water, 5% thioanisole, 2.5% ethanedithiol, 1% anisole, and 1% triisopropylsilane in trifluoroacetic acid (TFA)] at room temperature for 60

dichloromethane, and methanol before drying for storage at −20 °C.

Library Screening. In a micro-BioSpin column (0.8 mL, Bio-Rad), 100 mg of the pY library was swollen in dichloromethane, washed extensively with methanol, ddH₂O, and HBST buffer (30 mM HEPES, pH 7.4, 150 mM NaCl, and 0.05% Tween 20), and blocked for 1 h with 800 μL of HBST buffer containing 0.1% gelatin. The resin was drained and resuspended in 800 μL of a biotinylated MBP-SH2 domain of interest (10−50 nM final concentration) in HBST buffer plus 0.1% gelatin. After overnight incubation at 4 °C with gentle mixing, the resin was drained and resuspended in 800 μL of SAAP buffer (30 mM Tris, pH 7.6, 1 M NaCl, 10 mM MgCl₂, 70 μM ZnCl₂, and 20 mM potassium phosphate) containing 1 μL of streptavidin−alkaline phosphatase (Prozyme, ~1 mg/mL). After 10 min of gentle mixing at 4 °C, the resin was rapidly drained and washed with 400 μL of SAAP buffer, 400 μL of HBST buffer, and 400 μL of staining buffer (30 mM Tris, pH 8.5, 100 mM NaCl, 5 mM MgCl₂, and 20 μM ZnCl₂). The resin was then transferred into a 35 mm Petri dish by rinsing with 5 × 300 μL of the staining buffer. Upon the addition of 80 μL of 5 mg/mL BCIP in the staining buffer, intense turquoise color developed on positive beads in ~45 min, when the staining reaction was quenched by the addition of 3 mL of 8 M guanidine hydrochloride. The resin was transferred back into the BioSpin column, extensively washed with water, and replated in the Petri dish, from which colored beads were picked manually using a pipet under a dissecting microscope. The positive beads were sorted by color intensity into "intense", "medium", and "light" categories. Control experiments with biotinylated MBP produced no colored beads under identical conditions.

Partial Edman Degradation and Peptide Sequencing. The positive beads from each color intensity category were pooled and subjected to partial Edman degradation as previously described (*18*). The beads were suspended in 66% pyridine (aq) containing 0.1% Et₃N, to which was added an equal volume of 5% phenyl isothiocyanate (PITC) in pyridine containing a variable amount of Nic-OSU. After rapid mixing, the reaction was allowed to proceed for 6 min. The beads were washed with methanol, dichloromethane, and TFA and suspended in TFA (2 × 6 min). After extensive washing with CH₂Cl₂ and pyridine, the cycle was repeated. An optimized procedure was established for this library by trial and error using unselected beads and employed varying PITC/Nic-OSU ratios as follows: 6:1 for the N-terminal T and A; 4.5:1 for the N-terminal random positions; no Nic-OSU during pY degradation; and 5:1 for the C-terminal random positions. Finally, the linker sequence was capped by Nic-OSU in the absence of PITC. The beads were then treated for 20 min with ~1 mL of TFA containing NH₄I (10 mg) and Me₂S (20 μL) on ice to reduce any oxidized methionine. The beads were washed with ddH₂O, placed in individual microcentrifuge tubes, and treated overnight in the dark with 20 μL of 70% TFA containing CNBr (20 mg/ mL). After evaporation to dryness, the peptides were dissolved in 5 μL of 0.1% TFA in water. One microliter of the peptide solution was mixed with 2 μL of 0.1% TFA in 50% acetonitrile saturated with 4-hydroxy-α-cyanocinnamic acid and spotted onto a 96-well sample plate. Mass spectrometry was performed on a Bruker Reflex III MALDI-

TOF instrument in an automated manner. Sequence determination from the mass spectra was performed manually.

Synthesis of Biotinylated pY Peptides. All pY peptides contained a common C-terminal linker, -LNBKR-NH₂. Each peptide was synthesized on ~65 mg of CLEAR-amide resin using standard Fmoc/HBTU/HOBt chemistry. The N-terminus was acetylated by the treatment of Ac₂O. Cleavage and deprotection were carried out using reagent K as described above. Approximately 3 mg of the crude peptide was dissolved in a minimal volume of DMSO (300−500 μL, with sonication) and reacted with 1 equiv of NHS-PEG₄-biotin (Quanta Biochem) in 25 μL of DMSO. After 45 min at room temperature, the mixture was triturated twice with 20 volumes of Et₂O. The precipitate was collected and dried under vacuum. The biotinylated pY peptide was purified by reversed-phase HPLC on a C₁₈ column (Vydac 300 Å, 4.6 × 250 mm). The identity of each peptide was confirmed by MALDI-TOF mass spectrometric analysis. This procedure resulted in the addition of a 15-atom hydrophilic linker between the side chain of the C-terminal lysine and the carboxyl group of biotin.

Determination of Dissociation Constants by Surface Plasmon Resonance (SPR). All measurements were made with the isolated SH2 domains containing an N-terminal histidine tag at room temperature on a BIAcore 3000 instrument. A sensorchip containing immobilized streptavidin was conditioned with 1 M NaCl in 50 mM NaOH (aq) according to manufacturer's instructions. The biotinylated pY peptides were immobilized onto the sensorchip by flowing 6 μL of ~8 μM pY peptide solution in HBS-EP buffer (10 mM HEPES, pH 7.4, 150 mM NaCl, 3 mM EDTA, and 0.005% polysorbate 20). Data for the secondary plot analysis were acquired by passing increasing concentrations (0−5 μM) of an SH2 protein in HBS-EP buffer over the sensorchip for 2 min at a flow rate of 15 μL/min. A blank flow cell (no immobilized pY peptide) was used as control to correct for any signal due to the solvent bulk and/or nonspecific binding interactions. In fact, neither significant bulk effect nor nonspecific binding was observed. In between two runs, the sensorchip surface was regenerated by flowing a strip solution (10 mM NaCl, 2 mM NaOH, and 0.025% SDS in H₂O) for 5−10 s at a flow rate of 100 μL/min. The equilibrium response unit (RU_{eq}) at a given SH2 protein concentration was obtained by subtracting the response of the blank flow cell from that of the sample flow cell. The dissociation constant (K_D) was obtained by nonlinear regression fitting of the data to the equation:

$$RU_{eq} = RU_{max}[SH2]/(K_D + [SH2])$$

where RU_{eq} is the measured response unit at a certain SH2 protein concentration and RU_{max} is the maximum response unit.

Peptide Pull-Down Assays. Briefly, Raw 264.7 cells were lysed in TN1 lysis buffer (50 mM Tris, pH 8.0, 10 mM EDTA, 10 mM Na₄P₂O₇, 10 mM NaF, 1% Triton X-100, 125 mM NaCl, 10 mM Na₃VO₄, and 10 μg/mL each of aprotinin and leupeptin). Nuclei were removed by centrifugation for 10 min at 13000 rpm at 4 °C. Equal amounts of protein from each sample were incubated overnight with 5 μg of biotinylated pY peptides at 4 °C. Streptavidin−agarose beads were added to the samples, which were then incubated

for 1 h at 4 °C. Beads were washed twice in TN1 buffer and boiled in SDS—PAGE sample-loading buffer (60 mM Tris, pH 6.8, 2.3% SDS, 10% glycerol, 0.01% bromophenol blue, and 1% 2-mercaptoethanol) for 5 min, and the eluted proteins were separated by SDS—PAGE. Following gel electrophoresis, proteins were transferred to nitrocellulose membranes and incubated overnight at 4 °C with anti-SHP1 (rabbit polyclonal antibody from Upstate Biotechnology), anti-SHP2 (rabbit polyclonal antibody from Santa Cruz Biotechnology), or anti-SHIP (rabbit polyclonal antibody, a kind gift from Dr. K. Mark Coggeshall, Oklahoma Medical Research Foundation, Oklahoma City, OK). After washing, the blots were incubated with horseradish peroxidase-conjugated secondary antibodies, washed again, and briefly incubated in ECL (Amersham) for chemiluminescent detection on X-ray films. For experiments involving purified SHP-1 and SHP-2 proteins, 5 μg of biotinylated pY peptide was incubated with 1 μg of the purified proteins in TN1 buffer. The pY peptide—protein complexes were captured with streptavidin—agarose beads and analyzed as described above.

RESULTS

Library Design, Synthesis, and Screening. To demonstrate the effectiveness of the combinatorial method, we chose to determine the sequence specificity for the SH2 domains of protein tyrosine phosphatases SHP-1 and SHP-2 and inositol phosphatase SHIP. SHP-1 and SHP-2 belong to a subfamily of PTPs which each contain two SH2 domains N-terminal to their catalytic domain, whereas SHIP contains a single SH2 domain. All three proteins are involved in a variety of signaling pathways (*19*). Despite their sequence homology, SHP-1 and SHP-2 have very different in vivo functions. For example, SHP-2 generally acts as a *positive* regulator for the various signaling pathways, whereas SHP-1 primarily acts as a *negative* regulator of signaling events (*19*). Some studies show that SHP-1, SHP-2, and SHIP recognize distinct pY motifs on various receptors via their SH2 domains, while others report that the three enzymes can compete for binding to a common receptor bearing one or more immunoreceptor tyrosine-based inhibition motifs (ITIMs) (*20*). These data suggest that the SH2 domains in SHP-1, SHP-2, and SHIP have distinctive but partially overlapping specificities. Therefore, a detailed study on their sequence specificities would be very helpful in identifying their physiological targets and determining their cellular functions.

The specificity of an SH2 domain is primarily determined by the pY residue and the three residues immediately C-terminal to pY (*21*—*23*), although it has been reported that, for a few SH2 domains including those of SHP-1 and SHP-2, the −2 position (two residues N-terminal to pY, which is position 0) is also important for high-affinity interaction (*15, 24*). Thus, we designed a pY library, H$_2$N-TAXXpYXXX-LNBBRM-resin, where X represents norleucine (Nle) or any of the 18 natural amino acids except for Met and Cys and B is β-alanine. The N-terminal dipeptide (TA) helps to reduce potential bias caused by electrostatic interactions between an SH2 protein and the free N-terminus (which is required for peptide sequencing). At the C-terminus, a methionine permits the release of peptides from the resin by CNBr treatment prior to sequencing, while arginine serves to increase peptide solubility and sensitivity during MALDI-

two β-alanines add flexibility to the peptides, making them more accessible to a protein target. The dipeptide LN is added to shift the masses of the peptides to >600 Da, so that their mass spectral peaks do not overlap with matrix signals (vide infra). Methionine is excluded from the randomized positions to avoid internal cleavage during CNBr treatment and is replaced by the isosteric Nle residue. The library was synthesized on TentaGel S NH$_2$ resin ($\sim$90 μm in diameter and $\sim$2.86 $\times$ 10^6 beads/g) using the split-pool method (*7, 16, 17*) with each bead carrying $\sim$100 pmol of a unique sequence. This method ensures equal representation of all possible sequences in the library.

The theoretical diversity of the above library is 19^5 or 2.5 $\times$ 10^6. A typical screening involved $\sim$100 mg of resin, which covers $\sim$11% of the sequence space. The resin was incubated with a small amount of an SH2 domain protein (10—50 nM final concentration), constructed as an MBP fusion protein, and biotinylated on a surface lysine residue(s). Binding of the biotinylated SH2 domain to a resin-bound pY peptide recruits a streptavidin—alkaline phosphatase conjugate to the surface of that bead. Upon the addition of BCIP, the bound alkaline phosphatase cleaves BCIP into an indole, which dimerizes to form a turquoise precipitate deposited on the bead surface. As a result of this reaction cascade, beads that carry high-affinity SH2 ligands become colored. The number of colored beads depends on the binding affinity and specificity of the protein domain as well as the stringency of the screening conditions (e.g., SH2 domain concentration, number of washings, and length of staining time). The screening reactions were controlled so that 10—100 colored beads were obtained from 100 mg of resin ($\sim$286000 beads). The number of positive beads was quite reproducible when multiple screenings were performed against the same SH2 domain. Positive beads were manually removed from the library using a micropipet with the aid of a dissecting microscope.

Peptide Sequencing by Partial Edman Degradation and Mass Spectrometry. Individual sequence determination for a large number of selected beads presented an insurmountable challenge in the past, because Edman sequencing is both expensive and time-consuming. To this end, we have recently developed an inexpensive, high-throughput peptide sequencing technique, termed "partial Edman degradation", which is ideally suited for sequencing resin-bound peptides (*18*). Briefly, resin-bound peptides are treated with a $\sim$5:1 mixture of PITC and Nic-OSU followed by TFA (Figure 1a). This results in the removal of the N-terminal amino acid from 90% to 95% of the peptides (Edman degradation); for the remaining 5—10% of the peptides on each bead, reaction with Nic-OSU results in permanent N-terminal acylation and retention of the N-terminal residue (no degradation). Repetition of the above procedure produced a peptide ladder, which was subsequently analyzed by MALDI mass spectrometry. Figure 1b shows the mass spectrum of a single bead carrying the sequence TA(Nle)YpYATILNBBRM. Note that the isobaric residues Nle, Leu, and Ile are unambiguously resolved in the spectra by their appearance as a singlet (Ile) vs doublet peaks (Nle and Leu) (*18*).

Specificity of the C-SH2 Domain of SHP-2. Screening of the above library (100 mg) against 10 nM C-terminal SH2 domain of SHP-2, MBP-CSH2, resulted in 14 intensely
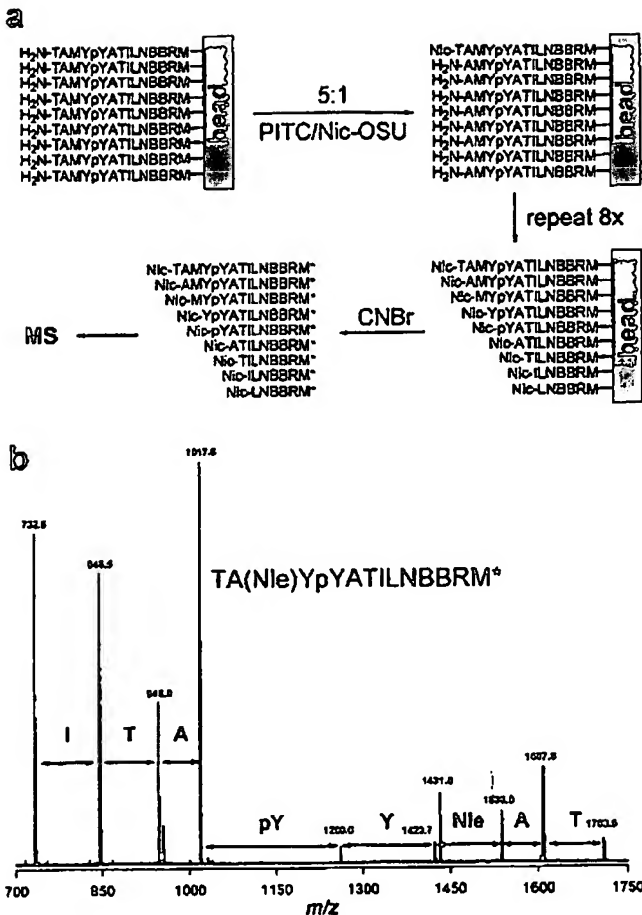
FIGURE 1: Peptide sequencing by partial Edman degradation and mass spectrometry. (a) Scheme showing the reactions involved in the degradation of a resin-bound peptide, TAMYpYATILNBBRM. (b) MALDI mass spectrum of the peptide and its truncation products (derived from a single 90 μm bead). A doublet at m/z 1423.7 and 1431.8 indicates that the residue N-terminal to tyrosine is a norleucine. Key: M, methionine at the C-terminus or norleucine at internal positions; M*, homoserine lactone.

Table 1: Selected SHP-2 C-SH2 Domain-Binding Sequences (77 Total)[a]

VIpYANI	VLpYAII	VTpYSQI	TRpYAVV
VIpYANI	VYpYAII	*YTpYSQI*	TYpYAVV
IEpYAQI	VYpYAII	*VEpYSEI*	VTpYAIV
YTpYAQI	TQpYAII	TYpYSMI	*IHpYATV*
AIpYASI	SNpYAII	TFpYSRI	*TVpYASV*
YSpYASI	MYpYAII	YYpYSRI	*TRpYAKV*
IWpYASI	YQpYAII	TRpYTQI	IIpYSQV
THpYASI	INpYAMI	VIpYTQI	VIpYSSV
TIpYATI*	THpYAMI	VTpYTSI	VIpYSVV
TSpYATI	TMpYAMI	VFpYTTI	TQpYSIV
VTpYATI	TTpYAAI	HFpYTTI	TVpYSIV
VGpYATI	*YKpYARI*	TIpYTVI	TIpYSMV
LYpYATI	*YMpYAHI*	TIpYTII	TVpYSEV
*NApYATI**	YMpYAEI	TYpYTMI	TVpYTEV
VApYAVI	ILpYSTI	TIpYTEI	TVpYASL
VHpYAVI	TTpYSTI	TYpYVEI	VYpYATL
IApYAVI	VHpYSTI	IQpYVQI	YLpYATL
IHpYAVI	TYpYSSI	TKpYVVI	IQpYAVL
PIpYAVI	IVpYSQI	TLpYAVV	TApYAIL
NMpYAVI			

[a] All sequences were obtained from a screening experiment performed with 10 nM SHP-2 C-SH2 domain. Key: bold type, peptides from the most intensely colored beads: roman type, peptides from beads of medium color intensity; italic type, sequences from the lightly colored beads; *, peptides selected for SPR analysis; M, norleucine.

intermediate color intensity. The beads (79 total) were separated into three pools according to their color intensity ("intense", "intermediate", and "light"), placed in three different vessels, and subjected to partial Edman degradation. The degraded beads were then separated into individual microcentrifuge tubes and treated with CNBr, and the released peptides were analyzed by MALDI-TOF MS. Out of the 79 samples, 77 produced high-quality spectra, allowing for unambiguous determination of their peptide sequences (Table 1). The mass spectra for the remaining two beads had one or more peaks missing, preventing complete sequence assignment. The 77 sequences were sorted according to the frequency of amino acid occurrence at position +3 followed by alphabetical order at positions +1 and +2 using the Microsoft Excel program. Inspection of selected sequences indicates that this SH2 domain strongly prefers a nonpolar aliphatic residue at the +3 position, with isoleucine being the most preferred amino acid (present in 57 selected peptides), followed by valine (present in 15 peptides) and leucine (present in 5 sequences) (Figure 2). The +1 position has the second most stringent requirement, strongly preferring an alanine (present in 46 peptides) or other small amino acids such as serine (present in 18 sequences), threonine (present in 10 sequences), and valine (present in 3 sequences). The −2 position is also critical for binding to the C-SH2 domain

threonine, valine, and isoleucine, which are occasionally replaced by a tyrosine. There is a weak preference for a β-branched residue at the +2 position and virtually no selectivity at the −1 position.

To test whether the library screening result is reproducible, the above experiment was repeated with 50 nM MBP-CSH2 protein under otherwise identical conditions. Ninety intensely colored and ~150 less colored beads were obtained and sequenced (see Table S1 in Supporting Information for individual sequences). A plot of the frequency of appearance for each amino acid (based on the 90 intensely colored beads) produced a pattern indistinguishable from that derived from the 10 nM screening (Figure 2). These results allow us to draw the following conclusions. First, the SHP-2 C-SH2 domain recognizes a single consensus sequence (T/V/I/y)-XpY(A/s/t/v)X(I/v/l), where lower case letters represent less frequently selected residues and X is any amino acid except for glycine and proline. Second, the screening method is highly reproducible and robust. Finally, one can unambiguously determine the sequence specificity of an SH2 domain by screening just a fraction of the complete library (~11% in this case), because not all of the randomized positions are crucial for SH2 binding. The same conclusion (the validity of using incomplete libraries) was also borne out of our earlier work with FHA domains (25). This greatly reduces the cost and time required for the characterization of each SH2 domain.

Specificity of the N-SH2 Domain of SHP-2. Initial screening of 100 mg of the library against 10 nM SHP-2 N-SH2 domain gave rather surprising results; the N-SH2 domain appeared to bind pY peptides of several distinct classes. To obtain additional sequences for more reliable analysis, the screening experiment was repeated twice, once at 10 nM and another at 50 nM N-SH2 protein. Again, the results were highly reproducible, with all three screenings producing the same types of sequences. All together, 150 intensely colored
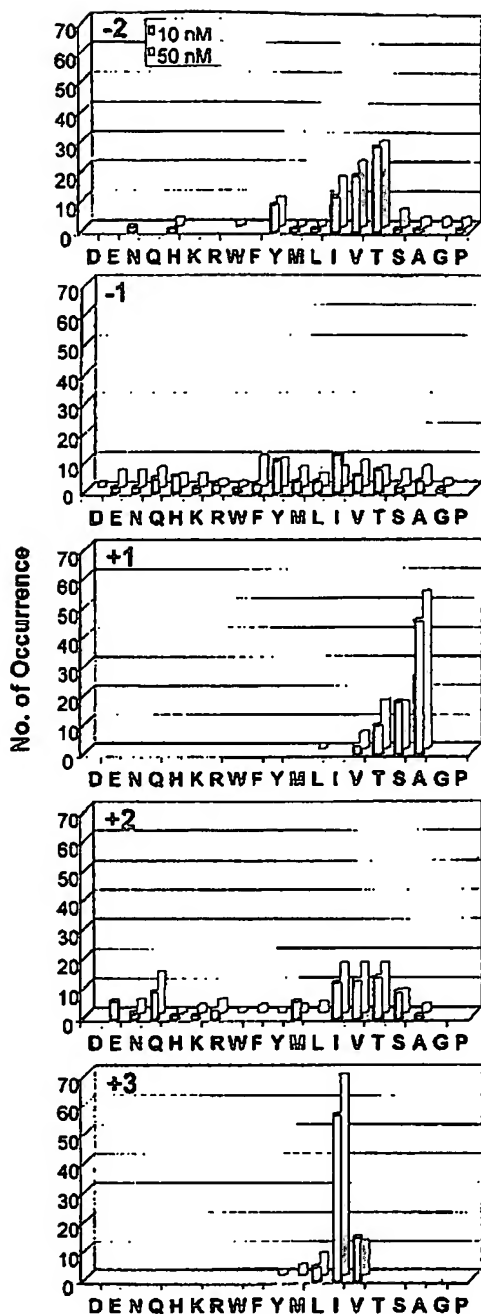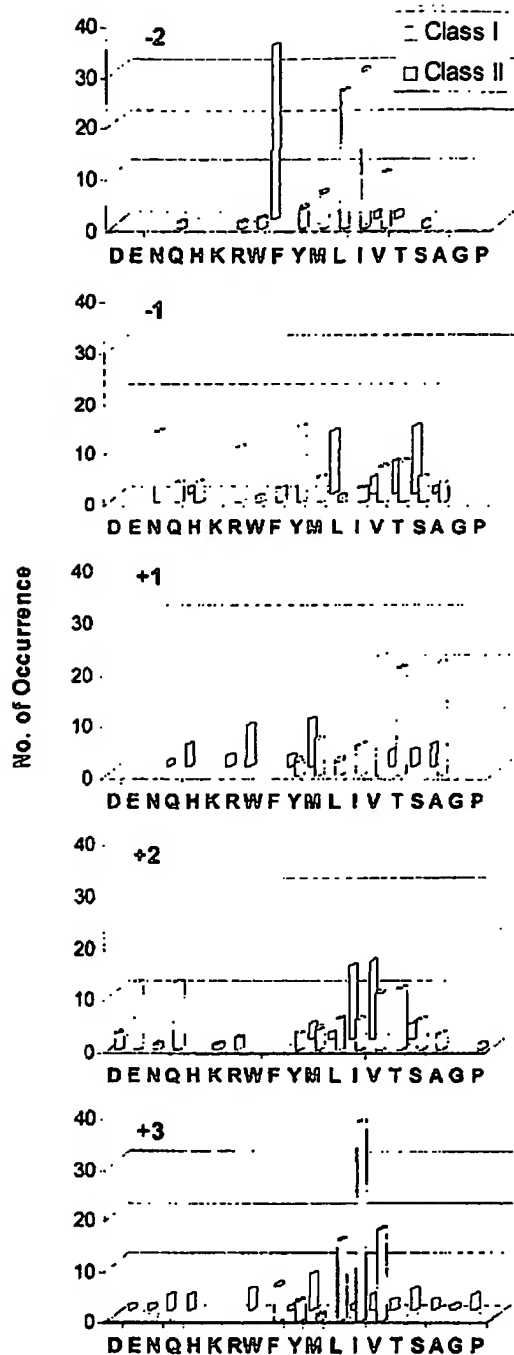
FIGURE 2: Specificity of the C-SH2 domain of SHP-2. Displayed are the amino acids identified at each position from −2 to +3 relative to pY (position 0). Number of occurrence on the y axis represents the number of selected sequences that contain a particular amino acid at a certain position. Key: open bar, results from screening at 10 nM C-SH2 protein (total 77 sequences); closed bar, results from screening at 50 nM C-SH2 protein (total 90 sequences); M, norleucine.

Table 2: Selected SHP-2 N-SH2 Domain-Binding Sequences (150 Total)[a]

class I		class II	class III	class IV
IVpYADI	LRpYIQV	WIpYFIR	ITpYLIG	LVpYMGP
LFpYAEI	IFpYTAV	VQpYFIR	YTpYLVA	LHpYMGP
VMpYAEI	ILpYTEV	WMpYKIY	IHpYLYA*	ALpYMIP
LHpYAII	ITpYTEV	WSpYKIY	TLpYLYA	ILpYMIP
VVpYAII	LVpYTEV*	WMpYNIG	LNpYLYM	WMpYMMP
VTpYALI	IYpYTPV	WTpYQIL*	VLpYLYP	VLpYMQP*
LYpYANI	YIpYTTV	WTpYQIT	IFpYLYS	VMpYMQP
IRpYAQI	IRpYTYV	WVpYRID	VMpYLYS	TEpYMVP
MYpYARI	MNpYVIV	WMpYRII*	IVpYLYT	ILpYFIP
SYpYASI	WSpYVLV	WIpYTIG	PMpYMIA	IVpYFVP
LVpYATI*	MHpYVQV	WVpYTIN	VVpYMYS	VIpYFVP*
LYpYATI	LRpYVRV	WTpYVIT	VTpYMYT	IIpYFYP
MYpYATI	LHpYVSV	WVpYYIG	VVpYMYT	
MYpYATI	LRpYVSV	WMpYYIQ	IIpYTIG	
YApYATI	WMpYYQV	WVpYYIR	IKpYTYP	
LNpYAVI	LRpYAKL	WMpYQLS	IMpYTYP	
LRpYAVI	IVpYAML	WVpYRLE	ITpYTYP*	
ISpYIEI	VIpYAQL	WMpYRLI	YVpYTYT	
LNpYIVI	LRpYMQL	ITpYRLV		
LYpYLQI	IQpYMVL	WMpYRLY		
LNpYMTI	IVpYTLL	WTpYSLA		
IFpYTAI	VNpYTTL	WTpYSLQ		
YVpYTAI	IApYVEL	WTpYSLY		
IMpYTDI	IRpYVEL	WMpYTLN		
IYpYTDI	VApYVEL*	WTpYVLY		
VYpYTEI	IQpYVML	WTpYYLF		
IMpYTII	IQpYVML	WTpYYLI		
VTpYTII	JNpYVQL	WMpYYLT		
VTpYTLI	VTpYVQL	WMpYYLY		
VYpYTQI	MNpYVTL	WMpYRMN		
ISpYTYI	RApYIVM	WTpYVTS		
ITpYTYI	LYpYATF	WIpYYTR		
INpYVEI	LNpYMTF*	WVpYYTY		
IHpYVMI	MSpYMVF	WTpYQYV		
INpYVQI	YNpYMVF	WMpYRYQ		
IWpYVSI	LYpYTSF	WTpYSYT		
LRpYVSI	LNpYVIF			
LTpYVTI	LNpYVLF			
IIpYVVI	ITpYLVY			
LYpYAQV	LRpYLVY			
INpYIEV	QMpYYLY			
ISpYIEV	LYpYYQY			

[a] Boldfaced sequences represent the intensely colored beads from screenings under the most stringent conditions (10 nM N-SH2 domain). Peptides labeled with asterisks were selected for SPR analysis. M = norleucine.

preferred residues for the N-SH2 domain. At the +1 position, while the C-SH2 domain strongly prefers alanine to serine, threonine, or valine. the N-SH2 domain selected threonine, valine, and alanine with equal frequency (but not serine). Sequence covariance is also observed, with pY(A/T)XI, pY-(T/V)XV, pYVXL, and pY(M/V)XF motifs being frequently selected.

The second most abundant class of peptides (class II) has the consensus of W(M/T/v)pY(y/r)(I/L)X, where the −2 residue is almost always a tryptophan and the −1 position is usually norleucine, threonine, or valine (Table 2 and Figure 3). Remarkably, while the +2 position is highly variable among class I peptides, it is the most invariant position on the C-terminal side of pY for class II peptides. The identity of the most preferred residues (Ile and Leu) suggests that the +2 side chain is engaged in hydrophobic interactions with the SH2 domain. Consistent with this binding mode, the selected +1 and +3 residues are variable and contain predominantly hydrophilic (e.g., Tyr, Arg, Gln, and Thr) or

sequences are listed in Table 2 (the most colored beads from 10 nM screenings are shown in boldface). Additional sequences from less colored beads are listed in Table S2 under Supporting Information. The selected sequences can be sorted into four different classes using the Excel program by grouping homologous sequences together. The most abundant class (class I) has a consensus sequence of (I/L/V/m)XpY(T/V/A)X(I/V/L/f), which is similar to that of the C-SH2 domain, albeit with some subtle differences at the −2 and +1 positions (Figure 3). While the C-SH2 domain most prefers a threonine at the −2 position, threonine was not found among any of the N-SH2-binding peptides (class I). On the other hand, leucine is seldom selected at the −2

FIGURE 3: Specificity of the N-SH2 domain of SHP-2. Displayed are the amino acids identified at each position (−2 to +3). Number of occurrence on the y axis represents the number of selected sequences that contain a particular amino acid at a certain position. Key: open bar, class I peptides; closed bar, class II peptides; M, norleucine.

Table 3: pY Peptides Selected against the SHIP SH2 Domain (158 Total)[a]

TMpYAFI	FApYSYL	VYpYYYL	AGpYVFM
PYpYSFI	VYpYSYL	IKpYYYL	DGpYVLM
PFpYSFI	NYpYSYL	FMpYYYL	HPpYVLM
PApYSMI	**VYpYTLL**	QTpYFLM	PLpYVLM
PFpYSVI	TGpYTLL	SGpYFLM	YDpYVLM
PApYSYI	IQpYTLL	YGpYFLM	LGpYVMM
VYpYSYI	YMpYTLL	PPpYSFM	WApYVMM
AYpYSYI	FFpYTLL	AMpYSFM	EGpYVYM
TYpYTFI	SSpYTLL	YQpYSIM	VGpYVYM
PYpYTLI	NGpYTLL	**FVpYSLM**	GGpYYFM
PFpYTLI	NMpYTLL	YFpYSLM	EGpYYFM
GYpYTLI	GApYVFL	PPpYSMM	**GTpYYLM**
GPpYTLI	**VGpYVLL**	YGpYSMM	GYpYYLM
GGpYTMI	SLpYVLL	QGpYSMM	AVpYYLM
YYpYTYI	HKpYVLL	PMpYSTM	AHpYYLM
VGpYYFI	QGpYVLL	**PRpYSTM**	TRpYYLM
PGpYYLI	TSpYVLL	PRpYSVM	MQpYYLM
TGpYYLI	VSpYVLL	PRpYSYM	FKpYYLM
AGpYYMI	MGpYVML	VYpYTLM	HPpYYLM
VGpYYMI	QGpYVML	PMpYTLM	SApYYMM
FNpYYMI	WGpYVML	PRpYTLM	VTpYYMM
GGpYYVI	**AYpYYLL**	LPpYTLM	MKpYYMM
SFpYYYI	PIpYYLL	YVpYTLM	GIpYYYM
TSpYYYI	TGpYYLL	YGpYTLM	**ATpYYYM**
PFpYFLL	TGpYYLL	FTpYTLM	TGpYYYM
TVpYFLL	VGpYYLL	MTpYTLM	AGpYFYV
KGpYQLL	VKpYYLL	AHpYTLM	PRpYSLV
TMpYSFL	LGpYYLL	SApYTLM	VYpYSLV
PLpYSIL	MGpYYLL	SPpYTLM	PKpYSYV
AVpYSIL	FNpYYLL	HPpYTLM	YApYSYV
PFpYSLL*	FYpYYLL	HYpYTLM	YLpYSYV
HSpYSLL	WYpYYLL	RWpYTLM	AGpYYFV
LYpYSLL	HPpYYLL	WLpYTLM	AYpYYLV
VLpYSLL	QIpYYLL	TIpYTMM	WVpYYLV
VYpYSLL	LQpYYML	FQpYTMM	SApYYYV
TLpYSLL	FApYYML	GGpYTMM	SYpYYYV
RGpYSML	YGpYYML	ALpYTMM	LLpYYYV
PLpYSTL	NApYYML	QYpYTMM	MVpYYYV
TYpYSVL	GIpYYYL	FTpYTYM	
PKpYSYL	TTpYYYL	STpYTYM	

[a] Boldfaced sequences were from the most intensely colored beads from 10 nM SH2 domain screening; the sequence with an asterisk was selected for SPR analysis; M = norleucine.

solvent. Class III peptides have the consensus sequence of (I/V)XpY(L/M/T)Y(A/P/T/S/g) (Table 2). A distinctive feature of this class is that they have a tyrosine (or occasionally isoleucine) at the +2 position and a small residue at the +3 position. Finally, class IV peptides have a consensus sequence of (I/V/L)XpY(F/M)XP (Table 2). Interestingly, although the class III and IV peptides were less abundant overall, they were disproportionately represented among the most intensely colored beads (boldfaced sequences in Table 2). Class III and IV peptides bind to the SHP-2 N-SH2 domain with exceptionally high affinity (vide infra).

Specificity of the SHIP SH2 Domain. The SH2 domain from SHIP was screened against the pY library at two

the peptide sequences from the 158 intensely colored beads were determined (Table 3). The SHIP SH2 domain recognizes a single consensus of pY(Y/S/T/v)(L/y/nle/f)(L/Nle/i/v) (Figure 4). Its specificity overlaps with those of SHP SH2 domains but also has a number of unique features. First, on the N-terminal side of pY, the SHIP SH2 domain does not require specific residues for high-affinity binding, although among the selected sequences there appears to be a higher than expected number of small residues (e.g., Gly, Pro, and Ala) at the −2 and −1 positions. Second, high-affinity binding to the SHIP SH2 domain requires a hydrophobic residue at the +2 position, with leucine being the most preferred, followed by tyrosine, norleucine, and phenylalanine. The latter feature had previously been noted by other investigators (26). Third, while alanine is among the most preferred amino acids at the +1 position for SHP SH2 domains, it is not favored by the SHIP SH2 domain. Among the nearly 200 SHIP SH2-binding sequences selected from the pY library (Table 3 and Table S3 in Supporting Information), only two had an alanine at the +1 position (TMpYAFI and TVpYALM).

Comparison with Previous Method: Specificity of the

FIGURE 4: Specificity of SHP SH2 domain. Displayed are the amino acids identified at each position (−2 to +3). Occurrence on the y axis represents the number of selected sequences that contain a particular amino acid at a certain position. Key: M, norleucine.

Table 4: pY Sequences Selected against the SHP-1 C-SH2 Domain (95 Total)[a]

VApYACL	TApYCML	IRpYASM	TRpYTRV
VYpYACL	ACpYCML	YWpYATM	YCpYTTV
IKpYAKL	TEpYCML	TQpYAVM	TRpYTTV
TQpYAML	VEpYCML	IRpYAVM	TQpYTRI
HRpYAML	SHpYCML	HRpYCKM	AIpYTLC
YYpYAQL	THpYCML	ALpYCLM	
TApYARL	IKpYCQL	TEpYCRM	SRpYHWF
HHpYARL	TSpYCQL	VVpYCRM	MHpYWRF
FRpYARL	QHpYCRL	TQpYCWM	TVpYSNK
YWpYARL	VHpYCRL	TRpYCWM	WWpYRVN
HVpYATL	TNpYCRL	TRpYCWM	VFpYHPQ
TApYAVL	VNpYCRL	TApYTCM	IWpYHPQ
TApYAVL	AApYCVL	TYpYTRM	YApYNFR
SHpYAVL	AApYCVL	VApYAVV	GHpYTFR
TQpYAVL	CApYCVL	TApYCCV	YHpYWQR
VHpYCCL	TApYCVL	TQpYCLV	YSpYYAR
TCpYCEL	TApYCVL	MYpYCRV	FTpYYAR
ACpYCIL	TFpYTAL	SCpYCSV	MYpYYNR
YRpYCKL	TIpYTTL	TYpYSCV	YGpYRYS
IApYCLL	IApYACM	AMpYSLV	YRpYFQY
VNpYCLL	YNpYAKM	VTpYTKV	WYpYKRY
TTpYCLL	TQpYAKM	VMpYTLV	TVpYRFY
VTpYCNL	VApYAMM	IMpYTNV	KRpYWFY
HApYCML	VRpYAMM	ITpYTQV	MFpYYRY

[a] Sequences were obtained from two screening experiments performed at 10 nM SHP-1 C-SH2 domain. C = α-aminobutyric acid; M = norleucine.

of their β-branching and bulky side-chain protecting group (tert-butyl for threonine), Fmoc-Thr(tBu)-OH and Fmoc-Val-OH are hindered and react slowly during coupling, resulting in a higher percentage of chain termination (reaction with Ac-Gly) and smaller amounts of full-length peptides on the bead surface. To test this notion and to demonstrate the advantage of our current method, we rescreened another pY library, which includes α-aminobutyric acid (Abu) as a cysteine surrogate at the random positions but is otherwise identical to the pY library described above, against the C-SH2 domain of SHP-1 (10 nM). Out of a total of 95 sequences obtained from 150 mg of resin, 77 belong to the class with a consensus sequence of (T/v/i)XpY(Abu/A/t)X-(L/m/v) (Table 4 and Figure 5). This is in general agreement with the previous result (15), but with a few subtle differences. The most notable difference is at the −2 position. The previous study suggested valine, isoleucine, leucine, and tyrosine as the most preferred residues, whereas the current data show that threonine is the most preferred amino acid, followed by valine and isoleucine (Figure 5). At positions +1 and +2, the current method also selected a larger number of threonine residues as compared to the previous method. The simplest explanation for the observed discrepancy is that the previous method biased against threonine-containing sequences. At the +1 position, the previous study produced almost exclusively alanine, whereas the current work shows that Abu is the most preferred amino acid, followed by alanine and threonine. Note that the previous library did not contain Abu at the random positions (15). The remaining 18 sequences do not show a clear consensus (Table 4). Some of the sequences were likely selected due to their binding directly to SA-AP (e.g., pYHPQ) (16), whereas others show some resemblance to the type II sequences previously selected against the SHP-1 C-SH2 domain (e.g., pYYXR) (15). Further work is underway to assess whether some of

sequence specificity of SHP-1 N- and C-SH2 domains using a different method (15). In our previous method, the full-length peptide on a bead was encoded by generating a series of sequence-specific chain-termination products (a peptide ladder) during library synthesis (27). The sequence of the full-length peptide was determined through MALDI-TOF analysis of the peptide ladder in a manner similar to that described above. We felt that the previous method might bias library screening against sequences that contain slow-

FIGURE 5: Comparison of the specificity of the SHP-1 C-SH2 domain as determined by the previous (open bar) vs current method (closed bar). Displayed are the amino acids identified at each position (−2 to +3). Number of occurrence on the *y* axis represents the number of selected sequences that contain a particular amino acid at a certain position (the previous *y* axis values were amplified by a factor of 2 to facilitate comparison). Key: C, aminobutyric acid; M, norleucine.

FIGURE 6: SPR analysis of the binding of the SHP-2 N-SH2 domain to peptide IHpYLYA. (a) Overlaid sensorgrams at indicated concentrations of N-SH2 protein (0.08−5.2 μM). (b) Plot of resonance signal under equilibrium binding conditions against SH2 concentration. The data were fitted to the equation $RU_{eq} = RU_{max}[SH2]/(K_D + [SH2])$.

Affinity Measurements of Selected Sequences. To verify the screening results, representative peptides from each consensus group (peptides labeled with asterisks in Tables 1−3) were individually synthesized and tested for binding to the five SH2 domains of SHP-1, SHP-2, and SHIP using the surface plasmon resonance (SPR) technique (BIAcore) (Figure 6). Two SHP-2 C-SH2 domain-binding peptides (TIpYATI and NApYATI), which were derived from intensely and lightly colored beads, respectively, were chosen to test whether the color intensity of a bead during screening correlates with the binding affinity of the peptide it carries. A predicted tight binding sequence was selected for the SHIP SH2 domain (PFpYSLL). For the SHP-2 N-SH2 domain, a total of 10 representative sequences with at least two from each class (both predicted tight and weaker binding sequences) were chosen for further analysis. A total of 65 equilibrium dissociation constants (K_D) were measured and

following conclusions. First, all of the tested pY peptides bind to their cognate SH2 domains with high affinity (K_D = 0.044−9.7 μM) and have, in general, the highest affinity to the SH2 domain used in their selection. For example, peptide VIpYFVP was selected by the N-terminal SH2 domain of SHP-2 (class IV). It binds exceptionally tightly to the N-SH2 domain (K_D = 0.044 μM) but interacts with the other four SH2 domains with 23−360-fold lower affinity. Likewise, peptide PFpYSLL binds to the SHIP SH2 domain (which selected the former in the screening) with high affinity (K_D = 0.20 μM) but much less tightly to the other four SH2 domains (K_D = 5.6−14 μM). A few peptides (e.g., LVpYATI), however, can associate with all five SH2 domains with similar K_D values (2−5 μM), consistent with the previous observation that the five SH2 domains have overlapping sequence specificities. Second, for peptides within the same consensus group, there is a general correlation between bead color intensity and binding affinity (e.g., compare TIpYATI vs NApYATI for the C-SH2 domain and WMpYRII vs WTpYQIL, IHpYLYA vs ITpYTYP, and VIpYFVP vs VLpYMQP for the N-SH2 domain). The only exception is VApYVEL, which was derived from an intensely colored bead but binds SHP-2 N-SH2 domains with slightly lower affinity than LVpYATI and LVpYTEV (both from medium-colored beads). For peptides in the different classes, this correlation may not exist. For example, peptide VLpYMQP, a class IV peptide from a medium-colored bead, has a much higher affinity for the SHP-2 N-SH2 domain than class II peptide WMpYRII, which was from an intensely colored bead. This is because the color intensity of a bead is determined not only by the equilibrium K_D value but also by the kinetics of association and dissociation and possibly

Table 5: Dissociation Constants (μM) of Selected pY Peptides toward SHP-1, SHP-2, and SHIP SH2 Domains^a

	SHP-2		SHP-1		
	N-SH2	C-SH2	N-SH2	C-SH2	SHIP SH2
(1) TIpYATI	3.9 ± 0.3	0.60 ± 0.07*	6.4 ± 0.4	2.4 ± 0.1	2.2 ± 0.2
(2) NApYATI	34 ± 3	3.9 ± 0.4*	28 ± 3	16 ± 2	10 ± 0.5
(3) PFpYSLL	9.7 ± 0.9	9.2 ± 1.5	5.6 ± 0.5	14 ± 4	0.20 ± 0.03*
(4) LVpYATI	1.9 ± 0.1*	2.0 ± 0.2	1.6 ± 0.5	5.2 ± 0.5	3.5 ± 0.2
(5) LVpYTEV	1.4 ± 0.1*	8.5 ± 1.2	3.2 ± 0.2	8.8 ± 1.3	3.8 ± 0.3
(6) VApYVEL	3.6 ± 0.1*	3.7 ± 0.1	4.9 ± 0.1	10 ± 1	5.2 ± 0.2
(7) LNpYMTF	2.4 ± 0.2*	8.9 ± 0.8	2.7 ± 0.2	>50	6.7 ± 0.9
(8) WTpYQIL	9.7 ± 0.3*	10 ± 1	17 ± 1	59 ± 4	3.8 ± 0.3
(9) WMpYRII	3.0 ± 0.4*	20 ± 6	8.5 ± 1.0	23 ± 5	6.3 ± 0.4
(10) IHpYLYA	0.28 ± 0.04*	12 ± 3	7.0 ± 0.4	27 ± 7	13 ± 1
(11) ITpYTYP	2.4 ± 0.2*	9.7 ± 1.9	2.1 ± 0.1	11 ± 3	3.2 ± 0.2
(12) VLpYMQP	0.11 ± 0.01*	4.9 ± 0.7	3.9 ± 0.2	>16	9.0 ± 0.9
(13) VIpYFVP	0.044 ± 0.014*	11 ± 2	1.0 ± 0.1	>16	3.8 ± 0.4

^a The reported errors represent uncertainties from nonlinear regression fitting. For most of the interactions, at least two independent sets of measurements were performed to ensure the reproducibility of the measurements. All pY peptides are N-terminally acetylated and contain a C-terminal linker, LNBKR-NH$_2$. The lysine side chain was acylated with a PEG$_4$-biotin moiety for immobilization. SH2 domains were constructed as N-terminal six-histidine fusion proteins. Key: M, norleucine; bold type, peptides from most intensely colored beads; italic type, peptides from lightly colored beads. The asterisk indicates the SH2 domain by which each peptide was selected.
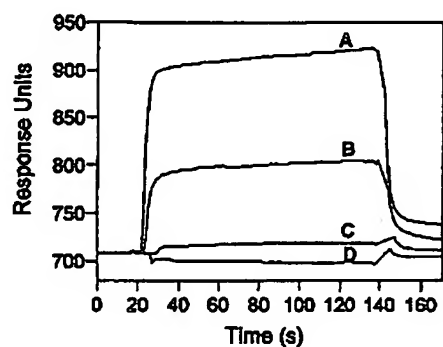
FIGURE 7: Competition of pY peptides for binding to the SHP-2 N-SH2 domain. Biotinylated peptide IHpYLYA was immobilized onto a sensorchip, and the N-SH2 domain in HBS-EP buffer (pH 7.4) was flowed over the chip surface at a flow rate of 15 μL/min. Key: (A) 0.3 μM SHP-2 N-SH2 protein alone; (B) 0.3 μM N-SH2 + 100 μM WMpYRII; (C) 0.3 μM N-SH2 + 100 μM LNpYMTF; (D) 0.3 μM N-SH2 + 100 μM LVpYTEV.

different binding modes and kinetics. For example, SPR analyses showed that the SHP-2 N-SH2 domain dissociated more slowly from immobilized peptides IHpYLYA and WMpYRII than peptide TIpYATI (data not shown). For peptides with similar K_D values, those with slower dissociation rates are expected to produce higher color intensity.

Competition Binding Experiments. To determine whether the four classes of pY peptides all bind to the same site on the SHP-2 N-SH2 domain surface, the peptides were subjected to binding competition to the SH2 domain by SPR. Peptide IHpYLYA (class III) was immobilized onto a sensorchip, and the N-SH2 protein was flowed over the chip surface. In the absence of competitor peptide, the N-SH2 domain (0.3 μM) bound to the immobilized IHpYLYA peptide, resulting in a large increase in resonance units (RU) (tracing A in Figure 7). However, when the N-SH2 domain (0.3 μM) was preincubated with 100 μM peptide LNpYMTF or LVpYTEV (class I), the binding was completely abolished (tracings C and D). Peptide WMpYRII (class II) reduced the amount of the N-SH2 domain bound to the sensorchip (tracing B), although it is less effective than the class I peptides. Peptides VLpYMQP and VIpYFVP (class IV) also effectively competed with the immobilized IHpYLYA for

suggest that all four classes of pY peptides bind to the same site on the SH2 domain surface.

Binding of Selected pY Peptides to Intact SHP-1, SHP-2, and SHIP. To determine whether the pY peptides selected from the combinatorial library are capable of binding to full-length SHP-1, SHP-2, and SHIP proteins, peptide pull-down assays were performed with crude cell lysates derived from a murine cell line (Raw 264.7). Peptide TIpYATI and a positive control peptide (pITIM) from FcγRIIb (biotin-aminohexanoyl-EAENTITpYSLLKH-NH$_2$) (*14*) effectively precipitated both SHP-1 and SHP-2 from the cell lysate (Figure 8a). Peptide LVpYATI also precipitated SHP-1 and SHP-2 but was less effective. A negative control (G4), which is derived from the phosphorylated ITAM on the Fc receptor γ-subunit (biotin-aminohexanoyl-LLPDQLpYQPLKDRED-DQpYSHLQ-NH$_2$) (*28*), did not pull down any of the proteins. Surprisingly, peptides IHpYLYA and WMpYRII, which are selective ligands for the SHP-2 N-SH2 domain, failed to precipitate SHP-2 from the lysate. We noted that, in some experiments, these two peptides precipitated small amounts of proteins of lower molecular masses (data not shown). We reasoned that the N-SH2 domain-specific peptides might have disengaged the intramolecular association between the N-SH2 domain and the PTP domain, resulting in the SHPs in their open, active conformation (*29, 30*), which were presumably cleaved into smaller species by protease(s) during the overnight incubation. Addition of common serine protease inhibitors did not prevent proteolysis. To this end, the pull-down assays were repeated with purified recombinant full-length SHP-1 and SHP-2. All of the tested pY peptides precipitated SHP-2, although IHpY-LYA was less effective than the other peptides (Figure 8b). The lower effectiveness of IHpYLYA is most likely due to its marginal aqueous solubility. The pY peptides also precipitated SHP-1, albeit less effectively. None of the peptides bound to SHIP. These results demonstrate that the pY peptides selected against the isolated SH2 domains are indeed capable of selectively binding to the corresponding intact proteins.

Database Search of Potential SHP-1/SHP-2-Binding Pro-
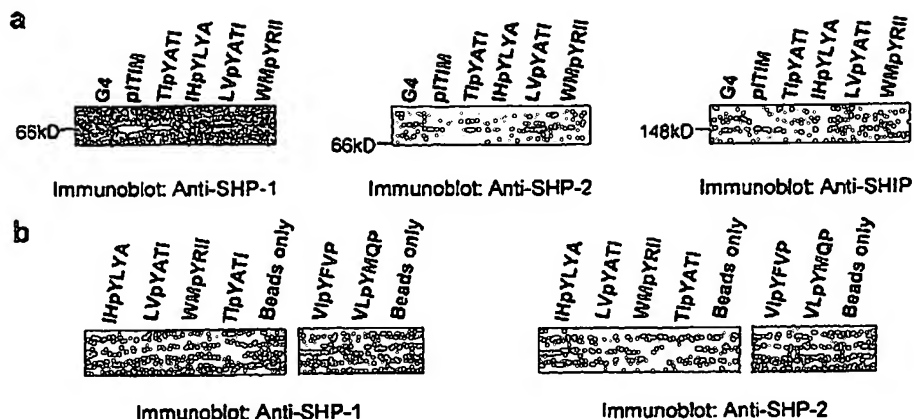
FIGURE 8: Pull-down assay of the interactions between pY peptides and full-length SHP-1, SHP-2, and SHIP. Biotinylated pY peptides were incubated with crude cell lysate (panel a) or purified protein (panel b). The peptide—protein complexes were captured by streptavidin—agarose beads and analyzed by western blotting. Key: G4, an ITAM peptide (negative control); pITIM, an ITIM peptide (positive control); beads only, no pY peptide added.

to search protein databases for potential SHP-1/2-binding proteins at the Protein Information Resource (PIR; web site, http://pir.georgetown.edu/). Since our initial searches with a single consensus motif resulted in a large number of "hits" (usually a few thousand) and both N- and C-SH2 domains of SHP-1/2 are often engaged in simultaneous interaction with tandem pY motifs, we narrowed our search using a tandem consensus sequence motif, [VIL]XY[ASTVI]X[ILV]X$_{1-50}$[TVIY]XY[ASTV]X[IVL], where X is any amino acid and the letters in brackets indicate the amino acids allowed at a given position. The two individual motifs were designed to encompass the N- (class I) and C-SH2 domain consensus sequences of both SHP's and were separated by anywhere from 1 to 50 residues. Any protein containing a sequence stretch that matches the tandem motif is considered as a positive "hit". A search of the human proteins resulted in 420 hits, representing ~100 unique proteins (many proteins appeared multiple times under different names or as fragments). After removing those proteins that we thought as "obvious" false positives (e.g., secreted proteins or transmembrane proteins with the consensus motifs in the extracellular environment), we obtained 77 proteins as potential SHP-1/SHP-2 targets (Table 6). Out of the 77 candidate proteins, 26 proteins have previously been shown to bind to SHP-1 and/or SHP-2 in a pY-dependent manner (31—62).

A literature search revealed that a total of 68 human proteins have previously been shown to interact with the SH2 domain(s) of SHP-1 and/or SHP-2 in the pY-dependent manner (Table 6 and Table S4 in Supporting Information). Thus, the above search has failed to identify the other 42 SHP-1/2-binding proteins. Sequence analysis of these proteins shows that 37 of these proteins contain one or more ITIM or ITIM-like motifs. The majority of them bind to SHP-1 and/or SHP-2 through a single ITIM or ITIM-like motif [e.g., CD72 (63, 64), death receptor (65), epidermal growth factor receptor (66), erythropoietin receptor (67—69), leptin receptor (70), PD-1 (71, 72), and platelet-derived growth factor receptor (73)]. Other proteins contain two or more ITIM motifs, but with one or more of their ITIM motifs containing a nonoptimal amino acid(s) at a critical position. For example, Gab-1, Gab-2, and Gab-3 each bind to SHP-2 via two ITIM motifs, [V/L]XpYLXL and VDpYVXV (74—76). The first ITIM motif has a leucine at the +1 position,

domains (Figures 2 and 3) and was not included in the tandem motif used in the above database search. When a single consensus motif, [VIL]XY[ASTVI|X|ILV], was used to search the human protein database, 24 out of the 37 ITIM-containing proteins were recovered among the hits, in addition to the 26 proteins identified from the first search. Therefore, our searches against the class I consensus sequence identified 50 out of the 68 known SHP-1/2 targets (74%). Five of the 42 proteins are known to interact with SHP-1 and/or SHP-2, but not through classical ITIM motifs. These include c-Kit (YVpYIDP) (77), CTLA-4 (QPpYFIP) (78), E-selectin (GSpYQKP) (79), prolactin receptor (LD-pYLDP) (80), and STAT3 (putatively LVpYLYP) (81). Note that these motifs are very similar to the class III (pYLYP) and IV sequences (pYIDP, pYLDP, pYFIP, pYQKP) selected against SHP-2 N-SH2 domains (Table 2). These peptides can also bind tightly to the SHP-1 N-SH2 domain (Table 5) and indeed appeared among the class I sequences selected by the N-SH2 domain of SHP-1 (15).

DISCUSSION

The combinatorial library method reported in this work has for the first time provided a *complete* solution to the problem of identifying linear peptide motifs that interact with a given protein or nonprotein receptor. Compared to previously reported methods, our method has many significant advantages. First, our method identifies individual binding sequences; this feature is crucial for understanding the specificity of receptors that recognize multiple consensus sequences. For example, when the four classes of binding sequences of the SHP-2 N-SH2 domain were combined and plotted in the same manner as in Figure 2 to give a composite histogram, the specificity pattern was dominated by class I sequences (see Figure S1 in Supporting Information). It was impossible to winnow out the less abundant class III and IV sequences from the histogram, although they bind to the N-SH2 domain with higher affinity than class I peptides. Even for a receptor that has a single consensus sequence, individual sequences are useful in revealing the subtle covariance of sequences. For example, among the pY peptides that bind to the SHP-2 C-SH2 domain, when the +3 residue is isoleucine, alanine is most frequently found at the +1 position; however, when valine is the +3 residue, a serine is most preferred at the +1 position (Table 1).

Table 6: Human Proteins Predicted To Bind to SHP-1 and/or SHP-2 via SH2 Domains

protein	binding motif(s)	ref
activating NK cell receptor 2B4[b]	TIYSMI, TLYSLI	31
adenylate cyclase, type VI	VSYVVL, IAYTLL	
adipocyte G protein-coupled receptor 175	LVYSLV, YVVYAGI	
alternative splicing factor-1	VCYADV, TAYIRV	
alternative splicing factor-3	VCYADV, VGYTRI	
B and T lymphocyte attenuator[a,b]	LLYSLL, IVYASL, TEYASI	34
β-hexosaminidase β-subunit	IEYARL, TTYSFL	
biliary glycoprotein-1 (CD66, CEACAM-1)[a,b]	VTYSTL, IIYSEV	33
coagulation factor II (thrombin) receptor	VCYVSI, VHYSFL, YVVYSIL	
dol-P-man-dependent α(1−3)-mannosyltransferase	VAYTEI, YDYTQL	
Ewing's sarcoma protein-1	LVYTSI, YPYSVL	
exportin-7, ran-binding protein-16	IGYSSV, TFYTAL, SYYSLL	
G protein-coupled receptor RDC1	VLYSFI, TEYSAL	
G6b-B protein of MHC III[a,b]	LLYADL, TIYAVV	35
H-rev107-like protein (HRLP-5)	VKYSRL, VQYSLI	
human germinal-center-associated lymphoma protein	LCYTLI, TEYSLL	
immune receptor expressed on myeloid cells-1 (polymeric immunoglobulin receptor)[a]	LCYADL, VEYVTM, ISYASL, TEYSTI	36, 37
immunoglobulin superfamily receptor translocation associated-1 (IFGP-2)	LVYSEI, VVYSEV	
immunoglobulin superfamily receptor translocation associated-2	VVYSEV, IIYSEV	
immunoglobulin-like transcript 2, leukocyte immunoglobulin-like receptor-1 (MIR-7)[a]	VTYAEV, VTYAQL	38
immunoglobulin-like transcript 3 (LIR-5)[a]	VTYAKV, VTYAQL	39
immunoglobulin-like transcript 5 (LIR-3)	VTYAPV, VTYAQL	
inhibitory receptor protein 60 (IRC-1)[a,b]	LHYANL, VEYSTV, LHYASV	40
interleukin 8 receptor α (CXCR-1)	IAYALV, ILYSRV, IIYAFI	
interleukin 8 receptor β (CXCR-2)	IIYALV, ILYSRV, LIYAFI	
killer cell Ig-like receptor 2DL1 (p58, NKAT-1)[a,b]	VTYTQL, IVYTEL	41, 42
killer cell Ig-like receptor 2DL2 (NKAT-6)	VTYTQL, IVYAEL	
killer cell Ig-like receptor 2DL3 (NKAT-2)	VTYAQL, IVYTEL	
killer cell Ig-like receptor 3DL1 (p70, NKB-1, NKAT-3)[a,b]	VTYAQL, ILYTEL	43
leucine-rich neuronal protein (LRCH-4)	VFYVVL, VTYTRL	
leukocyte antigen (CD84)[a,b]	TIYTYI, TVVYSEV	44
leukocyte-associated immunoglobulin-like receptor-1[a,b]	VTYAQL, ITYAAV	45
lipid phosphate phosphorylase-1 (phosphatidic acid phosphatase-2a)	LPYVAL, IPYALL	
metabotropic glutamate receptor-2	LCYILL, VCYSAL	
metabotropic glutamate receptor-3	LCYILL, ICYSAL	
metabotropic glutamate receptor-4	LSYVLL, ISYAAL	
metabotropic glutamate receptor-7	LSYVLL, ISYAAL	
multiple C2-domain and transmembrane region protein-2	LRYIIL, VQYAEL	
natural killer inhibitory receptor NKG2-A[a,b]	VIYSDL, ITYAEL	46
natural killer-.T-, B-cell antigen receptor[a,b]	LEYVSV, TVYASV, TIYSTI	47
neuropeptides B/W receptor type 1 (GPR7)	VVYAVL, VLYVLL	
novel protein similar to PRAME	LSYVLL, IHYSQL	
olfactory receptor 1F1	LFYSTI, VLYTVV	
olfactory receptor 8D1	ILYSIL, VFYTTV	
olfactory receptor 12D2	LRYTVI, LFYAPV, IMYTVV	
olfactory receptor 12D3	ISYSSV, LRYTVI, IMYSAV	
olfactory receptor 51B5	ISYVLI, VFYVTV	
olfactory receptor 51V1	TVYTVL, LRYSSI	
osteoblast-specific factor-2	IKYIQI, IKYTRI	
paired immunoglobin-like type 2 receptor α (FDF03)[a,b]	IVYASL, TLYSVL	48, 49
phosphoribosyl transferase domain containing-1	LEYVLI, IGYSDI	
PIG-M mannosyltransferase	VRYTDI, YRYTPL	
platelet endothelial cell adhesion molecule-1 (CD31)[a,b]	VQYTEV, TVVYSEV	50
polycystin-1, polycystic kidney disease-related protein-1	VTYTPV, VQYVAL, LNYTLL	
protein KIAA0319 (contains polycystic kidney disease 1 domains)	IFYVTV, TKYTIL	
protein zero related[b]	VIYAQL, VVYADI	51, 52
R3H domain protein-1	IPYTSV, VYYSVI	
ran-binding protein-17	VGYILL, TFYTAL, TSYTML, ICYSAL	
SH2 domain-containing phosphatase anchor protein-1[a]	VVYSQV, VIYSSV	53
sialic acid binding Ig-like lectin-2 (CD22)[a]	VTYSAL, IHYSEL, VDYSEL	54, 55
sialic acid binding Ig-like lectin-3 (CD33)[a,b]	LHYASL, TEYSEV	56
sialic acid binding Ig-like lectin-5 (OBBP-2)	LHYASL, TEYSEI	
sialic acid binding Ig-like lectin-6 (OBBP-1)	LHYAVL, TEYSEI	
sialic acid binding Ig-like lectin-9 (FOAP-9)[a]	LQYASL, TEYSEI	57
sialic acid binding Ig-like lectin-11[a,b]	LHYASL, TEYSEI	32
sialic acid binding Ig-like lectin-12 (S2V)[a,b]	IQYASL, YEYSEI	58
signal regulatory protein α-1 (SHPS-1, BIT, MyD-1, PTPNS-1)[a,b]	ITYADL, TEYASI, LTYADL	59, 60
signaling lymphocytic activation molecule (CD150)[b]	TIpYAQV, TVpYASV	61
sodium channel type V α subunit (cardiac muscle α-subunit)	LNYTIV, IMYAAV, TTYIII, IEYSVL	
sodium channel type XI α subunit (peripheral nerve sodium channel 5, hNaN)	INYTII, IIYAAV, VSYIII, IKYSAL	
solute carrier family 19, member 3 (SLC19A3)	LNYVQI, VGYVKV	
somatostatin receptor 1[b]	VIYVIL, VLYTFL, LCYVLI	62
spastic ataxia of Charlevoix−Saguenay	IHYTLL, YTYAII	
trace amine receptor-5 (GPR102)	LTYSGA, ILYSKI	
ubiquitin-specific protease-9, X chromosome (DFFRX)	VMYANL, YQYAEL	
ubiquitin-specific protease-9, Y chromosome (DFFRY)	VMYANL, YQYAEL	
zinc finger protein 521	VGYTSV, VTYSCI	

[a] Proteins that have previously been shown to bind to SHP-1 via its SH2 domains. [b] Proteins that have previously been shown to bind to SHP-2

library peptides, as each bead contains roughly the same amount of peptide molecules (~100 pmol). This is not the case with pY peptide libraries displayed on a phage surface, because such libraries are biased against sequences that are poor substrates of the tyrosine kinases used to phosphorylate the phage (10, 11). Youngquist et al. reported another method in which the peptide sequence on each bead is encoded by generating a set of chain-termination products during library synthesis, and the sequence of the full-length peptide is determined by mass spectrometric analysis of the set of chain-termination products (27). Unfortunately, due to different reactivities of the 20 amino acids, the amount of chain termination varies with peptide sequence. As a result, the amount of full-length peptide on each bead also varies, biasing the screening against peptides containing slow-coupling amino acids (e.g., Thr and Ile). Indeed, a comparison of the peptides selected by the Youngquist method vs the current method showed that the former caused an underrepresentation of Thr-containing sequences (Figure 5). Third, because our method employs chemically synthesized libraries, modified (e.g., pY) and/or unnatural amino acids (e.g., D-amino acids) can be easily incorporated into the libraries. Fourth, our method is high-throughput and cost-effective. By employing partial Edman degradation, we can routinely sequence 20–30 beads in an hour, at a cost of ~$0.50 per bead. Fifth, as demonstrated with all four SH2 domains from SHP-1, SHP-2, and SHIP, our method is highly reproducible. It is readily applicable to other protein or nonprotein receptors. We have recently applied this method to determine the sequence specificity of BIR domains, WW domains, and chromodomains (unpublished results). Finally, it is worth noting that abundance in the library does not correlate with high affinity, especially when comparing two different classes of peptides. In fact, the opposite trend appears to be true, as demonstrated here by the class I and IV sequences for the SHP-2 N-SH2 domain. Presumably, a high-affinity interaction requires a better fit between the protein and peptide structures, necessarily limiting the number of possible choices in the library. This further underscores the importance of obtaining individual binding sequences.

The five SH2 domains of SHP-1, SHP-2, and SHIP have overlapping specificities, and yet each domain possesses some unique features. There are major differences between SHP and SHIP SH2 domains. SHP SH2 domains require a hydrophobic residue at the −2 position, whereas the SHIP SH2 domain can tolerate most of the amino acids at the N-terminal side of pY. On the C-terminal side, SHIP SH2 strongly prefers a Leu at the +2 position, but SHP SH2 domains have no such requirement (except for class II peptides of the SHP-2 N-SH2 domain). There are also more subtle differences at the +1 position; while SHP SH2 domains all prefer an alanine at this position, alanine was seldom found at this position among all of the SHIP SH2-binding sequences. Among the four SHP SH2 domains, the two N-terminal SH2 domains have similar specificities, and the two C-SH2 domains are highly analogous to each other. Most of the class I and II peptides selected by SHP-2 N-SH2 also bind to the SHP-1 N-SH2 domain with similar affinities (Table 5). However, many of the class III and IV peptides (e.g., IHpYLYA, VLpYMQP, and VIpYFVP) show excellent

SHP-1 N-SH2 domain with >20-fold lower affinities and with even lower affinity to the other three SH2 domains. The two C-SH2 domains have two subtle differences (Figures 2 and 5). At the +3 position, SHP-1 most prefers leucine, whereas SHP-2 prefers isoleucine. At the +1 position, SHP-2 accepts serine as the second most preferred residue, whereas serine is disfavored by SHP-1.

The SH2 specificity data should be very useful in providing a molecular basis for different functions of SHP-1, SHP-2, and SHIP in cell signaling. For example, immunoreceptor PD-1 has been shown to co-immunoprecipitate with endogenous SHP-2 but not SHP-1 (71, 72). The pY motif responsible for SHP-2 binding is TEpYATIVF, which matches perfectly with the consensus sequence of the SHP-2 C-SH2 domain (Figure 2). Our data predict that it should bind only weakly to the SHP-1 C-SH2 domain, which only occasionally selected an isoleucine at the +3 position (Figure 5). Indeed, a synthetic peptide containing the TEpYATIVF motif bound SHP-2 much more strongly than SHP-1 in vitro (72). SHIP has been reported as the main inhibitory molecule for the immunoglobulin G Fc receptor signaling pathway by binding to the pYSLL motif on the Fc receptor (26, 82). The pYSLL motif matches the consensus sequence of the SHIP SH2 domain and binds the SHIP SH2 domain with much higher affinity than the SH2 domains of SHP-1 or SHP-2 (Table 5). Many receptors, however, contain multiple ITIM motifs that match the specificities of both SHP-1 and SHP-2. For example, the first ITIM motif of human Siglec-11 (LHpYASL) closely matches the consensus sequence of SHP-1 SH2 domains, whereas its second ITIM, TEpYSEI, matches the consensus of the SHP-2 C-SH2 domain (32). Some receptors contain ITIM motifs whose sequences represent a compromise between the consensus of SHP-1 and SHP-2 SH2 domains. Biliary glycoprotein 1 (CD66), which is known to bind both SHP-1 and SHP-2, is such an example (33). Its two ITIM motifs (VTpYSTL and IIpYSEV) match the overlapping specificities of SHP-1 and SHP-2 SH2 domains.

The specificity data can also be used to predict the interaction partners of the SH2 domain-containing proteins. As described above, simple database searches have identified 74% of the known SHP-1 and SHP-2 interacting proteins (Table 6 and Table S4 in Supporting Information). It is highly probable that some of the other predicted proteins in Table 6 will prove to be bona fide SHP-1 and SHP-2 binding proteins. Although at the present time, database searches using a single consensus motif generate too many false positives, the number of false positives can be greatly reduced by applying additional constraints. One such constraint is tissue distribution and subcellular localization. Another restriction is phosphorylation, which is required for binding for the vast majority of SH2 domains. Databases on phosphorylation sites and kinase specificity are becoming increasingly available in recent years (web sites: http://www.cbs.dtu.dk/databases/PhosphoBase/; http://phospho.e-lm.eu.org/about.html). Finally, one can make educated guesses on the basis of the function of a protein. Indeed, many of the 68 SHP-1/2-binding proteins have been discovered by the presence of ITIM motif(s) in their sequences. Additionally, this work has uncovered a new recognition motif, [IVL]XpY[LMF]XP, for the N-SH2 domains of

nature has utilized the class II and other class III motifs for binding to SHP-1 and SHP-2.

In summary, a powerful combinatorial library method has now been developed for the systematic determination of sequence specificities of protein interaction domains such as SH2 domains. The specificity information generated by this method will be very useful in understanding the cellular function of proteins that contain these interaction domains and the design of specific inhibitors against such protein domains.

SUPPORTING INFORMATION AVAILABLE

Additional SH2 domain-binding sequences, comparison of specificities of SHP-1/2 and SHIP SH2 domains, and a list of known SHP-1/2-interacting proteins. This material is available free of charge via the Internet at http://pubs.acs.org.

REFERENCES

1. Pawson, T., and Nash, P. (2003) Assembly of cell regulatory systems through protein interaction domains, *Science 300*, 445–452.
2. Venter, J. C., et al. (2001) The sequence of the human genome, *Science 291*, 1304–1351.
3. Bork, P., Schultz, J., and Ponting, C. P. (1997) Cytoplasmic signaling domains: the next generation, *Trends Biochem. Sci. 22*, 296–298.
4. Songyang, Z., Shoelson, S. E., Chaudhuri, M., Gish, G., Pawson, T., Haser, W. G., King, F., Roberts, T., Ratnofsky, S., Lechleider, R. J., Neel, B. G., Birge, R. B., Fajardo, J. E., Chou, M. M., Hanafusa, H., Schaffhausen, B., and Cantley, L. C. (1993) SH2 domains recognize specific phosphopeptide sequences, *Cell 72*, 767–778.
5. De Souza, D., Fabri, L. J., Nash, A., Hilton, D. J., Nicola, N. A., and Baca, M. (2002) SH2 domains from suppressor of cytokine signaling-3 and protein tyrosine phosphatase SHP-2 have similar binding specificities, *Biochemistry 41*, 9229–9236.
6. Muller, K., Gombert, F. O., Manning, U., Grossmuller, F., Graff, P., Zaegel, H., Zuber, J. F., Freuler, F., Tschopp, C., and Baumann, G. (1996) Rapid identification of phosphopeptide ligands for SH2 domains: Screening of peptide libraries by fluorescence-activated bead sorting, *J. Biol. Chem. 271*, 16500–16505.
7. Houghten, R. A., Pinilla, C., Blondelle, S. E., Appel, J. R., Dooley, C. T., and Cuervo, J. H. (1991) Generation and use of synthetic peptide combinatorial libraries for basic research and drug discovery, *Nature 354*, 84–86.
8. Scott, J. K., and Smith, G. P. (1990) Searching for peptide ligands with an epitope library, *Science 249*, 386–390.
9. Rickles, R. J., Botfield, M. C., Weng, Z., Taylor, J. A., Green, O. M., Brugge, J. S., and Zoller, M. J. (1994) Identification of Src, Fyn, Lyn, PI3K, and Abl SH3 domain ligands using phage display libraries, *EMBO J. 13*, 5598–5604.
10. Gram, H., Schmitz, R., Zuber, J. F., and Baumann, G. (1997) Identification of phosphopeptide ligands for the Src-homology 2 (SH2) domain of Grb2 by phage display, *Eur. J. Biochem. 246*, 633–637.
11. King, T. R., Fang, Y., Mahon, E. S., and Anderson, D. H. (2000) Using a phage display library to identify basic residues in A-Raf required to mediate binding to the Src homology 2 domains of the p85 subunit of phsophatidylinositol 3′-kinase, *J. Biol. Chem. 275*, 36450–36456.
12. Ganesan, L. P., Wei, G., Pengal, R. A., Moldovan, L., Moldovan, N., Ostrowski, M. C., and Tridandapani, S. (2004) The serine/threonine kinase Akt promotes Fcγ receptor-mediated phagocytosis in murine macrophages through the activation of p70S6 kinase, *J. Biol. Chem. 279*, 54416–54425.
13. Sugimoto, S., Lechleider, R. J., Shoelson, S. E., Neel, B. G., and Walsh, C. T. (1993) Expression, purification, and characterization of SH2-containing protein tyrosine phosphatase, SH-PTP2, *J. Biol. Chem. 268*, 22771–22776.
14. Tridandapani, S., Kelley, T., Pradhan, M., Cooney, D., Justement, L. B., and Coggeshall, K. M. (1997) Recruitment and phosphorylation of SHIP and Shc to the B cell Fc gamma ITIM peptide

15. Beebe, K. D., Wang, P., Arabaci, G., and Pei, D. (2000) Determination of binding specificity of the SH2 domains of protein tyrosine phosphatase SHP-1 through the screening of a combinatorial phosphotyrosyl peptide library, *Biochemistry 39*, 13251–13260.
16. Lam, K. S., Salmon, S. E., Hersh, E. M., Hruby, V. J., Kazmierski, W. M., and Knapp, R. J. (1991) A new type of synthetic peptide library for identifying ligand-binding activity, *Nature 354*, 82–84.
17. Furka, A., Sebestyen, F., Asgedom, M., and Dibo, G. (1991) General method for rapid synthesis of multicomponent peptide mixtures, *Int. J. Pept. Protein Res. 37*, 487–493.
18. Sweeney, M. C., and Pei, D. (2003) An improved method for rapid sequencing of support-bound peptides by partial Edman degradation and mass spectrometry, *J. Comb. Chem. 5*, 218–222.
19. Neel, B. G., Gu, H., and Pao, L. (2000) The 'Shp'ing news: SH2 domain-containing tyrosine phosphatases in cell signaling, *Trends Biochem. Sci. 28*, 284–293.
20. Ravetch, J. V., and Lanier, L. L. (2000) Immune inhibitory receptors, *Science 290*, 84–89.
21. Waksman, G., Kominos, D., Robertson, S. C., Pant, N., Baltimore, D., Birge, R. B., Cowburn, D., Hanafusa, H., Mayer, B. J., Overduin, M., Resh, M. D., Rios, C. B., Silverman, L., and Kuriyan, J. (1992) Crystal structure of the phosphotyrosine recognition domain SH2 of v-src complexed with tyrosine-phosphorylated peptides, *Nature 358*, 646–653.
22. Eck, M. J., Atwell, S. K., Shoelson, S. E., and Harrison, S. C. (1994) Structure of the regulatory domains of the Src-family tyrosine kinase Lck, *Nature 368*, 764–769.
23. Lee, C.-H., Kominos, D., Jacques, S., Margolis, B., Schlessinger, J., Shoelson, S. E., and Kuriyan, J. (1994) Crystal structures of peptide complexes of the amino-terminal SH2 domain of the Syp tyrosine phosphatase, *Structure 2*, 423–438.
24. Burshtyn, D. N., Yang, W., Yi, T., and Long, E. O. (1997) A novel phosphotyrosine motif with a critical amino acid at position −2 for the SH2 domain-mediated activation of tyrosine phosphatase SHP-1, *J. Biol. Chem. 272*, 13066–13072.
25. Liao, H., Yuan, C., Su, M.-I., Yongkiettrakul, S., Qin, D., Li, H., Byeon, I.-J. L., Pei, D., and Tsai, M.-D. (2000) Structure of the FHA1 domain of yeast Rad53 and identification of binding sites for both FHA1 and its target protein Rad9, *J. Mol. Biol. 304*, 941–951.
26. Bruhns, P., Vely, F., Malbec, O., Fridman, W. H., Vivier, E., and Daeron, M. (2000) Molecular basis of the recruitment of the SH2 domain-containing inositol 5-phosphatases SHIP1 and SHIP2 by FcγRIIB, *J. Biol. Chem. 275*, 37357–37364.
27. Youngquist, R. S., Fuentes, G. R., Lacey, M. P., and Keough, T. (1995) Generation and screening of combinatorial peptide libraries designed for rapid sequencing by mass spectrometry, *J. Am. Chem. Soc. 117*, 3900–3906.
28. Pengal, R. A., Ganesan, L. P., Fang, H., Marsh, C. B., Anderson, C. L., and Tridandapani, S. (2003) SHIP-2 inositol phosphatase is inducibly expressed in human monocytes and serves to regulate Fcγ receptor-mediated signaling, *J. Biol. Chem. 278*, 22657–22663.
29. Pei, D., Lorenz, U., Klingmuller, U., Neel, B. G., and Walsh, C. T. (1994) Intramolecular regulation of protein tyrosine phosphatase SH-PTP1: A new function for Src homology 2 domains, *Biochemistry 33*, 15483–15493.
30. Hof, P., Pluskey, S., Dhe-Paganon, S., Eck, M. J., and Shoelson, S. E. (1998) Crystal structure of the tyrosine phosphatase SHP-2, *Cell 92*, 441–450.
31. Tangye, S. G., Lazetic, S., Woollatt, T. E., Sutherland, G. R., Lanier, L. L., and Phillips, J. H. (1999) Cutting edge: Human 2B4, an activating NK cell receptor, recruits the protein tyrosine phosphatase SHP-2 and the adaptor signaling protein SAP, *J. Immunol. 162*, 6981–6985.
32. Angata, T., Kerr, S. C., Greaves, D. R., Varki, N. M., Crocker, P. R., and Varki, A. (2002) Cloning and characterization of human Siglec-11, *J. Biol. Chem. 277*, 24466–24474.
33. Huber, M., Izzi, L., Grondin, P., Houde, C., Kunath, T., Veillette, A., and Beauchemin, N. (1999) The carboxyl-terminal region of biliary glycoprotein controls its tyrosine phosphorylation and association with protein-tyrosine phosphatases SHP-1 and SHP-2 in epithelial cells, *J. Biol. Chem. 274*, 335–344.
34. Gavrieli, M., Watanabe, N., Loftin, S. K., Murphy, T. L., and Murphy, K. M. (2003) Characterization of phosphotyrosine

attenuator required for association with protein tyrosine phosphatases SHP-1 and SHP-2, *Biochem. Biophys. Res. Commun. 312*, 1236–1243.

35. De Vet, E. C. J. M., Aguado, B., and Campbell, R. D. (2001) G6b, a novel immunoglobulin superfamily member encoded in the human major histocompatibility complex, interacts with SHP-1 and SHP-2, *J. Biol. Chem. 276*, 42070–42076.

36. Sui, L., Li, N., Liu, Q., Zhang, W., Wan, T., Wang, B., Luo, K., Sun, H., and Cao, X. (2004) IgSF13, a novel human inhibitory receptor of the immunoglobulin superfamily, is preferentially expressed in dendritic cells and monocytes, *Biochem. Biophys. Res. Commun. 319*, 920–928.

37. Alvarez-Errico, D., Aguilar, H., Kitzig, F., Brckalo, T., Sayos, J., and Lopez-Botet, M. (2004) IREM-1 is a novel inhibitory receptor expressed by myeloid cells, *Eur. J. Immunol. 34*, 3690–3701.

38. Fanger, N. A., Cosman, D., Peterson, L., Braddy, S. C., Maliszewski, C. R., and Borges, L. (1998) The MHC class I binding proteins LIR-1 and LIR-2 inhibit Fc receptor-mediated signaling in monocytes, *Eur. J. Immunol. 28*, 3423–3434.

39. Cella, M., Dohring, C., Samaridis, J., Dessing, M., Brockhaus, M., Lanzavecchia, A., and Colonna, M. (1997) A novel inhibitory receptor (ILT3) expressed on monocytes, macrophages, and dendritic cells involved in antigen processing, *J. Exp. Med. 185*, 1743–1751.

40. Cantoni, C., Bottino, C., Augugliaro, R., Morelli, L., Marcenaro, E., Castriconi, R., Vitale, M., Pende, D., Sivori, S., Millo, R., Biassoni, R., Moretta, L., and Moretta, A. (1999) Molecular and functional characterization of IRp60, a member of the immunoglobulin superfamily that functions as an inhibitory receptor in human NK cells, *Eur. J. Immunol. 29*, 3148–3159.

41. Burshtyn, D. N., Scharenberg, A. M., Wagtmann, N., Rajagopalan, S., Berrada, K., Yi, T., Kinet, J.-P., and Long, E. O. (1996) Recruitment of tyrosine phosphatase HCP by the killer cell inhibitory receptor, *Immunity 4*, 77–85.

42. Olcese, L., Lang, P., Vely, F., Cambiaggi, A., Marguet, D., Blery, M., Hippen, K. L., Biassoni, R., Moretta, A., Moretta, L., Cambier, J. C., and Vivier, E. (1996) Human and mouse killer-cell inhibitory receptors recruit PTP1C and PTP1D protein tyrosine phosphatases, *J. Immunol. 156*, 4531–4534.

43. Fry, A. M., Lanier, L. L., and Weiss, A. (1996) Phosphotyrosines in the killer cell inhibitory receptor motif of NKB1 are required for negative signaling and for association with protein tyrosine phosphatase 1C, *J. Exp. Med. 184*, 295–300.

44. Lewis, J., Eiben, L. J., Nelson, D. L., Cohen, J. I., Nichols, K. E., Ochs, H. D., Notarangelo, L. D., and Duckett, C. S. (2001) Distinct interactions of the X-linked lymphoproliferative syndrome product SAP with cytoplasmic domains of members of the CD2 receptor family, *Clin. Immunol. 100*, 15–23.

45. Verbrugge, A., de Ruiter, T., Clevers, H., and Meyaard, L. (2003) Differential contribution of the immunoreceptor tyrosine-based inhibitory motifs of human leukocyte-associated Ig-like receptor-1 to inhibitory function and phosphatase recruitment, *Int. Immunol. 15*, 1349–1358.

46. Carretero, M., Palmieri, G., Llano, M., Tullio, V., Santoni, A., Geraghty, D. E., and Lopez-Botet, M. (1998) Specific engagement of the CD94/NKG2-A killer inhibitory receptor by the HLA-E class Ib molecule induces SHP-1 phosphatase recruitment to tyrosine-phosphorylated NKG2-A: Evidence for receptor function in heterologous transfectants, *Eur. J. Immunol. 28*, 1280–1291.

47. Bottino, C., Falco, M., Parolini, S., Marcenaro, E., Augugliaro, R., Sivori, S., Landi, E., Biassoni, R., Notarangelo, L. D., Moretta, L., and Moretta, A. (2001) NTB-A, a novel SH2D1A-associated surface molecule contributing to the inability of natural killer cells to kill Epstein–Barr virus infected B cells in X-linked lymphoproliferative disease, *J. Exp. Med. 194*, 235–246.

48. Mousseau, D. D., Banville, D., L'Abbe, D., Bouchard, P., and Shen, S. H. (2000) PILRα, a novel immunoreceptor tyrosine-based inhibitory motif-bearing protein, recruits SHP-1 upon tyrosine phosphorylation and is paired with the truncated counterpart PILRβ. *J. Biol. Chem. 275*, 4467–4474.

49. Fournier, N., Chalus, L., Durand, I., Garcia, E., Pin, J.-J., Churakova, T., Patel, S., Zlot, C., Gorman, D., Zurawski, S., Abrams, J., Bates, E. E. M., and Garrone, P. (2000) FDF03, a novel inhibitory receptor of the immunoglobulin superfamily, is expressed by human dendritic and myeloid cells, *J. Immunol. 165*, 1197–209.

50. Wong, M. X., and Jackson, D. E. (2004) Regulation of B cell activation by PECAM-1: Implications for the development of

51. Zhao, Z. J., and Zhao, R. (1998) Purification and cloning of PZR, a binding protein and putative physiological substrate of tyrosine phosphatase SHP-2, *J. Biol. Chem. 273*, 29367–29372.

52. Zhao, R., and Zhao, Z. J. (2000) Dissecting the interaction of SHP-2 with PZR, an immunoglobulin family protein containing immunoreceptor tyrosine-based inhibitory motifs, *J. Biol. Chem. 275*, 5453–5459.

53. Xu, M. J., Zhao, R., and Zhao, Z. J. (2001) Molecular cloning and characterization of SPAP1, an inhibitory receptor, *Biochem. Biophys. Res. Commun. 280*, 768–775.

54. Doody, G. M., Justement, L. B., Delibrias, C. C., Matthews, R. J., Lin, J., Thomas, M. L., and Fearon, D. T. (1995) A role in B cell activation for CD22 and the protein tyrosine phosphatase SHP, *Science 269*, 242–244.

55. Law, C.-L., Sidorenko, S. P., Chandran, K. A., Zhao, Z., Shen, S.-H., Fischer, E. H., and Clark, E. A. (1996) CD22 associates with protein tyrosine phosphatase 1C, Syk, and phospholipase C-γ1 upon B cell activation, *J. Exp. Med. 183*, 547–560.

56. Taylor, V. C., Buckley, C. D., Douglas, M., Cody, A. J., Simmons, D. L., and Freeman, S. D. (1999) The myeloid-specific sialic acid-binding receptor, CD33, associates with the protein-tyrosine phosphatases, SHP-1 and SHP-2, *J. Biol. Chem. 274*, 11505–11512.

57. Ikehara, Y., Ikehara, S. K., and Paulson, J. C. (2004) Negative regulation of T cell receptor signaling by siglec-7 (p70/AIRM) and siglec-9, *J. Biol. Chem. 279*, 43117–43125.

58. Yu, Z., Lai, C. M., Maoui, M., Banville, D., and Shen, S. H. (2001) Identification and characterization of S2V, a novel putative siglec that contains two V set Ig-like domains and recruits protein-tyrosine phosphatase SHPs, *J. Biol. Chem. 276*, 23816–23824.

59. Fujioka, Y., Matozaki, T., Noguchi, T., Iwamatsu, A., Yamao, T., Takahashi, N., Tsukda, M., Takada, T., and Kasuga, M. (1996) A novel membrane glycoprotein, SHPS-1, that binds the SH2-domain-containing protein tyrosine phosphatase SHP-2 in response to mitogens and cell adhesion, *Mol. Cell. Biol. 16*, 6887–6899.

60. Veillette, A., Thibaudeau, E., and Latour, S. (1998) High expression of inhibitory receptor SHPS-1 and its association with protein-tyrosine phosphatase SHP-1 in macrophages, *J. Biol. Chem. 273*, 22719–22728.

61. Howie, D., Simarro, M., Sayos, J., Guirado, M., Sancho, J., and Terhorst, C. (2002) Molecular dissection of the signaling and costimulatory functions of CD150 (SLAM): CD150/SAP binding and CD150-mediated costimulation, *Blood 99*, 957–965.

62. Florio, T., Thellung, S., Arena, S., Corsaro, A., Bajetto, A., Schettini, G., and Stork, P. J. S. (2000) Somatostatin receptor 1 (SSTR-1)-mediated inhibition of cell proliferation correlates with the activation of the MAP kinase cascade: role of the phosphatase SHP-2, *J. Physiol. 94*, 239–250.

63. Wu, Y., et al. (1998) The B-cell transmembrane protein CD72 binds to and is an in vivo substrate of the protein tyrosine phosphatase SHP-1, *Curr. Biol. 8*, 1009–1017.

64. Adachi, T., Flaswinkel, H., Yakura, H., Reth, M., and Tsubata, T. (1998) Cutting edge: The B cell surface protein CD72 recruits the tyrosine phosphatase SHP-1 upon tyrosine phosphorylation, *J. Immunol. 160*, 4662–4665.

65. Daigle, I., Yousefi, S., Colonna, M., Green, D. R., and Simon, H.-U. (2002) Death receptors bind SHP-1 and block cytokine-induced anti-apoptotic signaling in neutrophils, *Nat. Med. 8*, 61–67.

66. Keilhack, H., Tenev, T., Nyakatura, E., Godovac-Zimmermann, J., Nielsen, L., Seedorf, K., and Bohmer, F. D. (1998) Phosphotyrosine 1173 mediates binding of the protein-tyrosine phosphatase SHP-1 to the epidermal growth factor receptor and attenuation of receptor signaling, *J. Biol. Chem. 273*, 24839–24846.

67. Klingmuller, U., Lorenz, U., Cantley, L. C., Neel, B. G., and Lodish, H. F. (1993) Specific recruitment of SH-PTP1 to the erythropoietin receptor causes inactivation of JAK2 and termination of proliferative signals, *Cell 80*, 1445–1454.

68. Tauchi, T., Damen, J. E., Toyama, K., Feng, G.-S., Broxmeyer, H. E., and Kryatal, G. (1996) Tyrosine 425 within the activated erythropoietin receptor binds Syp, reduces the erythropoietin required for Syp tyrosine phosphorylation, and promotes mitogenesis, *Blood 87*, 4495–4501.

69. Mason, J. M., Beattie, B. K., Liu, Q., Dumont, D. J., and Barber, D. L. (2000) The SH2 inositol 5-phosphatase Ship1 is recruited in an SH2-depedent manner to the erythropoietin receptor, *J. Biol. Chem. 275*, 4398–4406.

70. Bjorbaek, C., Lavery, H. J., Bates, S. H., Olson, R. K., Davis, S.

feedback inhibition of the leptin receptor via Tyr-985. *J. Biol. Chem.* 275, 40649−40657.

71. Okazaki, T., Maeda, A., Nishimura, H., Kurosaki, T., and Honjo, T. (2001) PD-1 immunoreceptor inhibits B cell receptor-mediated signaling by recruiting src homology 2-domain-containing tyrosine phosphatase 2 to phosphotyrosine, *Proc. Natl. Acad. Sci. U.S.A.* 98, 13866−13871.

72. Sheppard, K.-A., Fitz, L. J., Lee, J. M., Benarder, C., George, J. A., Wooters, J., Qiu, Y., Jussif, J. M., Carter, L. L., Wood, C. R., and Chaudhary, D. (2004) PD-1 inhibits T-cell receptor induced phosphorylation of the ZAP70/CD3ζ signalosome and downstream signaling to PKCθ, *FEBS Lett.* 574, 37−41.

73. Baznet, C. E., Gelderloos, J. A., and Kazlauskas, A. (1996) Phosphorylation of tyrosine 720 in the platelet-derived growth factor α receptor is required for binding of Grb2 and SHP-2 but not for activation of Ras or cell proliferation, *Mol. Cell. Biol.* 16, 6926−6936.

74. Cunnick, J. M., Mei, L., Doupnik, C. A., and Wu, J. (2001) Phosphotyrosines 627 and 659 of Gab1 constitutes a bisphosphoryl tyrosine-based activation motif (BTAM) conferring binding and activation of SHP-2, *J. Biol. Chem.* 276, 24380−24387.

75. Yu, W.-M., Hawley, T. S., Hawley, R. G., and Qu, C.-K. (2002) Role of the docking protein Gab2 in β1-integrin signaling pathway-mediated hematopoietic cell adhesion and migration, *Blood* 99, 2351−2359.

76. Wolf, I., Jenkins, B. J., Liu, Y., Seiffert, M., Custodio, J. M., Young, P., and Rohrshneider, L. R. (2002) Gab3, a new DOS/ Gab family member, facilitates macrophage differentiation, *Mol. Cell. Biol.* 22, 231−244.

77. Kozlowski, M., Larose, L., Lee, F., Le, D. M., Rottapel, R., and Siminovitch, K. A. (1998) SHP-1 binds and negatively modulates the c-Kit receptor by interaction with tyrosine 569 in the c-Kit juxtamembrane domain, *Mol. Cell. Biol.* 18, 2089−2099.

78. Guntermann, C., and Alexander, D. R. (2002) CTLA-4 suppresses proximal TCR signaling in resting human CD4+ T cells by inhibiting ZAP-70 Tyr-319 phosphorylation: A potential role for tyrosine phosphatases, *J. Immunol.* 168, 4420−4429.

79. Hu, Y., Szente, B., Kiely, J.-M., and Gimbrone, M. A., Jr. (2001) Molecular events in transmembrane signaling via E-selectin, *J. Biol. Chem.* 276, 48549−48553.

80. Ali, S., and Ali, S. (2000) Recruitment of the protein-tyrosine phosphatase SHP-2 to the C-terminal tyrosine of the prolactin receptor and to the adaptor protein Gab2, *J. Biol. Chem.* 275, 39073−39080.

81. Gunaje, J. J., and Bhat, G. J. (2001) Involvement of tyrosine phosphatase PTP1D in the inhibition of interleukine-6-induced Stat3 signaling by α-thrombin, *Biochem. Biophys. Res. Commun.* 288, 252−257.

82. Kiener, P. A., Lioubin, M. N., Rohrschneider, L. R., Ledbetter, J. A., Nadler, S. G., and Diegel, M. L. (1997) Co-ligation of the antigen and Fc receptors gives rise to the selective modulation of intracellular signaling in B cells, *J. Biol. Chem.* 272, 3838−3844.

Extraordinary variation in a diversified family of immune-type receptor genes

Noel A. Hawke*†, Jeffrey A. Yoder†‡§¶, Robert N. Haire‡, M. Gail Mueller¶, Ronda T. Litman‡, Ann L. Miracle‡, Tor Stuge‖**, Linling Shen‖, Norman Miller‖, and Gary W. Litman*‡§¶††

Departments of *Medical Microbiology and ‡Pediatrics, University of South Florida Children's Research Institute, 140 Seventh Avenue South, St. Petersburg, FL 33701; §H. Lee Moffitt Cancer Center, 12902 Magnolia Drive, Tampa, FL 33612; ¶All Children's Hospital, 801 Sixth Street South, St. Petersburg, FL 33701; and ‖Department of Microbiology, University of Mississippi, 2500 North State Street, Jackson, MS 39216-4505

Immune inhibitory receptor genes that encode a variable (V) region, a unique V-like C2 (V/C2) domain, a transmembrane region, and a cytoplasmic tail containing immunoreceptor tyrosine-based inhibition motifs (ITIMs) have been described previously in two lineages of bony fish. In the present study, eleven related genes encoding distinct structural forms have been identified in *Ictalurus punctatus* (channel catfish), a well characterized immunological model system that represents a third independent bony fish lineage. Each of the different genes encodes an N-terminal V region but differs in the number of extracellular Ig domains, number and location of joining (J) region-like motifs, presence of transmembrane regions, presence of charged residues in transmembrane regions, presence of cytoplasmic tails, and/or distribution of ITIM(s) within the cytoplasmic tails. Variation in the numbers of genomic copies of the different gene types, their patterns of expression, and relative levels of expression in mixed leukocyte cultures (MLC) is reported. V region-containing immune-type genes constitute a far more complex family than recognized originally and include individual members that might function in inhibitory or, potentially activatory manners.

Extended multigene families belonging to the Ig gene super-family (IgSF) account for a diverse range of immunological functions including recognition of antigens and antigenic pep-tides by both somatically rearranging Ig and T cell antigen receptor (TCR) genes, as well as by major histocompatibility complex (MHC) molecules. The origins of the three diverse systems of effector molecules can be traced through analyses of these genes in extant species of representative early, jawed vertebrates (1). Recently, multigene families which encode novel immune-type receptors (*NITR/nitr*) have been described in *Spheroides nephelus* (Southern pufferfish; ref. 2) and *Danio rerio* (zebrafish; ref. 3). The *NITR* genes described in these species encode two extracellular Ig domains [a variable (V) domain and a V-like C2 (V/C2) domain], a transmembrane region, and most often, immunoreceptor tyrosine-based inhibition motifs (ITIMs) in the cytoplasmic tail. The general structural characteristics of the NITR V domain are common to the corresponding regions of both Ig and TCR (4); whereas ITIMs are found in several inhibitory receptors, which are encoded at the leukocyte recep-tor cluster (LRC) on human chromosome 19q13.3–13.4 and at a corresponding location on mouse chromosome 7 and include natural killer (NK) receptors, such as killer cell Ig-type receptors (KIRs) (5). Unlike *NITR* genes, LRC genes do not encode V regions. A number of questions arise regarding the distribution of the *NITR* genes in vertebrate phylogeny, their function, and the relatedness of *NITR* genes to other families of genes that are involved in immune function, specifically, the immune inhibitory receptors of the mammalian LRC.

The lack of immunologically relevant *in vitro* culture systems in pufferfish and zebrafish severely limits functional assessments. In contrast, *in vitro* immunological phenomena can be studied in *Ictalurus punctatus* (channel catfish), and specific functions have been assigned to cells possessing defined cell surface phenotypes

(6). Furthermore, functionally distinct clonal macrophage, B, T and NK-like cell lines (7–10) are available. In this study, genes related to *NITRs* have been identified in *Ictalurus* and are shown to encode for an extraordinary continuum of structural variation, including gene products that lack ITIMs and possess a positively charged residue in the transmembrane region, reminiscent of activating receptors of the LRC as well as TCRα/β (11–13). Different *NITR* genes exhibit both tissue- and lineage-specific expression patterns, and their expression is differentially regu-lated during the course of *in vitro* immune stimulation.

Materials and Methods

General Methods. For RNA isolation, poly(A)$^+$ selection, and construction of λDASH II (Stratagene) genomic, λZAP II (Stratagene), and λ TrpI-Ex2 (CLONTECH) cDNA libraries, we used standard technology (2). Libraries were screened with probes complementing *NITR* sequences from zebrafish, puffer-fish, trout (J.A.Y., unpublished observations), and *Ictalurus*. Rapid amplification of cDNA ends (RACE) was performed by using *Ictalurus* head kidney mRNA and the GeneRacer kit (Invitrogen). The methods used for automated DNA sequenc-ing, directional deletion of genomic clones, sequence alignments, identity searches, and assignment of protein domains have been described (2, 3).

RNA and DNA Blot Analyses. RNA blots were prepared as described by using Zetaprobe-GT (Bio-Rad; ref. 2). Probes complement-ing the V regions of *IpNITRs* 1–5 (labeled to equivalent specific activity) were hybridized in Expresshyb (CLONTECH) at 68°C and washed according to the manufacturer's specifications.

Genomic DNA (5 μg) was digested to completion with *Eco*RI or *Hin*dIII and subjected to electrophoresis in 1% LE agarose, transferred to Zetaprobe-GT under denaturing conditions, and UV crosslinked. Blots were hybridized either in Expresshyb (see above) or in 0.6 M NaCl/0.2 M Tris/0.02 M EDTA/0.5% SDS

Fig. 1. (A) CLUSTALW alignment of the predicted translation products of IpNITRs 1–4. The prototypic pufferfish (SN6A) and zebrafish (Nitr3.1) are shown for comparison. Identical residues are reverse image (black), functionally equivalent residues are in reverse image (gray). Leader (L), V, V/C2, J (FGXG), transmembrane (TM), CDR1 (111111), and CDR2 (222222) are indicated. Conserved cysteines are shaded with blue. Positively charged residues within the TM are shaded with red. Consensus ITIMs are shaded with yellow and ITIM-related sequences are shaded with orange. (B) CLUSTALW alignment of the predicted translation products of the single Ig domain-containing IpNITRs 5–11. The zebrafish Nitr3r.1 and portions of IpNITR1 in which the V/C2 region has been removed (circles) are shown for comparison; note the high level of identity of the C-terminal regions of IpNITRs 1, 6, 8, and 9. Labeling is as in A.

(conventional conditions) at 65°C and washed in 0.15 M NaCl/0.015 M Na citrate at 52°C.

In Vitro Allogeneic Stimulation. *In vitro* allogeneic stimulations were performed by using peripheral blood leukocytes (PBLs) from outbred *Ictalurus* as effectors and γ-irradiated 1G8 clonal B cells as stimulators, at a 5:2 effector to stimulator ratio (14). Allogeneic stimulation was monitored both by [³H]thymidine uptake and allospecific cytotoxicity as measured by ⁵¹Cr release from 5 × 10⁴ labeled 1G8 (as homologous targets) or 3B11 (as heterologous targets) B cells exposed to varying numbers of mixed leukocyte culture (MLC) effectors. MLC cytotoxic effectors were cloned subsequently by limiting dilutions in the presence of homologous target cells and yielded the 3H9 NK-like cell line, among others (9, 15).

Results and Discussion

Identification of Ictalurus NITRs. Heterologous screening of *Ictalurus* cDNA libraries (activated PBL, normal spleen, and head kidney) by using pufferfish *NITR* probes resulted in the identification of IpNITR2 and IpNITR4 (Fig. 1A; designations are based on the predicted level of structural complexity; see below). IpNITR3 was identified by heterologous screening of a second, higher representation *Ictalurus* head kidney cDNA library by using a probe complementing a V/C2 domain of a trout *NITR*. In addition, an IpNITR3-like genomic clone also was identified

and a two-round RACE strategy was used to identify the corresponding cDNA; however, multiple, closely related cDNA products were identified. Only cDNAs encoding an entire ORF were characterized further and include: IpNITR1 (Fig. 1A) as well as four additional transcripts (IpNITRs 5, 6, 8, and 9; Fig. 1B). IpNITRs 5, 6, 8, and 9 are distinguished by the presence of only a single (V) Ig domain. A fifth gene containing a single V domain (IpNITR7; Fig. 1B) was identified in a cDNA library screen by using an IpNITR3 probe. IpNITR10 and IpNITR11 were identified in the course of screening a 3H9 (an NK-like cell line) cDNA library with IpNITR3 and IpNITR5 V domain probes. Notwithstanding the variation that has been recognized in the overall organization of NITR genes, the particular methods used in studies to date with *Ictalurus* are not exhaustive in terms of defining all related genes, nor have been the strategies used previously to identify related genes in pufferfish (2) and zebrafish (3). Finally, although the degree of structural variation described herein is extreme, the designation *NITR* is used throughout to describe the *Ictalurus* genes based on the similarities of their Ig domains to the prototypic genes that were identified in the two other species of bony fish.

IpNITRs Exhibit Structural Diversity. Comparisons of predicted peptide structures of *Ictalurus* NITRs show considerable variation (Fig. 2). Specifically, mammalian Ig J motifs (FGXG), resembling those described previously in the V and V/C2

Hawke et al.
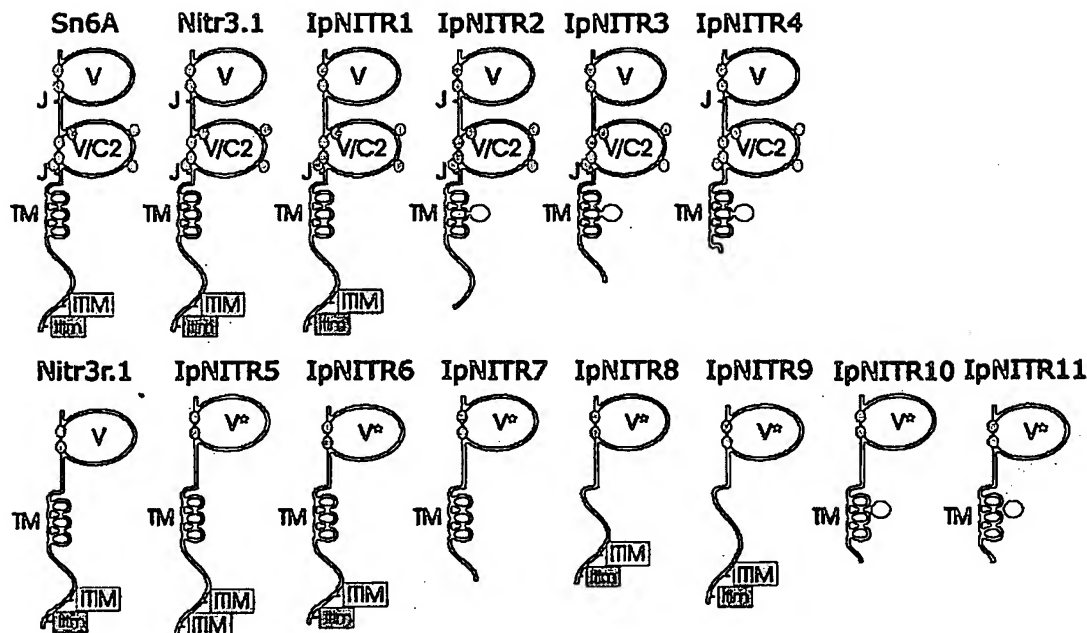
Fig. 2. Diversity in IpNITR structure. V, V/C2, joining (J; FGXG), and transmembrane (TM) regions are indicated. Consensus ITIMs are highlighted in yellow, ITIM-like sequences are highlighted in orange. Conserved cysteines are indicated with a blue oval. Conserved positively charged residues (+) are highlighted in red. The sequences of the Ig domains of IpNITRs 5–11 are related closely and indicated by ●. Pufferfish SN6A (2) and zebrafish Nitr3.1 and Nitr3r.1 (3) are shown for comparison.

domains of NITRs found in other species of bony fish (2, 3), are present in the V regions of IpNITR2 and IpNITR4, as well as in the V/C2 domains of IpNITRs 1–3 (Fig. 1A). Cysteines C^{25} and C^{109} (assignment based on IMGT V region nomenclature; http://imgt.cines.fr) are predicted to provide a second disulfide bridge between the β-pleated sheets of the V/C2 domain and are conserved in IpNITRs 1–4 as well as in nearly all NITRs from other species (refs. 2 and 3; Fig. 1A).

The use of a charged group within a hydrophobic transmembrane region to stabilize interactions with adaptor proteins and/or signaling complexes is a common mechanism in certain activatory members of the LRC, as well as TCR and Ig (12). The ITIM-containing NITRs described here, as well as all of the other NITRs characterized to date, lack intramembranous charged groups. However, IpNITRs 2–4 contain an arginine in their transmembrane region (Fig. 1A). By analogy to the activatory signaling complexes that form between certain NK receptors and DAP family members (12), this charged group could potentially interact with an as yet unidentified adaptor protein. Overall, IpNITRs 1–4 vary in the (i) number of J-like sequences, (ii) presence of a positively charged residue in the transmembrane region, (iii) length of the cytoplasmic tail, and (iv) presence of ITIM and ITIM-like sequences (Figs. 1A and 2). It is likely that these structural differences are associated with functional variation (see below).

In contrast, IpNITRs 5–11 possess single V domains, which are ≈85–100% related. The V domain of *IpNITR6* (selected as the reference) and the corresponding portions of *IpNITRs* 5 and 7–11 are from ≈91–99% related at the nucleotide sequence level. Variation is limited largely to two highly similar patterns in the second complementarity determining region (CDR2); one includes IpNITRs 6, 8, and 9 and the other includes IpNITRs 5, 7, 10, and 11. The single V-containing IpNITRs are most

structurally similar to the zebrafish receptor Nitr3r.1(3) (Figs. 1B and 2).

The sequences of the transmembrane regions of IpNITRs 5–7, 10, and 11 are very similar; however, the transmembrane region of both IpNITR10 and IpNITR11 possess a single, positively charged residue. Although IpNITR10 and IpNITR11 lack extended C-terminal sequence, several positively charged residues are immediately C-terminal of their transmembrane regions. These charged residues are conserved in IpNITRs 5–7, as well as IpNITRs 1–3; positively charged residues also are present in roughly corresponding positions in IpNITR8 and IpNITR9, which lack transmembrane regions. In addition, C-terminal sequences of IpNITR8 and IpNITR9 are nearly identical to IpNITR6 and IpNITR1. The ITIM and ITIM-like sequences in IpNITRs 6, 8, and 9, as well as IpNITR1, are identical, as is the more N-terminal ITIM in IpNITR5. IpNITR5 is the only NITR-related gene characterized thus far that possesses two consensus ITIMs (Fig. 1).

Genomic Analyses. Owing to the variation in the overall structure of *IpNITRs*, single exon probes (V-domain) were used in Southern blot analyses. Relatively few fragments hybridized with the *IpNITR* 1, 2, and 4 probes. Differences in the numbers of hybridizing elements in the EcoRI and HindIII digests can be accounted for by EcoRI sites in the V regions of *IpNITR1* and *IpNITR2* and a HindIII site in the V region of *IpNITR4* (Fig. 3). It is likely that only one or two copies of *IpNITRs* 1, 2, and 4 are present. In contrast, multiple fragments hybridize with the *IpNITR3* and *IpNITR5* V probes (which are ≈67% identical at the nucleotide level). Although similarities in hybridization patterns are evident when using Expresshyb (Fig. 3A), there also are unique features—e.g., an ≈9-kb band in the EcoRI-digest probed with *IpNITR3* is not prominent with the *IpNITR5* probe. Under conventional conditions, only the IpNITR5 "family"
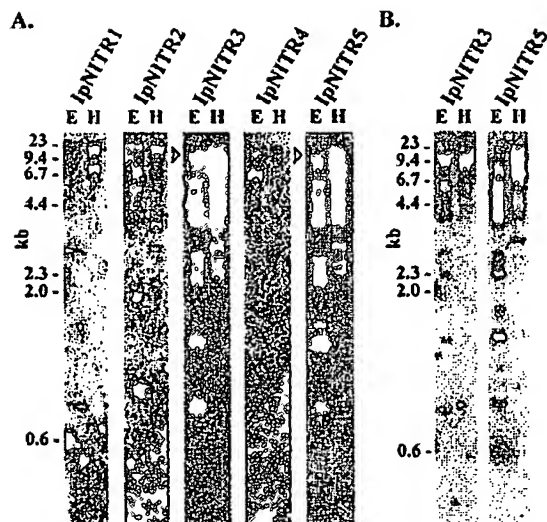
Fig. 3. Genomic complexity of *IpNITRs*. Southern blot transfers were hybridized in Expresshyb (*A*) or under conventional conditions (*B*) with probes complementing the V domains of IpNITRs 1–5 labeled to equivalent specific activity. Arrowheads are used to emphasize certain positions; size standards are indicated. Restriction sites for *Eco*RI and *Hind*III within V domains account for the differences in hybridization intensity for individual probes.

appears to be highly complex (Fig. 3*B*). This observation is consistent with the documented nucleotide sequence identities between the structurally distinct *IpNITRs* 5–11 and the likelihood that there are additional related types of genes.

The genomic organization of several IpNITRs has been determined (Fig. 4). The predicted exon structures (splice donor and acceptor sites, termination codons, and polyadenylation signal sequences) are entirely consistent with the cDNA sequences. The overall genomic organization of *IpNITRs* 1–4 resembles that of *NITR* genes that have been identified in pufferfish (2) and zebrafish (3), with the exception of cytoplasmic exons in IpNITRs 2–4. The possibility remains that variation in the structure of NITRs could derive in part through differential RNA processing, which has been proposed for the *nitr4* genes in zebrafish (3); however, there is no other evidence for alternative RNA processing contributing to the variability of *NITRs*. *IpNITR2* and *IpNITR4* are separated by an ≈3-kb
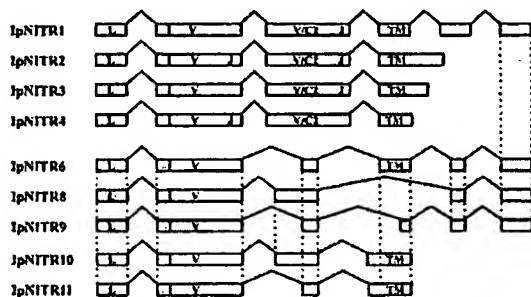
Fig. 4. Exon organization of IpNITRs. Exons are boxed, Intergenic sequence similarity is indicated by vertical dotted lines; leader (L), V, V/C2, joining (J), and transmembrane (TM) regions are indicated. Some components of the genomic organization of IpNITRs 1, 6, 8, and 9 are inferred from highly related genes.
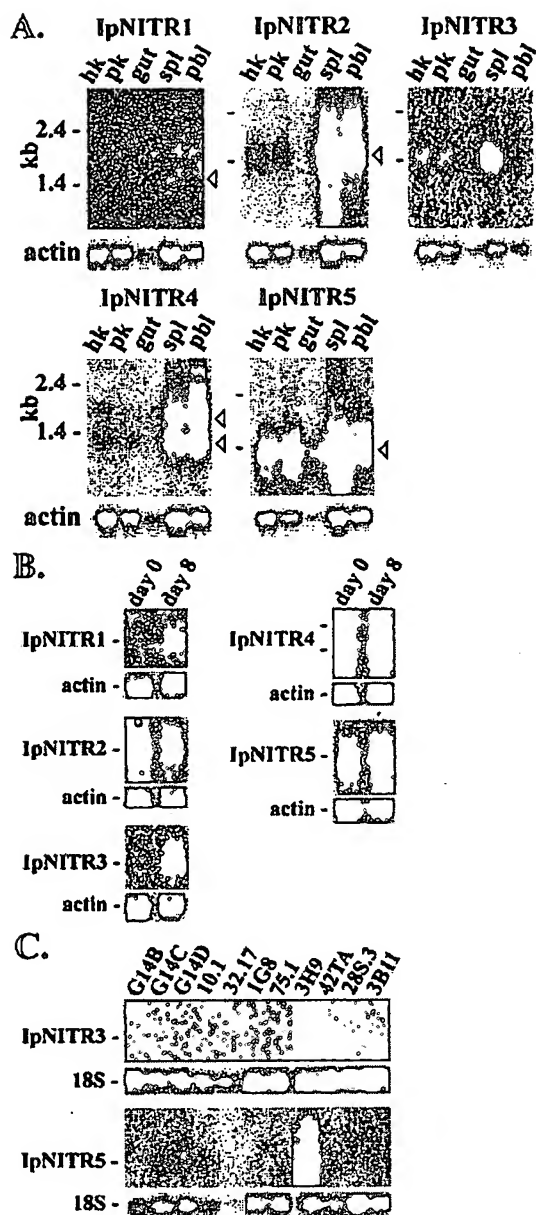
Fig. 5. Expression patterns of *IpNITRs*. (*A*) RNA blot [~1 μg/track of poly(A)⁺ mRNA] of head kidney (hk), posterior kidney (pk), gut, spleen (spl), and peripheral blood leukocytes (pbl). Probes complementing the V region of *IpNITRs* 1–5 were labeled to equivalent specific activity. Predominant transcripts are indicated with arrowheads. β-actin was used as a loading control; size standards are indicated. (*B*) RNA blot comparing expression of *IpNITRs* 1–5 at time 0 and after day 8 of one-way MLC. Total RNA (10 μg) was loaded into each track. Probes, hybridization, and loading controls are as in *A*. (*C*) RNA blot comparing expression of *IpNITRs* 1–5 in *Ictalurus* cell lines derived from peripheral blood leukocytes. Cell lines used include TCRα/β⁺ T cells (G14B, G14C, G14D, 32.17, and 28S.3), IgM⁺IgD⁻ B cells (1G8), IgM⁺IgD⁺ B cells (3B11), TCRαβ⁻, Ig⁻ cytotoxic cells (10.1, 75.1, and 3H9), and macrophages (42TA). Total RNA (2 μg) was loaded into each track. Probes and hybridization are as in *A*. 18S RNA served as a loading control.

intervening sequence; no evidence has been found for physical linkage between additional NITR elements. Extensive genomic sequencing such as that conducted previously in pufferfish (2) and which currently is in progress through the Zebrafish Genome Project likely will be needed to fully interpret the overall organization of IpNITRs.

IpNITR Genes Exhibit Tissue-Specific Expression. RNA blots are consistent with differential expression of IpNITR genes (Fig. 5A). Several conclusions can be drawn: (i) strong hybridization signals can be detected with the IpNITR 2–5 probes; (ii) IpNITR1 is detected only in spleen and at very reduced levels relative to the other IpNITR genes; (iii) different hybridization patterns occur with each of the aforementioned probes (based on genomic analysis, similarities in the IpNITR3 and IpNITR5 hybridization patterns are likely probe-related); (iv) two different RNA populations consistently hybridize with the IpNITR2 and IpNITR4 probes and this result could be reproduced by using RNA extracted from different animals; and (v) the broadest expression pattern is achieved with the IpNITR5 probe, which also produces the most complex genomic hybridization pattern in the Southern blot analyses.

Expression of IpNITR Genes in the MLC. One-way MLC using PBL responders and γ-irradiated clonal (1G8) B cell stimulators was performed and the kinetics of [³H]thymidine uptake were quantitated. Thymidine uptake predictably increased between one and six days, with a plateau achieved by day 9 (14). A biphasic increase in TCRα expression was observed relative to β-actin and likely is due to activation in primary allospecific T cells and T helper cells, with a later apparent increase as those T cells expand clonally in the effector population (data not shown). RNA analyses were carried out on mRNA isolated from an 8-day MLC as well as from an unstimulated day 0 control employing probes complementing IpNITRs 1–5 (Fig. 5B). The increase in expression of IpNITRs 1, 3, and 5 is consistent with an expansion of the lineage(s) expressing these genes through the course of the MLC. Significant levels of basal expression are evident for IpNITR2 and IpNITR4, which are expressed abundantly in PBLs (Fig. 5A). The expression of IpNITR2 decreases and the expression of IpNITR4 remains roughly equivalent in the 8-day MLC. These expression patterns reflect the kinetics of the

MLC reaction; IpNITR2 and IpNITR4 are likely expressed in several different cell types, of which some die off and others expand. Con A-stimulation failed to increase expression of IpNITRs (data not shown), which is inconsistent with expression of these receptors on T lymphocytes.

RNA from different Ictalurus cell lines also was hybridized with probes complementing the five different NITR families (Fig. 5C). Although expression of IpNITRs 1, 2, and 4 was not detected in any of the cell lines tested (data not shown), a high level of expression of IpNITR3 and IpNITR5 was noted for cell line 3H9, which was derived from PBLs through repeated allogeneic stimulation by using irradiated 1G8 cells and cloned by limiting dilution; considerably weaker hybridization was noted for cell lines G14C and G14D (both T cell lines derived from a gynogenetically derived channel catfish), as well as for 10.1 (NK-like cells; ref. 9). Functionally, 3H9 is cytotoxic toward a number of allogeneic cell lines (15). Because 3H9 is negative for both TCRα/β and IgM messages, and expresses the ligand for mAb CC41 (15), which is hypothesized to correspond to CD56, a mammalian NK marker, it might represent a NK equivalent or alternatively a γδT cell. Although 3H9 cells are negative for IgM mRNA, they show positive immunofluorescence to mAbs specific to the IgM heavy chain (Igμ) and both isotypes of Ictalurus Ig light chains (F and G) (15). Simultaneous expression of two light chain isotypes and the ability to modulate IgM off the cell surface by using anti-Ictalurus Igμ and replace it with affinity-purified Ictalurus antitrinitrophenol IgM antibodies are consistent with surface IgM being bound to a putative Fc receptor.

Limited screening of a 3H9 cDNA library resulted in the identification of IpNITR10, IpNITR11, several copies of IpNITR5, and three cDNAs corresponding to partially processed IpNITR3 and IpNITR5. The length variation in these various forms explains, in part, the disperse band observed in RNA blot analyses (Fig. 5C). Whereas function cannot be inferred from the expression patterns of NITRs, their expression in cytotoxic effectors and likely in other cell types further supports their possible role(s) in regulating various immune effector functions, as well as other recognition processes.

Relatedness of the NITRs and Relationships to the LRC. Various NITRs described to date possess characteristics of the inhibitory receptors encoded at the mammalian LRC, including Ig domains
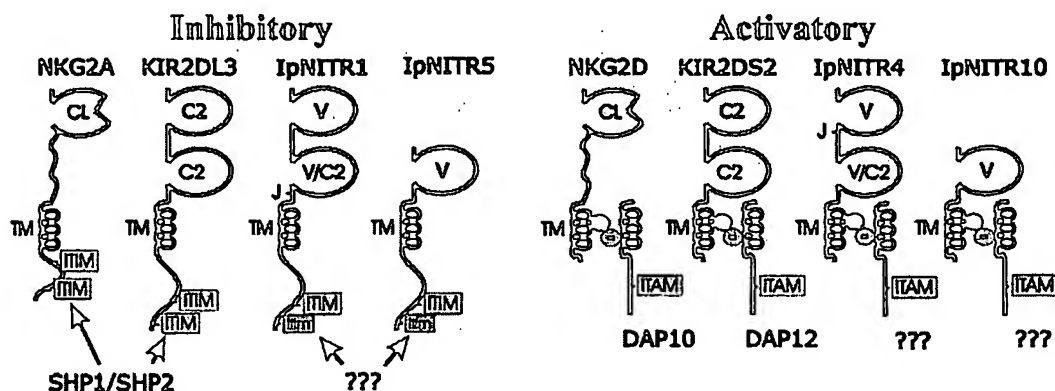
Fig. 6. Hypothetical signaling relationships of V domain-containing IpNITRs to LRC gene products. IpNITR1 and IpNITR5 are depicted as immune inhibitory receptors, which use two potential ITIMs and might signal through interactions with SHP1 and/or SHP2 as demonstrated previously for the mammalian receptors NKG2A and KIR2DL3. In contrast, IpNITR4 and IpNITR10 are depicted as immune activatory receptors lacking an ITIM and possessing an intramembranous positively charged residue and might functionally correspond to the mammalian receptors NKG2D and KIR2DS2 (13), which are associated with the negative charge-containing adaptors DAP10 and DAP12, respectively. Abbreviations are as in Fig. 2. C-type lectin domains (CL) and immunoreceptor tyrosine-based activation motifs (ITAM) also are shown.

and ITIM-mediated inhibition of MAPK (3) as well as NK killing (transfected mammalian cell lines) *in vitro* (J. Djeu, S. Wei, J. A. Y., and G. H. L., unpublished observations). The NITR variants described here expand the range of related gene products. IpNITRs 1–4 possess two extracellular Ig domains, a transmembrane region, and cytoplasmic tails of varying lengths (with or without ITIMs), and resemble most closely the NITRs described in pufferfish and zebrafish: IpNITRs 2–4, which possess charged intramembranous residues and for which equivalents have not yet been identified in the two other teleost fish systems, could potentially associate with adaptor molecules and function in an activatory pathway rather than in the postulated inhibitory pathway of the ITIM-containing NITR genes (Fig. 6). The identification of single Ig domain receptors that also possess charged intramembranous residues (IpNITR10 and IpNITR11) suggests that such pairings might be a basic feature of the NITRs. Identification of suitable adaptor molecules in this species would strengthen such proposals. As a family, NITRs exhibit potential for the type(s) of highly regulated positive and negative signals associated with the LRC gene products (ref. 4; see below).

IpNITRs 5–11 possess a single V domain and can be grouped into four potential functionally significant categories: transmembrane-containing with and without inhibitory motifs, transmembrane-containing with positively charged residues, and transmembrane-lacking. Structural comparisons can be made to several recently described mammalian single Ig domain containing receptors, PD-1 (16) and NKP44 (17), or pairs of receptors, CMRF-35 and CMRF-35-H9 (18), as well as PILRa/ FDF03/FDF03-ΔTM and PILRb (19, 20). These receptors are encoded outside the LRC and each receptor or pair of receptors is on a different chromosome. Of these, PILRa and PILRb appear most related to IpNITRs 5–11; PILRa is a single Ig domain receptor with a cytoplasmic tail containing two ITIM motifs (a putative inhibitory form). PILRb is a very similar receptor (90% amino acid identity through the first three exons) containing both a short highly charged cytoplasmic tail and a charged lysine in the transmembrane (a putative activatory form). Two alternatively spliced variants of the membrane-bound PILRa containing identical leader sequences and lacking TM regions are likely secreted in a manner similar to IpNITR8 and IpNITR9. However, unlike mammalian forms, all of the IpNITRs encode V regions, which are related closely.

Evolution of the NITR Genes. Collectively, the results reported here define a continuum of variation in form and presumably function for the NITRs. At this stage in the analysis of NITRs it is not possible to determine whether the V region serves a primary

recognition capacity similar to that seen in Ig and TCR, or whether these receptors recognize a common ligand—e.g., major histocompatibility complex (MHC)—as do several products of the LRC. What relationships, if any, the single V domain receptors have to the more typical diversified NITRs also remains to be determined.

Ictalurus and *Danio* (zebrafish) are representative members of a large assemblage the Ostariophysans, which encompass one of the four phylogenetic infrastructures of bony fish. *Spheroides* (pufferfish) represents a highly divergent lineage within that group. The studies reported here both confirm the presence of *NITR* genes in a third lineage of bony fish and expand the range of genes that possess an *NITR* character to now include eleven different members. Even in the absence of large-scale genomic scanning or a more comprehensive cDNA cloning strategy, a remarkable continuum of structural variation is defined. High levels of relatedness between exons that have been identified in different genes appear to be a common feature of the *IpNITR* genes and are consistent with gene duplication and exon exchange (2, 4). Whether the single Ig domain-containing genes found in *Ictalurus* diverged from or potentially gave rise to the genes possessing two extracellular domains is not apparent; however, extensive genomic sequencing available for the zebrafish *nitr* gene locus suggests that the single Ig domain gene *nitr3r.1* derived from a two-Ig-domain *nitr3* precursor (J.A.Y., unpublished observations).

The introduction of the *IpNITR* data provides additional possible precursor gene structures that might have factored in the evolution of rearranging immune receptors. Defining hierarchical relationships of the divergent forms of *NITRs* seen in extant bony fish would benefit from information about related genes present in species that diverged earlier in vertebrate phylogeny. This being the case, efforts are underway in our laboratory to identify gene structures related to the *NITRs* in cartilaginous fish, jawless vertebrates, and protochordates that are requiring the development of novel technologies to exploit the limited sequence identities between the highly diverse *NITR* genes.

1. Litman, G. W., Anderson, M. K. & Rast, J. P. (1999) *Annu. Rev. Immunol.* **17**, 109–147.
2. Strong, S. J., Mueller, M. G., Litman, R. T., Hawke, N. A., Haire, R. N., Miracle, A. L., Rast, J. P., Amemiya, C. T. & Litman, G. W. (1999) *Proc. Natl. Acad. Sci. USA* **96**, 15080–15085.
3. Yoder, J. A., Mueller, M. G., Wei, S., Corliss, B. C., Prather, D. M., Willis, T., Litman, R. T., Djeu, J. Y. & Litman, G. W. (2001) *Proc. Natl. Acad. Sci. USA* **98**, 6771–6776. (First Published May 29, 2001; 10.1073/pnas.121101598)
4. Litman, G. W., Hawke, N. A. & Yoder, J. A. (2001) *Immunol. Rev.* **181**, 250–259.
5. Barten, R., Torkar, M., Haude, A., Trowsdale, J. & Wilson, M. J. (2001) *Trends Immunol.* **22**, 52–57.
6. Miller, N., Wilson, M., Bengten, E., Stuge, T., Warr, G. & Clem, W. (1998) *Immunol. Rev.* **166**, 187–197.
7. Vallejo, A. N., Miller, N. W. & Clem, L. W. (1992) *Annu. Rev. Fish Dis.* **2**, 73–89.
8. Miller, N. W., Rycyzyn, M. A., Wilson, M. R., Warr, G. W., Naftel, J. P. & Clem, L. W. (1994) *J. Immunol.* **152**, 2180–2189.
9. Stuge, T. B., Wilson, M. R., Zhou, H., Barker, K. S., Bengten, E., Chinchar, G., Miller, N. W. & Clem, L. W. (2000) *J. Immunol.* **164**, 2971–2977.
10. Clem, L. W., Bly, J. E., Wilson, M., Chinchar, V. G., Stuge, T., Barker, K., Luft, C., Rycyzyn, M., Hogan, R. J., van Lopik, T. & Miller, N. W. (1996) *Vet. Immunol. Immunopathol.* **54**, 137–144.
11. Ravetch, J. V. & Lanier, L. L. (2000) *Science* **290**, 84–89.
12. Lanier, L. L. (2001) *Nat. Immunol.* **2**, 23–27.
13. Blery, M., Olcese, L. & Vivier, E. (2000) *Hum. Immunol.* **61**, 51–64.
14. Stuge, T. B., Yoshida, S. H., Chinchar, V. G., Miller, N. W. & Clem, L. W. (1997) *Cell. Immunol.* **177**, 154–161.
15. Shen, L., Stuge, T. B., Zhou, H., Khayat, M., Barker, K. S., Quiniou, S. M. A., Wilson, M., Bengten, E., Chinchar, V. G., Clem, L. W. & Miller, N. W. (2001) *Dev. Comp. Immunol.*, in press.
16. Finger, L. R., Pu, J., Wasserman, R., Vibhakar, R., Louie, E., Hardy, R. R., Burrows, P. D. & Billips, L. G. (1997) *Gene* **197**, 177–187.
17. Cantoni, C., Bottino, C., Vitale, M., Pessino, A., Augugliaro, R., Malaspina, A., Parolini, S., Moretta, L., Moretta, A. & Biassoni, R. (1999) *J. Exp. Med.* **189**, 787–796.
18. Green, B. J., Clark, G. J. & Hart, D. N. (1998) *Int. Immunol.* **10**, 891–899.
19. Mousseau, D. D., Banville, D., L'Abbe, D., Bouchard, P. & Shen, S.-H. (2000) *J. Biol. Chem.* **275**, 4467–4474.
20. Fournier, N., Chalus, L., Durand, I., Garcia, E., Pin, J. J., Churakova, T., Patel, S., Zlot, C., Gorman, D., Zurawski, S., *et al.* (2000) *J. Immunol.* **165**, 1197–1209.

CD85j (Leukocyte Ig-Like Receptor-1/Ig-Like Transcript 2) Inhibits Human Osteoclast-Associated Receptor-Mediated Activation of Human Dendritic Cells[1]

Claudya Tenca,[2]* Andrea Merlo,[2,3]* Estelle Merck,[†] Elizabeth E. M. Bates,[†] Daniele Saverino,* Rita Simone,* Daniela Zarcone,* Giorgio Trinchieri,[4†] Carlo E. Grossi,* and Ermanno Ciccone[5]*

Immature dendritic cells (DCs) derived from freshly isolated human monocytes were used to evaluate the effect of the inhibiting receptor CD85j (leukocyte Ig-like receptor-1/ILT2) on activation induced by cross-linking of the human osteoclast-associated receptor (hOSCAR). CD85j and hOSCAR were expressed consistently at the same density on monocytes and on monocyte-derived DCs (both immature and mature). Cross-linking of hOSCAR, which activates via the FcR-associated γ-chain, induced Ca^{2+} flux in DCs. Concomitant cross-linking of anti-CD85j mAb abolished this early activation event. Likewise, CD85j stimulation strongly reduced IL-8 and IL-12 production by hOSCAR-activated DCs. Inhibition of DCs via CD85j also impaired their ability to enhance Ag-specific T cell proliferation induced by hOSCAR. Finally, because hOSCAR prevents apoptosis of DCs in the absence of growth/survival factors, CD85j cross-linking was able to counteract completely this antiapoptotic effect and to reduce Bcl-2 expression enhanced by hOSCAR stimulation. Thus, CD85j is an inhibiting receptor that is functional in human DCs. *The Journal of Immunology*, 2005, 174: 6757–6763.

D
endritic cells (DCs)[6] are APCs that play a central role in the initiation of primary immune responses (1, 2). Upon stimulation, DCs secrete cytokines that are crucial for the regulation of innate resistance and adaptive immunity and undergo a process of maturation characterized by remarkable morphological and functional changes. The maturational state affects the ability of DCs to take up, process, and present Ags. Immature DCs located in peripheral tissues act as immune sentinels and are able to capture and process Ags due to their high endocytic activity (3, 4). Following activation and maturation induced by proinflammatory signals, DCs migrate to the T cell areas of secondary lymphoid organs, where they are able to present Ags to naive T cells. The outcome of the immune response (immune priming or toler-

ance) depends on the maturational status of DCs (5), which is generally believed to be regulated by endogenous factors such as proinflammatory cytokines (TNF and IL-1) (3, 6–8) or by exogenous factors such as pathogen-associated molecular patterns (e.g., LPS, dsRNA, and Cpg-DNA) (9, 10) recognized by specific receptors on the DC surface, such as the family of TLRs.

DC activity also can be regulated by both activating and inhibiting receptors that transduce signals via ITAM (11) and ITIM (12, 13), respectively. ITIM-bearing receptors negatively regulate cell functions when coligated with stimulating receptors that signal through ITAM. This growing family of receptors was described first in lymphocytes (14–16). However, in recent years, an increasing number of receptors that are members of the lectin family and of the Ig superfamily and are linked to ITAM/ITIM signaling have been described on myeloid cells and DCs, such as FcγR, C-type lectin receptors (DC immunoactivating receptor), Ig-like transcript (ILT)3, ILT4, and FDF03 (17–22).

Among ITIM-bearing inhibiting receptors, the leukocyte Ig-like receptor (LIR)/ILT molecular family (Ref. 23 and reviewed in Ref. 24) is encoded by at least 10 genes, and these proteins belong to the Ig superfamily. The products of some of these genes, such as LIR-1/ILT2 (CD85j), are surface membrane inhibiting receptors. CD85j/LIR-1/ILT2 is detected on the surface of a proportion of NK cells (23–77%) and of T lymphocytes (20%), on all B lymphocytes, monocytes, and myeloid DCs (14, 25–27). CD85j consists of four C2 Ig domains and exhibits a molecular mass of 110 kDa under both reducing and nonreducing conditions, suggesting that it is a noncovalently linked monomer (25, 26). Its inhibiting function is mediated by tyrosine phosphorylation of four ITIM-like sequences in its cytoplasmic tail. Tyrosine phosphorylation by p56^{lck} in T cells leads to recruitment of Src homology protein (SHP)-1, SHP-2, and Src homology 2 domain-containing inositol phosphatases (22). Recruitment of these phosphatases down-regulates the signaling mediated by activating receptors (23, 27, 28).

We have described previously that CD85j is present and functional in the cytoplasm of all T cells, independently of its surface expression (14, 29). Ligands for CD85j include the nonclassical class I HLA-G protein (30), some alleles of *HLA-A* and *-B* loci, and the human CMV *UL18* gene product, a viral homolog of HLA class I (26). CD85j shows a differential affinity for these ligands, e.g., 1000 times higher for UL18 than for HLA-A2 and 4 times higher for HLA-G than for classical HLA molecules (31, 32). Although it is unknown whether the different affinity could play a role in CD85j function, the interaction of CD85j with UL18 leads to activation of T lymphocytes, resulting in the lysis of human (h)CMV-infected cells, despite the defined inhibiting functions of CD85j (33). Likewise, UL18-expressing transfectants are lysed by human NK clones (34).

Several groups have reported the presence of the LIR/ILT family of receptors on APCs. It has been shown that these receptors function as negative regulators of monocyte and DC activation, presumably through recruitment of SHP-1 (20, 27, 35).

We recently described the human osteoclast-associated receptor (hOSCAR), a novel immune receptor associated with the FcRγ chain (FcRγ) and involved in endocytosis and Ag presentation through the MHC class II pathway in monocyte-derived DCs (mono-DC) (36). Its association with the ITAM-bearing FcRγ confers to hOSCAR the capacity to activate myeloid cells as shown by its ability to trigger calcium flux and cytokine release (36). We also showed that hOSCAR ligation induced phenotypic and functional maturation of DCs, elicited cytokine and chemokine secretion, and synergistically amplified the TLR-induced ability of DCs to prime naive T cell proliferation (37). Unlike hOSCAR, mouse (m)OSCAR is expressed only on osteoclasts (38), which, like certain DC subsets, derive from the myeloid lineage. Data from different groups strongly suggest that in vivo ligation of mOSCAR on osteoclasts is essential for the differentiation of these cells. The existence of an endogenous ligand for mOSCAR on osteoblasts has been inferred from this work (38).

In this study, mono-DCs have been activated by cross-linking of several surface molecules (CD1a, HLA-DR, and hOSCAR) with mAb, and the inhibiting ability of CD85j has been tested subsequently. hOSCAR (36, 37) provided the strongest activating signal for DCs and was therefore chosen for all of the experiments. We show that CD85j inhibits intracellular calcium mobilization and cytokine secretion triggered by ligation of hOSCAR. Moreover, CD85j prevents the rescue from apoptosis and the cooperation between DCs and Ag-specific T cells that is mediated by hOSCAR.

Materials and Methods
Cell cultures

Human peripheral blood samples were obtained from healthy donors according to institutional guidelines. PBMCs were purified by Ficoll-Hypaque density gradient centrifugation. Monocytes and CD4⁺ T lymphocytes were isolated by positive selection with magnetic beads coated with mAb to CD14 and CD4 (MACS; Miltenyi Biotec). To induce DC differentiation, purified monocytes were cultured for 5 days in the presence of 200 ng/ml recombinant human GM-CSF and 10 ng/ml recombinant human IL-4 (Schering-Plough Research Institute). These cells are termed immature DCs. Maturation was achieved by culturing immature DCs for an additional 24 h in the presence of 10 ng/ml LPS (Sigma-Aldrich). Cells were cultured in RPMI 1640 supplemented with 10% heat-inactivated FCS, 5 mM L-glutamine, and 50 IU/ml penicillin-streptomycin (from here on referred to as complete medium).

Antibodies

mAb used for immunophenotypic and functional analyses were as follows: anti-CD85j purified Ab (clone GHI/75; BD Pharmingen) or ascites (clone HP-F1, provided by Dr. M. Lopez-Botet, Molecular Immunopathology Unit, Universitat Pompeu Fabra, Barcelona, Spain); anti-OSCAR mAb 11.1CN5; anti-CTLA-4 (CH7.3-624 ascites, provided by Dr. A. Lanzavec-

chia, Institute for Research in Biomedicine, Bellinzona, Switzerland); anti-CD31 (clone Moon-1, provided by Dr. F. Malavasi, Laboratory of Immunogenetics, University of Torino, Italy); anti-HLA-DR (DI.12, a gift from Dr. C. Gelin, Institut National de la Santé et de la Recberche Médicale, Unité 396, Institut d'Hématologie, Hôpital Saint-Louis, Paris, France); and anti-Bcl-2 (DakoCytomation). Other mAb used for surface phenotype analysis were PE-conjugated anti-CD14, anti-CD1a, and anti-HLA-DR (BD Pharmingen).

Flow cytometry

The surface phenotype of monocytes and mono-DCs was assessed by flow cytometric analysis (FACSCalibur; BD Biosciences). The secondary reagent was PE-labeled goat anti-mouse (GAM) antiserum (Southern Biotechnology Associates).

Measurement of intracellular Ca^{2+} flux

Intracellular Ca^{2+} mobilization was determined as described previously (19), with modifications. Briefly, mono-DCs were loaded with 10 μM Fluo-3AM and 5 μM Pluronic F-27 (Molecular Probes) for 30 min at 37°C. mAb (10 μg/ml) was added to human serum-saturated cells and then cross-linked with 20 μg/ml GAM antiserum (Jackson ImmunoResearch). For inhibition experiments where anti-hOSCAR was used in combination with HP-F1, anti-CTLA-4, or anti-CD31, the latter mAb were added 30 s before anti-hOSCAR. Cells were analyzed subsequently by flow cytometry (FACSCalibur) to detect Ca^{2+} fluxes. Only viable cells (based on forward scatter criteria) and Fluo-3AM-loaded cells (based on 405- vs 530-nm emission spectra) were analyzed. A positive control was obtained by addition of ionomycin.

Cell activation and cytokine assays

Anti-hOSCAR, purified anti-CD85j, and anti-CD31 (as isotype- matched control Ab) were coated overnight at 4°C on flat-bottom plates at a final concentration of 20 μg/ml in PBS. The ascites HP-F1 and anti-CTLA-4 (as ascites control) were used at 1/100 dilution. In inhibition experiments, HP-F1 and purified anti-CD85j, or anti-CD31 and anti-CTLA-4, were coated in the same well together with anti-hOSCAR at the concentrations indicated above. Immature DCs were plated at 1 × 10⁶ cells/ml. *Escherichia coli* LPS was used at the final concentration of 10 ng/ml. Supernatants were collected after 24 h and tested for the presence of IL-8 and IL-12 p40 by ELISA (Diaclone Research).

Proliferation assays

DCs and CD4⁺ T lymphocytes were obtained as described above. Immature DCs were prelabeled with 10 μg/ml mAb and cross-linked with GAM antiserum (Jackson ImmunoResearch) for 30 min in the cold, washed, and pulsed with recall Ags (*Candida albicans* bodies, 3 × 10⁵/ml, or purified protein derivative, 10 μg/ml). Proliferative responses were measured by culturing 3 × 10⁴ pretreated immature DCs in the presence of 10⁵ CD4⁺ autologous T lymphocytes in 0.2 ml of complete medium, in 96-well flat-bottom microtiter plates. Cultures were pulsed with 0.5 μCi of [³H]thymidine (Amersham Biosciences) on day 4 and harvested 18 h later. Dry filters with scintillation fluid were counted in a gamma counter.

Detection of apoptosis

After DC differentiation, cells were collected and washed four times with PBS to remove GM-CSF and IL-4. Immature DCs were stimulated for 3 days with coated mAb in complete medium, as described above. Cultures were harvested, and the apoptotic cells were detected using the Annexin Vᶠᴵᵀᶜ kit (BD Pharmingen). To measure mitochondrial membrane potential, another indicator of apoptosis, cells were incubated in complete medium containing 25 nM 3,3-dihexylaxocarbocyanine iodide (DiOC₆) (Molecular Probes) for 30 min at 37°C in the dark, followed by flow cytometric analysis. Intracellular labeling with FITC-conjugated mAb to Bcl-2 (DakoCytomation) was performed as described elsewhere (39).

Statistical analyses

Differences in cell proliferation and cytokine production between hOSCAR-activated DCs and DCs treated concomitantly with anti-CD85j and anti-hOSCAR mAb were observed. To assess their statistical significance, Student's *t* test was used with a level of $p < 0.05$.

Results

CD85j is expressed on the surface of freshly isolated monocytes and of immature and mature DCs

Fresh monocytes, isolated by positive selection using magnetic beads coated with anti-CD14 mAb, were cultured for 5 days with GM-CSF and IL-4 (immature DCs), and further stimulated for 1 day with LPS (mature DCs). Cells were tested for the expression of cell surface markers. Freshly isolated monocytes and immature and mature DCs from 15 donors consistently expressed the inhibiting receptor CD85j and the activating receptor hOSCAR, at similar levels (Fig. 1). CD14, an LPS receptor, was down-regulated upon differentiation toward DCs and remained low in both immature and mature DCs, whereas CD1a and HLA-DR were up-regulated sharply in comparison with fresh monocytes. All cell types also expressed CD31 at about the same level (Fig. 1).

In the experiments described below, immature DCs have been used because they yield the best response to both activating and inhibiting stimuli.

CD85j inhibits Ca^{2+} flux induced by the activating receptor hOSCAR

Ligation of hOSCAR was a better activating stimulus than CD1a and HLA-DR (data not shown). As shown in Fig. 2, ligation of hOSCAR triggered a rapid Ca^{2+} flux in immature DCs (a). hOSCAR-induced Ca^{2+} flux was prevented completely in the presence of anti-CD85j mAb (HP-F1 or GHI/75) (Fig. 2b). In contrast, Ca^{2+} flux induced by cross-linking of hOSCAR was not affected by ligation of the inhibiting receptor CTLA-4 and of CD31 (Fig. 2, c and d). mAb to CTLA-4 that is not expressed on the DC surface (data not shown) and to CD31 were used in the form of ascites and of purified Abs, respectively, and thus provided isotype-matched controls for the inhibition experiments using HP-F1 (ascites) and GHI/75 (purified Abs). HP-F1 alone did not cause Ca^{2+} mobilization (Fig. 2e), whereas ligation of activating molecules, such as CD1a or HLA-DR (22, 27), yielded a low level of Ca^{2+} flux (Fig. 2f) that was inhibited by anti-CD85j mAb (data not shown). Thus, the strong signal produced by hOSCAR was used as a model of activation in all of the experiments.

CD85j down-regulates cytokine production induced by hOSCAR

Because stimulation via hOSCAR triggered the production of high amounts of IL-8 and IL-12 p40 by immature DCs (36, 37), we investigated the ability of CD85j cross-linking to inhibit the release of these cytokines. Cell stimulation was obtained by mAb coated onto culture plates to avoid the use of GAM antiserum that could interfere with cytokine detection in the supernatants. Concomitant coating with anti-CD85j, used both as purified mAb and as ascites, yielded a significant decrease of IL-8 and IL-12 p40 secretion (Fig. 3), when compared with stimulation with anti-hOSCAR alone. Cross-linking of CTLA-4 and of CD31 did not affect cytokine secretion mediated by hOSCAR (Fig. 3). In addition, as a positive control for immature DC functions, stimulation via LPS was also performed (Fig. 3). LPS, as shown previously (36), yielded the highest level of cytokine production that was not inhibited by coligation of CD85j (data not shown).

CD85j inhibits the ability of DCs to stimulate Ag-specific T cells

Because cross-linking of CD85j with other receptors decreases cytokine secretion by DCs, we investigated whether inhibition via this receptor affected the cooperation of DCs with T cells.

Because CD85j also inhibits T cell function (14), to prevent a direct effect of HP-F1 mAb on T lymphocytes, immature DCs were pulsed with HP-F1 mAb and GAM antiserum, washed to remove unbound Abs, and then added to purified autologous $CD4^+$ T cells stimulated with recall Ags. In the presence of recall Ags, anti-hOSCAR mAb enhanced $CD4^+$ cell proliferation that was abrogated by the concomitant cross-linking of CD85j on DCs (Fig. 4). Similarly to cytokine secretion, T cell proliferation was not affected by cross-linking of CTLA-4 and CD31. DCs not stimulated by Ag, and DCs or $CD4^+$ T cells alone did not proliferate (Fig. 4).

CD85j prevents the rescue from apoptosis mediated by hOSCAR

In the absence of survival factors such as GM-CSF and IL-4, immature DCs underwent apoptosis from which they were rescued by
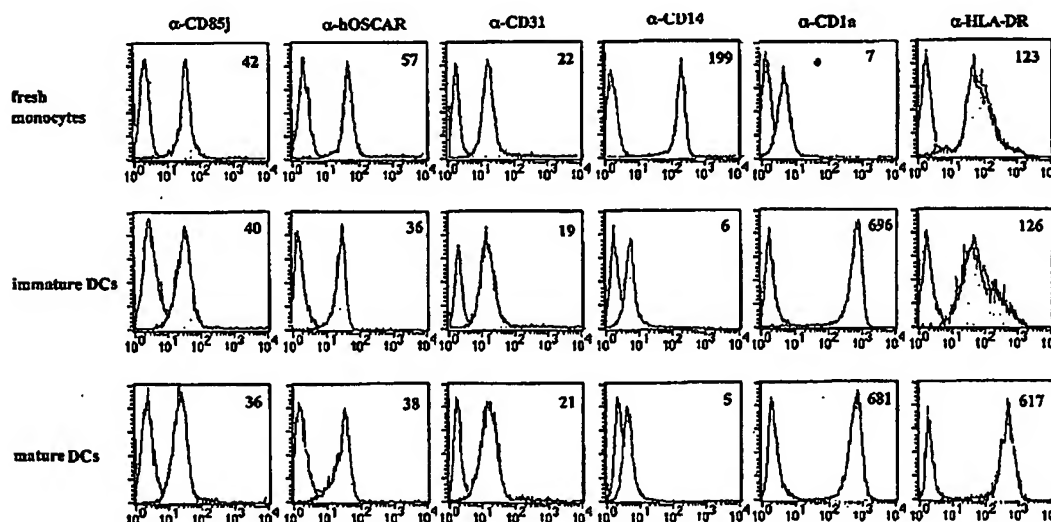
FIGURE 1. Surface phenotype of freshly isolated monocytes and immature and mature DCs. Flow cytometry analyses show that CD85j, hOSCAR, and CD31 are expressed at similar density on freshly isolated monocytes, on cells cultured for 5 days with GM-CSF and IL-4 (immature DCs), and following 24-h stimulation with LPS (mature DCs). In contrast, CD14 is sharply down-regulated on DCs in comparison with monocytes, whereas CD1a and HLA-DR are up-regulated. Numbers indicate mean fluorescence intensity (shaded histograms) with an identical setting of the instrument for all cells analyzed. Empty histograms refer to the binding of an isotype-matched control mAb.
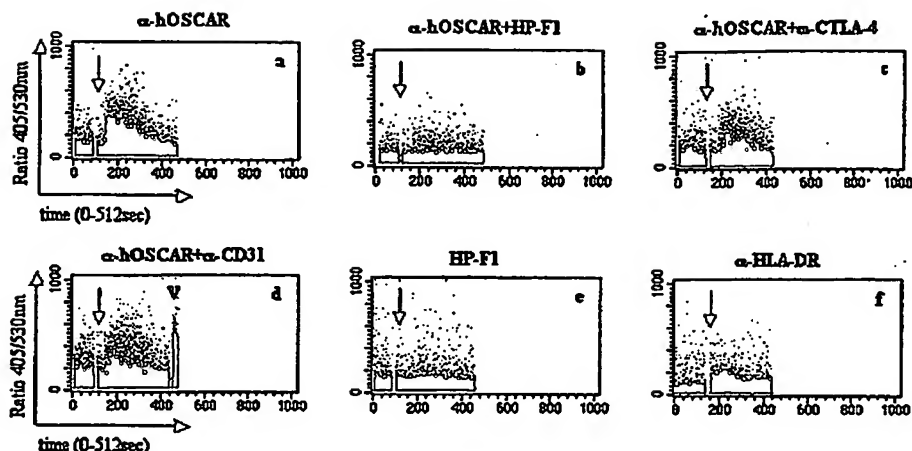
FIGURE 2. Ligation of CD85j in immature DCs inhibits hOSCAR-mediated intracellular Ca^{2+} mobilization. Intracellular Ca^{2+} flux, as determined by the 405/530-nm ratio in Fluo-3AM-loaded cells, is measured from the onset of the experiment. Primary Ab binding and the addition of GAM antiserum is used to allow receptor cross-linking (arrows). In these conditions, cross-linked anti-hOSCAR leads to intracellular Ca^{2+} mobilization (a) that is abrogated by concomitant addition of HP-F1 (b). Cross-linking of CTLA-4 (c), as ascites control, and of CD31 (d), as isotype-matched control Ab, does not affect Ca^{2+} influx induced by anti-hOSCAR. Ligation of HP-F1 alone has no effect on Ca^{2+} mobilization (e). Cross-linking of HLA-DR yields a moderate Ca^{2+} flux (f). Arrowhead in d corresponds to the positive control obtained after ionomycin addition. Data are from one representative experiment of five performed.

cross-linking of hOSCAR (37). The ability of CD85j to prevent the rescue of DC apoptosis mediated by hOSCAR was therefore investigated.

Immature DCs were cultured with medium alone and in the presence of plastic-coated mAb. In these conditions or in the presence of irrelevant mAb, immature DCs underwent spontaneous apoptosis after 3 days of culture. DC stimulation via hOSCAR

significantly reduced the number of apoptotic cells, detected by Annexin V^{FITC} staining or $DiOC_6$ uptake (see Fig. 5 and Ref. 37). The concomitant cross-linking of CD85j and hOSCAR reconstituted DC apoptosis to levels similar to those of cells cultured in the absence of survival factors (Fig. 5). Likewise, CD85j cross-linking decreased the expression of Bcl-2, an antiapoptotic molecule, the expression of which is enhanced by hOSCAR stimulation (Fig. 5).

FIGURE 3. Cross-linking of CD85j in immature DCs down-regulates the secretion of IL-8 and IL-12 p40 induced by hOSCAR. Immature DCs are stimulated with coated mAb or LPS, as described in *Materials and Methods*. After 24 h, supernatants are tested by ELISA for the presence of IL-8 and IL-12 p40. Data are means ± SD of triplicate samples from one representative experiment of three performed with similar results. NS, Nonstimulated. *, Statistically significant differences ($p < 0.05$) between hOSCAR-stimulated DCs in the absence or presence of anti-CD85j mAb.
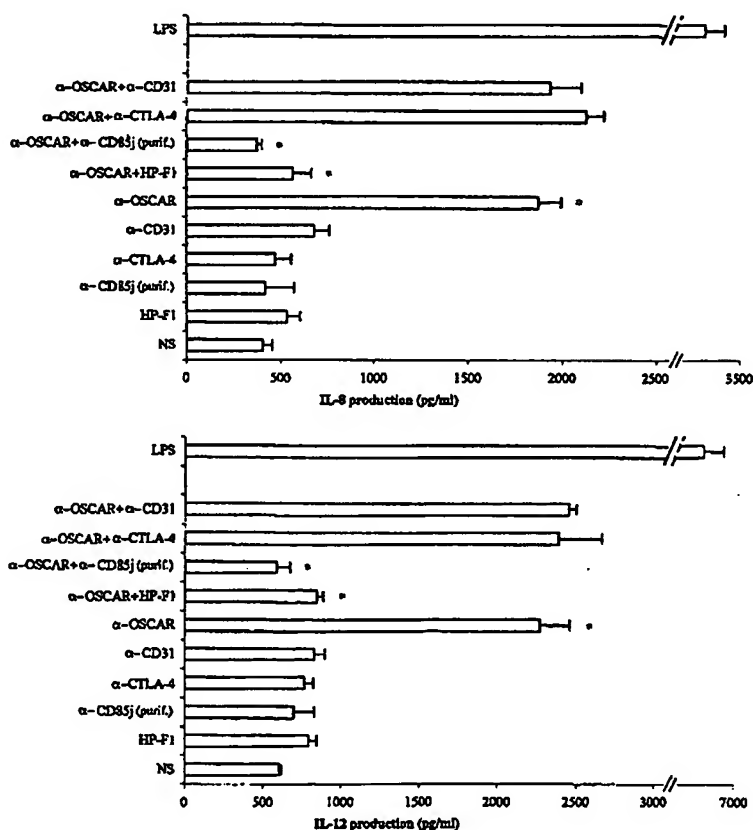
FIGURE 4. CD85j ligation on immature DCs inhibits hOSCAR-mediated proliferation of autologous Ag-specific CD4$^+$ T lymphocytes. Immature DCs are pretreated with the indicated mAb, washed, and pulsed using the recall Ags *C. albicans* (Ca) and purified protein derivative (PPD). Subsequently, autologous CD4$^+$ T lymphocytes are included in the assay. After 5-day culture, lymphocyte proliferation is measured by [^{3}H]thymidine uptake. hOSCAR-induced proliferation of CD4$^+$ cells, in the presence of recall Ags, is inhibited by the concomitant addition of HP-F1 mAb. CD4$^+$ T cells do not proliferate in the absence of Ag. Both stimulating factors, hOSCAR and Ag, are necessary on DCs for CD85j to inhibit T cell proliferation. Data are the means ± SD of triplicate samples from one representative experiment of three performed with similar results. *, Statistically significant difference ($p < 0.05$) of stimulation in the absence or presence of anti-CD85j mAb.
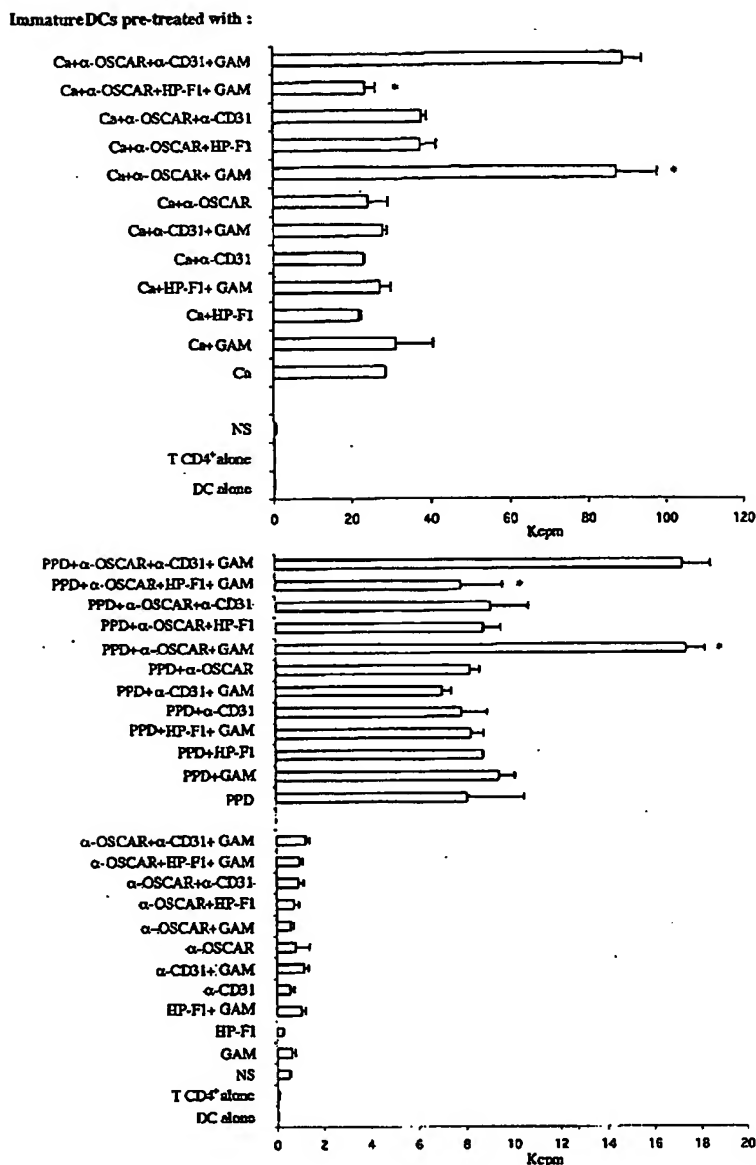
Discussion

In this study, the level of CD85j expression on DCs in the course of their differentiation from monocytes has been evaluated. CD85j was expressed in cells from all donors at similar levels and at all differentiation stages. These findings raised the issue of whether or not CD85j is functional in DCs. To evaluate the inhibitory function mediated by CD85j, hOSCAR was chosen among other activating molecules, such as CD1a and HLA-DR, because it provided the strongest activating signal for DCs. It is known that hOSCAR transduces an activating signal by interacting with an ITAM adapter, namely the FcR-associated γ-chain, providing a target for phosphatases recruited by CD85j. In immature DCs, the simultaneous cross-linking of CD85j, but not of CD31, significantly reduced hOSCAR-induced activation measured by Ca^{2+} flux or cytokine production. The only report on a regulation exerted by inhibiting receptors on cytokine production by monocytes and DCs deals with signal regulatory protein (SIRP)-α/CD47 ligation leading to inhibition of IL-12 and TNF-α, but not of IL-8 production induced by bacterially derived products such as *Staphylococcus*

aureus Cowan I or LPS (40, 41). In this study, we show that activated DCs produce lower amounts of IL-8 and IL-12 when CD85j is cross-linked. Thus, a role for CD85j in rendering DCs tolerogenic is conceivable.

The down-regulation of cytokine production by hOSCAR-stimulated DCs suggested that the cooperation with CD4$^+$ T lymphocytes might also be affected when CD85j is engaged. To gather information on this issue, immature DCs were pulsed with various mAb plus or minus GAM antiserum and washed to remove unbound Abs, to rule out a direct effect of the anti-CD85j mAb on T cells. Subsequently, Ab-primed DCs were added to purified autologous CD4$^+$ T cells in the presence of recall Ags. In these experimental conditions, CD85j cross-linking on DCs strongly reduced the proliferation of Ag-specific T cells. CD85j engagement did not down-regulate the expression of Ag-presenting molecules such as HLA-DR on DCs (data not shown). This suggests that CD85j did not impair the ability of DCs to process or present Ags but, rather, that the reduction of cytokine production affected T cell proliferation. In support of this contention, it should also be noted that,
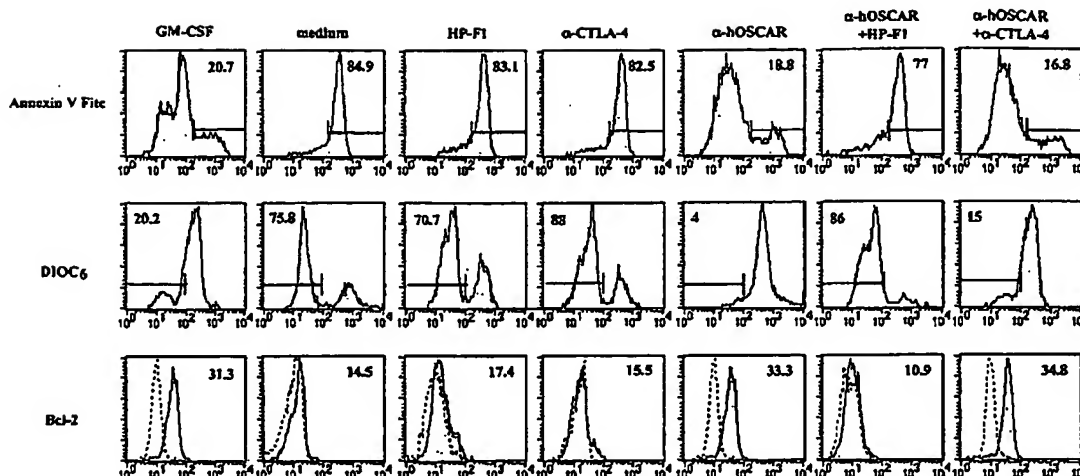
FIGURE 5. Cross-linking of CD85j abrogates hOSCAR-induced cell survival of immature DCs. Immature DCs are washed extensively to remove GM-CSF and IL-4, before stimulation with plastic-coated mAb, as described in *Materials and Methods*. After 3-day stimulation, cells are analyzed for annexin V binding, DiOC$_6$ uptake, and intracellular staining for Bcl-2. Numbers in the corner indicate the percentage of cells positive for annexin V and negative for DiOC$_6$ that correspond to early and late events of apoptosis, respectively. As for Bcl-2 staining, numbers indicate the specific mean fluorescence intensity of the different samples (shaded histogram), and the dotted lines show the binding of an isotype-matched control mAb. Data are representative of one of three independent experiments.

although T cells did not proliferate in the absence of recall Ags, the inhibiting effect of CD85j occurred when DCs were stimulated by both Ag and hOSCAR, and not when cells were stimulated by Ag alone. This suggests that hOSCAR sustains T cell proliferation indirectly by cytokine production that is down-regulated when CD85j is engaged. We also explored whether or not the loss of CD4$^+$ cell proliferation is due to the presence of Treg cells. However, no differences in the percentage of CD4$^+$CD25^{high} cells has been observed (data not shown).

In the absence of exogenous factors such as GM-CSF, DCs rapidly undergo apoptosis. Stimulation via hOSCAR yielded an antiapoptotic effect, as suggested by the up-regulated Bcl-2 expression in hOSCAR-stimulated DCs, and provided a survival signal to these cells. Engagement of CD85j prevented the rescue from apoptosis exerted by hOSCAR. Thus, CD85j could play a role in the termination of the immune response, because this is no longer sustained by Ag presentation conducted by DCs that undergo cell death following engagement of the receptor.

In conclusion, the inhibition mediated by CD85j was significant when activation was provided by hOSCAR. Therefore, it appears that CD85j interacts closely with hOSCAR on the cell surface. Phosphatases recruited by CD85j may exert an immediate and direct effect on kinases recruited by the ITAMs of FcRγ. Although CD31 (PECAM-1) is an adhesion molecule with ITIMs (42), CD31 was unable to block hOSCAR-FcRγ activation. This is probably due to the properties of the anti-CD31 mAb used. The Moon-1 mAb used in this study is specific for the second Ig domain of the CD31 molecule (43). This domain is not involved in Ca^{2+} mobilization that, instead, is triggered by fifth and sixth Ig domains (44).

Unlike the stimulation provided by hOSCAR, CD85j failed to inhibit the activation induced by LPS (data not shown). This is probably due to the maximum effect yielded by LPS, which recognizes at least two receptors on DCs, namely TLR4 (45) and CR3 (46), and provides activation using several distinct pathways (47). This could be relevant in vivo, during the acute phase of infection sustained by LPS-producing bacteria. In this phase, LPS activates DCs that sustain the immune response at the highest level. In contrast, when a successful immune response leads to bacterial clear-

ance and to lack of LPS, CD85j inhibits activating stimuli and therefore may contribute to the termination of the immune response. However, studies on SIRP-α inhibition of LPS stimulation suggest that PI3K activation via SIRP-α is essential to block cytokine production via TLR4 (41). Therefore, CD85j should not use this molecular pathway.

Although the ligand of hOSCAR is presently unknown, there is strong evidence from the data in mice that it is an endogenous molecule (38). Thus, it is conceivable that hOSCAR acts to induce DC maturation in the presence of its ligand. hOSCAR-activated DCs improve their survival and up-regulate the production of immune modulators, such as chemokines and cytokines (37). CD85j abrogated these responses and, consequently, could be a component of a regulatory loop that is active in a physiologic context. In addition, CD85j presumably inhibits other activating pathways and thus could play a more general role. CD85j broadly recognizes several HLA class I alleles and loci, including nonclassical class I molecules such as HLA-G (30–32). Interestingly, HLA-G is expressed strongly by fetal tissues and plays an essential role in maintaining the fetal graft during pregnancy by blocking locally the maternal immune response (48, 49). CD85j might therefore be involved in the abrogation of DC activation in the course of maternal tolerance.

Acknowledgments

Disclosures

The authors have no financial conflict of interest.

References

1. Banchereau, J., and R. M. Steinman. 1998. Dendritic cells and the control of immunity. *Nature* 392: 245–252.
2. Cella, M., F. Sallusto, and A. Lanzavecchia. 1997. Origin, maturation and antigen presenting function of dendritic cells. *Curr. Opin. Immunol.* 9: 10–16.
3. Sallusto, F., M. Cella, C. Danieli, and A. Lanzavecchia. 1995. Dendritic cells use macropinocytosis and the mannose receptor to concentrate macromolecules in the major histocompatibility complex class II compartment: down-regulation by cytokines and bacterial products. *J. Exp. Med.* 182: 389–400.
4. Steinman. R. M., and J. Swanson. 1995. The endocytic activity of dendritic cells. *J. Exp. Med.* 182: 283–288.

5. Lutz, M. B., and G. Schuler. 2002. Immature, semi-mature and fully mature dendritic cells: which signals induce tolerance or immunity? *Trends Immunol.* 23: 445–449.

6. Randolph, G. J., S. Beaulieu, S. Lebecque, R. M. Steinman, and W. A. Muller. 1998. Differentiation of monocytes into dendritic cells in a model of transendothelial trafficking. *Science* 282: 480–483.

7. Sallusto, F., and A. Lanzavecchia. 1994. Efficient presentation of soluble antigen by cultured human dendritic cells is maintained by granulocyte/macrophage colony-stimulating factor plus interleukin 4 and down-regulated by tumor necrosis factor α. *J. Exp. Med.* 179: 1109–1118.

8. Cella, M., A. Engering, V. Pinet, J. Pieters, and A. Lanzavecchia. 1997. Inflammatory stimuli induce accumulation of MHC class II complexes on dendritic cells. *Nature* 388: 782–787.

9. Verhasselt, V., C. Buelens, F. Willems, D. De Groote, N. Haeffner-Cavaillon, and M. Goldman. 1997. Bacterial lipopolysaccharide stimulates the production of cytokines and the expression of costimulatory molecules by human peripheral blood dendritic cells: evidence for a soluble CD14-dependent pathway. *J. Immunol.* 158: 2919–2925.

10. Hartmann, G., G. J. Weiner, and A. M. Krieg. 1999. CpG DNA: a potent signal for growth, activation, and maturation of human dendritic cells. *Proc. Natl. Acad. Sci. USA* 96: 9305–9310.

11. Cambier, J. C. 1995. Antigen and Fc receptor signaling: the awesome power of the immunoreceptor tyrosine-based activation motif (ITAM). *J. Immunol.* 155: 3281–3285.

12. Thomas, M. L. 1995. Of ITAMs and ITIMs: turning on and off the B cell antigen receptor. *J. Exp. Med.* 181: 1953–1956.

13. Cambier, J. C. 1997. Inhibitory receptors abound? *Proc. Natl. Acad. Sci. USA* 94: 5993–5995.

14. Saverino, D., M. Fabbi, F. Ghiotto, A. Merlo, S. Bruno, D. Zarcone, C. Tenca, M. Tiso, G. Santoro, G. Anastasi, et al. 2000. The CD85/LIR-1/ILT2 inhibitory receptor is expressed by all human T lymphocytes and down-regulates their functions. *J. Immunol.* 165: 3742–3755.

15. Lanier, L. L. 1998. NK cell receptors. *Annu. Rev. Immunol.* 16: 359–393.

16. Biassoni, R., C. Cantoni, D. Pende, S. Sivori, S. Parolini, M. Vitale, C. Bottino, and A. Moretta. 2001. Human natural killer cell receptors and co-receptors. *Immunol. Rev.* 181: 203–214.

17. Colonna, M. 2003. TREMs in the immune system and beyond. *Nat. Rev. Immunol.* 3: 445–453.

18. Chang, C. C., R. Ciubotariu, J. S. Manavalan, J. Yuan, A. I. Colovai, F. Piazza, S. Lederman, M. Colonna, R. Cortesini, R. Dalla-Favera, and N. Suciu-Foca. 2002. Tolerization of dendritic cells by T₅ cells: the crucial role of inhibitory receptors ILT3 and ILT4. *Nat. Immunol.* 3: 237–243.

19. Fournier, N., L. Chalus, I. Durand, E. Garcia, J. J. Pin, T. Churakova, S. Patel, C. Zlot, D. Gorman, S. Zurawski, et al. 2000. FDF03, a novel inhibitory receptor of the immunoglobulin superfamily is expressed by human dendritic and myeloid cells. *J. Immunol.* 165: 1197–1209.

20. Fanger, N., D. Cosman, L. Peterson, S. C. Braddy, C. R. Mailszewski, and L. Borges. 1998. The MHC class I binding protein LIR-1 and LIR-2 inhibit Fc receptor-mediated signaling in monocytes. *Eur. J. Immunol.* 28: 3423–3434.

21. Kanazawa, N., K. Tashiro, K. Inaba, and Y. Miyachi. 2003. Dendritic cell immunoactivating receptor, a novel C-type lectin immunoreceptor, acts as an activating receptor through association with Fc receptor γ chain. *J. Biol. Chem.* 278: 32645–32652.

22. Colonna, M., J. Samaridis, M. Cella, L. Angman, R. L. Allen, C. A. O'Callaghan, R. Dunbar, G. S. Ogg, V. Cerundolo, and A. Rolink. 1998. Cutting edge: human myelomonocytic cells express an inhibitory receptor for classical and nonclassical MHC class I molecules. *J. Immunol.* 160: 3096–3100.

23. Borges, L., M. L. Hsu, N. Fanger, M. Kubin, and D. Cosman. 1997. A family of human lymphoid and myeloid Ig-like receptors, some of which bind to MHC class I molecules. *J. Immunol.* 159: 5192–5196.

24. Long, E. O. 1999. Regulation of immune responses through inhibitory receptors. *Annu. Rev. Immunol.* 17: 875–904.

25. Lopez-Botet, M., P. Navarro, and M. Llano. 1999. How do NK cells sense the expression of HLA-G class Ib molecules? *Semin. Cancer Biol.* 9: 19–26.

26. Cosman, D., N. Fanger, L. Borges, M. Kubin, W. Chin, L. Peterson, and M. L. Hsu. 1997. A novel immunoglobulin superfamily receptor for cellular and viral MHC class I molecules. *Immunity* 7: 273–282.

27. Colonna, M., F. Navarro, T. Bellon, M. Llano, P. Garcia, J. Samaridis, L. Angman, M. Cella, and M. Lopez-Botet. 1997. A common inhibitory receptor for major histocompatibility complex class I molecules on human lymphoid and myelomonocytic cells. *J. Exp. Med.* 186: 1809–1818.

28. Cosman, D., N. Fanger, and L. Borges. 1999. Human cytomegalovirus, MHC class I and inhibitory signalling receptors: more questions than answers. *Immunol. Rev.* 168: 177–185.

29. Nikolova, M., P. Musette, M. Bagot, L. Boumsell, and A. Bensussan. 2002. Engagement of ILT2/CD85j in Sézary syndrome cells inhibits their CD3/TCR signaling. *Blood* 100: 1019–1025.

30. Navarro, F., M. Llano, T. Bellon, M. Colonna, D. E. Geraghty, and M. Lopez-Botet. 1999. The ILT2(LIR1) and CD94/NKG2A NK cell receptors respectively recognize HLA-G1 and HLA-E molecules co-expressed on target cells. *Eur. J. Immunol.* 29: 277–283.

31. Willcox, B. E., L. M. Thomas, and P. J. Bjorkman. 2003. Crystal structure of HLA-A2 bound to LIR-1, a host and viral major histocompatibility complex receptor. *Nat. Immunol.* 4: 913–919.

32. Shiroishi, M., K. Tsumoto, K. Amano, Y. Shirakihara, M. Colonna, V. M. Braud, D. S. Allan, A. Makadzande, S. Rowland-Jones, B. Willcox, et al. 2003. Human inhibitory receptors Ig-like transcript 2 (ILT2) and ILT4 compete with CD8 for MHC class I binding and bind preferentially to HLA-G. *Proc. Natl. Acad. Sci. USA* 100: 8856–8861.

33. Saverino, D., F. Ghiotto, A. Merlo, S. Bruno, L. Battini, M. Occhino, M. Maffei, C. Tenca, S. Pileri, L. Baldi, et al. 2004. Specific recognition of the viral protein UL18 by CD85j/LIR1/ILT2 on CD8⁺ T cells mediates the non-MHC-restricted lysis of human cytomegalovirus-infected cells. *J. Immunol.* 172: 5629–5637.

34. Leong, C. C., T. L. Chapman, P. J. Bjorkman, D. Formankova, E. S. Mocarski, J. H. Philips, and L. L. Lanier. 1998. Modulation of natural killer cell cytotoxicity in human cytomegalovirus infection: the role of endogenous class I major histocompatibility complex and a viral class I homology. *J. Exp. Med.* 187: 1681–1687.

35. Cella, M., C. Dohring, J. Samaridis, M. Dessing, M. Brockhaus, A. Lanzavecchia, and M. Colonna. 1997. A novel inhibitory receptor (ILT3) expressed on monocytes, macrophages, and dendritic cells involved in antigen processing. *J. Exp. Med.* 185: 1743–1751.

36. Merck, E., C. Gaillard, D. M. Gorman, F. Montero-Julian, I. Durand, S. M. Zurawski, C. Menetrier-Caux, G. Carra, S. Lébeque, G. Trinchieri, and E. E. Bates. 2004. OSCAR is an FcRγ-associated receptor expressed by myeloid cells involved in antigen presentation and activation of human dendritic cells. *Blood* 104: 1386–1395.

37. Merck, E., B. de Saint-Vis, M. Scuiller, C. Gaillard, C. Caux, G. Trinchieri, and E. E. Bates. Fc receptor γ-chain activation via hOSCAR induces survival and maturation of dendritic cells and modulates Toll-like receptor responses. *Blood. In press.*

38. Kim, N., M. Takami, J. Rho, R. Josien, and Y. Choi. 2002. A novel member of the leukocyte receptor complex regulates osteoclast differentiation. *J. Exp. Med.* 195: 201–209.

39. Cremer, I., M. C. Dieu-Nosjean, S. Marechal, C. Dezutter-Dambuyant, S. Goddard, D. Adams, N. Winter, C. Menetrier-Caux, C. Sautes-Fridman, W. H. Fridman, and C. G. Mueller. 2002. Long-lived immature dendritic cells mediated by TRANCE-RANK interaction. *Blood* 100: 3646–3655.

40. Latour, S., H. Tanaka, C. Demeure, V. Mateo, M. Rubio, E. J. Brown, C. Maliszewski, F. P. Lindberg, A. Oldenborg, A. Ulrich, et al. 2001. Bidirectional negative regulation of human T and dendritic cells by CD47 and its cognate receptor signal-regulator protein-α: down-regulation of IL-12 responsiveness and inhibition of dendritic cell activation. *J. Immunol.* 167: 2547–2554.

41. Smith, R. E., V. Patel, S. D. Seatter, M. R. Dochan, M. H. Brown, G. P. Brooke, H. S. Goodridge, C. J. Howards, K. P. Rigley, W. Harnett, and M. M. Harnett. 2003. A novel MyD-1 (SIRP-1α) signaling pathway that inhibits LPS-induced TNFα production by monocytes. *Blood* 102: 2532–2540.

42. Newman, P. J. 1999. Switched at birth: a new family for PECAM-1. *J. Clin. Invest.* 103: 5–9.

43. Deaglio, S., M. Morra, R. Mallone, C. M. Ausiello, E. Prager, G. Garbarino, U. Dianzani, H. Stockinger, and F. Malavasi. 1998. Human CD38 (ADP-ribosyl cyclase) is a counter-receptor of CD31, an Ig superfamily member. *J. Immunol.* 160: 395–402.

44. Wei, H., J. Song, L. Fang, G. Li, and S. Chatterjee. 2004. Identification of a novel transcript of human PECAM-1 and its role in the transendotelial migration of monocytes and Ca²⁺ mobilization. *Bichem. Biophys. Res. Commun.* 320: 1228–1235.

45. Pålsson-Mcdermott, E. M., and L. A. O'Neil. 2004. Signal transduction by the lypopolysaccharide receptor, Toll-like receptor-4. *Immunology* 113: 153–162.

46. Ingalls, R. R., and D. T. Golenbock. 1995. CD11c/CD18, a transmembrane signaling receptor for lipopolysaccharide. *J. Exp. Med.* 181: 1473–1479.

47. Noubir, S., Z. Hmama, and N. E. Reiner. 2004. Dual receptor and distinct pathways mediate interleukin-1 receptor-associated kinase degradation in response to lipopolysaccharide: involvement of CD14/TLR4, CR3, and phosphatidylinositol 3-kinase. *J. Biol. Chem.* 279: 25189–25195.

48. Thellin, O., B. Coumans, W. Zorzi, A. Igout, and E. Heinen. 2000. Tolerance to the foetal-placental "graft": ten ways to support a child for nine months. *Curr. Opin. Immunol.* 12: 731–737.

49. Hviid, T. V. 2004. HLA-G genotype is associated with fetoplacental growth. *Hum. Immunol.* 65: 586–593.

SPAP2, an Ig family receptor containing both ITIMs and ITAMs☆

Ming-jiang Xu, Runxiang Zhao, Hongxi Cao, and Zhizhuang Joe Zhao*

Hematology/Oncology Division, Department of Medicine, Vanderbilt-Ingram Cancer Center, Vanderbilt University, 547, PRB, 2220 Pierce Ave., Nashville, TN 37232-6305, USA

Abstract

This study reports cloning and characterization of SPAP2, a novel transmembrane protein. The extracellular portion of SPAP2 contains six immunoglobulin-like domains and its intracellular segment has two immunoreceptor tyrosine-based activation motifs (ITAMs) and two immunoreceptor tyrosine-based inhibition motifs (ITIMs). We also identified four alternatively spliced products. Sequence alignment with the genomic database revealed that the SPAP2 gene contains 16 exons and is localized at chromosome 1q21. PCR analyses demonstrated that SPAP2 mRNA is expressed in restricted human tissues including the kidney, salivary gland, adrenal gland, uterus, and bone marrow. Tyrosine-phosphorylated SPAP2 is specifically associated with SH2 domain-containing tyrosine kinases Syk and Zap70 and SH2 domain-containing tyrosine phosphatases SHP-1 and SHP-2. Site-specific mutagenesis studies revealed that tyrosyl residues 650 and 662 embedded in the ITIMs are responsible for the binding of Syk and Zap70 while tyrosyl residues 692 and 722 embedded in the ITIMs are involved in interactions with SHP-1 and SHP-2. Finally, recruitment of SHP-1 to the tyrosine-phosphorylated ITIMs led to a marked activation of the enzyme. © 2002 Elsevier Science (USA). All rights reserved.

Keywords: ITIM; ITAM; Tyrosine phosphatase; Tyrosine kinase; Ig family protein

Phosphorylation of specific cellular proteins on tyrosyl residues is one of the most fundamental regulatory mechanisms in signal transduction that dictates cell fate and regulates cell function [1]. This process alters the activity of proteins and/or provides docking sites to recruit signaling molecules such as proteins containing SH2 or PTB domains [2]. Tyrosine phosphorylation occurs at specific sites that are usually embedded in certain peptide motifs. The immunoreceptor tyrosine-based inhibition motif (ITIM) [3–5] and the immunoreceptor tyrosine-based activation motif (ITAM) represent two well-characterized tyrosine phosphorylation motifs [6,7].

ITIM was initially defined by Burshtyn et al. as a V/IxYxxL consensus sequence [8,9]. It is found in many hematopoietic cell receptors such as FcγRIIB (CD32), KIR, LAIR-1, CD22, PIR-B, CD33, gp49, and gp91 [10–17] and in widely distributed cell surface molecules including SIRP/SHPS-1 and PZR [18–20]. This motif usually exists in pairs with 20–30 amino acid residues between the tyrosyl residues. The tyrosyl residues can be phosphorylated and thereby recruit SH2 domain-containing phosphatases, including protein tyrosine phosphatases (PTPs) SHP-1 and SHP-2 and inositol-phosphatase SHIP. The association of ITIM-bearing receptors with terminating phosphatases is believed to represent a critical step in the inhibitory function of ITIM-bearing receptors. Emergence of an increasing number of ITIM-bearing receptors in recent years further emphasizes the important role of this motif in various signal transduction pathways and subsequent cellular responses [21–31].

ITAM was identified by analyzing the sequence elements responsible for the stimulatory signaling properties of the transducing subunits of B-cell and T-cell

---

receptors. With a $(D/E)x^2Yx^2Lx^{7-8}Yx^2L/I$ consensus sequence, ITAMs are present in a number of cellular signal-transducing molecules, including TCR-ζ, Igα, Igβ, CD3γ, CD3δ, and FcεIγ [6,7,32]. It has been well accepted that ITAMs are necessary and sufficient for the coupling of extracellular signals to intracellular signaling molecules. Upon stimulation, the tyrosine residues within the ITAMs become phosphorylated thereby permitting the binding of SH2 domain-containing protein tyrosine kinases (PTKs) such as Src family kinases, Zap70 and Syk [6,7,32–34].

Recently, we have cloned a novel member of the ITIM-bearing receptor family, designated SPAP1a for SH2 domain-containing phosphatase anchor protein-1a, which is specifically expressed in B-cells and recruits SHP-1 upon phosphorylation [35]. Here, we report the molecular cloning and characterization of another novel member of the ITIM-bearing receptor family, designated SPAP2a. SPAP2a belongs to the Ig-superfamily and its fifth and sixth Ig-domains share an 84% sequence identity with the Ig domain of SPAP1a. Importantly, the intracellular part of SPAP2a contains two ITIMs and two ITAMs. Our study shows that tyrosine-phosphorylated ITIMs and ITAMs of SPAP2a are able to recruit both SH2 domain-containing PTPs and SH2 domain-containing PTKs, respectively. To our knowledge, this is the first example of this type of signaling protein.

Materials and methods

Materials. Human embryonic kidney 293 cells, uterine cervical carcinoma HeLa cells, HT-1080 fibrosarcoma cells, Jurkat T cells, HL-60 promyelocytic cells, Human B cell lines BC-1, and BC-2 cells were obtained from the American Type Culture Collection. HeLa, 293 and HT-1080 cells were maintained in DMEM while all the other cells were cultured in RPMI. The media were supplemented with 10% fetal bovine serum and 50 U/ml each of penicillin and streptomycin. Monoclonal antibodies against Zap70 and Lck and rabbit polyclonal antibodies against SHP-1, SHP-2, Syk, and Lyn were purchased from Santa Cruz Biotechnology (Santa Cruz, CA). SHP-1 was purified by using an adenovirus expression system, as previously described [36].

Molecular cloning of SPAP2. Recently, we cloned SPAP1a, a novel member of the ITIM-bearing receptor family expressed in B-cells [35]. A search of the human expressed sequencing tag (EST) database with the SPAP1a sequence by using the BLAST program resulted in the identification of several homologous EST sequences. These EST sequences share more than 80% amino acid identity with SPAP1a, but apparently are derived from different genes. Among them, an EST sequence with a GenBank Accession Number AW500471 encodes a peptide containing an Ig domain with about 85% amino acid identity with the Ig domain of SPAP1a. Further search of the EST database with the AW500471 DNA sequence yielded another two EST sequences (GenBank Accession Numbers AW500429 and AW503702) that partially overlap with AW500471. This enabled us to deduce a 755-bp DNA sequence which potentially encodes a novel protein but lacks the 5′ and 3′ ends. To obtain the full-length DNA sequence, we followed a rapid amplification of the cDNA end (RACE) strategy with nested PCR. Considering that the ESTs were derived from germinal center B cells, we employed the human bone marrow cell Marathon-ready cDNA library from Clontech Laboratories (Palo Alto, CA) as a

template. The 5′ RACE primers were: 5′-GAGGACAGGGTGAGAT ACCGGAA and 5′-CACGTGCTGAGGATGGGGCT. The 3′ RACE primers utilized were: 5′-GGAGTGAGTCTCAGGGTCACAGTTC-3′ and 5′-TGGAAACTACTCCTGTGATGCAGAC-3′. PCR was performed by using the Advantage-GC PCR Kit (Clontech Laboratories, Palo Alto, CA). The PCR products were cloned into the TA cloning pCR2.1 vector (Invitrogen). The cDNA clones were sequenced by using the automated DNA sequencing facility of the Vanderbilt-Ingram Cancer Center.

Production of anti-SPAP2a antibodies. A 69-amino acid extracellular segment (amino acids 85–153) of SPAP2a was expressed in *Escherichia coli* as a glutathione-S-transferase (GST) fusion protein by using the pGex-2T vector (Pharmacia). The fusion protein was purified with a glutathione–Sepharose column and used to immunize rabbits. The rabbit serum was used for immunoprecipitation and Western blot analysis of SPAP2.

Expression of SPAP2a in 293 cells and stimulation of cells. The entire coding region of SPAP2a cDNA was amplified by PCR and then cloned into the pcDNA3 vector (Invitrogen). Cell transfection was carried out according to the standard calcium phosphate co-precipitation technique as described [31]. Briefly, 293 cells were grown to ~30% confluency and 1–5 µg of plasmid DNAs was used to transfect cells in each 6-well plate. The cells were harvested 48 h after transfection. To induce tyrosine phosphorylation of SPAP2a, the cells were treated with 0.1 mM pervanadate for 30 min. A 50-mM stock solution of pervanadate was made by mixing equal volumes of 0.1 M sodium vanadate and 0.2 M H_2O_2 and incubating this at room temperature for 20 min before adding it to the cells [27]. Stimulated cells were washed with ice-cold phosphate-buffered saline and then were subjected to extraction, as described below.

Cell extraction, immunoprecipitation, and Western blotting. Cells were washed with cold phosphate-buffered saline and then lysed in Buffer A containing 25 mM β-glycerol phosphate (pH 7.3), 5 mM EDTA, 5 mM EGTA, 0.5 mM sodium vanadate, 0.1 µM microcystin, 10 mM β-mercaptoethanol, 1 mM benzamidine, 0.1 mM phenylmethylsulfonyl fluoride, 2 µg/ml leupeptin, 1 µM pepstatin A, 1 µg/ml aprotinin, 0.1 M NaCl, and 1% Triton X-100. Extracts were cleared by centrifugation and then were immunoprecipitated with antibodies pre-bound to protein A–Sepharose. Following overnight incubation, the beads were washed three times with the extraction buffer supplemented with 0.15 M NaCl. For Western blot analyses, samples were separated by 10% SDS–PAGE and transferred to polyvinylidene difluoride (PVDF) membranes. The membranes were probed with various primary antibodies and detected by using the ECL system with horseradish peroxidase-conjugated secondary antibodies.

Determination of expression of SPAP2 in human tissues and cell lines. To determine the expression level of SPAP2 in various tissues and cell lines, we used the Rapid-Scan Gene Expression Panels from OriGene Technologies [35,37,38] and single-stranded cDNAs prepared from cell lines with the NucleoSpin RNA Kit (Clontech Laboratories). SPAP2 was amplified by using the primers of 5′-GAAAATATG GTCCTTATTTGCTCAGTA-3′ and 5′-TGTGACTAGATGTTCCA GTGGCAGA-3′ corresponding to 1078–1104 and 1990–2014 of the SPAP2a cDNA sequence, respectively. The primers were expected to give rise to a 937-bp PCR product. PCR was performed with thermo-DNA polymerase Pfu (Stratgene) for 35 cycles. The conditions were 94°C for 30 s, 60°C for 30 s, and 72°C for 75 s. The products were analyzed on 1% agarose gels and detected by staining with ethidium bromide.

Expression of GST fusion proteins and site-specific mutagenesis. The intracellular domain of SPAP2 (corresponding to aa 597–734 of SPAP2a) was expressed as a GST fusion protein by using the pGex-2T vector (Pharmacia). For functional analysis of the ITAMs and ITIMs, we also constructed five mutant forms of the fusion protein, as illustrated in Fig. 1. The mutation sites corresponded to tyrosine residues 650 and 662 embedded in the ITAMs and residues 692 and 722 embedded in the ITIMs. The tyrosyl residues were mutated to phenyl-
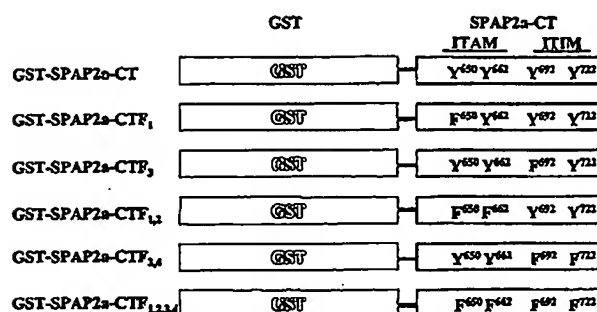
Fig. 1. Constructs of various Tyr-to-Phe mutants of GST fusion proteins containing the intracellular domain of SPAP2.

alanine by PCR and all the mutants were confirmed by DNA sequencing. The GST fusion protein constructs were used to transform DE3-LysS *E. coli* cells. To induce tyrosine phosphorylation of the fusion proteins, the *E. coli* cells were co-transformed with a c-Src construct carried by a pET9a vector (Novagen) which has a kanamycin-resistant gene, as described in our previous studies [39]. Expression of the recombinant proteins was induced by 0.5 mM isopropyl-1-thio-β-D-galactopyranoside for 3.5 h at 37 °C. *E. coli* cells were broken up by sonication in a buffer containing 25 mM Tris–Cl, pH 7.5, 10 mM β-mercaptoethanol, 1 mM EDTA, and 1 mM EGTA, 1 mM benzamidine, 0.1 mM phenylmethylsulfonyl fluoride, 2 μg/ml leupeptin, 1 μM pepstatin A, and 1 μg/ml aprotinin. GST fusion proteins were purified from the cell extracts by incubating with glutathione–Sepharose beads which were extensively washed with extraction buffer supplemented with 0.15 M NaCl.

GST fusion protein binding analyses. Jurkat cell extracts made in the aforementioned Buffer A were used for in vitro "pull-down" assays. Glutathione–Sepharose beads carrying GST fusion proteins were incubated with the Jurkat cell extracts for two hours and then washed, as described for immunoprecipitation as described above. Proteins bound to the beads were analyzed by Western blotting with specific antibodies. For control experiments, we used non-phosphorylated GST-SPAP2a-CT purified from cells expressing pGex-2T-SPAP2aCT alone and GST purified from cells co-expressing pGex-2T vector and pET9a-c-Src.

Phosphatase activity assays. PTP activity assays were performed with 2 mM p-NPP at room temperature, as previously described [36]. The assay system contained 25 mM HEPES–NaOH (pH 7.0), 1.0 mM EDTA, 1.0 mM dithiothreitol, 70 μg/ml SHP-1, and 200 μg/ml GST-SPAP2a-CT or its Y-to-F mutants (see Fig. 1).

Results

Molecular cloning of SPAP2 and sequence analyses

ITIM-bearing proteins represent a rapidly expanding family of inhibitory molecules. We have recently added a new member, namely, SPAP1a, to the family [35]. By searching the human expression sequencing tag (EST) database with the BLAST program, we identified a DNA sequence that potentially encodes a novel protein homologous to SPAP1a. Since the sequence lacks both 5' and 3' ends, we employed the RACE (rapid amplification of cDNA ends) strategy to extend the cDNA as described in Materials and methods. This led to isolation of a full-length cDNA with an open reading frame

encoding a protein of 734 amino acid residues as shown in Fig. 2. We designate the protein as SPAP2a. The ATG initiation codon of the SPAP2a cDNA is preceded by three in-frame termination codons at the 5' end. At the 3' end, there is a polyadenylation sequence. SPAP2a is a typical type I transmembrane protein with a hydrophobic signal peptide at the N-terminus and a hydrophobic transmembrane sequence in the middle. Its extracellular region consists of six Ig-domains. Sequence alignment of SPAP2a with proteins in the GenBank database revealed that the fifth and sixth Ig domains were highly homologous to each other. They also share 80–85% amino acid identity with the Ig domain of SPAP1a and the seventh to ninth Ig domains of IRTA2c (Fig. 3A). SPAP1a and IRTA2c are both B-cell-specific ITIM-bearing receptors which have been recently cloned [35,40]. The first to fourth Ig domains of SPAP2a have no significant sequence homology to any protein in the GenBank database. The intracellular domain of SPAP2a contains four tyrosyl residues. Two of them are embedded in peptide segments that resemble the ITIMs and the other two are found in peptide sequences known as the ITAMs. This makes SPAP2a distinctly interesting since no other proteins are known to contain both ITIMs and ITAMs. A sequence alignment of ITIMs and ITAMs from several known proteins is shown in Fig. 3B and C.

Isolation of four alternatively spliced isoforms of SPAP2a

Along with the isolation of the entire coding region of SPAP2a by PCR, we also obtained four alternatively spliced isoforms of cDNA. We named the encoded protein products sequentially SPAP2b, c, d, and e (Fig. 4). Compared with SPAP2a, the SPAP2b cDNA has a 285-nucleotide deletion, which results in a short protein product of 639 aa without the third Ig domain. The SPAP2c cDNA has an 18-nucleotide in-frame insertion in the region corresponding to the junction of the fourth and fifth Ig domains and thereby encodes a longer protein with 740 amino acid residues. SPAP2d and SPAP2e cDNAs have a 234-nucleotide insertion and a 95-nucleotide deletion, respectively, within the sequence corresponding to the end of the second Ig domain. These cause an early termination of translation and result in 189 and 199 aa polypeptides, respectively. SPAP2a, b, and c are integral transmembrane proteins, while SPAP2d and SPAP2e lack the transmembrane segments and therefore likely represent soluble proteins.

Chromosomal organization of the SPAP2 gene

By searching the GenBank database with the BLAST program, we matched the sequences of SPAP2 to a 160-

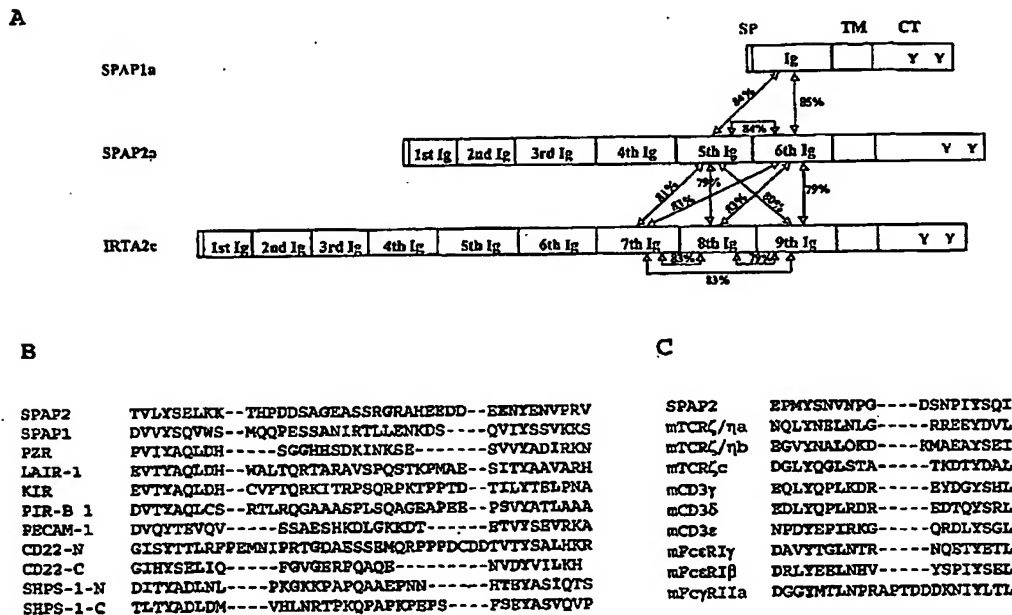Fig. 2. Nucleotide sequence and deduced amino acid sequence of human SPAP2a. The signal peptide and transmembrane region are underlined. Eight potential N-linked glycosylation sites and twelve cysteinyl residues involved in the disulfide bond formation in six immunoglobulin-like domains are bold-faced. ITIMs and ITAMs are underlined and bold-faced. Three 5′-in-frame termination codons and a 3′-polyadenylation signal sequence are double underlined. The inverted triangles indicate the positions of intron and exon juctions.

kb segment of human chromosome 1q21 deposited in the GenBank under the Accession Number AL356276. Sequence alignment revealed the genomic organization of SPAP2 as illustrated in Fig. 5. The SPAP2 gene consists of 16 exons and 15 introns spanning over 24 kb. The introns range from 76–6553 bp and all the intron–exon boundaries conformed to the GT-AG splicing rule. Exon 2 with a size of 127 bp contains the ATG translation initiation site and the signal peptide. The translation termination codon is located in exon 15. The transmembrane domain is found in exon 10. The tandem ITAMs correspond to a single exon 13, while the tandem ITIMs are entirely coded by a single exon 15. Sequence alignment with the SPAP2 genomic sequence also revealed the organization of the alternatively spliced forms of SPAP2. SPAP2b skips exon 6, while SPAP2c contains an alternatively spliced exon 8 (exon 8c). A larger exon 5 (exon 5d) and a smaller exon 6 (exon 6e) constitute SPAP2d and SPAP2e, respectively. The positions of splicing sites in SPAP2a are also indicated in Fig. 2. All the insertions and deletions in the alternatively spliced forms of SPAP2 occur at the intron–exon junctions.

Distribution of SPAP2 in human tissues and selected cell lines

To analyze the SPAP2 expression in human tissues, we employed the Rapid-Scan Gene Expression Panels (OriGene Technologies) which contained equal amounts of single-stranded cDNAs generated from 24 different human tissues. Previously, we had used the same cDNAs to demonstrate wide expressions of FYVE-DSP1 and FYVE-DSP2, and restricted expression of SPAP1, in bone marrow and spleen cells [35,37,38]. The 24-human tissues included brain, heart, kidney, spleen, liver, colon, lung, small intestine, muscle, stomach, testis, placenta, salivary gland, thyroid gland, adrenal gland, pancrease, ovary, uterus, prostate, skin, peripheral blood, bone marrow, fetal brain, and fetal liver. Fig. 6 shows that SPAP2 was restrictedly expressed in kidney, salivary gland, adrenal gland, and uterus. The fact that SPAP2 was not detected in bone marrow cells probably reflects its low expression level in this tissue. When the Marathon-ready bone marrow cDNA library from which we cloned SPAP2 was used as template, we were able to detect SPAP2 by PCR (Fig. 6, lower panel).

A

B

SPAP2	TVLYSELKK--THPDDSAGEASSRGRAHEEDD--EENYENVPRV
SPAP1	DVVYSQVWS--MQQPESSANIRTLLENKDS----QVIYSSVKKS
PZR	PVIYAQLDH-----SGGHHSDKINKSE-------SVVYADIRKN
LAIR-1	EVTYAQLDH--WALTQRTARAVSPQSTKPMAE--SITYAAVARH
KIR	EVTYAQLDH--CVFTQRKITRPSQRPKTPPTD--TILYTELPNA
PIR-B 1	DVTYAQLCS--RTLRQGAAASPLSQAGEAPEB--PSVYATLAAA
PECAM-1	DVQYTEVQV-----SSAESHKDLGKKDT-----BTVYSEVRKA
CD22-N	GISYTTLRFPPEMNIPRTGDAESSEMQRPPPDCDDTVTYSALHKR
CD22-C	GIHYSELIQ-----FGVGERPQAQE--------NVDYVILKH
SHPS-1-N	DITYADLNL----PKGKKPAPQAAAEPNN------HTBYASIQTS
SHPS-1-C	TLTYADLDM----VHLNRTPKQPAPKPEPS----FSEYASVQVP

C

SPAP2	EPMYSNVNPG----DSNPIYSQI
mTCRζ/ηa	NQLYNELNLG-----RREEYDVL
mTCRζ/ηb	EGVYNALOKD----KMAEAYSEI
mTCRζc	DGLYQGLSTA-----TKDTYDAL
mCD3γ	EQLYQPLKDR-----EYDGYSHL
mCD3δ	EDLYQPLRDR-----EDTQYSRL
mCD3ε	NPDYEPIRKG-----QRDLYSGL
mFcεRIγ	DAVYTGLNTR-----NQSTYETL
mFcεRIβ	DRLYEELNHV-----YSPIYSEL
mFcγRIIa	DGGYMTLNPRAPTDDDKNIYLTL

Fig. 3. (A) Schematic alignment of SPAP1a, SPAP2a, and IRTA2c. The Ig domains are sequentially numbered and amino acid sequence identities between homologous Ig domains are indicated. Transmembrane regions and signal peptides are shown as dashed blocks. Y denotes the conserved tyrosine residues embedded in ITIMs of the intracellular region. (B) Sequence alignment of tandem ITIMs. Conserved amino acid residues of ITIMs, plus glycine and proline residues between the tandem ITIMs, are bold-faced. (C) Sequence alignment of tandem ITAMs. Conserved amino acid residues of ITAMs are bold-faced.

Fig. 4. Protein sequence alignments of SPAP2a, SPAP2b, SPAP2c, SPAP2d, and SPAP2e. ":" denote identical amino acid residues. The signal peptides and transmembrane regions are underlined. ITIMs and ITAMs are boldfaced. The DNA sequences of SPAP2a, b, c, d, and e have been deposited into the GenBank database under Accession Numbers AF416901, AF416902, AF416903, AF416904, and AF416905, respectively.
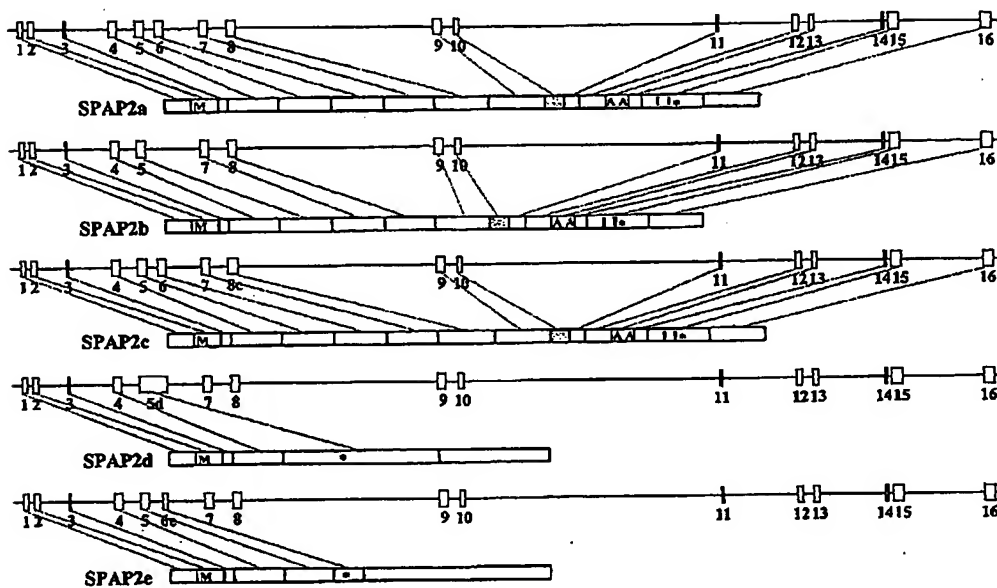
Fig. 5. Schematic diagram of the genomic organization of the SPAP2 gene that gives rise to five alternatively spliced products, namely, SPAP2a, SPAP2b, SPAP2c, SPAP2d, and SPAP2e. Exons are sequentially numbered. The AUG translation initiation sites (M), ITIMs (I), ITAMs (A), and the translation termination codons (*) are indicated. Transmembrane regions are shown as dashed blocks.

We also applied the same PCR strategy to examine the expression of SPAP2 in several human cell lines including 293 embryonic kidney, HeLa cervical carcinoma, HT-1080 fibrosarcoma cells of non-hematopoietic origin and Jurkat T cells, HL-60 promyelocytic cells, and the B cell lines BC-1 and BC-2. Only HeLa cells expressed a detectable level of SPAP2 mRNA (Fig. 6, lower panel). Note that the HeLa carcinoma cell line was derived from the uterine cervix and the data are thus consistent with the expression of SPAP2 in the uterus tissue. SPAP2 is apparently expressed in limited human tissues and cells. It should be pointed out that the PCR primers used for the expression screening do not discriminate between alternatively spliced forms of SPAP2.

Specific recruitment of SH2 domain-containing PTPs and PTKs to tyrosine-phosphorylated SPAP2a

To verify the identity of SPAP2a, we subcloned the entire coding region of the protein into the pCDNA3 vector for expression in mammalian cells. Upon transfection of human 293 embryonic kidney cells with the cDNA construct, expression of a 110-kDa protein was detected by anti-SPAP2 serum (Fig. 7A). The molecular size is larger than the calculated value of 80,855 Da based on the primary structure (including signal sequence). This is likely caused by glycosylation of the protein. Indeed, SPAP2a has eight putative N-linked glycosylation sites at the fifth and sixth Ig domains (see Fig. 2). The presence of tandem ITIMs in SPAP2a suggests that it may serve as an anchor protein for SH2

domain-containing tyrosine phosphatases SHP-1 and SHP-2. To verify this, SPAP2a-transfected 293 cells were treated with pervanadate, a tyrosine phosphatase inhibitor that has been shown to induce tyrosine phosphorylation of ITIM-bearing proteins [20,27,31,41]. As shown in Fig. 7B, this treatment produced tyrosine phosphorylation of SPAP2a and its association with SHP-1. The absence of tyrosine-phosphorylated SPAP2a and SHP-1 bands in vector control experiments essentially validated these assays. However, under the same assay conditions, we did not observe any binding of SHP-2 to tyrosine-phosphorylated SPAP2a although 293 cells expressed a substantial level of SHP-2. This may suggest a preferable association of SPAP2a with SHP-1. We further investigated the interaction of SPAP2a with SH2 domain-containing PTPs and PTKs by using GST-SPAP2aCT, a GST fusion protein containing the intracellular domain of SPAP2a. When co-expressed in *E. coli* cells with c-Src carried by the pET9a vector, GST-SPAP2aCT was heavily phosphorylated on tyrosine and represented virtually the only tyrosine-phosphorylated protein in the *E. coli* cell extracts (Fig. 8A, B). In contrast, GST alone was not phosphorylated by the co-expressed c-Src. This indicates that the intracellular domain of SPAP2a is an excellent substrate of c-Src. We therefore performed in vitro pull-down assays by using the tyrosine-phosphorylated GST-SPAP2aCT protein immobilized on glutathione–Sepharose beads. Upon incubation of the beads with Jurkat cell extracts, Western blotting analyses with specific antibodies revealed strong bindings of SHP-1, SHP-2, Syk, and
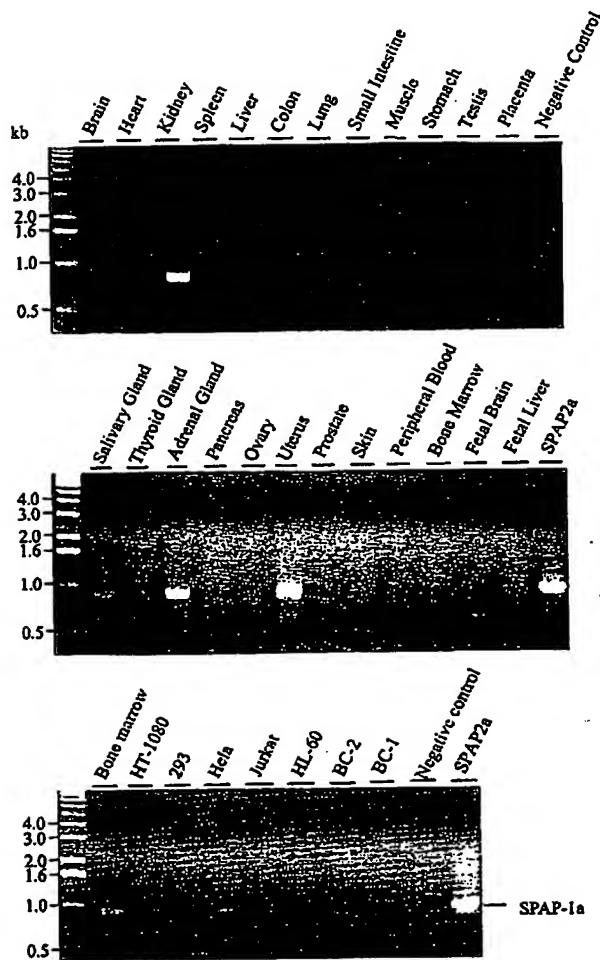
Fig. 6. Distribution of SPAP2 in human tissues and cell lines. First-strand cDNAs from 24 human tissues (concentrations at 100× from OriGene Technologies) and indicated human cell lines were amplified by PCR with a pair of specific primers. PCR products were resolved on 1% agarose gels and detected with ethidium bromide. The position of SPAP2 is indicated. Plasmid SPAP2a DNA and water were used as positive and negative controls, respectively. The bone marrow sample in the lower panel represents the human bone marrow Marathon-ready cDNA library from Clontech Laboratories.

Fig. 7. Expression of SPAP2a and its association with SHP-1. Human 293 cells were transfected with the pCDNA3 vector or the pCDNA3-SPAP2a construct for 48 h. The cells were non-treated (panel A and indicated lanes in panel B) or treated with 0.1 mM pervanadate for 30 min (indicated lanes in panel B). Cell extracts were immunoprecipitated with anti-SPAP2 serum. The immunoprecipitates were analyzed by immunoblotting with antibodies against phosphotyrosine, SHP-1, and anti-SPAP2 as indicated.

Zap70 (Fig. 8C). In control experiments, no association of these PTPs and PTKs with non-phosphorylated SPAP2a-CT or GST was observed. It should also be mentioned that we did not obtain any association of phosphorylated GST-SPAP2aCT with Src family kinases Lck and Lyn (data not shown). We also expressed SPAP2a in the Jurkat cells. Upon treatment with pervanadate, we observed an association of the protein with SHP-1 but not with Syk or Zap70 (data not shown). This may be due to the insufficient tyrosine phosphorylation of ITAMs. Therefore a physiological condition that induces phosphorylation of SPAP2a is required to study the in vivo interaction of SPAP2 in with Zap70 and Syk.

Functional analysis of the intracellular domain of SPAP2a

We further employed five Tyr-to-Phe mutant forms of SPAP2 (see Fig. 1) to verify the functions of ITIMs and ITAMs (Fig. 9). Anti-phosphotyrosine Western blotting analysis with anti-phopshotyrosine revealed that tyrosine phosphorylation remained at a considerable level after mutation of one or two tyrosyl residues, but mutation of all four sites abolished the phosphorylation. This indicates that these four tyrosyl residues (650, 662, 692, and 722) are responsible for the entire tyrosine phosphorylation of the cytoplasmic domain of SPAP2a. GST fusion protein pull-down assays demonstrated that mutations of Tyr^{650} and Tyr^{662} in the ITAMs diminished the binding of Zap70 but mutations of Tyr^{692} and Tyr^{722} in the ITIMs did not affect the binding at all. In contrast, mutations of ITAMs had essentially no effect on the interaction of SHP-1 with SPAP2a while mutations of ITIMs nearly diminished their interaction. Note that considerable binding of Zap70 remained after single mutation at Tyr^{650} but the interaction with SHP-1 was reduced to near basal levels by a single mutation at Tyr^{692}. We observed a similar binding of Syk to the ITAMs and SHP-2 to the ITIMs (data not shown). Together, these data demonstrated that the ITIMs and ITAMs in the intracellular domain of SPAP2 are functional. Finally, we also analyzed the effects of the GST-SPAP2a proteins on the activity of SHP-1 by using in vitro phosphatase assays. As shown in Fig. 10, tyrosine-phosphorylated GST-SPAP2a-CT produced an over 10-fold activation of SHP-1.
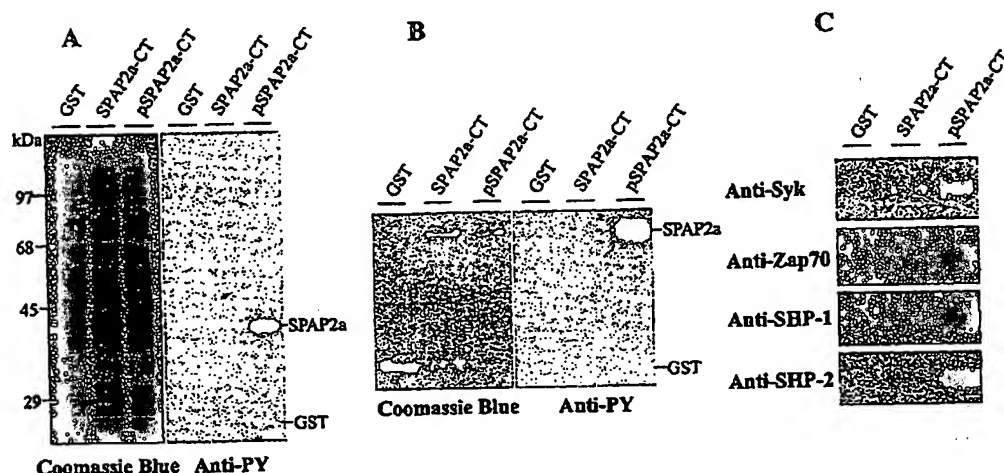
Fig. 8. Tyrosine phosphorylation of SPAP2a by c-Src and in vitro association of SPAP2a with SH2 domain-containing PTPs and PTKs. (A) GST and GST-SPAP2a-CT were expressed in DE3-LysS E. coli cells co-expressing c-Src carried by the pET9a vector. Cell extracts were resolved on SDS gels and analyzed by Coomassie blue staining and by immunoblotting with anti-phosphotyrosine. (B, C). Human Jurkat cell extracts were incubated with glutathione-Sepharose beads carrying GST, GST-SPAP2a-CT, and tyrosine-phosphorylated GST-pSPAP2a-CT for 2 h. The beads were washed and then dissolved in SDS sample buffer. After separation by SDS–PAGE, the samples were analyzed by immunoblotting with antibodies against phosphotyrosine, Syk, Zap70, SHP-1, and SHP-2 as indicated. The amounts of fusion proteins on the beads were determined by Coomassie blue staining.

Furthermore, while mutations of the tyrosyl residues in the ITAMs did not affect the stimulatory effects, mutations of the tyrosyl residues in the ITIMs almost diminished the activation. These data not only further confirm the specific interaction of SHP-1 with the ITIMs of SPAP2a but also suggest that SPAP2a is responsible for activation of SHP-1 in vivo.

Discussion

In the present study, we have isolated a novel cell surface protein, namely, SPAP2a. The distinct feature of SPAP2a is that it contains both ITIMs and ITAMs in the intracellular region. ITIMs are found in inhibitory receptors and they mediate the inhibitory functions of these receptors by recruiting terminating enzymes such as protein tyrosine phosphatases SHP-1 and SHP-2 and the inositol phosphatase SHIP. In contrast, ITAMs are present in various cell surface receptors that play a positive role in cell signaling. Tyrosine-phosphorylated ITIMs are responsible for the recruitment of tyrosine kinases Syk and Zap70 which further activate downstream signal transducers. In the present study, we have demonstrated that tyrosine-phosphorylated SPAP2a is able to bind SH2 domain-containing PTPs, namely, SHP-1 and SHP-2, as well as PTKs including Syk and Zap70. We further demonstrated that the ITIMs are responsible for binding of SHP-1 and SHP-2 while the ITAMs are involved in interactions with Syk and Zap70. Therefore SPAP2a may have both inhibitory and stimulatory functions. Whether the ITIMs and ITAMs of

SPAP2a have different responses to extracellular stimulation and whether they are sequentially or simultaneously activated are not known. It is possible that ITAMs are activated first and allow initiation of signal transduction. Activation of ITIMs thereafter should cause the automatic termination of the signaling process. Conversely, it is also possible that the ITIMs are phosphorylated first or constitutively phosphorylated. This could keep the total cellular tyrosine phosphorylation at a lower level. Then, any stimulation that boosts the tyrosine phosphorylation of ITAMs and suppresses those of ITIMs should initiate signal transduction. On the other hand, if the ITIMs and ITAMs are activated at the same time, they could constitute a futile cycle without a net effect on the level of tyrosine phosphorylation. However, this could at least raise the dynamic equilibrium of phosphorylation and dephosphorylation to a higher rate. In any case, PTKs and PTPs act in a coordinate way. Possession of both ITIM and ITAM makes SPAP2 distinctly important and by studying SPAP2, we may be able to reveal novel signal transduction mechanisms.

The fifth and sixth Ig domains of SPAP2a are highly homologous to each other and share over 80% sequence identity with the Ig domain of SPAP1a and the seventh, eighth, and ninth Ig domains of IRTA2c. Furthermore, all the three proteins contain tandem ITIMs in their intracellular segments. Therefore these proteins form a new subfamily of cell surface receptors. They may share identical or similar ligands that bind to the highly conserved Ig domains and the non-conserved Ig domains may play a regulatory role. This would be reminiscent of
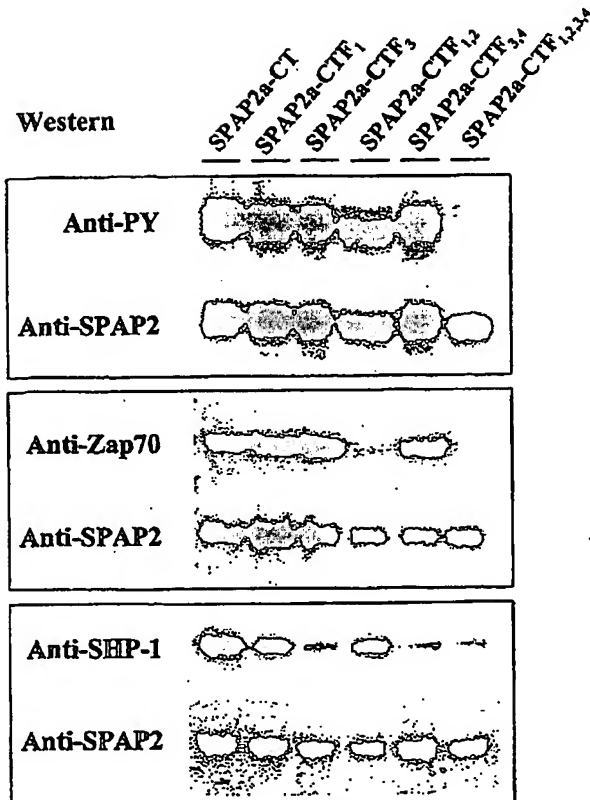
Fig. 9. Functional analyses of the ITAMs and ITIMs of SPAP2a. GST fusion proteins carrying the intracellular domain of SPAP2a in native or Tyr-to-Phe mutant forms were expressed in E. coli cells co-expressing c-Src. Top two panels. Cell extracts were subjected to Western blotting analyses with antiphosphotyrosine or anti-SPAP2. Bottom four panels. GST fusion proteins were immobilized on glutathione–Sepharose beads and the beads were incubated with Jurkat cell extracts. Proteins bound to the beads were analyzed by Western blotting with antibodies against phosphotyrosine (PY), SPAP2, Zap70, and SHP-1 as indicated.
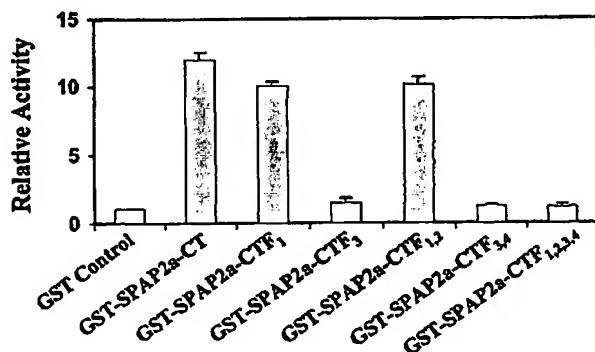
Fig. 10. Activation of SHP-1 by GST fusion proteins containing tyrosine-phosphorylated ITIMs of SPAP2. The activity of SHP-1 was analyzed in a reaction mixture containing 25 mM HEPES–NaOH (pH 7.0), 1 mM dithiothreitol, 1 mM EDTA, 2 mM pNPP, 50 µg/ml SHP-2, and 100 µg/ml GST-SPAP2a-CT or its Y-to-F mutants purified from E. coli cells co-expressing c-Src. Data represent relative activities.

the four members of fibroblast growth factor receptor family, which bind at least 19 structurally related polypeptides as ligands. The fibroblast growth factor receptors also belong to the Ig superfamily. The second Ig domain and the hinge region between the second and third Ig domains of the receptors are highly conserved and have been defined as the general binding sites for FGF [42,43]. The rest of the extracellular region may play a regulatory role. Finally, the soluble forms of SPAP2, namely, SPAP2d and 2e, corresponding to the first and second Ig domain, may also regulate the interaction of full-length SPAP2 with its ligands if not competing with it.

The genes of SPAP1, SPAP2, and IRTA2 are all localized on chromosome 1q21 in close proximity. As a common feature of B-cell malignancies, abnormalities in 1q21 are found in 39% of the marginal zone B-cell lymphomas and 10–15% of the B cell non-Hodgkin's lymphomas [44–46]. It has been recently reported that abnormal expression of IRTA2 is a frequent manifestation of the 1q21 abnormality [40]. Like IRTA2, SPAP1 expression appears to be restricted to B cells. Furthermore, we know that SPAP2 is also expressed in these cells because the EST sequences of SPAP2 were derived from germinal center B cell cDNAs. It will be of great interest to investigate the involvement of SPAP1 and SPAP2 in B cell malignancies. Different from SPAP1 and IRTA2, however, SPAP2 is also highly expressed in the uterus. Since abnormalities of 1q21 are also one of the most common karyotypic changes in malignancies of the uterine cervix [47], the study of the relation of SPAP2 to uterine cervical cancer is also worthy of further investigation.

Acknowledgments

References

[1] T. Hunter, Cell 80 (1995) 225–236.
[2] T. Pawson, J.D. Scott, Science 278 (1997) 2075–2080.
[3] F. Vely, E. Vivier, J. Immunol. 159 (1997) 2075–2077.
[4] E.O. Long, Annu. Rev. Immunol. 17 (1999) 875–904.
[5] J.V. Ravetch, L.L. Lanier, Science 290 (2000) 84–89.
[6] J.C. Cambier, J. Immunol. 155 (1995) 3281–3285.
[7] A. Weiss, D.R. Littman, Cell 76 (1994) 263–274.
[8] D.N. Burshtyn, A.M. Scharenberg, N. Wagtmann, S. Rajagopalan, K. Berrada, T. Yi, J.P. Kinet, E.O. Long, Immunity 4 (1996) 77–85.
[9] D.N. Burshtyn, E.O. Long, Trends Cell. Biol. 7 (1997) 473–479.
[10] T. Muta, T. Kurosaki, Z. Misulovin, M. Sanchez, M.C. Nussenzwcig, J.V. Ravetch, Nature 368 (1994) 70–73.
[11] M. Colonna, J. Samaridis, Science 268 (1995) 405–408.

[12] L. Meyaard, G.J. Adema, C. Chang, E. Woollatt, G.R. Sutherland, L.L. Lanier, J.H. Phillips, Immunity 7 (1997) 283–290.

[13] I. Stamenkovic, B. Seed, Nature 345 (1990) 74–77.

[14] M. Blery, H. Kubagawa, C.C. Chen, F. Vely, M.D. Cooper, E. Vivier, Proc. Natl. Acad. Sci. USA 95 (1998) 2446–2451.

[15] P.J. Newman, M.C. Berndt, J. Gorski, G.C. White, S. Lyman, C. Paddock, W.A. Muller, Science 247 (1990) 1219–1222.

[16] C. Cantoni, S. Verdiani, M. Falco, A. Pessino, M. Cilli, R. Conte, D. Pende, M. Ponte, M.S. Mikaelsson, L. Moretta, R. Biassoni, Eur. J. Immunol. 28 (1998) 1980–1990.

[17] Y. Yamashita, D. Fukuta, A. Tsuji, A. Nagabukuro, Y. Matsuda, Y. Nishikawa, Y. Ohyama, H. Ohmori, M. Ono, T. Takai, J. Biochem. (Tokyo) 123 (1998) 358–368.

[18] A. Kharitonenkov, Z. Chen, I. Sures, H. Wang, J. Schilling, A. Ullrich, Nature 386 (1997) 181–186.

[19] Y. Fujioka, T. Matozaki, T. Noguchi, A. Iwamatsu, T. Yamao, N. Takahashi, M. Tsuda, T. Takada, M. Kasuga, Mol. Cell. Biol. 16 (1996) 6887–6899.

[20] Z.J. Zhao, R. Zhao, J. Biol. Chem. 273 (1998) 29367–29372.

[21] L. Izzi, C. Turbide, C. Houde, T. Kunath, N. Beauchemin, Oncogene 18 (1999) 5563–5572.

[22] V.C. Taylor, C.D. Buckley, M. Douglas, A.J. Cody, D.L. Simmons, S.D. Freeman, J. Biol. Chem. 274 (1999) 11505–11512.

[23] T. Ulyanova, J. Blasioli, T.A. Woodford-Thomas, M.L. Thomas, Eur. J. Immunol. 29 (1999) 3440–3449.

[24] D.K. Newton-Nash, P.J. Newman, J. Immunol. 163 (1999) 682–688.

[25] T. Adachi, H. Flaswinkel, H. Yakura, M. Reth, T. Tsubata, J. Immunol. 160 (1998) 4662–4665.

[26] M. Falco, R. Biassoni, C. Bottino, M. Vitale, S. Sivori, R. Augugliaro, L. Moretta, A. Moretta, J. Exp. Med. 190 (1999) 793–802.

[27] M.J. Xu, R. Zhao, Z.J. Zhao, J. Biol. Chem. 275 (2000) 17440–17446.

[28] Z. Yu, C.M. Lai, M. Maoui, D. Banville, S.H. Shen, J. Biol. Chem. 276 (2001) 23816–23824.

[29] D.D. Mousseau, D. Banville, D. L'Abbe, P. Bouchard, S.H. Shen, J. Biol. Chem. 275 (2000) 4467–4474.

[30] N. Fournier, L. Chalus, I. Durand, E. Garcia, J.J. Pin, T. Churakova, S. Patel, C.J. Zlot, D. Gorman, S. Zurawski, J. Abrams, E.E. Bates, P. Garrone, Immunol. 165 (2000) 1197–1209.

[31] M.J. Xu, R. Zhao, X. Sui, F. Xu, Z.J. Zhao, Biochem. Biophys. Res. Commun. 267 (2000) 820–825.

[32] H. Flaswinkel, M. Reth, EMBO J. 13 (1994) 83–89.

[33] Z. Songyang, S.E. Shoelson, M. Chaudhuri, G. Gish, T. Pawson, W.G. Haser, F. King, T. Roberts, S. Ratnofsky, R.J. Lechleider, Cell 72 (1993) 767–778.

[34] R.L. Wange, L.E. Samelson, Immunity 5 (1996) 197–205.

[35] M.J. Xu, R. Zhao, Z.J. Zhao, Biochem. Biophys. Res. Commun. 280 (2001) 768–775.

[36] Z. Zhao, P. Bouchard, C.D. Diltz, S.H. Shen, E.H. Fischer, J. Biol. Chem. 268 (1993) 2816–2820.

[37] R. Zhao, Y. Qi, Z.J. Zhao, Biochem. Biophys. Res. Commun. 270 (2000) 222–229.

[38] R. Zhao, Y. Qi, J. Chen, Z.J. Zhao, Exp. Cell Res. 265 (2001) 329–338.

[39] R. Zhao, A. Guerrah, H. Tang, Z.J. Zhao, J. Biol. Chem. (2002) (in press).

[40] G. Hatzivassiliou, I. Miller, J. Takizawa, N. Palanisamy, P.H. Rao, S. Iida, S. Tagawa, M. Taniwaki, J. Russo, A. Neri, G. Cattoretti, R. Clynes, C. Mendelsohn, R.S. Chaganti, R. Dalla-Favera, Immunity 14 (2001) 277–289.

[41] R. Zhao, Z.J. Zhao, J. Biol. Chem. 275 (2000) 5453–5459.

[42] A.N. Plotnikov, S.R. Hubbard, J. Schlessinger, M. Mohammadi, Cell 101 (2000) 413–424.

[43] D.E. Johnson, L.T. Williams, Adv. Cancer. Res. 60 (1993) 1–41.

[44] J. Dierlamm, S. Pittaluga, I. Wlodarska, M. Stul, J. Thomas, M. Boogaerts, L. Michaux, A. Driessen, C. Mecucci, J.J. Cassiman, Blood 87 (1996) 299–307.

[45] K. Offit, G. Wong, D.A. Filippa, Y. Tao, R.S. Chaganti, Blood 77 (1991) 1508–1515.

[46] J. Whang-Peng, T. Knutsen, E.S. Jaffe, S.M. Steinberg, M. Raffeld, W.P. Zhao, P. Duffey, K. Condron, T. Yano, D.L. Longo, Blood 85 (1995) 203–216.

[47] C. Sreekantaiah, M.K. Bhargava, N.J. Shetty, Cancer 62 (1988) 1317–1324.

Expression of CD33-related siglecs on human mononuclear phagocytes, monocyte-derived dendritic cells and plasmacytoid dendritic cells

Kevin Lock[a], Jiquan Zhang[a], Jinhua Lu[b], Szu Hee Lee[b,1], Paul R. Crocker[a,*]

[a] Wellcome Trust Biocentre, School of Life Sciences, University of Dundee, Dow Street, Dundee, Scotland, UK
[b] Departments of Microbiology and Haematology, Faculty of Medicine, National University Hospital, National University of Singapore, Singapore

Abstract

Siglecs are sialic acid binding Ig-like lectins mostly expressed in the haemopoietic and immune systems. Amongst the 11 human siglecs, there are eight proteins highly related to CD33 which have biochemical features of inhibitory receptors, containing two conserved tyrosine-based inhibitory motifs. Five of these (CD33/siglec-3, -5, -7, -9 and -10) are expressed on circulating monocytes. Here we show that monocytes cultured to differentiate into macrophages using either GM-CSF or M-CSF retained expression of these siglecs and their levels were unaffected following stimulation with LPS. In comparison, monocyte-derived dendritic cells down-modulated siglec-7 and -9 following maturation with LPS. Plasmacytoid dendritic cells in human blood expressed siglec-5 only. On monocytes, siglec-5 was shown to mediate rapid uptake of anti-siglec-5 (Fab)$_2$ fragments into early endosomes. This suggests, in addition to inhibitory signalling, a potential role in endocytosis for siglec-5 and the other CD33-related siglecs. Our results show that siglecs are differentially expressed on mononuclear phagocytes and dendritic cells and that some can be modulated by stimuli that promote maturation and differentiation.
© 2004 Elsevier GmbH. All rights reserved.

Keywords: Phagocytes, dendritic cells, siglecs

Introduction

The sialic acid-binding Ig-like lectins (siglecs) (Crocker et al., 1998) are members of the Ig (I)-type lectin family (Powell and Varki, 1995) of type I transmembrane proteins implicated in adhesive and signalling functions at the plasma membrane. They are characterised by an N-terminal V-set Ig domain which contains the sialic acid binding site (May et al., 1998), followed by varying numbers of C2-set Ig domains (Fig. 1). All of the siglecs are expressed within the innate and adaptive immune systems with the notable exception of myelin associated glycoprotein (MAG), which is expressed by oligodendrocytes and Schwann cells of the

Fig. 1. The human siglec family. Diagram shows all known human siglecs and their domain organisation. The sialic acid binding site is contained with the N-terminal V-set domain and the inset shows the crystal structure of Sn V-set domain (ribbon) complexed with sialic acid (ball and stick). The circled Ys in the cytoplasmic regions represent putative tyrosine-based signalling motifs.

nervous system (Kelm et al., 1994). To date, 11 human siglecs (and 1 siglec-like protein) have been cloned and characterised. They can be divided into two subgroups based on sequence similarity in the extracellular and intracellular regions. Sialoadhesin (siglec-1), CD22 (siglec-2), and MAG constitute one subgroup, share only ~25–30% sequence identity in the extracellular region, and have divergent cytoplasmic tails. The second subgroup is made up of the CD33-related siglecs that include CD33 (siglec-3) and the recently discovered human siglecs 5–11 (Crocker, 2002). These proteins share 50–80% sequence similarity and have two highly conserved tyrosine-based motifs in their cytoplasmic tails. In humans, the CD33-related siglec genes are clustered on chromosome 19q13.3-4 and are separate from the genes encoding CD22, MAG (19q13.1), and sialoadhesin (20p).

Apart from siglec-6, which was discovered as a leptin binding protein (Patel et al., 1999), the only known ligands for CD33-related siglecs are sialylated glycans that can be presented on glycoproteins and glycolipids. Whilst each siglec exhibits a unique specificity for different glycans (Blixt et al., 2003), the ability of a given siglec to interact in trans with sialic acids on other cells is greatly influenced by cis interactions with sialic acids presented on the siglec-expressing cell, which mask

the sialic acid binding site (reviewed in Crocker and Varki, 2001). A recent study of CD22 expressed on B cells has shown, however, that when B cells interact with other B cells or with T cells, trans interactions can outcompete cis interactions (Collins et al., 2004). Further studies are required to investigate whether similar phenomena can occur with CD33-related siglecs expressed on myeloid cells.

In humans, the majority of siglecs, sialoadhesin being the exception, possess cytoplasmic tyrosine residues embodied within immune receptor tyrosine based inhibitory motifs (ITIM) and/or ITIM-like motifs. These are proposed to regulate cell function via tyrosine phosphorylation and recruitment of src homology 2 (SH2)-domain containing effector molecules (reviewed in Ravetch and Lanier, 2000). One study has shown transient phosphorylation of CD33 and recruitment of SH2-containing protein tyrosine phosphatase-1 (SHP-1) and -2 (SHP-2) following antibody-induced clustering (Taylor et al., 1999), but the usual strategy for inducing high-level phosphorylation of CD33-related siglecs has been to treat cells with sodium pervanadate. Pervanadate acts to irreversibly inhibit protein tyrosine phosphatases by specifically oxidising the catalytic cysteine to form cysteic acid (Huyer et al., 1997). In experiments using this approach, all CD33-related siglecs studied

thus far, have been shown to recruit SHP-1 and -2 in a phosphotyrosine-dependent manner (Falco et al., 1999; Kitzig et al., 2002; Paul et al., 2000; Taylor et al., 1999; Ulyanova et al., 1999). Several studies with monoclonal antibodies (mAb) have shown that some CD33-related siglecs can mediate inhibitory signalling. Co-clustering of CD33 and FcγRI (CD64) on mononuclear phagocytes results in decreased total protein tyrosine phosphorylation as well as a reduction in Ca^{2+} influx compared to clustering of CD64 alone (Paul et al., 2000; Ulyanova et al., 1999). Similarly, the cytotoxicity of natural killer (NK) cells is inhibited by clustering siglec-7 on the cell surface with mAbs (Falco et al., 1999) or with natural ligands (Nicoll et al., 2003). Other studies have shown that mAb ligation of CD33-related siglecs can result in reduced proliferation and apoptosis (Balaian et al., 2003; Nutku et al., 2003; Vitale et al., 2001) and modulate oxidative burst of neutrophils (Erickson-Miller et al., 2003). Unfortunately most of these studies were done with intact IgG, so the potential influence of FcR ligation on these functional activities cannot be excluded.

Thus, an emerging theme is that CD33-related siglecs containing ITIM-like motifs modulate activation functions of leukocytes and other cell populations that express them. The expression profiles of CD33-related siglecs and modulation of their expression are clearly key factors that determine the contribution of these proteins to cellular regulation within the immune system. In this paper, we present novel data on the expression of CD33-related siglecs on monocytes, macrophages and dendritic cells (DC). We show that these cell surface molecules in addition to transducing negative signals may mediate uptake of ligands. This may be important in the induction of tolerance to self or in generation of a protective immune response to invading microbes that carry cell surface sialic acid residues.

Materials and methods

Isolation of peripheral blood leucocytes and flow cytometry

Peripheral blood leucocytes were isolated from whole blood by incubation with four volumes of 1.5% dextran T500 in phosphate buffered saline (PBS) at room temperature for up to 1 h. Residual erythrocytes were lysed with RBC lysis solution (Sigma) at 37°C for 2 min followed by addition of 10 volumes of PBS. Cells were plated at a maximum of 1×10^6 cells/well in a 96-well, round-bottomed plate. For all subsequent steps, cells and buffers were maintained at 4°C. For the primary antibody incubations, PBS + 0.1% bovine

serum albumin (PBA) alone (no primary antibody control) or appropriate dilutions of irrelevant or specific mAb (either purified IgG or hybridoma supernatant) were added to the wells for up to 1 h. Cells were washed twice with PBA and incubated with PBA alone (no secondary antibody control) or anti-mouse IgG directly conjugated to fluorescein isothiocyanate (DAKO) for 45 min. Labelled cells were washed three times with PBA and either analysed immediately or fixed with 2% formaldehyde in PBS and stored at 4°C for subsequent analysis. For detection of siglecs on plasmacytoid DC (PDC), blood leucocytes were labelled with a mixture of phycoerythrin-conjugated anti-BDCA-2 (Miltenyi Biotec) and different Alexa-488-conjugated anti-siglec antibodies for 30 min at 4°C.

Differentiation of peripheral blood monocytes into macrophages and dendritic cells

Human monocytes were isolated from peripheral blood using Ficoll-paque Plus (Amersham Pharmacia Biotech) and following adherence to tissue culture plates (95% purity) were cultured at 1×10^6/ml in a humidified atmosphere at 37°C, 5% CO_2, in RPMI 1640 supplemented with 10% foetal calf serum (FCS) (HyClone), 100 units/ml penicillin, 100 µg/ml streptomycin, 2 mM L-glutamine, 1 mM sodium pyruvate, and 0.0012% (v/v) 2-mercaptoethanol. To generate DC, monocytes were cultured for 6 days in the presence of GM-CSF (20 ng/ ml) and IL-4 (20 ng/ml) with half of the medium being replaced by fresh medium every other day. Macrophages were obtained from isolated monocytes by cultivation in the presence of M-CSF (20 ng/ml). In some experiments, macrophages and DC were activated with *Escherichia coli* lipopolysaccharide (LPS) (0.5 µg/ml) for 48 h prior to analysis of CD33-related siglec expression by flow cytometry.

Endocytosis of anti-siglec-5 F(ab)₂ fragments and fluorescence microscopy

Adherent monocytes were incubated with Alexa-488 conjugated (Molecular Probes) polyclonal F(ab′)₂ fragments specific for siglec-5 at 4°C for 1 h. Excess antibody was removed by washing with PBS and cells were transferred to 37°C for the times indicated before fixing with 2% formaldehyde in PBS. Fixed cells were permeabilised with 0.1% saponin and the early endosomal compartment was localised by labelling with a Texas Red-conjugated antibody specific for EEA-1. Images were acquired using a DeltaVision Restoration Microscope (Applied Precision Inc., USA).
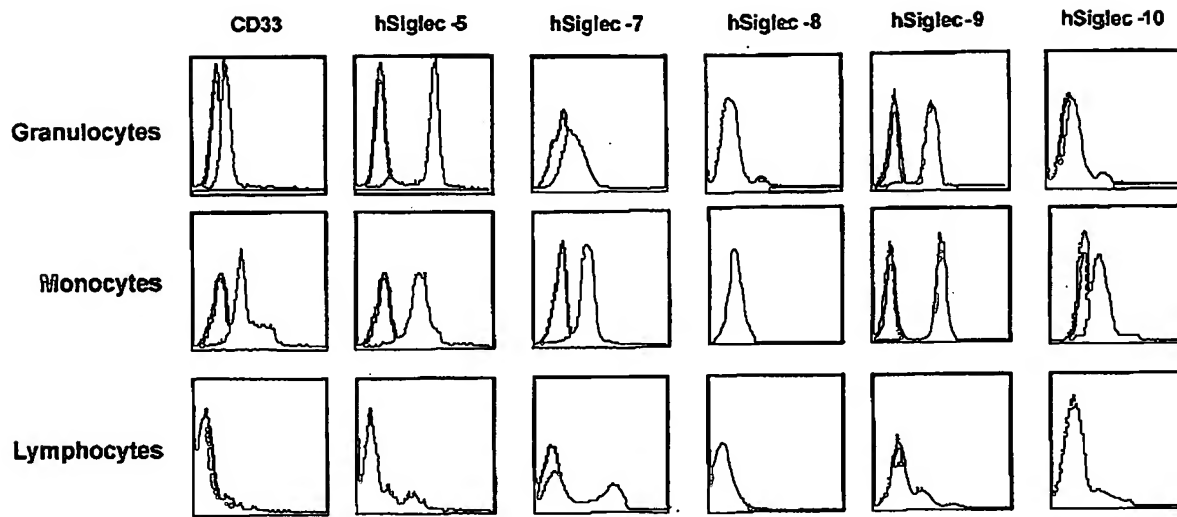
Fig. 2. Expression of CD33-related siglecs on human blood leucocytes. Blood leucocytes were stained with mAbs against the indicated siglecs followed by a secondary antibody coupled to FITC and analysed by flow cytometry (filled histograms). The fluorescence of cells labelled with an irrelevant unlabelled mAb is indicated by the unfilled histogram in each case. One of five experiments.

Results and discussion

Expression of CD33-related siglecs on blood leukocyte populations

Of the eight CD33-related siglecs encoded within the human genome (Fig. 1), seven can be detected at the surface of circulating white blood cells by flow cytometry (Fig. 2 and Patel et al., 1999). The exception is siglec-11 which is expressed on subsets of tissue macrophages (Angata et al., 2002). Analysis of different populations of blood leukocytes reveals broad expression of CD33-related siglecs on granulocytes and monocytes compared to lymphocytes. For example, the myeloid cell marker CD33/siglec-3 is found on monocytes and at low levels on granulocytes whilst siglec-5 is more abundant on granulocytes compared to monocytes (Fig. 2). Both populations express siglec-9, while siglec-7 is more abundant on monocytes than granulocytes and siglec-8 is found specifically on eosinophils (Fig. 2) (Floyd et al., 2000). Within the 'lymphocyte' population gated by side and forward scatter, siglec-7 is expressed on most NK cells, and siglec-5, -9 and -10 are expressed weakly on most B lymphocytes (Fig. 2). Conversely, CD33-related siglecs are largely absent from the majority of T lymphocytes, although a minor subset of CD8 T cells are positive for siglec-7 and -9 (Nicoll et al., 1999; Zhang et al., 2000). These results show that, with the notable exception of T cells, cells of the immune system express one or more siglecs with ITIM-like motifs.

An emerging theme is that inhibitory receptors on myeloid cells are important for preventing auto-reactivity to 'self' and unwanted bystander toxicity (Nathan and Muller, 2001). Sialic acids are good candidates as markers of 'self' to the immune system since they are largely absent from primitive organisms that could act as potential pathogens (reviewed in Crocker and Varki, 2001). The widespread expression of 'inhibitory' CD33-related siglecs on myeloid cells is consistent with a role of sialic acid in regulating leucocyte activation. For example, sialylated endothelial cell mucins lining the vasculature could interact with siglecs in trans and reduce the probability of spontaneous leucocyte activation in the circulation. Since T cells are activated physiologically in response to peptide-MHC complexes presented on the surface of antigen presenting cells, the absence of siglecs on T cells might be important for avoiding interactions with sialylated ligands that could modulate T cell activation responses in unpredictable ways. In comparison, it has been proposed that one of the functions of CD22/siglec-2 on B cells is to raise the threshold of B cell activation via interactions with sialylated ligands on cells presenting 'self' antigens that cross-react with B cell receptors (Lanoue et al., 2002). It is striking that B cells express not only CD22/siglec-2, but also siglec-5, -6, -9 and -10 supporting the concept that silencing of immune responses to self may be particularly important for B lymphocytes. Along these lines a recent study has proposed that clustering of CD22/siglec-2 at the junction between B cells and T cells might be important for preventing bystander B cell activation resulting from CD40–CD40L interactions (Collins et al., 2004). The additional CD33-related siglecs on B cells

Monocytes   Macrophages   Dendritic Cells
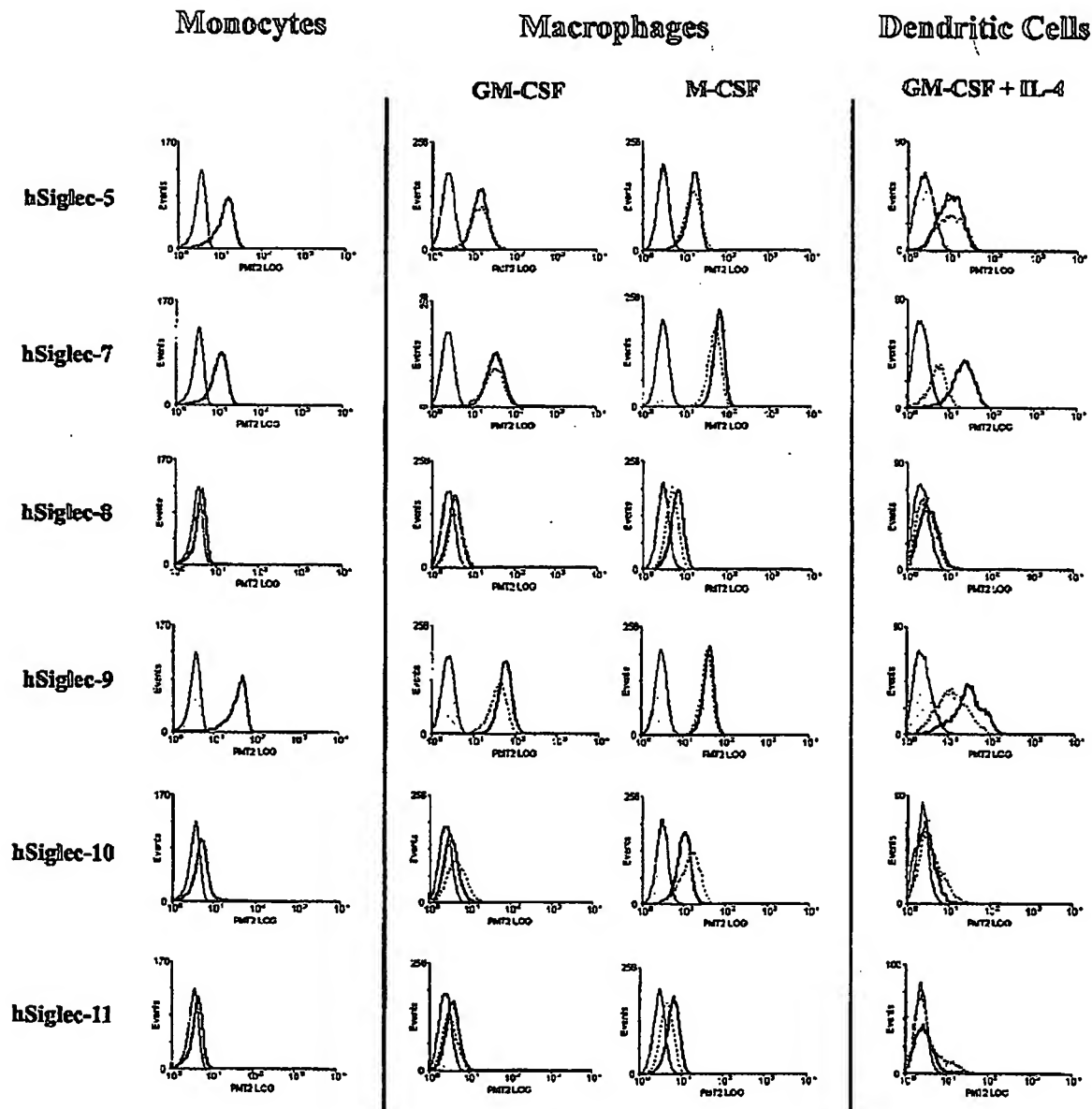
Fig. 3. Differential expression of CD33-related siglecs on monocytes, macrophages and dendritic cells. Freshly isolated monocytes, monocyte-derived macrophages or monocyte-derived DC were stained with the indicated mAb followed by FITC anti-mouse IgG. The fluorescence of unlabelled cells is indicated by the filled histogram in each case. Expression on unstimulated cells is shown by solid lines. The expression of CD33-related siglecs on macrophages and DC after stimulation with LPS is shown by dotted lines. One of three to four experiments.

may similarly contribute to inhibitory signalling during cell–cell interactions and antigen presentation.

Expression of CD33-related siglecs on monocytes, macrophages and DC

Since circulating monocytes have the potential to develop into both resident tissue macrophages and DC,

we were interested to determine whether monocyte differentiation affects expression of CD33-related siglecs. Human monocytes were isolated from peripheral blood and induced to differentiate into macrophages by the action of GM-CSF or M-CSF for 6 days, or into DC by incubation with GM-CSF and IL-4 (Fig. 3). Samples of both cell types were also activated by the addition of LPS into culture media for 48 h prior to analysis by flow cytometry. Expression levels of the siglecs on

monocyte-derived macrophages or DC did not appear to be significantly altered when compared with freshly isolated monocytes, except for slight up-regulation of siglec-10 on M-CSF-derived macrophages (Fig. 3). In contrast, LPS-activated DC revealed a significant down-modulation of siglec-7 and -9. Given the pivotal role played by DC in driving both T cell activation and T cell tolerance, the expression and modulation of inhibitory receptors on DC is of clear significance. Several inhibitory receptors such as immunoglobulin-like transcripts (ILTs/CD85) (Beinhauer et al., 2004; Cella et al., 1997), CEACAM· (Kammerer et al., 2001), FDF03 (Fournier et al., 2000), DCIR (Kanazawa et al., 2002) and LLIR (Huang et al., 2001) are expressed on human or mouse DC and in some cases they have been shown to modulate activation events. For example, ligation of PIR-B on mouse DC or its homologue ILT4 on human DC has been shown to inhibit responses to CD40 engagement, resulting in reduced T cell proliferation via inhibitory signalling in DC (Liang and Horuzsko, 2003). Interestingly, ILT4 expression was shown to be increased in response to maturation, whereas other inhibitory receptors such as LLIR are reduced (Beinhauer et al., 2004; Huang et al., 2001). It will be interesting to investigate whether siglecs can similarly modulate DC function. A down-modulation of siglec-7 and -9 in DC, as demonstrated here, may well lead to an enhanced activity of DC.

Expression of CD33-related siglecs on plasmacytoid dendritic cells

It has become increasingly clear that the DC are a heterogenous population of cells derived from more than one lineage. The natural IFN-α producing cells (IPC) previously identified in peripheral blood and comprising 0.1% of PBMC (Cederblad and Alm, 1990; Howell et al., 1994) were found to lack surface markers for monocytes, T, B or NK cells, but expressed high levels of HLA-DR (Abb et al., 1983; Fitzgerald-Bocarsly et al., 1988; Perussia et al., 1985). The large size, abundant cytoplasm and extensive endoplasmic reticulum (Feldman and Fitzgerald-Bocarsly, 1990; Ferbas et al., 1994; Ghanekar et al., 1996; Gobl et al., 1988) of these cells resembled antibody-producing plasma cells and they have now been re-named plasmacytoid dendritic cells (PDC) (reviewed in Fitzgerald-Bocarsly, 2002). Flow cytometry studies have also demonstrated these cells to be CD11c⁻, HLA-DR⁺ and CD123^bright and to express type II, C-type lectin blood DC antigen (BDCA)-2 (Dzionek et al., 2000). These observations have aided in the phenotypic characterisation of PDC and helped to distinguish them from other DC populations (e.g. the CD11c⁺ population of myeloid DC). To investigate CD33-related siglec expression on PDC,

freshly isolated blood leucocytes were labelled with a mAb against BDCA-2 to identify PDC and found to comprise approximately 0.1% of total cells, in agreement with previous findings (Cederblad and Alm, 1990; Howell et al., 1994) (Fig. 4). Expression of CD33-related siglecs on these rare cell types was found to be restricted to siglec-5, as demonstrated by flow cytometry (Fig. 4). It will be interesting to investigate whether siglec-5 ligation on PDC alters their functional properties.

Endocytosis mediated by CD33-related siglecs on monocytes

Besides a potential role in modulating cellular activation via recruitment of SHP-1 and -2 tyrosine phosphatases, the tyrosine-based motifs in CD33-related siglecs have the potential to function as signals for clathrin-dependent endocytosis. Generally, tyrosine-based signals are of the form NPXY or YXXØ (where X is any amino acid and Ø is an amino acid with a bulky hydrophobic side-chain) (Royle et al., 2002), which interact with the $\mu2$ subunit of adaptor protein-2 associated with clathrin in coated pits. To investigate whether CD33-related siglecs are capable of mediating endocytosis, F(ab)₂ fragments of an affinity-purified sheep polyclonal anti-siglec-5 IgG were prepared and labelled with Alexa-488. Freshly isolated monocytes were found to rapidly internalise the F(ab)₂ fragments, a fraction of which entered an early endosomal compartment, as shown by partial co-localisation with the EEA1 antigen (Fig. 5). These findings raise the possibility that CD33-related siglecs expressed by monocytes, macrophages and DC could be involved in the uptake and processing of sialylated glycoproteins. Further studies are needed to see if this could influence antigen processing and presentation by monocytes and dendritic cells in a similar way to that demonstrated for ILT-3 (Cella et al., 1997). For macrophages, uptake of sialylated glycoproteins by siglecs could be important for removal of antigenic epitopes from the immune system. Some pathogens have evolved the capacity to express surface sialic acids which have been proposed to protect pathogens from complement fixation and phagocytosis via electrostatic effects (reviewed· in Crocker and Varki, 2001). However, interactions with siglecs such as siglec-5 could lead to pathogen uptake and destruction, as proposed recently for sialylated forms of *Neisseria meningitidis* (Jones et al., 2003) and where studied, this has been closely linked to pathogenicity (reviewed in Crocker and Varki, 2001). Given the selective expression of siglec-5 on plasmacytoid DC, it is possible that uptake of such bacteria via this receptor may lead to efficient antigen presentation.
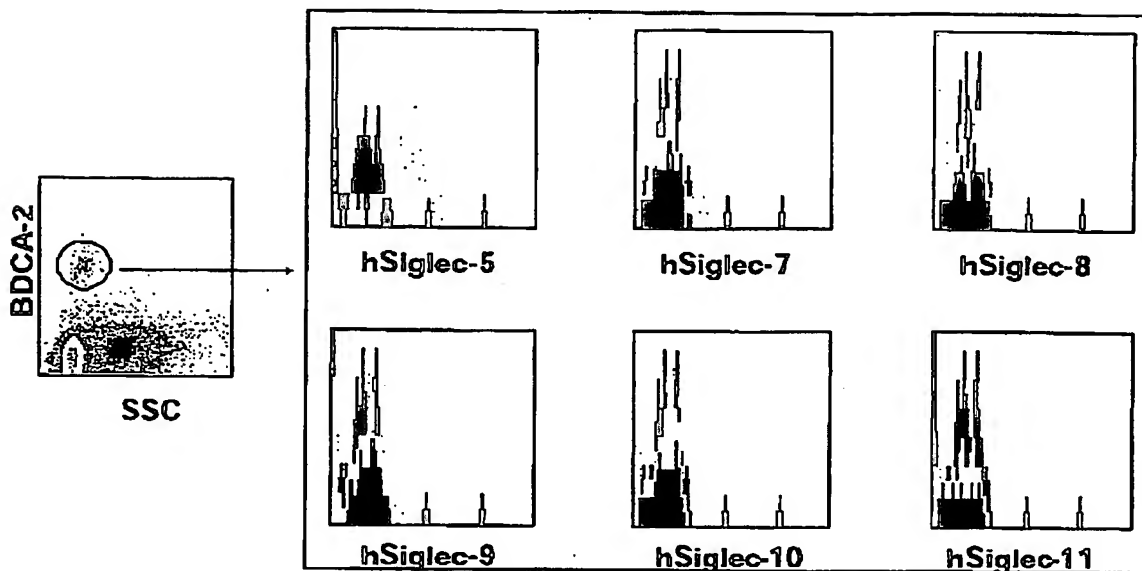
Fig. 4. Selective expression of siglec-5 by plasmacytoid dendritic cells. Peripheral blood leucocytes were labelled with anti-BDCA-2-PE and Alexa-488-labelled anti-siglec mAb and analysed by flow cytometry. The BDCA-2 positive cells (PDC) are also positive for siglec-5. The other CD33-related siglecs examined were not detectable on these cells. One of two experiments.
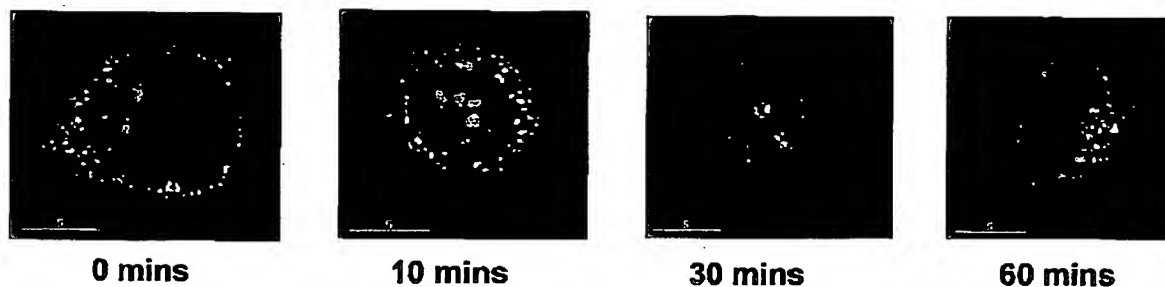

Fig. 5. Rapid internalisation of siglec-5 on adherent monocytes following antibody-mediated clustering. Adherent monocytes were labelled with sheep polyclonal anti-siglec-5 F(ab)₂ fragments conjugated to Alexa-488 at 4°C for 1 h before washing and transfer to 37°C for the times indicated (0–60 min). Cells were formaldehyde-fixed, permeabilised with saponin and stained with Texas Red-labelled antibody to EEA1 to identify early endosomal compartments. Cells were mounted and examined on a DeltaVision fluorescence microscope and images from the central z-section of representative cells are shown. For a colour version of this figure refer to the web version of the paper: [provide URL address]. One of three experiments.

Conclusions

Here we present data on expression of CD33-related siglecs on human monocytes, macrophages and dendritic cells. We show that all of these cells express at least one siglec, and apart from PDC which expressed only siglec-5, all populations examined expressed several siglecs simultaneously, especially siglec-3, -5, -7 and -9. This points to a significant degree of functional redundancy. However, several of these inhibitory receptors, particularly siglec-5, -7 and -9 show clear up- and down-modulation following exposure of cells to pharmacological and proinflammatory mediators. This suggests that these siglecs can be subject to transcriptional regulation during inflammatory and immune responses, and this could contribute to the fine-tuning of leucocyte activation thresholds. Further studies using animal models will clearly be of value in elucidating the in vivo functions of CD33-related siglecs on leucocytes.

References

Abb, J., Abb, H., Deinhardt, F., 1983. Phenotype of human alpha-interferon producing leucocytes identified by monoclonal antibodies. Clin. Exp. Immunol. 52, 179–184.

Angata, T., Kerr, S.C., Greaves, D.R., Varkin, N.M., Crocker, P.R., Varki, A., 2002. Cloning and characterization of human Siglec-11. A recently evolved signaling that can interact with SHP-1 and SHP-2 and is expressed by tissue macrophages, including brain microglia. J. Biol. Chem. 277, 24466–24474.

Balaian, L., Zhong, R.K., Ball, E.D., 2003. The inhibitory effect of anti-CD monoclonal antibodies on AML cell growth correlates with Syk and/or ZAP-70 expression. Exp. Hematol. 31, 363–371.

Beinhauer, B.G., McBride, J.M., Graf, P., Pursch, E., Bongers, M., Rogy, M., Korthauer, U., de Vries, J.E., Aversa, G., Jung, T., 2004. Interleukin 10 regulates cell surface and soluble LIR-2 (CD85d) expression on dendritic cells resulting in T cell hyporesponsiveness in vitro. Eur. J. Immunol. 34, 74–80.

Blixt, O., Collins, B.E., van den Nieuwenhof, I.M., Crocker, P.R., Paulson, J.C., 2003. Sialoside specificity of the siglec family assessed using novel multivalent probes: identification of potent inhibitors of myelin-associated glycoprotein. J. Biol. Chem. 278, 31007–31019.

Cederblad, B., Alm, G.V., 1990. Infrequent but efficient interferon-alpha-producing human mononuclear leukocytes induced by herpes simplex virus in vitro studied by immuno-plaque and limiting dilution assays. J. Interferon. Res. 10, 65–73.

Cella, M., Dohring, C., Samaridis, J., Dessing, M., Brockhaus, M., Lanzavecchia, A., Colonna, M., 1997. A novel inhibitory receptor (ILT3) expressed on monocytes, macrophages, and dendritic cells involved in antigen processing. J. Exp. Med. 185, 1743–1751.

Collins, B.E., Blixt, O., DeSieno, A.R., Bovin, N., Marth, J.D., Paulson, J.C., 2004. Masking of CD22 by cis ligands does not prevent redistribution of CD22 to sites of cell contact. Proc. Natl. Acad. Sci. USA 101, 6104–6109.

Crocker, P.R., 2002. Siglecs: sialic-acid-binding immunoglobulin-like lectins in cell-cell interactions and signalling. Curr. Opin. Struct. Biol. 12, 609–615.

Crocker, P.R., Varki, A., 2001. Siglecs, sialic acids and innate immunity. Trends Immunol. 22, 337–342.

Crocker, P.R., Clark, E.A., Filbin, M., Gordon, S., Jones, Y., Kehrl, J.H., Kelm, S., Le Douarin, N., Powell, L., Roder, J., Schnaar, R.L., Sgroi, D.C., Stamenkovic, K., Schauer, R., Schachner, M., van den Berg, T.K., van der Merwe, P.A., Watt, S.M., Varki, A., 1998. Siglecs: a family of sialic-acid binding lectins. Glycobiology 8: v.

Dzionek, A., Fuchs, A., Schmidt, P., Cremer, S., Zysk, M., Miltenyi, S., Buck, D.W., Schmitz, J., 2000. BDCA-2, BDCA-3, and BDCA-4: three markers for distinct subsets of dendritic cells in human peripheral blood. J. Immunol. 165, 6037–6046.

Erickson-Miller, C.L., Freeman, S.D., Hopson, C.B., D'Alessio, K.J., Fischer, E.I., Kikly, K.K., Abrahamson, J.A., Holmes, S.D., King, A.G., 2003. Characterization of Siglec-5 (CD170) expression and functional activity of anti-Siglec-5 antibodies on human phagocytes. Exp. Hematol. 31, 382–388.

Falco, M., Biassoni, R., Bottino, C., Vitale, M., Sivori, S., Augugliaro, R., Moretta, L., Moretta, A., 1999. Identification and molecular cloning of p75/AIRM1, a novel member

of the sialoadhesin family that functions as an inhibitory receptor in human natural killer cells. J. Exp. Med. 190, 793–802.

Feldman, M., Fitzgerald-Bocarsly, P., 1990. Sequential enrichment and immunocytochemical visualization of human interferon-alpha-producing cells. J. Interferon. Res. 10, 435–446.

Ferbas, J.J., Toso, J.F., Logar, A.J., Navratil, J.S., Rinaldo Jr., C.R., 1994. CD4+ blood dendritic cells are potent producers of IFN-alpha in response to in vitro HIV-1 infection. J. Immunol. 152, 4649–4662.

Fitzgerald-Bocarsly, P., 2002. Natural interferon-alpha producing cells: the plasmacytoid dendritic cells. Biotechniques (Suppl.), 16–29.

Fitzgerald-Bocarsly, P., Feldman, M., Mendelsohn, M., Curl, S., Lopez, C., 1988. Human mononuclear cells which produce interferon-alpha during NK(HSV-FS) assays are HLA-DR positive cells distinct from cytolytic natural killer effectors. J. Leukoc. Biol. 43, 323–334.

Floyd, H., Ni, J., Cornish, A.L., Zeng, Z., Liu, D., Carter, K.C., Steel, J., Crocker, P.R., 2000. Siglec-8. A novel eosinophil-specific member of the immunoglobulin superfamily. J. Biol. Chem. 275, 861–866.

Fournier, N., Chalus, L., Durand, I., Garcia, E., Pin, J.J., Churakova, T., Patel, S., Zlot, C., Gorman, D., Zurawski, S., Abrams, J., Bates, E.E., Garrone, P., 2000. FDF03, a novel inhibitory receptor of the immunoglobulin superfamily, is expressed by human dendritic and myeloid cells. J. Immunol. 165, 1197–1209.

Ghanekar, S., Zheng, L., Logar, A., Navratil, J., Borowski, L., Gupta, P., Rinaldo, C., 1996. Cytokine expression by human peripheral blood dendritic cells stimulated in vitro with HIV-1 and herpes simplex virus. J. Immunol. 157, 4028–4036.

Gobl, A.E., Funa, K., Alm, G.V., 1988. Different induction patterns of mRNA for IFN-alpha and -beta in human mononuclear leukocytes after in vitro stimulation with herpes simplex virus-infected fibroblasts and sendai virus. J. Immunol. 140, 3605–3609.

Howell, D.M., Feldman, S.B., Kloser, P., Fitzgerald-Bocarsly, P., 1994. Decreased frequency of functional natural interferon-producing cells in peripheral blood of patients with the acquired immune deficiency syndrome. Clin. Immunol. Immunopathol. 71, 223–230.

Huang, X., Yuan, Z., Chen, G., Zhang, M., Zhang, W., Yu, Y., Cao, X., 2001. Cloning and characterization of a novel ITIM containing lectin-like immunoreceptor LLIR and its two transmembrane region deletion variants. Biochem. Biophys. Res. Commun. 281, 131–140.

Huyer, G., Liu, S., Kelly, J., Moffat, J., Payette, P., Kennedy, B., Tsaprailis, G., Gresser, M.J., Ramachandran, C., 1997. Mechanism of inhibition of protein-tyrosine phosphatases by vanadate and pervanadate. J. Biol. Chem. 272, 843–851.

Jones, C., Virji, M., Crocker, P.R., 2003. Recognition of sialylated meningococcal lipopolysaccharide by siglecs expressed on myeloid cells leads to enhanced bacterial uptake. Mol. Microbiol. 49, 1213–1225.

Kammerer, R., Stober, D., Singer, B.B., Obrink, B., Reimann, J., 2001. Carcinoembryonic antigen-related cell adhesion

molecule 1 on murine dendritic cells is a potent regulator of T cell stimulation. J. Immunol. 166, 6537–6544.

Kanazawa, N., Okazaki, T., Nishimura, H., Tashiro, K., Inaba, K., Miyachi, Y., 2002. Dcir acts as an inhibitory receptor depending on its immunoreceptor tyrosine-based inhibitory motif. J. Invest. Dermatol. 118, 261–266.

Kelm, S., Pelz, A., Schauer, R., Filbin, M.T., Tang, S., Debellard, M.E., Schnaar, R.L., Mahoney, J.A., Hartnell, A., Bradfield, P., Crocker, P.R., 1994. Sialoadhesin, myelin-associated glycoprotein and CD22 define a new family of sialic acid-dependent adhesion molecules of the immuno-globulin superfamily. Curr. Biol. 4, 965–972.

Kitzig, F., Martinez-Barriocanal, A., Lopez-Botet, M., Sayos, J., 2002. Cloning of two new splice variants of Siglec-10 and mapping of the interaction between Siglec-10 and SHP-1. Biochem. Biophys. Res. Commun. 296, 355–362.

Lanoue, A., Batista, F.D., Stewart, M., Neuberger, M.S., 2002. Interaction of CD22 with alpha2,6-linked sialoglyco-conjugates: innate recognition of self to dampen B cell autoreactivity? Eur. J. Immunol. 32, 348–355.

Liang, S., Horuzsko, A., 2003. Mobilizing dendritic cells for tolerance by engagement of immune inhibitory receptors for HLA-G. Hum. Immunol. 64, 1025–1032.

May, A.P., Robinson, R.C., Vinson, M., Crocker, P.R., Jones, E.Y., 1998. Crystal structure of the N-terminal domain of sialoadhesin in complex with 3' sialyllactose at 1.85 Å resolution. Mol. Cell 1, 719–728.

Nathan, C., Muller, W.A., 2001. Putting the brakes on innate immunity: a regulatory role for CD200? Nat. Immunol. 2, 17–19.

Nicoll, G., Ni, J., Liu, D., Klenerman, P., Munday, J., Dubock, S., Mattei, M.G., Crocker, P.R., 1999. Identification and characterization of a novel siglec, siglec-7, expressed by human natural killer cells and monocytes. J. Biol. Chem. 274, 34089–34095.

Nicoll, G., Avril, T., Lock, K., Furukawa, K., Bovin, N., Crocker, P.R., 2003. Ganglioside GD3 expression on target cells can modulate NK cell cytotoxicity via siglec-7-dependent and -independent mechanisms. Eur. J. Immunol. 33, 1642–1648.

Nutku, E., Aizawa, H., Hudson, S.A., Bochner, B.S., 2003. Ligation of Siglec-8: a selective mechanism for induction of human eosinophil apoptosis. Blood 101, 5014–5020.

Patel, N., Brinkman-Van der Linden, E.C., Altmann, S.W., Gish, K., Balasubramanian, S., Timans, J.C., Peterson, D., Bell, M.P., Bazan, J.F., Varki, A., Kastelein, R.A., 1999. OB-BP1/Siglec-6. a leptin- and sialic acid-binding protein of the immunoglobulin superfamily. J. Biol. Chem. 274, 22729–22738.

Paul, S.P., Taylor, L.S., Stansbury, E.K., McVicar, D.W., 2000. Myeloid specific human CD33 is an inhibitory receptor with differential ITIM function in re-cruiting the phosphatases SHP-1 and SHP-2. Blood 96, 483–490.

Perussia, B., Fanning, V., Trinchieri, G., 1985. A leukocyte subset bearing HLA-DR antigens is responsible for in vitro alpha interferon production in response to viruses. Nat. Immunol. Cell Growth Regul. 4, 120–137.

Powell, L.D., Varki, A., 1995. I-type lectins. J. Biol. Chem. 270, 14243–14246.

Ravetch, J.V., Lanier, L.L., 2000. Immune inhibitory recep-tors. Science 290, 84–89.

Royle, S.J., Bobanovic, L.K., Murrell-Lagnado, R.D., 2002. Identification of a non-canonical tyrosine-based endocytic motif in an ionotropic receptor. J. Biol. Chem. 277, 35378–35385.

Taylor, V.C., Buckley, C.D., Douglas, M., Cody, A.J., Simmons, D.L., Freeman, S.D., 1999. The myeloid-specific sialic acid-binding receptor, CD33, associates with the protein-tyrosine phosphatases, SHP-1 and SHP-2. J. Biol. Chem. 274, 11505–11512.

Ulyanova, T., Blasioli, J., Woodford-Thomas, T.A., Thomas, M.L., 1999. The sialoadhesin CD33 is a myeloid-specific inhibitory receptor. Eur. J. Immunol. 29, 3440–3449.

Vitale, C., Romagnani, C., Puccetti, A., Olive, D., Costello, R., Chiossone, L., Pitto, A., Bacigalupo, A., Moretta, L., Mingari, M.C., 2001. Surface expression and function of p75/AIRM-1 or CD33 in acute myeloid leukemias: engagement of CD33 induces apoptosis of leukemic cells. Proc. Natl. Acad. Sci. USA 98, 5764–5769.

Zhang, J.Q., Nicoll, G., Jones, C., Crocker, P.R., 2000. Siglec-9, a novel sialic acid binding member of the immunoglo-bulin superfamily expressed broadly on human blood leukocytes. J. Biol. Chem. 275, 22121–22126.

KIR2DL4 Is an IL-2-Regulated NK Cell Receptor That Exhibits Limited Expression in Humans but Triggers Strong IFN-γ Production[1]

Akiko Kikuchi-Maki, Sei-ichi Yusa, Tracey L. Catina, and Kerry S. Campbell[2]

Killer cell Ig-like receptor (KIR)2DL4 (2DL4, CD158d) was previously described as the only KIR expressed by every human NK cell. It is also structurally atypical among KIRs because it possesses a basic transmembrane residue, which is characteristic of many activating receptors, but also contains a cytoplasmic immunoreceptor tyrosine-based inhibitory motif (ITIM). We expressed epitope-tagged 2DL4 in an NK-like cell line to study receptor function. Three distinct 2DL4 cDNA clones were analyzed: one encoding the "conventional" 2DL4 with the cytoplasmic ITIM (2DL4.1) and two encoding different cytoplasmic truncated forms lacking the ITIM (2DL4.2 and 2DL4*). Surprisingly, one truncated receptor (2DL4.2), which is the product of a prevalent human 2DL4 allele, was not expressed on the cell surface, indicating that some individuals may lack functional 2DL4 protein expression. Conversely, both 2DL4.1 and 2DL4* were expressed on the cell surface and up-regulated by IL-2. Analysis of primary NK cells with anti-2DL4 mAb confirmed the lack of surface expression in a donor with the 2DL4.2 genotype. Donors with the 2DL4.1 genotype occasionally expressed receptor only on CD56^{high} NK cells, although their expression was up-regulated by IL-2. Interestingly, Ab engagement of epitope-tagged 2DL4 triggered rapid and robust IFN-γ production, but weak redirected cytotoxicity in an NK-like cell line, which was the opposite pattern to that observed upon engagement of another NK cell activating receptor, NKp44. Importantly, both 2DL4.1 and 2DL4* exhibited similar activation potential, indicating that the ITIM does not influence 2DL4.1 activating function. The unique activation properties of 2DL4 suggest linkage to a distinct signaling pathway. *The Journal of Immunology*, 2003, 171: 3415–3425.

N atural killer cells play a vital role in the immune response to virus infection and cancer by providing linkage between innate and adaptive immunity. They can mediate direct lysis of susceptible target cells by releasing cytotoxic granules containing perforin and granzymes or by expressing ligands for apoptosis-inducing receptors on the target cell, such as Fas ligand (FasL)[3] and TNF-related apoptosis-inducing ligand (1–3). In addition, NK cells secrete cytokines, such as IFN-γ and TNF-α, during infection and inflammation (4). These cytokines are important for tumor and viral clearance, as well as lymphocyte recruitment and differentiation.

The physiological functions of NK cells are regulated by a balance of signals transmitted through activating receptors and inhibitory receptors (5, 6). A group of inhibitory receptors recognize MHC class I molecules on normal cells and dominantly suppress NK cell activation (7, 8). These MHC class I-binding inhibitory receptors contain at least one conserved immunoreceptor tyrosine-based inhibitory motif (ITIM) in their intracytoplasmic domain. In contrast, most NK cell-activating receptors are characterized by the presence of a basic amino acid in the transmembrane domain and the lack of an ITIM in the intracytoplasmic domain (9). The basic transmembrane residue associates noncovalently with acidic transmembrane residues in distinct signaling accessory proteins, named DAP10, DAP12, FcεRIγ, and TCRζ, which contain immunoreceptor tyrosine-based activation motifs or YxxM motifs in their cytoplasmic domains. KIRs constitute a family of polymorphic receptors with members that are activating or inhibitory (10). The activating forms possess a transmembrane lysine, exhibit short cytoplasmic domains that lack ITIMs, and are associated with DAP12, whereas inhibitory forms have long cytoplasmic domains with two ITIMs, lack a basic transmembrane residue, and lack DAP12 association.

KIR2DL4 (2DL4; CD158d) is the only member of the KIR family reportedly expressed in every NK cell clone analyzed from humans, as assessed by mRNA expression (11, 12), and has been identified in several lower primates (13–16). This broad expression profile and evolutionary conservation strongly implies that the receptor serves a critical role in the biological function of NK cells. Because a 2DL4-specific mAb has only recently been described (17), however, the surface expression and function of 2DL4 protein has not been fully clarified. Interestingly, 2DL4 is structurally unique among KIRs, because it exhibits elements of both inhibitory and activating NK cell receptors: 1) the cytoplasmic domain possesses a single ITIM and 2) the transmembrane domain contains a basic arginine residue (18). In accordance with this, both inhibitory and activating functional properties have been described for 2DL4 (17, 19, 20). The cytoplasmic domain of 2DL4, containing the single ITIM, can exhibit strong Src homology 2-containing

protein tyrosine phosphatase (SHP)-1-independent inhibitory function in isolation, when fused to the extracellular and transmembrane domains of KIR3DL1 (19) or when the 2DL4 transmembrane arginine residue is mutated (20). On the other hand, engagement of full-length 2DL4 has also been shown to trigger activating function with the unique capacity to induce IFN-γ production, but not cytotoxicity in resting NK cells (17). This is distinct among most NK cell-activating receptors, which usually trigger both functional responses.

The extracellular domain of 2DL4 exhibits both D0 and D2 Ig-like domains, which classifies the receptor as a type II KIR, along with KIR2DL5 (21). 2DL4 does not recognize classical MHC class I molecules, but instead two groups have reported that it binds to the nonclassical HLA-G (22–24). HLA-G is normally expressed only on fetal-derived trophoblast cells that invade the maternal decidua and appear to create a barrier for maternal NK cell attack of the HLA-mismatched fetus (25–27). An attractive hypothesis has been proposed suggesting that the engagement of 2DL4 by HLA-G might stimulate IFN-γ secretion but not cytotoxicity by uterine NK cells to support normal pregnancy and prevent fetal attack (24). In support of this hypothesis, NK cells are the predominant uterine lymphocyte population in pregnant women, and studies in mice by Croy and colleagues (28, 29) have shown that both NK cells and IFN-γ are essential for promoting optimal placental vascularity and development.

In this study, we utilized retroviral transduction to express N-terminal FLAG-tagged versions of 2DL4 in the NK-92 cell line. This allowed us to analyze the surface expression of 2DL4, as well as its function. To determine the role of the ITIM in the full-length receptor, three 2DL4 clones were analyzed: one that contains the cytoplasmic ITIM in frame (2DL4.1), and two others that contain cytoplasmic frame shifts resulting in truncated cytoplasmic domains that lack the ITIM (2DL4.2 and 2DL4*). We report the lack of surface expression of the product of a widely prevalent truncated receptor genotype (2DL4.2). In addition, the surface expression of 2DL4 on NK-92 cells and primary NK cells is shown to be up-regulated by IL-2. We further provide evidence that 2DL4 is indeed an activating receptor that strongly stimulates IFN-γ production and the up-regulation of cell surface activation markers. Interestingly, direct comparison between 2DL4 and NKp44 revealed significant differences in their activating capacities, with 2DL4 stimulating stronger IFN-γ production, but weaker redirected cytotoxicity. Importantly, the same activation potential was observed for 2DL4 isoforms that possess or lack the cytoplasmic ITIM, indicating that the ITIM does not influence activating function. Finally, engagement of 2DL4 can up-regulate FasL to trigger apoptosis of appropriate target cells.

Materials and Methods
Cells and culture

The IL-2-dependent NK-like cell line, NK-92 (a gift from Dr. C. Lutz, University of Iowa, Iowa City, IA), was maintained as previously described (19). NK-92 cells were passed with fresh IL-2-containing medium every 4 days. The murine mastocytoma, P815, was cultured as previously described (19). Jurkat T cells were cultured in RPMI 1640 medium (Life Technologies, Rockville, MD) containing 10% FBS (HyClone Laboratories, Logan, UT), 2 mM L-glutamine, 100 μg/ml penicillin, 100 μg/ml streptomycin, 10 mM HEPES (pH 7.4), 1 mM sodium pyruvate (all supplements from Life Technologies), and 50 μM 2-ME (Fisher, Pittsburgh, PA). The amphotropic retroviral packaging line, Phoenix-Ampho, was provided by Dr. G. Nolan (Stanford University, Stanford, CA). Phoenix-Ampho cells were cultured in DMEM medium (containing 10% FBS, 2 mM L-glutamine, 100 μg/ml penicillin, 100 μg/ml streptomycin, 50 μM 2-ME, and 10 mM HEPES) and passed before reaching confluence. NK3.3 cells were kindly provided by Dr. J. Kornbluth (St. Louis University School of Medicine, St. Louis, MO) and grown as previously described (19). For

analysis of primary NK cells, blood samples were obtained from volunteer adult donors that were recruited by written informed consent under procedures approved by our Institutional Review Board. PBMC were isolated with Ficoll-Hypaque (Amersham Biosciences, Uppsala, Sweden) and cultured in RPMI 1640 medium containing 5% autologous serum or human AB serum (ICN Biomedicals, Aurora, OH), nonessential amino acids, 2 mM L-glutamine, 100 μg/ml penicillin, 100 μg/ml streptomycin, 1 mM sodium pyruvate, 50 μM 2-ME, and 500 U/ml recombinant human IL-2 (Roche, Basel, Switzerland; generously provided by the Biological Resources Branch, National Cancer Institute, Frederick, MD). Primary cells were split with fresh IL-2 every 3 days, beginning on day 1 after initiation. All cell culture was performed at 37°C in humidified 7% CO_2 atmosphere.

Antibodies

The anti-FLAG mAb, M2, was purchased from Sigma-Aldrich (St. Louis, MO). PE-conjugated anti-CD69 mAb, biotin-conjugated anti-human FasL mAb (NOK1), and PE-conjugated anti-CD25 mAb were purchased from BD PharMingen (San Diego, CA). For intracellular staining, permeabilized cells were incubated with PE-conjugated anti-human IFN-γ mAb (B27) or an isotype control, PE-conjugated mouse IgG1 (Caltag Laboratories, Burlingame, CA). PE-conjugated goat anti-mouse κ (Southern Biotechnology Associates, Birmingham, AL) and PE-conjugated streptavidin (BD PharMingen) were used as secondary reagents. Protein G-purified anti-CD56 mAb, B159.5.2, and anti-NKp44 mAb, 3.43.13 (both mouse IgG1 isotypes) were prepared from the hybridomas, which were kindly provided by Dr. B. Perussia (Thomas Jefferson University, Philadelphia, PA) and Dr. M. Colonna (Washington University, St. Louis, MO), respectively. Anti-KIR2DL4 mAb (64, mouse IgM isotype) (17) was kindly provided by Dr. E. Long (National Institutes of Health, Rockville, MD). For the detection of 2DL4 on primary PBMC, cells were sequentially stained with anti-2DL4 (1 μl ascites/50 μl), biotinylated rat anti-mouse IgM (b-7-6, produced in our laboratory), and PerCP-conjugated streptavidin (BD PharMingen). For identification of the NK cell population (CD3⁻CD56⁺), PBMC were subsequently stained with FITC-conjugated anti-CD3 mAb (Immunotech, Marseilles, France) and PE-conjugated anti-CD56 mAb (Immunotech). All stained cells were analyzed on a FACScan (BD Biosciences, Mountain View, CA).

cDNA constructs

Total mRNA was extracted from NK3.3 cells with RNAzol reagent (Tel-Test, Friendswood, TX). The following gene specific primer sequences for KIR2DL4 were used to generate full-length cDNA from immediately after the leader by RT-PCR (C.therm. polymerase for RT-PCR; Boehringer Mannheim, Mannheim, Germany): forward primer containing EcoRI site 5'-TAGCTGAATTCACACGTGGGTGGTCAGGA-3' and reverse primer containing XhoI site 5'-TACGACTCGAGTGCTCTAAGATGGAGACT CAC-3'. RT-PCR products were subsequently amplified by PCR using the Pfx polymerase (Invitrogen). Three PCR products, subcloned from pBluescript, were named 2DL4.1 (corresponding to GenBank accession AF034772 containing a string of 11A at the beginning of the region encoding the cytoplasmic domain), 2DL4.2 (corresponding to GenBank accession BC028137 containing 10A) and 2DL4* (not found in GenBank, but 12A at the same location). The cDNAs were subcloned into the pFLAG-CMV3 vector (Sigma-Aldrich) to introduce a leader and N-terminal FLAG epitope tag (DYKDDDK) before the start of the mature polypeptide receptor (see Fig. 1A). NKp44 cDNA was cloned with the FLAG epitope sequence inserted between the endogenous leader and the mature polypeptide (see Fig. 1, A and B) as will be detailed elsewhere.[4] All four constructs containing leader and FLAG tag sequence were ligated into the bicistronic retroviral expression vector, pBMN-IRES-EGFP (generously provided by Dr. G. Nolan, Stanford University), to produce recombinant retrovirus for generation of NK cell lines with stably integrated cDNA. Cells transduced with this retroviral system coordinately express the introduced cDNA and enhanced green fluorescent protein (EGFP). Integrity of all constructs was confirmed by sequencing in the Fox Chase Cancer Center Automated DNA Sequencing Facility (Perkin-Elmer Applied Biosystems, Shelton, CT).
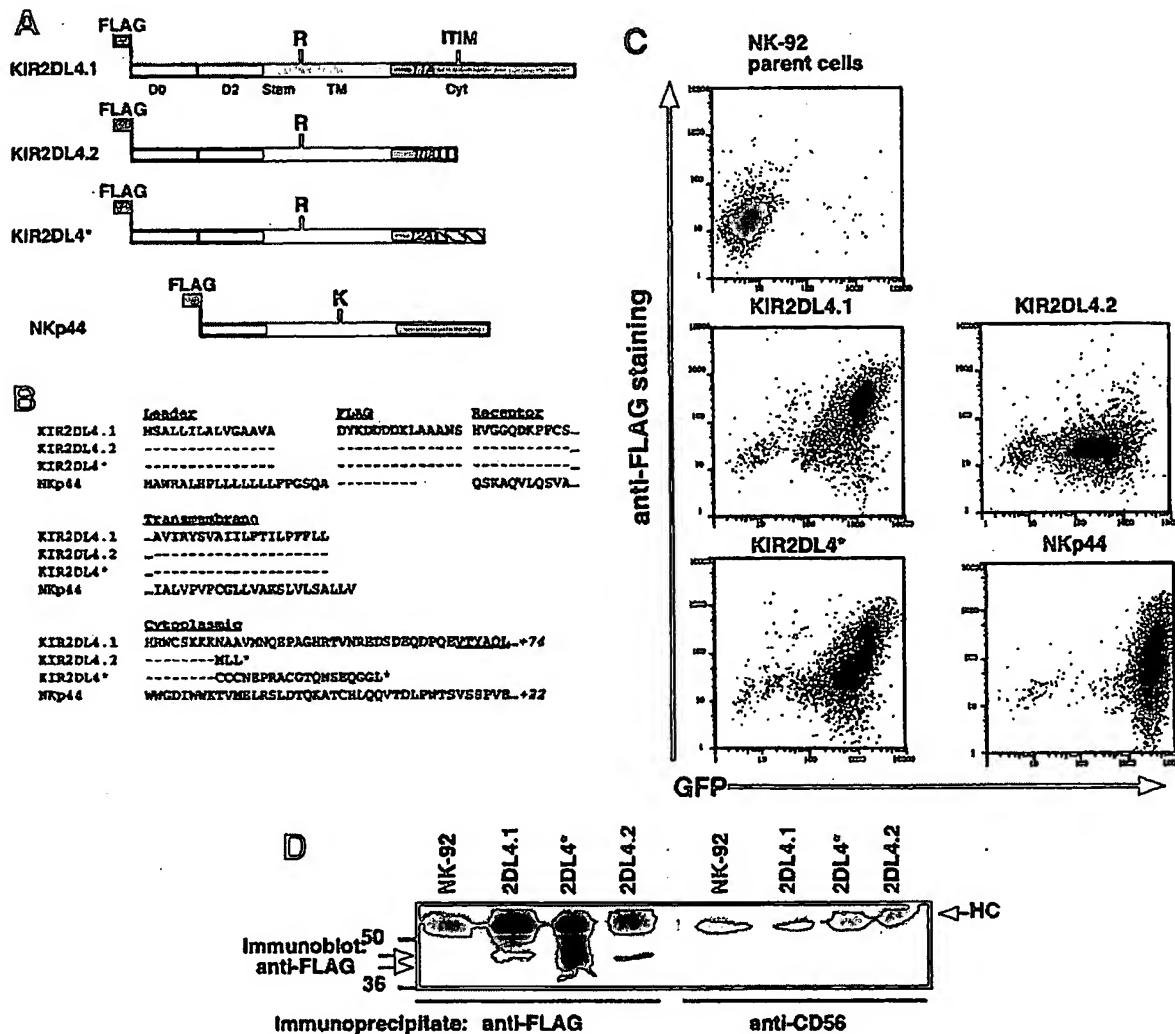
FIGURE 1. Protein structure and expression of FLAG-tagged 2DL4.1, 2DL4.2, 2DL4* and NKp44. *A*, Schematic representations of the protein products from the receptor cDNA constructs that were generated. D0 and D2 are highly conserved Ig-like domains in the KIR family, and transmembrane (TM) and cytoplasmic (Cyt) domains are shown. Hatched portions of cytoplasmic domains represent alternative cytoplasmic sequences that result from frame shifts. Each construct carried FLAG-epitope tags (at the N terminus) for detection and stimulation. *B*, Amino acid sequence of the amino terminal, transmembrane, and cytoplasmic domains of receptor constructs. Dashes represent identity and dots represent either intervening sequence or sequence that continues for 74 or 22 amino acids for 2DL4.1 and NKp44, respectively. An asterisk signifies a termination codon. Underlined sequence represents the position of the ITIM. The sequences of 2DL4.1, 2DL4.2, and NKp44 are representative of the GenBank accession numbers AF034772, BC028137, and AJ225109, respectively. The cDNA sequence of 2DL4.1 has a string of 11 adenines (11A) at the point of the cytoplasmic frame shift, whereas 2DL4.2 and 2DL4* have 10A and 12A, respectively. *C*, The surface expression of 2DL4.2 was not detected on NK-92 cells. The cDNAs encoding FLAG-tagged receptors were transduced into NK-92 cells with recombinant retrovirus. Parent cells and EGFP⁺ transduced cells were stained with anti-FLAG mAb in combination with PE-conjugated goat anti-mouse κ secondary reagent and analyzed by flow cytometry. Results are representative of numerous separate retroviral transduction experiments. *D*, 2DL4.2 protein was expressed in NK-92 cells. NK-92 cells and receptor-transduced NK-92 cells were lysed with 1% n-dodecyl β-D-maltoside and sequential immunoprecipitates were prepared with anti-CD56 and then anti-FLAG mAbs. Each lane represents immunoprecipitation from a lysate of 40 million cells. Samples were separated on 10% SDS-PAGE gels under reducing condition, and immunoblot analysis was performed with anti-FLAG mAb.

Retroviral transduction of NK-92 cells

Phoenix-Ampho cells were transfected with the pBMN vector containing one of the cDNA constructs using Lipofectamine Plus reagent (Life Technologies) as previously described (19). Supernatants (1 ml) of these transfectants grown for 2 days in serum-free Opti-MEM medium (Life Technologies) were collected, mixed with Lipofectamine Plus reagent, and added to 1–2 × 10⁶ NK-92 cells in a 24-well plate (3526, Corning, Corning NY), which was then centrifuged at 2000× g for 45 min at room temperature. After 5–7 days, EGFP-positive cells were sorted on a FACSVantage SE cell sorter (BD Biosciences) in the Fox Chase Cancer Center Cell Sorting Facility.

KIR2DL4 genotyping

Primers complementary to the 5' end of exon 6 of the KIR2DL4 gene (sense; 5'-CCA GAC ACC TGC ATG CTG-3') and the middle of intron 6 (antisense; 5'-TCC CTG TTC ACT GTT CTG TGT-3') were designed to amplify a 600-bp genomic product. Genomic DNA was prepared from IL-2 cultured PBMC from each donor with phenol/chloroform and ethanol precipitation. PCR mixtures contained 20 pmol of each primer, 40 nM MgCl₂, 4 nmol dNTP mix, 0.5 U AmpliTaq, 10× PCR buffer (all from Invitrogen) and 50–100 ng genomic DNA in a final reaction volume of 20 μl. The following thermal cycler conditions were used: 1 cycle of 3 min at 94°C, 35 cycles of 30 s at 94°C/30 s at 55°C/30 s at 68°C, and 1 cycle of 3 min

3418

POTENT IFN-γ PRODUCTION BY KIR2DL4

at 68°C. PCR products were purified directly with the Wizard PCR Preps DNA Purification System (Promega, Madison, WI) or from an agarose gel using a Gel Extraction kit (Qiagen, Valencia, CA). Products were directly sequenced in both directions using the sense primer (same as previously described, from exon 6) or a nested antisense primer (5'-TTG GGC CAG AGA CTT TCC TG-3') with the BigDye Terminator v3.1 Cycle Sequencing kit (Applied Biosystems, Foster City, CA) and analyzed on an ABI PRISM Model 377 DNA Sequencer in the Fox Chase Cancer Center DNA Sequencing Facility. Because polymerase slippage is common across long sequence repeats, especially poly(A) (30, 31), these events always accounted for minor peaks in our sequencing reactions after the poly(A) tract. Therefore, sequencing reactions were performed in both sense and antisense directions from at least three separate PCR to assure that the patterns were consistent and representative of the corresponding genomic DNA sequence.

Immunoprecipitation and immunoblotting

Parent NK-92 cells and 2DL4.1-, 2DL4.2-, and 2DL4*-transduced NK-92 cells (40 million/sample) were washed three times in HBSS (Life Technologies), and lysed for 30 min on ice in 1 ml/sample of lysis buffer, containing 1% n-dodecyl β-D-maltoside (ULTROL Grade; Calbiochem, La Jolla, CA), 150 mM NaCl (Fisher), 10 mM Tris-HCl (pH 7.5) (Fisher), 2 mM Na₃VO₄ (from 100X stock boiled 5 min before addition), 0.4 mM EDTA (Fisher), 10 mM sodium fluoride (Sigma-Aldrich), 1 mM Pefabloc (Roche, Indianapolis, IN), and 1 μg/ml each of leupeptin, aprotinin, and soybean trypsin inhibitor (Sigma-Aldrich). Lysates were cleared of nuclear/cytoskeletal components by centrifugation at 20,800 × g for 15 min at 4°C. Lysates were sequentially immunoprecipitated for 90 min at 4°C with anti-CD56 mAb (B159.5.2) and anti-FLAG mAb (2 μg/sample precoupled to 30 μl protein G-agarose). All immunoprecipitates were washed five times with ice-cold 0.2% n-dodecyl β-D-maltoside buffer (same components as lysis buffer) and resuspended in Laemmli reducing sample buffer (10% DTT). Immunoprecipitated samples were boiled for 3 min before separation on discontinuous 10% SDS-PAGE. Proteins were electrophoretically transferred to Immuno-Blot polyvinylidene difluoride membrane (Bio-Rad, Hercules, CA) and blocked with 5% skim milk (ACME, Salt Lake City, UT) in TBST buffer (10 mM Tris-HCl (pH 7.5), 150 mM NaCl, 0.05% Tween 20). Blocked membranes were probed initially with mouse anti-FLAG mAb (2 μg/ml) and secondarily with HRP-coupled donkey anti-mouse IgG (Jackson ImmunoResearch Laboratories, West Grove, PA). Immunoblotted proteins were visualized by chemiluminescence using the ECL detection reagents (Amersham, Arlington Heights, IL).

Cell stimulation with plate-bound Ab

Purified mAb (10 μg/ml in 0.1 M sodium carbonate/bicarbonate buffer, pH 9.5) was added at 50 μl/well to flat-bottom 96-well plates (PRO-BIND; BD Biosciences) or 500 μl/well to 24-well plates (3526, Corning). The plates were sealed with parafilm and incubated for 3 h at 37°C. Before use, the plates were washed twice with culture medium. 1–3 × 10⁵ cells/well were added to 96 flat-well plates or 5 × 10⁵ cells/well to 24-well plates, and plates were incubated at 37°C in a 7% CO₂ incubator.

Redirected cytotoxicity assay

NK-92 cells were tested for redirected cytotoxicity against the FcγRII/III⁺ P815 murine mastocytoma cell line in a 3–4 h ⁵¹Cr release assay in 200 μl medium/well. The P815 target cells (2 × 10⁶ cells) were labeled with 100 μCi ⁵¹Cr (5 mCi/ml, stock product 2030B; NEN, Boston, MA) for 60–90 min and incubated with effector cells in V-bottom 96-well plates (Costar, Cambridge, MA). Spontaneous release and maximal release of ⁵¹Cr were determined by incubating in medium alone or 1% Triton X-100, respectively. The percentage of specific lysis was determined as follows: [(mean cpm experimental release − mean cpm spontaneous release)/(mean cpm maximal release − mean cpm spontaneous release)] × 100. To engage specific receptors in the redirected assay, mAb (1 μg/ml) were mixed with P815 cells for 5 min before effector cell addition.

Intracellular staining for IFN-γ

NK-92 cells (5 × 10⁵/well: 24-well plate, 2 × 10⁵/well: 96-flat plate) were cultured with plate-bound anti-FLAG mAb or phorbol ester (PMA, 8 ng/ml) + Ca²⁺ ionophore (A23187, 0.1 μg/ml) for 3 or 6 h (entire period or last 4 h in the presence of brefeldin A (10 μg/ml; Sigma-Aldrich), respectively). After the incubation, the cells were fixed with 4% paraformaldehyde (Fisher), permeabilized with 0.1% saponin-containing PBS, stained with PE-conjugated anti-IFN-γ mAb or IgG1 control mAb, and analyzed on a FACScan.

ELISA for IFN-γ

NK-92 cells (2 × 10⁵ cells/well: 96 flat-well plate) were stimulated with plate-bound mAbs for 20 h, and IFN-γ release was measured in the supernatant by ELISA kit according to the manufacturer's instructions (BD PharMingen).

Fas-mediated DNA fragmentation assay

Target cell DNA fragmentation was measured using a modification of the JAM assay (32, 33). NK-92 cells were pelleted onto plate-bound mAb and incubated for 4 h. Jurkat T cells were separately labeled for 4 h with [³H]thymidine (1.0 mCi/ml; NEN) at a final concentration of 5 μCi/ml (5 × 10⁵ cells/ml). Just before the assay, Jurkat cells were gently pelleted and washed once with prewarmed medium. [³H]Thymidine labeled Jurkat T cells (1 × 10⁵ cells/well) were then pelleted with stimulated effector cells for 2 h in the presence or absence of EGTA/MgCl₂ (added to medium at 5 mM and 10 mM final concentrations, respectively) and DNA was harvested onto glass fiber filters (Packard Instrument, Meriden, CT). In some experiments, anti-CD56 (2 μg/ml) or anti-FasL (1:10 dilution of biotin-conjugated) mAbs were added to effector cells 30 min before addition of target cells. ³H retained on the filter (intact DNA) was assayed by scintillation counting (Top Count NXT; Packard Instruments) and percentage of specific DNA fragmentation was calculated using the following formula: percentage of DNA degradation = [(the total cpm in the Jurkat T cells alone − the number of cpm after incubation with NK-92 cells)/the total cpm in the Jurkat T cells alone] × 100. Statistical analysis by the Student t test was performed using the Excel X program for Mac (Microsoft, Redmond, WA).

Results

Expression of KIR2DL4 in the NK-92 cell line

To study 2DL4 in the absence of specific mAbs, we engineered N-terminal FLAG epitope-tagged forms of the receptor. We used RT-PCR to clone three versions of 2DL4 cDNAs from RNA derived from the human NK-like cell line NK3.3. We named the cDNAs 2DL4.1, 2DL4.2, and 2DL4* in the following study. These cDNAs encode proteins that differ substantially within the intracytoplasmic regions following lysine-246 (K246) (Fig. 1, A and B), due to frame shifts derived from variations in the number of a consecutive string of adenines in the cDNA, ranging from 10A to 12A. Several groups have previously reported cDNAs containing 10A or 11A sequences (34–36), and these are derived from distinct 2DL4 alleles that differ in the extreme 3' end of exon 6 (9A or 10A from exon 6 and an additional adenine from exon 7), for which multiple genomic sequences have been reported (9A exon 6, GenBank accession AC011501 and AF0031211; 10A exon 6, AL133414 and AF110035). The "conventional" allele of the 2DL4 cDNA, which we have named 2DL4.1 (11A, GenBank accession AF034772), encodes a protein with a cytoplasmic domain containing 115 amino acids, including a single ITIM. Another cDNA, which represents the widely reported alternative allele (10A, GenBank accession BC028137), encodes a short cytoplasmic domain containing only 11 amino acids and was named 2DL4.2. The profound intracytoplasmic difference and lack of the ITIM sequence suggest that the allele corresponding to 2DL4.2 exhibits alternative function. We also cloned a third cDNA named 2DL4* that contains a 12A sequence to encode 27 intracytoplasmic amino acids. Genomic or cDNA sequences corresponding to the 2DL4* cDNA have not previously been reported in GenBank. We cannot rule out that 2DL4* may have resulted from polymerase slippage during PCR, but it offered the capability to test a receptor with an alternative cytoplasmic domain, lacking the ITIM. In addition, we engineered a FLAG-tagged version of the NKp44 receptor (Fig. 1, A and B), which is an activating receptor that associates with DAP12 (37), and therefore, serves as a representative immunoreceptor tyrosine-based activation motif-coupled receptor for functional comparison with 2DL4.1.

We expressed the FLAG-tagged versions of 2DL4.1, 2DL4.2, 2DL4*, and NKp44 in the IL-2-dependent NK-like cell line, NK-92, using retroviral transduction with a bicistronic recombinant retrovirus that coordinately expresses both the cloned cDNA

and EGFP, as previously described (19). EGFP-positive transduced cells were sorted and stained for receptor surface expression with anti-FLAG mAb. As shown in Fig. 1C, 2DL4.1, 2DL4*, and NKp44 were expressed on the surface of NK-92 cells in parallel with EGFP expression. Surprisingly, however, 2DL4.2 was not detected on the cell surface (Fig. 1C), despite the presence of significant intracellular protein (Fig. 1D). This result suggests that the highly prevalent human allele corresponding to 2DL4.2 (34, 35) encodes a protein that is retained inside NK cells and is incapable of reaching the cell surface. Therefore, we used NK-92 cells transduced with either 2DL4.1, 2DL4*, or NKp44 for comparative functional analysis of these three receptors.

Regulation of KIR2DL4 surface expression on transduced NK-92 cells by IL-2

In contrast to our previous studies with the inhibitory receptor, KIR3DL1 (19), we noted that the surface expression of both 2DL4.1 and 2DL4* varied on transduced NK-92 cells. Therefore, we used anti-FLAG mAb staining to assess the surface expression levels of both forms of the receptors at various time intervals (day 1, 2, 3, and 4) after passing the cells into fresh IL-2 containing medium. This analysis revealed that the expression of both 2DL4.1 and 2DL4* on transduced NK-92 cells was dependent upon IL-2 stimulation, with the highest expression being detected on days 1 and 2 following the IL-2 stimulation (activated cells) and progressive decline on days 3 and 4 (resting cells, see Fig. 2). Restimulation with fresh IL-2-containing medium on day 4 always restored
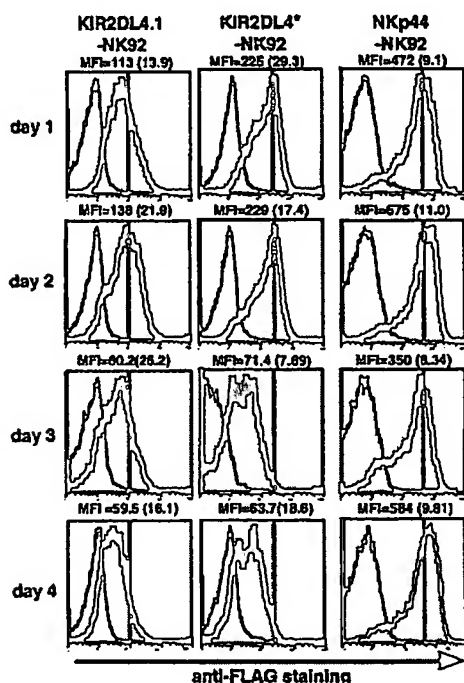
FIGURE 2. IL-2 dependent expression of 2DL4.1 and 2DL4* on NK-92 cells. Receptor-transduced NK-92 cells were stained with anti-FLAG mAb (thin histogram) or control mAb (thick histogram) in combination with PE-conjugated goat anti-mouse κ secondary reagent on various days of culture. On day 0, cells were passed into fresh IL-2-containing medium. The histograms represent staining profiles performed on the same day from independent cultures with staggered initiation days. MFI values of anti-FLAG staining and control secondary alone staining (in parentheses) are shown atop each panel. The results are representative of three time course experiments.

the expression of 2DL4.1 and 2DL4* to the maximal levels, but never resulted in the up-regulation of 2DL4.2 surface expression (data not shown). The expression of 2DL4.1 and 2DL4* on transduced cells was completely lost when cultured with a low dose of IL-2 in the medium or if cultures were extended for 5 days (data not shown). In contrast, the expression of FLAG-NKp44 was nearly unchanged in response to fresh IL-2 in the medium (Fig. 2). Similarly, CD56 expression levels were virtually unchanged on 2DL4.1 and 2DL4* transduced NK-92 cells during the same time course (data not shown). Therefore, IL-2 dependent 2DL4.1 and 2DL4* expression in NK-92 cells seems to be a unique property of these receptors. Furthermore, although driven from the same long-terminal repeat promoter of the retroviral vector, the expression level of EGFP in the transduced cells remained unchanged for the interval (data not shown), indicating that the IL-2 dependent surface expression of 2DL4.1 and 2DL4* on NK-92 cells is regulated post transcriptionally. In addition, the same expression pattern was observed for 2DL4.1 and 2DL4*, indicating that the regulation of expression is independent of the majority of the cytoplasmic domain and may alternatively be regulated through an associated accessory protein.

Up-regulation of KIR2DL4 by IL-2 on primary NK cells from only some donors

Next we tested whether surface expression of 2DL4 is also up-regulated by IL-2 on primary NK cells. PBMCs were isolated from six separate donors, cultured in IL-2, and stained every three days with anti-CD3 mAb, anti-CD56 mAb, and a recently described anti-2DL4-specific mAb that was kindly provided by Dr. Eric Long (17). When freshly isolated PBMCs were analyzed, they exhibited the typical pattern of a major $CD3^-CD56^+$ NK cell fraction and a minor $CD3^-CD56^{high}$ fraction (Fig. 3). Interestingly, only two of three donors (donors 3A and 3D) clearly expressed 2DL4 on freshly isolated NK cells, and expression was predominantly restricted to the $CD56^{high}$ fraction (Fig. 3). After culture in IL-2 for 12 days, CD56 levels progressively increased in the entire NK cell population and three distinct 2DL4 staining profiles were observed within the NK cell fraction: 1) the two donors that expressed 2DL4 on the freshly isolated $CD56^{high}$ fraction (donors 3A and 3D) expressed increased levels of 2DL4 on the entire NK cell fraction, 2) two donors that either initially lacked or marginally expressed 2DL4 (donors 3B and 2G, respectively) gradually expressed substantial levels of the receptor within three to six days of culture in IL-2, and 3) two donors (donors 3C and 3E) lacked the receptor on freshly isolated cells and only marginally expressed the receptor on some of the NK cell fraction after 12 days of culture in IL-2. Interestingly, subsequent analyses of donor 3D at 3 and 5 weeks later did not show 2DL4 expression on his freshly isolated $CD56^{high}$ NK cells, although expression was induced by culture in IL-2, indicating that expression may be influenced by certain environmental factors, possibly minor infections. We conclude from these results that 2DL4 is variably expressed on NK cells from different individuals, it is only found on the $CD56^{high}$ NK cell fraction when expressed, cell surface levels of the receptor can be up-regulated by IL-2, and some individuals only have marginal capacity to express the receptor on NK cells after 12 days of culture in IL-2. These primary NK cell results correlate directly with our observations in NK-92 cells transduced with 2DL4.1 or 2DL4.2.

Correlations between KIR2DL4 genotype and receptor surface expression

We next tested whether the lack of 2DL4 surface expression on primary NK cells from donors 3C and 3E corresponds to a KIR2DL4.2 homozygous genotype and the expression of 2DL4 in the other donors corresponds to a KIR2DL4.1 genotype. For this
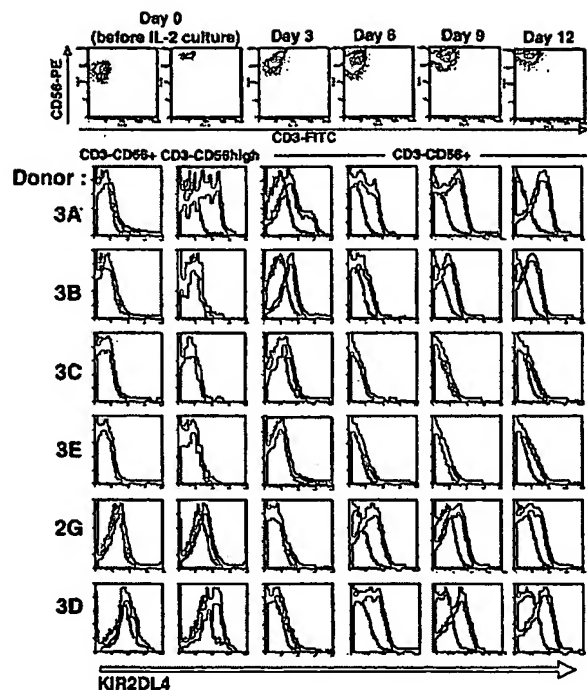
FIGURE 3. Analysis of KIR2DL4 expression on resting and IL-2 cultured primary NK cells. PBMCs were isolated from six healthy human donors (3A, 3B, 3C, 3D, 3E, and 2G) and cultured for 12 days with IL-2 as described in *Materials and Methods*. Cells were simultaneously stained with PE-conjugated anti-CD56, FITC-conjugated anti-CD3, and PerCP-conjugated anti-2DL4 mAb (64). Histograms of 2DL4 staining are shown for lymphocytes gated for the CD3⁻CD56⁺ fraction and the CD3⁻CD56ʰⁱᵍʰ fraction (freshly isolated cells on day 0) or the entire CD3⁻CD56⁺ fraction (days 3–12). CD3/CD56 staining profiles of the gated populations from a representative culture are shown in the *top panels* for each day of analysis. Gray lined histograms represent secondary alone staining (biotinylated anti-IgM + PerCP-Streptavidin) and dark line histograms indicate anti-2DL4 staining (with the same secondary reagents). Cells were split and supplemented with fresh IL-2 on days 0, 1, 4, 7, and 10. The different 2DL4 expression patterns did not correlate with specific age, gender, or race of the donors.

FIGURE 4. Genotype analysis of KIR2DL4 from donors analyzed in Fig. 3. The genomic sequences at the 3' end of exon 6 were amplified from PBMC of six donors (3A, 3B, 3C, 3D, 3E, and 2G) by PCR and sequenced to determine 2DL4 genotypes. Sequences with 10A and no subsequent frame displacement are characteristic of a homozygous 2DL4.1 genotype (3A, 3B, 3C, and 3D), 9A sequences with no subsequent displacement indicates a 2DL4.2 homozygous genotype (3E), and 9A sequences followed by frame displacement indicates a heterozygous genotype (2G). The sequence results in this region were also confirmed using an antisense sequencing primer and sequencing from at least three genomic PCR that were generated from the PBMC of each donor. The 2DL4 expression profile for these donors from the data in Fig. 3 is indicated on the *right*.

analysis, genomic DNA was prepared from each donor's NK cells and used as a template for PCR to synthesize a ~600 bp sequence spanning from exon 6 through intron 6 that encompasses the poly(A) tract at the 3' end of exon 6. These PCR products were sequenced in both directions and the sense sequencing reactions are shown in Fig. 4. Because one adenine in the transcribed mRNA is derived from the beginning of exon 7, a 10A genomic sequence in this region of exon 6 is characteristic of 2DL4.1 and a 9A genomic sequence corresponds to 2DL4.2. A distinct frame disruption in the sequence after 9A is characteristic of heterozygosity. Importantly, all donors that expressed 2DL4 on their NK cells were either homozygous for 2DL4.1 (10A, donors 3A, 3B, and 3D) or heterozygous for 2DL4.1 and 2DL4.2 (9A/10A, donor 2G). Further, the only donor that was homozygous for 2DL4.2 (9A, donor 3E) was incapable of expressing the receptor on NK cells. These results were consistent with our cDNA expression studies in NK-92 cells. Surprisingly, however, the other donor that did not express surface receptor was homozygous for 2DL4.1 (10A, donor 3C). We confirmed this phenotype and genotype in IL-2-stimulated NK cells prepared from a separate blood sample that was derived from donor 3C. Taken together, our results indicate that 2DL4.2 homozygous humans are incapable of expressing 2DL4,

although the presence of at least one allele of 2DL4.1 generally produces a receptor that can reach the NK cell surface. The results from donor 3C, however, clearly demonstrate that alternative mechanisms must be responsible for a lack of 2DL4 surface expression in some individuals.

KIR2DL4 exhibits unique activating function compared with NKp44

We next tested the biological impacts of 2DL4 engagement on receptor-transduced NK-92 cells. Our initial functional experiments were designed to test whether the transmembrane region of 2DL4, which contains an arginine, can link the receptor to activation signaling in NK-92 cells. To test the transmembrane region

independently of the cytoplasmic ITIM sequence, we first compared functional capacities of the frame-shifted FLAG-2DL4*, which lacks the ITIM, with the FLAG-NKp44 in distinct transduced NK-92 cell populations. These cell lines allowed us to manipulate the receptors under identical conditions with the common triggering reagent, anti-FLAG mAb. For consistency and to avoid nonspecific activation effects in our functional studies, we always tested the transduced NK-92 cells on day 3 after IL-2, which we refer to as "resting" NK cells.

To directly compare the stimulation capacities of 2DL4* and NKp44, we engaged the receptors on resting NK-92 cells with anti-FLAG mAb to test for Ab redirected cytotoxicity toward the FcγR$^+$ P815 target cells (Fig. 5A). Interestingly, NKp44 engagement stimulated strong target cell lysis, whereas only weak cell lysis was detected upon engagement of 2DL4* on NK-92 cells, despite similar levels of receptor expression as assessed by anti-FLAG staining (Fig. 5A). Furthermore, when triggered with an anti-NKp44 mAb, the same levels of cytotoxicity were observed for both receptor-transduced cell populations (data not shown). These observations demonstrate a significant difference in the cytolytic capacities triggered by NKp44 and 2DL4.

Next we assessed IFN-γ production by resting NK-92 cells after cross-linking the receptors with plate-bound anti-FLAG mAb for 3 h to 20 h by intracellular staining (3 h and 6 h) and ELISA (20 h). Strong intracellular staining of IFN-γ was detected at early time points in 2DL4* transduced NK-92 cells after anti-FLAG mAb engagement, whereas significantly lower levels were detected after the same treatment in the NKp44 transduced NK-92 cells (Fig. 5, B and C). In fact, significantly increased levels of IFN-γ staining were detectable in 2DL4*-transduced NK-92 cells after only 3 h of stimulation. Consistently, about twice as much IFN-γ secretion was detected by ELISA at later time points (20 h) in supernatants from NK cells stimulated through 2DL4 than through NKp44 (Fig. 5C). Interestingly, engagement of 2DL4* stimulated significantly more potent IFN-γ production despite about 10-fold lower levels of receptor surface expression when compared with that of NKp44, as assessed by anti-FLAG mAb staining (Fig. 5C). In summary, our data showed rapid and robust IFN-γ secretion in response to engagement of 2DL4* on NK-92 cells, which significantly exceeded that stimulated by the same mAb through NKp44 over a wide time course, despite significantly higher surface expression of NKp44.

We further tested whether stimulation through 2DL4* or NKp44 induces expression of several cell surface activation markers in cell NK-92 cells. Cross-linking of 2DL4* and NKp44 on resting transduced cells with plate-bound anti-FLAG mAb for 18 h resulted in the up-regulation of the cell surface activation markers CD69 (an activating receptor), CD25 (the IL-2Rα chain), and FasL (data not shown). The degrees of up-regulation were similar for both receptors.

The intracytoplasmic ITIM sequence does not influence activating function of KIR2DL4

We next compared the activating capacities of 2DL4.1 and 2DL4* to determine the impact of the ITIM on activating function. When engaged with plate-bound anti-FLAG mAb, both receptors stimulated the up-regulation of all three activation markers, CD25, CD69, and FasL (data not shown). Importantly, both forms of 2DL4 (with or without the ITIM) increased activation markers to similar degrees, indicating that the ITIM does not influence activation through the full-length "conventional" receptor. In addition, there was no difference in IFN-γ production stimulated through 2DL4.1 or 2DL4* when assayed by intracellular staining (3 or 6 h; Fig. 6A) or ELISA (12, 15, or 18 h; Fig. 6B), again indicating that the inhibitory ITIM domain does not influence receptor activating
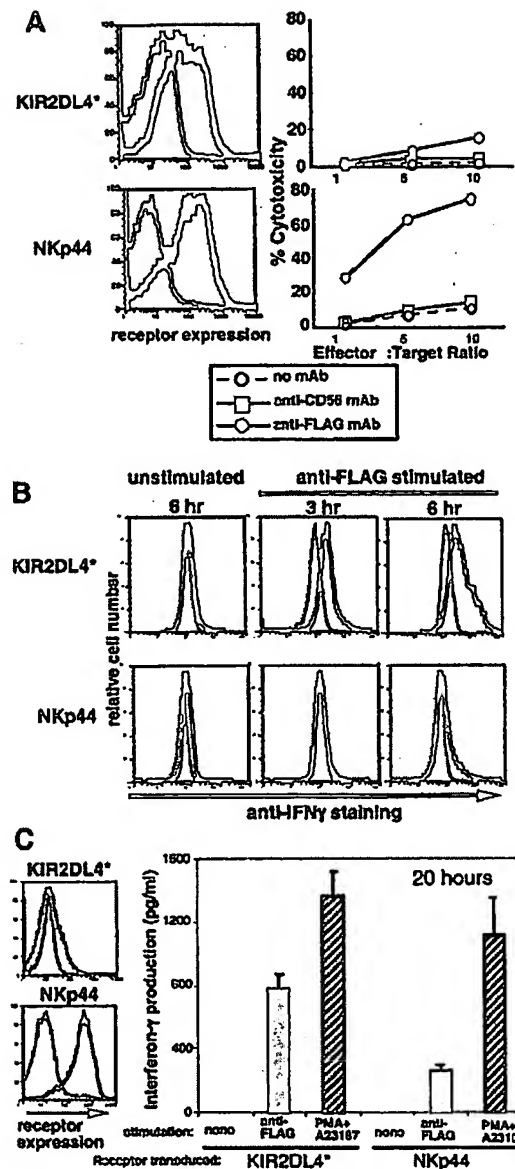

FIGURE 5. Differential activation capacity induced by the engagement of 2DL4* vs NKp44. A, Weak redirected cytotoxicity was induced by engagement of 2DL4*, but strong cytotoxicity was induced by NKp44 engagement. Resting transduced cells (day 3 after IL-2) were stained with anti-FLAG mAb (M2; dark lined histograms in left panels) and assayed for Ab-redirected cytotoxicity against ^{51}Cr-labeled FcγR$^+$ P815 target cells in the absence or presence of anti-CD56 mAb (B159, used as a negative control) or anti-FLAG mAb (M2) for 4 h (right panels). The results are representative of four experiments. B, IFN-γ production was routinely more robust through engagement of 2DL4* than through NKp44. Transduced cells were stimulated with or without plate-bound anti-FLAG mAb for 3 h or 6 h. After cell fixation and permeabilization, intracellular staining was performed with PE-anti-IFN-γ mAb (black histogram) or PE-mouse IgG1 (gray histogram; negative control). C, Late term IFN-γ production is more potent through 2DL4* despite lower cell surface receptor expression when compared with NKp44. FLAG-2DL4* and FLAG-NKp44 transduced NK-92 cells were stained with anti-FLAG mAb (black histogram) in combination with PE-conjugated goat anti-mouse κ secondary reagent or the secondary alone (gray histogram) on day 3 after IL-2. The same cells were stimulated with or without plate-bound anti-FLAG mAb or phorbol ester and calcium ionophore (PMA + A23187), culture supernatants were harvested after 20 h, and supernatants were analyzed by ELISA for IFN-γ concentration. The results are representative of three experiments.
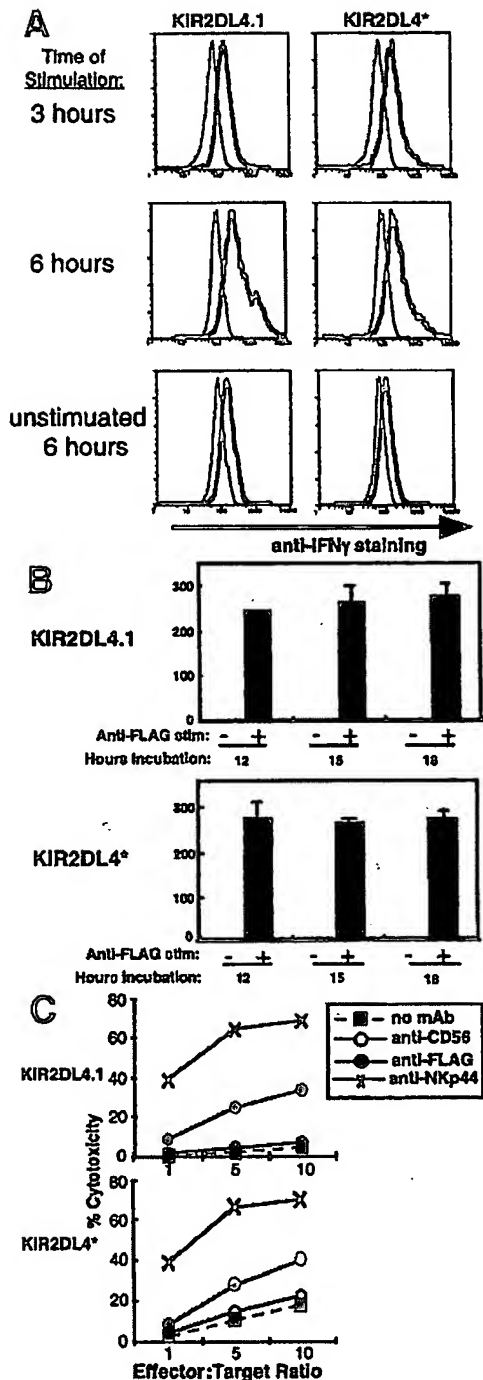
FIGURE 6. Similar activation capacities were observed for 2DL4.1 and 2DL4*. *A*, Comparable strong and rapid IFN-γ production through 2DL4.1 or 2DL4* engagement on resting NK-92 cells. Transduced NK-92 cells (day 3 after IL-2) were stimulated with or without plate-bound anti-FLAG mAb for 3 or 6 h. After cell fixation and permeabilization, intracellular staining was performed with PE-anti-IFN-γ mAb (thick line) or PE-mouse IgG1 (thin line, negative control). Results are representative of more than three experiments. *B*, Nearly identical induction of IFN-γ release by engagement of 2DL4.1 or 2DL4* in transduced NK-92 cells at several later time points. Transduced NK-92 cells (day 3 after IL-2) were engaged or not with plate-bound anti-FLAG mAb for 12, 15, or 18 h. Supernatants were harvested and assayed by ELISA for IFN-γ concentration. Error bars represent SD from the mean of three samples. Results are representative of
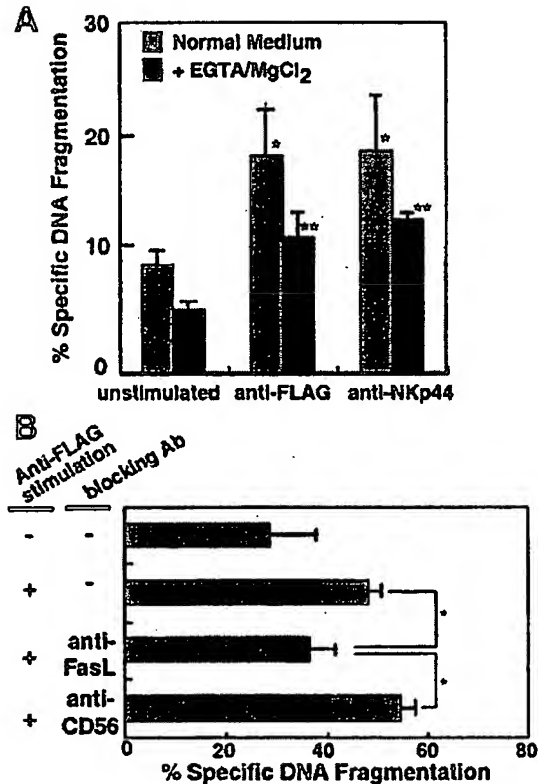
FIGURE 7. Cross-linking 2DL4.1 on NK-92 cells enhances DNA fragmentation of Fas⁺ Jurkat target cells in a FasL-dependent manner. *A*, 2DL4.1 and NKp44 transduced NK-92 cells were preincubated for 4 h with or without plate-bound anti-FLAG mAb. [³H]Thymidine-labeled Fas⁺ Jurkat cells were subsequently added for 2 h in the presence or absence of 2 mM EGTA/2.5 mM MgCl₂ (final concentration in medium) (E:T ratio = 1:1). [³H]Thymidine incorporation was then quantitated in harvested cells to determine percentage specific DNA fragmentation as in *Materials and Methods*. Student's *t* test was performed and bracketed bars with *normal medium or with **EGTA/MgCl₂ represent $p < 0.05$ compared with the corresponding unstimulated condition. *B*, 2DL4.1 transduced NK-92 cells were preincubated for 4 h with or without plate-bound anti-FLAG mAb and then pretreated with anti-FasL mAb (NOK1) or anti-CD56 mAb (as a negative control) for 30 min before the addition of [³H]thymidine-labeled Jurkat cells for 2 h (E:T ratio = 2:1). [³H]Thymidine incorporation was quantitated in harvested cells, and percentage-specific DNA fragmentation was calculated as described in *Materials and Methods*. Anti-FasL mAb and anti-CD56 mAb were present throughout the 2 h incubation. Student's *t* test was performed and bracketed bars marked with asterisk represent $p < 0.05$ compared with the anti-FasL mAb treated, stimulated condition.

function. Finally, neither form of 2DL4 exhibited substantial redirected cytotoxicity toward P815 target cells, particularly when compared with stimulating with anti-NKp44 mAb in the same NK-92 cell populations (Fig. 6*C*). Therefore, in several biological assays, we did not detect any substantial negative (or positive) influence on 2DL4.1 activating function that could be attributed to

more than three experiments. *C*, Comparatively weak redirected cytotoxicity was induced by Ab engagement of 2DL4.1 or 2DL4* on day 3 after IL-2 stimulation of NK-92 cells. Transduced cells (day 3 after IL-2) were assayed for mAb-redirected cytotoxicity against ⁵¹Cr-labeled FcγR⁺ P815 target cells in the absence or presence of anti-CD56 mAb (B159, negative control), anti-NKp44 mAb (3.43.13), or anti-FLAG mAb (M2) for 4 h. Results are representative of three experiments.

the cytoplasmic ITIM. These results indicate that signals from 2DL4.1 appear to be derived from an associated accessory protein and are not influenced by the ITIM or the majority of the receptor intracytoplasmic domain.

KIR2DL4 engagement can stimulate NK cells to trigger Fas-mediated DNA fragmentation in Jurkat cells

Because we observed the up-regulation of FasL in response to engaging 2DL4 on NK-92 cells, we tested whether stimulation of NK-92 cells through 2DL4.1 could promote Fas-mediated DNA fragmentation of Jurkat cell targets, which express Fas (32). In these experiments, 2DL4.1-transduced NK-92 cells were stimulated for 4 h with plate-bound anti-FLAG mAb or anti-NKp44 mAb to induce the expression of FasL and then incubated with [³H]thymidine-labeled Jurkat T cells for 2 h. DNA from the cultures was harvested to measure specific DNA fragmentation. In this assay, target cell DNA fragmentation was induced after stimulation through either receptor (Fig. 7A), even in the presence of EGTA/MgCl$_2$ to deplete calcium, which indicates that the elevated FasL promotes DNA fragmentation in Jurkat cells by a granule-independent mechanism. To confirm a role for FasL in this process, we assessed the effects of blocking FasL with specific mAb on the target cell DNA fragmentation. In these experiments, Jurkat DNA fragmentation induced by the stimulation of the NK cells through 2DL4.1 was inhibited partially by anti-FasL mAb, but not by anti-CD56 mAb (isotype control) (Fig. 7B). The results indicate that the FasL induced by 2DL4.1 engagement on NK-92 cells is functional and has the potential to promote DNA fragmentation in Fas$^+$ target cells.

Discussion

In this study, we utilized retroviral transduction to express and comparatively test the functions of FLAG epitope-tagged versions of the NK cell receptors 2DL4 or NKp44 in the human NK-like cell line, NK-92. The lack of FcγRIII (CD16) on NK-92 cells eliminated concerns of Fc-mediated activation events from the stimulating IgG mAbs, which allowed us to directly compare functions of the two receptors by engaging each with a common anti-FLAG mAb. Differential capacities of 2DL4* and NKp44 to trigger cytotoxicity and produce IFN-γ were observed under identical stimulation conditions in resting NK-92 cells. 2DL4* exhibited low redirected cytotoxicity and robust IFN-γ production (Fig. 5), which is consistent with a previous report (17), whereas NKp44 exhibited strong redirected cytotoxicity and modest IFN-γ production. Interestingly, we observed that 2DL4* stimulated more potent IFN-γ production throughout a broad time course, despite significantly lower surface expression, as compared with NKp44. These observations strongly suggest that the two receptors transduce distinct downstream signals, which are likely triggered through different associated accessory proteins. Although NKp44 associates with DAP12, the accessory protein associated with 2DL4 has not yet been identified.

Our results and those of Long and colleagues (20) demonstrate that 2DL4 is an activating receptor, despite the inhibitory cytoplasmic motif. In fact, our comparisons between two forms of 2DL4 with radically different cytoplasmic domains (2DL4.1 with the ITIM and 2DL4* lacking the ITIM) showed no major differences in activating capacity, suggesting that the ITIM does not suppress activating functions (Fig. 6). This was unexpected because strong inhibitory function was previously demonstrated by the 2DL4.1 ITIM in isolation using modified 2DL4 receptors, either by replacing the cytoplasmic domain of KIR3DL1 with that of 2DL4.1 or by mutating the transmembrane arginine of 2DL4.1 (19, 20)]. The inhibitory capacity of the 2DL4.1 ITIM appears to be

mediated through recruitment of the protein tyrosine phosphatase, SHP-2 (19). Whereas SHP-2 has been shown to contribute to negative signaling responses through some receptors (38, 39), recruitment of the phosphatase is more often involved in promoting positive signals through activating receptors (40, 41). Thus, it is important to consider the possibility that SHP-2 might contribute positive influences to 2DL4.1 function that are not evident in the functional assays used in this study. Further work is underway in our lab to address this possibility.

Our studies also demonstrated the lack of surface expression of a truncated form of 2DL4 (named 2DL4.2 in our studies) encoded by an allele that appears to be highly prevalent within the human population. Witt and colleagues (34) previously examined the frequency of the two 2DL4 alleles corresponding to 2DL4.1 and 2DL4.2 in two studies of Australian donors. Surprisingly, they found that both alleles were equally distributed in the donor populations, and 32.6% (n = 46) or 27.1% (n = 48) of individuals were homozygous for the 2DL4.2 genotype (35). Our results showed a lower representation of the 2DL4.2 allele, but our donor pool was limited. Although the identification of the two 2DL4 genotypes originally indicated differential function of receptors containing or lacking the intracytoplasmic ITIM, it is now apparent that the truncated form may not be expressed on the NK cell surface at all. Our studies of primary human cells support this possibility with only marginal expression of 2DL4 on NK cells from a donor (3E) exhibiting a homozygous 2DL4.2 phenotype, even after long-term culture in IL-2. Further, Witt et al. (35) showed that the predominant mRNA identified from NK cells of individuals homozygous for the 2DL4.2 genotype lacked the TM exon entirely, indicating further pressures against surface expression in those individuals. To standardize nomenclature for these allelic variations in this region of 2DL4, we propose adoption of the following: 1) KIR2DL4.1 (CD158d.1) for the ITIM-containing receptor (11A cDNA and 10A genomic exon 6) and 2) KIR2DL4.2 (CD158d.2) for the truncated receptor that is retained inside NK cells (10A cDNA and 9A genomic exon 6).

Our results complicate the attractive hypothesis that 2DL4 engagement with HLA-G plays an essential role in placental development by promoting IFN-γ release, because maintenance of this nonexpressed genotype does not seem to be selected against in humans. Clearly, the potential relevance of 2DL4 in human pregnancy is more complicated than currently understood. Importantly, despite diminished placental development (28, 29), IFN-γ-deficient and NK cell-deficient mice can still reproduce, and homozygosity of the 2DL4.2 allele in women does not correlate with the incidence of pre-eclampsia in later stages of pregnancy (35). Further, a recent report described a woman entirely lacking a 2DL4 gene who has had multiple normal pregnancies (42). It should also be noted that although two groups have published evidence that HLA-G is a ligand for 2DL4 (22–24), two additional reports have claimed that HLA-G is not the ligand (43, 44). These results indicate that alternative ligands may exist for 2DL4 and the receptor is not essential for normal pregnancy. It must be considered, however, that a beneficial role for 2DL4 in pregnancy is still possible under certain conditions. Therefore, the physiological impacts of the 2DL4.2 genotype on early stages of pregnancy should still be examined. However, it should also be considered that alternative 2DL4 ligands may mediate separate biological functions. For this reason, further population studies are also required to test whether different 2DL4 genotypes contribute to resistance to specific diseases, especially those that are more prevalent beyond childbearing ages, such as cancer.

The frame shift resulting from the missing adenine in the 2DL4.2 cDNA encodes only three subsequent amino acids before

early termination (Fig. 1B). Interestingly, these three amino acids are methionine-leucine-leucine, thereby introducing a dileucine motif, known to bind the AP-1 clathrin adaptor, which mediates intracellular sorting of proteins from the *trans*-Golgi network to endosomes and lysosomes (45–47). Additionally, the only trans-membrane 2DL4-like sequence identified in orangutan also ends prematurely with the methionine-leucine-leucine sequence (14), suggesting that this intracellular retention motif may serve some conserved biological purpose. Further analysis is necessary to confirm whether this motif contributes to the mechanism of intracellular retention of 2DL4.2. We cannot presently explain why one of our human blood donor (3C) exhibits a 2DL4.1-like genotype, yet does not express the receptor on the surface of NK cells, even after IL-2 culture. The result suggests that additional mechanisms may also prevent surface expression of 2DL4.1 in some individuals.

We also found that 2DL4 was only expressed on freshly isolated CD56^{high} NK cells from some individuals, and expression of the receptor was up-regulated by IL-2 stimulation in NK-92 and primary NK cells (Figs. 2 and 3). Taken together, our results indicate that despite the reports that all NK cells express 2DL4 mRNA (11, 12), the receptor appears to only reach the surface of activated NK cells. This result supports a previous report that used a polyclonal Ab preparation to show 2DL4 expression only on decidual and placental NK cells from pregnant mothers, which also express high levels of CD56 (23). Our results with retrovirus-driven expression also indicate that IL-2-mediated up-regulation of 2DL4 is independent of most of the cytoplasmic domain and is apparently due to either posttranscriptional regulation or regulation by an associated protein. We cannot rule out the possibility that an alternative accessory protein (not found in NK-92 cells or only weakly found in IL-2 stimulated NK cells) may allow surface expression of 2DL4.2 in certain NK cell populations, especially because marginal 2DL4 expression was noted on NK cells from previously negative donors after 12 days of culture with IL-2 (Fig. 3). By analogy, recent reports (48, 49) have demonstrated that alternative cytoplasmic domains in the NKG2D receptor mediate selective association with different transmembrane accessory proteins in NK cells at different activation states. Additional experiments will be required to understand the regulation of 2DL4 surface expression, the roles of accessory protein association in surface expression, and their functional significance.

We also showed that 2DL4.1 engagement induced the up-regulation of FasL, which was functional, because it promoted DNA fragmentation in Jurkat cells in a Ca^{2+}-independent manner that was partially blocked by anti-FasL mAb (Fig. 7). In the same way, previous studies have shown that upon stimulation with cytokines (50), appropriate target cells (3), or FcγRIIIA ligands (51), functional FasL is up-regulated on NK cells and can induce Fas-mediated target cell death. Because redirected assays in this and the previous report (17) consisted of short-term ^{51}Cr release assays, the importance of FasL-mediated killing triggered by 2DL4 may have been underestimated. Interestingly, a recent study of IL-12 plus IL-2 therapy suggested a unique beneficial interrelationship between IFN-γ and the Fas/FasL pathways in mediating apoptosis, inhibition of tumor neovasculation, and overall tumor regression (52). Therefore, in a similar manner, local IFN-γ production, such as that triggered through 2DL4, could sensitize tumor cells or virus infected cells to subsequent Fas-mediated bystander lysis by NK cells. In addition, our studies showed that anti-FasL mAb only partially blocked DNA fragmentation in Jurkat cells, suggesting the involvement of other apoptosis-inducing elements, such as TNF-related apoptosis-inducing ligand (2) or other TNF family members (53–55). It should also be noted that 2DL4-induced expression of CD25 (IL-2Rα chain) and CD69 (an activation recep-

tor) (56, 57) indicates that, in addition to promoting strong IFN-γ production and Fas-mediated target cell cytotoxicity, engagement of the receptor may prime NK cells to respond subsequently to IL-2 and target cells in vivo.

Functionally, our data show that 2DL4.1 can stimulate rapid and potent IFN-γ production by resting NK cells that is not influenced by its cytoplasmic ITIM motif. Potent IFN-γ production through 2DL4.1 may play at least two important functional roles in vivo: support of pregnancy and/or contribution to a cytokine-specific innate immune response. Interestingly, uterine NK cells express high levels of CD56, which is characteristic of NK-92 cells and the CD56^{high} NK cell subset that exclusively expressed 2DL4 in our studies of primary cells. Importantly, the CD56^{high} CD16$^{low/−}$ cells are an important minor subset of the NK cell pool because they produce abundant immunoregulatory cytokines, such as IFN-γ, TNF-α, and IL-10, are less effective mediators of Ab-dependent cellular and natural cytotoxicity, and can escape the vasculature to access lymph nodes and presumably reach sites of primary tumors and viral infections (58–62). IFN-γ has been shown to provide effective antiviral and antitumor innate immune functions (63, 64). Therefore, although questions of ligands and surface expression remain, appropriate engagement of 2DL4.1 can selectively stimulate NK cells to elicit a strong IFN-γ response, which has the potential to contribute significant biological benefits, but only in individuals capable of expressing this receptor.

Note added in proof. Goodridge et al. (65) recently published similar evidence for differential expression and IL-2-mediated up-regulation of KIR2DL4 that is consistent with our results.

Acknowledgments

References

1. Moretta, A., R. Biassoni, C. Bottino, M. C. Mingari, and L. Moretta. 2000. Natural cytotoxicity receptors that trigger human NK-cell-mediated cytolysis. *Immunol. Today 21:228.*
2. Takeda, K., M. J. Smyth, E. Cretney, Y. Hayakawa, N. Kayagaki, H. Yagita, and K. Okumura. 2002. Critical role for tumor necrosis factor-related apoptosis-inducing ligand in immune surveillance against tumor development. *J. Exp. Med. 195:161.*
3. Mori, S., A. Jewett, K. Murakami-Mori, M. Cavalcanti, and B. Bonavida. 1997. The participation of the Fas-mediated cytotoxic pathway by natural killer cells is tumor-cell-dependent. *Cancer Immunol. Immunother. 44:282.*
4. Biron, C. A., K. B. Nguyen, G. C. Pien, L. P. Cousens, and T. P. Salazar-Mather. 1999. Natural killer cells in antiviral defense: function and regulation by innate cytokines. *Annu. Rev. Immunol. 17:189.*
5. Campbell, K. S., and M. Colonna. 2001. Human natural killer cell receptors and signal transduction. *Int. Rev. Immunol. 20:333.*
6. Lanier, L. L. 1998. NK cell receptors. *Annu. Rev. Immunol. 16:359.*
7. Long, E. O. 1999. Regulation of immune responses through inhibitory receptors. *Annu. Rev. Immunol. 17:875.*
8. McVicar, D. W., and D. N. Burshtyn. 2001. Intracellular signaling by the killer immunoglobulin-like receptors and Ly49. *Sci. STKE 2001:RE1.*
9. Moretta, A., C. Bottino, M. Vitale, D. Pende, C. Cantoni, M. C. Mingari, R. Biassoni, and L. Moretta. 2001. Activating receptors and coreceptors involved in human natural killer cell-mediated cytolysis. *Annu. Rev. Immunol. 19:197.*
10. Vilches, C., and P. Parham. 2002. KIR: diverse, rapidly evolving receptors of innate and adaptive immunity. *Annu. Rev. Immunol. 20:217.*
11. Valiante, N. M., M. Uhrberg, H. G. Shilling, K. Lienert-Weidenbach, K. L. Arnett, A. D'Andrea, J. H. Phillips, L. L. Lanier, and P. Parham. 1997. Functionally and structurally distinct NK cell receptor repertoires in the peripheral blood of two human donors. *Immunity 7:739.*
12. Uhrberg, M., N. M. Valiante, B. P. Shum, H. G. Shilling, K. Lienert-Weidenbach, B. Corliss, D. Tyan, L. L. Lanier, and P. Parham. 1997. Human diversity in killer cell inhibitory receptor genes. *Immunity 7:753.*
13. Rajalingam, R., M. Hong, E. J. Adams, B. P. Shum, L. A. Guethlein, and P. Parham. 2001. Short KIR haplotypes in pygmy chimpanzee (*Bonobo*) resemble

the conserved framework of diverse human KIR haplotypes. *J. Exp. Med.* 193:135.

14. Guethlein, L. A., L. R. Flodin, E. J. Adams, and P. Parham. 2002. NK cell receptors of the orangutan (*Pongo pygmaeus*): a pivotal species for tracking the coevolution of killer cell Ig-like receptors with MHC-C. *J. Immunol.* 169:220.

15. Khakoo, S. I., R. Rajalingam, B. P. Shum, K. Weidenbach, L. Flodin, D. G. Muir, F. Canavez, S. L. Cooper, N. M. Valiante, L. L. Lanier, and P. Parham. 2000. Rapid evolution of NK cell receptor systems demonstrated by comparison of chimpanzees and humans. *Immunity* 12:687.

16. Hershberger, K. L., R. Shyam, A. Miura, and N. L. Letvin. 2001. Diversity of the killer cell Ig-like receptors of rhesus monkeys. *J. Immunol.* 166:4380.

17. Rajagopalan, S., J. Fu, and E. O. Long. 2001. Cutting edge: induction of IFN-γ production but not cytotoxicity by the killer cell Ig-like receptor KIR2DL4 (CD158d) in resting NK cells. *J. Immunol.* 167:1877.

18. Selvakumar, A., U. Steffens, and B. Dupont. 1996. NK cell receptor gene of the KIR family with two IG domains but highest homology to KIR receptors with three IG domains. *Tissue Antigens* 48:285.

19. Yusa, S., T. L. Catina, and K. S. Campbell. 2002. SHP-1- and phosphotyrosine-independent inhibitory signaling by a killer cell Ig-like receptor cytoplasmic domain in human NK cells. *J. Immunol.* 168:5047.

20. Faure, M., and E. O. Long. 2002. KIR2DL4 (CD158d), an NK cell-activating receptor with inhibitory potential. *J. Immunol.* 168:6208.

21. Vilches, C., R. Rajalingam, M. Uhrberg, C. M. Gardiner, N. T. Young, and P. Parham. 2000. KIR2DL5, a novel killer-cell receptor with a D0–D2 configuration of Ig-like domains. *J. Immunol.* 164:5797.

22. Cantoni, C., S. Verdiani, M. Falco, A. Pessino, M. Cilli, R. Conte, D. Pende, M. Ponte, M. S. Mikaelsson, L. Moretta, and R. Biassoni. 1998. p49, a putative HLA class I-specific inhibitory NK receptor belonging to the immunoglobulin superfamily. *Eur. J. Immunol.* 28:1980.

23. Ponte, M., C. Cantoni, R. Biassoni, A. Tradori-Cappai, G. Bentivoglio, C. Vitale, S. Bertone, A. Moretta, L. Moretta, and M. C. Mingari. 1999. Inhibitory receptors sensing HLA-G1 molecules in pregnancy: decidua-associated natural killer cells express LIR-1 and CD94/NKG2A and acquire p49, an HLA-G1-specific receptor. *Proc. Natl. Acad. Sci. USA* 96:5674.

24. Rajagopalan, S., and E. O. Long. 1999. A human histocompatibility leukocyte antigen (HLA)-G-specific receptor expressed on all natural killer cells. *J. Exp. Med.* 189:1093.

25. King, A., and Y. W. Loke. 1991. On the nature and function of human uterine granular lymphocytes. *Immunol. Today* 12:432.

26. Pazmany, L., O. Mandelboim, M. Vales-Gomez, D. M. Davis, H. T. Reyburn, and J. L. Strominger. 1996. Protection from natural killer cell-mediated lysis by HLA-G expression on target cells. *Science* 274:792.

27. Mincheva-Nilsson, L., V. Baranov, M. M. Yeung, S. Hammarstrom, and M. L. Hammarstrom. 1995. Immunomorphologic studies of human decidua-associated lymphoid cells in normal early pregnancy. *Adv. Exp. Med. Biol.* 371A:367.

28. Ashkar, A. A., J. P. Di Santo, and B. A. Croy. 2000. Interferon γ contributes to initiation of uterine vascular modification, decidual integrity, and uterine natural killer cell maturation during normal murine pregnancy. *J. Exp. Med.* 192:259.

29. Guimond, M. J., B. Wang, and B. A. Croy. 1998. Engraftment of bone marrow from severe combined immunodeficient (SCID) mice reverses the reproductive deficits in natural killer cell-deficient tg ε 26 mice. *J. Exp. Med.* 187:217.

30. Shinde, D., Y. Lai, F. Sun, and N. Arnheim. 2003. Taq DNA polymerase slippage mutation rates measured by PCR and quasi-likelihood analysis: (CA/GT)n and (A/T)n microsatellites. *Nucleic Acids Res.* 31:974.

31. Tuntiwechapikul, W., and M. Salazar. 2002. Mechanism of in vitro expansion of long DNA repeats: effect of temperature, repeat length, repeat sequence, and DNA polymerases. *Biochemistry* 41:854.

32. Matzinger, P. 1991. The JAM test: a simple assay for DNA fragmentation and cell death. *J. Immunol. Methods* 145:185.

33. Duke, R. C. 2000. Methods of analyzing chromatin changes accompanying apoptosis of target cells in killer cell assays. *Methods Mol. Biol.* 121:125.

34. Witt, C. S., A. Martin, and F. T. Christiansen. 2000. Detection of KIR2DL4 alleles by sequencing and SSCP reveals a common allele with a shortened cytoplasmic tail. *Tissue Antigens* 56:248.

35. Witt, C. S., J. M. Whiteway, H. S. Warren, A. Barden, M. Rogers, A. Martin, L. Beilin, and F. T. Christiansen. 2002. Alleles of the KIR2DL4 receptor and their lack of association with pre-eclampsia. *Eur. J. Immunol.* 32:18.

36. Steffens, U., Y. Vyas, B. Dupont, and A. Selvakumar. 1998. Nucleotide and amino acid sequence alignment for human killer cell inhibitory receptors (KIR). *Tissue Antigens* 51:398.

37. Cantoni, C., C. Bottino, M. Vitale, A. Pessino, R. Augugliaro, A. Malaspina, S. Parolini, L. Moretta, A. Moretta, and R. Biassoni. 1999. NKp44, a triggering receptor involved in tumor cell lysis by activated human natural killer cells, is a novel member of the immunoglobulin superfamily. *J. Exp. Med.* 189:787.

38. Lee, K. M., E. Chuang, M. Griffin, R. Khattri, D. K. Hong, W. Zhang, D. Straus, L. E. Samelson, C. B. Thompson, and J. A. Bluestone. 1998. Molecular basis of T cell inactivation by CTLA-4. *Science* 282:2263.

39. Fournier, N., L. Chalus, I. Durand, E. Garcia, J. J. Pin, T. Churakova, S. Patel, C. Zlot, D. Gorman, S. Zurawski, J. Abrams, E. E. Bates, and P. Garrone. 2000. FDF03, a novel inhibitory receptor of the immunoglobulin superfamily, is expressed by human dendritic and myeloid cells. *J. Immunol.* 165:1197.

40. Tomic, S., U. Greiser, R. Lammers, A. Kharitonenkov, E. Imyanitov, A. Ullrich, and F. D. Bohmer. 1995. Association of SH2 domain protein tyrosine phosphatases with the epidermal growth factor receptor in human tumor cells: phospha-

tidic acid activates receptor dephosphorylation by PTP1C. *J. Biol. Chem.* 270:21277.

41. Ugi, S., H. Maegawa, A. Kashiwagi, M. Adachi, J. M. Olefsky, and R. Kikkawa. 1996. Expression of dominant negative mutant SHPTP2 attenuates phosphatidylinositol 3'-kinase activity via modulation of phosphorylation of insulin receptor substrate-1. *J. Biol. Chem.* 271:12595.

42. Gomez-Lozano, N., R. De Pablo, S. Puente, and C. Vilches. 2003. Recognition of HLA-G by the NK cell receptor KIR2DL4 is not essential for human reproduction. *Eur. J. Immunol.* 33:639.

43. Boyson, J. E., R. Erskine, M. C. Whitman, M. Chiu, J. M. Lau, L. A. Koopman, M. M. Valter, P. Angelisova, V. Horejsi, and J. L. Strominger. 2002. Disulfide bond-mediated dimerization of HLA-G on the cell surface. *Proc. Natl. Acad. Sci. USA* 99:16180.

44. Allan, D. S., M. Colonna, L. L. Lanier, T. D. Churakova, J. S. Abrams, S. A. Ellis, A. J. McMichael, and V. M. Braud. 1999. Tetrameric complexes of human histocompatibility leukocyte antigen (HLA)-G bind to peripheral blood myelomonocytic cells. *J. Exp. Med.* 189:1149.

45. Zhu, Y., B. Doray, A. Poussu, V. P. Lehto, and S. Kornfeld. 2001. Binding of GGA2 to the lysosomal enzyme sorting motif of the mannose 6-phosphate receptor. *Science* 292:1716.

46. Bresnahan, P. A., W. Yonemoto, S. Ferrell, D. Williams-Herman, R. Geleziunas, and W. C. Greene. 1998. A dileucine motif in HIV-1 Nef acts as an internalization signal for CD4 downregulation and binds the AP-1 clathrin adaptor. *Curr. Biol.* 8:1235.

47. Rapoport, I., Y. C. Chen, P. Cupers, S. E. Shoelson, and T. Kirchhausen. 1998. Dileucine-based sorting signals bind to the β chain of AP-1 at a site distinct and regulated differently from the tyrosine-based motif-binding site. *EMBO J.* 17:2148.

48. Gilfillan, S., E. L. Ho, M. Cella, W. M. Yokoyama, and M. Colonna. 2002. NKG2D recruits two distinct adapters to trigger NK cell activation and costimulation. *Nat. Immun.* 3:1150.

49. Diefenbach, A., E. Tomasello, M. Lucas, A. M. Jamieson, J. K. Hsia, E. Vivier, and D. H. Raulet. 2002. Selective associations with signaling proteins determine stimulatory versus costimulatory activity of NKG2D. *Nat. Immun.* 3:1142.

50. Tsutsui, H., K. Nakanishi, K. Matsui, K. Higashino, H. Okamura, Y. Miyazawa, and K. Kaneda. 1996. IFN-γ-inducing factor up-regulates Fas ligand-mediated cytotoxic activity of murine natural killer cell clones. *J. Immunol.* 157:3967.

51. Eischen, C. M., J. D. Schilling, D. H. Lynch, P. H. Krammer, and P. J. Leibson. 1996. Fc receptor-induced expression of Fas ligand on activated NK cells facilitates cell-mediated cytotoxicity and subsequent autocrine NK cell apoptosis. *J. Immunol.* 156:2693.

52. Wigginton, J. M., J. K. Lee, T. A. Wiltrout, W. G. Alvord, J. A. Hixon, J. Subleski, T. C. Back, and R. H. Wiltrout. 2002. Synergistic engagement of an ineffective endogenous anti-tumor immune response and induction of IFN-γ and Fas-ligand-dependent tumor eradication by combined administration of IL-18 and IL-2. *J. Immunol.* 169:4467.

53. Wallach, D., E. E. Varfolomeev, N. L. Malinin, Y. V. Goltsev, A. V. Kovalenko, and M. P. Boldin. 1999. Tumor necrosis factor receptor and Fas signaling mechanisms. *Annu. Rev. Immunol.* 17:331.

54. Kashii, Y., R. Giorda, R. B. Herberman, T. L. Whiteside, and N. L. Vujanovic. 1999. Constitutive expression and role of the TNF family ligands in apoptotic killing of tumor cells by human NK cells. *J. Immunol.* 163:5358.

55. Kayagaki, N., N. Yamaguchi, M. Nakayama, K. Takeda, H. Akiba, H. Tsutsui, H. Okamura, K. Nakanishi, K. Okumura, and H. Yagita. 1999. Expression and function of TNF-related apoptosis-inducing ligand on murine activated NK cells. *J. Immunol.* 163:1906.

56. Sancho, D., A. G. Santis, J. L. Alonso-Lebrero, F. Viedma, R. Tejedor, and F. Sanchez-Madrid. 2000. Functional analysis of ligand-binding and signal transduction domains of CD69 and CD23 C-type lectin leukocyte receptors. *J. Immunol.* 165:3868.

57. Pisegna, S., A. Zingoni, G. Pirozzi, B. Cinque, M. G. Cifone, S. Morrone, M. Piccoli, L. Frati, G. Palmieri, and A. Santoni. 2002. Src-dependent Syk activation controls CD69-mediated signaling and function on human NK cells. *J. Immunol.* 169:68.

58. Cooper, M. A., T. A. Fehniger, and M. A. Caligiuri. 2001. The biology of human natural killer-cell subsets. *Trends Immunol.* 22:633.

59. Cooper, M. A., T. A. Fehniger, S. C. Turner, K. S. Chen, B. A. Ghaheri, T. Ghayur, W. E. Carson, and M. A. Caligiuri. 2001. Human natural killer cells: a unique innate immunoregulatory role for the CD56bright subset. *Blood* 97:3146.

60. Fehniger, T. A., M. A. Cooper, G. J. Nuovo, M. Cella, F. Facchetti, M. Colonna, and M. A. Caligiuri. 2002. CD56bright natural killer cells are present in human lymph nodes and are activated by T cell derived IL-2: a potential new link between adaptive and innate immunity. *Blood* 12:12.

61. Loza, M. J., and B. Perussia. 2001. Final steps of natural killer cell maturation: a model for type 1-type 2 differentiation? *Nat. Immun.* 2:917.

62. Ross, M. E., and M. A. Caligiuri. 1997. Cytokine-induced apoptosis of human natural killer cells identifies a novel mechanism to regulate the innate immune response. *Blood* 89:910.

63. Biron, C. A., and L. Brossay. 2001. NK cells and NKT cells in innate defense against viral infections. *Curr. Opin. Immunol.* 13:458.

64. Tannenbaum, C. S., and T. A. Hamilton. 2000. Immune-inflammatory mechanisms in IFNγ-mediated anti-tumor activity. *Semin. Cancer Biol.* 10:113.

65. Goodridge, J. P., C. S. Witt, F. T. Christiansen, and H. S. Warren. 2003. KIR2DL4 (CD158d) genotype influences expression and function in NK cells. *J. Immunol.* 171:1768.

Inhibitory NK Receptor Ly49Q Is Expressed on Subsets of Dendritic Cells in a Cellular Maturation- and Cytokine Stimulation-Dependent Manner[1]

Noriko Toyama-Sorimachi,[2]*[†] Yoshiki Omatsu,[‡] Atsuko Onoda,[†] Yusuke Tsujimura,*[†] Tomonori Iyoda,[‡] Akiko Kikuchi-Maki,* Hiroyuki Sorimachi,[¶] Taeko Dohi,* Shinsuke Taki,[§] Kayo Inaba,[‡] and Hajime Karasuyama[†]

Ly49Q is a member of the Ly49 family that is expressed on Gr-1^{+} cells but not on NK and NKT cells. Ly49Q appears to be involved in regulating cytoskeletal architectures through ITIM-mediated signaling. We provide evidence that dendritic cells (DCs) of certain maturational states expressed Ly49Q, and that IFN-α plays an important role in its regulation. Freshly prepared murine plasmacytoid pre-DCs as well as Flt3L-induced plasmacytoid pre-DCs expressed Ly49Q, whereas freshly prepared myeloid DCs did not. However, GM-CSF-induced myeloid DCs showed low levels of Ly49Q expression, and this was significantly enhanced by IFN-α. In contrast, other cytokines and ligands for TLRs such as TNF-α, IL-6, LPS, and CpG-ODN had little or no effect on Ly49Q expression. Plasmacytoid pre-DCs in all mouse strains examined expressed Ly49Q. Constitutive expression of Ly49Q on myeloid DCs was observed in three restricted mouse strains including 129, NZB, and NZW. As can be seen in other Ly49 family members, Ly49Q expression was affected by MHC class I expression. At the same time, Ly49Q possessed polymorphisms, including at least three alleles. The polymorphic residues lay within the stalk and carbohydrate recognition domain, and two of them, in loop 3 and loop 6 of the carbohydrate recognition domain, are located in the region implicated in the interaction of Ly49A with H-2D^d. Therefore, depending on IFN-α, our results imply that Ly49Q serves a role for the biological functions of certain DC subsets through recognition of MHC class I or related molecules. *The Journal of Immunology*, 2005, 174: 4621–4629.

The Ly49 family is one of the subfamilies of NK receptors. As with other NK receptor families, the Ly49 family plays a crucial role in self-nonself discrimination by NK cells through its ability to recognize MHC class I or related molecules (1–3). When NK cells recognize MHC class I molecules on target cells, signals transduced by ITIM-bearing inhibitory NK receptors inhibit cytotoxic function and cytokine production (4–8). Ly49Q is an ITIM-bearing inhibitory receptor, which is classified in the Ly49 family because of its high structural similarities and chromosomal location (9). However, Ly49Q has unique features, distinguishing it from other Ly49 family members. We have recently reported that Ly49Q is not expressed on NK and NKT cells, but is predominantly expressed on Gr-1^{+} myeloid lineage cells and activated macrophages (9). Expression of Ly49Q on mono-

cytes/macrophages was regulated during their ontogeny and is significantly up-regulated by treatment with IFN-γ, which is produced by a wide variety of cells in response to infectious or inflammatory stimuli. Ly49Q has the ability to associate with both Src homology region 2 domain-containing phosphatase 1 and 2 in a tyrosine phosphorylation-dependent manner. Cross-linking of Ly49Q by a specific Ab to Ly49Q triggers rapid cell adhesion and spreading, resulting in the formation of cell polarity in macrophages. Furthermore, Ly49Q can induce tyrosine phosphorylation of various cellular proteins in an ITIM-dependent manner. Therefore, Ly49Q potentially functions as a surface receptor involved in regulation of the cytoskeletal architecture of macrophages, which is essential to macrophage functions such as migration, phagocytosis, production of cytokines, synthesis of bactericidal materials, including O$_2^-$ and NO.

Dendritic cells (DCs)[3] are the most potent APCs and are essential for the link between innate and acquired immunity (10–13). Murine DCs are characterized by the expression of CD11c and are divided into two major subsets: the CD11c^{+}CD11b^{+} conventional myeloid DCs and CD11c^{+}CD11b^{-}B220^{+} plasmacytoid pre-DCs, or type I IFN-producing cells (14, 15). Both subsets are distributed throughout various tissues and play different roles in immune responses. Conventional myeloid DCs are able to polarize an adoptive immune response toward a Th1-type response (16). Plasmacytoid pre-DCs are characterized by their ability to secrete high levels of IFN-α, conferring resistance to viruses (14, 15). Both types of DCs express a wide range of receptors, including TLRs and C-type lectins, for the recognition and the subsequent internalization of microbes (17–21). Distinct sets of TLRs and C-type

*Department of Gastroenterology, Research Institute, International Medical Center of Japan, Tokyo, Japan; [†]Department of Immune Regulation, Tokyo Medical and Dental University Graduate School, Tokyo, Japan; [‡]Department of Animal Development and Physiology, Graduate School of Biostudies, Kyoto University, Kyoto, Japan; [¶]Department of Enzymatic Regulation for Cell Functions, Tokyo Metropolitan Institute of Medical Science, Tokyo, Japan; and [§]Department of Immunology and Infectious Diseases, Shinshu University Graduate School of Medicine, Nagano, Japan

[2] Address correspondence and reprint requests to Dr. Noriko Toyama-Sorimachi, Department of Gastroenterology, Research Institute, International Medical Center of Japan, 1-21-1, Toyama, Shinjuku-ku, Tokyo 162-8655, Japan. E-mail address: nsorima@ri.imcj.go.jp

lectins are expressed on different subsets of DCs depending on their tissue localization and maturational states. Therefore, each differential subset of DCs is specialized to respond to specific stimuli by viruses or microbes.

An increasing number of C-type lectins possessing a carbohydrate recognition domain (CRD) have been identified in both human and mouse DCs (18–21). Their CRD recognizes self or pathogenic structures of glycoproteins. Several C-type lectins, including DC-specific ICAM-3 grabbing nonintegrin, DEC-205, and blood DC Ag 2 are responsible for the endocytosis of a broad array of foreign materials following presentation of Ags to T cells (22–24). However, another C-type lectin known as DC immunoreceptor has a cytoplasmic ITIM, and hence seems to be involved in the negative regulation of DC functions (25). DCs also express structurally different groups of inhibitory receptors, including paired Ig-like receptor B and paired Ig-like type L receptor α/FDF03, which belong to the Ig-superfamily (26, 27). These inhibitory receptors play crucial roles in tuning the DC functions. For example, DCs were aberrantly activated in PIR-B$^{-/-}$ mice, exacerbating graft-vs-host disease (28). Although ligands of these inhibitory receptors and their exact function in DCs should be further investigated, inhibitory receptors might play important roles in maintaining the homeostasis, initiation, amplification, and termination of DC functions, as observed in other types of immune cells.

In this study, we report that an inhibitory C-type lectin, Ly49Q, was expressed on certain developmental/maturational stages of murine DCs, which was primarily regulated by IFN-α. Our findings illustrate a common recognition system in APCs, such as macrophages and DCs, through the inhibitory receptor Ly49Q.

Materials and Methods

Mice

C57BL/6, BALB/c, C3H, DBA1, and DBA2 mice were purchased from CLEA Japan. A/J, AKR/N, 129SvJ NZB, NZW, and NZBWF$_1$ mice were purchased from Japan SLC. SJL mice were purchased from Charles River Japan. C57BL/6 β$_2$m$^{-/-}$ mice were purchased from Taconic Farms. JF1 and MSM mice were gifts from Dr. T. Shiroishi (National Institute of Genetics, Shizuoka, Japan). All experiments were performed according to the Guidelines for Animal Use and Experimentation as set out by our institute.

Abs and reagents

Anti-Ly49Q mAb was produced as previously described (9). The following mAbs were purchased from BD Pharmingen: FITC-conjugated anti-CD11b (Mac-1), anti-Gr-1 (Ly6C/G), anti-Ly6C, anti-CD40, anti-CD86, anti-I-A^b, anti-CD4, and anti-CD8α; PE-Cy5.5-conjugated anti-CD11c and streptavidin; biotin-conjugated CD11c; PE-conjugated anti-B220; and allophycocyanin-conjugated streptavidin. Flt3L and GM-CSF were purchased from R&D Systems. IFN-α and IFN-γ were purchased from PeproTech. Peptide glycan, LPS, and poly(I:C) were purchased from Sigma-Aldrich. CpG-ODN (TCA TTG GAA AAC GTT CTT CGG GGC G) was phosphorothioate-modified (Hokkaido System Science). Collagenase type III and collagenase D were purchased from Worthington Biochemical and Boehringer Mannheim, respectively.

Cell preparation and culture

In vitro culture of plasmacytoid pre-DCs was performed as described previously (29). Briefly, bone marrow (BM) cells were isolated by flushing femurs and tibiae of euthanized mice with RPMI 1640 medium supplemented with 5% heat-inactivated FCS (Moregate lot no. 49300124; Australia). The BM cells were treated with a Tris-ammonium chloride buffer to lyse RBC and plated at a concentration of 10^6 cells/ml into a six-well culture dish in culture medium consisting of RPMI 1640 medium supplemented with 10% FCS, 10 mM HEPES, 2 mM L-glutamine, 1 mM sodium pyruvate, 50 μM 2-ME, 1% (v/v) nonessential amino acids, 100 U/ml penicillin, 100 μg/ml streptomycin, and 100 ng/ml murine Flt3L. Every 4 days of culture, half of the medium was removed and fresh cytokine-supplemented culture medium was added back into the cultures. For preparation of BM-derived myeloid DCs, BM cells were cultured at 2 × 10^6 cells in 10 ml of the culture medium supplemented with 20 ng/ml GM-CSF.

Twenty-four hours after seeding, 10 ml of fresh medium containing GM-CSF was added, and every 3 days of culture, half of the medium was exchanged. In some experiments, Flt3L- or GM-CSF-induced BM DCs were treated with IFN-α (100 U/ml), IFN-γ (20 ng/ml), TNF-α (50 ng/ml), LPS (1 μg/ml), CpG-ODN D19 (10 μg/ml), or peptide glycan (10 μg/ml) for 18 h, and flow cytometry analysis was performed.

Preparation of DCs from the spleen was performed as previously described (30). Briefly, organs were treated with 1 mg/ml type III collagenase for 30 min at 37°C. After the addition of 10 mM EDTA to the collagenase treated organs, they were further incubated at 37°C for 5 min, and dispersed by gentle pipetting. CD11c$^+$ cells were enriched using AutoMACS cell sorter with anti-CD11c mAb-conjugated microbeads.

Flow cytometry analysis

Immunofluorescence analysis was performed as previously described (9). For staining hemopoietic lineage cells, cells were preincubated with 20% heat-inactivated normal rat serum for 15 min on ice. Incubation of cells with Abs was conducted in the presence of purified 2.4G2 Ab. Cytoplasmic staining was performed in accordance with the company's protocol using BD Cytofix/Cytoperm kit (BD Biosciences). Stained cells were analyzed with the FACSCalibur system (BD Biosciences).

RT-PCR analysis of Ly49Q transcription and its polymorphisms

Primers for amplifying the full-length Ly49Q sequence were: 5′-CCG GAATTCATGAGTGAGCAGGAGGTCACTTATTCAAC-3′ and 5′-CGC GGATCCTTAACTGTTGTTGGGGAGCGAATCAGGA-3′. RNA was prepared from Gr-1$^+$ BM cells and subjected to RT-PCR with these primers. The integrity of mRNAs and successful cDNA synthesis were verified for each sample by monitoring hypoxanthine phosphoribosyltransferase. In some experiments, prepared RNA was treated with RNA-free DNase to eliminate genomic DNA. The PCR products were cloned into a pBS vector using BamHI and EcoRI recognition sites, and then sequenced using an ABI PRISM 310 Genetic Analyzer (Applied Biosystems). Sequences were deposited with GenBank under the following accession numbers: Ly49q1$^{129 × 1/Sv}$ (AB190779), Ly49q1$^{A/J}$ (AB190780), Ly49q1^{AKR} (AB190781), Ly49q1$^{C3H/HeN}$ (AB190782), Ly49q1^{DBA1} (AB190783), Ly49q1^{DBA2} (AB190784), Ly49q1JF1 (AB190785), Ly49q1^{MSM} (AB190786), Ly49q1$^{SJL/J/On}$ (AB190787), Ly49q1^{NZW} (AB190788), and Ly49q1^{NZB} (AB190789).

To classify and confirm nucleotide substitutions in Ly49Q cDNA prepared from various mouse strains, PCR products were digested with the restriction enzymes indicated and analyzed using gel electrophoresis.

Genomic PCR

Genomic DNA was extracted by incubating mouse tail tissues in an extraction buffer (10 mM Tris, pH 8.3, 50 mM KCl, 1.5 mM MgCl$_2$, 1 mg/ml gelatin, 0.45% Nonidet P-40, 0.45% Tween 20, 0.4 mg/ml proteinase K) at 50°C overnight. PCR primers for amplifying Ly49q1 and Ly49q2 were: 5′-GACAGGGACTATGCAGTTACATGCTCT (5′ primer in Fig. 4A) and 5′-CCTGTACTACACTCTAGAGGC-3′ (3′ primer in Fig. 4A). PCR products were cloned into the pBS vector followed by sequence analysis as described above. In some experiments, PCR products were digested with PstI restriction enzyme and analyzed using gel electrophoresis. To determine partial sequences of Ly49q3 (intron 3-exon 4), PstI-digested PCR products obtained from 129 mice were cloned into the pBS vector followed by sequence analysis. The sequences were deposited with GenBank (Ly49q2, AB193835; Ly49q3, AB193834).

Identification of isoforms and new exons

RT-PCR products corresponding to full-length Ly49Q obtained from JF1, MSM, and 129 × 1/Sv mice were cloned into the pBS vector and cDNA sequences of several independent clones which have different sizes of inserts were determined. Existence of sequences corresponding to the newly identified exons was confirmed by searching sequences in the Ensemble genomic sequences of mouse chromosome 6 including Klra17 (Ensemble gene ID: ENSMUSG00000014543). GenBank accession numbers of isoforms and exons are as follows: Cyt, AB193830; CDR1, AB193831; CDR2, AB193832; and CDR3, AB193833.

Vectors and cDNA transfection

The Ly49Q cDNA modified to add a FLAG tag at the N terminus of Ly49Q was inserted into the eukaryotic expression vector pME18S and then transfected into COS7 cells by electroporation (9). Forty-eight hours after transfection, Ly49Q expression was analyzed using flow cytometry or Western blot analysis.

Results

Expression of Ly49Q on subsets of DCs

Our previous study indicated that a small portion of Gr-1^{low} fraction in BM also expressed Ly49Q (Fig. 1A). To identify these Ly49Q$^+$Gr-1^{low} cells, further flow cytometry analysis was performed using a panel of Abs against lineage markers. Ly49Q$^+$Gr-1^{low} cells expressed CD11c as well as B220, suggesting that these cells were plasmacytoid pre-DCs (Fig. 1A, data not shown). As shown in Fig. 1B, most of the B220$^+$CD11c$^+$ plasmacytoid pre-DCs in the BM were specifically stained with anti-Ly49Q mAb. RT-PCR analysis indicated that the mRNA of Ly49Q was also detected in sorted Ly49Q$^+$B220$^+$ cells (data not shown). The expression level of Ly49Q on plasmacytoid pre-DCs exhibited over a 10-fold higher mean fluorescence intensity than that on Gr-1$^+$ cells in BM (9).

Previous studies demonstrated that mouse DCs could be generated in vitro by culturing BM cells with Flt3L or GM-CSF (29, 31). We further confirmed the expression of Ly49Q on plasmacytoid pre-DCs using cultured DCs. Flt3L-induced BM DCs contained several populations, which were divided into groups according to the expression of CD11b and B220. As shown in Fig. 1C, a large portion of CD11c$^+$CD11b$^-$B220$^+$ plasmacytoid pre-DCs expressed Ly49Q on their surface. CD11c$^+$CD11b$^+$B220$^-$ myeloid DCs also expressed Ly49Q, although the levels from these myeloid DCs were lower than from Flt3L-induced plasmacytoid pre-DCs.

Regulation of Ly49Q expression by IFN-α

We previously reported that Ly49Q expression on monocytes/macrophages is regulated during their differentiation and activation (9). To examine whether the Ly49Q expression is regulated during the DC differentiation/activation process, Flt3L-induced plasmacytoid pre-DCs and GM-CSF-induced myeloid DCs were treated with a panel of cytokines or ligands for TLRs and examined for their expression of Ly49Q. When cells were treated with IFN-α, we observed significant enhancement of Ly49Q expression, as

well as MHC class II expression, on CD11c$^+$CD11b$^+$ myeloid DCs (Fig. 2A, right panels, and data not shown). RT-PCR analysis for Ly49Q mRNA by RT-PCR confirmed higher transcription of the Ly49q gene in IFN-α-treated myeloid DCs than in untreated myeloid DCs (Fig. 2, B and C). As for plasmacytoid pre-DCs, Ly49Q expression was slightly enhanced in the presence of IFN-α, IFN-γ, or LPS (Fig. 2A, left and middle panels). In both myeloid and plasmacytoid pre-DCs, IFN-γ was less effective than IFN-α in enhancing the expression of Ly49Q. The enhanced expression of Ly49Q was not observed when both types of DCs prepared from IFNαR$^{-/-}$ mice were treated with IFN-α, even though IFN-γ induced a slight increase of Ly49Q expression on these cells (Fig. 2A and data not shown). Notably, other cytokines and a panel of ligands of TLRs, including TNF-α, CpG, poly(I:C), peptide glycan, and anti-CD40 mAb had little effect on the expression of Ly49Q, even though these stimuli induced an increased expression of MHC class II (Fig. 2A and data not shown).

We further analyzed Ly49Q expression levels on plasmacytoid pre-DCs in IFNαR$^{-/-}$ mice. However, Ly49Q expression pattern differences on plasmacytoid pre-DCs between IFNαR$^{-/-}$ and wild-type mice was not observed in both the BM and spleen (Fig. 2D).

Expression of Ly49Q in various mouse strains

Previous studies have shown that some members of the Ly49 family are not expressed in some mouse strains, as genes encoding for certain Ly49 were deleted during their diversification (32, 33). Therefore, we investigated the expression of Ly49Q in various mouse strains. Ly49Q was expressed in splenic B220$^+$CD11c$^+$ plasmacytoid pre-DCs prepared from 10 strains of laboratory mice: SJL (H-2^b), A/J (H-2^b), AKR (H-2^k), BALB/c (H-2^d), C3H (H-2^k), DBA1 (H-2^q), DBA2 (H-2^d), NZB (H-2^d), NZW (H-2^z), and 129 × 1/SvJ (H-2^b). Plasmacytoid pre-DCs in wild mice, such as JF1 and MSM, also expressed Ly49Q (data not shown). Correlations between the expression levels and MHC class I haplotypes were not observed, although the expression levels slightly
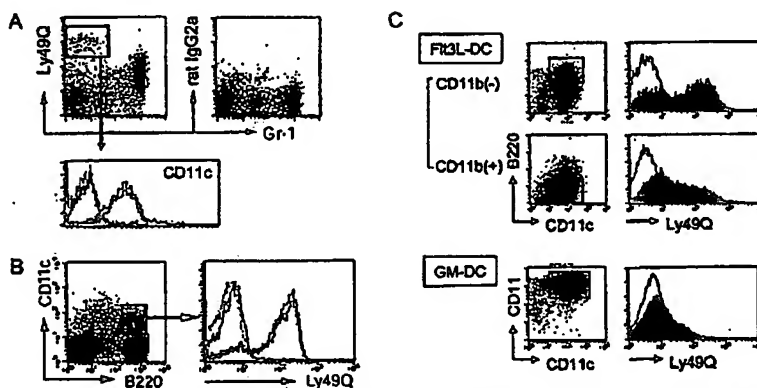

FIGURE 1. Ly49Q expression on plasmacytoid pre-DCs. A, Three-color flow cytometric analysis of BM cells. BM cells were stained with FITC-conjugated anti-Gr-1 and PE-conjugated anti-CD11c mAbs in combination with biotin-conjugated anti-Ly49Q or control rat IgG2a Abs. CD11c expression on Ly49Q$^+$Gr-1$^+$ cells was analyzed. A thick line in the histogram indicates staining by anti-CD11c. A thin line indicates staining by control Ab, and a dashed line indicates a pattern in the absence of Ab. B, Three-color flow cytometric analysis of BM cells. BM cells were stained with FITC-conjugated anti-CD11c and PE-conjugated anti-B220 mAbs in combination with biotin-conjugated anti-Ly49Q (thick line) or biotin-conjugated rat IgG2a (thin line) revealed by allophycocyanin-conjugated streptavidin. A dashed line indicates the staining pattern in the absence of first Ab. C, Ly49Q expression on BM-derived DCs with Flt3L or GM-CSF. BM-derived DCs were prepared by culturing BM in the presence of Flt3L or GM-CSF as described in Materials and Methods. CD11b$^+$ and CD11b$^-$ DCs were purified from FLt3L-induced BM cells using an AutoMACS cell sorter, and then stained with FITC-conjugated anti-CD11c and PE-conjugated anti-B220 mAbs in combination with biotin-conjugated anti-Ly49Q (shaded histograms) or with biotin-conjugated rat IgG2a (open histograms) revealed by allophycocyanin-conjugated streptavidin. GM-CSF-induced DCs were stained with FITC-conjugated anti-CD11c and PE-conjugated anti-CD11b mAbs in combination with biotin-conjugated anti-Ly49Q (shaded histogram) or biotin-conjugated rat IgG2a (open histogram) revealed by allophycocyanin-conjugated streptavidin.
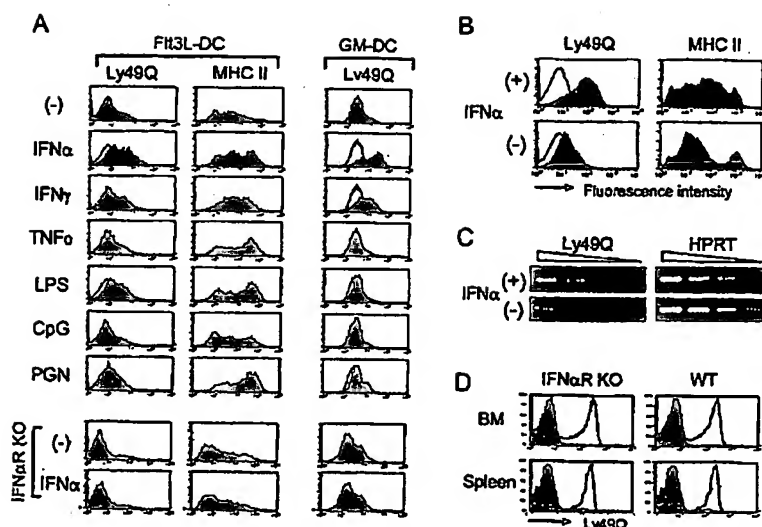
FIGURE 2. Enhancement of Ly49Q expression by IFN-α or IFN-γ. *A.* Flt3L- or GM-CSF-induced BM DCs prepared from wild-type C57BL/6 or IFNαR⁻/⁻ mice were treated for 18 h with various cytokines or the TLR ligands indicated. Because cells obtained from the cultures contain various subsets, CD11c⁺CD11b⁻ plasmacytoid pre-DCs in Flt3L-induced DCs and CD11c⁺CD11b⁺ myeloid DCs in GM-CSF-induced DCs were analyzed for the expression of Ly49Q or MHC class II. Cells were stained with FITC-conjugated CD11c and PE-conjugated anti-CD11b in combination with biotin-conjugated anti-Ly49Q (shaded histograms) or biotin-conjugated rat IgG2a mAbs (solid line in the (−) histogram) revealed by streptavidin-PC5. For MHC class II staining, cells were stained with PE-conjugated anti-CD11c and PC5-conjugated anti-CD11b mAbs in combination with FITC-conjugated anti-MHC class II (shaded histograms) or control mAbs (open histograms). All shaded histograms except for (−) histograms are overlaid with open histograms; these indicate patterns of untreated DCs stained with anti-Ly49Q mAb (solid lines). *B,* GM-CSF-induced BM DCs were treated with IFN-α for 18 h and stained with anti-Ly49Q or anti-MHC class II mAbs as described above. Shaded histograms indicate staining patterns with anti-Ly49Q or anti-MHC class II mAbs. Open histograms indicate staining patterns with isotype-matched control mAbs. *C,* mRNA was prepared from IFN-α-stimulated myeloid DCs, and then RT-PCR was performed using primer sets specific for Ly49Q as described previously (9). Templates were used in serial 5-fold dilutions. *D,* DCs were prepared from BM and spleens of IFNαR⁻/⁻ and control mice, and Ly49Q expression was examined by flow cytometry analysis.

differed by strains (Fig. 3). Interestingly, however, no detectable level of Ly49Q expression on B220⁻CD11c⁺ conventional myeloid DCs was observed in most mouse strains, although significant expression of Ly49Q was detected on GM-CSF-induced BM-derived myeloid DCs as described above (Fig. 3*B*). Exceptionally, in three strains, NZB, NZW, and 129 × 1/SvJ, all myeloid DCs expressed significant yet low, levels of Ly49Q relative to plasmacytoid pre-DCs.

Makrigiannis et al. (32) reported that the 129 × 1/SvJ strain has the *Ly49q2* gene with a high sequence similarity with *Ly49q1*. We further examined the possibility that these three strains have the *Ly49q2* gene or other related genes, and that myeloid DCs in these strains express them on their surface. Although *Ly49q1* and *Ly49q2* are highly homologous, these two genes can be discriminated using the *PstI* restriction enzyme (Fig. 4*A*). Genomic PCR

analysis and subsequent *PstI* treatments indicated that NZB and NZW mice did not have the *Ly49q2* gene in the NK complex (Fig. 4*B*). Only 129 × 1/SvJ and SJL/J strains have the *Ly49q2* gene. In these two mouse strains, we also identified the *Ly49q3* gene, which has a high sequence similarity to *Ly49q1* and *Ly49q2*. Because NZB and NZW strains do not have *Ly49q2* and *Ly49q3* genes, it was strongly suggested that Ly49Q1 proteins were expressed on myeloid DCs in these two strains.

Effect of MHC class I on Ly49Q expression

It has been demonstrated that Ly49 expression levels in NK cells are influenced by MHC class I expression (34–36). To examine whether this is also true for Ly49Q, Ly49Q expression levels on plasmacytoid pre-DCs were compared between C57BL/6 and
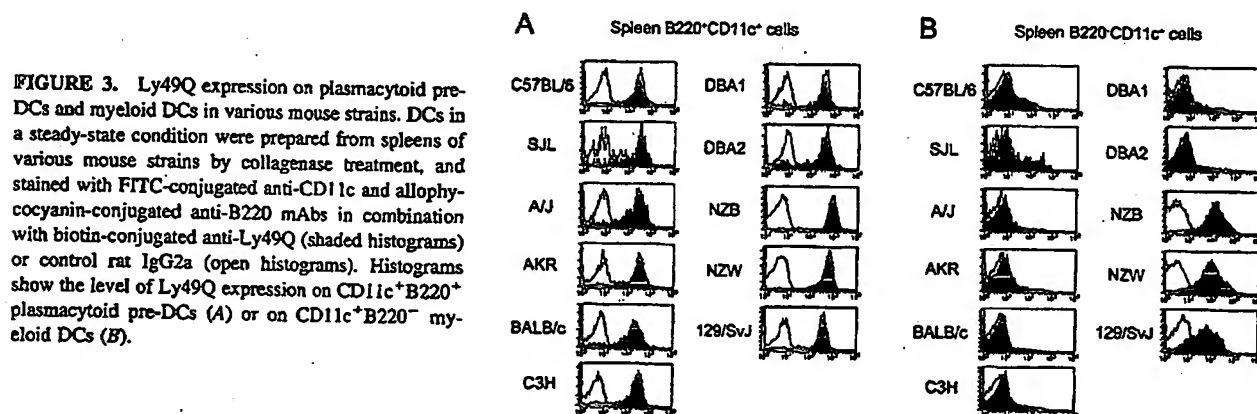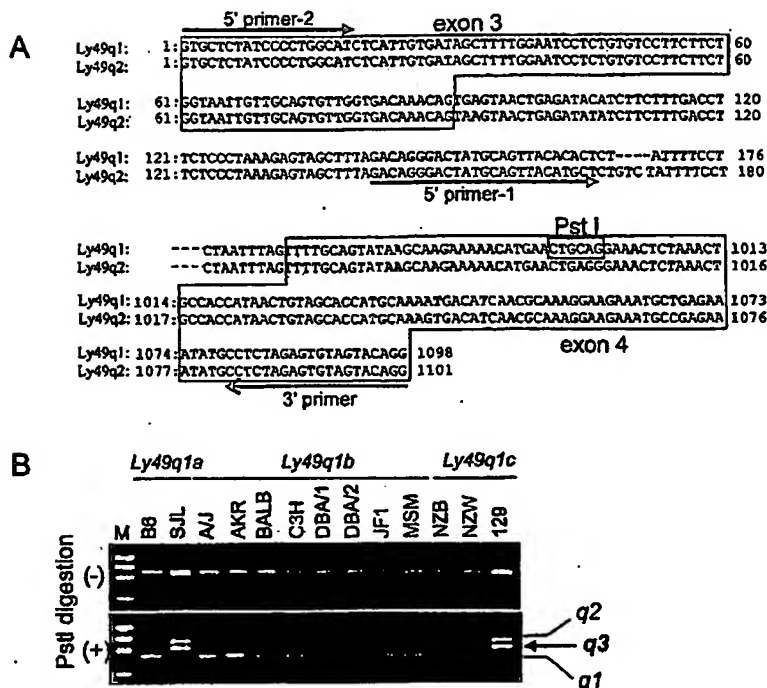

FIGURE 3. Ly49Q expression on plasmacytoid pre-DCs and myeloid DCs in various mouse strains. DCs in a steady-state condition were prepared from spleens of various mouse strains by collagenase treatment, and stained with FITC-conjugated anti-CD11c and allophycocyanin-conjugated anti-B220 mAbs in combination with biotin-conjugated anti-Ly49Q (shaded histograms) or control rat IgG2a (open histograms). Histograms show the level of Ly49Q expression on CD11c⁺B220⁺ plasmacytoid pre-DCs (*A*) or on CD11c⁺B220⁻ myeloid DCs (*B*).

FIGURE 4. Genomic PCR analysis of *Ly49q1* and *Ly49q2*. *A*, Partial nucleotide sequences of *Ly49q1* and *Ly49q2*. *Sequence of Ly49q2*[129] (exon 3–4) was retrieved from GenBank (AF425087). The sequence corresponding to *Ly49q1*[129] was retrieved from the Ensemble genomic sequence of mouse chromosome 6 including *Klra17* (Ensemble gene ID: ENSMUSG00000014543). As *Ly49q1* and *Ly49q2* are highly homologous, *Ly49q2*-specific primers could not be set. However, *Ly49q1* has a recognition site for the *Pst*I restriction enzyme in exon 4. Therefore, these highly homologous genes could be discriminated using *Pst*I treatment of intron 3-exon 4 PCR products amplified using primers as indicated in *A*. *B*, Detection of *Ly49q1*, *q2*, and *q3* genes in various mouse strains by genomic PCR. PCR products derived from *Ly49q2* gene can be identified by the treatment of the products with *Pst*I. Sequence analysis indicated that *Pst*I-resistant PCR products were identical to the *Ly49q2* sequence retrieved from GenBank (AF425087). Only mouse strains 129 and SJL have the *Ly49q2* gene. In addition, a novel gene that is highly homologous to *Ly49q2*, designated *Ly49q3*, was identified in these strains. *Pst*I-treated PCR products were cloned, and sequences of *Ly49q3* were determined. GenBank accession numbers of the *Ly49q3* from 129 × 1/Sv were AB193834.

C57BL/6 β_2m$^{-/-}$ mice. Ly49Q expression levels in splenic plasmacytoid pre-DCs were higher in the C57BL/6 β_2m$^{-/-}$ mice than in control C57BL/6 mice (Fig. 5). Interestingly, however, difference in Ly49Q expression levels in BM was not observed. Therefore, the Ly49Q expression levels on plasmacytoid pre-DCs appear to be affected by the expression of β_2-microglobulin (β_2m)-associated, MHC class I-like molecules in periphery.

Polymorphisms and isoforms of Ly49Q

To obtain clues for a possible ligand for Ly49Q, a polymorphic variation of Ly49Q was examined. Ly49Q cDNA was additionally cloned from 10 laboratory and 2 wild mouse strains, and we determined their nucleotide sequences. To exclude the possibility that nucleotide substitutions in obtained sequences were PCR artifacts, multiple independent clones were used for determining the sequences. Furthermore, restriction enzymes that could discriminate nucleotide substitutions in different alleles were chosen by comparing sequences, and allelic variations in mouse strains were
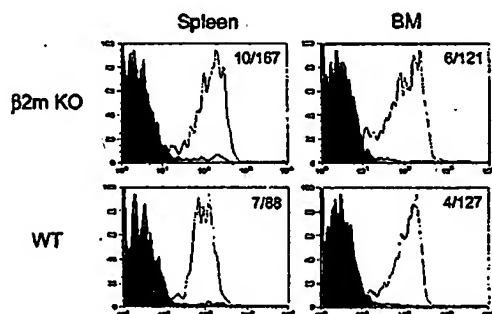

FIGURE 5. Comparison of Ly49Q expression levels between β_2m$^{-/-}$ and control mice. DCs were prepared from the spleen and BM as described in *Materials and Methods*. CD19$^-$B220$^+$ cells were gated and Ly49Q expression was examined. Numeric data in histograms indicate the mean fluorescence intensity of histograms representing staining patterns using control (*left sides*) or anti-Ly49Q (*right sides*) mAbs.

confirmed by digesting the PCR products corresponding to Ly49Q with restriction enzymes (Fig. 6). We identified at least three alleles, tentatively termed *Ly49q1a*, *q1b*, and *q1c*, possessing nucleotide variations at 10 residues and amino acids variations at 7 residues (Fig. 7A). Four of the seven amino acid variations were identified within stalk regions, and three within the CRD region. The cytoplasmic regions, including ITIMs, were completely conserved. No correlations between MHC haplotypes and Ly49Q allele types were observed (Fig. 7B). Based on previous studies showing crystal structures of Ly49A and Ly49C, polymorphisms at position 229 and at position 253, respectively, resided in loops 3 and 6, which are important for recognition of MHC class I and β_2m by Ly49A (Fig. 7C) (37–39).

We further identified three additional exons in the *Ly49q1* gene and four additional splice variants of Ly49Q1 in mouse strains 129, JF1, and MSM (Fig. 8, *A* and *B*). To examine the surface expression of newly identified alleles and isoforms, FLAG-tagged Ly49Q1 cDNA was introduced into COS7 cells, their expression was tested using anti-Ly49Q and anti-FLAG mAbs (Fig. 8C). All three alleles of *Ly49q1* were expressed on the surface and recognized by anti-Ly49Q mAb as well as by anti-FLAG mAb, although the efficiency of Ly49Q1c expression was lower than that of other two alleles. Expression of the four isoforms was not detected using anti-Ly49Q mAb and anti-FLAG mAb. In biochemical analysis of these isoforms, degradation products derived from FLAG-tagged proteins was detectable, suggesting that these isoforms are not stably expressed in cells (data not shown).

Discussion

We have demonstrated that an ITIM-bearing inhibitory receptor, Ly49Q, was expressed on DC subsets. Freshly isolated plasmacytoid pre-DCs expressed Ly49Q on their surface. In contrast, in most mouse strains, freshly prepared myeloid DCs did not express Ly49Q. However, GM-CSF-induced myeloid DCs prepared from BM expressed low but significant levels of Ly49Q. Of particular interest, expression of Ly49Q was greatly enhanced when DCs were treated with IFN-α or IFN-γ. A panel of ligands for TLRs

FIGURE 6. Detection of allelic variations of *Ly49q1* genes using digestion with restriction enzymes. *A,* Recognition sites of restriction enzymes identified in three different alleles. *B,* Comparison of restriction maps of Ly49Q between C57BL/6, BALB/c, and 120 × 1/Sv mice. These three alleles can be discriminated by the electrophoretic mobility of DNA fragments obtained by enzyme treatments with PCR products corresponding to the full-length Ly49Q. *C,* Electrophoretic patterns of Ly49Q PCR products treated with restriction enzymes indicated. Full-length cDNA of Ly49Q1 was amplified from BM of C57BL/6 and BALB/c using *Ly49q*-specific primers as described in *Materials and Methods,* and treated with restriction enzymes. Allelic variations at indicated positions were detectable by this treatment.
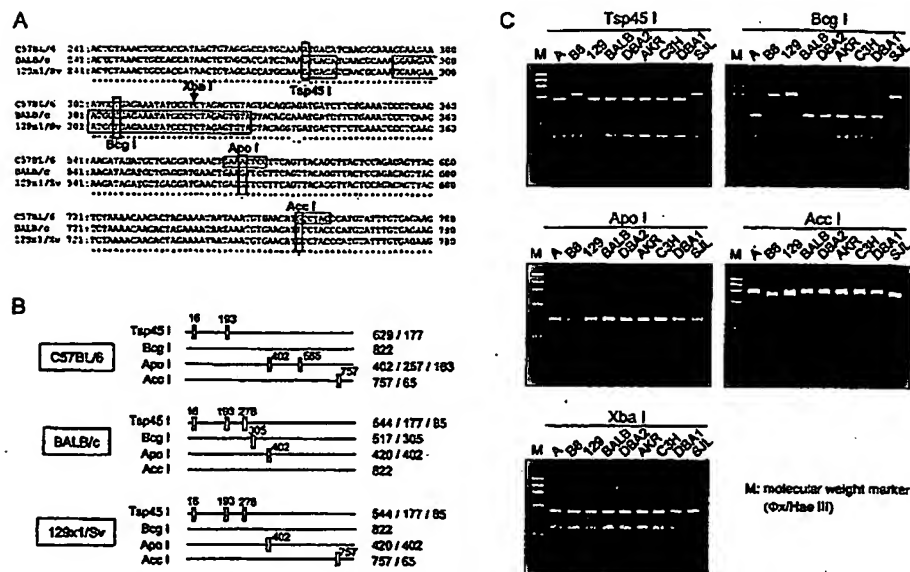
bad minimal effect on Ly49Q expression in our assay conditions. Therefore, DCs express Ly49Q depending on their maturational/activation states and on their cytokine environments. This also implies a potential role of Ly49Q in immune responses under certain circumstances such as virus infection.

Ly49Q expression seems to be regulated through the differentiation and activation process of DC subsets, as has been observed in monocytes/macrophages (9). Flt3L-induced BM-derived plasmacytoid pre-DCs expressed lower levels of Ly49Q than freshly prepared plasmacytoid pre-DCs from the BM or spleen. Based on their lower levels of surface expression of CD80, CD86, and MHC class II and of their lower production of IFN-α, plasmacytoid pre-DCs in Flt3L-cultured BM cells are considered less mature than those in peripheral lymphoid organs (40). Therefore, expression of Ly49Q on plasmacytoid pre-DCs appears to be enhanced as they mature. Compared with plasmacytoid pre-DCs, myeloid DCs showed a different pattern of Ly49Q expression. Because detect-

able levels of Ly49Q were observed on GM-CSF-cultured BM-DCs but not on freshly prepared myeloid DCs from spleens, we speculate that the surface expression of Ly49Q decreases during differentiation in myeloid DCs. Treatment of GM-CSF-cultured BM-DCs with IFN-α induced a substantial increase in Ly49Q expression, suggesting that myeloid DCs re-express Ly49Q in the presence of IFN-α. In addition, myeloid DCs in some mouse strains expressed Ly49Q on their surface. Taken together, it is likely that Ly49Q plays a role not only in plasmacytoid pre-DCs, but also in myeloid DCs in some circumstances. Expression of other inhibitory receptors such as PIR-A/B and SIRP on GM-CSF- and Flt3L-cultured BM-DCs, as well as Ly49A, Ly49C, and CD94 on NK cells, was not affected by the treatment with IFN-α (data not shown). The selective enhancement of Ly49Q expression by IFN-α or IFN-γ may imply potential roles for Ly49Q in immune responses elicited by virus infections. Further investigations are necessary to clarify this.
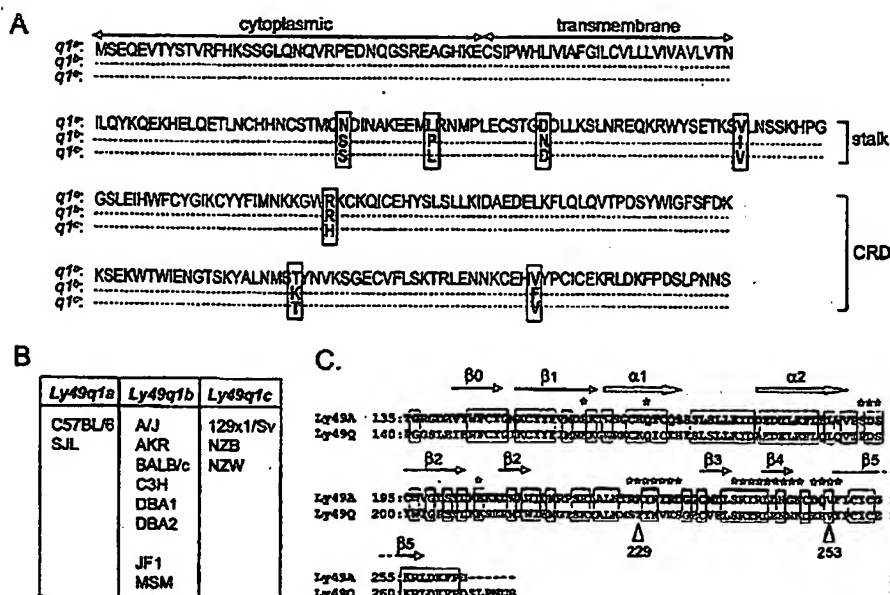

FIGURE 7. Alignment of *Ly49q1* sequences from various mouse strains. *A,* Amino acid sequences of the *Ly49q1* gene from various mouse strains were determined. Amino acids possessing allelic variations are shown in boxes. Three alleles of *Ly49q1* were identified. *B,* Types of *Ly49q1* alleles in various mouse strains are shown. *C,* Positions of polymorphic residues of Ly49Q. Asterisks denote contact sites of Ly49A with H-2D^d (37). Lys^{224} and Val^{24N} of Ly49A, respectively correspond to Thr/Lys^{229} and Val/Phe^{253} polymorphic residues in Ly49Q.

FIGURE 8. Spliced variants of Ly49Q. *A,* Schematic presentation of the exon-intron organization of the *Ly49q1* gene. Exons are boxed. Shaded boxes denote newly identified exons in 129, JF1, and MSM mice. Asterisks denote translation stop codons. GenBank accession numbers for newly identified isoforms are as follows: Cyt, AB193830; CDR1, AB193831; CDR2, AB193832; and CDR3, AB193833. *B,* Sequences of splice junctions. Sequences corresponding to boundaries between exons and introns were retrieved from the genome sequence of mouse chromosome 6 including KIra17 (Ensemble gene ID: ENS-MUSG00000014543). *C,* Reconstitution of Ly49Q allelic variants and isoforms in COS7 cells. FLAG-tagged Ly49Q cDNA encoding allelic variants and isoforms were introduced into COS7 cells. Cells were stained 48 h after transfection with biotin-conjugated anti-Ly49Q or anti-FLAG mAbs. Biotin-conjugated mAbs were revealed using PE-conjugated streptavidin.
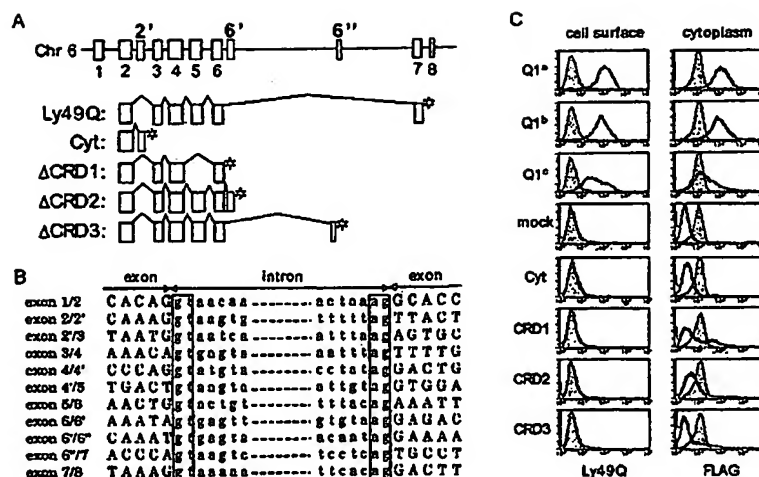
Transitional expression of Ly49Q during differentiation/maturation processes of myeloid DCs seems to parallel that of monocytes/macrophages (9). Gr-1^{+} immature myeloid cells, including immature monocytes, expressed high levels of Ly49Q in the BM. Expression of Ly49Q seemed to disappear in circulating monocytes in peripheral blood, and then appeared after activation. Similarity of Ly49Q expression patterns suggests similar functions of Ly49Q in DCs and in macrophages. Our previous study demonstrated that Ly49Q itself introduces signals from extracellular to intracellular to rearrange the cytoskeleton, resulting in rapid spreading and formation of pseudopods in IFN-γ-activated macrophages (9). We observed a similar effect of anti-Ly49Q mAb on the morphology of IFN-α-stimulated plasmacytoid pre-DCs (data not shown). We also observed that anti-Ly49Q mAb used in this study had no effect on the production of IFN-α and other cytokines by plasmacytoid pre-DCs (data not shown). Although further analysis is required to clarify the function of Ly49Q in macrophages and DC subsets, our findings suggest a unique common regulatory mechanism in professional APCs, such as macrophages and DCs, for regulating cytoskeleton and cell adhesiveness through an inhibitory receptor.

Compared with other C-type lectins expressed on DCs, such as DEC-205 and DC-SIGN, Ly49Q seems to play distinct roles. DEC-205, Langerin (CD207), Lox-1, and mouse macrophage galactose-type C-type lectin recognize carbohydrate profiles on microorganisms, and are involved in internalization, processing and presentation of foreign Ags (41–45). Although Ly49Q does not possess a typical leucine-based internalization motif in its cytoplasmic region, the YxxL sequence in its cytoplasmic ITIM could be related with a tyrosine-based internalization motif Yxxϕ, where ϕ is any bulky hydrophobic residue (46). However, involvement of Ly49Q in Ag uptake may be less possible. Incubation of murine macrophage cell lines with anti-Ly49Q mAbs together with anti-rat IgG did not induce an internalization of this molecule from the surface of macrophage cell lines (A. Kikuchi-Maki and N. Toyama-Sorimachi, unpublished observation). Therefore, Ly49Q appears not to be involved in Ag uptake or internalization. In addition, Ly49Q, like other Ly49 family members, does not contain either the essential motif necessary for recognition of mannose- or galactose-containing carbohydrates, or amino acid residues involved in calcium binding, which is conserved in other calcium-dependent lectins. Therefore, it is reasonable to assume that Ly49Q is not associated with recognition and internalization of microbes via carbohydrate structures.

We now know that inhibitory Ly49 family members expressed on NK and NKT cells recognize MHC class I molecules and are responsible for self-nonself discriminations (1–3). Based on the high structural similarity between Ly49Q and other conventional Ly49 family members expressed on NK and T cell subsets, we hypothesize that Ly49Q also recognizes MHC class I or its related molecules. Based on this point of view, it is of particular interest to determine whether Ly49Q possesses allelic polymorphisms. Sequence analysis of Ly49Q cDNA isolated from various mouse strains indicated that Ly49Q is a polymorphic receptor, similar to other Ly49 family members, suggesting that the ligand for Ly49Q may be a polymorphic molecule. Structural analysis from crystallography indicated that loops 1, 5, and β-sheet 4 are important in the recognition of MHC class I by both Ly49A and Ly49C (37, 38). In addition, in the case of Ly49A, loops 3 and 6 are important for the recognition of MHC class I and the associated β_2m (37). In the case of Ly49A, valine at position 253 is especially important in interaction with β_2m. Importantly, amino acid substitutions between polymorphic alleles at position 239 and 253 reside in loops 3 and 6, respectively. Therefore, we speculate that the polymorphic variations in Ly49Q may influence its ligand recognition.

Previous studies have demonstrated that expression levels of other Ly49 molecules on NK cells were apparently regulated by corresponding MHC class I molecules (receptor calibration model) (34–36). Our comparison of expression levels of Ly49Q in various mouse strains showed that there was no correlation between the expression levels of Ly49Q and MHC class I haplotypes. However, expression levels of Ly49Q were affected by the lack of β_2m, suggesting that a ligand for Ly49Q is a β_2m-associated molecule. Interestingly, the effect of β_2m on Ly49Q expression was observed only in the spleen, implying that Ly49Q expression was conditioned during the plasmacytoid pre-DC maturation process. Although a ligand for Ly49Q is yet to be unidentified, it is likely that both the ligand and the cytokine environment exert an influence on the Ly49Q expression level because IFNs greatly enhanced the Ly49Q expression levels.

Ly49Q expression was widely observed in plasmacytoid pre-DCs in all mouse strains examined, suggesting the importance of this molecule in these cells. Of interest, freshly prepared myeloid DCs in mouse strains 129, NZB, and NZW expressed considerably higher levels of Ly49Q in a steady state. Our analysis indicated that Ly49Q1 has several isoforms and alleles. In addition, *Ly49q2* and *q3* genes exist in some mouse strains. Therefore, exceptional staining of myeloid DCs by anti-Ly49Q mAb may be due to the

expression of Ly49Q1-related molecules including Ly49Q2, Q3, and isoforms of Q1. However, genomic and RT-PCR analysis demonstrated that Ly49Q2 and Q3 were not expressed in DCs in mouse strains 129, NZB, and NZW. Furthermore, in our reconstitution experiments, Ly49Q1 isoforms appeared not to be expressed. Therefore, rather than being due to cross-reactivity of anti-Ly49Q mAb to Ly49Q1-related molecules on myeloid DCs, it seems to be more likely that Ly49Q1 expression is elicited on myeloid DCs because of cytokine environment differences present in these three mice strains. Previous observation showing that that 129 mice produce a higher amount of IFN-α compared with other laboratory mouse strains may support this notion (47).

In conclusion, Ly49Q is an inhibitory receptor expressed on DC subsets. Expression is regulated during DC differentiation/maturation. IFN-α is the most potent inducer of Ly49Q, suggesting important roles of this molecule in combating viral infection. The possible roles of Ly49Q in regulation of the cytoskeleton are particularly interesting because reorganization of cytoskeleton is an important event in DC functions including migration, Ag presentation, and cytokine production. Further investigation to gain insights into the physiological roles of Ly49Q will help elucidate cytoskeletal regulation of DCs as well as a novel recognition mechanism for DCs through a MHC class I receptor.

Acknowledgements

Disclosures

References

1. Lanier, L. L. 1998. NK cell receptors. *Annu. Rev. Immunol.* 16:359.
2. Takei, F., K. L. McQueen, M. Maeda, B. T. Wilhelm, S. Lohwasser, R. H. Lian, and D. L. Mager. 2001. Ly49 and CD94/NKG2: developmentally regulated expression and evolution. *Immunol. Rev.* 181:90.
3. Anderson, S. K., J. R. Ortaldo, and D. W. McVicar. 2001. The ever-expanding Ly49 gene family: repertoire and signaling. *Immunol. Rev.* 181:79.
4. Karlhofer, M., R. K. Ribaudo, and W. M. Yokoyama. 1992. MHC class I alloantigen specificity of Ly-49$^+$ IL-2-activated natural killer cells. *Nature* 358:66.
5. Mason, L. H., J. R. Ortaldo, H. A. Young, V. Kumar, M. Bennett, and S. K. Anderson. 1995. Cloning and functional characteristics of murine large granular lymphocyte-1: a member of the Ly-49 gene family (Ly-49G2). *J. Exp. Med.* 182:293.
6. Yu, Y. Y. L., T. George, J. R. Dorfman, J. Roland, V. Kumar, and M. Bennett. 1996. The role of Ly49A and 5E6 (Ly49C) molecules in hybrid resistance mediated by murine natural killer cells against normal T cell blasts. *Immunity* 4:67.
7. Nakamura, M. C., E. C. Niemi, M. J. Fisher, L. D. Shultz, W. E. Seaman, and J. C. Ryan. 1997. Mouse Ly-49A interrupts early signaling events in natural killer cell cytotoxicity and functionally associates with the SHP-1 tyrosine phosphatase. *J. Exp. Med.* 185:673.
8. Hanke, T., H. Takizawa, C. W. McMahon, D. H. Busch, E. G. Pamer, J. D. Miller, J. D. Altman, Y. Liu, D. Cado, F. A. Lemonnier, et al. 1999. Direct assessment of MHC class I binding by seven Ly49 inhibitory NK receptors. *Immunity* 11:67.
9. Toyama-Sorimachi, N., Y. Tsujimura, M. Maruya, A. Onoda, T. Kubota, S. Koyasu, K. Inaba, and H. Karasuyama. 2004. Ly49Q, a member of the Ly49 family that is selectively expressed on myeloid lineage cells and involved in regulation of cytoskeletal architecture. *Proc. Natl. Acad. Sci. USA* 101:1016.
10. Banchereau, J., F. Briere, C. Caux, J. Davoust, S. Lebecque, Y. J. Liu, B. Pulendran, and K. Palucka. 2000. Immunology of dendritic cells. *Annu. Rev. Immunol.* 18:767.
11. Lanzavecchia, A., and F. Sallusto. 2001. The instructive role of dendritic cells on T cell responses: lineages, plasticity and kinetics. *Curr. Opin. Immunol.* 13:291.
12. Guermonprez, P., J. Valladeau, L. Zitvogel, C. Thery, and S. Amigorena. 2002. Antigen presentation and T cell stimulation by dendritic cells. *Annu. Rev. Immunol.* 20:621.

13. Steinman, R. M., D. Hawiger, K. Liu, L. Bonifaz, D. Bonnyay, K. Mahnke, T. Iyoda, J. Ravetch, M. Dhodapkar, K. Inaba, and M. Nussenzweig. 2003. Dendritic cell function in vivo during the steady state: a role in peripheral tolerance. *Ann. NY Acad. Sci.* 987:15.
14. Nakano, H., M. Yanagishita, and M. D. Gunn. 2001. CD11c$^+$ B220$^+$ Gr-1$^+$ cells in mouse lymph nodes and spleen display characteristics of plasmacytoid dendritic cells. *J. Exp. Med.* 194:1171.
15. Asselin-Paturel, C., A. Boonstra, M. Dalod, I. Durand, N. Yessaad, C. Dezutter-Dambuyant, A. Vicari, A. O'Garra, C. Biron, F. Briere, and G. Trinchieri. 2001. Mouse type I IFN-producing cells are immature APCs with plasmacytoid morphology. *Nat. Immunol.* 2:1144.
16. Kelsall, B. L., E. Stuber, M. Neurath, and W. Strober. 1996. Interleukin-12 production by dendritic cells: the role of CD40-CD40L interaction in Th1 T-cell responses. *Ann. NY Acad. Sci.* 795:116.
17. Kaisho, T., and S. Akira. 2001. Dendritic-cell function in Toll-like receptor-and MyD88-knockout mice. *Trends Immunol.* 22:78.
18. Figdor, C. G., Y. van Kooyk, and G. J. Adema. 2002. C-type lectin receptors on dendritic cells and Langerhans cells. *Nat. Rev. Immunol.* 2:77.
19. Engering, A., T. B. Geijtenbeek, and Y. van Kooyk. 2002. Immune escape through C-type lectins on dendritic cells. *Trends Immunol.* 23:480.
20. van Kooyk, Y., and T. B. Geijtenbeek. 2003. DC-SIGN: escape mechanism for pathogens. *Nat. Rev. Immunol.* 3:697.
21. Cambi, A., and C. G. Figdor. 2003. Dual function of C-type lectin-like receptors in the immune system. *Curr. Opin. Cell Biol.* 15:539.
22. Geijtenbeek, T. B., D. S. Kwon, R. Torensma, S. J. van Vliet, G. C. van Duijnhoven, J. Middel, I. L. Cornelissen, H. S. Nottet, V. N. KewalRamani, D. R. Littman, et al. 2000. DC-SIGN, a dendritic-cell-specific HIV-1-binding protein that enhances trans-infection of T cells. *Cell* 100:587.
23. Geijtenbeek, T. B., R. Torensma, S. J. van Vliet, G. C. van Duijnhoven, D. J. Adema, Y. van Kooyk, and C. G. Figdor. 2000. Identification of DC-SIGN, a novel dendritic cell-specific ICAM-3 receptor that supports primary immune responses. *Cell* 100:575.
24. Dzionek, A., A. Fuchs, P. Schmidt, S. Cremer, M. Zysk, S. Miltenyi, D. W. Buck, and J. Schmitz. 2000. BDCA-2, BDCA-3, and BDCA-4: three markers for distinct subsets of dendritic cells in human peripheral blood. *J. Immunol.* 165:6037.
25. Kanazawa, N., T. Okazaki, H. Nishimura, K. Tashiro, K. Inaba, and Y. Miyachi. 2002. DCIR acts as an inhibitory receptor depending on its immunoreceptor tyrosine-based inhibitory motif. *J. Invest. Dermatol.* 118:261.
26. Kubagawa, H., C. C. Chen, L. H. Ho, T. S. Shimada, L. Gartland, C. Mashburn, T. Uehara, J. V. Ravetch, and M. D. Cooper. 1999. Biochemical nature and cellular distribution of the paired immunoglobulin-like receptors, PIR-A and PIR-B. *J. Exp. Med.* 189:309.
27. Fournier, N., L. Chalus, I. Durand, E. Garcia, J. J. Pin, T. Churakova, S. Patel, C. Zlot, D. Gorman, S. Zurawski, et al. 2000. FDF03, a novel inhibitory receptor of the immunoglobulin superfamily, is expressed by human dendritic and myeloid cells. *J. Immunol.* 165:1197.
28. Nakamura, A., E. Kobayashi, and T. Takai. 2004. Exacerbated graft-versus-host disease in Pirb$^{-/-}$ mice. *Nat. Immunol.* 5:623.
29. Gilliet, M., A. Boonstra, C. Paturel, S. Antonenko, X.-L. Xu, G. Trinchieri, A. O'Garra, and Y.-J. Liu. 2002. The development of murine plasmacytoid dendritic cell precursors is differentially regulated by FLT3-ligand and granulocyte/macrophage colony-stimulating factor. *J. Exp. Med.* 195:953.
30. Inaba, K., M. Pack, M. Inaba, H. Sakuta, F. Isdell, and R. M. Steinman. 1997. High levels of a major histocompatibility complex II-self peptide complex on dendritic cells from the T cell areas of lymph nodes. *J. Exp. Med.* 186:665.
31. Inaba, K., M. Inaba, N. Romani, H. Aya, M. Deguchi, S. Ikehara, S. Muramatsu, and R. M. Steinman. 1992. Generation of large numbers of dendritic cells from mouse bone marrow cultures supplemented with granulocyte/macrophage colony-stimulating factor. *J. Exp. Med.* 176:1693.
32. Makrigiannis, A. P., A. T. Pau, P. L. Schwartzberg, D. W. McVicar, T. W. Beck, and S. K. Anderson. 2002. A BAC contig map of the Ly49 gene cluster in 129 mice reveals extensive differences in gene content relative to C57BL/6 mice. *Genomics* 79:437.
33. Proteau, M.-F., E. Rousselle, and A. P. Makrigiannis. 2004. Mapping of the BALB/c Ly49 cluster defines a minimal natural killer cell receptor gene repertoire. *Genomics* 84:669.
34. Sundback, J., K. Karre, and C. L. Sentman. 1996. Cloning of minimally divergent allelic forms of the natural killer (NK) receptor Ly-49C, differentially controlled by host genes in the MHC and NK gene complexes. *J. Immunol.* 157:3936.
35. Salcedo, M., A. D. Diehl, M. Y. Olsson-Alheim, J. Sundback, L. van Kaer, K. Karre, H.-G. Ljunggren. 1997. Altered expression of Ly-49 inhibitory receptors on natural killer cells from MHC class I-deficient mice. *J. Immunol.* 158:3174.
36. Olsson, M. Y., K. Karre, C. L. Sentman. 1995. Altered phenotype and function of natural killer cells expressing the major histocompatibility complex receptor Ly-49 in mice transgenic for its ligand. *Proc. Natl. Acad. Sci. USA* 92:1649.
37. Tormo, J., K. Natarajan, D. H. Margulies, and R. A. Mariuzza. 1999. Crystal structure of a lectin-like natural killer cell receptor bound to its MHC class I ligand. *Nature* 402:623.
38. Dam, J., R. Guan, K. Natarajan, N. Dimasi, L. K. Chlewicki, D. M. Kranz, P. Schuck, D. H. Margulies, and R. A. Mariuzza. 2003. Variable MHC class I engagement by Ly49 natural killer cell receptors demonstrated by the crystal structure of Ly49C bound to H-2K^b. *Nat. Immunol.* 4:1213.

39. Dimasi, N., M. W. Sawicki, L. A. Reineck, Y. Li, K. Natarajan, D. H. Margulies, and R. A. Mariuzza. 2002. Crystal structure of the Ly49I natural killer cell receptor reveals variability in dimerization mode within the Ly49 family. *J. Mol. Biol.* 320:573.

40. Brawand, P., D. R. Fitzpatrick, B. W. Greenfield, K. Brasel, C. R. Maliszewski, and T. De Smedt. 2002. Murine plasmacytoid pre-dendritic cells generated from Flt3 ligand-supplemented bone marrow cultures are immature APCs. *J. Immunol.* 169:6711.

41. Jiang, W., W. J. Swiggard, C. Heufler, M. Peng, A. Mirza, R. M. Steinman, and M. C. Nussenzweig. 1995. The receptor DEC-205 expressed by dendritic cells and thymic epithelial cells is involved in antigen processing. *Nature* 375:151.

42. Mahnke, K., M. Guo, S. Lee, H. Sepulveda, S. L. Sain, M. Nussenzweig, and R. M. Steinman. 2000. The dendritic cell receptor for endocytosis, DEC-205, can recycle and enhance antigen presentation via major histocompatibility complex class II-positive lysosomal compartments. *J. Cell Biol.* 151:673.

43. Takahara, K., Y. Yashima, Y. Omatsu, H. Yoshida, Y. Kimura, Y. S. Kang, R. M. Steinman, C. G. Park, and K. Inaba. 2004. Functional comparison of the mouse DC-SIGN, SIGNR1, SIGNR3 and Langerin, C-type lectins. *Int. Immunol.* 16:819.

44. Denda-Nagai, K., N. Kubota, M. Tsuiji, M. Kamata, and T. Irimura. 2002. C-type lectin on bone marrow-derived immature dendritic cells is involved in the internalization of glycosylated antigens. *Glycobiology* 12:443.

45. Delneste, Y., G. Magistrelli, J. Gauchat, J. Haeuw, J. Aubry, K. Nakamura, N. Kawakami-Honda, L. Goetsch, T. Sawamura, J. Bonnefoy, and P. Jeannin. 2002. Involvement of LOX-1 in dendritic cell-mediated antigen cross-presentation. *Immunity* 17:353.

46. Bonifacino, J. S., and E. C. Dell'Angelica. 1999. Molecular bases of the recognition of tyrosine-based sorting signals. *J. Cell Biol.* 145:923.

47. Asselin-Paturel, C., B. Geraldine, J.-J. Pin, F. Briere, and G. Trinchieri. 2003. Mouse strain differences in plasmacytoid dendritic cell frequency and function revealed by a novel monoclonal antibody. *J. Immunol.* 171:6466.

TREMS IN THE IMMUNE SYSTEM AND BEYOND

Marco Colonna

Triggering receptors expressed by myeloid cells (TREMs) belong to a rapidly expanding family of receptors that include activating and inhibitory isoforms encoded by a gene cluster linked to the MHC. TREM1 and TREM2 activate myeloid cells by signalling through the adaptor protein DAP12. TREM1 triggers phagocyte secretion of pro-inflammatory chemokines and cytokines, amplifying the inflammation that is induced by bacteria and fungi. TREM2 activates monocyte-derived dendritic cells and regulates osteoclast development. Remarkably, TREM2 deficiency leads to a severe disease that is characterized by bone cysts and demyelination of the central nervous system, which results in dementia, implying that the function of TREM2 extends beyond the immune system.

*Department of Pathology and Immunology, Washington University School of Medicine, 660 South Euclid Avenue, St Louis, Missouri 63110, USA.
e-mail: mcolonna@pathbox.wustl.edu*
doi:10.1038/nri1106

During the onset of an infection, the host must launch a rapid innate response to control pathogen proliferation and spread until the adaptive response of specific T and B cells has fully developed. This first line of defence is provided by the coordinate action of several effector cell types, including phagocytes and natural killer (NK) cells. These cells express a large array of cell-surface receptors, some of which detect pathogens and trigger responses to infectious and/or inflammatory stimuli. The germline encoded Toll-like receptors (TLRs) allow the direct recognition of distinct microbial structures that are shared by microorganisms, such as lipopolysaccharide (LPS), lipoteichoic acid (LTA), flagellin and bacterial DNA[1–4]. The mannose, scavenger and dectin receptors mediate binding and phagocytosis of microorganisms and foreign particles[5–7]. Fc, complement and scavenger receptors further facilitate the clearance of microorganisms that are coated with opsonic proteins, such as immunoglobulins, complement fragment C3b and mannose-binding lectin[5,8,9].

Innate immune cells also express receptors of the immunoglobulin and lectin-like superfamilies that recognize ubiquitously expressed endogenous molecules, including MHC class I molecules[10,11], CD47 (REF. 12), CD200 (REFS 13–15) and sialic acids[16]. These receptors contain cytoplasmic immunoreceptor tyrosine-based
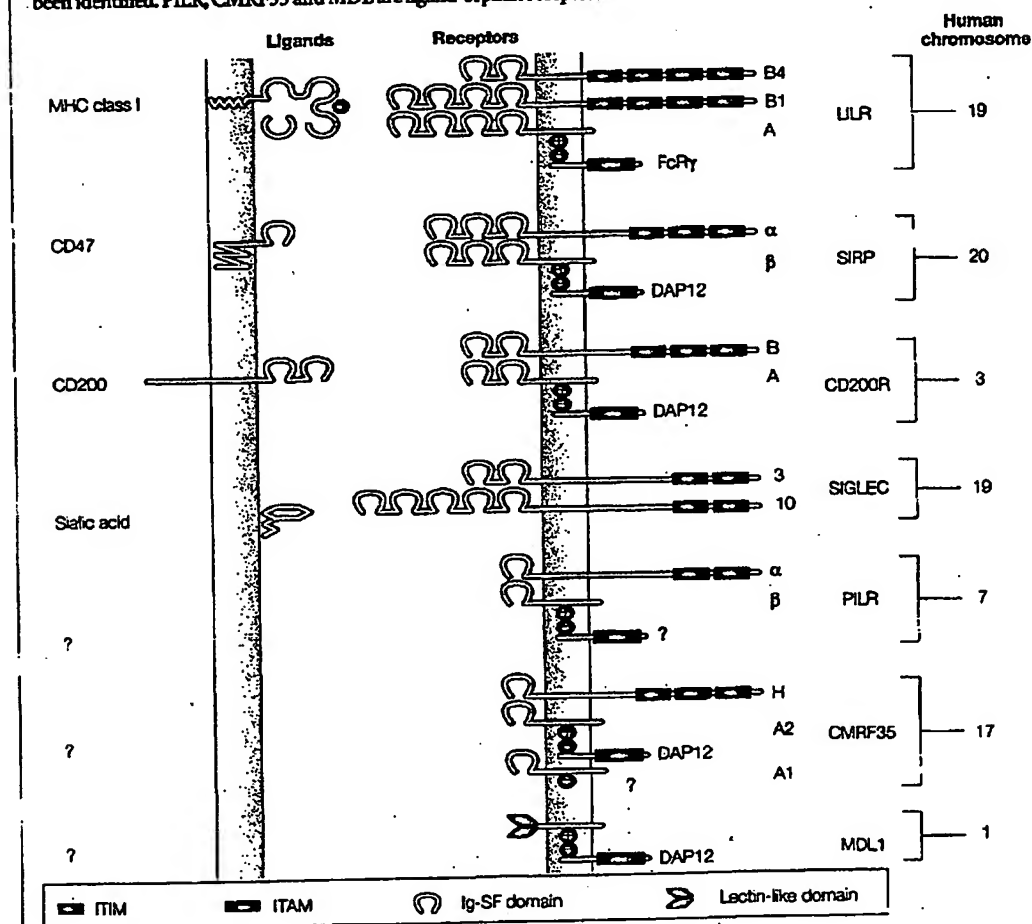
inhibitory motifs (ITIMs), which recruit protein tyrosine phosphatases that mediate inhibition. So, phagocytes and NK cells normally receive continuous 'off' signals that are generated by inhibitory receptors interacting with their cognate ligands. These constant inhibitory signals provide tolerance to 'self'. During infection, activating signals that are delivered by the pathogen receptors overrule those that are transmitted by inhibitory receptors, promoting innate responses. Furthermore, certain pathogens induce the downregulation of expression of inhibitory ligands, thereby enabling activation of phagocytes and NK cells. Therefore, innate responses to pathogens and tolerance to self depend on a dynamic equilibrium between the activating signals that are transduced by pathogen receptors and the inhibitory signals that are mediated by self receptors.

Intriguingly, inhibitory receptors are usually encoded in clusters that also include genes encoding activating isoforms[17]. Inhibitory and activating isoforms are similar in their extracellular domains. Activating receptors, however, lack cytoplasmic signalling elements, but contain a charged residue in their transmembrane domain that facilitates the association with transmembrane adaptor proteins. Most of these adaptors, including the γ-chain of Fc receptors, DAP12 and

Box 1 | Activating and inhibitory receptor pairs expressed by myeloid cells

- Human leukocyte immunoglobulin-like receptors (LILRs)[67] comprise at least five inhibitory (LILRB1–5) and three activating (LILRA1–3) receptors. LILRB1 and LILRB2 recognize virtually all human MHC class I molecules[67–73]. LILRB1 also binds the human cytomegalovirus (HCMV)-encoded class-I-like molecule UL18 (REF. 69). LILRA1 binds the free heavy-chain form of HLA-B27 (REF. 72). LILRAs deliver activating signals through the Fc receptor for IgG (FcγR)[73]. The mouse counterparts of LILRs are the paired immunoglobulin-like receptors (PIRs)[74].

- Signal regulatory proteins (SIRPs)[75] include SIRP-α1, SIRP-β1 and SIRP-β2. SIRP-α1 binds CD47 (also known as integrin-associated protein)[76] and inhibits macrophages and dendritic cells. Accordingly, CD47-deficient red blood cells, which fail to engage SIRP-1α, are phagocytosed by spleen macrophages[81]. SIRP-β1 activates myeloid cells through DAP12 (REFS 78,79). Its ligand specificity is unknown. Potential SIRP ligands include poxvirus-encoded homologues of CD47.

- CD200 receptors (CD200Rs) comprise one inhibitory isoform that recognizes CD200 and inhibits macrophages[80–82]. Accordingly, lack of CD200–CD200R interaction facilitates the activation of macrophages and exacerbates experimental allergic encephalomyelitis (EAE)[80–82]. CD200Rs also include an activating isoform that signals through DAP12 (J. H. Philips et al., unpublished observations). Its ligand specificity is unknown. Potential ligands of CD200Rs include a human herpesvirus-8-encoded homologue of CD200.

- Sialic-acid-binding immunoglobulin-like lectins (SIGLECs) are characterized by an amino-terminal V-set immunoglobulin-like domain that binds to sialic-acid residues followed by a variable number of C2-set immunoglobulin-like domains ranging from 1 to 16 (REF. 16). SIGLEC 3 (CD33), 5, 7, 8 and 9 are expressed by myeloid cells and deliver inhibitory signals.

- Paired immunoglobulin-like receptors (PILRs) include PILRα (also known as FDF03), which inhibits Ca²⁺ mobilization that is triggered by the low-affinity receptor for IgG (FcγRII). PILRβ is a putative activating receptor[83,84].

- CMRF35 receptors comprise one inhibitory receptor (CMRF35H) and six putative activating receptors (CMRF35A1–A6)[31–33,85]. Whereas one activating receptor (CMRF35A2) signals through DAP12, the others have a transmembrane glutamic-acid residue and therefore might use as-yet-unknown signalling adaptors.

- The myeloid DAP12-associated receptor 1 (MDL1) triggers cell activation[96]. MDL1 inhibitory counterparts have not been identified. PILR, CMRF35 and MDL are ligand-orphan receptors.
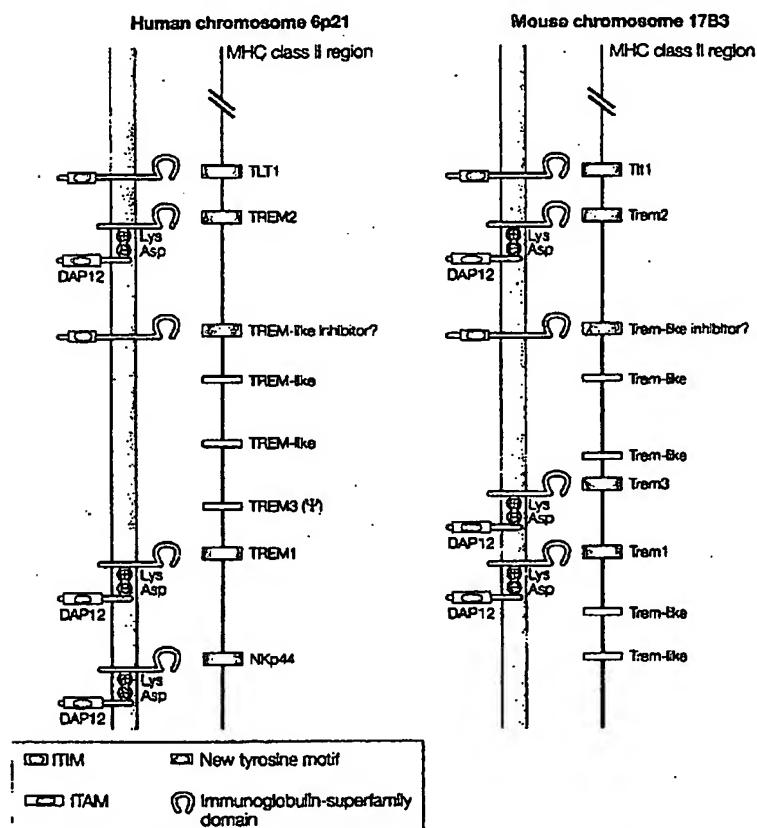
Human chromosome 6p21

MHC class II region

TLT1
TREM2
DAP12
TREM-like Inhibitor?
TREM-like
TREM-like
TREM3 (Ψ)
TREM1
DAP12
NKp44
DAP12

Mouse chromosome 17B3

MHC class II region

Tlt1
Trem2
DAP12
Trem-like inhibitor?
Trem-like
Trem-like
Trem3
DAP12
Trem1
DAP12
Trem-like
Trem-like

ITIM
ITAM
New tyrosine motif
Immunoglobulin-superfamily domain

Figure 1 | **Organization of the human and mouse TREM gene cluster.** Schematic diagram that compares the order of genes in the TREM (triggering receptors expressed by myeloid cells) clusters in humans and mice. Genes encoding activating TREMs and NKp44 are shown as purple boxes. There is a putative inhibitory gene TREM-like transcript 1 (TLT1), which encodes a potential immunoreceptor tyrosine-based inhibitory motif (ITIM) in the cytoplasmic domain. An additional TREM-like gene (orange box) with unusual cytoplasmic tyrosine motifs and TREM-like immunoglobulin domains (white boxes) have been annotated in the completed human and mouse Genome Projects carried out by the National Centre for Biotechnology Information. TREM genes are closely linked to the MHC class II region. TREM3 is a pseudogene (Ψ) in humans. Models of the encoded molecules are shown below the genes. The DAP12 adaptor for activating forms is also shown.

In this article, I review studies on a recently discovered family of receptors, known as triggering receptors expressed by myeloid cells (TREMs), which comprise at least one inhibitory and two activating receptors of the immunoglobulin gene family. The activating iso-forms of this family are unique in that one receptor, TREM1, controls inflammation, whereas another, TREM2, regulates the development and function of dendritic cells (DCs), as well as MICROGLIA and osteoclasts. Moreover, a genetic defect in TREM2 results in a human disease that is characterized by brain and bone abnormalities, providing the first example of an activating receptor that affects the function of both immune and non-immune cells.

Molecular characterization of TREMs

Human TREM1 and TREM2 are transmembrane glyco-proteins that consist of a single extracellular immuno-globulin-like domain of the V-type, a transmembrane region with a charged lysine residue and a short cyto-plasmic tail[24] (FIG. 1). Both receptors associate with DAP12 for signalling and function[24,25]. The cytoplasmic domain of DAP12 contains an ITAM, which, after phos-phorylation, provides a docking site for the tyrosine kinases ζ-chain-associated protein 70 (ZAP70) and spleen tyrosine kinase (SYK). These promote the recruitment and tyrosine phosphorylation of adaptor complexes that contain CBL and growth factor receptor binding protein 2 (GRB2), which activate phosphatidy-linositol 3-kinase (PI3K), phospholipase Cγ1 and p44-p42 extracellular-signal-regulated kinase (ERK) pathways[26]. The triggering of these pathways ultimately leads to intracellular Ca²⁺ mobilization, rearrangement of the actin cytoskeleton and activation of several tran-scription complexes. An alternative messenger RNA splice variant of TREM1 (TREM1sv) has also been detected, which lacks the transmembrane and cytoplas-mic domains. If translated, it might generate a secreted TREM1 decoy that could potentially modulate TREM1-mediated signalling and activation[27]. Mouse counterparts of TREM1 and TREM2 have been identified, as well as a third complementary DNA that encodes Trem3, which exists only as a pseudogene in humans[24,28,29] (FIG. 1). Mouse Trem2 and Trem3 associate with endogenous DAP12 in transfected macrophage cell lines and promote cellular activation and release of nitric oxide[28,29].

TREM1 and TREM2 have limited homology with other members of the immunoglobulin gene superfam-ily. The closest TREM relative is NKp44, an activating NK-cell receptor that is encoded by a gene closely linked to the TREM genes[30]. More distant relatives of TREMs include the CMRF35-family members[31-33]. The posi-tively charged lysine residue that is common to the transmembrane regions of TREMs, NKp44 and two CMRF-related cDNAs is important, because it is required for the association with DAP12 (REF. 34). The receptor for polymeric immunoglobulin (pIgR) also has homology with the extracellular region of TREM. However, none of the TREMs, CMRF35 or NKp44 binds immunoglobulin. In fact, all of these receptors are as yet poorly understood in terms of binding specificity.

CD3ζ, contain immunoreceptor tyrosine-based activa-tion motifs (ITAMs), which function as docking sites for protein tyrosine kinases that mediate activation[18] (FIG 1).

How the activating isoforms of self receptors func-tion remains enigmatic. Recent studies on the mouse Ly49 family of receptors indicate that activating iso-forms have evolved to recognize virus-encoded mol-ecules that mimic inhibitory ligands — for example, the mouse cytomegalovirus (MCMV)-encoded class I homologue m157 (REFS 19,20). This strategy would provide the host with pathogen-specific activating receptors. Activating receptors might also contribute to first-line surveillance by recognizing endogenous molecules that are expressed at high levels mainly by virus-infected and transformed cells, as are the MHC class-I-chain-related molecules MICA and MICB, H60 and retinoic acid early inducible genes Rae1α–Rae1δ[21-23].

Several paired activating and inhibitory receptors that are expressed by myeloid cells have been identified (BOX 1).

MICROGLIA
Bone-marrow-derived macrophage lineage cells that are present in the CNS.

The genes that encode TREMs, together with NKp44, map to human chromosome 6p21 and mouse chromosome 17 and are linked to the MHC[35] (FIG. 1). The TREM gene cluster includes at least one other gene that encodes a TREM-related molecule with an ITIM motif in its cytoplasmic tail, which might therefore function as an inhibitory receptor (FIG. 1). Accordingly, this TREM-related receptor has been shown to recruit SH2-domain-containing protein tyrosine phosphatase 1 (SHP1) in transfected cells[36]. So, the TREM gene cluster encodes both activating and inhibitory receptors, as do other immune gene clusters[17]. Additional TREM-like genes and pseudogenes have been predicted by computational analysis of the TREM genomic region (FIG. 1). This cluster arrangement indicates that TREMs might have evolved from the repeated duplication of an ancestral gene and diverged under selective pressure, perhaps for resistance to pathogenic infections.

TREM1: an amplifier of acute inflammation

Human TREM1 is expressed by blood neutrophils and a subset of monocytes/macrophages, which are the main effector cells in innate responses[24]. In normal tissues, TREM1 is selectively expressed by alveolar macrophages[37]. These are long-lived effector cells that are present in the lung, which are specialized for the recognition and clearance of pathogens, phagocytosis of apoptotic or damaged cells and the removal of macromolecules. Furthermore, TREM1 is expressed at high levels by neutrophilic infiltrates and epithelial cells in human skin and lymph nodes that are infected by Gram-positive and -negative bacteria, as well as fungi[38]. The tissue distribution of TREM1 expression has indicated a role in inflammation. Consistent with this, engagement of TREM1 expressed by granulocytes and monocytes with agonist monoclonal antibodies has been shown to stimulate the production of pro-inflammatory chemokines and cytokines[24,39]. Production of interleukin-8 (IL-8, CXCL8), a potent chemoattractant for neutrophils, is strongly induced by the engagement of TREM1, followed by the production of monocyte chemoattractant protein 1 (MCP1, CCL2), MCP3 (CCL7) and macrophage inflammatory protein 1α (MIP1α, CCL3). Triggering of TREM1 also induces granulocytes to release myeloperoxidase[24], but does not induce phagocytosis[39]. A marked upregulation of the production of tumour-necrosis factor (TNF) and IL-1α by monocytes in response to monoclonal antibodies specific for TREM1 is observed when LPS is used as a co-stimulus, showing that TREM1 can amplify inflammatory responses that are initiated by TLRs. In addition, LPS and other TLR ligands upregulate the expression of TREM1, indicating that TREM1 and TLRs cooperate to produce an inflammatory response[38] (N. A. Begum et al., unpublished observations). This cooperation could occur at several levels, as illustrated in FIG. 2. Expression of TREM1 might be controlled by nuclear factor-κB (NF-κB), which is activated by the TLR signalling pathway[1–4]. Conversely, TREM1-mediated tyrosine phosphorylation, activation

of mitogen-activated protein kinases (MAPKs) and mobilization of Ca^{2+} might lead to the activation of transcription complexes, which synergize with NF-κB in promoting the transcription of pro-inflammatory genes (FIG. 2).

The role of TREM1 as an amplifier of inflammation has been confirmed by in vivo studies. In an animal model of LPS-induced shock, blocking signalling through TREM1 with a soluble TREM1–immunoglobulin fusion protein reduced hyperresponsiveness and death[38]. In models of septic shock, including intraperitoneal injection of live Escherichia coli and CAECAL LIGATION AND PUNCTURE (CLP), blocking TREM1 also protected mice against shock and death[38]. Furthermore, transgenic mice that overexpress DAP12 develop high numbers of blood neutrophils, as well as large macrophage infiltrates in the lungs, and are highly susceptible to LPS-induced shock[40]. This phenotype might be explained, in part, by the constitutive activation of the TREM1–DAP12-dependent pathway. Together, these results highlight the crucial role of TREM1 in the amplification of inflammatory responses to bacteria, and implicate TREM1 as a potential target for therapeutic intervention in human diseases that are caused by excessive inflammatory responses to infection, such as septic shock.

Sepsis and septic shock constitute a systemic response to infection that is characterized by a combined hyperinflammatory and immunosuppressive state. The excessive inflammatory response is mediated by increased systemic levels of pro-inflammatory cytokines, such as TNF, IL-1β, high mobility group 1 (HMG1) protein and macrophage migration inhibitory factor (MIF)[41,42]. The coexisting immunosuppressive state is indicated by increased circulating levels of IL-10, transforming growth factor-β (TGF-β) and soluble receptor antagonists, such as IL-1Rα and soluble TNF receptors. Strategies for the treatment of sepsis and septic shock by blocking or attenuating TNF and IL-1 activity have shown partial benefit[43]. So, modulation of TREM1 signalling might help to control the outcome in patients with sepsis. Similarly, TREM1 might be a therapeutic target in other inflammatory syndromes, such as acute lung injury, in which the accumulation of neutrophils leads to a marked release of pro-inflammatory cytokines, loss of epithelial and endothelial integrity and the development of interstitial pulmonary oedema[44].

In summary, the available data indicate that TREM1 amplifies TLR-initiated responses to microbial challenges. Clearly, identifying the natural ligands for TREM1 is essential for understanding its physiological relevance during innate responses. TREM1 could recognize bacterial products, similar to other pattern-recognition receptors. Alternatively, TREM1 might recognize soluble proteins that are secreted during inflammation, such as acute-phase reaction proteins or cell-surface molecules that are expressed at high levels following the initial inflammatory response. Whatever the answer, targeted activation or blockade of TREM1 and its ligand(s) might help to increase the efficacy of existing treatments for sepsis.

TREM1: linking innate and adaptive immunity

Recent evidence indicates that there is a direct link between TREM1 and adaptive immune responses[39]. This hypothesis is supported by the ability of TREM1 to augment monocyte production of chemokines, which recruit effector lymphocytes to the site of inflammation. IL-8, CCL2 and CCL3 are all involved in the recruitment of pro-inflammatory T helper 1 (T_H1) cells. In addition, engagement of TREM1 has recently been shown to induce the differentiation of a subset of primary monocytes into DCs that express CD1A, low levels of CD14, and high levels of MHC class II molecules and CD86. These DCs have a markedly higher capacity to present antigens to naive T cells *in vitro* and to stimulate the production of interferon-γ (IFN-γ) by T_H1 cells, compared with monocytes. Given this, TREM1 might have a role in the adaptive response, as well as in the innate response. Generation of *Trem1*-deficient mice by gene targeting will be crucial to test these models.

TREM2 and partial DC maturation

Whereas the main role of TREM1 is in granulocyte and monocyte/macrophage responses, TREM2 mainly controls the function of other myeloid cells, including DCs, osteoclasts and microglia. Human TREM2 is expressed by immature monocyte-derived DCs[25]. These cells are considered to be the *in vitro* counterparts of DCs that actively sample normal proteins and incoming pathogens in peripheral tissues *in vivo*[45]. When exposed to microbial products, TNF and TNF-related proteins, such as CD40L and TNF-related activation-induced cytokine (TRANCE), immature DCs are activated through the TLRs, TNF receptor (TNFR), CD40 and TRANCE receptor (TRANCER), respectively[45]. Activated DCs downregulate the expression of TREM2 (REF. 25) and antigen-capturing molecules, such as the Fc receptor for IgG (FcγR). At the same time, DCs express the CC-chemokine receptor CCR7, which guides the migration of DCs to the T-cell areas of the lymph nodes.
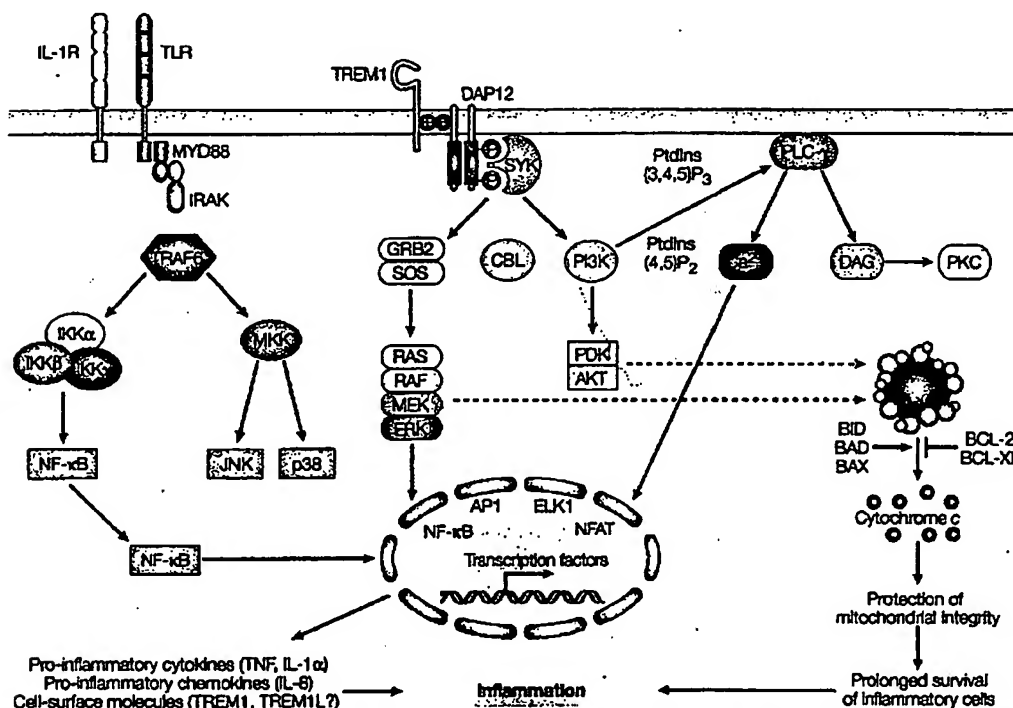

Figure 2 | **Schematic presentation of the role of TREM1 in inflammatory responses.** TREM1 is expressed as a transmembrane receptor complex with the DAP12 chain subunit. The complex is stabilized through a unique electrostatic interaction between a negatively charged (–) amino acid in DAP12 and a positively charged (+) amino acid in TREM chains. After TREM crosslinking, the DAP12 immunoreceptor tyrosine-based activation motif (ITAM) tyrosines (Y) are phosphorylated, possibly by a protein tyrosine kinase of the SRC family, providing a docking site for protein tyrosine kinases of the SYK family. SYK recruits and phosphorylates CBL and growth factor receptor binding protein 2 (GRB2), leading to activation of phosphatidylinositol 3-kinase (PI3K) and extracellular-signal-regulated kinase (ERK) pathways. These pathways induce Ca^{2+} mobilization and activation of transcription factors, including ELK1, nuclear factor of activated T cells (NFAT), activator protein 1 (AP1) and nuclear factor-κB (NF-κB), which transcribe genes that encode pro-inflammatory cytokines, pro-inflammatory chemokines and cell-surface molecules. PI3K and ERK pathways that are triggered by TREM1 also promote mitochondrial integrity and cell survival by inactivating pro-apoptotic factors — BH3-interacting domain death agonist (BID), BCL-2-antagonist of cell death (BAD) and BCL-2-associated X protein (BAX). The TREM signalling cascade synergizes with the interleukin-1 receptor (IL-1R)–Toll-like receptor (TLR) signalling pathways. Engagement of TLR and IL-1R activates a signalling pathway that leads to activation of NF-κB. NF-κB induces the transcription and upregulation of expression of TREM1 by granulocytes and monocytes. In addition, expression of TREM1 ligands might also be upregulated at the inflammatory site. The TREM1 signalling cascade reinforces the production of inflammatory mediators that are initiated by TLR and IL-1R signalling. DAG, diacylglycerol; IRAK, interleukin-1-receptor-associated kinase; IKK, inhibitor of NF-κB kinase; PDK, phosphoinositide-dependent kinase; PKC, protein kinase C; TNF, tumour-necrosis factor; TRAF6, TNF-receptor-associated factor; TREM, triggering receptors expressed by myeloid cells.

In addition, DCs upregulate the expression of MHC, co-stimulatory and adhesion molecules, allowing them to present antigen to rare naive T cells and induce their proliferation[45].

Ligation of TREM2 with agonist monoclonal antibodies on immature DCs *in vitro* has been shown to induce incomplete maturation, in which expression of CCR7 and some co-stimulatory molecules are upregulated, whereas adhesion molecules, such as intercellular adhesion molecule 1 (ICAM1) are not and no IL-12 is released[25]. A similar pattern of DC maturation has also been observed when DCs are activated through the FcγR, which also signals through an ITAM-containing adaptor protein[46]. This partial activation of DCs could be due to selective triggering of the protein tyrosine kinase (PTK), ERK and Ca^{2+} pathways by TREM2 and FcγR[25], whereas TLRs, TNFR, CD40 and TRANCER induce the activation of NF-κB and stress-activated protein kinase (SAPK) or JUN N-terminal kinase (JNK). These observations indicate that maturation of DCs requires many pathways that are independently regulated, rather than an integrated cohort of events. Importantly, distinct patterns of DC activation might influence not only the degree of expansion of naive T-cell populations, but also the subsequent differentiation of helper T cells. Consistent with a role for TREM2 and DAP12 in the migration and activation of DCs, DAP12-deficient mice accumulate DCs in the skin and mucosa and have impaired T$_H$1-cell responses[47,48]. So, TREM2, and probably other DAP12-associated receptors that are expressed by DCs, including the signal regulatory protein-β1 (SIRP-β1)[49], might regulate T-cell responses *in vivo* by activating professional antigen-presenting cells.

TREM2 in osteoclast and glial function

Although TREM2 was originally identified and characterized in DCs that were derived *in vitro* from monocytes, recent evidence indicates that it might be important in brain function and bone modelling. This hypothesis has been triggered by studies of a rare disease known as Nasu-Hakola disease (NHD) or polycystic lipomembranous osteodysplasia with sclerosing leukoencephalopathy (PLOSL)[50-52]. Nasu-Hakola disease is an autosomal recessive disease, which was originally discovered in families from Finland and Japan, and is characterized by a combination of presenile dementia and bone cysts. The brain pathology is characterized by leukodystrophy due to the accumulation of lipidic material, sclerosing leukoencephalopathy with demyelination, axonal loss and massive gliosis[52]. The bone cysts are mainly located in the extremities and are described as cystic spaces that are filled with triglycerides and membranes[52]. On the basis of the pathological changes, Nasu-Hakola disease was originally hypothesized to result from an enzyme deficiency that causes lipid accumulation, similar to the build-up of foamy cells with sphingomyelin that is characteristic of Nieman-Pick syndrome, which is caused by a defect in sphingomyelinase[53].

An original study of Nasu-Hakola disease in Finland reported linkage of the disease to a region of chromosome 19q13 (REFS 54,55). Analysis of potential candidate genes in this chromosomal region, surprisingly, indicated a homozygous deletion of exons 1–4 of the gene encoding DAP12 (REF. 56). Confirming the role of DAP12, five out of six Japanese patients with Nasu-Hakola disease were found to have a loss-of-function DAP12 mutation[57]. In addition, DAP12-deficient mice have Nasu-Hakola disease-like lesions, including osteopetrosis and thalamic hypomyelinosis with synaptic degeneration[58]. However, as DAP12 associates with various cell-surface receptors that are expressed by NK and myeloid cells, the specific receptor(s) involved in the pathogenesis of Nasu-Hakola disease remained unclear. Unexpectedly, recent analysis of patients with Nasu-Hakola disease, who have an intact gene encoding DAP12 and normal expression levels of DAP12, indicated loss-of-function mutations in TREM2 (REF. 59). So, TREM2 and DAP12 seem to be crucially involved in bone modelling and brain myelination. If this is the case, how do TREM2 and DAP12 regulate non-immune functions? Most probably, TREM2 and DAP12 are expressed by a broad range of myeloid cells, including osteoclasts and microglia, which are crucial for bone modelling and brain function, respectively.

In agreement with this hypothesis, expression of TREM2 and DAP12 has recently been detected in osteoclasts and shown to be involved in osteoclast development[58]. Osteoclasts are multinucleated giant cells with the capacity to resorb mineralized tissues[60]. Normal osteoclasts are derived from the fusion of mononuclear myeloid precursors in the presence of two cytokines — macrophage colony-stimulating factor (MCSF) and TRANCE[61]. However, monocytic precursors that are derived from TREM2- and DAP12-deficient patients do not differentiate *in vitro* into mature osteoclasts. As a result, immature osteoclasts resorb bone inefficiently (M. Cella *et al.*, and J. Paloneva *et al.*, unpublished observations). Similarly, DAP12-deficient mice develop osteopetrosis, and the differentiation of DAP12-deficient osteoclasts from bone-marrow precursors is blocked *in vitro*[58].

Expression of TREM2 and DAP12 has also been detected in the brain[59] and microglia[62]. Microglia respond to many physiological and stress stimuli by secreting cytokines and neurotrophic factors. In addition, they contribute to tissue repair by phagocytosing damaged

---

Box 2 | Outstanding questions for TREM biology

• What are the ligands of the triggering receptors expressed by myeloid cells, TREM1 and TREM2? Do TREMs recognize endogenous molecules or microbial products?

• Are Trem1-knockout mice resistant to sepsis?

• Is TREM1 a useful target for therapeutic intervention in septic shock?

• Do Trem2-knockout mice develop symptoms that are similar to Nasu-Hakola disease?

• What is the signalling pathway that allows TREM2 to regulate osteoclast development?

• Why do TREM2-deficient patients develop bone cysts?

• Why do TREM2-deficient patients develop demyelination of the central nervous system and dementia?

• Why do TREM2- and DAP12-deficient patients not develop immune deficiencies?

• What is the function of the inhibitory TREM, TREM-like transcript 1 (TLT1)?

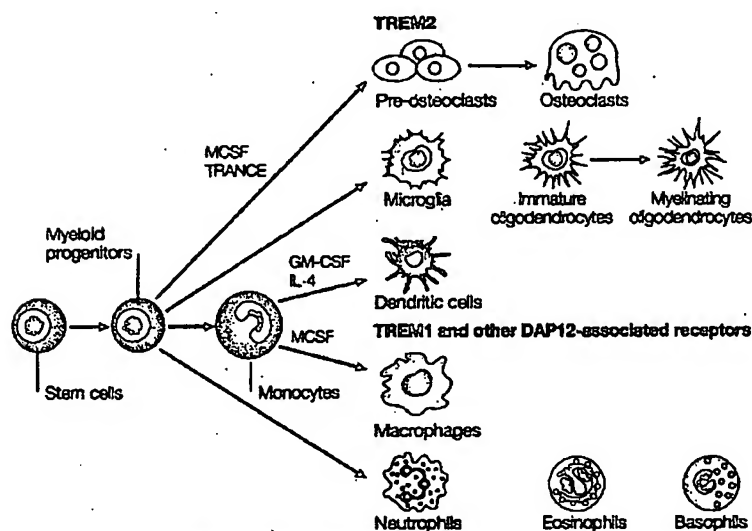• Are TREM mutations responsible for any of the MHC-linked autoimmune diseases?

Figure 3 | TREM regulation of myeloid-cell differentiation. DAP12-associated receptors might regulate myeloid-cell development from a common myeloid progenitor. TREM2 is expressed by monocyte-derived dendritic cells (DCs), immature osteoclasts, microglia and, perhaps, oligodendrocytes. It is required for the differentiation of osteoclast precursors into mature osteoclasts, and might have a role in the differentiation of glial cells and induce the differentiation of monocytes towards a DC pathway, rather than towards a macrophage pathway[58,59]. TREM1 is expressed by mature neutrophils, monocytes and macrophages. Triggering of TREM1 and other DAP12-associated receptors might be crucial for inducing the final differentiation of neutrophils and macrophages and promoting their inflammatory function[40,65]. TREMs might guide myeloid-cell differentiation by modulating the responsiveness to certain cytokines or reinforcing signalling pathways that are triggered by cytokine receptors or integrins. GM-CSF, granulocyte-macrophage colony-stimulating factor; IL-4, interleukin-4; MCSF, macrophage colony-stimulating factor; TREM, triggering receptors expressed by myeloid cells.

neurons[63]. However, so far, no microglial abnormalities have been detected in patients with Nasu-Hakola disease or in DAP12-deficient mice. Unexpectedly, DAP12 is also expressed by normal oligodendrocytes, despite their neuroepithelial origin. Oligodendrocytes form the myelin sheath that surrounds neuron axons, enhancing nerve-signal conductance in the central nervous system and ensuring axonal integrity. It is possible that the TREM2–DAP12 pathway induces the differentiation of immature oligodendrocytes into mature myelin sheath-forming cells. Consistent with this, DAP12-deficient mice have markedly reduced myelination of axons, synapse degeneration and accumulation of synaptic vesicles (especially in the medial thalamus), together with the accumulation of immature oligodendrocytes in areas that surround the thalamus. The expression of DAP12 by oligodendrocytes is surprising, as these cells are thought to be of neuroepithelial rather than myeloid origin. It is possible, however, that DAP12 is expressed only by a particular subset of oligodendrocytes, and that these might originate in the myeloid lineage. Further studies are required to determine whether TREM2 and DAP12 are also expressed by human oligodendrocytes.

Finally, in vitro studies indicate that differentiation of human TREM2-deficient myeloid precursors to DCs is also inefficient (M. Cella et al., unpublished observations). TREM2-deficient monocytes that are cultured in vitro with granulocyte-macrophage colony-stimulating factor

(GM-CSF) and IL-4 differentiate into two distinct cell subsets: a small subset that expresses the DC marker CD1A and a larger population that expresses the macrophage marker CD16, but lacks expression of CD1A. So, TREM2-deficient monocytes seem to favour a macrophage differentiation pathway. Only prolonged treatment with GM-CSF and IL-4 overcomes this bias, eventually driving differentiation towards a DC pathway that is characterized by the acquisition of the CD1A⁺CD16⁻ phenotype typical of monocyte-derived DCs.

In summary, present data indicate that the TREM2–DAP12 pathway directs the differentiation of myeloid precursors towards the formation of mature DCs, osteoclasts, microglia and possibly oligodendrocytes. So far, it is unclear how TREM2 and DAP12 can influence myeloid development. They might modulate cell responsiveness to certain cytokines or reinforce signalling pathways that are triggered by cytokine receptors or integrins. Consistent with this hypothesis, the TREM2–DAP12 signalling pathway might also trigger changes in actin polymerization and cytoskeleton organization, which are required for the fusion of osteoclast precursors into a mature multinucleated osteoclast and to ensure that the cellular processes of oligodendrocytes contact and wrap around the neuron axons.

Another potential role of TREM2 might be promoting the removal of apoptotic cells, organic matrix components and macromolecules by microglia. If so, a defect of TREM2 would lead to the accumulation of toxic products that cause brain damage. Intriguingly, it has been reported recently that a soluble chimaeric protein, which includes the extracellular region of mouse TREM2 and the Fc portion of human IgG, can bind to bacteria, yeast and bacterial products, such as LPS and LTA. Furthermore, this binding is blocked by anionic carbohydrate molecules, including dextran sulphate. Thereby, TREM2 might function as a sort of scavenger receptor for polyanionic macromolecules[64]. The discovery of the ligands for TREM2 and other DAP12-associated receptors will be crucial to verify these hypotheses and to characterize precisely the many contributions of DAP12 to immune and non-immune functions. BOX 2 outlines some of the unresolved questions regarding the biology of TREMs.

Concluding remarks

Among the immune-receptor families that include inhibitory and activating receptors, TREMs seem to be unique in terms of their role in the regulation of myeloid-cell development and function (FIG. 3). Under homeostatic conditions, engagement of TREM2 promotes DC, osteoclast, microglia and oligodendrocyte differentiation (FIG. 3). So, the absence of TREM2 signalling in an immature myeloid-cell precursor results in a partial deficit of these cells and/or their functions. During inflammatory conditions, TREM2 is downregulated, whereas other DAP12-associated receptors, such as TREM1, are upregulated and redirect myeloid-cell differentiation and function, promoting inflammatory responses by granulocytes, monocytes and macrophages (FIG. 3). Accordingly, overexpression of DAP12 by a monocytic cell line induces macrophage differentiation

in vitro[65,66]. Moreover, DAP12-transgenic mice develop neutrophilia *in vivo*[40].

Another unique feature of TREMs is the role of TREM2 deficiency in Nasu–Hakola disease. As DAP12 and TREM2 deficiencies result in virtually identical diseases, TREM2, remarkably, seems to be the main receptor among all the DAP12-associated receptors. It will be important to investigate further the polymorphism of

TREM2, the plasticity of the TREM region in the human population — for example, the variation of gene number and polymorphisms — and the possible association of TREM diversity with other human diseases. Among these, multiple sclerosis is an obvious candidate, given the role of TREM2 in brain myelination, the association of multiple sclerosis with MHC class II molecules, and the linkage of TREMs with the MHC.

1. Hoffmann, J. A., Kafatos, F. C., Janeway, C. A. & Ezekowitz, R. A. Phylogenetic perspectives in innate immunity. *Science* 284, 1313–1318 (1999).
2. Medzhitov, R. Toll-like receptors and innate immunity. *Nature Rev. Immunol.* 1, 135–145 (2001).
3. Poltorak, A. et al. Defective LPS signaling in C3H/HeJ and C57BL/10ScCr mice: mutations in Tlr4 gene. *Science* 282, 2085–2088 (1998).
4. Akira, S., Takeda, K. & Kaisho, T. Toll-like receptors: critical proteins linking innate and acquired immunity. *Nature Immunol.* 2, 675–680 (2001).
5. Aderem, A. & Underhill, D. M. Mechanisms of phagocytosis in macrophages. *Annu. Rev. Immunol.* 17, 593–623 (1999).
6. Linehan, S. A., Martinez-Pomares, L. & Gordon, S. Mannose receptor and scavenger receptor: two macrophage pattern recognition receptors with diverse functions in tissue homeostasis and host defense. *Adv. Exp. Med. Biol.* 479, 1–14 (2000).
7. Brown, G. D. et al. Dectin-1 is a major β-glucan receptor on macrophages. *J. Exp. Med.* 196, 407–412 (2002).
8. Barrington, R., Zhang, M., Fischer, M. & Carroll, M. C. The role of complement in inflammation and adaptive immunity. *Immunol. Rev.* 180, 5–15 (2001).
9. Fraser, I. P., Koziel, H. & Ezekowitz, R. A. The serum mannose-binding protein and the macrophage mannose receptor are pattern recognition molecules that link innate and adaptive immunity. *Semin. Immunol.* 10, 363–372 (1998).
10. Lanier, L. L. NK cell receptors. *Annu. Rev. Immunol.* 16, 359–393 (1998).
11. Dietrich, J., Nakajima, H. & Colonna, M. Human inhibitory and activating Ig-like receptors which modulate the function of myeloid cells. *Microbes Infect.* 2, 323–329 (2000).
12. Oldenborg, P. A. et al. Role of CD47 as a marker of self on red blood cells. *Science* 288, 2051–2054 (2000).
13. Wright, G. J. et al. Lymphoid/neuronal cell surface OX2 glycoprotein recognizes a novel receptor on macrophages implicated in the control of their function. *Immunity* 13, 233–242 (2000).
14. Hoek, R. M. et al. Down-regulation of the macrophage lineage through interaction with OX2 (CD200). *Science* 290, 1768–1771 (2000).
15. Barclay, A. N., Wright, G. J., Brooke, G. & Brown, M. H. CD200 and membrane protein interactions in the control of myeloid cells. *Trends Immunol.* 23, 285–290 (2002).
16. Crocker, P. R. & Varki, A. Siglecs, sialic acids and innate immunity. *Trends Immunol.* 22, 337–342 (2001).
17. Trowsdale, J. Genetic and functional relationships between MHC and NK receptor genes. *Immunity* 15, 363–374 (2001).
18. Tomasello, E., Bléry, M., Vély, E. & Vivier, E. Signaling pathways engaged by NK cell receptors: double concerto for activating receptors, inhibitory receptors and NK cells. *Semin. Immunol.* 12, 139–147 (2000).
19. Arase, H., Mocarski, E. S., Campbell, A. E., Hill, A. B. & Lanier, L. L. Direct recognition of cytomegalovirus by activating and inhibitory NK cell receptors. *Science* 296, 1323–1326 (2002).
20. Smith, H. R. et al. Recognition of a virus-encoded ligand by a natural killer cell activation receptor. *Proc. Natl Acad. Sci. USA* 99, 8826–8831 (2002).
21. Bauer, S. et al. Activation of NK cells and T cells by NKG2D, a receptor for stress-inducible MICA. *Science* 285, 727–729 (1999).
22. Diefenbach, A., Jamieson, A. M., Liu, S. D., Shastri, N. & Raulet, D. H. Ligands for the murine NKG2D receptor: expression by tumor cells and activation of NK cells and macrophages. *Nature Immunol.* 1, 119–126 (2000).
23. Cerwenka, A. et al. Retinoic acid early inducible genes define a ligand family for the activating NKG2D receptor in mice. *Immunity* 12, 721–727 (2000).

24. Bouchon, A., Dietrich, J. & Colonna, M. Cutting edge: inflammatory responses can be triggered by TREM-1, a novel receptor expressed on neutrophils and monocytes. *J. Immunol.* 164, 4991–4995 (2000).
    This paper reported the original cloning of the triggering receptors expressed by myeloid cells (TREMs).
25. Bouchon, A., Hernandez-Munain, C., Cella, M. & Colonna, M. A DAP12-mediated pathway regulates expression of CC chemokine receptor 7 and maturation of human dendritic cells. *J. Exp. Med.* 194, 1111–1122 (2001).
    A paper that characterized the function of TREM2 in dendritic cells.
26. McVicar, D. W. et al. DAP12-mediated signal transduction in natural killer cells. A dominant role for the Syk protein-tyrosine kinase. *J. Biol. Chem.* 273, 32934–32942 (1998).
27. Gingras, M. C., Lapillonne, H. & Margolin, J. F. TREM-1, MDL-1, and DAP12 expression is associated with a mature stage of myeloid development. *Mol. Immunol.* 38, 817–824 (2002).
28. Daws, M. R., Lanier, L. L., Seaman, W. E. & Ryan, J. C. Cloning and characterization of a novel mouse myeloid DAP12-associated receptor family. *Eur. J. Immunol.* 31, 783–791 (2001).
    The first group to characterize mouse Trems.
29. Chung, D. H., Seaman, W. E. & Daws, M. R. Characterization of TREM-3, an activating receptor on mouse macrophages: definition of a family of single Ig domain receptors on mouse chromosome 17. *Eur. J. Immunol.* 32, 59–66 (2002).
30. Cantoni, C. et al. NKp44, a triggering receptor involved in tumor cell lysis by activated human natural killer cells, is a novel member of the immunoglobulin superfamily. *J. Exp. Med.* 189, 787–796 (1999).
31. Jackson, D. G., Hart, D. N., Starling, G. & Bell, J. I. Molecular cloning of a novel member of the immunoglobulin gene superfamily homologous to the polymeric immunoglobulin receptor. *Eur. J. Immunol.* 22, 1157–1163 (1992).
32. Green, B. J., Clark, G. J. & Hart, D. N. The CMRF-35 mAb recognizes a second leukocyte membrane molecule with a domain similar to the poly Ig receptor. *Int. Immunol.* 10, 891–899 (1998).
33. Speckman, R. A. et al. Novel immunoglobulin superfamily gene cluster, mapping to a region of human chromosome 17q25, linked to psoriasis susceptibility. *Hum. Genet.* 112, 34–41 (2003).
34. Wu, J., Cherwinski, H., Spies, T., Phillips, J. H. & Lanier, L. L. DAP10 and DAP12 form distinct, but functionally cooperative, receptor complexes in natural killer cells. *J. Exp. Med.* 192, 1059–1068 (2000).
35. Allcock, R. J., Barrow, A. D., Forbes, S., Beck, S. & Trowsdale, J. The human TREM gene cluster at 6p21.2 encodes both activating and inhibitory single IgV domain receptors and includes NKp44. *Eur. J. Immunol.* 33, 567–577 (2003).
36. Washington, A. V., Quigley, L. & McVicar, D. W. Initial characterization of TREM-like transcript (TLT)-1: a putative inhibitory receptor within the TREM cluster. Triggering receptors expressed on myeloid cells. *Blood* 100, 3822–3824 (2002).
37. Colonna, M. & Facchetti, F. TREM-1: a new player in acute inflammatory responses. *J. Infect. Dis.* (in the press).
38. Bouchon, A., Facchetti, F., Weigand, M. A. & Colonna, M. TREM-1 amplifies inflammation and is a crucial mediator of septic shock. *Nature* 410, 1103–1107 (2001).
    Identification of the pro-inflammatory function of TREM1.
39. Bleharski, J. R. et al. A role for triggering receptor expressed on myeloid cells-1 in host defense during the early-induced and adaptive phases of the immune response. *J. Immunol.* 170, 3812–3818 (2003).
40. Lucas, M. et al. Massive inflammatory syndrome and lymphocytic immunodeficiency in KARAP/DAP12-transgenic mice. *Eur. J. Immunol.* 32, 2653–2663 (2002).

41. Wang, H. et al. HMG-1 as a late mediator of endotoxin lethality in mice. *Science* 285, 248–251 (1999).
42. Bernhagen, J. et al. MIF is a pituitary-derived cytokine that potentiates lethal endotoxaemia. *Nature* 365, 756–759 (1993).
43. Tracey, K. J. & Abraham, E. From mouse to man: or what have we learned about cytokine-based anti-inflammatory therapies? *Shock* 11, 224–225 (1999).
44. Ware, L. B. & Matthay, M. A. The acute respiratory distress syndrome. *N. Engl. J. Med.* 342, 1334–1349 (2000).
45. Banchereau, J. & Steinman, R. M. Dendritic cells and the control of immunity. *Nature* 392, 245–252 (1998).
46. Regnault, A. et al. Fcγ receptor-mediated induction of dendritic cell maturation and major histocompatibility complex class I-restricted antigen presentation after immune complex internalization. *J. Exp. Med.* 189, 371–380 (1999).
47. Tomasello, E. et al. Combined natural killer cell and dendritic cell functional deficiency in KARAP/DAP12 loss-of-function mutant mice. *Immunity* 13, 355–364 (2000).
48. Bakker, A. B. et al. DAP12-deficient mice fail to develop autoimmunity due to impaired antigen priming. *Immunity* 13, 345–353 (2000).
49. Dietrich, J., Cella, M., Seiffert, M., Buhring, H. J. & Colonna, M. Cutting edge: signal-regulatory protein β1 is a DAP12-associated activating receptor expressed in myeloid cells. *J. Immunol.* 164, 9–12 (2000).
50. Hakola, H. P., Jarvi, O. H. & Sourander, P. Osteodysplasia polycystica hereditaria combined with sclerosing leucoencephalopathy, a new entity of the dementia presenilis group. *Acta Neurol. Scand.* 46, S79 (1970).
51. Nasu, T., Tsukahara, Y. & Terayama, K. A lipid metabolic disease — 'membranous lipodystrophy' — an autopsy case demonstrating numerous peculiar membrane-structures composed of compound lipid in bone and bone marrow and various adipose tissues. *Acta Pathol. Jpn* 23, 539–558 (1973).
52. Verloes, A. et al. Nasu–Hakola syndrome: polycystic lipomembranous osteodysplasia with sclerosing leucoencephalopathy and presenile dementia. *J. Med. Genet.* 34, 753–757 (1997).
53. Kitajima, I. et al. Nasu–Hakola disease (membranous lipodystrophy). Clinical, histopathological and biochemical studies of three cases. *J. Neurol. Sci.* 91, 35–52 (1989).
54. Pekkarinen, P. et al. Assignment of the locus for PLO-SL, a frontal-lobe dementia with bone cysts, to 19q13. *Am. J. Hum. Genet.* 62, 362–372 (1998).
55. Pekkarinen, P. et al. Fine-scale mapping of a novel dementia gene, PLOSL, by linkage disequilibrium. *Genomics* 54, 307–315 (1998).
56. Paloneva, J. et al. Loss-of-function mutations in TYROBP (DAP12) result in a presenile dementia with bone cysts. *Nature Genet.* 25, 357–361 (2000).
57. Kondo, T. et al. Heterogeneity of presenile dementia with bone cysts (Nasu–Hakola disease): Three genetic forms. *Neurology* 59, 1105–1107 (2002).
58. Kaifu, T. et al. Osteopetrosis and thalamic hypomyelinosis with synaptic degeneration in DAP12-deficient mice. *J. Clin. Invest.* 111, 323–332 (2003).
    This study characterizes the role of DAP12 in the development of osteoclasts and oligodendrocytes in vivo and in vitro.
59. Paloneva, J. et al. Mutations in two genes encoding different subunits of a receptor signaling complex result in an identical disease phenotype. *Am. J. Hum. Genet.* 71, 656–662 (2002).
    Original identification of TREM2 mutations as the basis of Nasu–Hakola disease.
60. Teitelbaum, S. L. Bone resorption by osteoclasts. *Science* 289, 1504–1508 (2000).
61. Wong, B. R., Josien, R. & Choi, Y. TRANCE is a TNF family member that regulates dendritic cell and osteoclast function. *J. Leukocyte Biol.* 65, 715–724 (1999).

62. Schmid, C. D. *et al.* Heterogeneous expression of the triggering receptor expressed on myeloid cells-2 on adult murine microglia. *J. Neurochem.* **83**, 1309–1320 (2002).

63. Kreutzberg, G. W. Microglia: a sensor for pathological events in the CNS. *Trends Neurosci.* **19**, 312–318 (1996).

64. Daws, M. R., Sullam, P. M., Niemi, E. C., Chen, T. T. & Seaman, W. E. Pattern recognition by TREM-2: binding of anionic ligands. *J. Immunol.* (in the press).
The first identification of a TREM2 ligand.

65. Aoki, N. *et al.* The role of the DAP12 signal in mouse myeloid differentiation. *J. Immunol.* **165**, 3790–3796 (2000).

66. Aoki, N. *et al.* DAP12 ITAM motif regulates differentiation and apoptosis in M1 leukemia cells. *Biochem. Biophys. Res. Commun.* **291**, 296–304 (2002).

67. Samaridis, J. & Colonna, M. Cloning of novel immunoglobulin superfamily receptors expressed on human myeloid and lymphoid cells: structural evidence for new stimulatory and inhibitory pathways. *Eur. J. Immunol.* **27**, 660–665 (1997).

68. Colonna, M. *et al.* A common inhibitory receptor for major histocompatibility complex class I molecules on human lymphoid and myelomonocytic cells. *J. Exp. Med.* **186**, 1809–1818 (1997).

69. Colonna, M. *et al.* A novel immunoglobulin superfamily receptor for cellular and viral MHC class I molecules. *Immunity* **7**, 273–282 (1997).

70. Colonna, M. *et al.* Human myelomonocytic cells express an inhibitory receptor for classical and nonclassical MHC class I molecules. *J. Immunol.* **160**, 3096–3100 (1998).

71. Borges, L., Hsu, M. L., Fanger, N., Kubin, M. & Cosman, D. A family of human lymphoid and myeloid Ig-like receptors, some of which bind to MHC class I molecules. *J. Immunol.* **159**, 5192–5196 (1997).

72. Allen, R. L., Raine, T., Haude, A., Trowsdale, J. & Wilson, M. J. Leukocyte receptor complex-encoded immunomodulatory receptors show differing specificity for alternative HLA-B27 structures. *J. Immunol.* **167**, 5543–5547 (2001).

73. Nakajima, H., Samaridis, J., Angman, L. & Colonna, M. Human myeloid cells express an activating ILT receptor (ILT1) that associates with Fc receptor γ-chain. *J. Immunol.* **162**, 5–8 (1999).

74. Kubagawa, H., Burrows, P. D. & Cooper, M. D. A novel pair of immunoglobulin-like receptors expressed by B cells and myeloid cells. *Proc. Natl Acad. Sci. USA* **94**, 5261–5266 (1997).

75. Kharitonenkov, A. *et al.* A family of proteins that inhibit signaling through tyrosine kinase receptors. *Nature* **386**, 181–186 (1997).

76. Brown, E. J. & Frazier, W. A. Integrin-associated protein (CD47) and its ligands. *Trends Cell Biol.* **11**, 130–135 (2001).

77. Oldenborg, P. A. *et al.* Role of CD47 as a marker of self on red blood cells. *Science* **288**, 2051–2054 (2000).

78. Dietrich, J., Cella, M., Seiffert, M., Bühring, H. J. & Colonna, M. Cutting edge: signal-regulatory protein β1 is a DAP12-associated activating receptor expressed in myeloid cells. *J. Immunol.* **184**, 9–12 (2000).

79. Tomasello, E. *et al.* Association of signal-regulatory proteins β with KARAP/DAP-12. *Eur. J. Immunol.* **30**, 2147–2156 (2000).

80. Wright, G. J. *et al.* Lymphoid/neuronal cell surface OX2 glycoprotein recognizes a novel receptor on macrophages implicated in the control of their function. *Immunity* **13**, 233–242 (2000).

81. Hoek, R. M. *et al.* Down-regulation of the macrophage lineage through interaction with OX2 (CD200). *Science* **290**, 1768–1771 (2000).

82. Barclay, A. N., Wright, G. J., Brooke, G. & Brown, M. H. CD200 and membrane protein interactions in the control of myeloid cells. *Trends Immunol.* **23**, 285–290 (2002).

83. Fournier, N. *et al.* FDF03, a novel inhibitory receptor of the immunoglobulin superfamily, is expressed by human dendritic and myeloid cells. *J. Immunol.* **165**, 1197–1209 (2000).

84. Mousseau, D. D., Banville, D., L'Abbe, D., Bouchard, P. & Shen, S. H. PILRα, a novel immunoreceptor tyrosine-based inhibitory motif-bearing protein, recruits SHP-1 upon tyrosine phosphorylation and is paired with the truncated counterpart PILRβ. *J. Biol. Chem.* **275**, 4467–4474 (2000).

85. Cantoni, C. *et al.* Molecular and functional characterization of IRp60, a member of the immunoglobulin superfamily that functions as an inhibitory receptor in human NK cells. *Eur. J. Immunol.* **29**, 3148–3159 (1999).

86. Bakker, A. B., Baker, E., Sutherland, G. R., Phillips, J. H. & Lanier, L. L. Myeloid DAP12-associating lectin (MDL)-1 is a cell surface receptor involved in the activation of myeloid cells. *Proc. Natl Acad. Sci. USA* **96**, 9792–9796 (1999).

Online links

DATABASES

The following terms in this article are linked online to:
LocusLink: http://www.ncbi.nlm.nih.gov/LocusLink/
CBL | CCL2 | CCL3 | CCL7 | CCR7 | CD1A | CD3ζ | CD16 | CD40L | DAP12 | GM-CSF | GRB2 | H60 | HMG1 | ICAM1 | IFN-γ | IL-1α | IL-1β | IL-4 | IL-8 | IL-10 | JNK | MCSF | MICA | MICB | MIF | NF-κB | NKp44 | PTK | SHP1 | SIRP-β1 | SYK | TGF-β | TNF | TRANCE | ZAP70
OMIM: http://www.ncbi.nlm.nih.gov/Omim/
Nasu-Hakola disease

FURTHER INFORMATION

LILR nomenclature web site:
http://www.gene.ucl.ac.uk/nomenclature/genefamily/lilr.html
KIR nomenclature web site:
http://www.gene.ucl.ac.uk/nomenclature/genefamily/kir.html
Access to this interactive links box is free online.